Application of Ring-Closing Metathesis to the Synthesis of Unsaturated 14-Membered Lactams and the Marine Alkaloids Motuporamines A-C

by

WILLIAM PETER DONALD GOLDRING

B.Sc. (Hons.), The University of Toronto, 1995

A THESIS SUBMITTED IN PARTIAL FULFILLMENT OF
THE REQUIREMENTS FOR THE DEGREE OF
DOCTOR OF PHILOSOPHY

in

THE FACULTY OF GRADUATE STUDIES
(Department of Chemistry)

We accept this thesis as conforming to the required standard

THE UNIVERSITY OF BRITISH COLUMBIA
August, 2000

In presenting this thesis in partial fulfilment of the requirements for an advanced degree at the University of British Columbia, I agree that the Library shall make it freely available for reference and study. I further agree that permission for extensive copying of this thesis for scholarly purposes may be granted by the head of my department or by his or her representatives. It is understood that copying or publication of this thesis for financial gain shall not be allowed without my written permission.

Department of CHEMISTRY

The University of British Columbia
Vancouver, Canada

Date 28/8/00

ABSTRACT

The construction of unsaturated 14-membered lactams **77-92** via ring-closing metathesis (RCM) of a series of diene-amides using Grubbs' benzylidene **3** was examined as part of an ongoing study in our laboratory into the chemistry and formation of macrocyclic compounds. Specifically, nine contiguous sites for ring closure were examined to explore the factors governing the yield and the resulting diastereomeric ratio of the newly formed olefin. The position of the olefin within the lactam products was confirmed with 2D NMR experiments, and the configuration was determined with ^{1}H NMR homonuclear decoupling experiments. The diene-amide substrates were in turn synthesized from simple carboxylic acids, alkenyl amines, and alkenyl halides using amidation or amide alkylation methods.

Further exploration of the factors governing these reactions was conducted by studies into the effects of additives, reaction conditions, and structural modifications to the diene-amide. With respect to the latter, selected diene-amides were protected with a BOC group, and in one case a diene was differentially substituted with respect to the double bonds to provide the only observed formation of lactams **91** and **92** via RCM.

The observed trend in yield for the series of RCM reactions was rationalized based on relative enthalpies of ring closure, relative product energies, and the formation of unproductive intramolecular catalyst complexes. The latter appeared to be the predominant factor governing cyclization. Cyclization yields increased with the distance between the amide group and the terminal double bonds of the diene-amide.

The observed *E*/*Z* ratios at each site of ring closure from the RCM reactions were rationalized by comparison to calculated *E*/*Z* ratios based on the energy difference between molecular mechanics calculated global minimum energy conformations for each pair of isomeric lactams. The moderate to high correlation between the observed and calculated ratios suggested that the relative transition state energies were reflected in the relative energies of the (*E*)- and (*Z*)-lactam products. Olefin isomerization of selected lactams with ruthenium methylidene **4** was attempted, and the isomeric ratios were found to be different from those obtained from the RCM reactions.

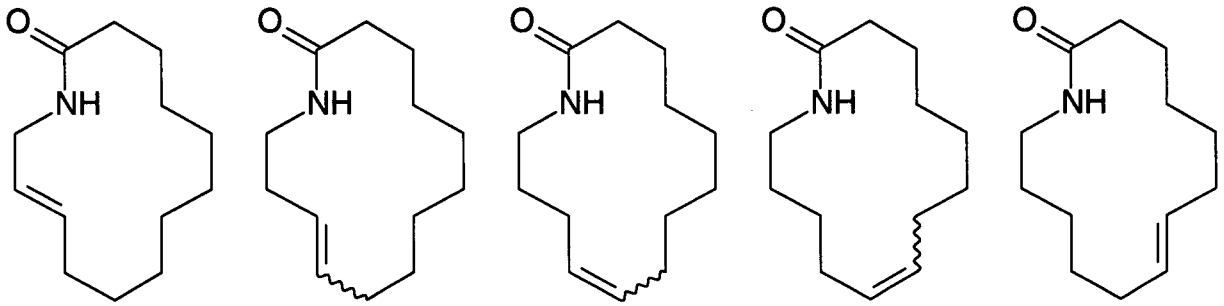

77

(*Z*)-**78**
(*E*)-**79**

(*Z*)-**80**
(*E*)-**81**

(*E*)-**82**
(*Z*)-**83**

84

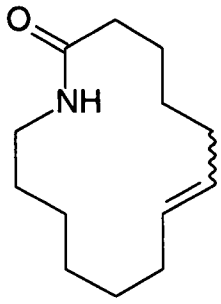

(*Z*)-**85**
(*E*)-**86**

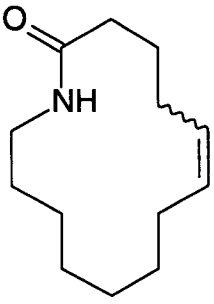

(*Z*)-**87**
(*E*)-**88**

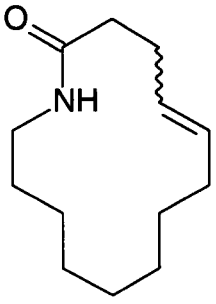

(*E*)-**89**
(*Z*)-**90**

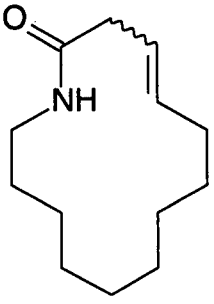

(*E*)-**91**
(*Z*)-**92**

The knowledge gained from the previous studies was applied to the total synthesis of the cytotoxic marine alkaloids motuporamines A (**33**), B (**34**), and C (**39**) and the respective diacetylated derivatives **36**, **37**, and **41**. The macrocyclic amine units of motuporamines B and C were constructed via RCM, and the spermidine-like unit common to all three natural products was constructed using Michael addition and amidation methods. Lactams **83**, **85**, and **86** were constructed via RCM and applied in the synthesis of motuporamine B. The structural ambiguity of motuporamine C, with respect to the position of the olefin within the macrocyclic amine unit, prompted the synthesis of the two positional isomers **39** and **40**. These compounds were synthesized from the 15-membered lactams **171** and **162** respectively, which were in turn constructed from the corresponding diene-amides via RCM.

Comparisons were made between the spectral data of the authentic and synthetic compounds. Minor differences between compounds **37** and **37**·TFA, and authentic diacetylmotuporamine B were observed. This indicated that the structure assigned to motuporamine B was incorrect. Compounds **36**·TFA and **41**·TFA were found to be identical to authentic diacetylmotuporamines A and C, respectively. This indicated that the authentic compounds were isolated as the ammonium trifluoroacetate

salts. The position of the olefin within authentic motuporamine C was assigned to the C-14/C-15 bond position, as represented in compound **39**.

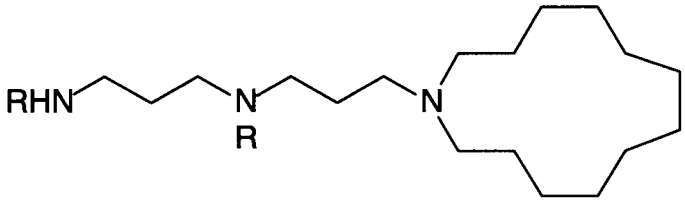

33 R = H (motuporamine A)
36 R = Ac

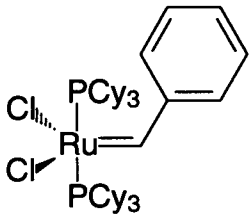

3

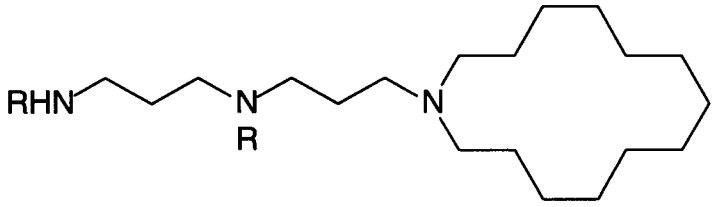

34 R = H (motuporamine B)
37 R = Ac

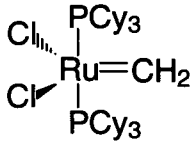

4

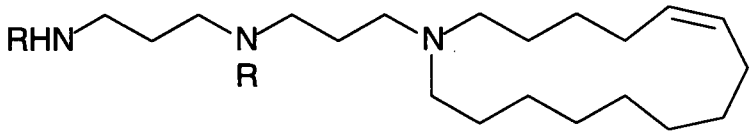

39 R = H (motuporamine C)
41 R = Ac

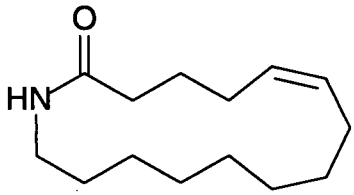

171

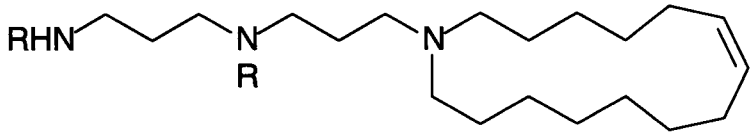

40 R = H
42 R = Ac

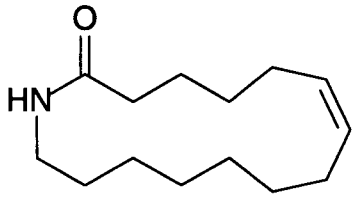

162

TABLE OF CONTENTS

LIST OF SCHEMES

LIST OF FIGURES

LIST OF TABLES

LIST OF ABBREVIATIONS

1D 1-dimensional
2D 2-dimensional
Ac ..... acetyl
ADMET ..... acyclic diene metathesis
Bn ..... benzyl
BOC ..... *tert*-butoxycarbonyl
bp ..... boiling point
bs ..... broad singlet
Bu ..... butyl
CBZ ..... carbobenzyloxy
CI ..... chemical ionization
COSY ..... correlation spectroscopy
Cp ..... cyclopentadienyl
Cy ..... cyclohexyl
d ..... doublet
DCC 1,3-dicyclohexylcarbodiimide
DCI ..... desorption chemical ionization
dd ..... doublet of doublets
ddt ..... doublet of doublet of triplets
DMAP ..... *N*,*N*-dimethylaminopyridine
DMF ..... *N*,*N*-dimethylformamide
DNMR ..... dynamic nuclear magnetic resonance
dt ..... doublet of triplets
EI ..... electron ionization
Et ..... ethyl
eq. ..... equivalents
FAB ..... fast-atom bombardment
FLC ..... flash liquid chromatography
Fmoc 9-fluorenylmethyloxycarbonyl
G ..... Gibbs free energy

GC ..... gas chromatography

H ..... enthalpy

Hz ..... hertz

h ..... hour(s)

HMBC ..... heteronuclear multiple bond connectivity spectroscopy

HMQC ..... heteronuclear multiple quantum coherence spectroscopy

HOBt 1-hydroxybenzotriazole

HPLC ..... high performance liquid chromatography

HRMS ..... high resolution mass spectrum or spectrometry

i-Pr ..... isopropyl

IR ..... infrared (spectroscopy)

J ..... coupling constant

k ..... Boltzmann constant (1.38066×10^{-23} JK^{-1})

LAH ..... lithium aluminum hydride

LDA ..... lithium diisopropylamide

LRMS ..... low resolution mass spectrum or spectrometry

LSIMS ..... liquid secondary ion mass spectrum or spectrometry

M ..... Molar, moles per Litre

m ..... multiplet

M^+ ..... molecular ion

m/z ..... mass-to-charge ratio

Me ..... methyl

Ms ..... methanesulfonyl

N ..... Avogadro constant (6.02214×10^{23} mol^{-1})

^{1}H NMR ..... nuclear magnetic resonance (proton)

^{13}C NMR ..... nuclear magnetic resonance (carbon)

^{19}F NMR ..... nuclear magnetic resonance (fluorine)

p ..... para

PG ..... protecting group

Ph ..... phenyl

PhH ..... benzene

ppm ..... parts per million

pyr ..... pyridine

q ..... quartet

quant. ..... quantitative

quint..... quintet

R..... Molar gas constant (8.3145 $JK^{-1}mol^{-1}$)

RCM ..... ring-closing metathesis

R_f ..... retention factor or ratio-to-front

RLC ..... radial liquid chromatography

ROMP..... ring opening metathesis polymerization

rt ..... room temperature

S..... entropy

s..... singlet

T ..... Temperature

t..... tertiary

t ..... time or
triplet (spectroscopy)

TBDPS ..... *tert*-butyldiphenylsilyl

TCBOC..... 2,2,2-trichloro-*tert*-butoxycarbonyl

TEA ..... triethylamine

Tf ..... trifluoromethanesulfonyl

TFA..... trifluoroacetic acid or trifluoroacetate

THF ..... tetrahydrofuran

TLC..... thin layer chromatography

tosyl..... *p*-toluenesulfonyl

tosylate ..... *p*-toluenesulfonate

Ts ..... *p*-toluenesulfonyl

ACKNOWLEDGMENTS

I wish to express my gratitude to the now late Professor Larry Weiler, my Ph.D. supervisor. Your guidance, support, generosity, and patience both scientific and otherwise were extraordinary. Your presence and effect on this world is greatly missed.

This work could not have been accomplished without assistance from the NMR Laboratory (Liane and Marietta), Mass Spectrometry Laboratory, Microanalysis Laboratory (Mr. Peter Borda), Computer Services (Mr. Jason Gozjolko), and Glass Shop (Mr. Steve Rak). I thank Dr. Nick Burlinson and Mr. Dean Clyne (now Dr.) for their assistance and helpful discussions regarding various aspects of NMR spectroscopy.

Following the passing of Professor Weiler, I thank Dr. Michael Pungente for supervision and Professor Martin Tanner for reading this thesis during the writing process. Their hard work and support facilitated the completion of this thesis.

I thank the members of the Weiler lab, both past and those of us who remained, for many helpful and stimulating discussions, and for the mutual support of our loss.

Special thanks to Mr. André Hodder (M. le H) for his friendship, and providing a challenging and often crazy research environment.

I owe the maintenance of my sanity throughout this degree to Jamie Morris. Thank you for your friendship and many memorable adventures. Special thanks to Andrea Nicholson for her friendship, and her excellent research contribution to our laboratory that allowed me to learn how to teach. What up dog? I also thank Sitki: and Autonomica for allowing me to bring a little of this world into theirs.

Financial support provided by NSERC and UBC (UGF) is also acknowledged.

For her strength and patience I am eternally indebted to my fiancée Sherry. Thank you for not only encouraging and inspiring, but also participating in this process.

Why, for example, should a group of simple, stable compounds of carbon, hydrogen, oxygen and nitrogen struggle for billions of years to organize themselves into a professor of chemistry? What's the motive? If we leave a chemistry professor out on a rock in the sun long enough the forces of nature will convert him into simple compounds of carbon, oxygen, hydrogen and nitrogen, calcium, phosphorous, and small amounts of other minerals. It's a one-way reaction. No matter what kind of chemistry professor we use and no matter what process we use we can't turn these compounds back into a chemistry professor. Chemistry professors are unstable mixtures of predominantly unstable compounds which, in the exclusive presence of the sun's heat, decay irreversibly into simpler organic and inorganic compounds. That's a scientific fact.

The question is: Then why does nature reverse this process? What on earth causes the inorganic compounds to go the other way? It isn't the suns energy. We just saw what the sun's energy did. It has to be something else. What is it?

Robert M. Pirsig from *Lila*

DEDICATION

To Sherry, my parents, and
to the memory of Dr. Larry Weiler.

I also dedicate this thesis to those who challenge
themselves beyond what they already know.

CHAPTER 1
INTRODUCTION

The sciences are but one philosophical approach humans choose to understand the universe in which we exist. Such tools of rational thought provide a systematic method for investigating physical phenomenon from macroscopic to microscopic levels. Chemistry is the study of the microscopic level, and specifically the properties, interactions, and bonding of and between atoms and molecules. Through human intervention, the construction and deconstruction of molecules, an ensemble of bonded atoms, provides a better understanding of these characteristics. Organic chemistry specifically studies molecules containing, but not necessarily limited to, carbon, hydrogen, oxygen, and nitrogen atoms. Such molecules are most commonly found in biological systems, such as human beings, and an investigation of their physical properties constitutes an approach to understanding living systems on the molecular level. In synthetic organic chemistry such molecules are in one way better understood through the development of methods for constructing, deconstructing, or rearranging their structural features. Furthermore, these methods are applied to the construction of molecules obtained from biological systems, termed natural products, and the synthesis of such compounds is a branch of organic chemistry called natural product synthesis.

Natural product total syntheses are often conducted to provide a significant amount of an otherwise rare compound of biological interest, due to the limited availability from natural sources. This allows further study of the physical, chemical, and biological properties. The synthesis of natural products also provides an opportunity to develop and test synthetic methods that were otherwise unavailable. Synthetic methods development is often inspired by novel structural features within molecules, and by existing methods and the potential for improvement. Conducted in consort, a synergetic relationship develops as each requires and perpetuates the other. Natural products often have interesting biological properties with potential applications to issues of human health. Some examples include epothilones A and B, Sch 38516, manzamine A, and roseophilin. The synthesis of such compounds in the laboratory often involves elements of efficiency, economy, and elegance. The excitement over potential

biological activity and applications often leads to competitive synthetic efforts to construct these molecules. However,

> It's not unusual for compounds that attract so much synthetic interest to ultimately prove disappointing from a therapeutic standpoint and to drop off scientists' radar screens soon after the excitement of total synthesis has died down.[1]

One method that has recently been developed, but is not necessarily new to organic synthesis, is ring-closing metathesis (RCM). This reaction allows the construction of cyclic compounds from acyclic precursors. Application of this method to the construction of the natural products mentioned above is indicated on the structures below. RCM has received much attention from both areas of methodological development and natural product total synthesis. Although much of the attention has come from high profile total syntheses, the true highlight of this reaction is the facile application in a number of areas of chemistry such as molecular recognition and self-assembly, solid phase synthesis, transition metal catalysis, and of course natural product total synthesis.

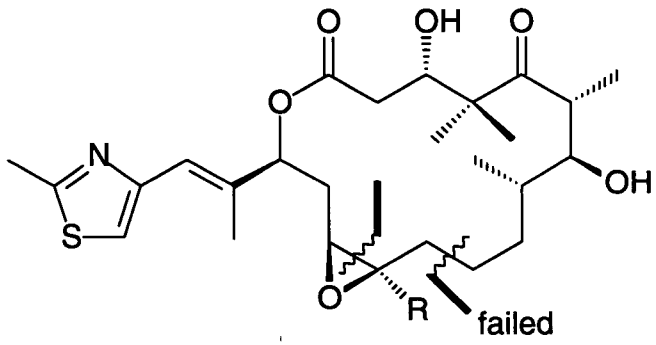

epothilone A (R = H)
epothilone B (R = CH_3)

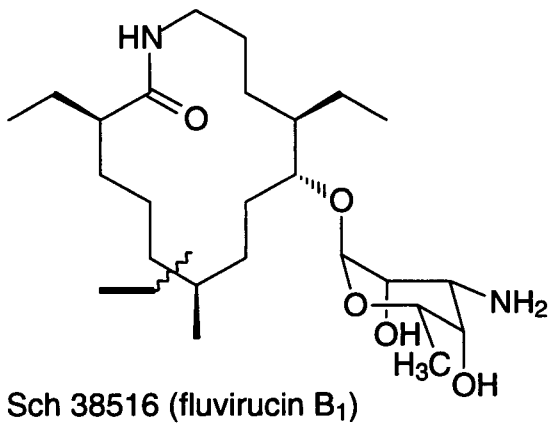

Sch 38516 (fluvirucin B_1)

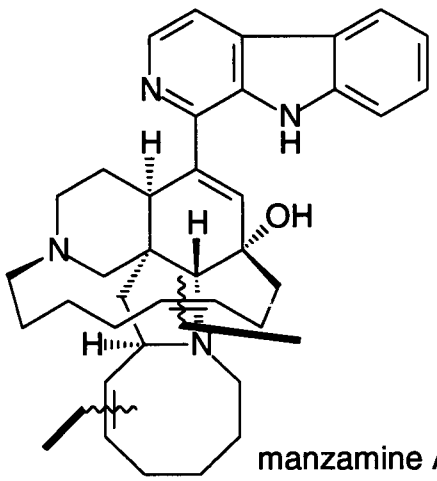

manzamine A

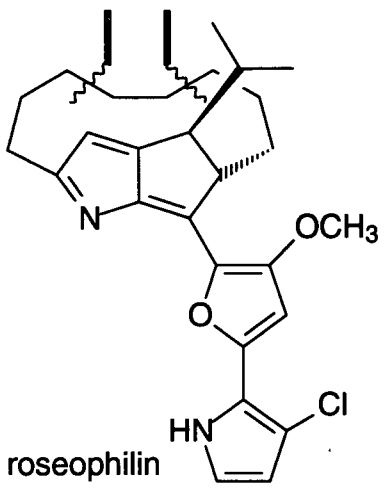

roseophilin

1.1 Ring-Closing Metathesis

The development of carbon-carbon bond forming reactions constitutes one of the most important methods for constructing organic molecules. The coupling of two carbon atoms to form a carbon-carbon double bond has the added benefit of introducing a reactive functional group, which can be used to further elaborate the molecule. In the context of a cyclization process, this reaction would allow entry to unsaturated cyclic structures that possess an increased level of complexity and a similar ability for structural elaboration. In the early 1990's, renewed interest in the ring-closing metathesis (RCM) reaction has led to the development of such a reliable, efficient, and well-defined process.

The RCM reaction belongs to a family of carbon-carbon double bond forming reactions more generally referred to as olefin metathesis.[2] These reactions involve the formation of double bonds via a metal alkylidene catalyzed reaction between two simple olefins. It is worth noting the reaction requires a substrate with two double bonds and only a catalytic amount of the metal alkylidene. The catalytic nature of the process, the readily available alkene subunits required for construction of the diene substrate, and the increased level of complexity and function of the resulting unsaturated cyclic compound makes this a very appealing method for the construction of such compounds.

1.1.1 Olefin Metathesis

> **me·tath·e·sis** (mə tath′i sis) *n.*, *pl.* **–ses** (-sēz′). **1** the transposition of sounds, syllables, or letters in a word. **2** *Chemistry.* the interchange of atoms between two molecules. **3** a transposition; reversal. [< LL < Gk. *metathesis* transposition, ult. < *meta-* over + *tithenai* set][3]

Olefin metathesis, as the definition suggests, involves an interchange of alkylidene groups between two substituted olefins. A catalytic amount of a metal alkylidene mediates this process. For diene substrates containing functional groups, generally represented by X, this method can be applied to three types of processes (Figure 1): (a) ring-closing metathesis (RCM), (b) ring opening metathesis polymerization (ROMP), and (c) acyclic diene or cross metathesis (ADMET). Until the early 1990's olefin metathesis was almost exclusively applied to ROMP type reactions. This process involves the opening of an unsaturated ring system and subsequent intermolecular reaction with a second cyclic molecule. The reaction is

thermodynamically favoured due to the relief in strain associated with opening of the unsaturated ring system, and increasingly so for more strained bicyclic systems. The intermolecular reaction between two substituted olefins (ADMET) has received much less attention. Two issues complicate the outcome of this process. The first involves the regioselectivity of the reaction. When two different substituted olefins are applied, often the reaction produces a mixture of cross- and self-metathesis products. The second issue involves the stereoselectivity of the reaction. Usually the geometry of the resulting olefin cannot be controlled. Finally, the RCM reaction involves intramolecular reaction between two double bonds contained within the same acyclic diene.

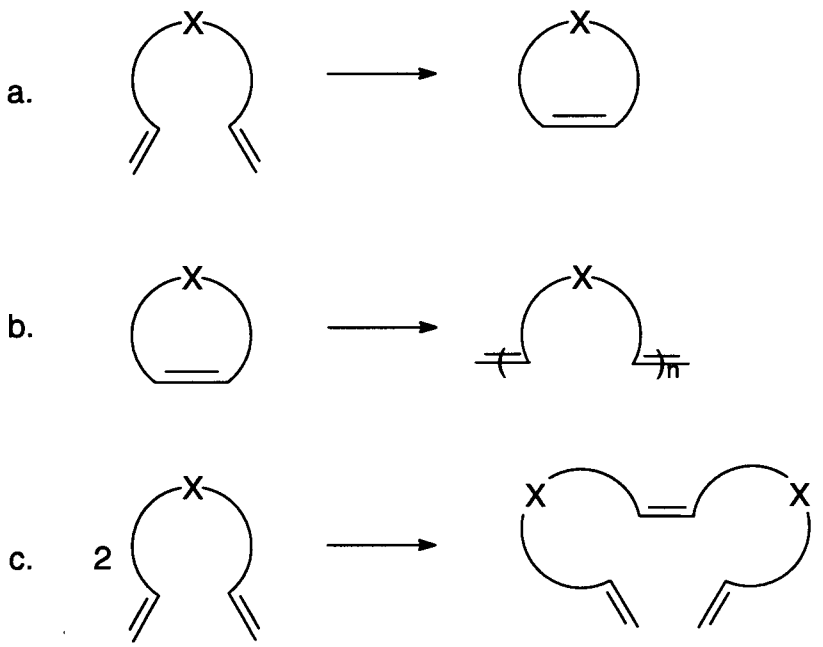

Figure 1. Types of olefin metathesis reactions using dienes possessing functional groups X: (a) ring-closing metathesis (RCM), (b) ring opening metathesis polymerization (ROMP), and (c) acyclic diene or cross metathesis (ADMET).

The discussion that follows will focus on the RCM reaction, and in particular how it applies to the construction of macrocyclic compounds. However, the two other types of metathesis processes, in the context of ring-closure, deserve some attention. The outcome of the reaction depends on the probability of intermolecular reactions between diene molecules, thus leading to dimeric (ADMET) and/or cyclic dimeric (tandem ADMET-RCM) products. The stereochemical outcome of the reaction depends upon

the ability of the newly formed unsaturated ring to undergo reversible ring opening and ring closing, and also on mechanistic considerations which will be discussed later in this chapter. Furthermore, the ring opening process might divert the product to ADMET and ROMP pathways, thus complicating the outcome of the reaction. The factors favouring productive RCM, and disfavouring the other two types of processes, will be discussed in due course.

The lack of highly active and well-defined olefin metathesis catalysts, coupled with the issues introduced above, might have contributed to the limited attention the RCM reaction received up until the early 1990's. At this time a new class of highly active and well-defined metathesis catalysts were developed that led to intense research interest in this field.

1.1.2 Olefin Metathesis Catalysts

Early applications of the olefin metathesis reaction to cyclization processes employed catalyst/co-catalyst systems such as; $WCl_6/SnMe_4$,[4] and WCl_6/Cp_2TiMe_2 and $WOCl_4/Cp_2TiMe_2$.[5,6] However, these catalyst systems are unstable in air, have a low tolerance towards a number of polar functional groups, and require Lewis acidic co-catalysts. In fact, early attempts to carry out a self-metathesis of *N,N*-diethyl-10-undecenamide failed when using the $WCl_6/SnMe_4$ and $WCl_6/PhSiH_2$ catalyst systems.[7] However, the analogous methyl ester and nitrile reacted without difficulty, which suggested metathesis catalysts of this type were not tolerant to amide groups. Subsequently, Schrock and co-workers developed the well-defined molybdenum imido alkylidene complex **1** (Figure 2).[8] The recent intense research activity and advances in ring-closing metathesis, and the general acceptance of this reaction by organic chemists as a reliable and efficient method for the construction of cyclic molecules can largely be attributed to the introduction of this complex. Today, alkylidene complex **1** remains one of the most commonly used metathesis catalysts in organic synthesis. However, this complex is sensitive to polar groups, requires rigorous removal of oxygen and water from the reaction medium, and is difficult to prepare. Such characteristics prompted further investigation of more efficient and stable metathesis catalysts.

Within a few years, Grubbs and co-workers developed a class of metathesis catalysts based on ruthenium. Ruthenium alkylidene **2**[9] and most notably ruthenium

benzylidene **3** (Figure 2),[10,11] the latter of which is referred to as Grubbs' precatalyst, have been widely applied in olefin metathesis reactions and RCM in particular. Due to the more impressive activity of ruthenium benzylidene **3**, it has stood out as a reliable alternative to Schrock's molybdenum alkylidene **1**. However, both these complexes have favourable conditions to which they are individually applied. In comparison, **3** is easier to prepare, more tolerant to a wider range of functional groups, and is stable to air as a solid. It does decompose in solution, but requires less rigorous removal of oxygen and water from the reaction medium prior to use. These characteristics have made **3** more appealing for general use in the realm of organic synthesis.

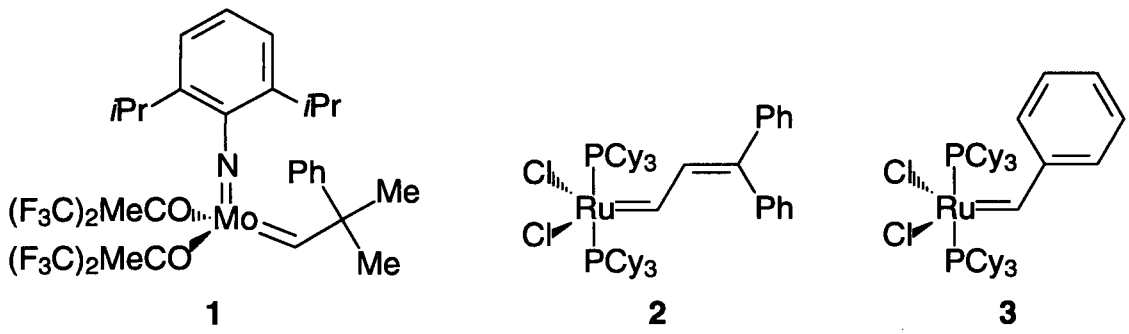

1 **2** **3**

Figure 2. Well-defined metathesis precatalysts.

The success of Schrock's and Grubbs' metathesis precatalysts have spawned a number of variations within these classes. For instance, water-soluble[12] and recyclable[13] ruthenium benzylidenes, and ruthenium allenylidenes[14] have been developed. The potential for catalyzed kinetic resolution and enantioselective desymmetrization reactions in RCM was realized through the development of chiral molybdenum alkylidene complexes.[15] These few examples illustrated not only the versatility and modular nature of these systems, but also the diverse structures, conditions, and studies to which they can be applied.

The development of these well-defined metathesis catalysts led to intense research activity, most notably for their application in RCM. In particular, further insight into the scope and applicability of this reaction to the construction of macrocyclic compounds was gained. The factors governing this reaction and the expected outcome

are best understood through examining the mechanism by which these catalysts act, and thermodynamic and kinetic effects.

1.1.3 RCM Mechanism: Thermodynamic and Kinetic Considerations

In principle, the formation of macrocyclic compounds via RCM of diene substrates involves a series of reversible processes, and therefore is governed by thermodynamic factors. The assembly of a macrocyclic ring via RCM involves an increase in enthalpy or strain energy of the molecule. This results from unfavourable torsional bond opposition forces (Pitzer strain), bond angle deformation (Baeyer strain), and transannular steric interactions. Usually the entropy of macrocyclic ring formation is negative due to the reduction in the freedom of molecular motion required to bring two ends of the acyclic chain together. However, an entropic gain is associated with the RCM reaction due to bisection of the diene substrate. It is this gain in entropy and the subsequent evaporative loss of the by-product ethylene that drives the reaction. A successful RCM reaction is dependent on the favourable balance between the entropy and enthalpy of ring closure.

The generally accepted mechanism for the RCM of a diene involves the formation and cleavage of metallacyclobutane intermediates, in which the former occurs via a [2+2] cycloaddition reaction between a metal alkylidene and a double bond from the diene. Hérisson and Chauvin first proposed the metallacyclobutane intermediate in 1970,[16] however it is still unknown if the cycloaddition/cycloreversion processes occur in a concerted or stepwise manner. This issue alone can significantly affect the stereochemical outcome of the reaction. More recent studies suggested that formation of the *anti*-metallacyclobutane intermediate is favoured due to the predominant formation of (*E*)-alkene cross metathesis products.[17] With respect to the construction of macrocyclic compounds, the conformation of the incipient ring might play a larger role in the stereochemical determining event, and thus the resulting *E*/*Z* ratio of the cyclized product.

The most commonly used metathesis catalysts are technically precatalysts or initiators of the catalytic cycle. The first step involves reaction between the precatalyst and one of the double bonds from the diene **A** (Figure 3). Productive cleavage of the resulting metallacyclobutane intermediate **B** liberates a simple alkene and substrate alkylidene **C**. It is at this point that the catalytic cycle begins. Intramolecular reaction

between substrate alkylidene **C** and the distal double bond provides the [n.2.0]-bicyclic intermediate **D** that contains a fused metallacyclobutane. Productive cleavage of **D** gives the desired macrocycle **E**, which contains an olefin at the site of ring closure, and a metal methylidene, the catalytic species. For example, if ruthenium benzylidene **3** was employed as the precatalyst, then ruthenium methylidene **4** would emerge as the catalytic species. Continuing, the catalytic species reacts with another molecule of diene **A** to eventually liberate ethylene and substrate alkylidene **C**. The catalytic cycle subsequently repeats the same series of steps as described above.

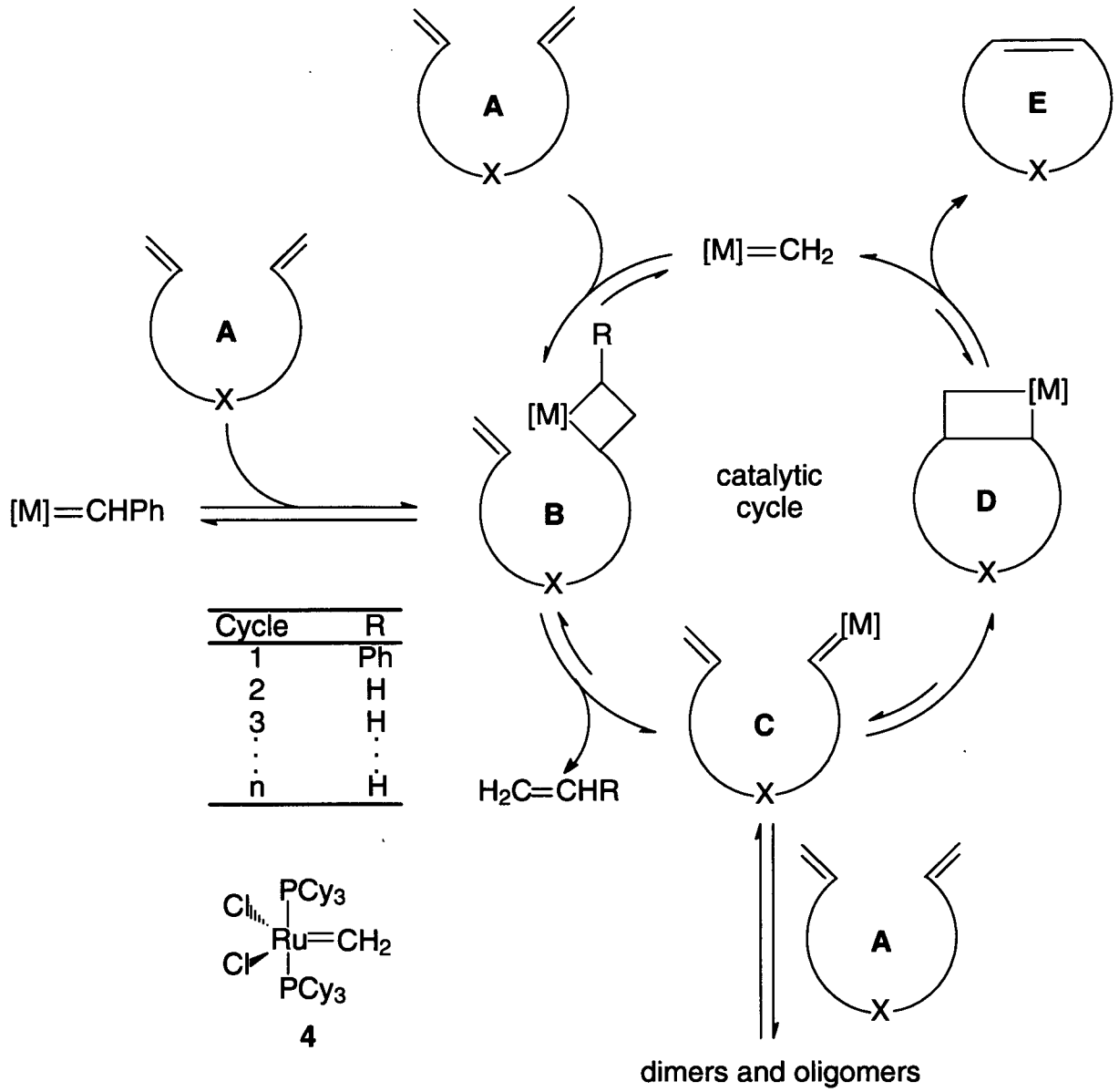

Figure 3. Mechanism for ring-closing metathesis of a diene.

Propagation of the catalytic cycle depends upon the lifetime of the catalytic species and the formation of by-products, such as dimeric compounds. The activity of an olefin metathesis catalyst decreases over time due to catalyst decomposition and the formation of unproductive catalyst complexes. The latter involves an intramolecular complex between the substrate alkylidene and polar functional groups present within the substrate. This process will be explained in more detail later in this chapter. Poor yields often result from slow reactions due to the competitive rates of productive metathesis and catalyst decomposition. The inevitable loss of catalyst activity suggests that the yields of such reactions can only be improved by the addition of fresh catalyst.

In addition to catalyst decomposition, unproductive reaction pathways can adversely affect propagation of the catalytic cycle. Dimer and oligomer formation may competitively remove the substrate and substrate alkylidene from the catalytic cycle. The formation of such compounds is often problematic when constructing macrocyclic compounds. Usually, such reactions are conducted at high dilution to limit the probability of intermolecular interactions. With respect to RCM, the rate of the intermolecular reaction is dependent on the concentrations of substrate **A** and substrate alkylidene **C** (Figure 4).[18] The rate of the intramolecular reaction, corresponding to cyclization, is solely dependent upon the concentration of substrate alkylidene **C**. Therefore, a decrease in the concentration of substrate **A** (high dilution) leads to a reduction in the rate of dimer product **F** formation, while the rate of cyclic product **E** formation remains relatively unaffected. Therefore, RCM reactions conducted at high dilution should kinetically favour the formation of monomeric cyclic products and disfavour the formation of dimers.

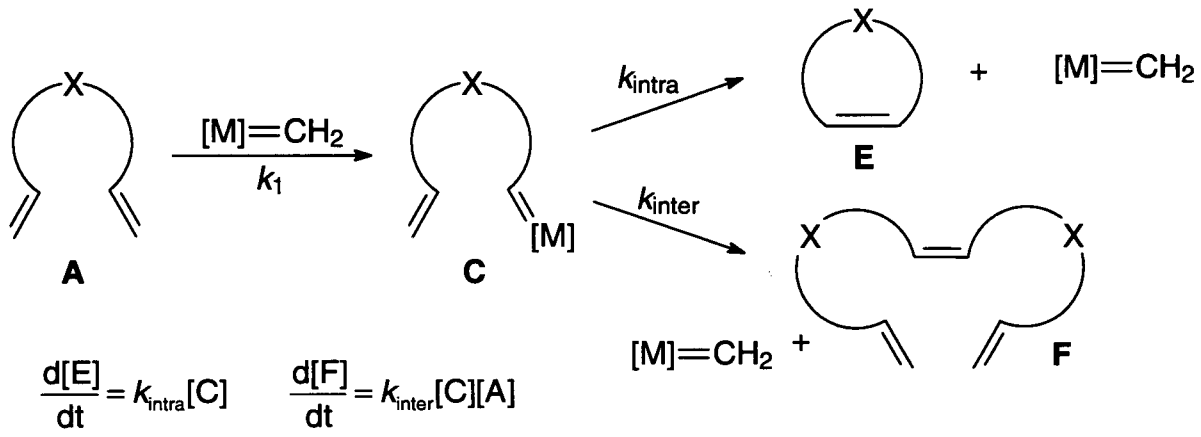

Figure 4. The kinetics of diene ring-closing versus dimerization (from reference 18).

The construction of monomeric macrocyclic compounds in the RCM reaction is favoured based on the thermodynamic factors governing the process, the evaporative loss of ethylene, and the kinetic effect of high dilution. However, catalyst decomposition and the formation of unproductive catalyst complexes might inhibit the catalytic cycle and thus productive cyclization. Such complexes result by formation of an intramolecular complex between the Lewis basic functional group and the metal attached to the substrate alkylidene. The strength of such a complex might depend on the proximity between the two groups within the substrate. These factors should be considered when employing a strategy involving RCM.

During the latter half of the 1990's numerous reports described the facile construction of cyclic compounds, from small to macrocyclic rings, containing a wide variety of functionality.[2] Key studies conducted earlier that decade provided the impetus for this research. The historical developments in RCM prior to and during this period, paying particular attention to the formation of macrocyclic lactams, provides a perspective on the course of the current developments in this field.

1.2 Construction of Macrocyclic Compounds and Lactams via Ring-Closing Metathesis

Villemin reported the first synthesis of a macrocyclic compound via RCM in 1980.[4] The construction of unsaturated 15- and 16-membered lactones from the corresponding diene-esters, using WCl_6 as catalyst and $SnMe_4$ as co-catalyst, were described. For example, cyclization of diene-ester **5** gave 16-membered lactone **6** as a

mixture of *E* and *Z* isomers in 65% yield (Figure 5). Hydrogenation of lactone **6** gave exaltolide (**7**), the musk component of the angelica root. Within the same year, Tsuji and Hashiguchi reported the synthesis of unsaturated 19- and 21-membered lactones via RCM using the WCl_6/Cp_2TiMe_2 catalyst system in 18% and 12% yield respectively.[5] These seminal reports introduced the application of olefin metathesis to the construction of macrocyclic compounds.

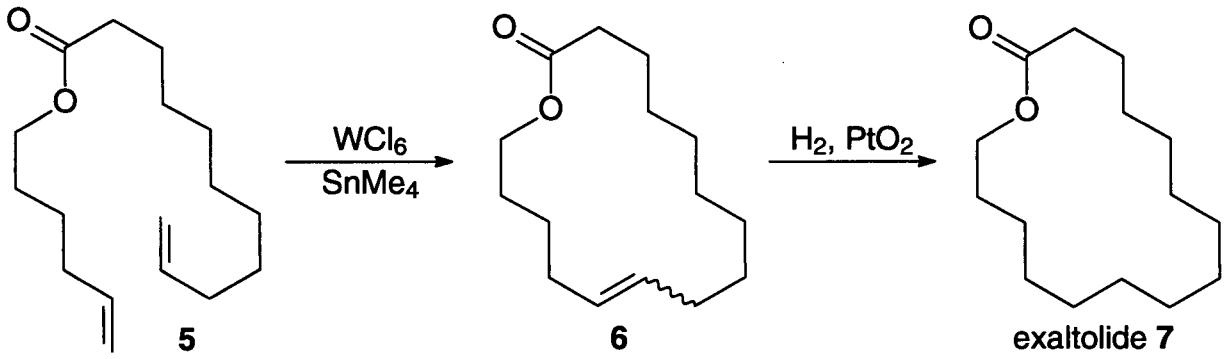

Figure 5. Total synthesis of exaltolide (**7**) via RCM (from reference 4).

It was more than a decade after these results were disclosed that the RCM reaction was further applied to the construction of a macrocyclic compound. In 1993, Junga and Blechert cyclized a diene-ester, similar to the one employed by Villemin, using CH_3ReO_3 to afford the 16-membered lactone **6** in 35% yield.[19] The poor yield observed in the examples discussed above, and the lack of well-defined metathesis catalysts might account for the absence of the RCM reaction in the literature during this time. However, it was the development of Schrock's alkylidene **1**, and seminal research conducted by Grubbs and Fu shortly thereafter, that prompted the intense research interest in RCM today.

In three reports Grubbs and Fu described the construction of unsaturated 5- to 7-membered cyclic ethers,[20] cyclic amines and lactams,[21] and carbocycles[22] using 2-10 mol% of Schrock's alkylidene **1**. In particular, their report on the synthesis of 5- and 6-membered *N*-benzyl lactams **10** and **11** highlighted one of the limitations of this reaction. For example, diene-amides **8** and **9** derived from acrylic acid and vinyl acetic acid respectively failed to cyclize (Figure 6).[21] Presumably, the formation of unproductive intramolecular catalyst complexes such as **G** and **H**, with the appropriate

heteroatom and double bond proximity, accounted for the failure of diene-amides **8** and **9** to undergo cyclization. Grubbs and Fu reasoned that the precatalyst could react at either double bond in the first metathesis event. Since the rate of metathesis for monosubstituted double bonds is higher than that for disubstituted double bonds, they also reasoned that differential substitution of the diene double bonds might facilitate cyclization due to the competitive rates of the first metathesis event. Accordingly, differentially substituted diene-amides **12** and **13** possessing methyl or ethyl substitution at the carboxyl alkene terminus respectively were prepared. These compounds cyclized smoothly using 4-10 mol% of alkylidene **1** to give lactams **10** and **11** in 74% and 80% yield respectively.

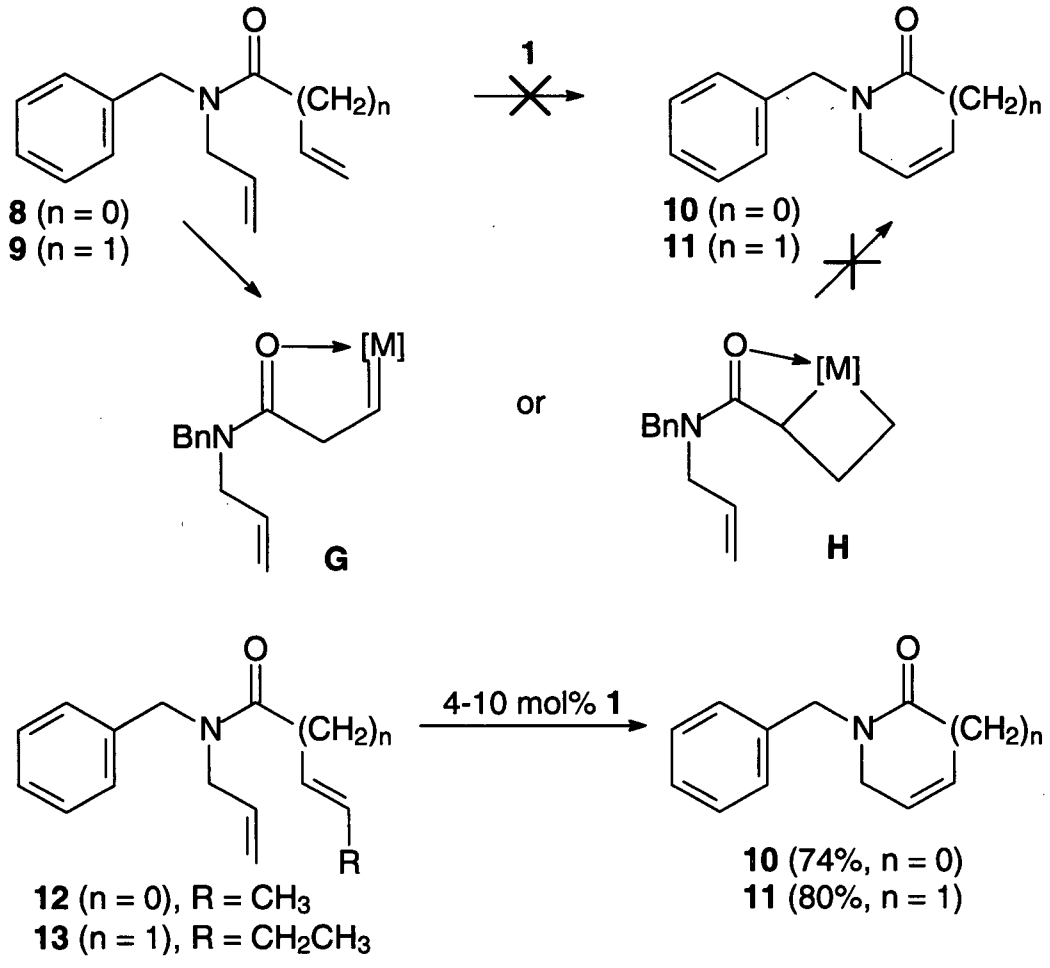

Figure 6. RCM construction of 5- and 6-membered lactams and unproductive catalyst complex formation (from reference 21).

These three reports illustrated the facile and efficient construction of small ring size carbo- and heterocycles via RCM. They also provided the first examples of efficient and accessible RCM reactions applicable to organic synthesis, and subsequently spawned a number of reports detailing novel applications and usage in the total synthesis of natural products.

Within the next few years the RCM reaction was applied in approaches to the total synthesis of two macrocyclic natural products and to the construction of macrocyclic peptides.[23] Hoveyda and co-workers employed the RCM reaction in the construction of the 14-membered lactam core of Sch 38516 **15** (Fluvirucin B_1), an antifungal agent effective against the influenza A virus (Figure 7).[24] Cyclization of the diene-amide aglycon proceeded smoothly using 20 mol% of Schrock's alkylidene **1**, however glycosylation of the resulting macrocyclic lactam was not possible. Fortunately, the reaction also proceeded smoothly using the carbohydrate containing diene-amide **14**. Cyclization of either diene-amide substrate gave the corresponding product lactam in 90-91% yield. Hoveyda attributed the success of these cyclization reactions to the conformational restraint afforded by the stereogenic centres, thus facilitating predisposition of the diene-amides to cyclization.[24c]

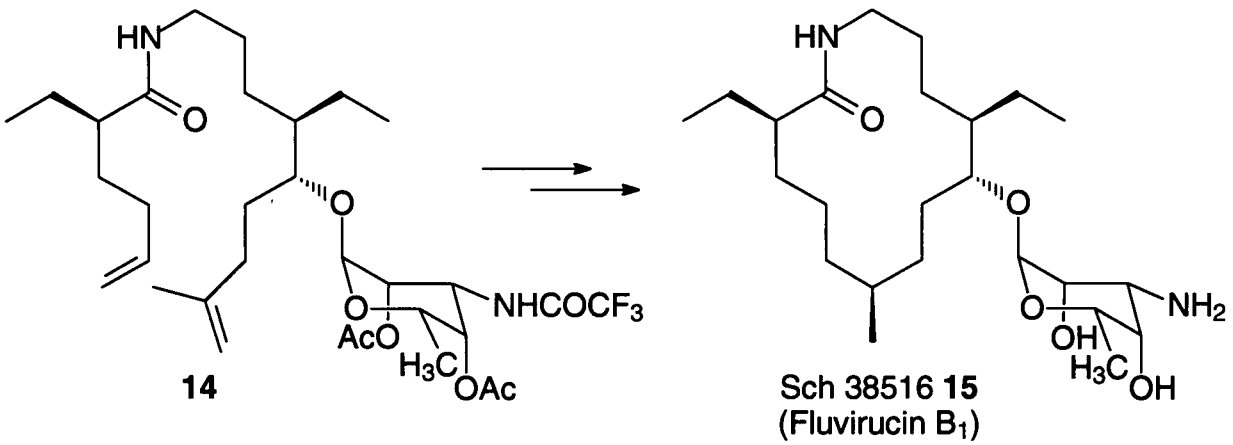

Figure 7. Construction of the macrolactam core of Sch 38516 **15** (Fluvirucin B_1) via RCM (from reference 24c).

In another application of the RCM reaction in natural product synthesis, the research groups of Pandit and Martin concurrently conducted studies towards the total synthesis of manzamine A (**16**), a marine alkaloid that exhibits potent antitumor activity.

Both of these groups applied the RCM reaction to the construction of the 13- and 8-membered **D** and **E** rings respectively.[25] Pandit and co-workers utilized Grubbs' alkylidene **2** in the construction of the 13-membered **D** ring from diene **17**,[25b] while Martin and co-workers utilized Schrock's alkylidene **1** in the construction of the 8-membered **E** ring from diene **18** (Figure 8).[25a] More recently Martin and co-workers constructed the **D** ring from a substrate similar to **17**, but obtained the cyclized product in more than double the yield (67%) using benzylidene **3**.[25e] With respect to both syntheses of the 13-membered **D** ring, it is interesting to note that the *Z* isomer was isolated as the major product. Similar to the assertion made by Hoveyda, cyclization to the larger ring might have been facilitated by the conformational predisposition of the diene substrates. However, the biased formation of the (*Z*)-alkene suggested that factors beyond the formation of the favoured *anti*-metallacyclobutane intermediate,[17] that would give the (*E*)-alkene, influenced the stereoselectivity of the reaction.

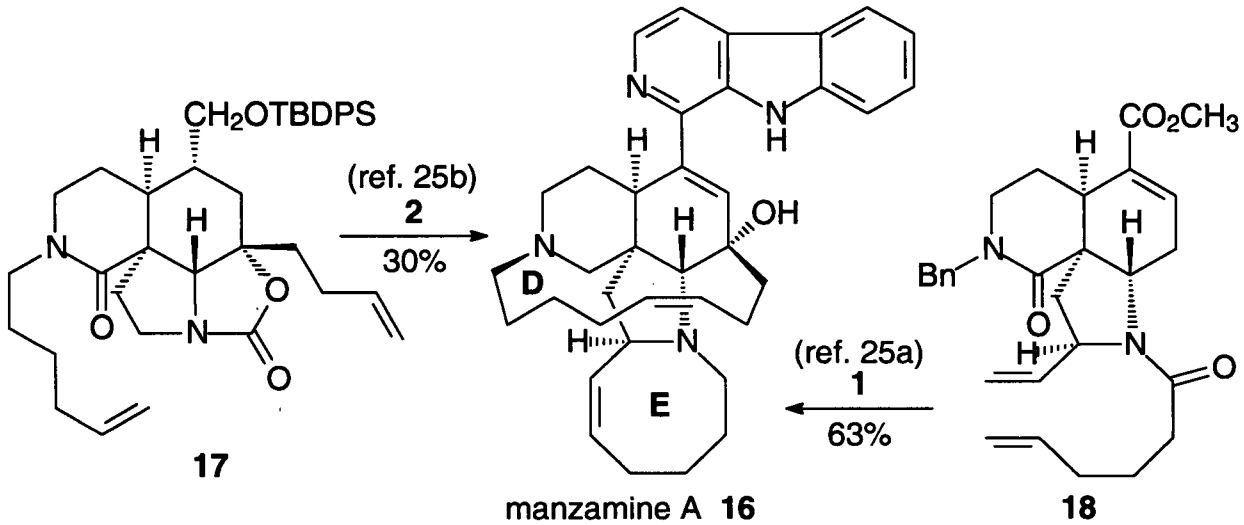

Figure 8. Applications of RCM in approaches to the total synthesis of manzamine A (**16**) (from references 25a and 25b).

Grubbs and co-workers applied the RCM reaction to construct and study constrained peptide structures. β-Turns are a key secondary structure found in peptides and are often stabilized by disulfide bridges resulting from the covalent linkage between two cysteine residues. An examination into the nature of these structures prompted an application of the RCM reaction to the construction of rigidified macrocyclic

tetrapeptides, which contain a carbon-carbon double bond in place of the disulfide bridge and therefore act as β-turn mimetics.[26,27] Figure 9 illustrates one example in which 14-membered tetrapeptide **20** was formed in 60% yield from the corresponding acyclic bis-allylglycine tetrapeptide **19** using 20 mol% of ruthenium alkylidene **2**. Of all possible diastereomers, only diene **19** would cyclize. For example, the reaction of a mixture of all four possible diastereomers of **19** led exclusively to the formation of macrocyclic tetrapeptide **20**. This suggested that only one diastereomer, diene **19**, underwent cyclization, which possessed the same absolute and relative configuration as in the analogous natural disulfide.[28] In addition to the macrocyclic tetrapeptide shown below, other tetrapeptides that possessed different amino acid substitution were constructed in comparable yield using 20-30 mol% of either ruthenium alkylidene **2** or benzylidene **3**.[27] The success of these cyclization reactions was attributed to the conformational predisposition of the dienes towards cyclization. This process was assisted by an intramolecular hydrogen bond, and the restrictive nature of the substituents and their relative configuration both favouring cyclization of the diene. Similarly, for the diastereomers that did not cyclize, these factors might have restricted the diene to conformations disfavouring cyclization.

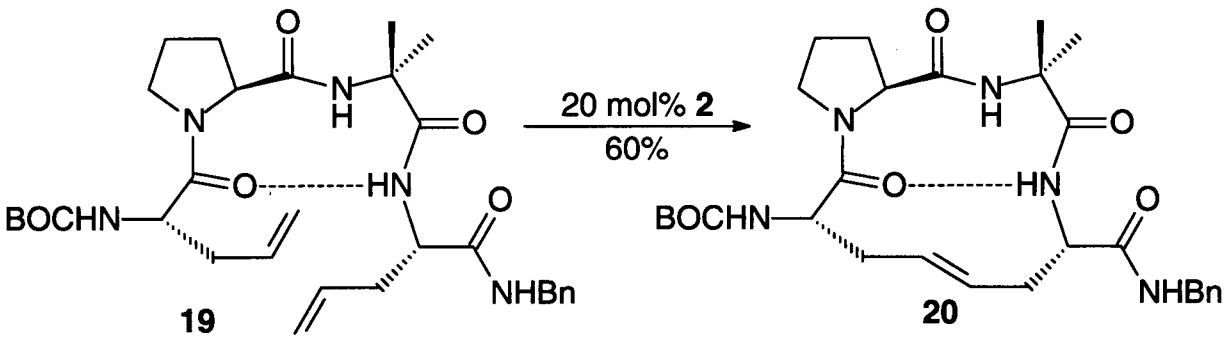

Figure 9. Synthesis of a rigidified macrocyclic tetrapeptide β-turn mimetic via RCM (from reference 26).

Two analogous macrocyclic tetrapeptides were constructed on solid supports following two different strategies. One involved construction of the support bound bis-allylglycine tetrapeptide using standard solid phase peptide synthesis techniques, followed by RCM cyclization and subsequent cleavage of the macrocyclic tetrapeptide.[27] An ingenious approach to a similar macrocyclic tetrapeptide involved a

cyclization-cleavage strategy whereby the acyclic tetrapeptide resembled a differentially substituted diene.[29] In this case the disubstituted double bond was covalently attached to the solid support, and RCM cyclization and concomitant cleavage gave the macrocyclic tetrapeptide. A similar strategy was applied to the construction of seven-membered lactams.[30] Using such a strategy, undesirable ADMET processes were disfavoured due to the pseudo-dilution effect of the solid support, and therefore the reactions were conducted at higher concentrations.

The conformation of the amide groups in the previous examples presumably played a significant role in facilitating access to conformations predisposed for ring closure. This effect was observed in the construction of six- and eight-membered lactams. For example, bis(*N*-allyl) dipeptide **22** was cyclized using 10 mol% of alkylidene **2** to give lactam **24** in 51% yield, however the analogous diene-ester **21** failed to give lactone **23** under similar conditions (Figure 10).[31] Similarly, *N*-allyl-*N*-methyl amide **27** underwent a tandem ring opening-RCM reaction using 10 mol% of benzylidene **3** to provide the tricyclic compound **30** in 95% yield.[32] However, the analogous ether **25** and ester **26** failed to give the corresponding tricyclic compounds **28** and **29** under similar conditions. The successful and exclusive cyclization of amide substrates **22** and **27** was attributed to the ability of the amide group to adopt energetically accessible conformations that favoured cyclization.

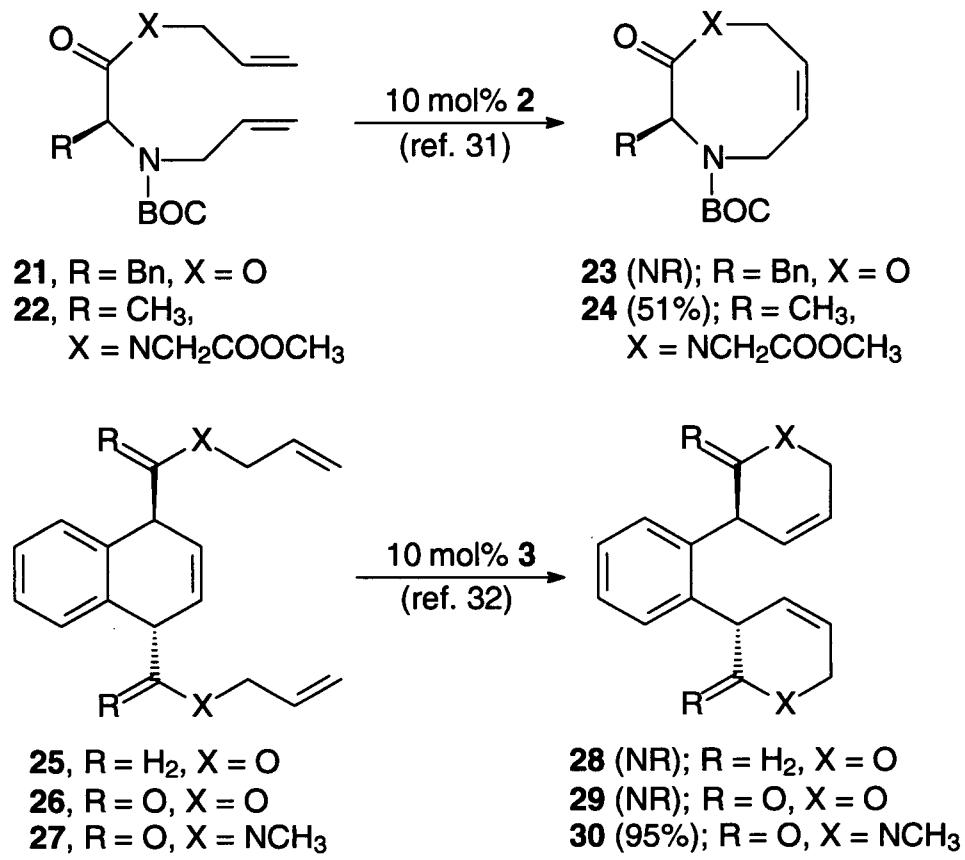

Figure 10. Effect of amide conformation in the construction of eight- and six-membered lactams (from references 31 and 32).

Finally, Clark and Ghadiri reported a very interesting application of the olefin metathesis reaction in which construction of a peptide cylinder was facilitated by intermolecular hydrogen bonds.[33] Two identical C_2 symmetric cyclic peptide molecules, each containing two L-homoallylglycine residues, combined to form the hydrogen bonded ensemble **31** (Figure 11). In Figure 11, the remainder of the substituents on **31** were omitted for simplicity. Ensemble **31** was covalently captured via sequential olefin metathesis reactions using 20-25 mol% of alkylidene **2** to give **32** in 65% yield as a mixture of stereoisomers with respect to the double bonds. This example clearly illustrated the tolerance of ruthenium based metathesis catalysts to multiple amide groups, but also provided a source of concern with regard to the nature of the ensemble. In the context of conventional diene-amide RCM intermolecular hydrogen bonding might cause ADMET processes to be more competitive relative to the desired RCM process, and lead to the formation of dimeric and cyclic dimeric products.

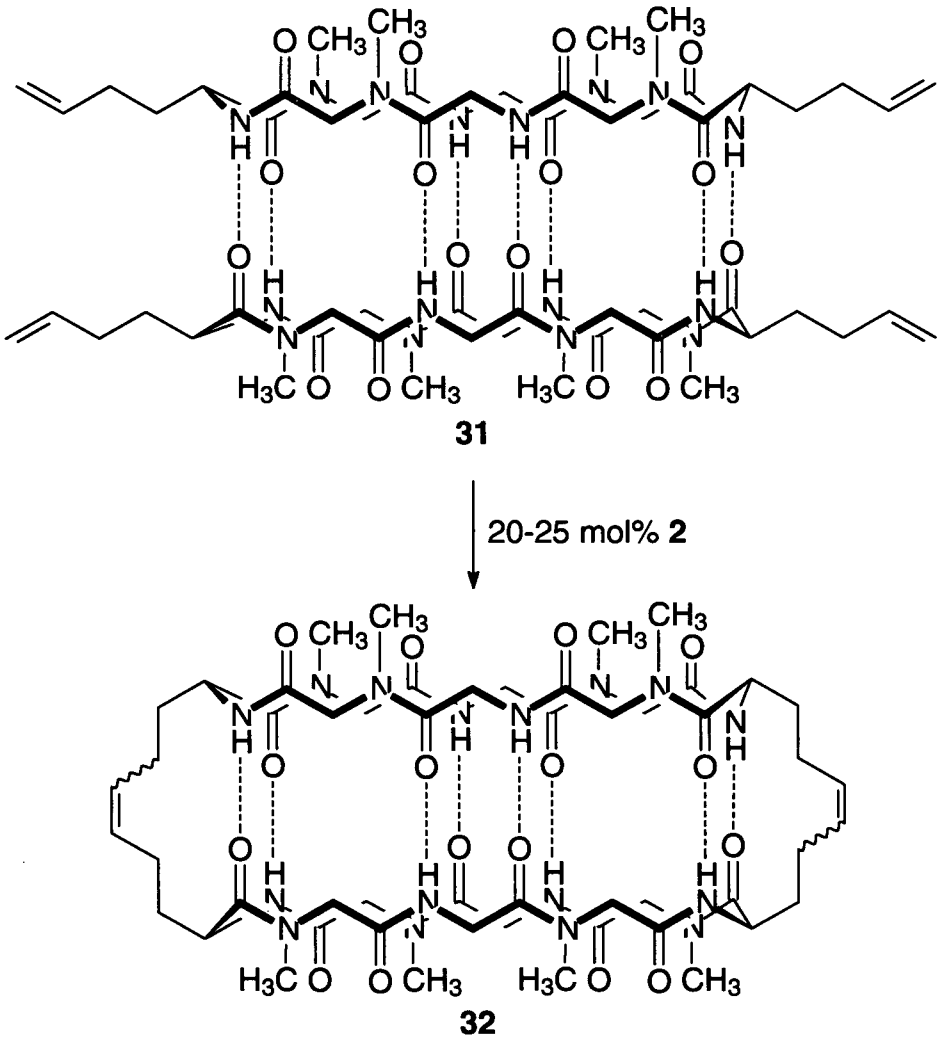

31

32

Figure 11. Construction of a peptide cylinder via hydrogen bond promoted intermolecular metathesis (from reference 33).

These examples illustrated the amide group tolerance of the precatalysts developed by Schrock and Grubbs. However, for diene-amides the proximity between the Lewis basic heteroatoms of the amide and the terminal double bonds played a significant role in the formation of unproductive intramolecular catalyst complexes. In addition, high catalyst loading (ca. 20-30 mol%) was required in some cases. The apparent need for stereogenic centres, intramolecular hydrogen bonding, or other elements of conformational restraint to predispose the diene for cyclization was also illustrated. In terms of the latter, the amide group appeared to possess a greater ability to access productive ring closing conformations, relative to ester and ether groups. Finally, exclusive formation of the *Z* isomer, and the lack of selectivity observed in some

cases suggested that factors beyond the formation of the favoured *anti*-metallacyclobutane governed the stereoselectivity of macrocyclization via RCM.

The preceding discussion provided an overview of the historical developments in the RCM reaction up to the mid-1990's, and in particular as it applied to the construction of macrocyclic compounds. It was at this time that investigations in our laboratory commenced, exploring the RCM formation of 14-membered lactones and lactams.

1.3 Proposed Studies of Unsaturated 14-Membered Lactam Formation via RCM

A number of the examples discussed in the previous section illustrated some of the problems associated with the RCM reaction as it applied to macrocyclization. A few examples were marked by low yields and high catalyst loading (ca. 20-30 mol%). The stereochemical outcome in some cases, as well as others that will be discussed in due course, did not favour a particular alkene configuration and often gave a mixture of stereoisomers. This suggested that the site of ring closure and the associated conformation of the incipient ring might play a critical role in the stereochemical determining event. These examples suggested that further examination of this process was necessary. In particular, our interest in this reaction was directed towards the construction of 14-membered lactams.

The examples discussed in the previous section also illustrated some of the factors governing the formation of macrocyclic compounds via RCM, and prompted us to further examine these factors on a more fundamental level. We felt it would be of interest to study the reactions of conformationally unbiased diene substrates to determine if productive ring closure required any level of conformational preorientation within the diene substrate. This was accomplished using diene-amides that only possessed an amide group and the requisite terminal double bonds. These diene-amides lacked stereogenic centres, intramolecular hydrogen bonds, and other structural elements of conformational restraint that would otherwise facilitate cyclization. We were also interested in exploring what effect the proximity between the terminal double bonds and the amide group within the diene-amide, thus the site of ring closure, had on the yield and stereochemical outcome of the RCM reaction. This effect was examined through a systematic study of ring closure at nine different yet contiguous sites within the 14-membered lactam, shown below. Through such a systematic study,

we were hopeful that an increased understanding of the factors governing the RCM reaction would be gained.

In addition to the studies proposed above, the synthesis of unsaturated 14-membered cyclic amines via RCM of the corresponding diene-amines was also of interest. However, our primary goal was the construction of the 14-membered lactams.

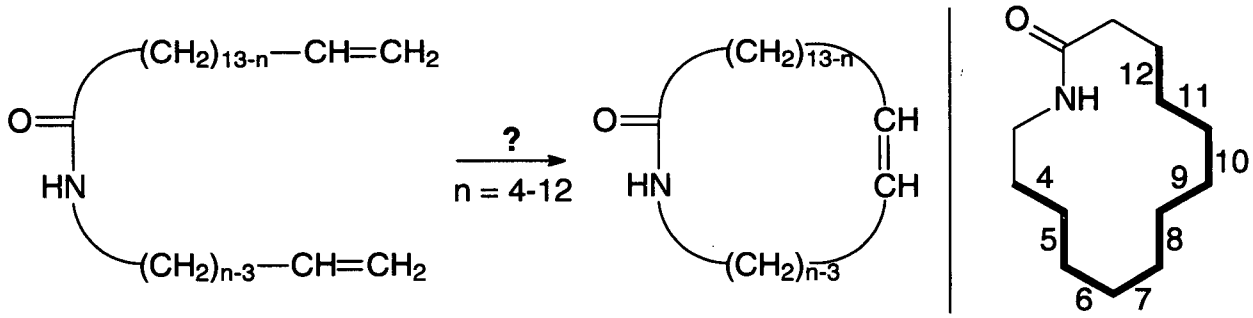

Applications of the RCM reaction to the synthesis of natural and unnatural products of biological interest were illustrated in the previous section. Such applications could benefit from the studies outlined above, which might provide additional criteria for successful macrocyclization, therefore providing a basis for the development of synthetic plans incorporating this reaction. A related study of the self-metathesis of terminally unsaturated amines of varying carbon chain length found that the product yield increased with the distance between the double bond and the amine.[34] However, a maximum yield was obtained when these groups were separated by three methylene units. This trend was attributed to favourable intramolecular stabilization complexes between the metal alkylidene and nitrogen atom. How this would relate to the relative proximity between the site of ring closure and the amide group in the formation of 14-membered lactams was a question of interest.

Many interesting developments in this field were reported during the course of our investigations. In fact, this reaction was applied to the construction of unsaturated cyclic sulfides and disulfides,[35] siloxanes,[36,37] silaketals,[38,39] phosphonates,[40] alkenylboronates,[41] and stannane-substituted ethers.[42] Most noteworthy were reports from the Fürstner research group in which issues similar to those discussed above were explored regarding the formation of macrocyclic compounds via RCM. Reports from this and other groups disclosed the facile ring closure of conformationally unbiased diene-esters[43,44] and a diene-amide[45] to give 14-, 16-, 20-, and 21-membered lactones,

and an 18-membered lactam, each as isomeric mixtures with respect to the newly formed olefin. The construction of macrocyclic ethers,[46] polyethers,[47,48] and bicyclic carbohydrate derivatives[49] were also reported. It is interesting to note that formation of the *E* isomer was favoured in each of these studies, however it was not known whether this selectivity resulted from local olefin stability or global conformational stability. The details of these reports will be addressed in due course as they relate to the studies discussed in the following chapter. However, a fundamental aspect of the RCM reaction as it applies to the construction of macrocyclic compounds was illustrated. The ability to predict or control the resulting stereochemical ratio from the RCM reaction was not possible. It seemed likely that the stereochemical determining event might be governed in part by the conformation of the incipient ring. A better understanding of the factors governing this process might be gained through studies of ring closure at nine contiguous sites within the 14-membered lactam, the resulting stereochemical outcome at each site, and an understanding of the well-defined conformational properties of 14-membered rings.

1.4 Conformational Properties of 14-Membered Rings

The structure of the unsaturated lactam products, resulting from the RCM of diene-amide substrates, can be examined on three levels. The first involves the order and way in which the atoms are bonded within the molecule. In reference to the unsaturated lactam products, this constitutional arrangement of atoms will differ based on the position of the olefin within the ring, which in turn depends on the site of ring closure. The term positional isomer also applies in this instance. The second level involves the bonding arrangement of the atoms in space, for a molecule of given constitution. This refers to the *E* (*trans*) or *Z* (*cis*) configuration of the olefin at each position, which in turn depends upon the stereochemical outcome of the reaction. The third level involves the conformation or spatial arrangement of the atoms, within a given constitution and configuration. Usually conformational isomers cannot be isolated at room temperature due to the rapid interconversion via rotation about single bonds in the molecule. However, a basic knowledge of the conformational properties of 14-membered rings might provide a better understanding of the factors governing the stereoselectivity of the RCM reaction. Furthermore, the low strain associated with this ring size was expected to favour cyclization.

Today, our understanding of the low energy conformations of medium and large ring saturated cycloalkanes, and their tendency to adopt diamond-lattice conformations, can largely be attributed to research conducted by Dale. A diamond-lattice is an extended tetrahedral array of carbon atoms, which possesses ideal carbon-carbon bond lengths, and ideal bond and dihedral angles (Figure 12). In 1961 Dunitz and co-workers reported the construction and solid state structures of cyclodecane derivatives.[50] Dale recognized the diamond-lattice conformation adopted by these compounds in the solid state and extended his analysis to include cycloalkanes of various ring sizes.[51] A conformation that was superimposable on the diamond-lattice was predicted to possess minimum bond angle (Baeyer) and torsional (Pitzer) strain. Subsequently, Dale proposed minimum energy conformations for 9- to 16-membered cycloalkanes, and conducted semi-quantitative calculations of conformational enthalpy using Fieser-Dreiding models.[52] For each ring size, the model was manually adjusted to minimize the strain energy associated with each dihedral angle by correlation with a specific energy from a potential energy curve of butane. Of the ring sizes examined, only the even-membered cycloalkanes adopted diamond-lattice conformations, and of these, the structure that possessed the least strain was the minimum energy diamond-lattice conformation of cyclotetradecane (bold lines, Figure 12). This lowest energy conformation was considered "strain free", with respect to bond angle and torsional strain, and correlated with the solid[53] and solution[54] state structures.

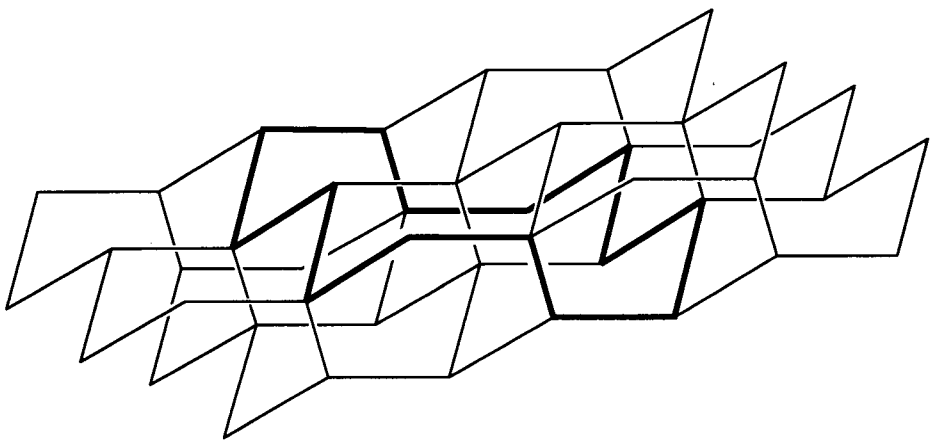

Figure 12. Lowest energy diamond lattice conformation of cyclotetradecane.

The "strain free" conformation of cyclotetradecane does however possess elements of strain. Of the four different types of methylene groups, methylenes 1, 2, and 4 experience varying degrees of transannular steric interactions (Figure 13). These three groups each have one proton directed into the ring, which experiences one, two, or three transannular interactions with other such protons. The endocyclic proton on methylene 1 experiences the most severe of these interactions. The protons attached to methylene 3, which is denoted the corner atom and defined by the two adjacent gauche dihedral angles of the same sign, point away from the ring and do not experience any transannular interactions. Accordingly, geminal substitution at this position is favoured.[55]

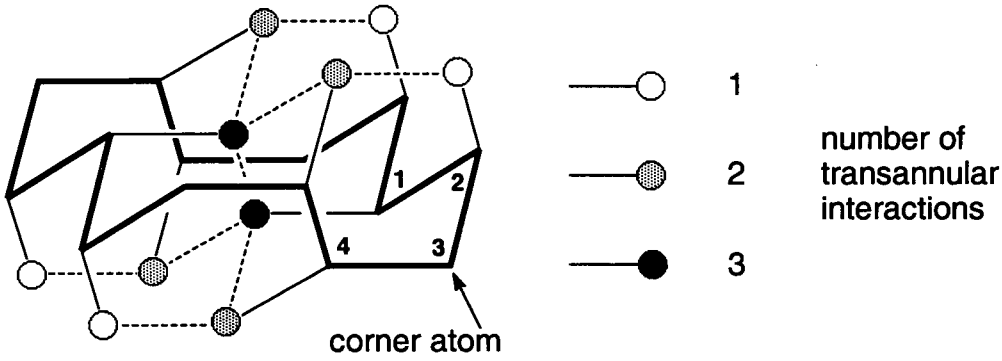

Figure 13. Transannular hydrogen interactions in cyclotetradecane.

The substitution of methylene groups with other atoms and functional groups can have varying effects on the strain associated with the ring.[51,56] For instance, heteroatoms such as nitrogen or oxygen will have little effect on the conformation of the ring, but when properly situated they can give rise to a reduction in the number of transannular interactions. A similar effect occurs upon substitution of two adjacent methylenes with an amide group. However, electron delocalization gives the C-N bond partial double bond character leading to planarity of these atoms with the two adjacent methylene carbons, thus causing a deformation of the conformation from the strain free diamond-lattice. Although introduction of a double bond further reduces the number of transannular interactions, it also prohibits the ring from adopting a strain free conformation due to the imposed planarity mentioned above. However, in the case of a

14-membered ring, if the amide and double bond are diametrically situated, a strain free conformation can be adopted.

The overall reduction in transannular interactions depends on the relative position of these groups and how they are situated within the ring, as illustrated below. However, the introduction of such conformationally rigid groups also deforms the conformation of the ring away from the preferred stain free diamond-lattice. In comparing the relative stability between two related cyclic compounds, a higher melting point is often associated with the more stable compound that can adopt more favourable conformations.[56] Since high cyclization yields and high melting points have often been correlated,[51] the yield of RCM cyclization might, in part, depend on the conformational stability of the incipient ring. Therefore, the site of ring closure might have a significant effect on the yield of the reaction.

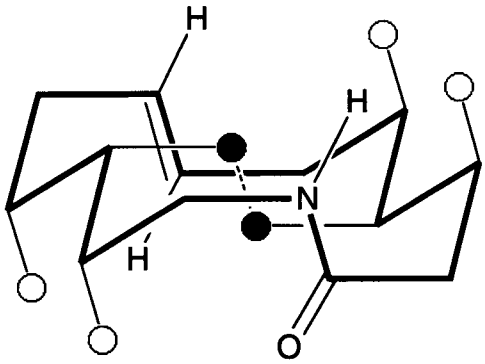

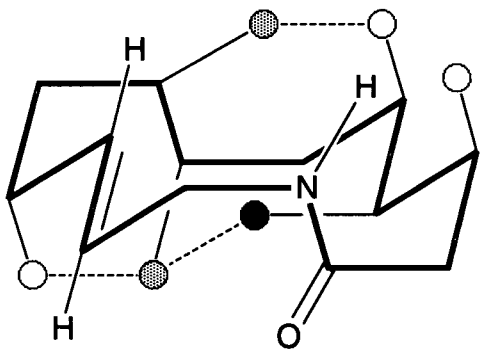

Through the course of these studies our increased understanding of the RCM reaction, as it applied to the formation of 14-membered lactams, prompted application of this knowledge to the total synthesis of a natural product of biological interest. The synthetic target was chosen based on two criteria. Primarily, the natural product should possess a macrocyclic structural element, preferably a lactam, to which the RCM reaction could be applied. Secondly, it would be of interest for the natural product to exhibit a promising level of biological activity with the potential for treatment of an issue of human health. Concurrent to our studies into the RCM formation of 14-membered lactams, researchers at the University of British Columbia isolated a family of compounds that met these criteria. The remainder of this chapter is devoted to a discussion of the marine alkaloids motuporamines A-C and the proposed synthetic plan.

1.5 Cytotoxic Marine Alkaloids Motuporamines A-C

Methodological studies are conducted for a number of reasons. Often such studies are carried out to develop and build upon existing methods. Numerous studies directed towards novel applications of the RCM reaction, some of which were discussed previously in this chapter, are exemplary. Methodological studies are also conducted during and specifically for the synthesis of natural products and other compounds of biological interest. In these cases new methods are often required to form novel structures. For example, during the course of the total syntheses of epothilone A[57] and Sch 38516 (Fluvirucin B_1)[24] studies directed towards forming macrocyclic precursors to these natural products via RCM were conducted.

Regarding the research discussed herein, studies were conducted to obtain a better understanding of the RCM reaction and broaden its usage as it applied to the construction of 14-membered lactams. Correspondingly, the methods utilized for 14-membered lactam formation via RCM were applied to a total synthesis of the cytotoxic marine alkaloids motuporamines A-C.

1.5.1 Biological Properties, Isolation, and Structural Elucidation of Motuporamines A-C

Marine organisms are a rich source of biologically active and structurally novel compounds that have attracted much research interest and effort. For instance, novel cytotoxic alkaloids, some of which are discussed below, have been isolated from a variety of marine sponges. Such interest stems from the potential for these compounds to lead to new anticancer drugs and other medicinal agents. Off Motupore Island, Papua New Guinea, the marine sponge *Xestospongia exigua* (Kirkpatrick) was obtained. The crude extracts from *X. exigua* exhibited selective in vitro cytotoxicity against a panel of human cancer cell lines. Motuporamines A (**33**), B (**34**), and C (**35**) (Figure 14) were isolated from these crude extracts through bioassay-guided fractionation.[58] Unfortunately, the mixture of motuporamines exhibited modest in vitro cytotoxicity. This suggested that the crude extracts might have contained other more active compounds, or compounds that when in combination with motuporamines A-C led to the more impressive cytotoxic activity of the crude extracts.

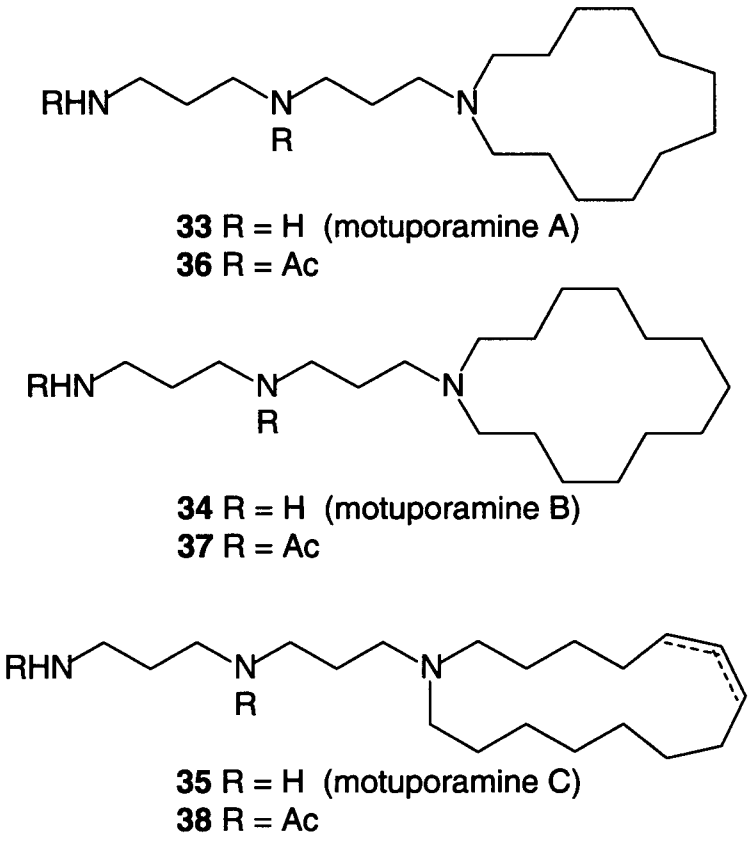

Figure 14. Motuporamines A (**33**), B (**34**), and C (**35**).

The waters off the coast of Papua New Guinea are host to a number of marine sponges that contain a variety of cytotoxic alkaloids. The protein phosphatase-1 inhibitor and cytotoxin motuporin, a cyclic pentapeptide, was isolated from the marine sponge *Theonella swinhoei* that in turn was collected off Motupore Island.[59] This is the same area where the marine sponge containing motuporamines A-C was obtained. Also collected from the coastal waters of Papua New Guinea was the marine sponge *Xestospongia ingens* (Thiele) which contained the cytotoxic pentacyclic alkaloids ingenamine[60] and madangamine A.[61] Prior to their isolation, the existence of this class of alkaloids was suggested by an elegant biogenetic scheme proposed for manzamines A-C put forth by Baldwin and Whitehead (Figure 15).[62,63] Following this scheme, the structure of manzamine C[64] was reduced to the four units, tryptophan, acrolein, ammonia and a symmetrical dialdehyde. This hypothesis was later supported in part by the isolation of the azamacrocyclic containing marine alkaloids keramaphidin C and

keramamine C from *Amphimedon* sp.,[65] both of which appeared to be biogenetic precursors of manzamine C.

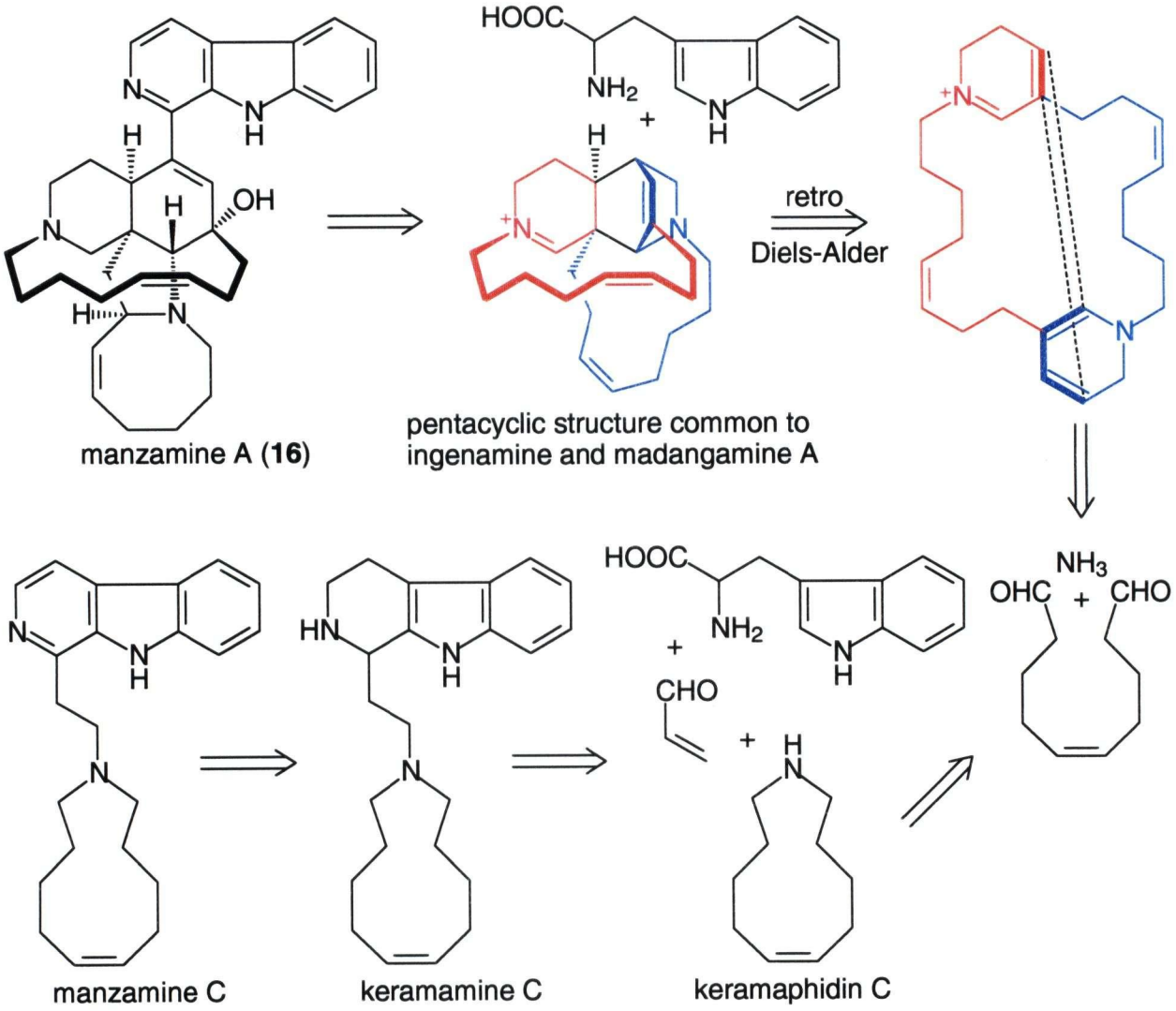

Figure 15. Proposed biogenesis of manzamines A and C, and related biogenetic precursors (from references 62 and 65).

Andersen and co-workers suggested that manzamine C was also biogenetically related to the motuporamines and proposed a biogenesis for these compounds based on the Baldwin and Whitehead pathway (Figure 16).[58] The azamacrocyclic structure contained within the motuporamines, keramaphidin C and keramamine C has also appeared in other marine alkaloids. Two such examples are haliclorensin[66] and the cytotoxic halitulin,[67] both isolated from the Indo-Pacific sponge *Haliclona tulearensis*. However, the spermidine-like side chain distinguishes motuporamines A-C from these natural products.

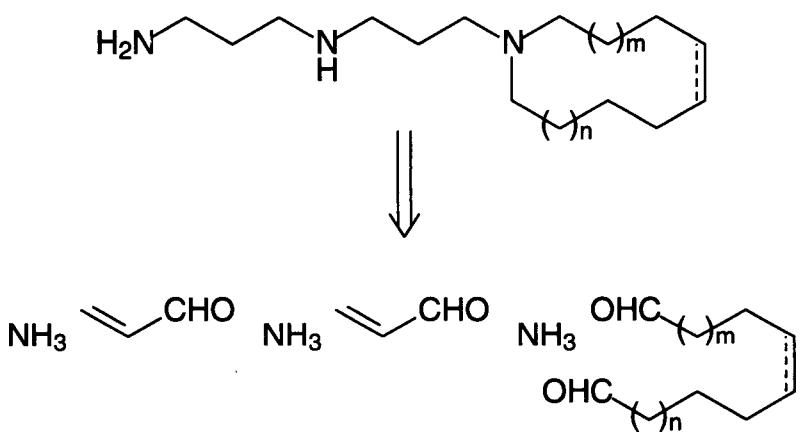

Figure 16. Proposed biogenesis of motuporamines A-C (from reference 58).

Returning to the mixture of motuporamines A-C, attempts to isolate the individual compounds were not successful.[58] Diacetylated derivatives were prepared from this mixture by reaction with acetic anhydride in pyridine. The resulting derivatives were easily separated by reversed-phase HPLC, and provided pure samples of diacetylmotuporamines A (**36**), B (**37**), and C (**38**) (see Figure 14).

NMR and mass spectral data were collected and analyzed in order to determine the structures of these compounds. The molecular formula for each compound was determined by analysis of high-resolution FAB mass spectral data. Analysis of the ^{1}H, ^{13}C, and 2D NMR spectral data led to the elucidation of the structures for diacetylmotuporamines A (**36**) and B (**37**), and tentative elucidation of the structure for diacetylmotuporamine C (**38**). The diacetylated derivatives **36**, **37**, and **38** possessed, respectively, a 13-, 14-, and 15-membered macrocyclic amine, and each compound contained the same spermidine-like unit.

Each diacetylated compound was reportedly isolated as the free base, however in the ^{1}H NMR spectrum of these compounds the signals assigned to the methylene protons adjacent to the tertiary nitrogen atom were conspicuously found downfield (ca. δ 3.05-3.20) from the expected values for such protons (ca. δ 2.40).[68] These signals appeared in a region more commonly observed for such protons in the chemical environment of an ammonium salt (ca. δ 3.05)[68] and not the free base as reported. Considering that the diacetylated derivatives were purified by reversed-phase HPLC, with 60% water and 1% trifluoroacetic acid in methanol as eluant, it is possible that

these compounds were isolated as the ammonium salts with trifluoroacetate as a counter ion.

In addition to ring size, diacetylmotuporamine C (**38**) differed from **36** and **37** by the presence of an olefin within the macrocyclic amine. Proton homonuclear decoupling NMR experiments indicated that the olefin had the *Z* configuration, with $J = 10.9$ Hz. However, it was not possible to determine the position of the olefin within the macrocyclic amine unit of **38**. Analysis of the 2D NMR data obtained for **38** eliminated all possible positional isomers but two, represented in compounds **41** and **42** (Figure 17). Assuming one of these two compounds is identical to authentic diacetylmotuporamine C (**38**), its positional isomer will be referred to in this text as isomotuporamine C and the diacetylated derivative as diacetylisomotuporamine C.

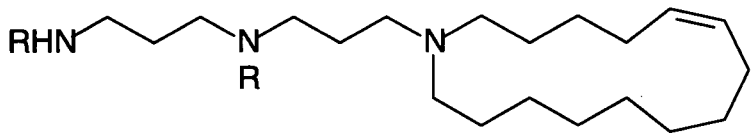

39 R = H
41 R = Ac

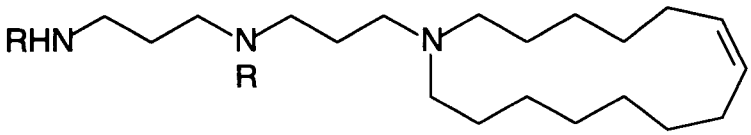

40 R = H
42 R = Ac

Figure 17. Positional isomers **41** and **42**, possible structures of authentic diacetylmotuporamine C (**38**).

The unusual structure and biological properties of the motuporamines, combined with the unresolved structural ambiguity related to motuporamine C (**35**), prompted the synthesis of these compounds. In order to elucidate the structure of motuporamine C, isomeric compounds **41** and **42** were synthesized. It was hoped that a comparison between these compounds and authentic diacetylmotuporamine C (**38**) would conclusively determine the position of the olefin. Interest in these compounds was not restricted to this work alone. Concurrent to our preparation of a manuscript describing the work discussed herein,[69] a report on the synthesis of motuporamines A (**33**) and B (**34**) by Baldwin and co-workers appeared.[70] Subsequent to our publication describing

the work discussed herein,[69] a report of an alternate synthesis of isomeric triamines **39** and **40**, isolated as the bishydrochloride salts, appeared.[71] The synthetic strategy employed by these groups differs considerably from the approach taken in our laboratory, as outlined in the next section.

1.5.2 Synthetic Plan

The synthesis of motuporamines A-C could provide a number of research opportunities. Biological studies performed on the individual compounds might provide key information as to which compounds or structural motifs gave rise to the in vitro cytotoxicity of the mixture. Recall that biological studies were not conducted on the individual compounds, however the synthesis of the motuporamines in large quantities would allow such studies to be conducted. The RCM reaction that was studied as part of this thesis could be applied to the synthesis of the macrocyclic amine portions of these compounds, via formation of the appropriate lactam. This would provide an opportunity to assess the applicability and scope of this method, by applying the knowledge gained from those studies. As synthetic targets, these compounds are by no means complex, however they are novel and of research interest. The synthesis of these compounds would also provide an opportunity to verify the structures assigned to the authentic compounds. This is especially important in the case of diacetylmotuporamine C (**38**) in which the exact position of the olefin within the macrocyclic amine unit could not be determined from the spectral data.

Motuporamines A-C are comprised of two simple subunits, one being a macrocyclic amine. Motuporamines A (**33**) and B (**34**) contain a 13- and 14-membered macrocyclic amine, respectively. Motuporamine C (**35**) contains a 15-membered macrocyclic amine with an endocyclic olefin in one of two possible positions. The second structural feature common among these compounds is a spermidine-like unit extending from the nitrogen atom of the macrocyclic amine. Spermidine consists of a 3-aminopropyl unit attached to a nitrogen atom of 1,4-butanediamine. In reference to the motuporamines, the term spermidine-like refers to a bis-propanediamine unit, or more specifically, a 3-aminopropyl unit attached to a nitrogen atom of 1,3-propanediamine.

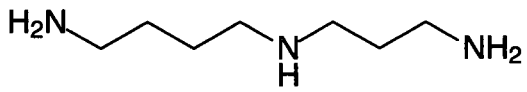

spermidine

Retrosynthetic analysis of the general motuporamine structure involved separating the molecule into spermidine-like and macrocyclic amine units. Such a disassembly of the motuporamines in two different ways is illustrated in Figure 18. The first, shown in the lower retrosynthetic scheme, involved a two step disconnection starting with a retro amidation reaction followed by a retro Michael addition to reveal the macrocyclic amine and two simple three-carbon units. In this way the spermidine-like unit would be built up from the nitrogen atom of the macrocyclic amine in a linear fashion.

The second and more convergent approach involved the same locations of bond disconnection, but in the opposite order, shown in the upper retrosynthetic scheme (Figure 18). Following this approach, the spermidine-like side chain would be preformed from two simple subunits. Baldwin and co-workers formed the spermidine-like unit of motuporamines A (**33**) and B (**34**) in this manner.[70] Disconnection of the spermidine-like side chain from the macrocyclic amine could be accomplished by a retro alkylation, amidation, or reductive amination reaction. The requisite spermidine-like unit would require the appropriate introduction and removal of leaving and protecting groups, and must incorporate a nitrogen atom concealed as an azide, nitrile, or protected amine. Disassembly of the spermidine-like unit could be accomplished by similar retro transformations.

One disadvantage to the second approach is the number of steps involved, due to the addition and removal of protecting and leaving groups. For this reason, it seemed appropriate to follow the linear approach. Although the side chain would have to be prepared for each motuporamine compound, examination of the methods available suggested this would be a more efficient route.

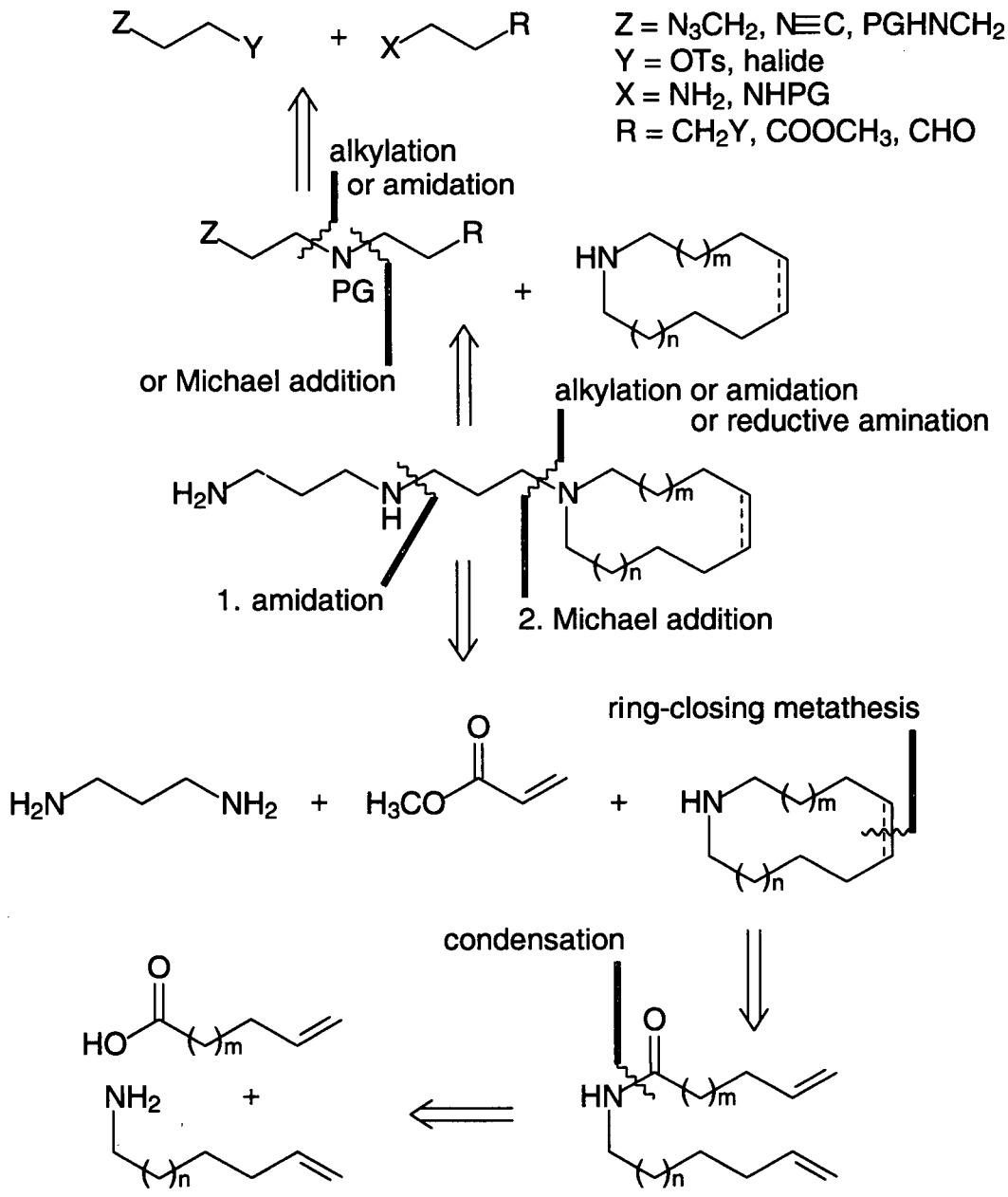

Figure 18. Retrosynthetic analysis for the synthesis of Motuporamines A-C.

What remained was to consider the key bond disconnection of the macrocyclic amine. Lactamization and ring expansion are obvious methods for assembling the macrocyclic amine units. The latter was chosen by Baldwin and co-workers in their synthesis of motuporamine B (**34**).[70] Since recent work in our laboratory involved studying the scope of the RCM reaction as it applied to macrocyclic lactone and lactam formation,[72] it seemed appropriate to form the ring portions of the motuporamines in this way. Since the motuporamine C isomers **39** and **40** both contain an olefin, differing only

in position, this method would be especially appropriate for forming the ring portions of these compounds. Accordingly, disconnection of the general macrocyclic amine structure by a retro ring-closing metathesis reaction reveals the diene-amide precursor (Figure 18). The appropriate reductive transformations, to form the desired macrocyclic amine from the unsaturated lactam, would have to be considered. Disassembly of the diene-amide through a retro condensation reaction leads to the requisite amine and carboxylic acid.

The syntheses of the motuporamines were conducted to accomplish two main goals. The first was to synthesize these compounds, in part, using the RCM reaction studied herein to form the macrocyclic amine units. The second goal was to compare the spectral data of the authentic and synthetic compounds in order to verify the structures assigned to the motuporamines. This included a determination of the position of the olefin within motuporamine C (**35**). In addition to the main goals, a few ancillary goals were considered. It was of interest to synthesize these compounds in an efficient manner, without the use of protecting groups. It was also of interest to determine if the diacetylated derivatives were isolated as the ammonium salts, or the free bases as reported. The synthesis of the motuporamine C isomers **39** and **40** was also intended to test the RCM reaction, studied herein for 14-membered lactam formation, as it applied to 15-membered lactam formation. Considering the variety of approaches that could be taken to assemble the spermidine-like unit, it seemed appropriate to examine the methods available. Selections of these are discussed in the next section. Taking into consideration the goals discussed above, one of these methods was chosen to assemble the spermidine-like portion of the motuporamines.

1.5.3 Synthetic Approaches to Spermidine and Spermidine-like Units

Spermine and its component structure spermidine, as well as spermine-like and spermidine-like structures are common to a number of alkaloids. Such compounds have attracted the interest of synthetic chemists due to their novel structures and biological activity. A number of alkaloids contain these structures as part of a macrocyclic backbone. Some of these include the spermine containing budmunchiamines,[73] and the spermidine containing (*S*)-(+)-dihydroperiphylline[74] and (-)-(4*R*)-dihydroisomyricoidine,[75] the latter being a synthetic compound. As for acyclic alkaloids, homocaldopentamine[76] and the family of Nephilatoxins[77] are spider toxins that

represent just a few of the alkaloids that contain the spermidine structure. A number of the compounds discussed above were the subjects of total syntheses. Examination of these syntheses would provide insight into the methods employed to form such structures, and how these methods may be adapted to the synthesis of the spermidine-like unit of the motuporamines.

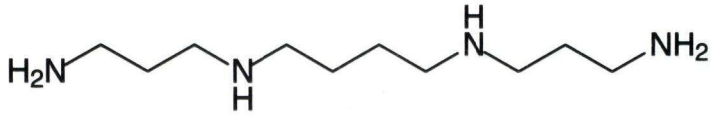

spermine

Successive amine alkylation is a typical strategy employed in the formation of spermidine-like structures. For example, synthesis of a portion of (S)-(+)-dihydroperiphylline involved such a strategy.[74] Alkylation of aminopropanol **43** with 4-bromobutyronitrile provided spermidine-like alcohol **44** (Figure 19). Alkylation of a primary amine with the triflate of **44** formed compound **45** that contained the spermidine-like structure, shown in bold red.

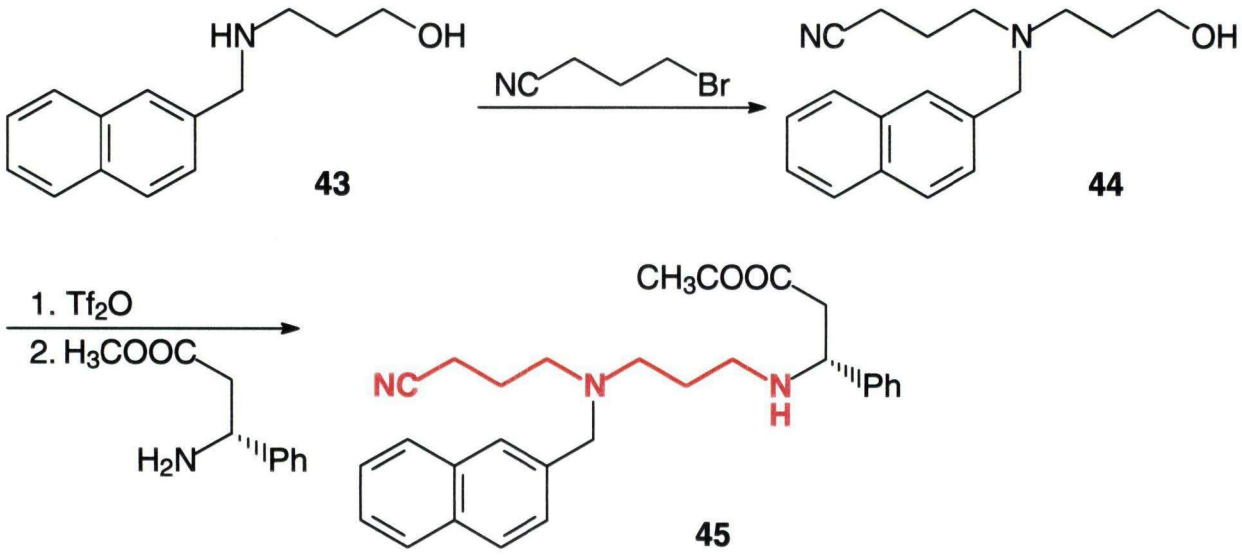

Figure 19. Synthesis of the spermidine-like portion, shown in bold red, of (S)-(+)-dihydroperiphylline (from reference 74).

The synthesis of penta-*N*-protected homocaldopentamine employed a similar strategy to construct the acyclic polyamine structure.[76] Synthesis of a spermidine-like

unit more closely resembling the one contained in the motuporamines began with modifications to 3-chloropropan-1-ol (**46**). Sequential treatment of **46** with sodium azide and *p*-toluenesulfonyl chloride formed **47** (Figure 20). Alkylation of 3-aminopropan-1-ol with **47** followed by *N*-carbamation and *O*-tosylation provided spermidine-like tosylate **48**. Finally, alkylation of a secondary amine with **48** formed **49**, which contained the spermidine-like structure shown in bold red.

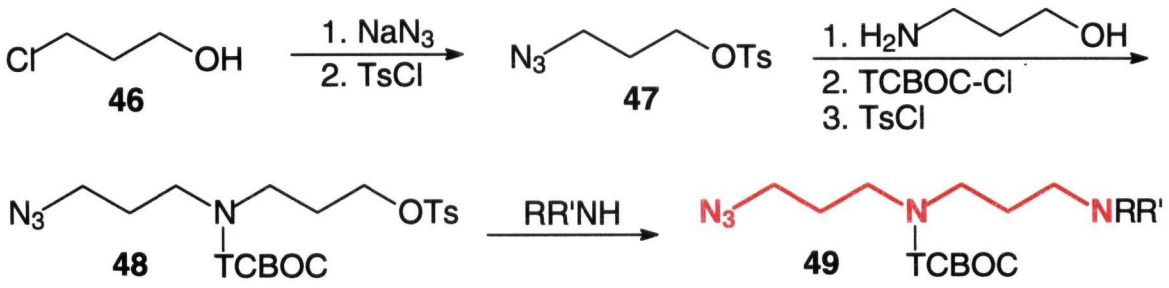

Figure 20. Synthesis of the spermidine-like portion, shown in bold red, of homocaldopentamine (from reference 76).

The previous two examples suggested that either compound **48** or a modified version of the triflate of **44** (Figure 19) might function as an alkylating agent in the motuporamine syntheses. Baldwin and co-workers employed a similar unit in the synthesis of motuporamines A (**33**) and B (**34**).[70] A similar alkylation strategy was employed to couple the subunits of the spermidine-like structure, but reductive amination was used to complete its formation. The synthesis of the spermidine-like structure of motuporamines A (**33**) and B (**34**) began with *N*-carbamation followed by *O*-tosylation of 3-aminopropan-1-ol (**50**) to form tosylate **51** (Figure 21). Substitution of **51** with 3-aminopropan-1-ol (**50**) and subsequent *N*-carbamation of the resulting secondary amine, followed by oxidation of the hydroxyl, resulted in the formation of spermidine-like aldehyde **52**. Reductive amination of the appropriate macrocyclic amine with aldehyde **52** gave the protected triamine **53**. Subsequent to this work, an alternate synthesis of isomeric triamines **39** and **40** utilized an aldehyde analogous to **52**, bearing BOC groups in place of CBZ groups.[71]

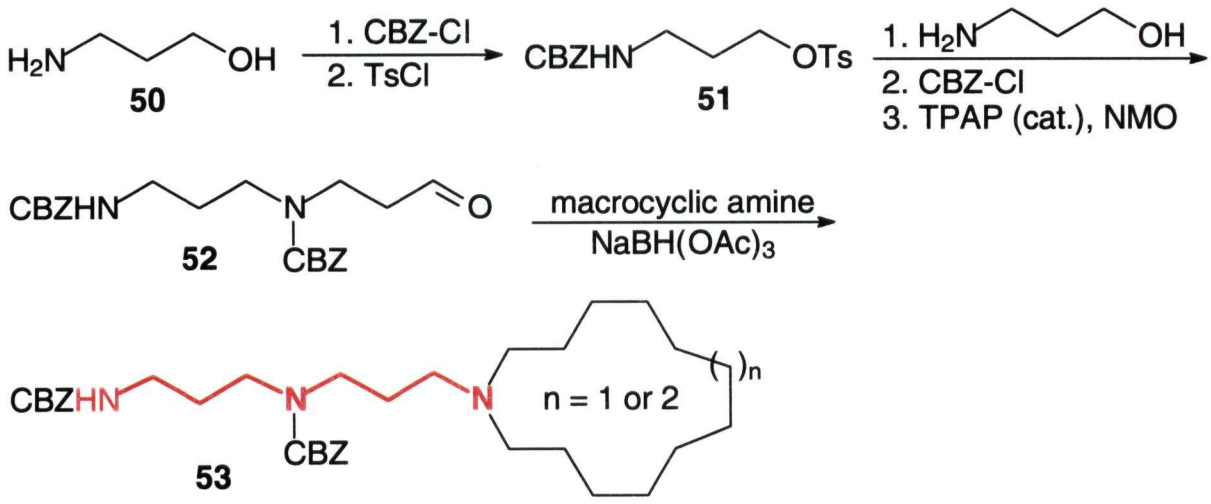

Figure 21. Synthesis of the spermidine-like portion, shown in bold red, of motuporamines A (**33**) and B (**34**) by Baldwin et al. (from reference 70).

One drawback to the approaches illustrated in the previous three examples was the necessity of several protecting and leaving groups. The need for such substituents adds additional steps to a synthesis and results in the waste of material. Consequently, a different approach to these structures was examined. The total synthesis of spider neurotoxins Nephilatoxins (NPTX-10 and NPTX-12) employed Michael chemistry to couple the subunits and amidation to introduce the third nitrogen of the spermidine-like structure.[77] The synthesis of the spermidine-like portion of these natural products began with Michael addition of 4-aminobutan-1-ol (**54**) to methyl acrylate followed by BOC protection of the resulting β-amino ester to form compound **55** (Figure 22). Mesylation of **55** followed by substitution with sodium azide resulted in the formation of azide **56**. Alkaline hydrolysis of the methyl ester within **56** followed by esterification with *p*-nitrophenol and DCC, and finally amidation with a primary amine resulted in the formation of **57**, in which the spermidine-like structure is shown in bold red. Although the synthesis of this portion of the Nephilatoxin structure was accomplished following a strategy different to those described earlier, the use of protecting and leaving groups was still required.

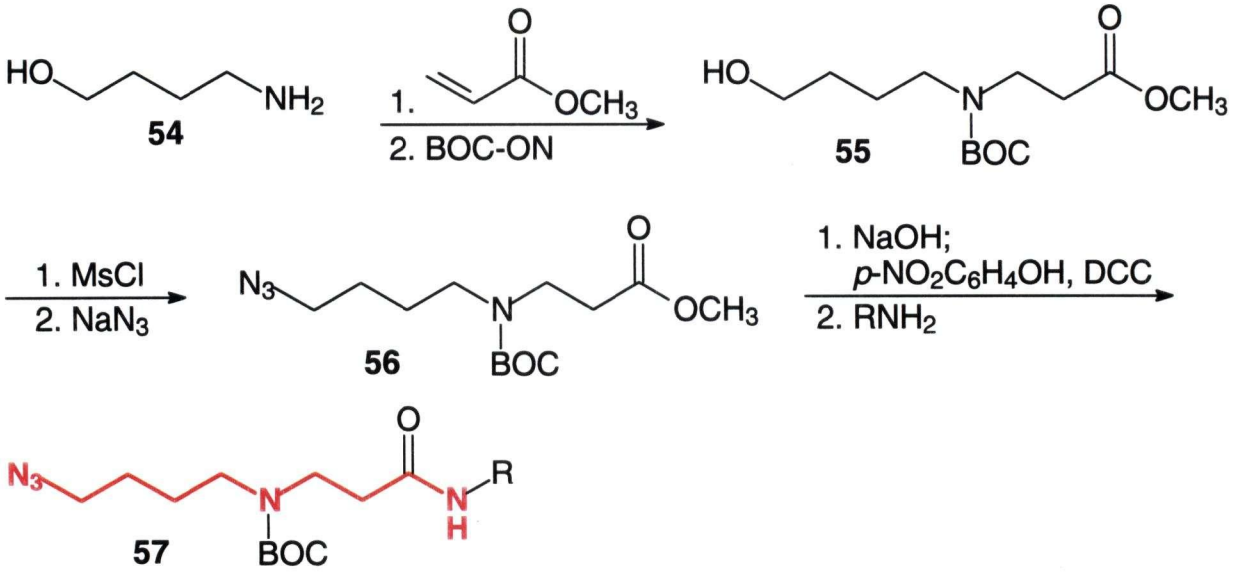

Figure 22. Synthesis of the spermidine-like portion, shown in bold red, of Nephilatoxins (NPTX-10 and NPTX-12) (from reference 77).

Although most of the methods presented thus far followed a linear approach to these types of structures, few met the criteria of our synthetic plan and were better suited to the convergent approach. The use of Michael addition and amidation chemistry in the previous example provided a source of inspiration for an alternate route. It would be appealing to utilize these steps without the use of protecting and leaving groups. Further inspection of the literature provided such an example.

Dendrimers are a class of branched oligomeric molecules. These compounds possess an initiator core with a number of repeating units radially attached to it. Branching usually occurs at the terminus of each repeating unit within each layer, or generation, thus providing the dendritic or tree-like structure. The synthesis of such a dendrimer provided some of the methods necessary to construct the spermidine-like unit of the motuporamines. The first stage in the synthesis of this dendrimer began with exhaustive Michael addition of ammonia with methyl acrylate forming triester **58** (Figure 23).[78] Exhaustive amidation of **58** with ethylenediamine formed the amine-terminated star-branched oligomer **59** that possessed the spermidine-like structure, shown in bold red for one of the radially repeating units. Each repetition of these two steps would introduce the next layer or generation of the dendrimer.

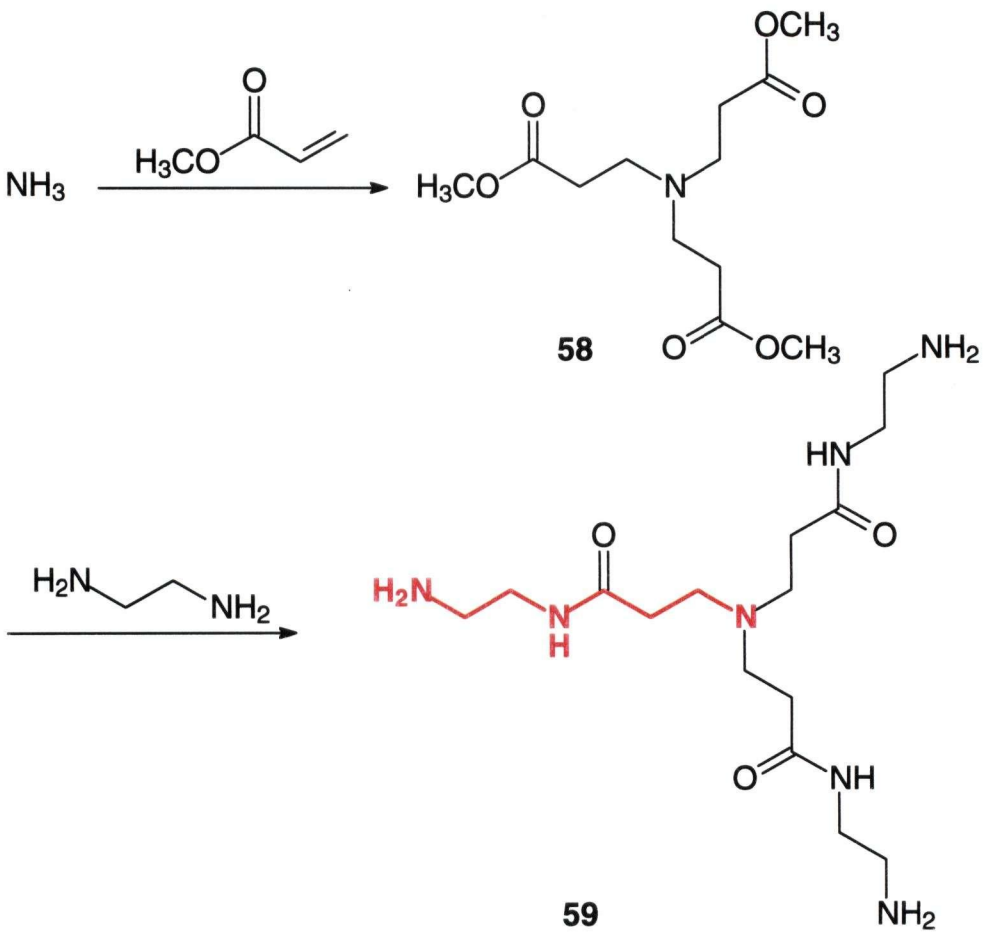

Figure 23. Synthesis of an amine-terminated star-branched oligomer (from reference 78).

It was considered that this method could be adapted for the synthesis of the motuporamines. In order to form the correct structure, substitution of ethylenediamine with 1,3-diaminopropane would be required. Since this method would be applied to a secondary amine, exhaustive Michael addition would not be a concern. Addition of excess 1,3-diaminopropane during the amidation step would be required to prevent the formation of diacylated products. A number of other features make this an attractive method to form the spermidine-like unit. Both reactions can be carried out in the same reaction vessel and the purification after each step simply involves removal of the excess reagents and solvent in vacuo. Finally, this method does not require the use of protecting groups. This reduces the number of steps and reagents required for installation of the side chain. Considering the simplicity and efficiency of this method, it seemed appropriate to form the spermidine-like unit of the motuporamines in this manner.

1.5.4 Precedence of 15-Membered Lactam Formation by RCM

The formation of macrocyclic compounds via RCM was discussed earlier in this chapter. Although a few examples of ring formation by this method were sited, none of these specifically involved 15-membered lactam formation, which is required for the synthesis of the lactam precursors to the motuporamine C isomers **39** and **40**. 15-Membered macrocyclic ketones,[45] polyethers,[47] lactones,[79] and urethanes[80] have been formed with varying success by RCM using Grubbs' benzylidene **3** (Table 1). Formation of this ring size also appeared in the ingenious synthesis of acyclic (2S,7R)-2,7-diaminosuberic acid, an isosteric dicarba analogue of cystine peptides,[81,82] via a cyclic precursor (Entry 5), and in the total synthesis of the 15-membered azamacrolide epilachnene.[45,83] With exception of Entries 1 and 6, the RCM reactions were slow and required moderate to high catalyst loading (ca. 10-50 mol%) to form these macrocyclic compounds in reasonable yield. Furthermore, little to no stereoselectivity was observed, with the exception of the macrocyclic urethanes (Entry 4) in which the *Z* isomer was formed exclusively.

The problems associated with forming these macrocyclic compounds and how that could affect the synthesis of motuporamine C isomers **39** and **40** must be addressed. Since an odd-membered ring cannot adopt a strain free diamond-lattice conformation, the strain associated with formation of a 15-membered ring might affect the yield of the reaction or the catalyst loading (see Section 1.4). The high yields obtained for the majority of the products presented in Table 1 suggest that conformational stability was not a significant factor governing cyclization. However, the high precatalyst loading required for the formation of the urethanes (Entry 4) and the macrocyclic precursor to 2,7-diaminosuberic acid (Entry 5) indicated some difficulty in forming these compounds. The effects of the proximity between the double bond and the carbonyl in the former and areas of steric congestion in the latter, rather than conformational stability, might account for the high precatalyst loading. Both of these factors have been shown to hinder RCM. The azamacrolide precursors to epilachnene (Entry 6) more closely resemble the lactams required for the synthesis of motuporamine C isomers **39** and **40**, considering how remote the olefin is from the carbonyl and areas of steric congestion. The high yields and low catalyst loading in these cases suggest that similar results might be obtained for **39** and **40**. Another problem to consider is the lack of stereocontrol of the resulting olefin.

Table 1. Formation of Various 15-Membered Macrocyclic Compounds by RCM.

Entry	RCM product	mol% **3**	Yield (%)[a]	*E*:*Z*	Ref.
1	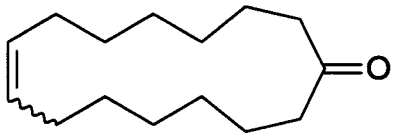	2-5	72	4.6:1	45
2	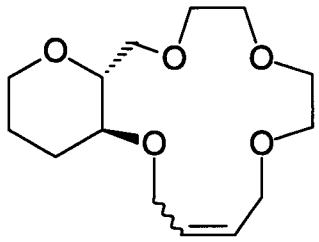	10	85	10:3	47
3	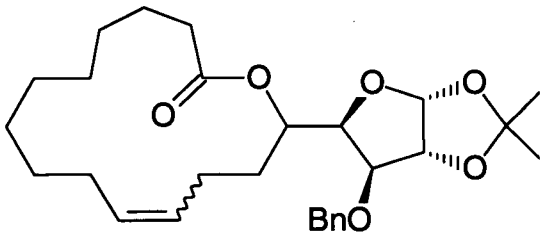	10-20 10-20	66 (5*S*) 46 (5*R*)	1:3	79
4	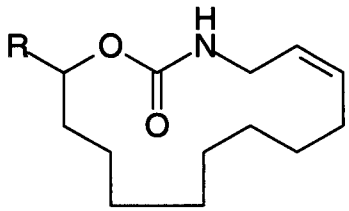	50 50	69 R=Me 58 R=H	0:100	80
5	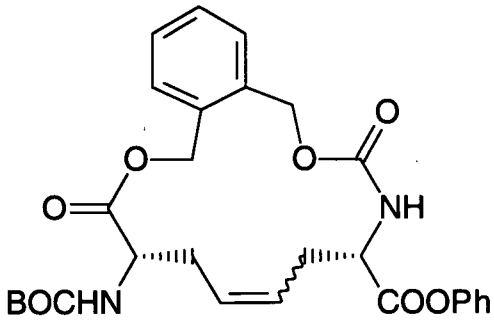	40	83	1:1	81
6	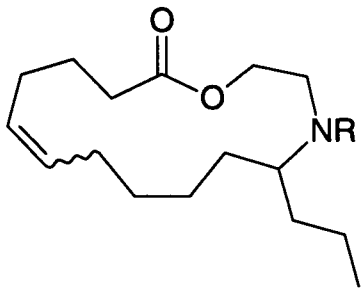	5	89 R=Fmoc 89 R=BOC 83 R=H·HCl	2:1	45

[a] Refers to isolated yields after chromatography.

The inability to control or even predict the configuration of the olefin resulting from RCM is a fundamental problem associated with this approach to macrocyclization that has yet to be resolved. The macrocyclic compounds formed by RCM presented in Table 1 are exemplary of this problem. Although the macrocyclic urethanes were formed exclusively with the *Z* configuration, this result was neither expected nor predicted. The remaining compounds in this table were formed with little or no stereoselectivity. This fundamental aspect of macrocycle formation by RCM was anticipated to be a problem for the formation of the lactam precursors to the motuporamine C isomers **39** and **40**. Recall the ring portion of both these compounds contained an olefin with the *Z* configuration. Therefore, formation of each lactam via RCM would require exclusive or highly selective formation of the olefin with the *Z* configuration. The selectivity would likely depend on the position of the resulting olefin within the lactam. The RCM studies discussed in the next chapter would provide some insight into this issue.[72]

These examples, although none are specific to lactams, suggest it is reasonable to form the 15-membered lactam precursors to the motuporamine C isomers **39** and **40** by RCM. Support for this supposition also comes from the examples of 13-, 14- and 18-membered lactam formation by RCM that were discussed earlier in this chapter. So far it appears that the control or prediction of the configuration of the resulting olefin will not be possible.

1.5.5 Proposed Synthesis of Diacetylmotuporamines A-C

The linear assembly of the spermidine-like side chain proposed for our syntheses of the motuporamines does not require the use of protecting groups, can be conducted in the same reaction vessel, and involves a simple yet efficient purification. When the number of steps involved in the preparation of such a side chain is considered for a convergent approach, including the addition and removal of protective groups, the linear approach appears to be more simple and efficient.

Baldwin and co-workers chose to synthesize motuporamines A (**33**) and B (**34**) in a convergent manner,[70] which involved coupling of the spermidine-like aldehyde **52** to the appropriate macrocyclic amine. Their synthesis began with a one-carbon ring expansion of cyclododecanone (**60**), followed by Beckmann rearrangement of the corresponding oxime **61** to give lactam **62** (Scheme 1). Reduction of lactam **62**

provided macrocyclic amine **63**. Macrocyclic amine **66** was prepared by reduction of the commercially available lactam **65**. Reductive coupling of **52** and a macrocyclic amine (**63** or **66**) resulted in formation of diprotected motuporamines **64** or **67**. Deprotection followed by diacetylation provided diacetylmotuporamines A (**36**) and B (**37**). These compounds were reportedly isolated as the free base and found to be identical to the authentic material.

Scheme 1. Synthesis of Diacetylmotuporamines A (**36**) and B (**37**) by Baldwin and Co-workers (from reference 70)[a]

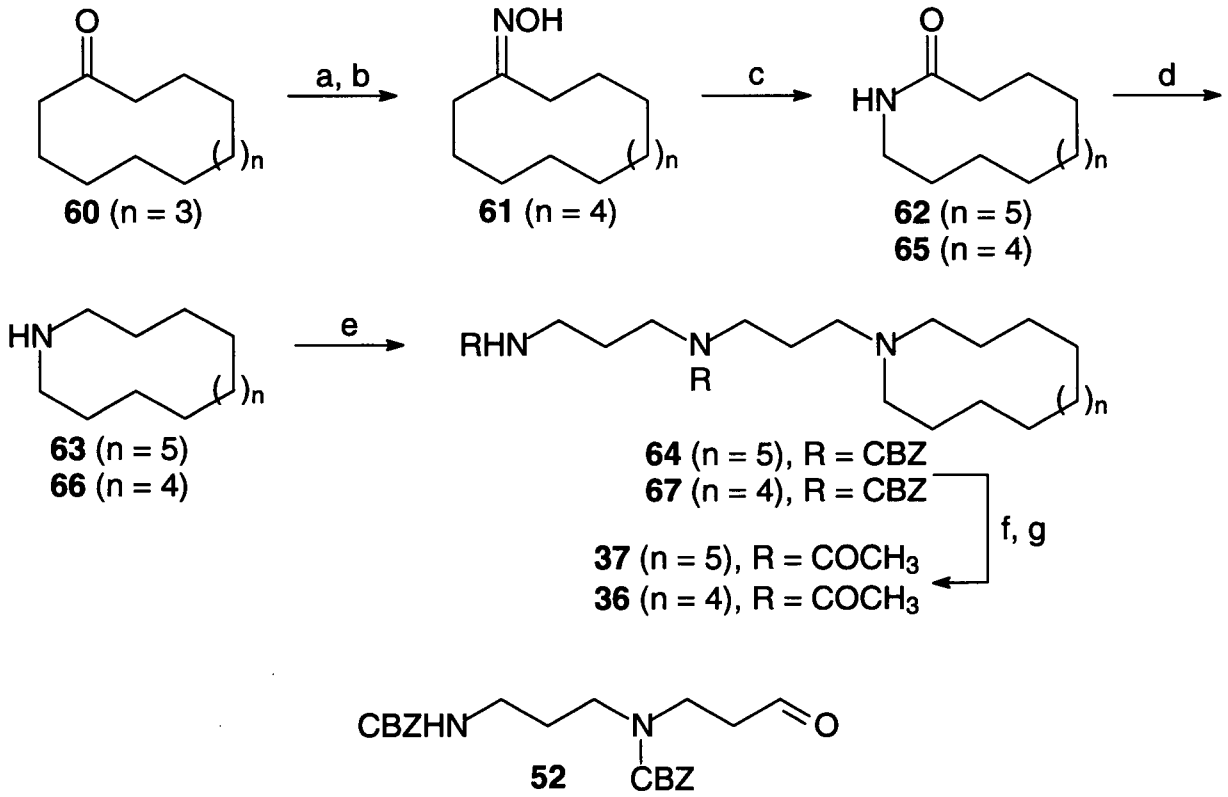

[a]Key: (a) Me_3SiCHN_2, $BF_3{\cdot}Et_2O$, CH_2Cl_2, 77%; (b) $NH_2OH{\cdot}HCl$, $NaHCO_3$, MeOH, 91%; (c) P_2O_5, CH_3SO_3H, 100%; (d) LAH, THF, reflux, 97% (**66**) or 60% (**63**); (e) aldehyde **52**, $NaBH(OAc)_3$, 1,2-dichloroethane, 100% (**67**) or 66% (**64**); (f) Pd/C, H_2, MeOH, 85% (**33**) or 100% (**34**); (g) Ac_2O, Et_3N, pyr, 76% (**36**) or 78% (**37**).

A linear approach to the synthesis of motuporamines A-C was proposed for our work. In general, the appropriate macrocyclic amine is added to methyl acrylate in a Michael fashion followed by amidation of the resulting β-amino ester with

1,3-diaminopropane (Figure 24). Reduction of the resulting amide followed by diacetylation would provide the desired diacetylmotuporamine. This route has certain advantages over the previous synthesis of motuporamines A (**33**) and B (**34**). Four fewer steps are required to introduce the spermidine-like unit to the macrocyclic amine. Also, the Michael addition and amidation steps are performed in the same reaction vessel and the purification only involves removal of the excess reagents and solvent in vacuo. Clearly this process, although linear, is more simple and efficient.

Similar to the synthesis of these compounds by Baldwin and co-workers, the 13-membered macrocyclic amine **66** could be prepared by reduction of commercially available lactam **65**. Recall that Baldwin and co-workers synthesized the 14-membered macrocyclic amine **63** in part by ring expansion and Beckmann rearrangement. Considering that the RCM methodological studies reported in this thesis involved the synthesis of a series of unsaturated 14-membered lactams, it seemed appropriate that macrocyclic amine **63** should be derived from one or a combination of these products. It was anticipated that the chemistry developed from these studies could be applied to the synthesis of the 15-membered lactam precursors of the motuporamine C isomers **39** and **40**. In general, coupling of the appropriate carboxylic acid and amine followed by RCM of the resulting diene-amide would form the corresponding unsaturated lactam (Figure 24). Reduction(s) of the appropriate lactam would result in formation of the desired 14- and 15-membered macrocyclic amines. The spermidine-like side chain could be added to these macrocyclic amines as discussed above.

The lack of control over the configuration of the resulting olefin in the RCM reaction would only affect the synthesis of motuporamine C isomers **39** and **40**. This was not anticipated to be an issue for the synthesis of motuporamine B (**34**) since configurational or positional olefin isomers of the unsaturated 14-membered lactams obtained by RCM would be reduced through hydrogenation. As discussed previously, formation of the 15-membered lactams by RCM requires control over the configuration of the resulting olefin, preferably forming the *Z* isomer. The RCM studies conducted in our laboratory, some of which are presented herein, might provide some insight regarding this issue, in addition to the scope of this reaction. These and other results regarding the RCM formation of 14-membered lactams are discussed in the following chapter.

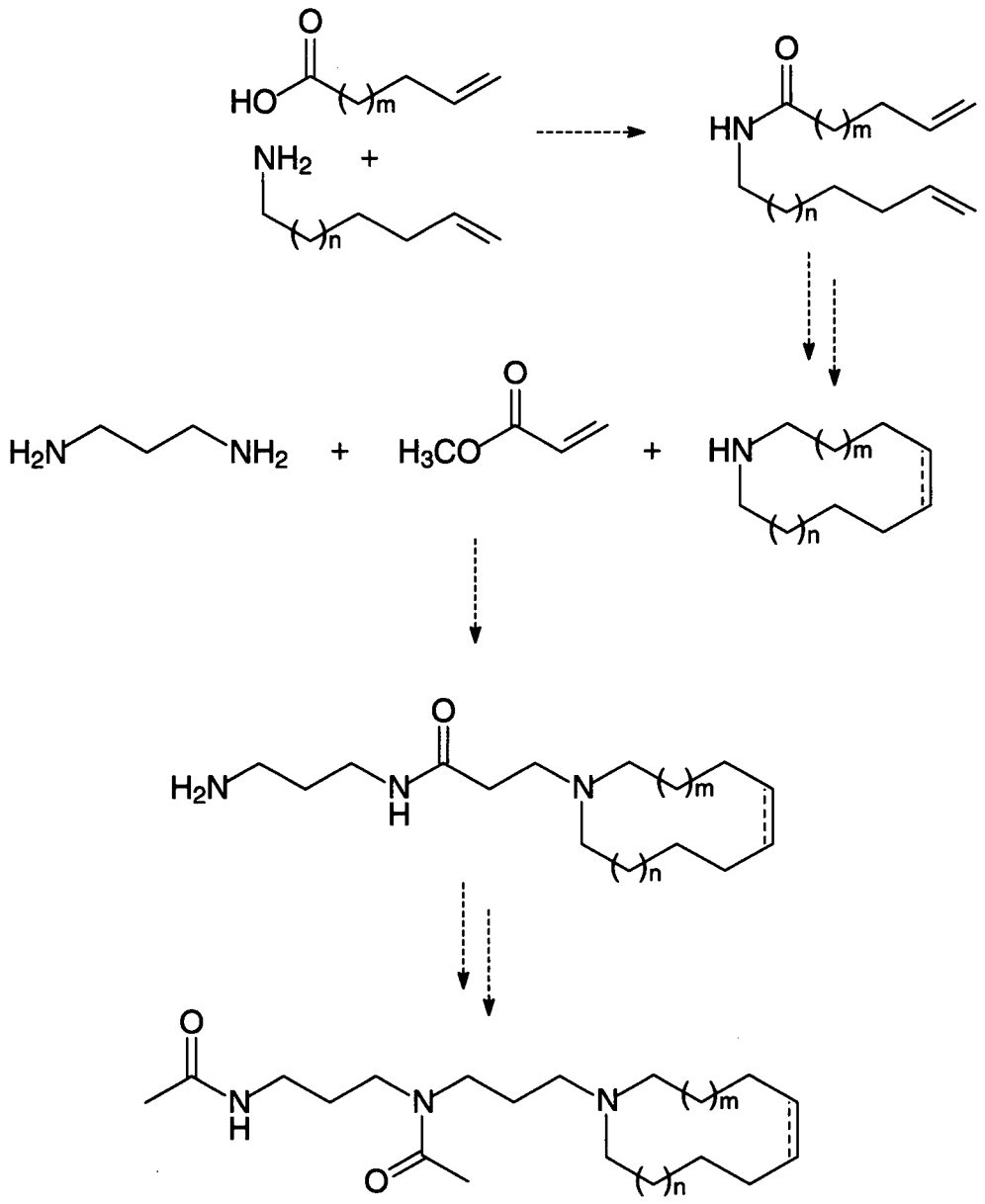

Figure 24. Proposed synthetic route to diacetylmotuporamines A-C.

CHAPTER 2
SYNTHESIS OF UNSATURATED 14-MEMBERED LACTAMS VIA RCM

Results and Discussion

The application of established polymerization metathesis catalysts and the development of a new class of catalysts early in the 1990's renewed research interest in the olefin metathesis reaction. Since this time numerous applications of this reaction as a cyclization process have appeared in the literature,[2] and a few examples of ring-closing metathesis (RCM) were discussed in Chapter 1. In particular, its usage in the formation of macrocyclic compounds from acyclic dienes has received much attention. A few studies have illustrated the facile formation of medium to large ring compounds, ranging in size from 10- to 36-membered rings, however a systematic study of a single ring size has yet to be carried out.

As part of an ongoing study in our laboratory into the chemistry of macrocyclic compounds, the synthesis of a series of unsaturated 14-membered lactams (**77-92**) by RCM of the corresponding series of diene-amides (**68-76**) using Grubbs' benzylidene **3** (Figure 25), was examined to explore nine logical sites for ring closure. In particular, it was anticipated that these studies would lead to a better understanding of the effect that the position of the terminal double bonds relative to the amide functional group would have on the yield of the reaction and on the resulting diastereomeric ratio of the newly formed olefin. The effects of reaction conditions, additives, and structural modifications to the diene were also explored. The relative energies of the product lactams were determined using molecular mechanics calculations to better understand the factors governing the resulting olefin configuration from RCM. For each site of ring closure the *E*/*Z* ratio observed from RCM was compared to a value obtained from molecular mechanics calculations. Finally, preliminary studies were conducted to probe the effect of the active form of the catalyst on the unsaturated lactam products.

Although our primary goal was the synthesis of unsaturated 14-membered lactams via RCM, we were also interested in exploring the synthesis of unsaturated macrocyclic amines from diene-amines using Grubbs' benzylidene **3**. At the onset of

these studies little was known of the functional group compatibility between **3** and the nitrogen atom of a tertiary amine.

Substitution of a methylene group in cyclotetradecane with an oxygen[84] or nitrogen[85] atom was shown to have little effect on the conformation of the ring. However, these atoms were situated in positions within the conformation to eliminate the greatest number of transannular interactions within the ring. With respect to unsaturated 14-membered lactams, the introduction of an amide group and an olefin was expected to have a similar effect. In an examination of conformationally controlled stereoselective reactions of monosubstituted 8- to 12-membered ketones and lactones, Still et al. noted that in comparison to smaller size rings, such as 6-membered rings:

> Functionalized macrocycles on the other hand typically have 3-dimensional structures which are significantly different from normal rings in that sp^2 centres tend to stand perpendicular to the plane of the ring where important transannular nonbonded interactions are minimized.[86]

The degree to which these interactions are minimized in unsaturated 14-membered lactams depends on the relative position of the amide and olefin groups, and on which positions they occupy within the conformation of the ring (see Section 1.4). Whether a minimization of transannular interactions, or lack there of, would have an effect on the yield of the RCM of diene-amides, and on the preferred configuration of the resulting olefin were questions of interest. In addition, the formation of unproductive catalyst complexes, resulting when a terminal double bond and an amide group are in close proximity, would have to be considered. Depending on the severity, this problematic interaction might hinder the determination of these transannular effects at olefin positions close to the amide group.

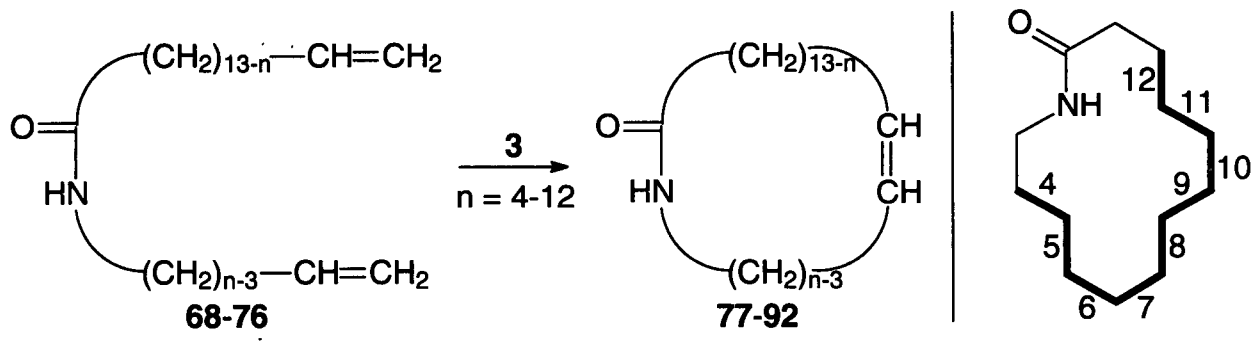

68-76 **77-92**

Figure 25. Proposed formation of unsaturated 14-membered lactams **77-92** via RCM of diene-amides **68-76** using Grubbs' benzylidene **3**.

2.1 Synthetic Plan for Diene-amide Construction

In order to conduct these studies the synthesis of a series of diene-amides was required. Since these compounds are all structurally related, and only differ by the length of the alkenyl chains extending from the amide functionality, a general synthetic approach was considered. Retrosynthetic analysis of the unsaturated lactam structure, using lactam **84** as an example, illustrated synthetic routes and methods applicable for the construction of these compounds. This analysis began with the ring opening of lactam **84** by a retro RCM reaction (Figure 26). Disconnection of the requisite diene-amide **72** was accomplished in two ways. The first, following path a, involved retro amidation to provide the requisite carboxylic acid **93** and amine **94**. Acid **93** was obtained by hydrolysis, and amine **94** by reduction, of the corresponding nitriles **95** and **96**. These nitriles were obtained either by lithioacetonitrile or nitrile addition to iodide **97**. The second key disconnection strategy, following path b, involved retro alkylation of diene-amide **72** to provide the requisite primary amide **98** and alkenyl iodide **99**. Iodide **99** was formed from alcohol **100** by an iodide substitution transformation. Retro amidation of primary amide **98** gave carboxylic acid **93**. In addition to the nitrile hydrolysis described above, an alternate route to acid **93** involved malonic ester alkylation with iodide **97**, followed by hydrolysis, and finally decarboxylation.

The retrosynthetic analysis discussed above illustrated a number of the methods that were applied in the synthesis of the diene-amides required for these studies. From this analysis, a synthetic strategy was inferred whereby two particular precursors could be derived from a single compound that possessed a dual reactivity. For instance, nitriles were used to form carboxylic acids as well as amines. The carboxylic acids could be used to form primary amides as well as the secondary diene-amides. One application that was not discussed above, but was found to be quite useful, was the formation of amines by reduction of the corresponding primary amides. In addition to this dual reactivity, compounds such as iodide **97** were common starting materials in the syntheses of various precursors to the requisite diene-amides via one- or two-carbon additions.

A number of concerns associated with macrocyclic ring formation via RCM were considered. Some of these included the choice of catalyst, the reactivity of this catalyst to the amide group, and the unbiased conformational mobility of the acyclic diene-amide due to the absence of any substituents. Prior to the synthesis of the diene-amides it

seemed appropriate to investigate the precedence set in the literature illustrating the formation of a macrocyclic compound by RCM.

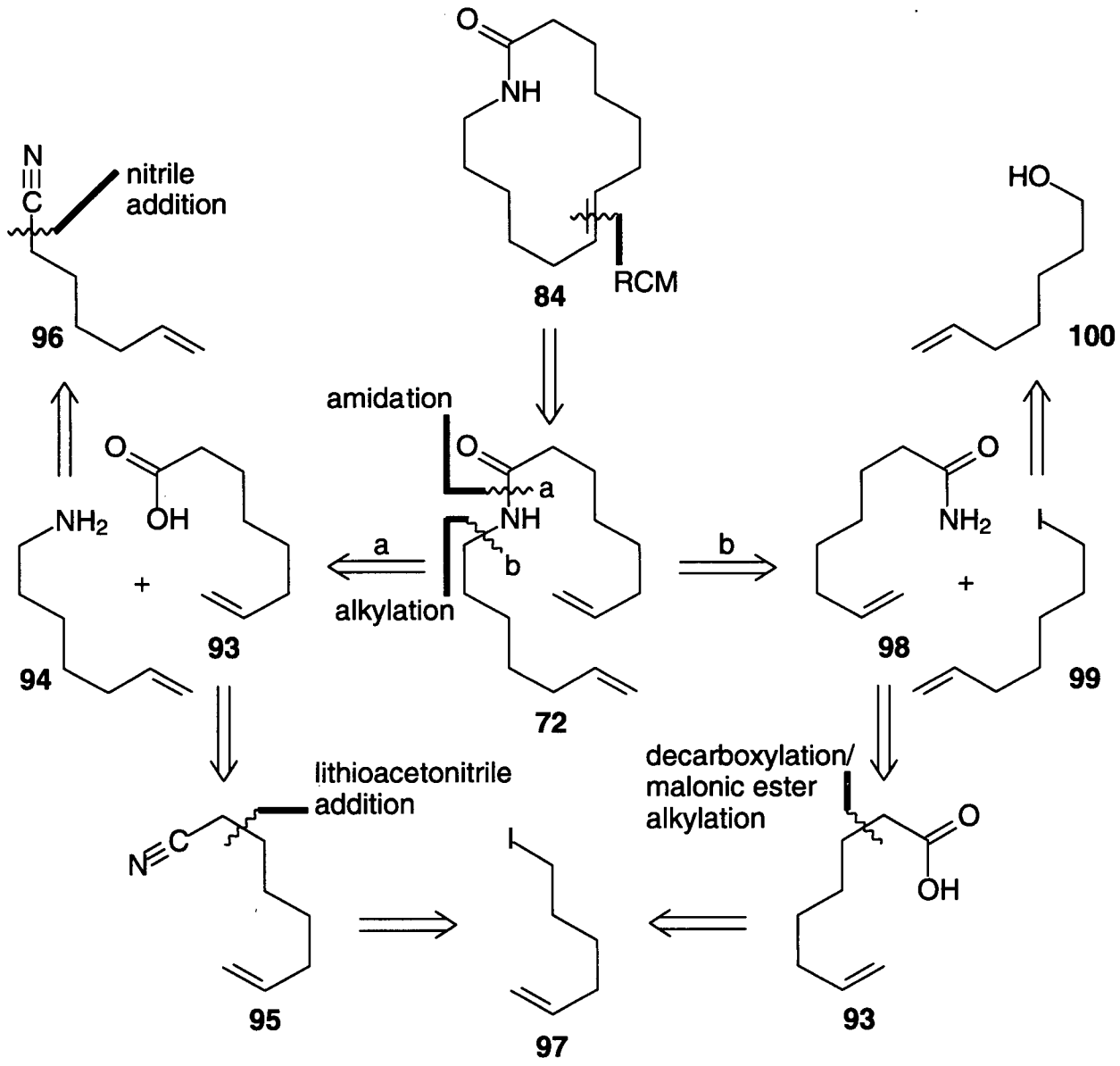

Figure 26. Retrosynthetic analysis for the synthesis of 2-azacyclotetradecenones, illustrated by analysis of (*E*)-2-azacyclotetradec-8-enone (**84**).

2.2 Preliminary Metathesis Studies

Recall the seminal applications of the RCM reaction in macrocyclic lactone construction discussed in Chapter 1 (see Section 1.2). In order to assess the viability of the catalyst and the conformationally unbiased diene substrate, attempts were made to reproduce the synthesis of the unsaturated 16-membered lactone **6** reported by Villemin,[4] starting from the commercially available alcohol **101** and carboxylic acid **102**. Coupling of these compounds using DCC gave diene-ester **5** in 14% yield (Scheme 2). Repeated attempts to cyclize **5** using the reaction conditions and $WCl_6/SnMe_4$ catalyst system employed by Villemin failed. Although these reactions were assembled in a glove box under an inert atmosphere, the possibility of contamination from oxygen was not ruled out. Furthermore, the activity of the tungsten catalyst was questionable. In light of this failure, a simpler system was chosen to test the applicability of these conditions to olefin metathesis.

Scheme 2. Attempted RCM of 5-Hexenyl 10-undecenoate (**5**)[a]

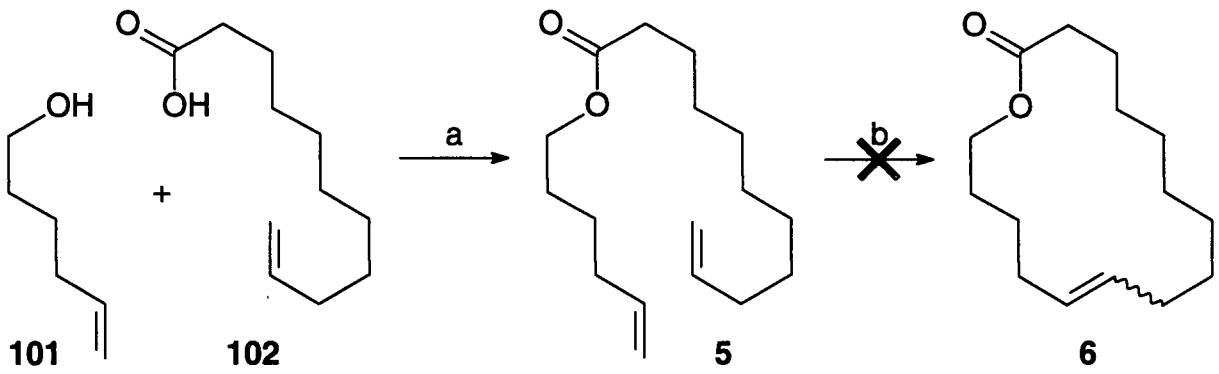

[a]Key: (a) DCC, TEA, acetonitrile, rt, 14%; (b) WCl_6, $SnMe_4$, chlorobenzene, 70 °C, 0%.

Concurrent to the report discussed above, the synthesis of unsaturated esters by intermolecular olefin metathesis was reported.[5,87] One example involved the intermolecular metathetic formation of unsaturated diacetate **105**. Attempts to reproduce this result began with the formation of 9-decenyl acetate (**104**) in 90% yield by acetylation of the commercially available alcohol **103** with acetyl chloride and DMAP (Scheme 3). Attempts to couple two molecules of **104** under conditions similar to those described above failed. This result, coupled with the failure of the previous attempt,

suggested the catalyst used for these studies was not fully active or was contaminated by the presence of oxygen.

Scheme 3. Attempted Intermolecular Metathesis of 9-Decenyl acetate (**104**)[a]

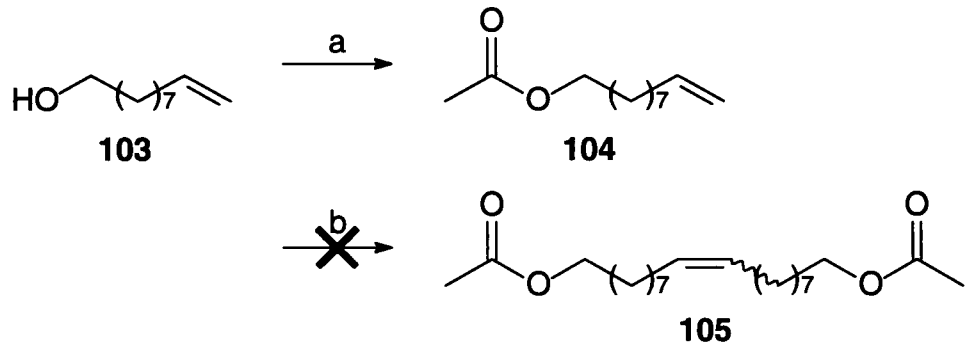

103 **104** **105**

[a]Key: (a) AcCl, DMAP, TEA, CH_2Cl_2, 0 °C to rt, 90%; (b) WCl_6, $SnMe_4$, PhH, 70 °C, 0%.

Considering the difficulty encountered with the $WCl_6/SnMe_4$ catalytic system, investigation of other catalysts amenable to olefin metathesis seemed appropriate. Recently, reports of new olefin metathesis catalysts that are tolerant to a wider variety of functional groups and reaction conditions have appeared. These include Schrock's molybdenum alkylidene **1**[8] and Grubbs' ruthenium benzylidene **3**.[10,11] For reasons that were discussed earlier, and will be elaborated on in due course, the latter precatalyst proved to be well suited for the purposes of our studies.

2.3 Preparation of Dichlorobis(tricyclohexylphosphine)ruthenium benzylidene (Grubbs' Benzylidene 3)

The synthesis of Grubbs' benzylidene **3** began with the preparation of hydrazone **107** by addition of *p*-toluenesulfonylhydrazide to benzaldehyde (**106**) (Scheme 4). Benzylidene **3** was prepared from **107** according to a modification[88] of the method of Schwab, Grubbs, and Ziller.[11] Hydrazone **107** was converted into phenyldiazomethane (**108**) with base. Due to the potentially explosive nature of this compound, it was not isolated neat but stored at -42 °C in a solution of hexane and toluene. Addition of **108** to dichlorotris(triphenylphosphine)ruthenium, in the initial step of a two-step one-pot process, gave the corresponding ruthenium benzylidene. In the same reaction vessel, phosphine exchange was accomplished by addition of tricyclohexylphosphine to provide analytically pure Grubbs' benzylidene **3** as a purple solid in a yield of 41% over two steps, after successive washing of the precatalyst with nitrogen sparged methanol. The lower yield of **3** obtained here, compared to yields reported in the literature (ca. 60-99%),[11,88] was attributed to excessive washing of the solids with methanol.

Scheme 4. Synthesis of Grubbs' Benzylidene **3**[a]

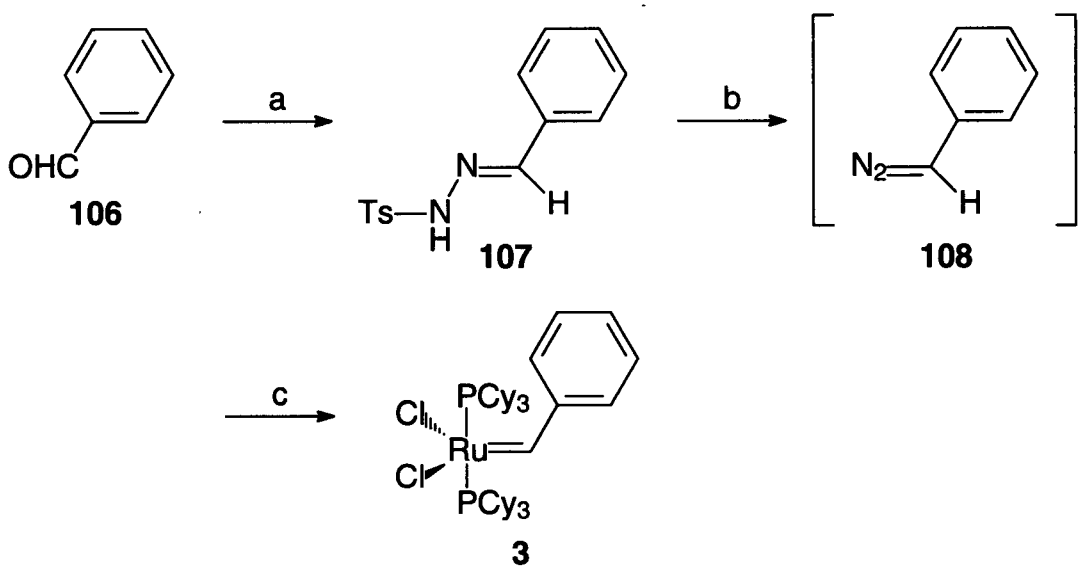

[a]Key: (a) $TsNHNH_2$, MeOH, 50 °C, 45%; (b) 3.8 M NaOH, $BnEt_3N^+Cl^-$, hexane, toluene, 70 °C; (c) $RuCl_2(PPh_3)_3$, CH_2Cl_2, -42 °C; then PCy_3, CH_2Cl_2, -15 °C, (41% for 2 steps).

2.4 Initial Studies and Method Development Towards Forming a Macrocyclic Amine and Macrocyclic Lactams via RCM Using Grubbs' Benzylidene 3

Prior to our studies of unsaturated 14-membered lactam formation via RCM, discussed later in this chapter, the possibility of forming unsaturated macrocyclic amines via RCM from the corresponding diene-amines was considered. At this time, little was known of the effect of a tertiary amine nitrogen atom on Grubbs' benzylidene **3**. However, in certain cases unproductive metallacyclobutane complexes were isolated. For example, Schrock and co-workers isolated metallacyclobutane complexes by reaction of neopentylidene complexes of the type M(CH-*t*-Bu)-(*N*-2,6-C_6H_3-*i*-Pr_2)($OC(CH_3)_2CF_3)_2$, where M = Mo or W, with methyl acrylate or *N,N*-dimethylacrylamide (Figure 27).[89] The formation of such complexes was expected to complicate the formation of the unsaturated lactams due to the carbonyl present in the diene-amide substrates. However, using tertiary amine substrates and Grubbs' benzylidene **3** such problematic reactivity was not anticipated due to the absence of a carbonyl in these substrates.

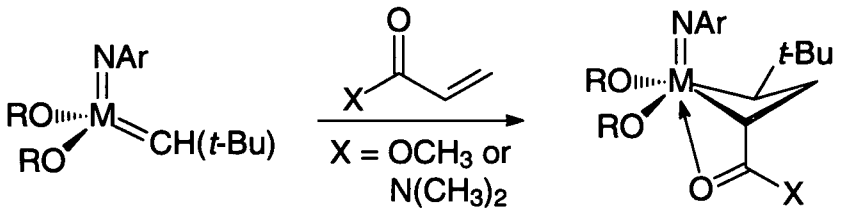

R = $C(CH_3)_2CF_3$, M = Mo or W, Ar = 2,6-C_6H_3-*i*-Pr_2

Figure 27. Metallacyclobutane complex formation (from reference 89).

2.4.1 Attempted RCM of *N*-Benzyl-*N*-(3-butenyl)-10-undecenylamine (111)

N-Benzyl protected diene-amine **111** was chosen as the first candidate for RCM based on the availability of the precursors in our laboratory. The synthesis of this compound began with the coupling of benzylamine and the commercially available acid **102** using DCC to afford amide **109** in 65% yield (Scheme 5). Reduction of amide **109** with LAH gave amine **110** in 90% yield. Diene-amine **111**, the requisite RCM precursor, was formed in 49% yield by alkylation of amine **110** with 4-bromobutene using potassium carbonate as base. Unfortunately, cyclization of diene-amine **111** using Grubbs' benzylidene **3** failed, and 77% of **111** was recovered.

Scheme 5. Attempted RCM of *N*-Benzyl-*N*-(3-butenyl)-10-undecenylamine (**111**)[a]

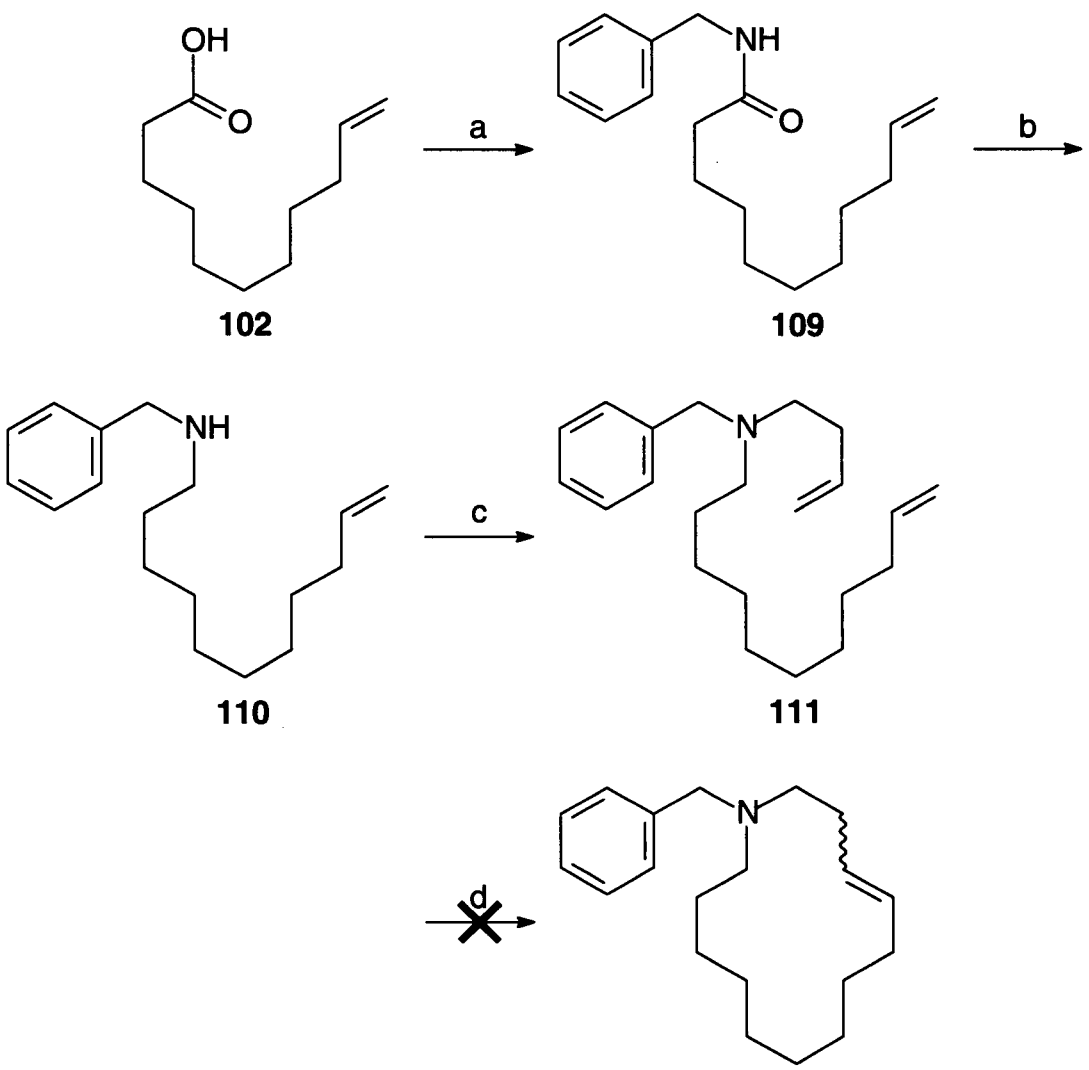

[a]Key: (a) $BnNH_2$, DCC, CH_2Cl_2, rt, 65%; (b) LAH, THF, 70 °C, 90%;
(c) $BrCH_2CH_2CH{=}CH_2$, K_2CO_3, acetonitrile, rt, 49%;
(d) 5 mol% **3**, CH_2Cl_2, 40 °C, 0%.

At this point the studies of diene-amine RCM were dispensed with to pursue the formation of unsaturated 14-membered lactams via diene-amide RCM. This decision may seem rather premature, however shortly after this work was attempted a number of reports appeared in the literature that illustrated how ruthenium benzylidene **3** was neither tolerant towards nor reactive in the presence of an amine. Complimentary to earlier studies of cyclic amine formation by RCM,[2a,21] more recent studies illustrated how secondary and tertiary amines can poison the activity of ruthenium based

metathesis catalysts.[35,90] In fact, it has become common practice to add triethylamine to a RCM reaction to deactivate any remaining active ruthenium catalyst.[27] In contrast, these studies illustrated the tolerance of molybdenum based metathesis catalysts towards amines.[2a,21,35] For ruthenium based metathesis catalysts this undesired reactivity towards amine substrates was avoided by the addition of electron withdrawing protecting groups to the nitrogen atom,[90] or by formation of the ammonium salt.[45,91] In retrospect, it is not surprising that ruthenium benzylidene **3** was not reactive towards diene-amine **111**.

Despite the failure of diene-amine **111** to undergo RCM, a significant quantity of amide **109**, used in the synthesis of **111**, remained. This and similar amides, of varying carbon chain length, appeared to be ideal compounds that would allow entry into the diene-amide structure required for the RCM studies of lactam formation. Accordingly, alkylation of a series of *N*-benzyl-ω-alkenamides with the appropriate ω-haloalkenes, followed by reductive cleavage of the benzyl group could provide the requisite diene-amides. Unfortunately, attempts to alkylate amide **109** under a variety of conditions[85,92-96] failed (Table 2). This failure was attributed to elimination of the alkenyl halide, which was facilitated by the base or the conjugate base of the amide.

Table 2. Attempted Alkylation of *N*-Benzyl-10-undecenamide (**109**) with 4-Bromobutene

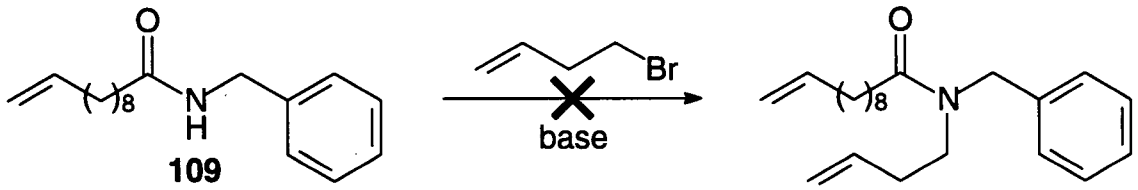

Entry	Reaction Conditions	Yield (%)[a]	Ref.[b]
1	1.5 eq. or 2.2 eq. *n*-BuLi, THF, -78 °C to rt	0	85
2	*t*-BuO^-K^+, THF, rt	0	92
3	NaH, THF, 0 °C to rt	0	93
4	KOH, DMSO, rt	0	94
5	NaOH, K_2CO_3, $Bu_4N^+HSO_4^-$, benzene, 60 °C	0	95
6	P4-phosphazene base, THF, -78 °C	0	96

[a] In all cases amide **109** was quantitatively recovered.
[b] Reference from which the reaction conditions were obtained.

After this series of disappointing results our efforts were directed towards studying the RCM of a series of diene-amides (**68-76**). The preliminary results of unsaturated 14-membered lactam formation via RCM and the development of an optimized RCM method are discussed in the following section.

2.4.2 Initial RCM Studies and Method Development

The preliminary studies of unsaturated 14-membered lactam formation by RCM began with diene-amide **76** as the first candidate in this systematic study. Two synthetic routes to diene-amide **76**, both involving the use of iodoalkene **113**, were considered and are discussed below. Iodoalkene **113** was formed from acid **102** in near quantitative yield over two steps (Scheme 6). This process involved reduction of acid **102** with LAH, followed by conversion of the resulting alcohol **112**[97] to iodide **113** with iodine, imidazole, and triphenylphosphine.

Scheme 6. Synthesis of 11-Iodoundecene (**113**)[a]

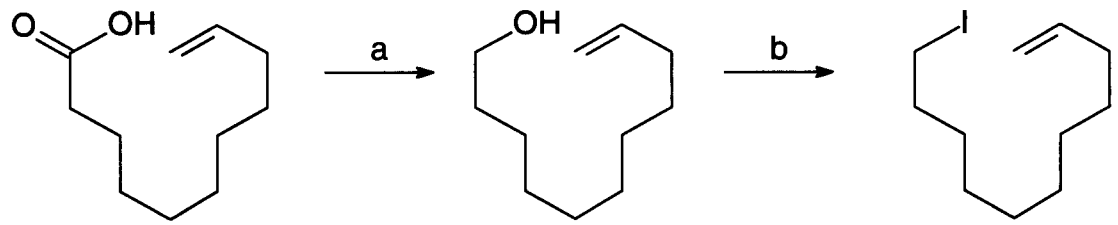

102 **112** **113**

[a]Key: (a) LAH, THF, -78 °C to rt, 99%; (b) I_2, imidazole, PPh_3, CH_2Cl_2, 0 °C to rt, 99%.

The formation of *N*-(10-undecenyl)-3-butenamide (**76**) began with the conversion of vinylacetic acid (**114**) to primary amide **115** (Scheme 7). This was accomplished by formation of the acid chloride of **114**, using oxalyl chloride, followed by amidation with ammonia. The resulting primary amide **115** was alkylated with iodoalkene **113** using NaOH, K_2CO_3, and tetrabutylammonium hydrogen sulfate to give diene-amide **76** in 25% yield. This reaction was not explored any further. The poor yield was mainly due to the predominant formation of dialkylated amide.

Scheme 7. Synthesis of *N*-(10-Undecenyl)-3-butenamide (**76**)[a]

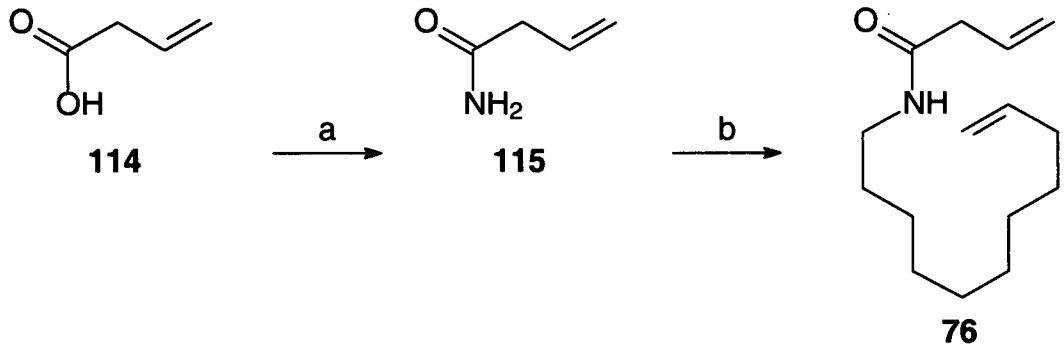

[a]Key: (a) $(ClOC)_2$, DMF, CH_2Cl_2, 0 °C to rt; then $NH_3(g)$, 0 °C to rt, 47%; (b) iodide **113**, NaOH, K_2CO_3, tetrabutylammonium hydrogen sulfate, toluene, 120 °C, 25%.

Due to the poor yield of the previous route to diene-amide **76**, an alternate route was explored. The commercially available alcohol **103** was converted to iodide **116** in 96% yield by treatment with iodine, triphenylphosphine, and imidazole (Scheme 8). Reaction of the resulting iodide **116** with potassium cyanide gave nitrile **117** in 93% yield. Nitrile **117** was quantitatively reduced with LAH. The resulting amine **118** was coupled with vinylacetic acid (**114**) using DCC to afford diene-amide **76** in 33% yield. Although the yield resulting from both synthetic routes was disappointing, enough material was obtained to conduct RCM studies of diene-amide **76**.

Scheme 8. Alternate Synthesis of *N*-(10-Undecenyl)-3-butenamide (**76**)[a]

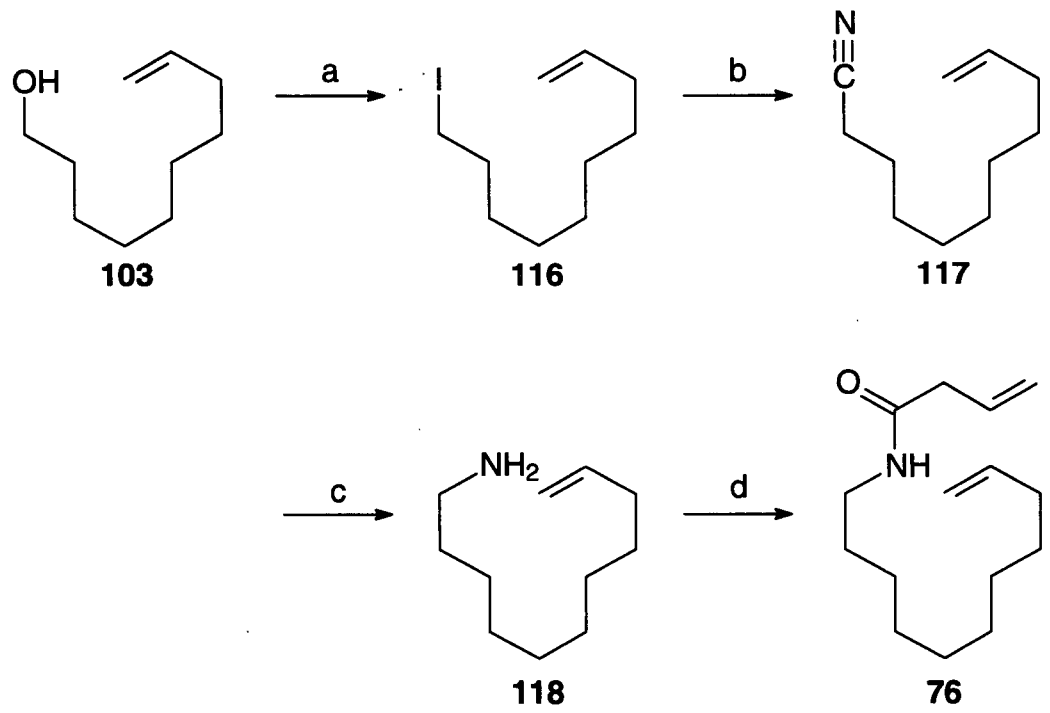

[a]Key: (a) I_2, imidazole, PPh_3, CH_2Cl_2, 0 °C to rt, 96%; (b) KCN, acetonitrile, 90 °C, 93%; (c) LAH, THF, 70 °C, quant.; (d) vinylacetic acid, DCC, CH_2Cl_2, 0 °C to rt, 33%;

With diene-amide **76** in hand, preliminary studies into the cyclization of this compound via RCM using Grubbs' benzylidene **3** were conducted. Recall the precedence of unproductive metallacyclobutane complexes formed by the reaction of metal alkylidene complexes with *N,N*-dimethylacrylamide (see Figure 27).[89] Diene-amide **76** was expected to exhibit similar reactivity towards precatalyst **3** due to the close proximity between the terminal double bond of the carboxyl chain and the amide carbonyl, a bond separation similar to that found in *N,N*-dimethylacrylamide. In terms of the applied method, separate solutions of **76** and **3**, both in nitrogen sparged dichloromethane, were slowly combined under high dilution conditions using a syringe pump. Unfortunately, none of the desired macrocyclic lactam was obtained using two different amounts of precatalyst (Table 3). However, there appeared to be a correlation between the amount of precatalyst used and the amount of recovered diene-amide **76**. This negative result suggested that the mass balance might be found in a catalyst complex such as the one shown in Figure 27.

Table 3. Attempted RCM of *N*-(10-Undecenyl)-3-butenamide (**76**)

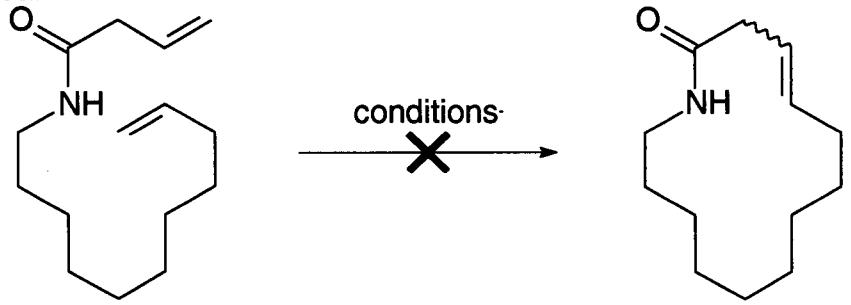

76 (*E*)-**91** / (*Z*)-**92**

Entry	Reaction Conditions	Yield (%)[a]
1	5 mol% **3**, 4.3 mM CH_2Cl_2, rt	0 (93)
2	20 mol% **3**, 5.0 mM CH_2Cl_2, rt	0 (71)

[a] Recovered diene-amide **76** after chromatography in parenthesis.

In order to minimize this proximity effect between the terminal double bond and amide group to the fullest extent, and hopeful to obtain a macrocyclic lactam by RCM, the metathesis precursor *N*-(6-heptenyl)-7-octenamide (**72**) was synthesized. The synthetic strategy chosen for the formation of this compound involved the preparation and coupling of the requisite amine and carboxylic acid, as shown below. The synthesis of diene-amide **72** began with the preparation of amine **94** (Scheme 9). Conversion of alcohol **101** with iodine, using conditions described earlier, and subsequent displacement of the resulting iodide **97** with potassium cyanide gave nitrile **96** in 90% overall yield over these two steps. Reduction of **96** with LAH gave the desired amine **94** in 88% yield.

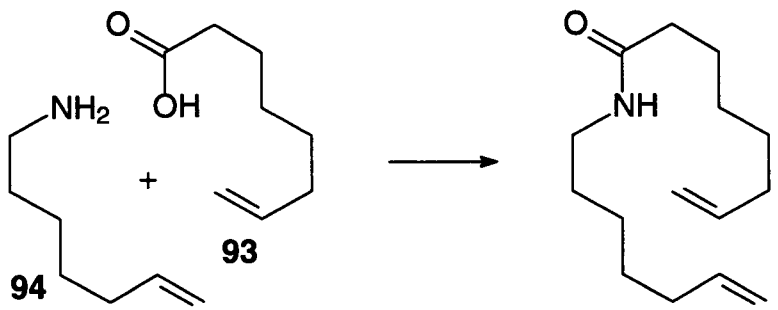

94 **93** **72**

Scheme 9. Synthesis of 6-Heptenylamine (**94**)[a]

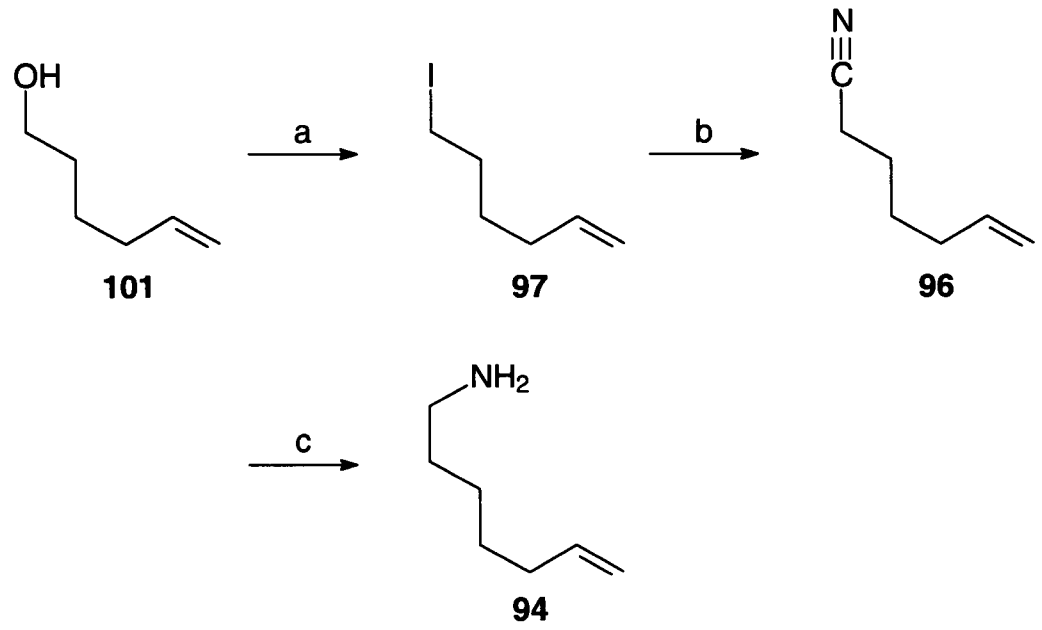

[a]Key: (a) I_2, imidazole, PPh_3, CH_2Cl_2, 0 °C to rt, 96%; (b) KCN, acetonitrile, 90 °C, 94%; (c) LAH, THF, 70 °C, 88%.

The synthesis of the requisite carboxylic acid **93** was accomplished using two different methods to assess their viability, both of which started from iodoalkene **97**. The first method involved alkylation of dimethyl malonate with **97** using sodium hydride (Scheme 10). Dihydrolysis of the resulting alkenylmalonate **119** in aqueous base, followed by treatment with aqueous acid and subsequent decarboxylation of the dicarboxylic acid gave acid **93** in 81% overall yield. An alternate synthesis of acid **93** began with a two-carbon addition to iodide **97** using lithioacetonitrile, which in turn was prepared by addition of *n*-butyllithium to acetonitrile at -78 °C in THF. Hydrolysis of the resulting nitrile **95** with potassium hydroxide in refluxing ethylene glycol gave acid **93** in 79% overall yield for two steps. In comparison, no advantage was offered by either method, and both gave acid **93** in comparable yield. The coupling of amine **94** with acid **93** was accomplished according to the method of Mukaiyama and co-workers,[98] using 2-bromo-1-methylpyridinium fluorosulphonate and triethylamine to give diene-amide **72** in 79% yield. In contrast, the coupling of amine **94** with acid **93** in the same manner using 2-chloro-1-methylpyridinium iodide as the coupling reagent gave diene-amide **72** in 44% yield.

Scheme 10. Synthesis of *N*-(6-Heptenyl)-7-octenamide (**72**)[a]

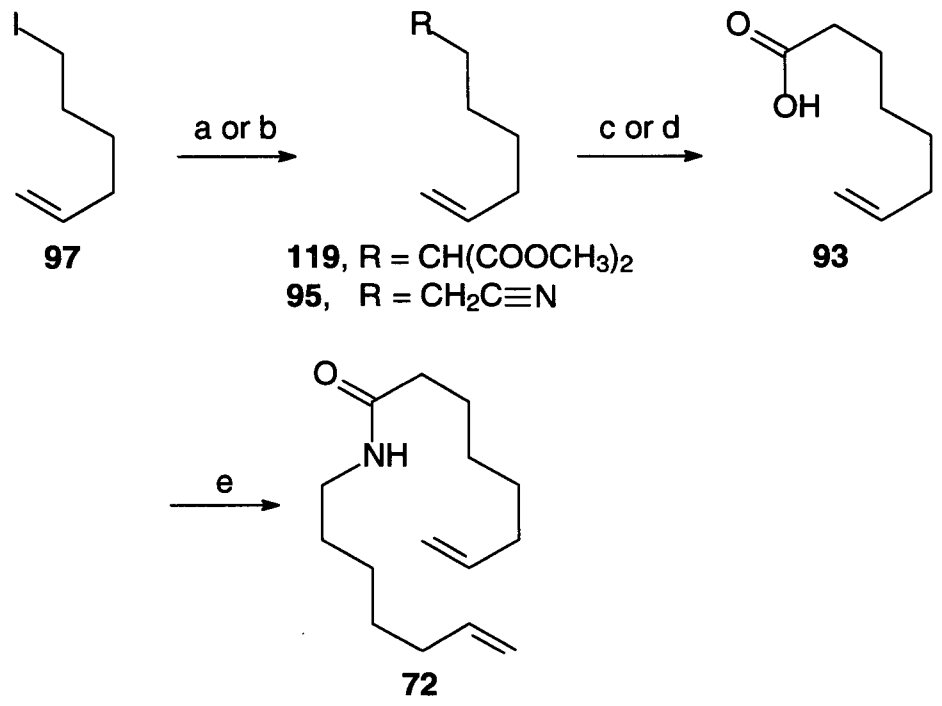

[a]Key: (a) NaH, $CH_2(COOCH_3)_2$, THF, DMF, 60 °C, 85% (**119**); (b) $LiCH_2CN$, THF, -78 °C to rt, 90% (**95**); (c) NaOH, H_2O, 90 °C; then conc. HCl; then neat, 100 °C, 95% from **119**; (d) KOH, $(HOCH_2)_2$, 150 °C, 88% from **95**; (e) amine **94**, TEA, 2-bromo-1-methylpyridinium fluorosulphonate, CH_2Cl_2, 40 °C, 79%.

In comparison to the other members of the series of diene-amides proposed for this study, the terminal double bonds of **72** were the farthest removed from either end of the amide group. Consequently, the problematic reactivity associated with diene-amide **76** was not expected. To our delight, the combination of separate solutions of **72** and **3**, both in dichloromethane, over twelve hours under high dilution conditions using a syringe pump, followed by an additional portion of **3** over another twelve hour period gave (*E*)-lactam **84** in 98% yield (Table 4, Entry 1). However, the product contained an undetermined quantity of cyclic dimer, which was inseparable from **84** by chromatography. The cyclic dimer was not observed in the ^1H and ^{13}C NMR spectra of the product mixture due to coincident chemical shift values. However, it was identified by a peak at 419 *m/z* in the mass spectrum obtained in positive-ion DCI mode. The intensity of this peak was 69% relative to the molecular ion of **84**, the base peak in the spectrum.

Table 4. Synthesis of (*E*)-2-Azacyclotetradec-8-enone (**84**) via RCM of *N*-(6-Heptenyl)-7-octenamide (**72**)

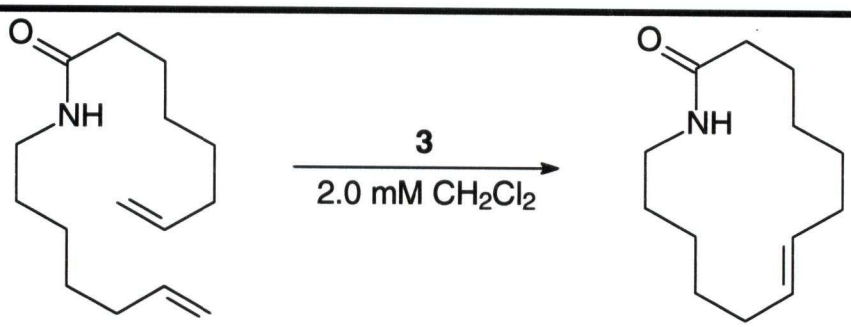

72 **84**

Entry	mol% **3**	T (°C)	Addition time (h)	Total time (h)	Yield (%)[a]
1	20	40	12 (X2)	43	98[b]
2	5	40	12 (X2)	47	97[b]
3	5	40	12	14	>99[b]
4	5	22	12	13	99[b]
5	5	22	3	4	94[b]
6	5	22	0	1	87 (12)
7	5	22	3	19	21 (79)[c]

[a] Isolated yield after chromatography, and recovered diene-amide **72** in parenthesis.
[b] Product contained an unknown amount of cyclic dimer.
[c] Reaction conducted under an ethylene atmosphere.

Although the formation of dimeric products was not desired, the excellent yield associated with the RCM of diene-amide **72** prompted further studies directed towards optimization of the reaction conditions. In terms of optimization, the variables of interest were the reduction of catalyst loading, reaction temperature, addition time, and total reaction time. Although a decrease in the amount of solvent required would add to the preparative appeal of this macrocyclization method, an increase of the substrate concentration seemed inappropriate due to the formation of cyclic dimeric products at the present concentration. An increase in concentration would increase the probability of intermolecular reactions that led to the formation of such dimeric products.

The scope of the RCM of diene-amide **72** was explored by conducting a series of experiments directed towards adjusting the variables discussed above, and the results are summarized in Table 4. These experiments were conducted in a manner similar to

the one discussed earlier (Entry 1). In addition, each reaction mixture was constantly sparged with nitrogen to prevent contamination by oxygen, which would promote the decomposition of the catalyst, and also to promote the evaporative loss of ethylene in an attempt to drive the reaction to completion. In all cases the cyclic monomer was formed exclusively as (*E*)-lactam **84**. Entries 2-5 clearly illustrate how a reduction of the catalyst loading, reaction temperature, addition time, and total reaction time did not significantly affect the yield of the RCM reaction. However, the cyclic dimer was still formed under these conditions. This was remedied by direct addition of a solution of Grubbs' benzylidene **3** to a solution of diene-amide **72**, both in dichloromethane, followed by quenching of the active catalytic species with triethylamine after one hour (Entry 6). In this case lactam **84** was obtained in 87% yield, and the recovery of **72** in 12% yield constituted the remainder of the mass balance.

An alternate method aimed at preventing the formation of cyclic dimeric products was explored. Hoveyda and co-workers encountered problematic acyclic dimer formation during studies of chromene formation by ruthenium-catalyzed rearrangement of styrenyl ethers.[99] Chromene **121** was formed by a ring-opening/ring-closing rearrangement of styrenyl ether **120** using ruthenium alkylidene **2** (Figure 28). Hoveyda and co-workers proposed that the terminal double bond contained in the product might undergo reaction with the corresponding ruthenium alkylidene to form acyclic dimer **122**. The amount of dimer, relative to monomer, was moderately reduced by conducting the reaction at half the concentration. However, when the reaction was conducted under an ethylene atmosphere, at the original concentration, the amount of acyclic dimer was significantly reduced. Applying a similar approach, the product obtained from the RCM reaction of diene-amide **72**, conducted under an ethylene atmosphere, did not contain any dimeric compounds. However, under these conditions lactam **84** was obtained in only 21% yield (Table 4, Entry 7). The recovery of **72** in 79% yield constituted the remainder of the mass balance. The introduction of ethylene apparently prevented the formation of dimeric products and acted to shift the equilibrium in favour of the starting diene-amide. This result validated the notion that the evaporative loss of ethylene, facilitated by a constant sparge of the reaction mixture with nitrogen, would drive the reaction towards completion. However, this did not constitute a practical method to prevent the formation of dimeric products due to the considerable reduction in yield of lactam **84**.

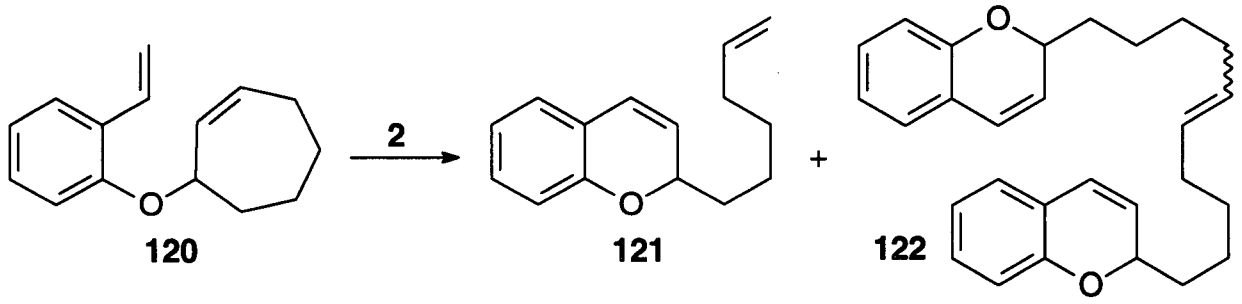

[2], M	C_2H_4	Yield (**121**;**122**, %)
0.1	-	45;56
0.05	-	50;29
0.1	1 atm	92;<2

Figure 28. Effects of concentration and ethylene atmosphere on chromene and acyclic chromene dimer formation by RCM (from reference 99).

The study presented in Table 4 led to a better understanding of the RCM of diene-amide **72**. The formation of cyclic dimeric products was dependent on the total reaction time. Dimerization might have occurred either directly from the newly formed substrate alkylidene or via ring opening of lactam **84**. In either case, the results suggested that the rate of dimerization was lower than the rate of monomer cyclization. It is interesting to note that the product yield was not adversely affected by most changes to the reaction conditions, and the diastereoselectivity remained unchanged throughout the series of experiments. This study clearly illustrated that this diene-amide could undergo RCM within one hour to form unsaturated lactam **84** in high yield. Since this reaction was considered enthalpically disfavoured due to the strain associated with ring formation, entropy, the formation of two molecules from one, and the evaporative loss of ethylene must be the driving force.

The optimization study conducted for the RCM of *N*-(6-heptenyl)-7-octenamide (**72**) led to reaction conditions that allowed the formation of lactam **84** in high yield at room temperature, within one hour, and at low precatalyst loading. Recall that the main goal of this work was to conduct a systematic study of the formation of a series of unsaturated 14-membered lactams, exploring nine logical sites for ring-closure, by RCM of the corresponding series of diene-amides (**68**-**76**). To allow reasonable comparisons within the series, it seemed appropriate to conduct this study using the same reaction conditions for each diene-amide. A number of the diene-amides were expected to

undergo RCM at a lower relative rate due to the competitive formation of unproductive catalyst complexes. Accordingly, the conditions from Entry 5 (Table 4) were applied to this study, with time and site of ring closure being the only variables. The syntheses of the remaining diene-amides required for the systematic study are discussed in the following section.

2.5 Synthesis of Constitutionally Isomeric Diene-amides

In addition to the two diene-amides **76** and **72**, whose preparations were described earlier, seven others were synthesized to comprise a series of nine diene-amides (**68-76**) in total. These compounds were prepared in order to study the effects of the ring-closing position on the RCM construction of unsaturated 14-membered lactams. These nine positions are represented as bonds 4 through 12 in the structure of 2-azacyclotetradecanone, shown below. The remaining five bond positions in this structure were not considered for this study since; three were not accessible via conventional RCM (positions 1, 2, and 14), one would involve the unlikely RCM of an acylated enamine (position 3), and the proximity of the remaining position, 13, was expected to disfavour RCM due to the competitive formation of internal catalyst complexes. For these reasons, the most logical sites for ring-closure were explored by conducting RCM reactions with diene-amides **68-76**.

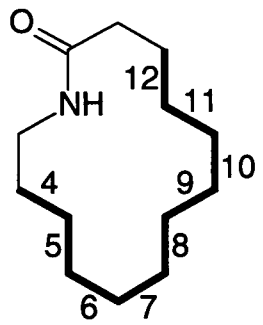

The construction of the remaining diene-amides followed the strategies outlined in the synthetic plan, and involved chemistry similar to that applied in the syntheses of **76** and **72**. The following sections discuss the synthesis of each, beginning with diene-amide **68**, the requisite RCM substrate predisposed to ring-closure at position 4.

2.5.1 Synthesis of *N*-(2-Propenyl)-11-dodecenamide (68)

The first step in the synthesis of *N*-(2-propenyl)-11-dodecenamide (**68**) involved alkylation of dimethyl malonate with iodide **116**, using sodium hydride as base, to give alkenylmalonate **123** in 93% yield (Scheme 11). Recall iodide **116** was obtained from the corresponding alcohol **103** during the synthesis of diene-amide **76** (see Section 2.4.2, Scheme 8). Hydrolysis of alkenylmalonate **123** in aqueous base, followed by treatment with aqueous acid and subsequent decarboxylation of the dicarboxylic acid gave acid **124**[100] in 93% overall yield. Coupling of allylamine with acid **124** using DCC gave diene-amide **68** in 34% yield. Similar yields were observed when this reaction was repeated using the same reagents and conditions. However, enough material was obtained for the RCM studies.

Scheme 11. Synthesis of *N*-(2-Propenyl)-11-dodecenamide (**68**)[a]

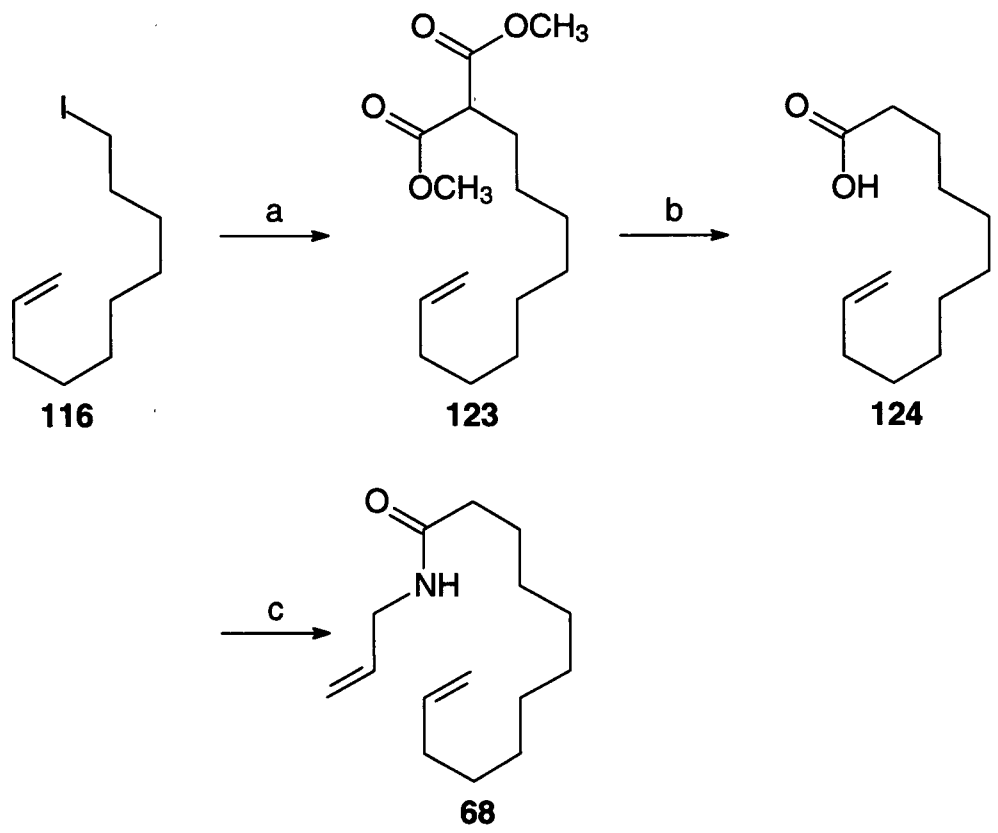

116 **123** **124** **68**

[a]Key: (a) NaH, $CH_2(COOCH_3)_2$, THF, DMF, 60 °C, 93%; (b) NaOH, H_2O, 90 °C; then conc. HCl; neat, 140 °C, 93%; (c) allylamine, DCC, CH_2Cl_2, 0 °C to rt, 34%.

2.5.2 Synthesis of *N*-(3-Butenyl)-10-undecenamide (69)

The alkenylamine required for the synthesis of *N*-(3-butenyl)-10-undecenamide (**69**) was derived from 4-bromobutene via a Gabriel type protocol applied by Marks and co-workers.[101] Substitution of 4-bromobutene with potassium phthalimide, followed by hydrolysis of the resulting alkenylphthalimide by sequential addition of hydrazine monohydrate and concentrated HCl, then treatment of the crude amine in dry diethyl ether with HCl gas gave crude 3-butenylammonium chloride. The crude 3-butenylammonium chloride was coupled with acid **102** using 2-bromo-1-methylpyridinium fluorosulphonate and triethylamine to give diene-amide **69** in 36% yield (Scheme 12). Although the yield obtained from this reaction was disappointing, enough material was obtained for the RCM studies.

Scheme 12. Synthesis of *N*-(3-Butenyl)-10-undecenamide (**69**)[a]

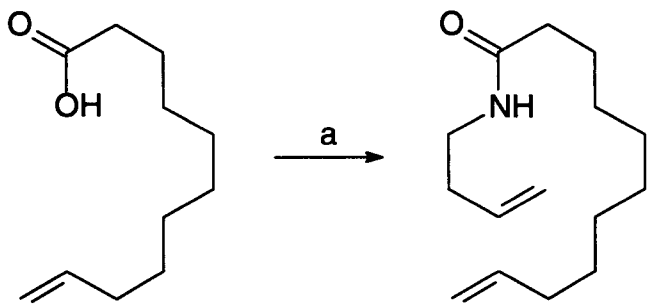

102 **69**

[a]Key: (a) 3-butenylammonium chloride, TEA, 2-bromo-1-methylpyridinium fluorosulphonate, CH_2Cl_2, 40 °C, 36%.

2.5.3 Synthesis of *N*-(4-Pentenyl)-9-decenamide (70)

The synthesis of *N*-(4-pentenyl)-9-decenamide (**70**) began with the oxidation of 9-decen-1-ol (**103**) using Jones' reagent to give acid **125**[102] in 97% yield (Scheme 13). Conversion of **125** to the acid chloride, using oxalyl chloride, followed by amidation with ammonia gave primary amide **126** in 95% yield. Amide **126** was alkylated with 5-bromopentene using NaOH, K_2CO_3, and tetrabutylammonium hydrogen sulfate to give diene-amide **70** in 71% yield. In comparison to the analogous alkylation of primary amide **115** (see Scheme 7), this alkylation was not complicated by the formation of a

dialkylamide. However, this was the only case in which alkylation of a primary amide provided the desired diene-amide in an acceptable yield.

Scheme 13. Synthesis of *N*-(4-Pentenyl)-9-decenamide (**70**)[a]

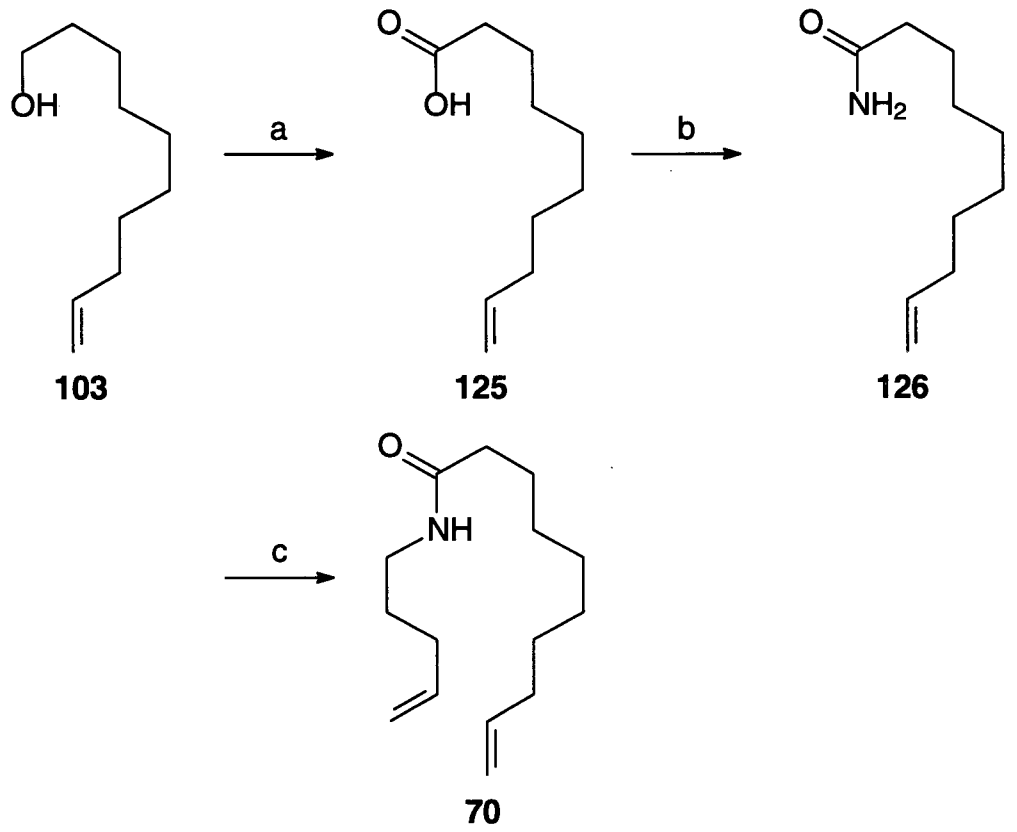

[a]Key: (a) Jones' reagent, acetone, rt, 97%; (b) $(ClOC)_2$, DMF, CH_2Cl_2, 0 °C to rt; then $NH_3(g)$, 0 °C to rt, 95%; (c) 5-bromopentene, NaOH, K_2CO_3, tetrabutylammonium hydrogen sulfate, toluene, 120 °C, 71%.

2.5.4 Synthesis of *N*-(5-Hexenyl)-8-nonenamide (71)

Following a number of steps that were described earlier, quantitative substitution of 8-bromooctene (**127**) with potassium cyanide, followed by hydrolysis of the resulting nitrile **128** with potassium hydroxide in refluxing ethylene glycol gave acid **129** in 96% yield (Scheme 14). Quantitative conversion of acid **129** into primary amide **130**, followed by alkylation with 6-bromohexene, conducting both steps as described earlier, gave diene-amide **71** in 27% yield. Similar to analogous alkylations, the poor yield was

due to the predominant formation of the dialkylamide. However, enough material was obtained for the RCM studies.

Scheme 14. Synthesis of *N*-(5-Hexenyl)-8-nonenamide (**71**)[a]

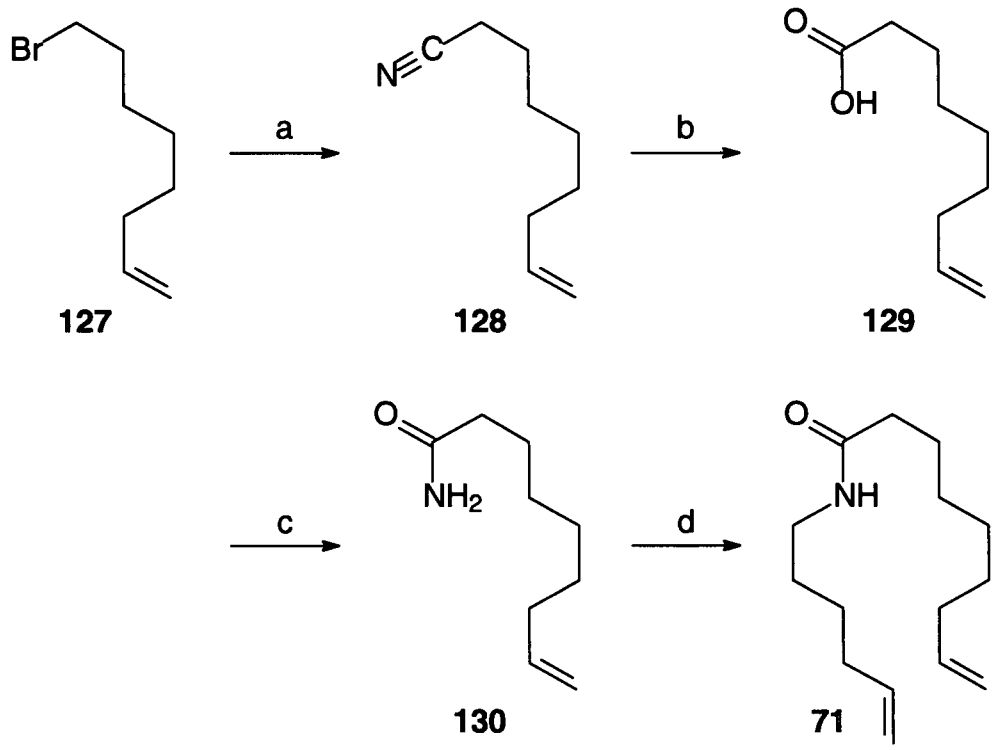

[a]Key: (a) KCN, 18-C-6, acetonitrile, 90 °C, quant.; (b) KOH, $(HOCH_2)_2$, 170 °C, 96%; (c) $(ClOC)_2$, DMF, CH_2Cl_2, 0 °C to rt; then $NH_3(g)$, 0 °C to rt, quant.; (d) 6-bromohexene, NaOH, K_2CO_3, tetrabutylammonium hydrogen sulfate, toluene, 120 °C, 27%.

2.5.5 Synthesis of *N*-(7-Octenyl)-6-heptenamide (73)

The synthesis of *N*-(7-octenyl)-6-heptenamide (**73**) began with the hydrolysis of nitrile **96** to give acid **131** in 93% yield (Scheme 15). The synthesis of nitrile **96** was illustrated earlier (see Scheme 9). Conversion of acid **131** to diene-amide **73**, via primary amide **132**, was accomplished in two steps as described earlier, in 39% overall yield. In contrast, the reduction of nitrile **95** using LAH, followed by coupling of the resulting amine **133** with acid **131** using 2-chloro-1-methylpyridinium iodide and triethylamine gave diene-amide **73** in 26% overall yield for the two steps.

Scheme 15. Synthesis of *N*-(7-Octenyl)-6-heptenamide (**73**)[a]

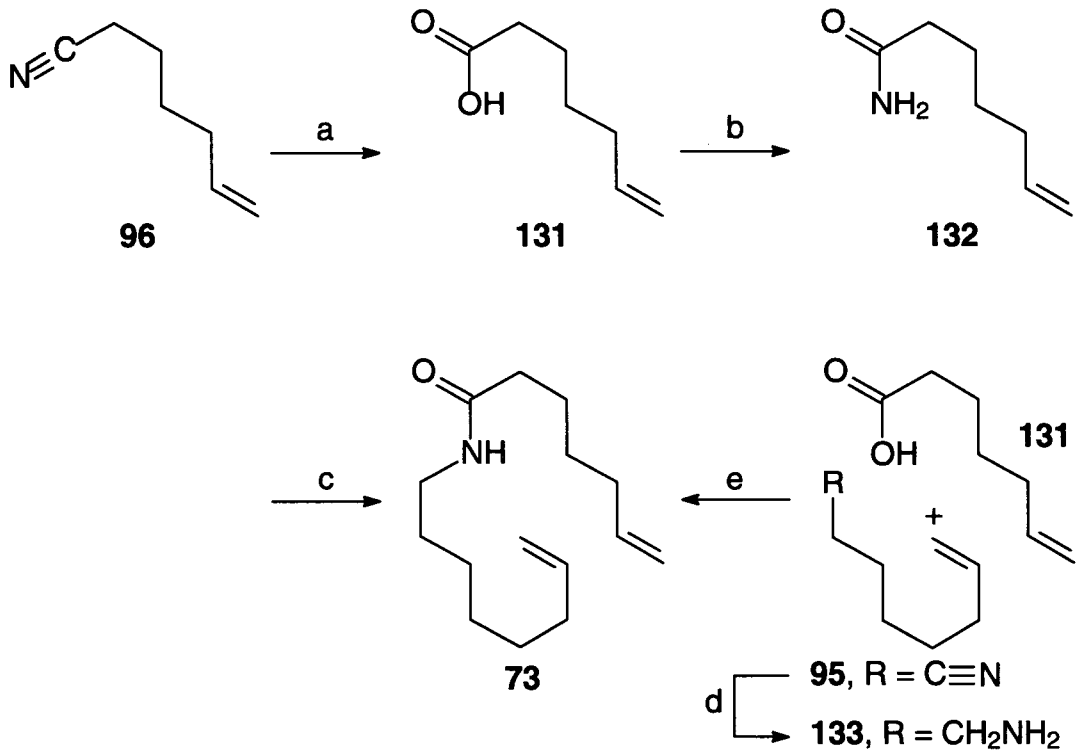

[a]Key: (a) KOH, $(HOCH_2)_2$, 150 °C, 93%; (b) $(ClOC)_2$, DMF, CH_2Cl_2, 0 °C to rt; then NH_3(g), 0 °C to rt, 86%; (c) 8-bromooctene, NaOH, K_2CO_3, tetrabutylammonium hydrogen sulfate, toluene, 120 °C, 45%; (d) LAH, THF, 0 °C to rt, 85%; (e) TEA, 2-chloro-1-methylpyridinium iodide, CH_2Cl_2, 40 °C, 30%.

2.5.6 Synthesis of *N*-(8-Nonenyl)-5-hexenamide (74)

During the course of the diene-amide syntheses, a number of the requisite subunits could be applied to more than just one target. For instance, amine **134**, a requisite subunit for the synthesis of *N*-(8-nonenyl)-5-hexenamide (**74**), was obtained by reduction of the corresponding primary amide **130** with LAH in 84% yield (Scheme 16). Recall amide **130** was constructed during the synthesis of diene-amide **71** (see Scheme 14).

Scheme 16. Synthesis of 9-Heptenylamine (**134**)[a]

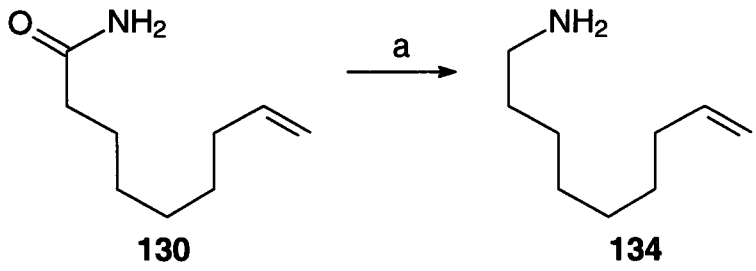

130 **134**

[a]Key: (a) LAH, THF, 70 °C, 84%.

The second subunit required for the synthesis of diene-amide **74** is acid **135**. Oxidation of commercially available 6-hexen-1-ol (**101**) with Jones' reagent gave acid **135**[100] in 98% yield (Scheme 17). Coupling of amine **134** with acid **135** according to the method of Mukaiyama and co-workers[98] gave diene-amide **74** in 75% yield.

Scheme 17. Synthesis of *N*-(8-Nonenyl)-5-hexenamide (**74**)[a]

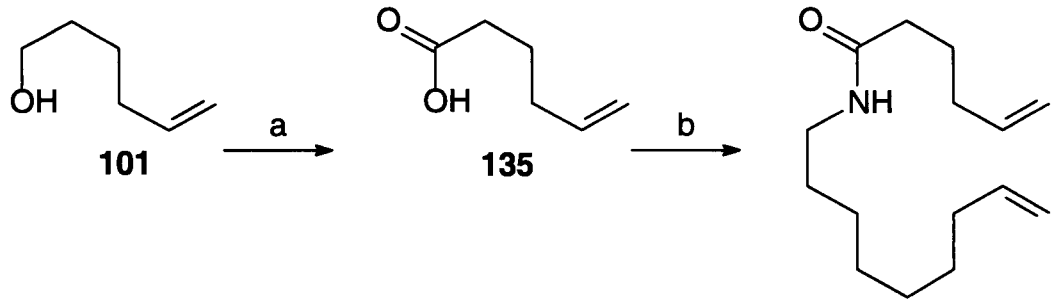

101 **135** **74**

[a]Key: (a) Jones' reagent, acetone, rt, 98%; (b) amine **134**, TEA, 2-chloro-1-methyl-pyridinium iodide, CH_2Cl_2, 40 °C, 75%.

2.5.7 Synthesis of *N*-(9-Decenyl)-4-pentenamide (75)

The last in the series of diene-amides synthesized for the RCM studies was constructed using two different strategies, the first of which involved primary amide alkylation. Conversion of commercially available 4-pentenoic acid (**136**) into primary amide **137** was accomplished using methods described earlier and in 80% yield (Scheme 18). Similar to previously described amide alkylations, **137** was alkylated with

iodoalkene **116** to give diene-amide **75** in 28% yield. Due to the poor yield of this alkylation step, an alternate route to the target compound was explored.

Scheme 18. Preliminary Synthesis of *N*-(9-Decenyl)-4-pentenamide (**75**)[a]

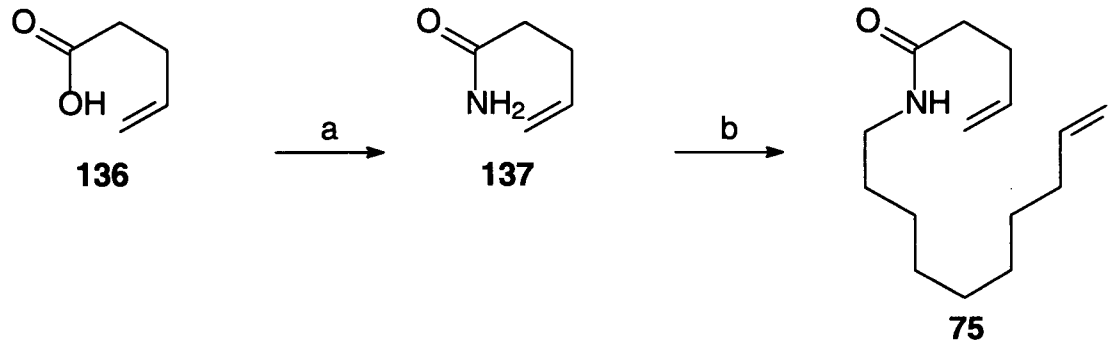

[a]Key: (a) $(ClOC)_2$, DMF, CH_2Cl_2, 0 °C to rt; then $NH_3(g)$, 0 °C to rt, 80%; (b) iodide **116**, NaOH, K_2CO_3, tetrabutylammonium hydrogen sulfate, toluene, 120 °C, 28%.

The alternate synthesis of diene-amide **75** involved coupling of the corresponding amine and carboxylic acid. Accordingly, primary amide **126**, used previously for the synthesis of diene-amide **70** (see Scheme 13), was reduced with LAH to give amine **138** in 88% yield (Scheme 19). Coupling of amine **138** with 4-pentenoic acid (**136**) using DCC gave diene-amide **75** in 74% yield. This was a considerable improvement in yield over the previous route.

Scheme 19. Synthesis of *N*-(9-Decenyl)-4-pentenamide (**75**)[a]

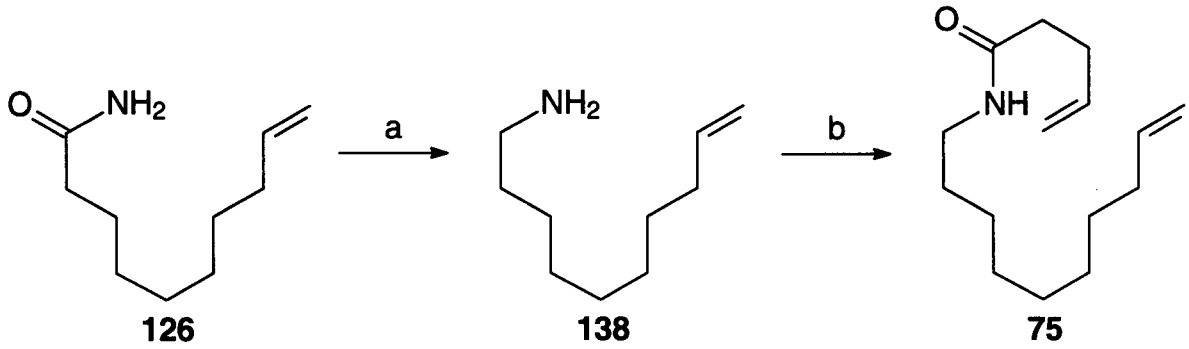

[a]Key: (a) LAH, THF, 70 °C, 88%; (b) 4-pentenoic acid, DCC, CH_2Cl_2, 0 °C to rt, 74%.

2.5.8 Summary

Regarding the syntheses of the nine diene-amides required for the proposed RCM studies, insight into the spectroscopic properties of and general synthetic strategies towards these compounds was gained. A general analysis of the spectral data obtained for each of the diene-amides provided evidence to confirm their structures. Furthermore, the synthetic routes chosen to construct these compounds, and the methods used therein, both deserve comment. The following discussion will begin with the analysis of the spectral data.

The structures of the nine diene-amides were confirmed by inspection of the spectral data obtained for each. The constitutionally isomeric relationship between these compounds was reflected in the similarity between the spectral data, and was used to facilitate this analysis. For instance, the ^{1}H NMR spectrum of each diene-amide contained two pairs of overlapping resonances; one pair at δ 5.7-5.8, typically observed as a doublet of doublet of triplets, and the second pair at δ 4.9-5.1 corresponding to the internal and terminal vinyl protons respectively. In addition to the signals in this region, a broad singlet was observed (ca. δ 5-6) corresponding to the N-H proton. Other characteristic resonances observed in the ^{1}H NMR spectra were a quartet at δ 3.1-3.3, a triplet at δ 2.1-2.2, and two overlapped resonances at δ 1.9-2.1 corresponding to the protons on the methylene carbons adjacent to the nitrogen atom, the carbonyl, and the two vinyl groups, respectively. Diene-amides **76** and **68** were exceptions to these trends due to the proximity of a terminal double bond to the carbonyl of the former, and to the nitrogen atom of the latter. The ^{13}C NMR spectrum of each diene-amide contained fifteen signals, except in cases where signals were coincident with respect to chemical shift. Signals characteristic of the carbonyl (ca. δ 170), the tertiary (ca. δ 137) and secondary (ca. δ 115) vinyl carbons, and the carbon adjacent to the nitrogen atom (ca. δ 39) were observed. The IR spectral data contained signals at approximately 3300 and 1640 cm^{-1} corresponding to N-H and carbonyl stretching frequencies, respectively. In addition, HRMS and chemical analysis results were found to be consistent with the composition of each diene-amide.

In terms of the diene-amide syntheses, the following comments are divided into three sections: general strategies, methods for subunit construction, and secondary amide formation. Of the two main strategies applied in the syntheses of these

compounds, those being amidation and primary amide alkylation, the latter was clearly the less appealing method. With the exception of diene-amide **70**, all other attempts to alkylate a primary amide were complicated by the predominant formation of the dialkylamide. The construction of the diene-amides by coupling of a carboxylic acid and an amine was more appealing due to the range of coupling methods available and the higher yields obtained in most cases. In terms of the subunit construction, most methods provided the requisite material in high yield. The formation of alkenenitriles, by one or two carbon addition to a bromo or iodoalkene, was a particularly attractive strategy as it allowed entry to the corresponding carboxylic acid by hydrolysis, or the corresponding amine by reduction.

With the nine diene-amides **68-76** in hand the proposed RCM study was conducted, the results of which are discussed in the next section.

2.6 Systematic Study of Unsaturated 14-Membered Lactam Formation via RCM

The RCM reactions of diene-amides **68-76** were conducted to investigate nine ring closure sites in the construction of the corresponding unsaturated 14-membered lactams. These ring closure sites constituted the contiguous bond positions 4 through 12 in the series of 2-azacyclotetradecenones. This study explored the effect the proximity between the terminal double bonds and amide group had on the yield of the RCM reaction as well as the configuration of the newly formed olefin.

The choice of solvent and metathesis precatalyst used for the RCM reactions was based on issues of practicality, and from reports in the literature. The choice of dichloromethane as the reaction solvent was primarily based on a report that indicated it provides the highest turnover number for ruthenium alkylidene precatalysts.[9] Also, compared to pentane, toluene, THF, methanol, and benzene, RCM reactions proceed with higher yields and reaction rates in dichloromethane.[40,80,103-105] Dichloromethane represents a compromise between reduced co-ordinating ability and increased solvating ability.[103] Furthermore, the choice of solvent was based upon analogous studies concurrently conducted in our laboratory into the construction of unsaturated 14-membered lactones via RCM of diene-esters. Due to the volatility of the unsaturated 14-membered lactone products, these compounds were best handled in dichloromethane. Although product volatility was not encountered with the lactam

products reported in this thesis, a comparison between the two series of RCM reactions would be valuable and more readily compared by utilizing the same reaction conditions.

The decision to use Grubbs' benzylidene **3** as the metathesis precatalyst was in accord with our desire to remain consistent with studies that were concurrently being conducted in our laboratory. In terms of practical usage, the stability of **3** to air and moisture in the solid state has been illustrated, making it easy to work with and store. Furthermore, it is the most active of the ruthenium based precatalysts.[10,11] In contrast, molybdenum based metathesis catalysts decompose when exposed to air and moisture, and the preparative methods available are tedious by comparison.[8] However, when in solution **3** will decompose due to the presence of oxygen.[10] This can easily be overcome by sparging the solvent prior to use with nitrogen gas for 20 minutes. When using Schrock's molybdenum alkylidene **1**, it appears that product yields can be improved by conducting the reactions in a glove box, in comparison to identical reactions conducted on the bench-top.[25d] However, it is interesting to note that when using **3** no added benefit resulted from the use of a glove box, glove bag, or Schlenk line techniques.[106] The activity of the catalyst could simply be maintained by a steady stream of nitrogen across the reaction mixture. Considering these characteristics, Grubbs' benzylidene **3** appeared to be an excellent choice for our purposes.

To allow a comparison of yield within the series of reactions, each diene-amide was subjected to the same reaction conditions, with the site of ring closure and reaction time being the only variables. The conditions applied in this study were developed during studies of the RCM of *N*-(6-heptenyl)-7-octenamide (**72**) (see Section 2.4.2). Specifically, separate solutions of a diene-amide and precatalyst **3** (5 mol%), both in dichloromethane, were added to a portion of dichloromethane (2.0 mM in total) over three hours under high dilution conditions using a syringe pump (see Table 4, Entry 5). Either thin layer chromatography or gas-liquid chromatography was used to monitor each reaction. A reaction was quenched when the starting material was consumed, or when it was no longer being consumed, up to a total reaction time of approximately 24 hours. The active form of the catalyst was quenched either by addition of TEA or bubbling air into the reaction mixture.

RCM of diene-amides **68-76** using Grubbs' benzylidene **3** resulted in formation of the corresponding unsaturated 14-membered lactams **77-90** in a range of low (7 to 11%), moderate (32 to 47%), and high (74 to 86%) yields (Table 5). Similar to previous

results, RCM of diene-amide **76** failed. The results of this study illustrated that the proximity of the amide group to the terminal double bonds affected the yield and total reaction time of the cyclization. In general, an increase in the distance between these groups resulted in a higher yield of lactam product and a shorter total reaction time. In addition to the isolation of the unsaturated lactams, recovery of the starting diene-amide typically constituted the remainder of the mass balance (see Table 5). Cyclic and acyclic dimeric products were not observed throughout this study, either by isolation or in the spectral data of the products.

The observed *E*/*Z* ratios for each pair of diastereomeric lactams, resulting from the RCM of the corresponding diene-amides, are also given in Table 5. Typically, the olefin isomers were separated by column or radial chromatography. However, the minor isomers (*E*)-**81**, (*E*)-**88**, and (*Z*)-**90** could not be separated from the respective major diastereomers. Each mixture gave satisfactory chemical analysis, and the assignment of the minor isomers was tentatively based on NMR and mass spectral data. It is interesting to note that the order of elution during chromatographic separation was not consistent throughout the series. For example, chromatographic separation of the isomeric lactams resulting from ring closure at bond position 7 began with elution of (*E*)-**82** followed by the isomer (*Z*)-**83**. The analogous products resulting from ring closure at bond position 9, (*Z*)-**85** and (*E*)-**86**, followed the opposite order of elution. This inconsistent behaviour was also observed with GC retention times.

The possibility was considered that the relative transition state energies for formation of the *E* and *Z* isomers might be reflected in the relative strain energies of the diastereomeric lactam products. Molecular mechanics calculations were performed,[107] using the MM3* force field, to calculate global minimum energy conformations for lactams **77**-**92** representing each member of the nine pairs of diastereomers. These calculated enthalpy values were used as an estimation of the relative free energy between pairs of diastereomers ($\Delta S = 0$). Based on this energy difference, the ratio of the isomeric products for each bond position was calculated using equation 1. Comparison of the calculated *E*/*Z* ratios with those observed from the RCM reactions revealed moderate to very high correlation (Table 5). Although we considered the entropy associated with each isomer within a diastereomeric pair to be similar, that is ΔS was assumed to be zero, these entropy values are not rigorously equivalent. Due to the simplification used here, and elsewhere in this thesis, the calculated *E*/*Z* ratios do

not include the entropy component of the free energy. Therefore, comparisons between the calculated and experimentally observed values should be made with caution.

Table 5. Formation of Unsaturated 14-Membered Lactams **77-90** via RCM of Diene-amides **68-76**

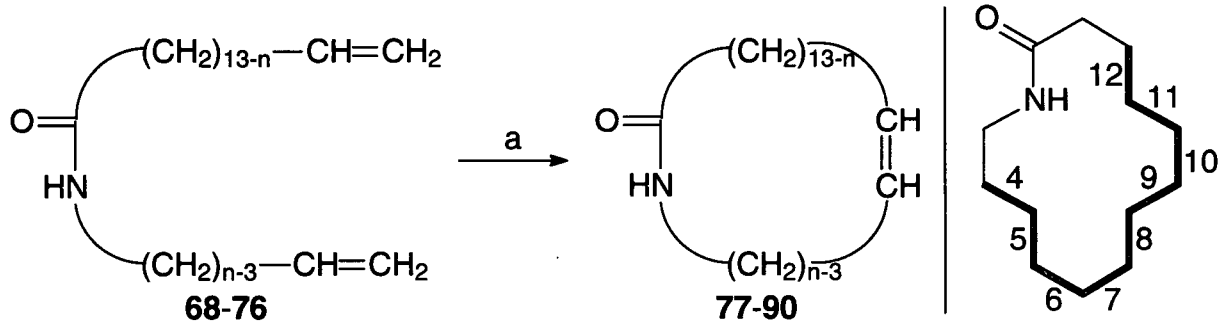

68-76 **77-90**

Position (n)	Substrate	Product(s) (*E*/*Z*)	t (h)	Yield (%)[b]	*E*/*Z*[c]	Calculated *E*/*Z*[d]
4	**68**	**77**/–	26	7 (83)	>99:1	63:37
5	**69**	**79/78**	20	32 (60)	72:28	95:5
6	**70**	**81/80**	22	47 (39)	16:84	16:84
7	**71**	**82/83**	7	86 (0)	54:46	48:52
8	**72**	**84**/–	1	87 (12)	>99:1	97:3
9	**73**	**86/85**	4	74 (9)	58:42	57:43
10	**74**	**88/87**	25	39 (32)	11:89	17:83
11	**75**	**89/90**	24	11 (75)	80:20	99:1
12	**76**		24	0 (82)		99:1

[a] Separate solutions of diene-amide and 5 mol% **3**, in CH_2Cl_2 at 2.0 mM in total, were added over three hours at rt, with the exception of **72** where the substrate and catalyst were added immediately.

[b] Isolated yield of analytically pure material after chromatography, and recovered diene-amide in parenthesis.

[c] Ratio of isomers was determined by GC, 500 MHz ^{1}H NMR, or by chromatographic separation.

[d] Calculated using Macromodel 4.5 (see reference 107).

$$\Delta G^{\circ}_{E} - \Delta G^{\circ}_{Z} = -RT \ln([E]/[Z]) \qquad (1)$$

It is worth noting that the RCM cyclization of diene-amide **74** was previously reported. Cyclization of **74** with 25 mol% of Schrock's molybdenum alkylidene **1** gave

exclusively, in terms of configuration, lactam (*Z*)-**87** in 41% yield, and a mixture of cyclic dimeric products in 20% yield.[24c] In comparison, cyclization of **74** with 5 mol% of Grubbs' benzylidene **3** gave a mixture of lactams (*E*)-**88** and (*Z*)-**87** in 39% yield, and in a ratio of 11:89 respectively (see Table 5, n = 10). Both yields were quite similar, although the five-fold increased loading of **1** suggests that **3** was more effective in this case. Furthermore, formation of the (*Z*)-lactam **87** was strongly favoured when using either precatalyst. This suggested that these catalysts have similar affects on the relative transition state energies for formation of the *E* and *Z* isomers. It also suggested that the conformation of the macrocyclic ring, rather than the metallacyclobutane ring, might play a larger role in the stereochemical determining event.

Additional experiments were conducted with diene-amides **71-73**, and these results are summarized in Table 6. Reactions were conducted in a manner similar to those summarized in Table 5, with the exception of the following parameters: addition time, reaction time, scale, and concentration. In comparison to Entries 2 and 9 (Table 6), those reactions conducted by an instantaneous combination of substrate and precatalyst (Entries 1 and 8), or with a three hour addition time and a longer reaction time (Entries 3 and 10) were characterized by lower yields and the formation of dimeric products. The isolation of acyclic and cyclic dimeric products was confirmed by the presence of peaks in the mass spectrum, obtained in positive-ion DCI mode, at 447 and 419 *m/z* (M^++1), respectively. These dimeric compounds were presumably isolated as mixtures of head-to-head and head-to-tail isomers, as well as configurational isomers with respect to disubstituted double bond(s). It is worth noting that nearly all RCM reactions reported in this chapter were conducted on a 25-100 mg scale. In comparison, reactions conducted on approximately a 1 g scale were characterized by lower yields (Entries 4, 7, and 11). Finally, the effect of concentration was dramatically illustrated by the RCM of diene-amide **71** at a concentration of 0.02 M (Entry 5), ten times the usual concentration. RCM at this higher concentration was marked by a reduction in the yield of the lactam products **82** and **83**, and a significant increase in yield of the cyclic dimer, both isolated in nearly a 1:1 ratio. This suggested that conducting the reaction at higher concentration increased the probability of intermolecular reactions that lead to the formation of dimeric products. It is interesting to note that regardless of the conditions applied, the observed *E*/*Z* ratios did not

significantly vary within a bond position, and remained comparable to the calculated *E/Z* ratios (see Table 5).

Table 6. Formation of Unsaturated 14-Membered Lactams **82-86**: A Study of Scale, Addition Time, and Reaction Time in the RCM of Diene-amides **71-73**

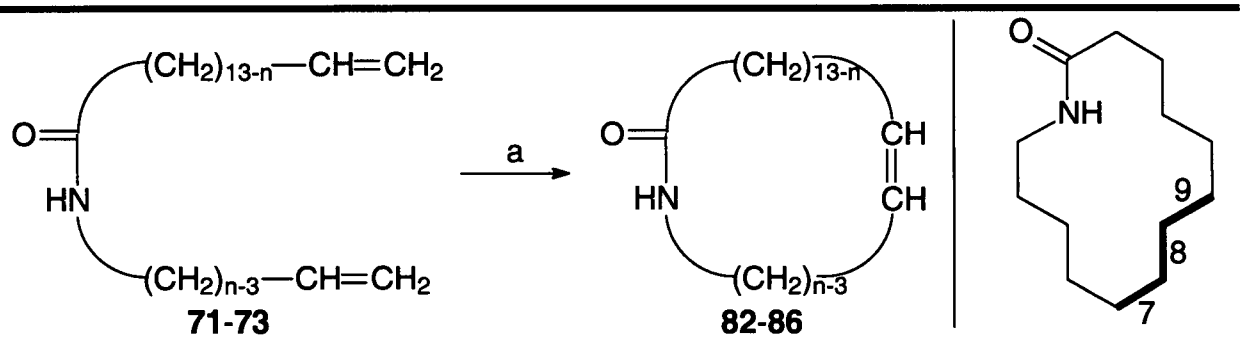

71-73 **82-86**

Entry	Position (n)	Substrate	Product(s) (*E/Z*)	t (h)[b]	Yield (%)[c]	*E/Z*[d]
1	7	**71**	**82/83**	3 (0)	81 (8, 11)	52:48
2	7	**71**	**82/83**	7 (3)	86 (0, 0)	54:46
3	7	**71**	**82/83**	25 (3)	79 (0, 19)	53:47
4	7	**71**	**82/83**	8 (3)	71 (13, 5)[e]	57:43
5	7	**71**	**82/83**	4 (0)	46 (0, 54)[f]	56:44
6	8	**72**	**84**/–	1 (0)	87 (12, 0)	>99:1
7	8	**72**	**84**/–	1 (0)	74 (14, 0)[e]	>99:1
8	9	**73**	**86/85**	3 (0)	50 (12, 22)	61:39
9	9	**73**	**86/85**	4 (3)	74 (9, 0)	58:42
10	9	**73**	**86/85**	7 (3)	62 (2, 0)	67:33
11	9	**73**	**86/85**	6 (3)	65 (7, 0)[e]	57:43

[a] Separate solutions of diene-amide and 5 mol% **3**, in CH_2Cl_2 at 2.0 mM in total, were combined at rt.
[b] Total reaction time, and addition time in parenthesis.
[c] Isolated yield of analytically pure material after chromatography, and recovered diene-amide followed by isolated dimeric products in parenthesis.
[d] Ratio of isomers were determined by GC, 500 MHz ^{1}H NMR, or by chromatographic separation.
[e] Reaction conducted on approximately a 1 g scale (cf. 25-100 mg).
[f] Reaction conducted at a concentration of 0.02 M.

The results presented in Table 6 provided further insights into the RCM formation of 14-membered lactams. Dilution effects retarded the formation of dimeric products, either by the slow addition of substrate, or by the overall concentration. Furthermore, the formation of dimeric products at longer reaction times suggested that the cyclic monomer ring opened under the reaction conditions, but at a lower rate than that of cyclization. However, slow dimerization of any remaining diene-amide must also have occurred. In either case, the results suggested that the rate of dimerization was lower than the rate of monomer cyclization. Based on molecular mechanics calculations that will be discussed in due course, each reaction was found to be endothermic. The low yield associated with a larger scale reaction might be attributed to a requirement for atmospheric heat energy that was more readily absorbed with a smaller scale reaction. In all, these experiments illustrated factors that influence the formation of the dimeric products.

The structures of the lactams synthesized in these studies were confirmed by the spectral data obtained for each. The isomeric relationship between these compounds was reflected in the similarity between the spectral data, and this was used to facilitate the analysis. It is important to note that the major difference between the ^{1}H NMR spectra of the diene-amide substrates and the macrocyclic lactam products was the absence of the vinyl methylene proton signals in the latter, corresponding to the terminal double bonds of the diene-amides. This contributed to evidence confirming that cyclization had occurred. The ^{1}H NMR spectrum of each lactam contained a pair of doublet of triplets at δ 5.2-5.6 corresponding to the vinyl methine protons. Also found in this region was a broad singlet (ca. δ 5.3-6.0) corresponding to the N-H proton. Other characteristic resonances observed in the ^{1}H NMR spectra were a doublet of triplets, which often appeared as a quartet at δ 3.1-3.4, a multiplet at δ 2.1-2.3, and two resonances at δ 2.0-2.2 and δ 1.9-2.0, which were overlapped in a few cases. These signals correspond to the protons on methylene groups adjacent to the nitrogen atom, the carbonyl, and either side of the olefin, respectively. Macrocyclic lactam **77** was an exception to this general trend due to the proximity of the olefin to the nitrogen atom. The ^{13}C NMR spectrum of each macrocyclic lactam contained thirteen signals, except in cases where signals were coincident with respect to chemical shift. Signals

characteristic of the carbonyl (ca. δ 173), the two vinyl carbons (ca. δ 127-133), and the carbon adjacent to the nitrogen atom (ca. δ 38-41) were observed. The IR spectra contained signals at approximately 3450 and 3350 cm^{-1}, and 1680 cm^{-1} corresponding to two different forms of hydrogen bonded N-H stretching frequencies, and a carbonyl stretching frequency, respectively. In addition to the data discussed above, HRMS and chemical analysis results were found to be consistent with the composition of each macrocyclic lactam.

The configuration of the olefin within each unsaturated 14-membered lactam was determined by 500 MHz ^1H NMR homonuclear decoupling experiments. These experiments were performed by separate irradiation of both allylic proton resonances (ca. δ 1.9-2.2) resulting in simplification of the adjacent vinyl proton resonance from a doublet of triplets to a doublet. In general, an olefin with J = 15.4 Hz was assigned the *E* configuration, and an olefin with J = 11.0 Hz was assigned the *Z* configuration. A few of the lactams had a coupling constant that deviated slightly from these values. Typically, the coupling constant for an (*E*)-alkene is found in the range 12-18 Hz, while a (*Z*)-alkene has a smaller coupling constant found in the range 6-12 Hz.[108] The observed coupling constants and the assigned configurations were consistent with these ranges.

The IR spectral data might also provide support for the configuration of each olefin suggested by the NMR decoupling data. In general, the stretching mode of a (*Z*)-alkene absorbs more strongly than the corresponding absorption in an (*E*)-alkene, due to the pseudosymmetry of the latter. However, the coincident overlap of carbonyl (amide I band) and alkene stretching frequencies in each IR spectrum prevented this determination.

A comparison between the allylic carbon resonances in the ^{13}C NMR spectrum of each lactam also provided support for the assignments suggested by the decoupling experiments. In general, the allylic carbon resonances of the (*E*)-lactams were found at lower field, by about 3-7 ppm, relative to the analogous resonances from the isomeric (*Z*)-lactams. For example, the allylic carbon resonances in lactam (*E*)-**82** were found at δ 31.51 and 30.51, whereas the corresponding resonances in the isomeric lactam (*Z*)-**83** were found at δ 26.04 and 24.66. This trend was consistently observed throughout the series of unsaturated lactams and is consistent with trends observed in the literature. Typically, the allylic carbon resonances of an (*E*)-alkene are found at lower field, by

about 4-6 ppm, relative to those of the (*Z*)-alkene, due to a stronger shielding effect experienced by the latter.[109,110] This shielding effect, known as the γ-effect and represented by the relationship $\delta_{\alpha(E)} > \delta_{\alpha(Z)}$, results from a steric perturbation of the C-H bond due to overlapping van der Waals radii between sets of allylic protons in a (*Z*)-alkene.[111] In conclusion, the configuration of the olefin within each macrocyclic lactam was determined by ^{1}H NMR homonuclear decoupling experiments, and the assignments were supported by a comparison between allylic carbon resonances in the ^{13}C NMR spectra of each diastereomeric lactam pair.

One concern regarding the unsaturated lactams formed via RCM was positional isomerization of the olefin prior to or after cyclization. This would result in smaller ring size lactam products, or unsaturated lactam products in which the olefin was situated in an unexpected position. Reports describing the construction of cyclic compounds that were one carbon unit smaller than anticipated,[112,113] and the positional isomerization of a vinyl glycine derivative,[26] both of which occurred under RCM conditions, warranted further inspection of the lactam products obtained during our studies. The formation of smaller ring size products was rejected by the mass spectral data and chemical analysis, however the possibility of positional isomerization was of concern. X-ray crystallography and 2D NMR analysis were used to verify the position of the olefin within the lactam products.

Lactams **77**-**90** were obtained as white solids, and it was hoped that the position and configuration of the olefin within each could be confirmed by X-ray crystallographic analysis. Unfortunately, only lactam **89** provided crystals suitable for such an analysis. The crystals obtained for the remaining lactam products were not suitable for this analysis, which provided some indication of the disorder in the solid state. It is interesting to note that the conformation of **89** in the solid state (Figure 29), determined by single-crystal X-ray diffraction, was nearly identical to the global minimum energy conformation obtained from a molecular mechanics conformational search. A comparison between the calculated and solid state conformations, represented in polar maps (Figure 30),[114] best illustrates their similarity. The solid state structure of lactam **89** confirmed the position and configuration of the olefin with in the ring. In addition, it suggested that the global minimum energy conformations obtained from gas phase molecular mechanics calculations might be representative of the solid state conformations, and offers support for our analysis of the observed *E*/*Z* ratios.

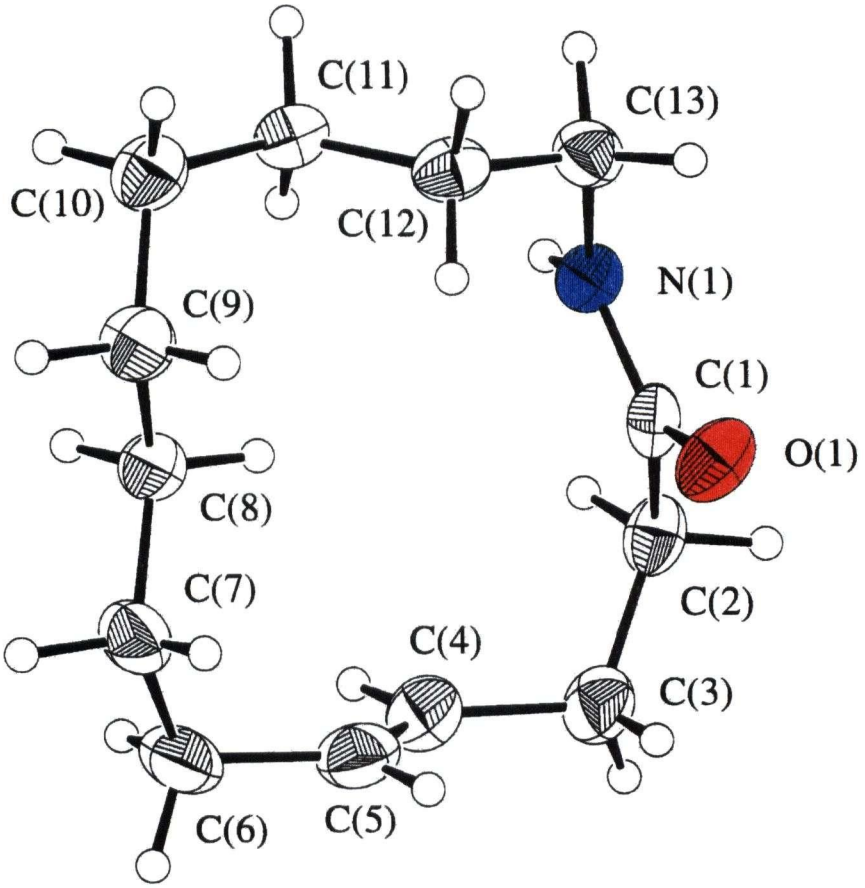

Figure 29. ORTEP representation of (*E*)-**89**, showing 50% probability ellipsoids and hydrogen atoms with arbitrary thermal parameters for clarity.

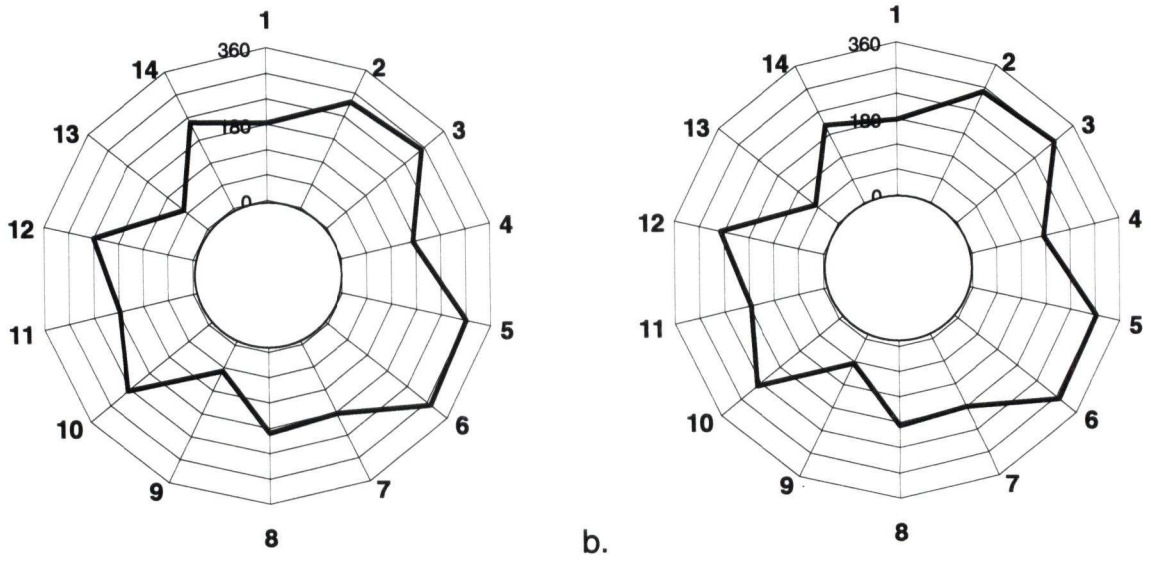

Figure 30. Polar plots of (a) solid state and (b) molecular mechanics global minimum energy conformations of lactam (*E*)-**89**.

The position of the olefin within each macrocyclic lactam was confirmed by a detailed analysis of the COSY, HMQC, and HMBC 2D NMR data. Using lactam (*E*)-**82** as an example, partial COSY and HMBC correlations are illustrated in Figure 31, where bold red bonds represent COSY correlations and blue arrows represent HMBC correlations. COSY correlations were observed between H-2 (δ 5.95) and H-3 (δ 3.16), which in turn was correlated to H-4 (δ 1.50). Furthermore, H-4 (δ 1.50) was correlated to the lower field resonance (ca. δ 1.38) contained within the multiplet of two unresolved resonances at δ 1.33-1.41. The resonance at δ 1.38 was tentatively assigned to H-5. COSY correlations between H-8 (δ 5.26) and H-7 (δ 5.48), which in turn was correlated to H-6 (δ 1.92), which was correlated to H-5 (δ 1.38) readily identified a portion of the ring extending from N-2 through to the olefin, and also confirmed the assignment of H-5. The location of the olefin, at bond position 7, was consummately confirmed. The assignment of the resonance at δ 1.38 to H-5 was also confirmed by analysis of the HMBC spectrum. For example, HMBC correlations between H-5 (δ 1.38) and carbons C-3 (δ 39.02) and C-6 (δ 30.51) provided further evidence to support the assignment of H-5. In contrast, HMBC correlations between H-10 (δ 1.34), the higher field resonance in the same multiplet containing H-5, and carbons C-9 (δ 31.51) and C-11 (δ 28.25) suggested the higher field signal was not related to H-5. Further analysis of the COSY spectrum provided correlations for the contiguous protons H-8 through H-14, and analysis of the HMBC spectrum facilitated the assignment of the remaining proton and carbon resonances. In conclusion, the preceding analysis provided complete correlations for the proton and carbon resonances associated with lactam (*E*)-**82**. Furthermore, this analysis confirmed the position of the olefin as assigned, and suggested that positional olefin isomerization processes had not occurred either during the RCM reactions or during the purification of the lactam products.

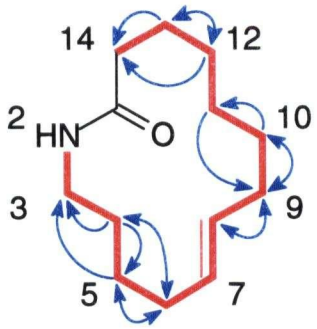

(*E*)-**82**

Figure 31. Partial 500 MHz COSY (bold red bonds) and HMBC (blue arrows) correlations for (*E*)-2-azacyclotetradec-7-enone (**82**).

Earlier in this section, a tentative rationale was provided regarding the product yield, reaction rate, and observed *E*/*Z* ratios resulting from the RCM of a series of diene-amides. This preliminary discussion will be expanded upon later in this chapter, including a more detailed attempt to rationalize the data. However, additional studies were conducted into the RCM formation of unsaturated 14-membered lactams that provided further insight into these reactions, and a discussion of these results should precede any further discussion regarding a rationale of the overall results. These additional studies focussed on improvements to the reactions that exhibited low yield and are discussed in the following section.

2.7 Improvements to Unsaturated 14-Membered Lactam Formation via RCM

Formation of the lactams obtained by ring closure at bond positions 7, 8, and 9 proceeded smoothly, in a short period of time, and in yields greater than 70%. In contrast, the lactams obtained by ring closure at bond positions 4 through 6 and 10 through 12 were obtained in very low yield and required longer reaction times. These observations illustrated the significance of the distance between the amide and both terminal double bonds, and its effect on the yield of these RCM reactions. To contribute to our understanding of the RCM reaction, and improve upon the results of the systematic study, attempts were made to increase the yield and rate of the reactions that gave the desired lactam products in poor yield (<50%).

Concurrent to our studies, efforts directed towards resolving issues of problematic reactivity in RCM appeared in the literature. For instance, studies involving

the use of additives to either increase the activity of the catalytic species[115,116] or to destabilize unproductive catalyst complexes[89,117,118] have appeared. Earlier in our studies, the tolerance of Grubbs' benzylidene **3** to a secondary amide was a concern. In contrast to the problematic reactivity associated with amines, early reports illustrated how ruthenium based metathesis precatalysts were tolerant to secondary amides during the construction of lactams,[26,90,119] cyclic peptides,[26,27,29] and more noteworthy in the formation of 14-[24a] and 18-membered[45] lactams. The tolerance of Grubbs' benzylidene **3** to the presence of a primary amide has also been established.[120] Earlier in this chapter the sensitivity of precatalyst **3** to diene-amine substrates and the required addition of an electron withdrawing group on the nitrogen atom of these compounds was discussed (see Section 2.4.1). Similarly, the addition of a protecting group to the nitrogen atom of a diene-amide can lead to an improvement in the yield of the product lactam resulting from RCM.[90,121,122]

Other modifications to the diene have involved the addition of an alkyl substituent to one of the two terminal double bonds providing a differentially substituted diene. In general, disubstituted olefins undergo intermolecular metathesis at a lower rate than monosubstituted olefins.[21,32,123] Substitution of the double bond closest to the functional group reduces the problematic effect of proximity due to the differences in reaction rates of both types of olefins in the differentially substituted diene. This type of modified diene was applied in the construction of cyclic amines,[124] lactams,[21] and macrocyclic lactones,[44] for which RCM of the corresponding bis-terminal diene failed. Further details of the studies discussed above will be presented in due course as it relates to our efforts towards improving the yield in the RCM reactions of selected diene-amides.

Prompted and inspired by these studies, experiments were designed that attempted to improve the yield of unsaturated 14-membered lactam formation via RCM. Through these experiments a better understanding was gained regarding the problematic reactivity exhibited by some of the diene-amides employed in this study. The propensity to form, and the relative stability of, unproductive metallacyclobutane complexes of type **I** and **J** and chelate complexes of type **K** and **L** (Figure 32), as well as the overall activity of the ruthenium catalyst were considered to be factors governing the RCM of diene-amides. Accordingly, to probe these factors experiments were designed to increase the catalyst activity, extricate unproductive catalyst complexes, and adjust the reactivity of the diene-amide. This was accomplished by exploring the

effects of additives, increased temperature, the introduction of an *N*-BOC protecting group, and the RCM of differentially substituted diene-amides.

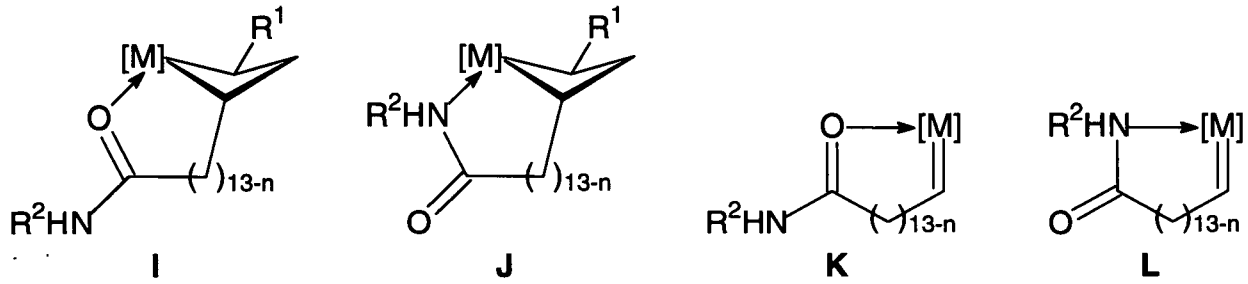

Figure 32. Unproductive catalyst complexes proposed to inhibit RCM.

2.7.1 RCM Using Additives

One approach to improving the yield of unsaturated 14-membered lactam formation via RCM, especially in those cases marked by low yields (n = 4-6 and 10-12), involved the use of additives. Two modes of action for such compounds involves either improving the activity of the metathesis catalyst, or competing with and effectively destabilizing unproductive catalyst complexes to allow the reaction to proceed more smoothly. In terms of the catalyst activity, Grubbs and co-workers observed improved catalyst activity upon addition of CuCl to the reaction mixture.[115,116] Presumably, the addition of CuCl promotes phosphine dissociation, a proposed step in the formation of a metallacyclobutane intermediate. In terms of destabilizing unproductive catalyst complexes two methods were reported. One involved the use of a Lewis acid, such as $Ti(O\textit{i}Pr)_4$, to compete with ruthenium for co-ordination to an ester group.[117] The second method relates to the formation of unproductive molybdenum and tungsten metallacyclobutane complexes discussed earlier in this chapter (see Section 2.4 and Figure 27). Reaction of the tungsten metallacyclobutane complex derived from methyl acrylate with trimethylphosphine effectively reversed its formation.[89] In contrast, similar complexes derived from *N,N*-dimethylacrylamide did not react with trimethylphosphine, and the stability of these complexes was attributed to the greater basicity of the amide carbonyl oxygen relative to that of the corresponding ester. Notwithstanding, the application of trialkylphosphines was explored.

Prompted by these developments, such methods were employed in preliminary studies directed towards improving the product yield from the RCM of selected diene-amides. RCM of diene-amide **68** using 5 mol% of Grubbs' benzylidene **3** in the presence of $Ti(O\textit{i}Pr)_4$ gave lactam **77** in 10% yield (Table 7, Entry 2). The same reaction conducted in the absence of $Ti(O\textit{i}Pr)_4$ gave a comparable product yield of 7% (Entry 1). It is interesting to note that RCM of a diene-urethane derived from allylamine, and analogous to **68**, gave no improvement in yield in the presence of $Ti(O\textit{i}Pr)_4$.[80] Similarly, RCM of the 4-pentenoic acid derived diene-amide **75** using 5 mol% of Grubbs' benzylidene **3** in the presence of $Ti(O\textit{i}Pr)_4$ did not lead to an improvement in yield (cf. Entries 5 and 6). In contrast, RCM of diene-esters derived from 4-pentenoic acid[117] and acrylic acid[118] gave improved yields of lactone products when conducted in the presence of $Ti(O\textit{i}Pr)_4$. RCM of **68** at 45 °C using 20 mol% of **3** gave lactam **77** in an improved yield of 22% (cf. Entry 1), and dimeric products in 23% yield (Entry 3). The same reaction conducted in the presence of tricyclohexylphosphine gave lactam **77** in 32% yield (Entry 4). Similar results were observed for the RCM of diene-amide **75** at higher temperature and precatalyst loading (Entry 7) and in the presence of tricyclohexylphosphine (Entry 8). It is worth noting that RCM reactions were unaffected by the presence of CuCl.

The results summarized in Table 7 illustrated the benefit of conducting RCM reactions at higher temperature and precatalyst loading. These results also illustrated that RCM of diene-amides conducted in the presence of $Ti(O\textit{i}Pr)_4$ and CuCl did not lead to an improvement in the product yield and reaction rate. In contrast, RCM in the presence of tricyclohexylphosphine gave a modest improvement in the product yield. It is interesting to note that a proposed mechanism for RCM involved dissociation of one of the two phosphine ligands from the catalyst during formation of the metallacyclobutane intermediate.[115] Reactions conducted in the presence of CuCl proceeded at a higher rate, which provided support for this proposed mechanism.[115,116] CuCl can sequester a phospine in an ill-defined copper complex,[125] therefore driving the equilibrium of a RCM reaction in the direction of product. However, under this proposed mechanism the addition of excess tricyclohexylphosphine should inhibit the catalytic cycle, and not lead to an improvement in yield (see Table 7). Further investigation into the RCM mechanism and the effect of excess phosphine ligand is required.

Table 7. Formation of Unsaturated 14-Membered Lactams **77**, and **89** and **90**: RCM of Diene-amides **68** and **75** in the Presence of Additives

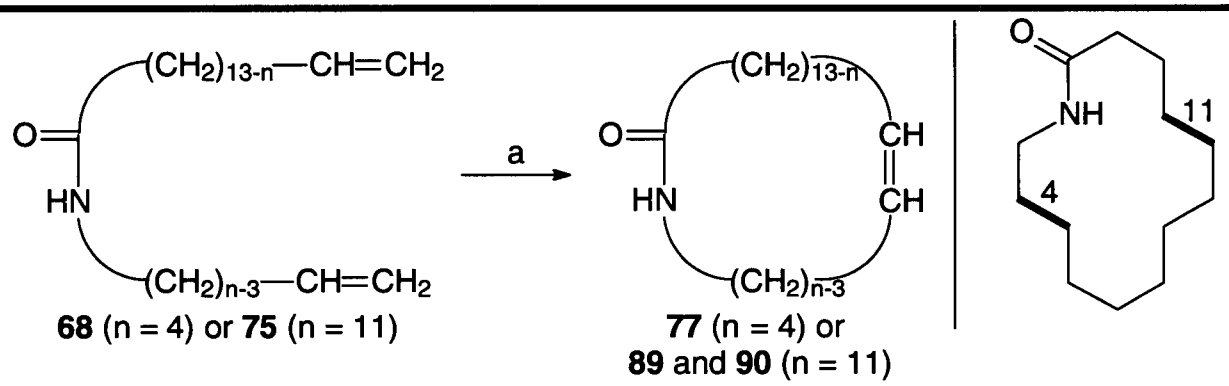

68 (n = 4) or **75** (n = 11) → **77** (n = 4) or **89** and **90** (n = 11)

Entry	Substrate/ Product(s)	mol% **3**	T (°C)	t (h)[b]	Additive (1 eq.)	Yield (%)[c]
1	**68 / 77**	5	rt	26 (3)		7 (83,0)
2	**68 / 77**	5	rt	24 (3)	$Ti(OiPr)_4$	10 (64,0)
3	**68 / 77**	20	45 °C	29 (24)		22 (27,23)
4	**68 / 77**	20	45 °C	42 (24)	PCy_3	32 (14,13)
5	**75 / 89,90**	5	rt	24 (3)		11 (75,0)
6	**75 / 89,90**	5	rt	24 (3)	$Ti(OiPr)_4$	7 (80,0)
7	**75 / 89,90**	20	45 °C	27 (24)		18 (33,32)
8	**75 / 89,90**	20	45 °C	48 (24)	PCy_3	27 (35,22)

[a] Slow addition of separate solutions of diene-amide and **3**, in CH_2Cl_2 at 2.0 mM.
[b] Total reaction time, and addition time in parenthesis.
[c] Isolated yield after chromatography, and recovered diene-amide followed by isolated dimeric products in parenthesis.

The RCM of diene-amides **68** and **75** at increased temperature and precatalyst loading led to an improvement in the yield of cyclized product. Although this improvement was more likely due to the increased catalyst loading, a number of reports have illustrated the effect of increased temperature on RCM. Further studies directed towards improving the product yield in the RCM formation of 14-membered lactams by increased reaction temperature follows in the next section.

2.7.2 RCM at Increased Temperature

Considering the somewhat poor results obtained with the additives studied in the previous section, a simpler and more general approach to an improvement of product yield was considered. The effect of increased temperature in RCM was shown to increase the rate of the reaction in general,[124,126] and improve the yield of cyclized product in some cases.[99a,117,127] However, the instability of ruthenium and molybdenum catalysts at elevated temperatures, due to the increased rate of decomposition, is well documented.[8-11,18] With this in mind, refluxing dichloromethane appeared to be a reasonable choice to allow for rate enhancement while limiting catalyst decomposition.

Selected diene-amides from the series studied previously, corresponding to ring closure at bond positions 4 through 6 and 10 through 12, were marked by low yield (<50%). In an attempt to improve upon these results, diene-amides **68-70** and **74-76** were subjected to the same RCM reaction conditions used previously (see Section 2.6), but at an increased temperature. The temperature was maintained using an oil bath heated to 45 °C. The results of these experiments are summarized in Table 8.

The effect of an increase in temperature on the RCM of these diene-amide substrates can be illustrated by a comparison of the results presented in Table 8 to those obtained for the identical reactions conducted at room temperature (see Table 5). At increased temperature the product yields were improved upon with varying success. Aside from position 12, which failed to yield cyclized product, all experiments led to an improved product yield, ranging from a 9% increase for diene-amide **75** (n = 11) to an 82% increase for diene-amide **74** (n = 10). The most significant increase in yield was observed for those bond positions farthest removed from the amide functional group (n = 5, 6, and 7). It is worth mentioning that the increased temperature did not affect the observed *E*/*Z* ratios for each pair of diastereomeric lactams (cf. Table 5 and Table 8). In addition to the improved product yield, rate enhancement was observed with the RCM of diene-amides **70** and **74**, however the other substrates were allowed to react for up to 24 hours in an attempt to maximize the product yield. Presumably, the increased product yield can be attributed to rate enhancement and the evaporative loss of ethylene, expedited by the increased temperature.

Table 8. Formation of Unsaturated 14-Membered Lactams **77-81** and **87-90**: RCM of Diene-amides **68-70** and **74-76** at Increased Temperature (45 °C)

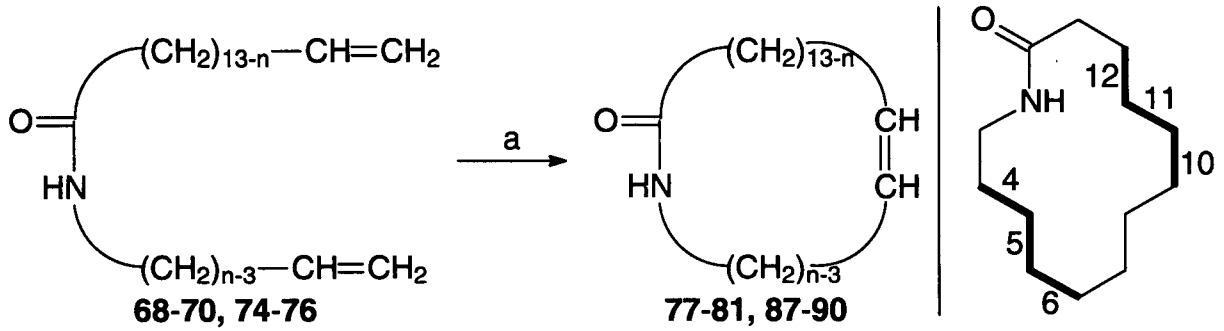

68-70, 74-76 **77-81, 87-90**

Position (n)	Substrate	Product(s) (*E*/*Z*)	t (h)	Yield (%)[b]	*E*/*Z*[c]	Calculated *E*/*Z*[d]
4	**68**	**77**/–	24	12 (67,13)	>99:1	63:37
5	**69**	**79/78**	24	56 (26,9)	71:29	95:5
6	**70**	**81/80**	8	71 (0,0)	14:86	16:84
10	**74**	**88/87**	9	71 (8,5)	13:87	17:83
11	**75**	**89/90**	24	12 (86,0)	73:27	99:1
12	**76**		24	0 (92,0)		99:1

[a] Separate solutions of diene-amide and 5 mol% **3**, in CH_2Cl_2 at 2.0 mM in total, were added over three hours and stirred at 45 °C.
[b] Isolated yield of analytically pure material after chromatography, and recovered diene-amide followed by isolated dimeric products in parenthesis.
[c] Ratio of isomers was determined by GC, 500 MHz ^{1}H NMR, or by chromatographic separation.
[d] Calculated using Macromodel 4.5 (see reference 107).

In addition to the isolation of the unsaturated lactams, recovery of the starting diene-amide and the isolation of acyclic and cyclic dimeric products typically constituted the remainder of the mass balance (Table 8). The dimeric products were presumably isolated as mixtures of head-to-head and head-to-tail isomers, as well as configurational isomers with respect to the disubstituted double bond(s). Recall that the isolation of dimeric products was not observed when the reactions were conducted at room temperature (see Table 5). This suggested that the rate of intermolecular reactions, the process of acyclic diene metathesis (ADMET), was increased relative to the rate of intramolecular reactions (RCM). In reports that appeared coincident to our own,[72] an increase in the amount of acyclic (ADMET) and cyclic (tandem ADMET-RCM) dimeric

products was observed upon increased reaction temperature.[46,99a,128] If dimer formation also occurred via cyclic monomer ring opening, then the rate of this process likely increased due to the increase in temperature. However, for the experiments presented in Table 8 the formation of dimeric products was of little consequence when compared to the improvement in yield of the desired lactam.

In summary, conducting the RCM reactions of selected diene-amides at increased temperature led to an increase in the yield of the desired lactam products, the formation of cyclic and acyclic dimeric products, and an improved reaction rate. Furthermore, the observed *E*/*Z* ratios were not affected in comparison to those observed at room temperature. Although more rapid catalyst decomposition occurs at higher temperature,[18] it was not a factor governing the RCM reactions due to the improved yields observed in most cases. This improvement might have resulted from either a higher reaction rate or the destabilization of unproductive catalyst complexes. Studies directed towards understanding the latter are discussed in the following two sections.

2.7.3 RCM of *N*-BOC Protected Diene-amides

The use of a protecting group on the amide nitrogen atom constituted another approach directed towards the improvement of product yield, particularly for those diene-amides marked by low yield (<50%). The temperature studies discussed in the previous section illustrated an effect upon rate, yield, and dimer formation in the RCM of selected diene-amides. Although the improved yield in some cases was a positive development, the question remained as to whether a rate enhancement or the destabilization of unproductive catalyst complexes effected this change. With respect to the latter, nitrogen atom protecting groups were assessed according to their potential to produce this destabilizing effect during RCM. Furthermore, the facile introduction and removal of such a group, and its stability to the RCM reaction conditions were of interest. Accordingly, the *tert*-butoxycarbonyl (BOC) group was chosen for these studies. This group was anticipated to hinder the formation of unproductive catalyst complexes in two ways. One involves the electronic nature of the BOC group. By reducing the electron density at the carbonyl oxygen and amide nitrogen atoms, due to electron delocalization, the propensity to form such a complex might be reduced. In fact, a comparison of the net atomic charge of these atoms between diene-amide **70**

and *N*-BOC diene-amide **141**, obtained from semi-empirical calculations employing the AM1 method,[129] suggested such a reduction in electron density (Figure 33). Steric bulk was the second way in which the BOC group was anticipated to hinder the formation of unproductive catalyst complexes. This might occur by hindering association between the electron deficient (Lewis acidic) ruthenium atom and either Lewis basic heteroatom from the amide group. This effect was anticipated to be limited to the nitrogen atom due to the stability associated with the *s*-trans conformation of the amide.[130,131] In this case, the steric demand of the BOC group would affect the carbonyl oxygen atom to a lesser extent. In related research, a remarkable increase in yield was observed in the RCM formation of a 6-membered lactam when incremental increases to the steric demand of an α-substituent, relative to the nitrogen atom, were made.[132]

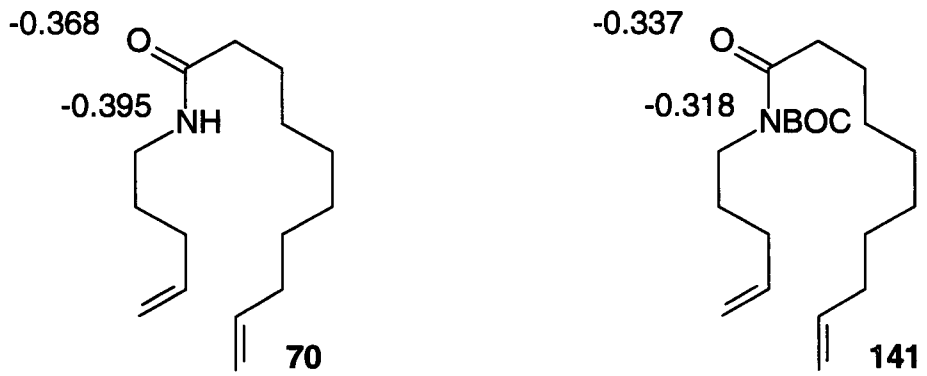

Figure 33. Semi-empirical calculated net atomic charge, employing the AM1 method, for the amide nitrogen and oxygen atoms of diene-amides **70** and **141**.

In order to conduct these studies the requisite *N*-BOC diene-amides **139-144** were obtained in yields of 57-92% by protection of the corresponding diene-amides **68-70** and **74-76** using di-*tert*-butyl dicarbonate in the presence of DMAP (Table 9). Our initial attempts to form 14-membered *N*-BOC lactams via RCM proceeded in improved yield. However, the olefin isomers could not be resolved which prevented a determination of the observed *E*/*Z* ratios resulting from RCM. This problem necessitated cleavage of the BOC group following cyclization. Accordingly, *N*-BOC diene-amides **139-144** were subjected to the same RCM reaction conditions used previously (see Section 2.6), and subsequently treated with trifluoroacetic acid to give the corresponding lactams **77-81** and **87-90**. These results are summarized in Table 9.

Table 9. Formation of Unsaturated 14-Membered Lactams **77-81** and **87-90**: Synthesis and RCM of *N*-BOC Diene-amides **139-144**

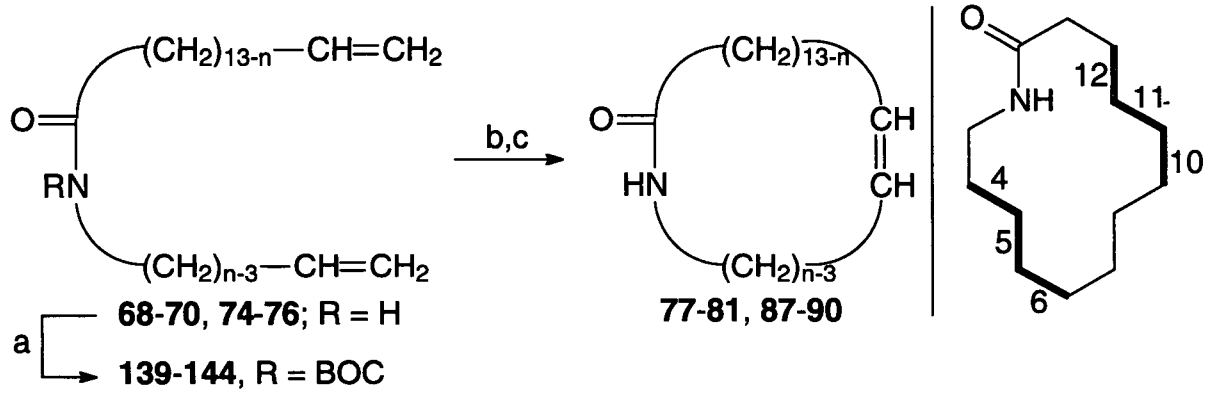

Position (n)	*N*-BOC Substrate	Yield (%)[d]	Product(s) (*E*/*Z*)	t (h)	Yield (%)[e]	*E*/*Z*[f]	Calculated *E*/*Z*[g]
4	**139**	92	**77**/–	24	20 (67,3)	>99:1	63:37
5	**140**	59	**79/78**	17	57 (5,20)	64:36	95:5
6	**141**	60	**81/80**	8	62 (11,17)	13:87	16:84
10	**142**	57	**88/87**	10	71 (8,21)	20:80	17:83
11	**143**	72	**89/90**	24	31 (42,23)	82:18	99:1
12	**144**	65		24	0 (93,0)		99:1

[a] BOC_2O, DMAP, THF, rt.
[b] Separate solutions of *N*-BOC diene-amide and 5 mol% **3**, in CH_2Cl_2 at 2.0 mM in total, were added over three hours at rt.
[c] The crude product was treated with CF_3COOH:CH_2Cl_2 (1:1) for 30 minutes.
[d] Isolated yield of analytically pure material after chromatography.
[e] Same as d, and recovered diene-amide followed by isolated dimeric products in parenthesis.
[f] Ratio of isomers was determined by GC, 500 MHz ^1H NMR, or by chromatographic separation.
[g] Calculated using Macromodel 4.5 (see reference 107).

The potential for problematic reactivity during the course of these experiments was anticipated. For instance, BOC cleavage during the RCM event or incomplete cleavage upon treatment with trifluoroacetic acid was of concern. Another concern was the potential for isomerization of the product olefin, either in position or configuration, due to the acidic conditions applied in the BOC cleavage step. However, cleavage products due to loss of the BOC group were not observed during the course of the RCM reactions when followed by TLC and GC. Furthermore, upon cleavage of the BOC

group none of the *N*-BOC protected compounds were detected using TLC and GC, or by spectral analysis of the product lactams. The spectral data of the lactam products obtained from these experiments were identical to those obtained from the analogous experiments using the unprotected diene-amides. These observations confirmed the stability of the BOC group to the reaction conditions, which was an important issue when considering the factors that influenced the results of these experiments. Furthermore, quantitative cleavage of the BOC group apparently occurred, and the conditions applied in this reaction did not lead to any detectable amount of products resulting from positional isomerization. The absence of configurational isomerization could not be confirmed, however such a process seems unlikely given the lack of positional isomerization that would presumably occur via the same protonated intermediate cation. In all, these observations diminished any concern regarding the stability of the BOC group and olefin to the reaction conditions.

The effect of the *N*-BOC group on the RCM reactions is best illustrated by a comparison of the results presented in Table 9 to those obtained for the RCM reactions of the corresponding unprotected diene-amide substrates (see Table 5). Similar to the results obtained for the reactions conducted at increased temperature (see Table 8), an improvement in yield was observed for those bond positions furthest removed from the amide functional group (n = 5, 6, and 10). This improvement became less pronounced at bond positions closer to the amide group (n = 4 and 11), and RCM of *N*-BOC diene-amide **144** (n = 12) failed, which was consistent with all previous attempts to cyclize at this bond position. It is worth noting that product formation via RCM of *N*-BOC diene-amides **139** (n = 4) and **143** (n = 11) led to a 54% and 182% increase in yield respectively, although the overall yield remained disappointingly low. In contrast, the analogous reactions conducted at elevated temperature using the unprotected diene-amides did not lead to such an improvement in product yield (cf. Table 8). Furthermore, the introduction of the BOC group had little affect on the observed *E*/*Z* ratios for each pair of diastereomeric lactams (cf. Table 5 and Table 9). Rate enhancement was observed for the RCM reactions of *N*-BOC diene-amides **140-142**, and the other substrates were allowed to react for 24 hours in an attempt to maximize product yield. The increased product yield observed in these experiments was tentatively attributed to rate enhancement, however each reaction was also dependent on the duration of the catalyst activity. It stands to reason that the BOC

group reduced the electron density at the carbonyl oxygen and amide nitrogen atoms, due to electron delocalization, thus reducing the electron donating ability of these atoms. Accordingly, the propensity to form, and stability of, unproductive catalyst complexes would be reduced. This would facilitate productive metathesis and was reflected in the higher rates and yields. Finally, it is interesting to note that the introduction of a second carbonyl, that of the BOC group, did not hinder these reactions, but in fact led to an improvement in product yield. This suggested that the nitrogen atom played a larger role in the formation of unproductive catalyst complexes than the carbonyl oxygen atom, at least for the *N*-BOC diene-amide substrates.

In addition to the isolation of the unsaturated lactams, recovery of the starting diene-amide and the isolation of a significant amount of acyclic and cyclic dimeric products typically constituted the remainder of the mass balance (Table 9). The identification and nature of the dimeric products was discussed earlier (see Section 2.6). The elimination of hydrogen bonding due to introduction of the BOC group was expected to significantly reduce the probability of dimer formation, since a mode of intermolecular interaction was removed. However, in comparison to the studies conducted at room temperature and elevated temperature, the ratio of dimeric products to the desired lactam products was greatest for the RCM reactions of the *N*-BOC diene-amides. The delocalization of the electron density throughout the amide group was expected to weaken unproductive catalyst complexes and lower the propensity to form them. However, this effect may also weaken proposed catalyst relay complexes of type **M**[45] that would otherwise increase the rate of cyclization, relative to those substrates lacking any functional group. With this in mind, a reduction in the rate of cyclization could result in a significant reduction in the difference between the relative rates of RCM and ADMET, thus leading to an increase in yield of the acyclic (ADMET) and cyclic (tandem ADMET-RCM) dimeric products. In accord with the dimer formation encountered during the temperature studies (see Section 2.7.2), the formation of such products was of little consequence when compared to the improvement in yield of the desired lactam.

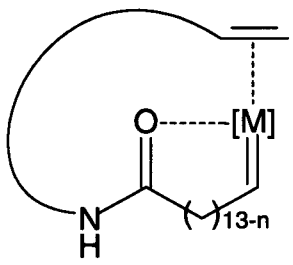

M

In summary, the RCM reactions of *N*-BOC diene-amides **139-144** led to an increase in yield of the desired lactam, the formation of dimeric products, and an improved rate of reaction, when compared to the unprotected diene-amides. Similar to the elevated temperature studies, the observed yields in this study were affected by the proximity of the terminal double bonds to the amide group, but to a lesser extent. Furthermore, the observed *E*/*Z* ratios were similar in comparison to previous results using the unprotected diene-amides. In reports that appeared coincident to our own,[72] and all of which compliment an earlier report,[90] improved yields were observed upon *N*-protection of a diene-amide.[121,122] It was tentatively proposed that the improved yield observed during these studies resulted from an increased reaction rate, which in turn was facilitated by the destabilization of unproductive catalyst complexes. It seemed logical that the destabilization of such complexes could have prolonged the activity of the catalyst and provided an improvement in the number of catalytic turnovers.

The discussion of an additional study directed towards hindering the formation of unproductive catalyst complexes, by means of employing differentially substituted diene-amides, follows in the next section.

2.7.4 RCM of Differentially Substituted Diene-amides: Substitution for a Sterically Hindered Disubstituted Double Bond

The failure of the unprotected and *N*-BOC diene-amides **76** and **144** (n = 12) to undergo RCM prompted further study of ring-closure at this position. Considering the terminal double bond closest to the carbonyl, and their respective proximity, it seemed likely that unproductive catalyst complexes of type **I-L** were formed (see Figure 32). The absence of products resulting from any metathesis events suggested that these complexes were highly stable and might be irreversibly formed. Such reactivity would account for the failure of these substrates to undergo RCM.

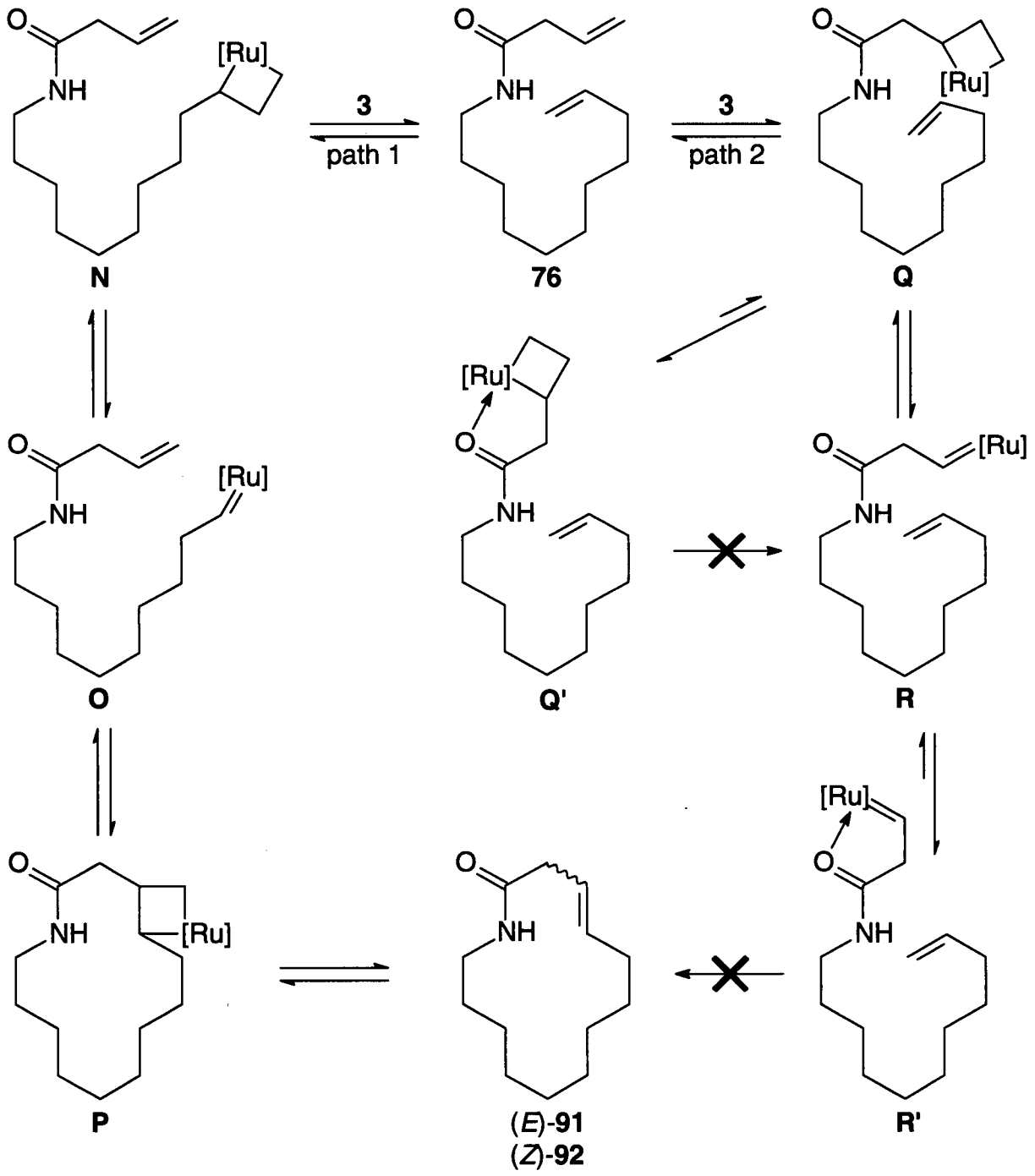

Figure 34. Possible reaction paths for the RCM of diene-amide **76**.

This undesired reactivity was perceived as a problem associated with the site of the first metathesis event. For example, if the first metathesis event occurred at the terminal double bond farthest removed from the amide group, it seemed reasonable that the reaction could proceed to the product lactam, via compounds **N** through **P** (path 1, Figure 34). However, if the first metathesis event occurred at the terminal double bond

closest to the amide group, it seemed likely that the catalyst would become sequestered in unproductive complexes such as **Q'** and **R'** (path 2, Figure 34). Even if some amount of metallacyclobutane **Q** was converted to alkylidene **R**, it seemed reasonable that the catalyst would become sequestered in unproductive complex **R'**.

The unproductive complex formation associated with diene-amide **76** might be disfavoured if the precatalyst was selective toward reaction with the double bond furthest removed from the amide group. It is known that disubstituted olefins undergo intermolecular metathesis at a lower rate than terminal olefins. Accordingly, addition of an alkyl substituent to the appropriate terminal double bond on diene-amide **76** might lead to a regioselective metathesis reaction.[21] Using such a differentially substituted diene-amide, the first metathesis event might be favoured to occur at the terminal double bond over the sterically demanding disubstituted double bond, due to a decrease in the relative rate of the latter, and eventually furnish the desired lactam. This strategy was put into practice by studying the RCM reactions of differentially substituted diene-amides **145** and **148**.

The synthesis of (*E*)-*N*-(10-undecenyl)-3-hexenamide (**145**) required only one step from readily available subunits. Coupling of amine **118** and commercially available (*E*)-3-hexenoic acid according to the method of Mukaiyama and co-workers[98] gave differentially substituted diene-amide **145** in 69% yield (Scheme 20). Recall amine **118** was constructed during the synthesis of diene-amide **76** (see Scheme 8).

Scheme 20. Synthesis of (*E*)-*N*-(10-Undecenyl)-3-hexenamide (**145**)[a]

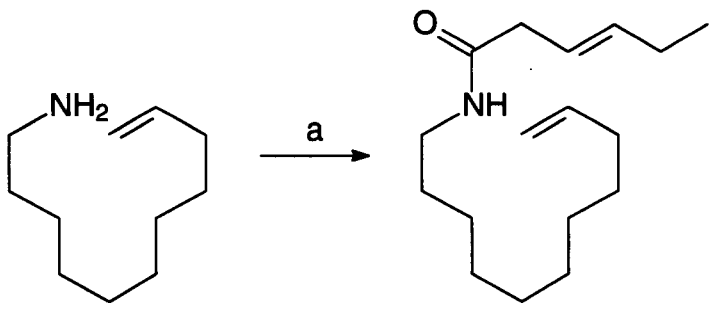

118 **145**

[a]Key: (a) (*E*)-3-hexenoic acid, TEA, 2-chloro-1-methylpyridinium iodide, CH_2Cl_2, 40 °C, 69%.

The primary goal of this study was to determine if ring closure was possible at bond position 12 via RCM of a differentially substituted diene-amide. In addition, exploring the effect of the configuration of the double bond on the RCM of such a substrate was of interest. Accordingly, commercially available (*Z*)-3-hexenol (**146**) allowed entry to (*Z*)-*N*-(10-undecenyl)-3-hexenamide (**148**), the configurational isomer of **145**. Oxidation of alcohol **146** using Jones' reagent gave acid **147** in 90% yield (Scheme 21). Coupling of amine **118** and acid **147** according to the method of Mukaiyama and co-workers[98] gave differentially substituted diene-amide **148** in 58% yield.

Scheme 21. Synthesis of (*Z*)-*N*-(10-Undecenyl)-3-hexenamide (**148**)[a]

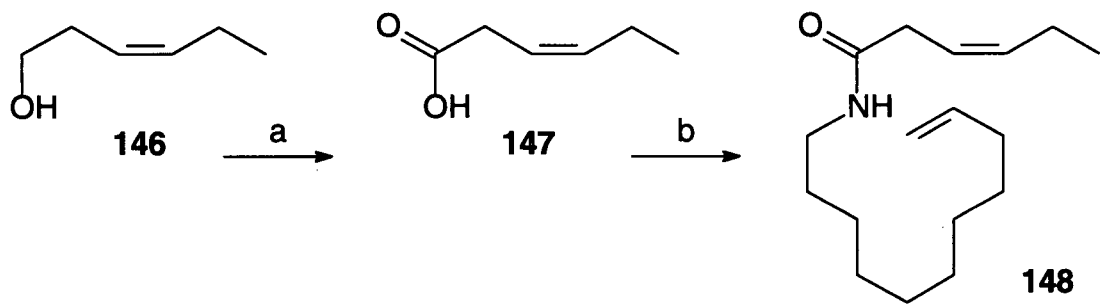

[a]Key: (a) Jones' reagent, acetone, rt, 90%; (b) amine **118**, TEA, 2-chloro-1-methyl-pyridinium iodide, CH_2Cl_2, 40 °C, 58%.

The RCM reactions of differentially substituted diene-amides (*E*)-**145** and (*Z*)-**148** provided the first observed formation of the unsaturated 14-membered lactam isomers **91** and **92** via RCM. Due to the reduction in rate associated with the metathesis of a disubstituted olefin, the reactions of these substrates were conducted under the same RCM reaction conditions applied in the temperature studies (see Section 2.7.2). Separate reactions of diene-amides (*Z*)-**148** and (*E*)-**145** with 5 mol% of precatalyst **3** gave inseparable mixtures of lactams **91** and **92** in 11% and 6% yield respectively (Table 10, Entries 1 and 3). The mixture of **91** and **92** gave satisfactory chemical analysis, and the assignment of both isomers was tentatively based on NMR and mass spectral data. The acyclic dimer was isolated in each case with a yield comparable to that of the lactam products. The significant yield of acyclic dimer was attributed to the temperature applied during these reactions, the effect of which was discussed earlier

(see Section 2.7.2), and to the lower rate of RCM associated with reaction of a disubstituted double bond. Recovery of the starting diene-amide typically constituted the remainder of the mass balance. Repeating these reactions using 20 mol% of **3** gave the lactam products in improved yields (Entries 2 and 4). The improvement in yield of the desired lactam products was greater using (*Z*)-diene-amide **148**, however the reaction of (*E*)-diene-amide **145** led to a more significant increase in the amount of dimeric products. It is worth mentioning that the substrate recovered from the reaction of (*Z*)-diene-amide **148** contained a mixture of **145** and **148**, whereas the substrate recovered from the reaction of (*E*)-diene-amide **145** only contained a small amount of the isomer **148**. The observed *E*/*Z* ratios for the pair of diastereomeric lactams were moderately consistent for each precatalyst loading, however the observed ratios did not correlate with the calculated values, although both favoured (*E*)-**91**.

Table 10. Synthesis of (*E*/*Z*)-2-Azacyclotetradec-12-enones (**91**) and (**92**) via RCM of Diene-amides **145** and **148**[a]

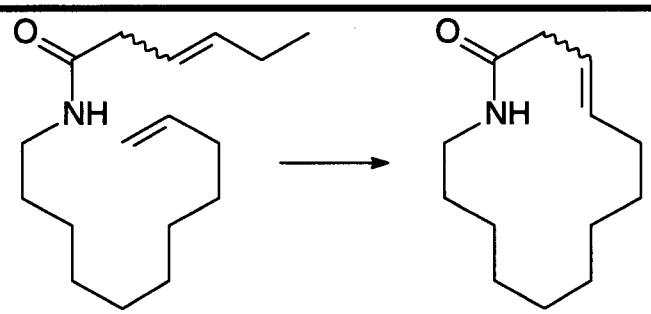

(*E*)-**145** or (*Z*)-**148** (*E*)-**91** and (*Z*)-**92**

Entry	Substrate	mol% **3**	Recovered Substrate		Yield (%)[d]	*E*/*Z*[c]	Calculated *E*/*Z*[e]
			Yield (%)[b]	**145**:**148**[c]			
1	(*Z*)-**148**	5	72	7:93	11 (10)	62:38	99:1
2	(*Z*)-**148**	20	42	44:56	37 (15)	80:20	99:1
3	(*E*)-**145**	5	86	99:1	6 (7)	69:31	99:1
4	(*E*)-**145**	20	52	93:7	11 (34)	77:23	99:1

[a] Separate solutions of diene-amide and **3**, in CH_2Cl_2 at 2.0 mM in total, were added over three hours and stirred at 45 °C for 24 hours.
[b] Recovery after chromatography.
[c] Ratio of isomers was determined by 200 or 500 MHz ^{1}H NMR.
[d] Isolated yield after chromatography, and yield of acyclic dimer in parenthesis.
[e] Calculated using Macromodel 4.5 (see reference 107).

Concurrent to the studies described above, a report describing attempts to form the analogous 13- and 14-membered lactones by similar means appeared. The RCM of diene-esters **149** and **150**, analogous to (*E*)-diene-amide **145**, using ruthenium alkylidene **2** gave 13-membered lactone **151** in 6% yield, and none of the corresponding 14-membered lactone **152** (Figure 35).[44] These results, in conjunction with the RCM of the corresponding diene-amides, illustrated the difficulty associated with the formation of macrocyclic lactones and lactams via RCM of substrates derived from vinylacetic acid and related disubstituted derivatives.

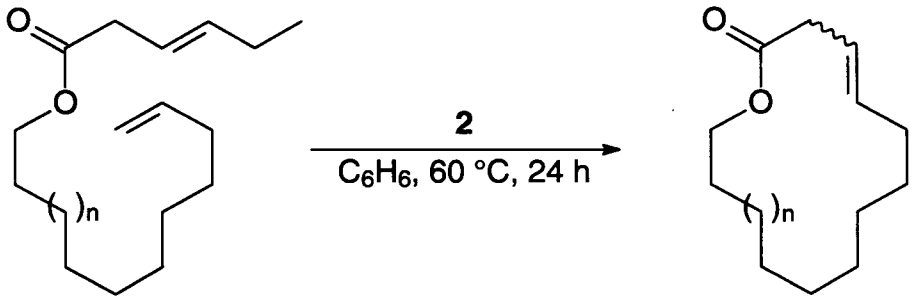

149 (n = 0)
150 (n = 1)

151 (n = 0, 6%)
152 (n = 1, 0%)

Figure 35. RCM of differentially substituted diene-esters **149** and **150** (from reference 44).

To account for the low yields observed in the formation of the macrocyclic lactones and lactams described above, the steric demand of the disubstituted double bond was considered. However, a report on the formation of a tetrasubstituted double bond in high yield via RCM, using a ruthenium based metathesis catalyst,[123] suggested that arguments solely based on steric demand could not account for the extent of the low yields. It seemed more likely that the rate of catalyst decomposition and dimer formation were competitive with the rate of RCM. The rate of the latter can be improved by increasing the catalyst loading,[18] and this effect was observed during our studies (Table 10, Entry 2). The activity of the ruthenium propylidene, the catalytic species in the RCM reactions of the differentially substituted dienes described above, is comparable to that of ruthenium benzylidene **3**. However, the activity of these compounds is lower relative to ruthenium methylidene **4**, the catalytic species in diene metathesis.[10,11] This suggests that the ruthenium propylidene had a negative effect on

the rate of productive metathesis, which is consistent with the low product yields and significant dimer formation observed in the RCM reactions of **145** and **148**.

In addition to the formation of lactams **91** and **92**, one of the more interesting observations was the higher yield associated with the RCM of (*Z*)-diene-amide **148**, in comparison to the isomer (*E*)-**145**. Also, the recovery of a mixture of isomeric diene-amides suggested that the starting material underwent isomerization, and to a more significant extent when using (*Z*)-**148**. These observations suggested that precatalyst **3**, or more specifically the substrate alkylidene, was more reactive towards (*Z*)-**148** than to (*E*)-**145**, and the greater strain associated with a (*Z*)-alkene might account for the observed difference in reactivity. The strained vinyl carbon atoms in a (*Z*)-alkene possess more *s* character, thus making these atoms more electronegative relative to the analogous carbon atoms in an (*E*)-alkene.[133] Reaction with a more electron rich olefin might facilitate a metathesis event, when the electron deficient nature of the ruthenium atom in precatalyst **3** is considered.

Since the products from the RCM reactions of (*E*)-**145** and (*Z*)-**148** are the same, it seemed reasonable that the difference between the observed product yields might be reflected in the difference between the free energy of the diene-amide substrates (equation 2).[31] Making the assumption that the entropy associated with each diene-amide was identical simplified the calculation, and presumes that the difference between the free energy of these compounds was primarily reflected in the difference between the enthalpy (equation 3). It is worth noting that the rigor and accuracy of this analysis is questionable since these reactions do not reach an equilibrium and the entropy changes are not necessarily equivalent. Molecular mechanics calculations were performed on compounds (*E*)-**145** and (*Z*)-**148** using the MM3* force field. The enthalpy of (*E*)-**145** was 3.2 kJ/mol lower than that for (*Z*)-**148**. The lower energy associated with (*E*)-**145** correlated with the lower yield observed using this substrate. Although a more rigorous analysis might provide more accurate results, it is interesting to note that the differences between the calculated enthalpies correlated with the relative facility of RCM within a diastereomeric pair of differentially substituted diene-amides.

$$\Delta G^{\circ}_{Z}(\mathbf{148}) - \Delta G^{\circ}_{E}(\mathbf{145}) = [\Delta H^{\circ}_{Z}(\mathbf{148}) - T\Delta S^{\circ}_{Z}(\mathbf{148})] - [\Delta H^{\circ}_{E}(\mathbf{145}) - T\Delta S^{\circ}_{E}(\mathbf{145})] \quad (2)$$

$$\Delta G^{\circ}_{Z}(\mathbf{148}) - \Delta G^{\circ}_{E}(\mathbf{145}) = \Delta H^{\circ}_{Z}(\mathbf{148}) - \Delta H^{\circ}_{E}(\mathbf{145}) \quad (3)$$

The addition of an alkyl substituent to the appropriate terminal double bond of diene-amide **76** gave differentially substituted diene-amides (*E*)-**145** and (*Z*)-**148**. Cyclization of these substrates via RCM led to the first observed formation of unsaturated 14-membered isomeric lactams **91** and **92** via RCM. Although this study provided the only conditions and structural modifications that allowed formation of these lactams, the significance of these results was diminished due to the low yield and significant amount of acyclic dimer formed. Additional studies and approaches to this problem are required to allow entry to macrocyclic lactams of this type in more reasonable yields and lower precatalyst loading.

2.8 Reactivity of Selected Unsaturated 14-Membered Lactams with Ruthenium Methylidene 4

Subsequent to the RCM studies discussed in the preceding sections, the focus of our efforts shifted from the formation of 14-membered lactams via RCM to a rationalization of the observed *E*/*Z* ratios resulting from these reactions. The implications of the isomerized diene substrates, recovered from the RCM reactions of differentially substituted diene-amides (*E*)-**145** and (*Z*)-**148**, to such a rationalization was significant. These results suggested that the factors governing the observed *E*/*Z* ratios from the RCM reactions might include isomerization of the resulting isomeric lactams by reaction with either precatalyst **3** or the active form of the catalyst, ruthenium methylidene **4**. This, in conjunction with the formation of dimeric and oligomeric material, significantly complicates this analysis from either a thermodynamic or kinetic perspective. It is generally accepted that the formation of a metallacyclobutane intermediate occurs via a [2+2] cycloaddition, and its subsequent breakdown to a newly formed metal alkylidene via a cycloreversion process. These processes likely occur in a concerted manner, however a stepwise mechanism would further complicate the issue. Upon consideration of the factors governing the observed product isomer distribution, preliminary studies were conducted that focussed on isomerization of selected lactam

products either using precatalyst **3** or the active form of the catalyst, ruthenium methylidene **4**.

Ring opening of the unsaturated 14-membered lactams was anticipated to be unfavourable for two reasons. One was suggested by the poor reactivity of the disubstituted diene-amides, which was discussed in the preceding section. The second is a two-fold thermodynamic argument. Ring opening would involve an unfavourable decrease in entropy, the formation of one molecule from two. In terms of enthalpy, ring strain is a driving force for ring opening. However, the lack of significant ring strain associated with the 14-membered lactams would also disfavour ring opening. Exposure of lactam (*E*)-**82** to 5 mol% of precatalyst **3** for 6 hours gave only the starting lactam in 78% recovery (Table 11, Entry 1). This experiment did not lend credence to the expected reactivity of the lactams since oligomer formation likely constituted the remainder of the mass balance, but this was not confirmed. A similar lack of reactivity was reported using Schrock's alkylidene **1**[112] and precatalyst **3**[46] in the attempted ring opening of macrocyclic ethers. Since ruthenium methylidene **4** was involved in the catalytic cycle of the RCM reactions, it seemed appropriate to use it for these studies. Accordingly, ruthenium methylidene **4** was synthesized by bubbling ethylene gas into a solution of precatalyst **3** in dichloromethane. In a matter of minutes the solution changed colour from purple to black, indicating the reaction was complete. This mixture was sparged with nitrogen to remove the dissolved ethylene that could affect the outcome of the isomerization experiments. This solution was directly added to a solution of the lactam in dichloromethane. Exposure of lactam (*E*)-**82** to 5 mol% of **4** for 20 hours gave a mixture of lactams (*E*)-**82** and (*Z*)-**83** in 86% yield (GC ratio, 82:18), and cyclic dimeric products in 14% yield (Entry 2). This reaction was repeated at ten times the concentration (0.02 M) and gave an increased amount of cyclic dimeric products, and the same ratio of lactam isomers (Entry 4). In comparison, the analogous RCM reactions of diene-amide **71** also gave significant amounts of cyclic dimeric products, but different *E*/*Z* ratios for the lactam products (Entries 3 and 5).

Table 11. Ruthenium Catalyzed Isomerization of Lactam (*E*)-**82**

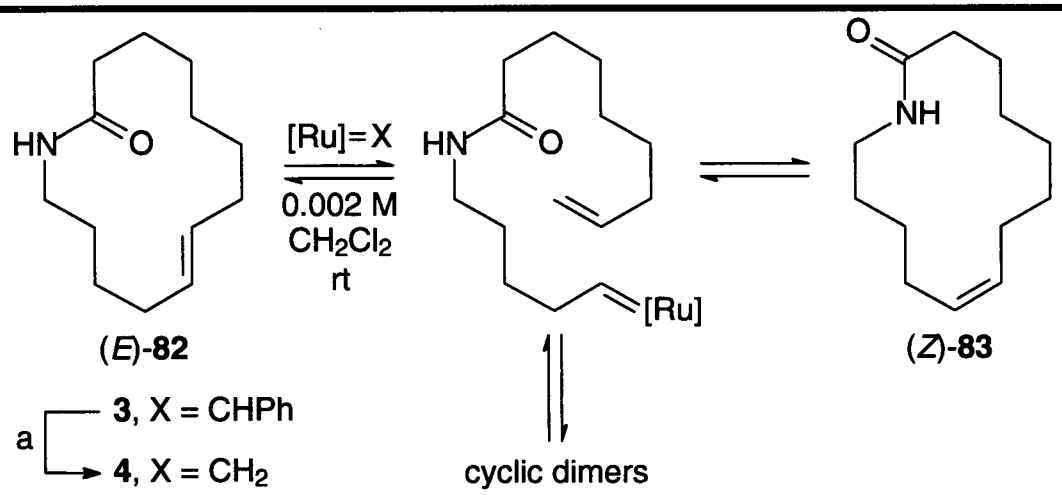

Entry	Substrate	X (mol%)	t (h)[b]	Yield (%)[c] (*E*)-**82**	(*Z*)-**83**	cyclic dimers	Ratio **82**:**83**[d]
1	(*E*)-**82**	CHPh (5)	6	78	0	0	100:0
2	(*E*)-**82**	CH_2 (5)	20	71	15	14	82:18
3	diene **71**	CHPh (5)	25	42	37	19	53:47
4	(*E*)-**82**[e]	CH_2 (5)	20	39	9	31	79:21
5	diene **71**[e]	CHPh (5)	4	26	20	54	56:44

[a] Grubbs' benzylidene **3**, ethylene, CH_2Cl_2, rt. Sparged with nitrogen prior to use.
[b] Ruthenium species in CH_2Cl_2 added immediately to lactam in CH_2Cl_2 (2.0 mM).
[c] Isolated yield after chromatography.
[d] Ratio of isomers was determined by GC.
[e] Reaction conducted at a concentration of 0.02 M.

Somewhat similar results were obtained using lactam (*Z*)-**80**. In comparison to the exposure of lactam (*E*)-**82** to 5 mol% of precatalyst **3**, exposure of lactam (*Z*)-**80** to 5 mol% of precatalyst **3** under an ethylene atmosphere for 30 minutes and then stirring under nitrogen for a total of 6 hours gave diene-amide **70** in 24% yield, cyclic dimers in 14% yield, and recovered (*Z*)-**80** in 60% yield (Table 12, Entry 1). This example clearly illustrated the necessity to purge the catalyst mixture of ethylene prior to addition to the lactam. Furthermore, the production of diene-amide **70** was consistent with previous observations (See Table 4, Entry 7). Exposure of lactam (*Z*)-**80** to 5 mol% of **4** for 20 hours gave a mixture of lactams (*Z*)-**80** and (*E*)-**81** in 88% yield (GC ratio, 83:17), and

cyclic dimeric products in 12% yield (Entry 2). In comparison, the observed *E*/*Z* ratios from the analogous RCM reaction of diene-amide **70** were similar, however products arising from dimerization processes were not observed (Entry 3).

Table 12. Ruthenium Catalyzed Isomerization of Lactam (*Z*)-**80**

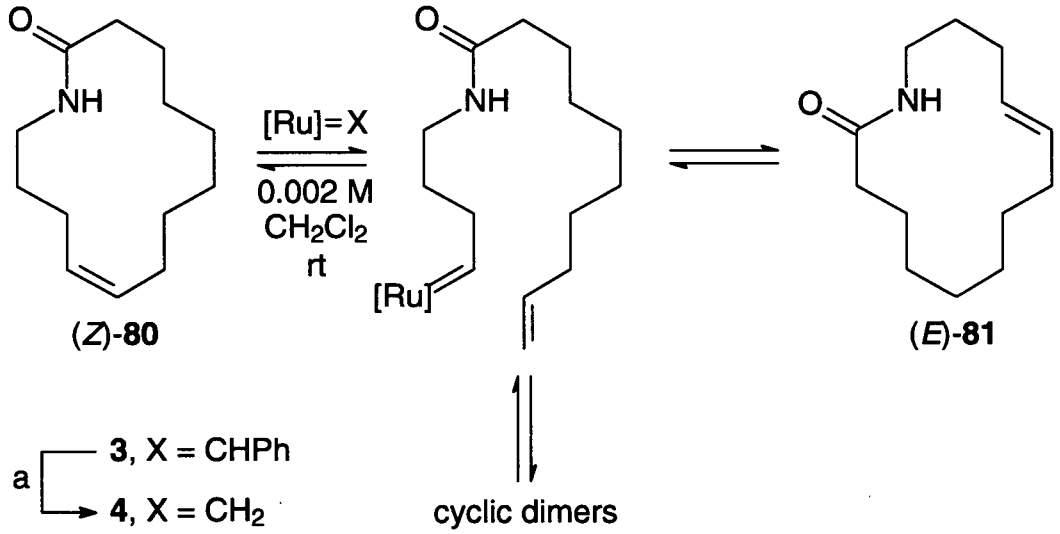

Entry	Substrate	X (mol%)	t (h)[b]	Yield (%)[c] (*Z*)-**80**	(*E*)-**81**	cyclic dimers	Ratio **80**:**81**[d]
1	(*Z*)-**80**[e]	CHPh (5)	6	60	0	14 (24)	100:0
2	(*Z*)-**80**	CH_2 (5)	20	73	15	12	83:17
3	diene **70**	CHPh (5)	22	39	8	0 (39)	84:16

[a] Grubbs' benzylidene **3**, ethylene, CH_2Cl_2, rt. Sparged with nitrogen prior to use.
[b] Ruthenium species in CH_2Cl_2 added immediately to lactam in CH_2Cl_2 (2.0 mM).
[c] Isolated yield after chromatography, and recovered diene in parenthesis.
[d] Ratio of isomers was determined by GC.
[e] Reaction conducted under ethylene atmosphere for 30 minutes.

These preliminary studies illustrated that exposure of unsaturated 14-membered lactams (*Z*)-**80** and (*E*)-**82** to ruthenium methylidene **4** resulted in isomerization of the lactam and formation of cyclic dimeric products. It is worth mentioning that in contrast to our observations, a 14-membered lactam analogous to (*Z*)-**87** did not react with the methylidene form of Schrock's alkylidene **1**, which was pre-treated with ethylene.[24c] When followed by TLC none of the dimeric products were observed up to five hours,

and isomerization was not observed up to three hours, when followed by GC. The RCM of a diene-amide (n = 7, 8, and 9) uninhibited by catalyst complex formation proceeds faster than these ring opening processes. A report of the isomeriation of a *Z,Z*-disilanyl analogue of 1,5-cyclooctadiene to the *E,E*-isomer, over 15 days using a ruthenium hydride complex, suggests that these ring opening and isomerization processes are slow.[134]

The low rate of dimerization was reflected in the RCM of selected diene-amides. For example, the RCM reaction of diene-amide **71**, conducted over 7 hours, gave only the corresponding lactam products (*E*)-**82** and (*Z*)-**83**, whereas the same reaction conducted over 25 hours led to the formation of a significant amount of cyclic dimeric products (see Table 6, Entries 2 and 3). However, the observed *E/Z* ratios were nearly identical. In contrast, the sluggish RCM of diene-amide **70**, conducted over 22 hours, gave only the lactam products (*Z*)-**80** and (*E*)-**81**. These observations, in conjunction with the isomerization experiments, suggested that isomerization and dimerization processes catalyzed by the ruthenium methylidene **4** mediated ring opening of the lactam products were slow, and could be avoided by adjusting the reaction time to the rate of RCM. In other words, RCM reactions that proceed to completion in less than 10 hours should be terminated, by the addition of air or triethylamine, to avoid undesired dimerization and isomerization processes that affect the lactam products. Those RCM reactions requiring prolonged reaction times due to the low rate of cyclization likely do not encounter these processes.

In summary, preliminary studies into the isomerization of selected unsaturated lactams with ruthenium methylidene **4** illustrated the formation of configurational isomers and cyclic dimeric products. It appeared that these processes were slow relative to RCM cyclization, and thus could be avoided by carefully monitoring the RCM reactions of diene-amides. These studies also suggested the observed *E/Z* ratios from RCM resulted from a combination of thermodynamic and kinetic factors. Kinetic factors would predominate with shorter reaction times. The thermodynamic process, involving the reaction of a newly formed lactam with **4**, was more likely to occur for reactions with prolonged reaction times. This was particularly true for reactions that were not quenched after completion.

2.9 Rationalization of Yield Obtained During RCM Studies

The factors governing RCM cyclization must be considered to rationalize the yields observed from the RCM reactions of diene-amides **68-76**, (*E*)-**145**, and (*Z*)-**148**. Since 1994, numerous reports have illustrated the facile formation of macrocyclic compounds via RCM, and initial reports suggested that the presence of stereogenic centres were needed for ring closure to occur readily.[24c] However, reports to the contrary, including the studies discussed herein,[72] illustrated the facile ring closure of conformationally mobile and unbiased diene substrates via RCM. Although stereogenic centres,[24c,31] intramolecular hydrogen bonding,[26,27] and chelation effects[135] might constrain the diene olefins to be in a proximity that facilitates RCM, such forms of conformational constraint and predisposition are not required.

The results discussed herein suggested one of the key factors governing the RCM formation of 14-membered lactams involved the proximity of the amide group to the terminal double bonds. The proximity effect might be related to the relative enthalpies of ring closure, the relative energies of the lactam products with respect to the position of the olefin, and the formation of unproductive catalyst complexes (see Figure 32).

The enthalpy change for ring closure at each site was calculated using equation 4 and gave the difference in energy between the global minimum energy conformations for diene-amides **68-76**, (*E*)-**145**, and (*Z*)-**148**, and the corresponding lactam products, including the formation of ethylene (Table 13). For the isomeric lactams at each olefin position, the lower energy configurational isomer was used for the calculations (see Section 2.6, Table 5). These calculated enthalpies of ring closure were used as an estimation of the free energies of ring closure ($\Delta S = 0$). Few correlations could be drawn between the enthalpy changes and the observed yields, however the decrease in enthalpy of ring closure for the series of diene-amides **76**, (*E*)-**145**, and (*Z*)-**148**, all equivalent in ring closing position, were reflected in the observed yields from RCM. In contrast, a similar analysis comparing the formation of bridged bicycloalkenes of different ring sizes did provide correlations between the enthalpies of ring closure and observed yield.[136]

$$[\Delta G^{\circ}\,(\text{lactam}) + \Delta G^{\circ}\,(\text{ethylene})] - \Delta G^{\circ}\,(\text{diene}) \cong [\Delta H^{\circ}\,(\text{lactam}) + \Delta H^{\circ}\,(\text{ethylene})] - \Delta H^{\circ}\,(\text{diene}) \quad (4)$$

Table 13. Ring Sizes of Unproductive Catalyst Complexes, Enthalpies of Ring Closure, and Relative Lactam Energies for RCM of Diene-amides **68-76**

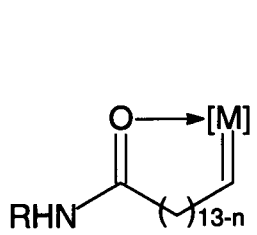

K

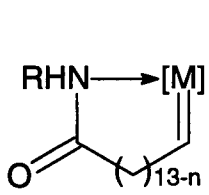

L

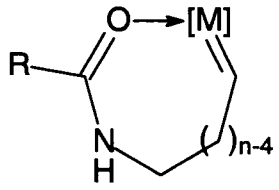

K'

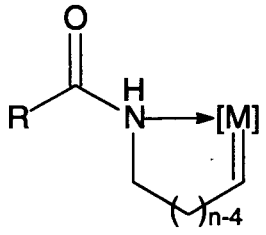

L'

Position (n)	Yield[a] (%)	Ring size: carboxyl alkylidene complex		Ring size: amino alkylidene complex		$\Delta H^{b,c}$ (kJ/mol)	Relative Energy[b,c] (kJ/mol)
		K	**L**	**K'**	**L'**		
4	7	13	13	6	4	19.0	0.0
5	32	12	12	7	5	14.3	18.0
6	47	11	11	8	6	18.5	2.4
7	86	10	10	9	7	18.0	5.4
8	87	9	9	10	8	15.5	3.2
9	74	8	8	11	9	17.5	5.5
10	39	7	7	12	10	15.1	3.4
11	11	6	6	13	11	15.7	5.8
12	0	5	5	14	12	12.1	27.3
12*E*[d]	6 (11)	5	5	14	12	11.5	27.3
12*Z*[d]	11 (37)	5	5	14	12	8.2	27.3

[a] Isolated yield of analytically pure material after chromatography, and yield when using 20 mol% **3** in parenthesis.
[b] Calculated using Macromodel 4.5 (see reference 107) and equation 4.
[c] Refer to Table 5 for the most stable isomer at each site of ring closure.
[d] RCM of differentially substituted diene-amide (*E*)-**145** or (*Z*)-**148**.

A comparison between the relative energies of the products in the series, differing in the position of the olefin within the ring, and the observed yields provided a stronger basis for a rationalization (Table 13). Similar to the calculations described above, the lower energy configurational isomer at each bond position was used. Although a general trend was not observed, the low yields observed at positions 5 and 12 in relation to the higher yields observed at positions 7, 8, and 9 correlate with the

relative energies of the products. The remaining positions in this set of calculated data did not correlate with the observed trend in yield (n = 4, 6, 10, and 11). A similar analysis was used to rationalize the contrast in efficiency between the RCM formation of two eight-membered cyclic ethers, differing only in the position of the olefin.[137] This analysis lends credence to our contention that the relative transition state energies for ring formation might be reflected in the relative strain energies of the lactam products (see Section 2.6). The calculated enthalpies of ring closure illustrated the endothermic nature of the reactions in this series, further suggesting a product-like transition state.

Often the melting point of a cyclized product directly correlates with the cyclization yield.[51] This in turn reflects the stability of the compound. It is interesting to note that such correlations were not observed between the product yields and lactam melting points within this series. Furthermore, correlations were not observed between each enthalpy of cyclization, or relative product energy, and the lactam melting point. It seems likely that factors beyond the relative stability of the lactam products governed the observed trend in yield throughout the series.

A more significant factor governing the RCM formation of 14-membered lactams appeared to be the formation of unproductive catalyst complexes. Complex formation might occur between the amide group and either the carboxyl alkylidene (type **K** and **L**), or the amino alkylidene (type **K'** and **L'**). The analogous metallacyclobutane complexes of type **I** and **J** (see Figure 32) were omitted to simplify the analysis, but each would lead to the same complex ring size. A general trend was observed upon comparison between the catalyst complex ring size and the observed yields (Table 13). This comparison suggested that complexes of seven-members or smaller, contained within the dashed lines in Table 13, might retard the catalytic process or stall it altogether, and the degree of which depends on the stability associated with the ring size. Trends that correlate ring size and stability are well documented,[138] and presumably the observed yields from the RCM reactions reflect a similar trend in the relative stability of the catalyst complexes. For example, the trend of decreasing yield observed upon ring closure at positions 9 through 12 might be reflected in the increasing stability of the eight- to five-membered catalyst complexes of type **K** and/or **L** respectively. A similar trend was observed at positions 7 through 4 with complexes of type **K'** and **L'**, however the contributions involving either N or O atom co-ordination differ within each ring closing position due to the different ring sizes of the complexes. For instance, a

comparison of yield between positions 7 (86%) and 6 (47%) suggested that a seven-membered complex of type **L'** affected the reaction very little, but the effect of the corresponding six-membered complex was presumably stronger and led to a reduction in yield. In the preceding analysis it was assumed that complexes of eight- to eleven-members (of types **K**, **K'**, and **L**, where n = 6 and 7) had no impact on the reactions. Throughout the series of RCM reactions these trends were consistently observed.

The relative basicity of the amide nitrogen and carbonyl oxygen atoms was also reflected in the yields observed from the RCM reactions. Semi-empirical calculations suggested that the net atomic charge at the nitrogen atom was slightly greater than the carbonyl oxygen for diene-amide **70** (see Figure 33). Therefore, catalyst complexes with nitrogen atom co-ordination were anticipated to be more stable, due to the greater electron donating ability, and thus have a more significant affect on the RCM reactions than the carbonyl oxygen complexes. However, the oxygen complexes appeared to affect the reactions more significantly. Recall that the seven-membered nitrogen complex **L'** proposed for position 7 had little effect on the reaction based on the observed yield of 86%. In contrast, at position 10 the seven-membered oxygen complex **K** must have significantly affected the reaction based on the observed yield of 39%. This assumes the analogous seven-membered nitrogen complex **L** at position 10 had little effect on the reaction. Although the net atomic charge was calculated to be greater on the nitrogen atom (see Figure 33), the observations described above suggest that oxygen complexes of type **K** and **K'** had a more significant affect on the RCM reactions.

The preceding analysis suggested that the formation and stability of unproductive catalyst complexes predominantly governed the trend in yield observed from the RCM of diene-amides **68-76**. The stability of such complexes was directly related to the relative position of the amide group to the terminal double bonds. However, at sites of ring closure far removed from the amide group the effects of such complexes were negligible and the enthalpy of ring closure and relative product stability might play a more significant role in the efficiency of ring closure.

These studies constitute the first systematic study of a single ring size exploring nine contiguous sites of ring closure via RCM. Future applications of the RCM reaction

towards the formation of macrocyclic lactams would benefit from maximizing the distance between the terminal double bonds and the amide group.

In a report on their efforts towards the total synthesis of sarain A, Weinreb and co-workers recently encountered these proximity effects, illustrating the relationship between the site of ring closure and the observed yield.[139] The construction of the "western" macrocyclic ring via RCM was attempted with three different diene-amide substrates corresponding to three different sites of ring closure (Figure 36). Steric and conformational effects, and the formation of unproductive catalyst complexes presumably were factors governing cyclization of these substrates. The contrast in yield between positions 8 and 9, analogous to positions 9 and 10 in our studies, might be explained by the formation of such complexes and their relative stability.

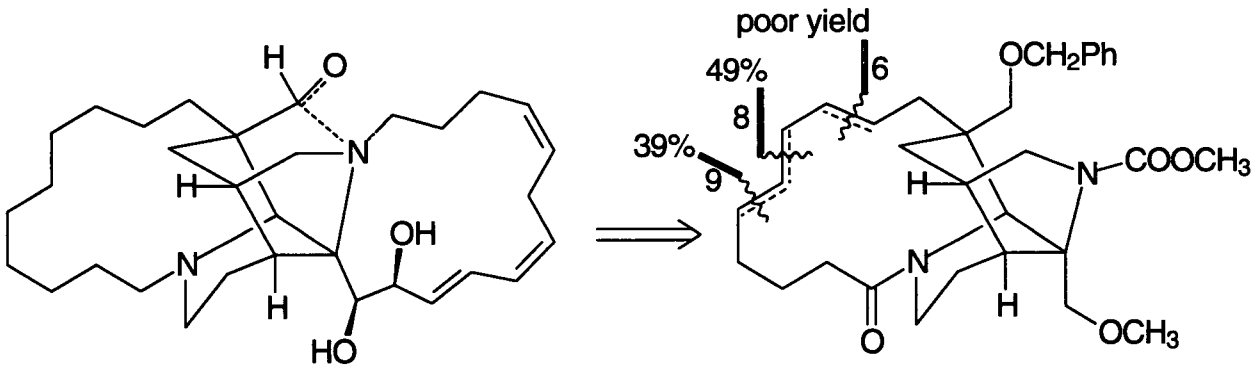

Figure 36. Sarain A, and sites of RCM formation of the "western" macrocyclic precursor (from reference 139).

2.10 Attempts to Rationalize the *E/Z* Ratios Obtained During the RCM Studies

Since the onset of our studies the application of RCM in the synthesis of macrocyclic compounds from diene substrates has become a practical and reliable method. The reaction conditions and substrate requirements have been well established. However, issues regarding the selectivity, or lack thereof, in the configuration about a newly formed disubstituted olefin has received little attention. This fundamental aspect of macrocycle formation via RCM is particularly unappealing when applied to the synthesis of compounds which necessitate the formation of a specific olefin stereochemistry at the site of ring closure. In some cases exclusive formation of a

specific configuration was observed upon formation of a trisubstituted double bond, however the ability to predict or control the resulting olefin configuration of a disubstituted olefin has yet to be established.

Epothilones A and B are perhaps the two most identifiable natural products to which RCM was applied in a total synthesis.[57] These compounds possess a macrocyclic lactone skeleton, and the construction of this ring via RCM was complicated by the formation of a mixture of olefin isomers. Although the formation of unnatural isomers might lead to a better understanding of the structure and activity of the natural product, it detracts from the appeal of the synthetic method. However, ring closure at a site that eventually becomes saturated simplifies the issue since the mixture, in whatever ratio, can be reduced by hydrogenation. In many cases this is not possible, and understanding the factors governing the observed *E*/*Z* ratio would be extremely valuable, and may eventually lead to the ability to control or at least predict the stereochemical outcome.

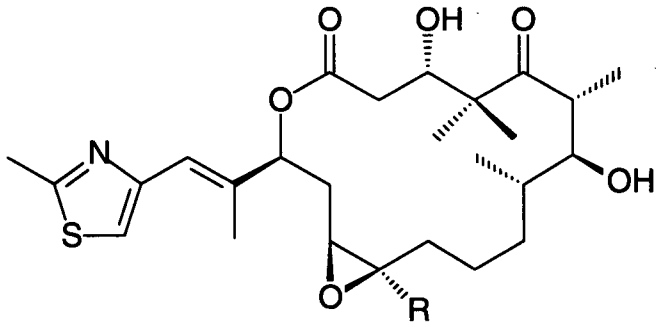

epothilone A (R = H)
epothilone B (R = CH_3)

The geometry of the olefin resulting from a RCM reaction depends on the process by which the metallacyclobutane intermediate is formed and cleaved. The cycloaddition reaction between a ruthenium alkylidene and a double bond, as well as the cycloreversion step, is believed to be a concerted process. This would suggest that the stereochemical determining event is the formation of the metallacyclobutane intermediate. Formation of the *anti*-intermediate would give the (*E*)-alkene exclusively upon productive cleavage of the ring, and similarly the *syn*-intermediate would give the (*Z*)-alkene (Figure 37). One of the factors governing this event involves the relationship

between the substituents on the ring. The *anti*-intermediate, leading to the (*E*)-alkene, is usually favoured due to the minimization of unfavourable steric interactions.[17]

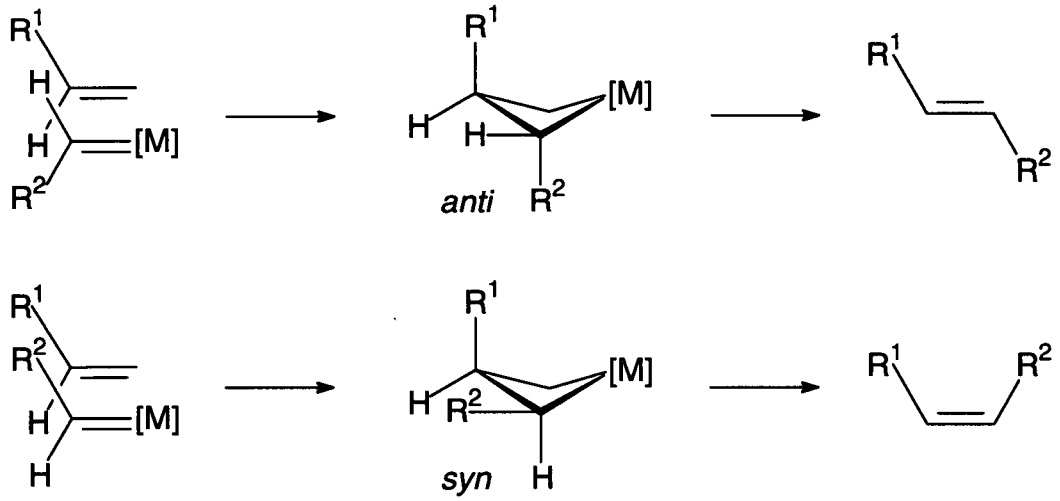

Figure 37. Concerted formation of (*E*)- and (*Z*)-alkenes from the corresponding *anti*- and *syn*-metallacyclobutane intermediates.

Rationalizing the stereochemical outcome if the reaction occurs in a stepwise manner is more difficult. Even if the metallacyclobutane intermediate forms in a concerted manner, stepwise cleavage gives a zwitterionic intermediate which can undergo bond rotation leading to an isomeric mixture of alkene products (Figure 38). Although the [2+2] cycloaddition reaction is commonly regarded as a concerted process in RCM, and will be assumed as such for this analysis, the possibility of a stepwise mechanism cannot be ignored.

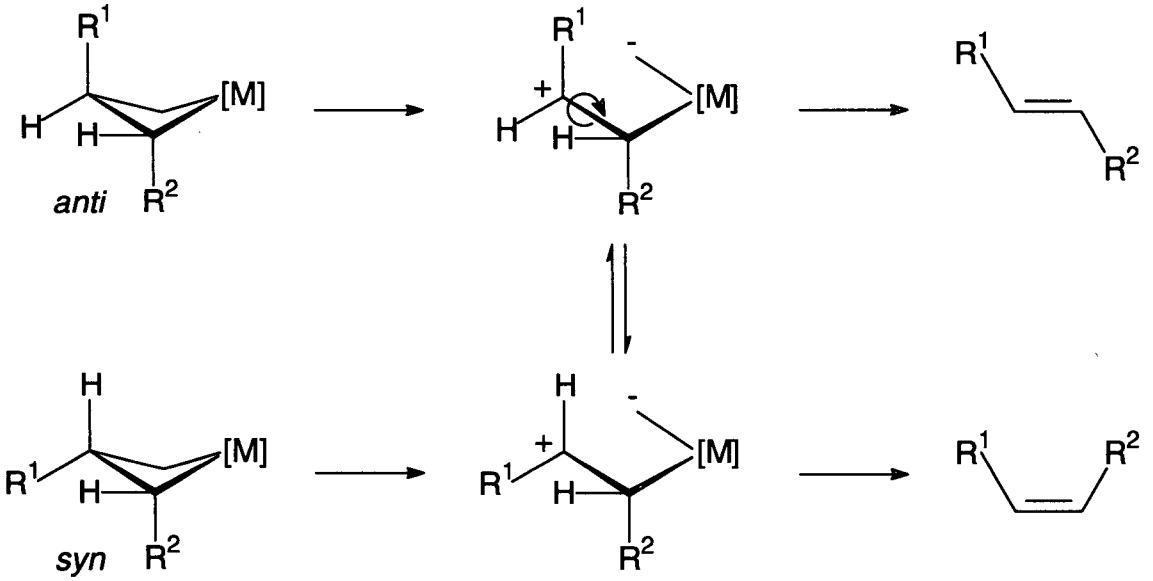

Figure 38. Stepwise formation of (*E*)- and (*Z*)-alkenes from *anti*- and *syn*-metallacyclobutane intermediates.

Another factor governing the stereochemical determining event might be conformational in origin. Although formation of the *anti*-metallacyclobutane intermediate might be favoured, the conformation of the incipient ring may dictate the outcome of this event. A simple analysis of the RCM formation of lactams (*Z*)-**85** and (*E*)-**89** illustrates this point (Figure 39). For the moment, assume the intermediates are biased to adopt the same conformation. The formation of (*Z*)-**85** might require the metal alkylidene to preorganize the conformation of the incipient ring. Formation of the *syn*-metallacyclobutane intermediate, through the lowest energy transition state, followed by productive cleavage would give (*Z*)-lactam **85**. The formation of (*E*)-**89** might require a similar conformational preorganization to give the *anti*-metallacyclobutane intermediate, through the lowest energy transition state, and subsequent cleavage to give (*E*)-lactam **89**. This analysis does not account for the contribution from other low energy conformations, but it does provide a basis for further analysis. This preliminary analysis suggests that the *E*/*Z* ratio observed from the RCM formation of an unsaturated 14-membered lactam depends on the site of ring closure, and the requirement for the diene substrate to adopt a conformation favouring the lowest energy transition state.

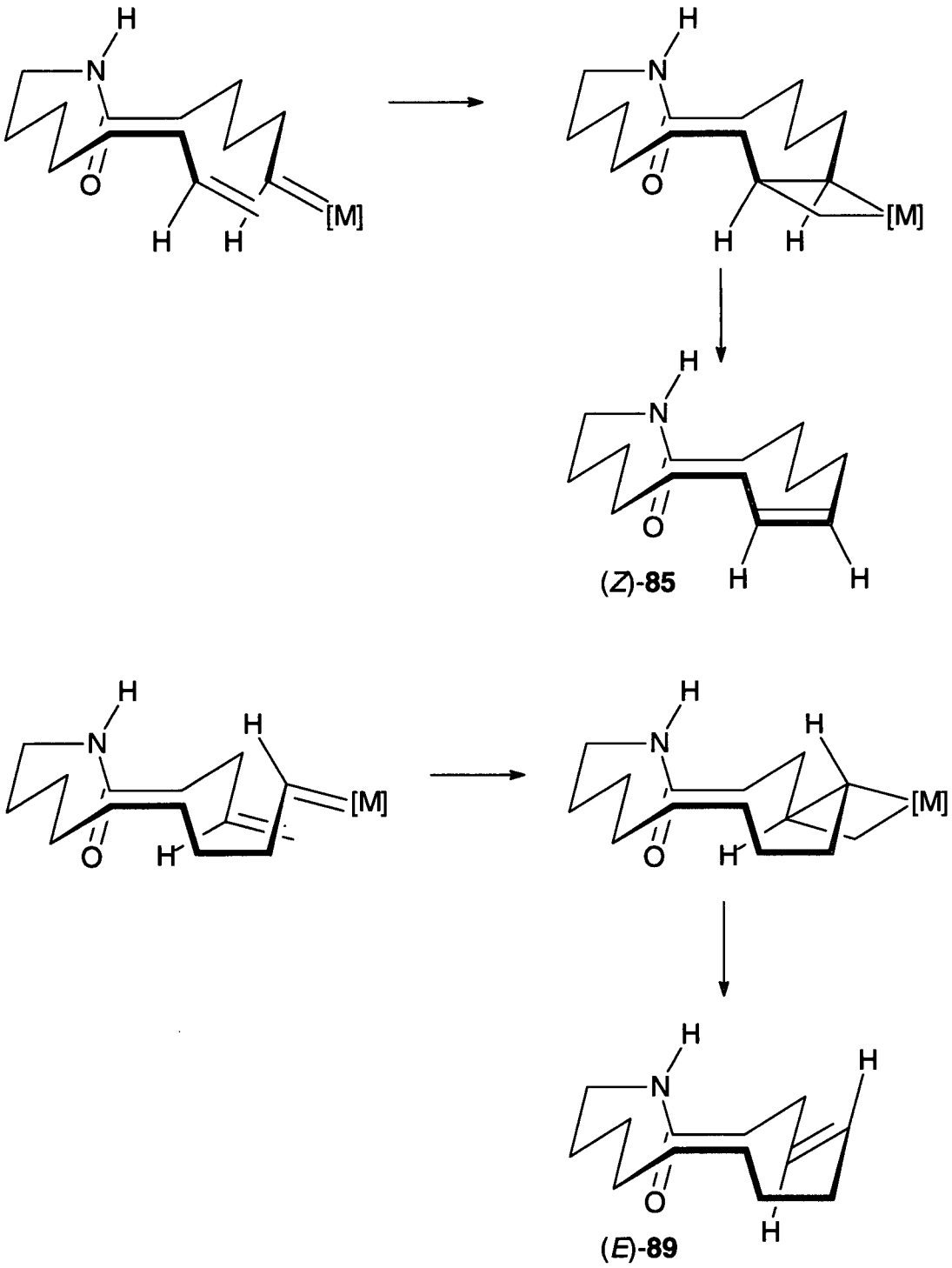

Figure 39. Conformational control involved in the RCM formation of lactams (*Z*)-**85** and (*E*)-**89**.

Attempts to rationalize the stereochemical outcome from the RCM reactions of diene-amides **68-76**, (*E*)-**145**, and (*Z*)-**148** were based on relative product energies from molecular mechanics calculations, and concepts from the preceding analyses. Due to

the transient nature of the metallacyclobutane intermediate, data concerning the conformation of the macrocyclic ring at this stage in the mechanism was not obtained. In fact, Grubbs and co-workers have never observed this intermediate that precedes cyclization.[115] However, in accord with the Curtin-Hammett principle[140] productive metathesis occurs selectively through the lowest energy transition state in the first cycle.[17] It is conceivable that the relative transition state energies for the formation of the *anti*- and *syn*-metallacyclobutane intermediates might be reflected in the relative energies of the (*E*)- and (*Z*)-lactam products. To explore this possibility, calculated *E*/*Z* ratios based on the energy difference between molecular mechanics calculated global minimum energy conformations for each pair of isomeric lactams (**77**-**92**) were obtained (see Section 2.6, Table 5). Comparison of the calculated *E*/*Z* ratios with those observed from the RCM reactions revealed moderate to very high correlation (Table 14). In those cases that compared moderately well (n = 4, 5, 11, and 12) the calculated ratios favoured the major isomer obtained from RCM. From this comparison it appeared that the relative transition state energies were reflected in the relative product energies.

The moderate correlation between the calculated and observed ratios for the bond positions near the amide warranted further analysis. A more detailed calculation of the *E*/*Z* ratios included an ensemble of several low energy conformations for each structure, up to 8.368 kJ/mol (2 kcal/mol) above the global minimum energy. This was in contrast to the previous calculations that merely compared the global minimum energy conformations. The contributions from these low energy conformations were calculated using the Boltzmann distribution law for noninteracting molecules (equation 5). In this equation, N_s represents the number of molecules in molecular state (conformation) s, ε_s is the energy of the molecular state (conformation) s, and k is the Boltzmann constant (1.38066×10^{-23} J K^{-1}).[141] The Boltzmann distribution expression was used to weight the contribution from each conformation, and a weighted enthalpy was calculated using equation 6. These calculated enthalpy values were used as an estimation of the relative free energy between the pairs of diastereomers ($\Delta S = 0$), and the ratio of the isomeric products for each bond position was calculated using equation 1 (see Section 2.6). The calculated *E*/*Z* ratios, taking into account the weight associated with each conformation, were either comparable to the ratios calculated using the global minimum energy conformations, or deviated further from the experimental ratios (Table 14). In contrast to the previous calculations, the more

detailed calculations, which account for the contributions from low energy conformations, did not provide any further insight into the observed *E*/*Z* ratios from the RCM reactions. The effect of solvent on the observed ratios, and the absence of solvation in either set of calculated ratios, might account for the discrepancy observed in some cases.

$$\frac{\langle N_s \rangle}{N} = \frac{e^{-\varepsilon_s/kT}}{\sum_r e^{-\varepsilon_r/kT}} \tag{5}$$

$$\Delta H^\circ = \sum_r \frac{\langle N_r \rangle}{N} \Delta H_r^\circ \cong \Delta G^\circ \tag{6}$$

Table 14. Calculated and Experimental *E*/*Z* Ratios for Lactams **77-92** from the RCM of Diene-amides **68-76**, (*E*)-**145**, and (*Z*)-**148**

			Calculated *E*/*Z* from conformations:		
Position (n)	Product(s) (*E*/*Z*)	Experimental *E*/*Z*[a]	Global minimum[b]	< 8.368 kJ/mol[b,c]	Saturated Lactam[d]
4	**77**/–	>99:1	63:37	53:47	92:8
5	**79**/**78**	72:28	95:5	95:5	79:21
6	**81**/**80**	16:84	16:84	18:82	34:66
7	**82**/**83**	54:46	48:52	47:53	50:50
8	**84**/–	>99:1	97:3	98:2	94:6
9	**86**/**85**	58:42	57:43	64:36	43:57
10	**88**/**87**	11:89	17:83	21:79	33:67
11	**89**/**90**	80:20	99:1	99:1	85:15
12			99:1	99:1	84:16
12*E*[c]	**91**/**92**	77:23	99:1	99:1	84:16
12*Z*[c]	**91**/**92**	80:20	99:1	99:1	84:16

[a] Ratio of isomers were determined by GC, 500 MHz ^{1}H NMR, or by chromatographic separation.
[b] Calculated using Macromodel 4.5 (see reference 107).
[c] Calculated in part using equations 5 and 6.
[d] Calculated using equation 7.

The possibility was considered that the conformation adopted by the incipient ring in the lowest energy transition state might not be reflected in the relative product energies, but might be reflected in the energy of conformations resembling the saturated ring, which attempts to adopt a diamond lattice conformation. Molecular mechanics calculations were performed, using the MM3* force field, to calculate the low energy conformations of 2-azacyclotetradecanone (**62**). The global minimum energy conformation of **62** is shown below. The Boltzmann distribution expression was used to weight the contribution from each conformation up to 8.368 kJ/mol (2 kcal/mol) above the global minimum energy. For a given conformation the torsional angle at each site of ring closure was presumed to reflect the propensity to form the corresponding olefin configuration. For example, a torsional angle of 180° might correspond to the formation of an (*E*)-alkene, and one of 0° to a (*Z*)-alkene. Those intermediate angles might reflect the favoured isomer or ratio obtained in a resulting mixture. Therefore, considering all conformations and a particular site for ring closure the weighted sum of the absolute torsional angles ($|\theta|$), relative to 180°, might correspond to the probability of forming the (*E*)-alkene (equation 7). Using equation 7, *E*/*Z* ratios were calculated for each site of ring closure from the torsional angles in each conformation and the weight attributed to each (Table 14). In comparison to the previous analyses based on the lowest energy conformations of the lactam products, this analysis provided the best correlations between the calculated and observed ratios at bond positions close to the amide (n = 4, 5, 11, and 12*Z* and 12*E*). Comparable ratios were also calculated for positions 7 and 8, however the ratios calculated for positions 6, 9, and 10 deviated from the observed ratios. This analysis suggested that at bond positions close to the amide the relative transition state energies were reflected in the low energy conformations of saturated lactam **62**.

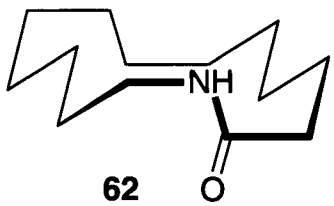

62

$$\%E = \sum_r \frac{\langle N_r \rangle}{N} |\theta_r| \Big/ 180 \qquad (7)$$

In summary, a comparison between the calculated and experimental *E*/*Z* ratios suggested that the relative transition state energies were reflected in the relative molecular mechanics calculated energies of the (*E*)- and (*Z*)-lactam products. Calculated ratios based on the global minimum energy conformations were found to correlate with the experimental ratios, and ratios based on a weighted distribution of low energy conformations provided similar correlations. Calculations based on the torsional angles from low energy conformations of the saturated lactam **62** provided better correlations at ring closure sites in close proximity to the amide group. It appeared that the conformation adopted in the transition state is product-like, and complements calculations indicating these reactions are endothermic (see Table 13). For the series of diene-amides studied (**68-76**), molecular mechanics calculations provided a basis to rationalize the stereochemical outcome of the unsaturated 14-membered lactam products. The validity of such an analysis was strengthened by comparable conformations observed for lactam **89** in the solid state and from molecular mechanics calculations.

It is not known whether the observed *E*/*Z* ratios resulted from the relative thermodynamic stability of the isomeric lactam products, a kinetic factor of conformational origin, or a combination of both. Preliminary evidence in support of a kinetic product distribution was obtained from the isomerization studies conducted with ruthenium methylidene **4** (Section 2.8), which indicated that the ring opening of the lactam products was slow relative to the rate of ring closure at closure sites far removed from the amide. Therefore, prolonged reaction times that may extend beyond the lifetime of the catalyst could result in a thermodynamic product distribution. It is interesting to note that the observed *E*/*Z* ratios correlated with the relative thermodynamic stability of the isomeric product lactams. This might be attributed to mere coincidence, or the coincidental reflection of the relative transition state energies in the relative energies of the isomeric products. However, this does not necessarily suggest that the outcome resulted from an established thermodynamic equilibrium. What remains very clear is that formation of macrocyclic compounds via RCM has emerged as a reliable and general method, only to be complicated by the inability to predict and control the stereochemical outcome of the reaction. Hopefully the preceding analysis provided a basis to further the understanding of this fundamental aspect of RCM.

2.11 Conclusions

The construction of a series of unsaturated 14-membered lactams (**77-92**), exploring ring closure at nine contiguous sites, was conducted via RCM of the corresponding diene-amides (**68-76**, (*E*)-**145**, and (*Z*)-**148**). The diene-amides were in turn synthesized from simple carboxylic acids, alkenyl amines, and alkenyl halides, which all commonly possessed a terminal olefin. Where applicable, subunits differing in functional group, but equal in chain length, were derived from a common precursor. For example, some carboxylic acids and alkenyl amines, possessing the same number of carbon atoms in the linear chain, were derived from the corresponding nitrile. Amidation and primary amide alkylation strategies were applied to the coupling of these subunits. The amide alkylation methods were less appealing due to the formation of dialkylated products. It is worth mentioning that construction of the diene-amides in a convergent manner added to the synthetic appeal of RCM.

Preliminary studies into the RCM formation of a macrocyclic amine and two lactams were met with varying success. The failed cyclizations of *N*-benzyl diene-amine **111**, and vinylacetic acid derived diene-amide **76** were attributed to the Lewis basic nature of the heteroatoms contained on these substrates causing deactivation of the metathesis catalyst. Cyclization of diene-amide **72**, in contrast, proceeded smoothly suggesting Grubbs' benzylidene **3** was tolerant to the amide group. Studies using this substrate found that the effects of catalyst loading, temperature, and addition and total reaction time could be minimized. These minimized conditions were applied to a systematic study of the RCM of diene-amides **68-76**.

The formation of lactams **77-90** via RCM of diene-amides **68-76** proceeded with varying results, yet followed a general trend. An incremental decrease in yield was observed throughout the series corresponding to one of the terminal double bonds in a diene-amide being incrementally closer to the amide group. This effect was most significantly illustrated by the failure of diene-amide **76** to undergo ring closure. The effect of the proximity between the terminal double bond and amide group was a significant factor governing RCM. The slow addition of precatalyst and substrate, and the appropriate reaction time and termination were also important factors favouring cyclization. The moderate to high correlation between the observed and molecular mechanics calculated *E*/*Z* ratios at each site of ring closure suggested the relative

transition state energies, leading to the *E* and *Z* isomeric products, were reflected in the relative product energies.

The structures of most lactam products were confirmed by spectroscopic and elemental analysis. The configuration of the olefins were determined by ^{1}H NMR homonuclear decoupling experiments and confirmed by a comparison of the allylic carbon resonances in the ^{13}C NMR spectrum. The position of the olefin within the macrocyclic ring was confirmed by analysis of COSY, HMQC, and HMBC 2D NMR data. Although lactams **77**-**90** were obtained as white solids, only lactam **89** provided crystals suitable for X-ray crystallographic analysis. The solid state structure confirmed the position and configuration of the olefin within **89**, and the conformation was nearly identical to the global minimum energy conformation obtained from molecular mechanics calculations.

Additional studies were conducted in attempts to improve the yield for the RCM reactions of those diene-amides more significantly affected by the proximity between the double bonds and the amide group. Such attempts explored the effects of additives, temperature, *N*-BOC amide protection, and differentially substituted diene-amides. In terms of additives, tricyclohexylphosphine was found to marginally improve the yield in some cases, but $Ti(O\textit{i}Pr)_4$ and CuCl had little to no effect. The phosphine may have disrupted unproductive catalyst complexes facilitating ring closure. Increased temperature and *N*-BOC amide protection improved the yield observed from RCM to a comparable extent. Rate enhancement in the former and reduced heteroatom basicity, corresponding to weaker unproductive catalyst complexes in the latter, was attributed to the improvement in yield. Both conditions also led to the formation of dimeric products, which was tentatively attributed to more competitive rates of intermolecular and ring opening reactions, relative to the desired intramolecular reaction. Finally, the application of differentially substituted diene-amides (*E*)-**145** and (*Z*)-**148** led to the only observed formation of isomeric lactams **91** and **92**, and (*Z*)-**148** gave a better yield of the desired products than the geometrical isomer (*E*)-**145**.

The general trend in yield throughout the series was governed by the formation of unproductive catalyst complexes. The extent to which the RCM reaction was inhibited depended on the ring size and thus the stability of such a complex, which was directly related to the distance between the amide group and the terminal double bonds. A number of comparisons within the series suggested that complexes with the carbonyl

oxygen were more stable relative to the analogous complexes with nitrogen. These observations complement those reported by Fürstner and co-workers.[45,91b,142,143] It appears that the factors governing the RCM formation of macrocyclic compounds include; (i) the relative proximity of the functional group and the terminal double bonds, (ii) the Lewis basicity of the heteroatoms on the functional group, and (iii) steric congestion near the terminal double bonds. These factors were reflected throughout our studies.

Finally, one of the more elusive issues concerns the observed *E*/*Z* ratios at each site of ring closure. Surprisingly little attention has been paid in the literature to the predicted and controlled formation of disubstituted olefins in macrocyclic systems via RCM. However, a few reports, including our own,[72] have illustrated that in certain cases either the (*E*)-alkene[144] or the (*Z*)-alkene[145] was serendipitously yet exclusively formed. The resulting ratio from a given RCM reaction might reflect the relative transition state energies leading to formation of the isomeric products. In fact, the observed and calculated ratios were in strong agreement, and suggested that the relative transition state energies were reflected in the relative product energies.

The preceding discussion illustrated the facile formation of 14-membered lactams via RCM of conformationally unbiased diene-amide substrates. The success of future applications of this method to the formation of macrocyclic compounds would best be suited to those diene substrates with terminal double bonds far removed from any functional group. Due to our inability to control the resulting *E*/*Z* ratio, this method is best applied to those macrocyclic targets in which the newly formed olefin can be reduced. Further studies are required to elucidate the nature of the transition state in these reactions, how it relates to the relative energies of the products, and how it can be affected to control the selectivity of the reaction. In the realm of natural product total synthesis this fundamental problem cannot be avoided since many naturally occurring macrocyclic compounds may require the formation of one particular olefin isomer upon application of RCM. One such example is the marine alkaloid motuporamine C (**35**). The total synthesis of motuporamines A-C, and the application of RCM to the construction of the macrocyclic rings of motuporamines B and C are discussed in the next chapter.

CHAPTER 3
SYNTHESIS AND STRUCTURAL VERIFICATION OF DIACETYLMOTUPORAMINES A-C

Results and Discussion

The ring-closing metathesis (RCM) methodology presented in Chapter 2 established this reaction as a viable method, under the appropriate conditions, for forming unsaturated 14-membered lactams. The extension of this chemistry to the formation of larger ring sizes was expected to proceed without difficulty. Accordingly, this chemistry was applied to the formation of one of the two structural features common among motuporamines A-C, the macrocyclic amine. Motuporamine A (**33**) was the only exception where the macrocyclic amine was derived from a commercially available lactam. In either case, reduction of the lactam furnished the desired macrocyclic amine. A spermidine-like unit was the other structural feature common among the motuporamines. A method for introducing this unit was taken from a synthetic strategy applied in the synthesis of a starburst dendrimer.[78] Prior to synthesizing the macrocyclic amine units the proposed chain addition strategy was tested. This was accomplished by synthesizing triamine **153**, a model motuporamine compound.

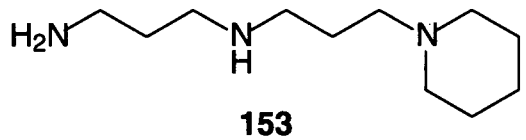

153

3.1 Synthesis of *N*-(3-Aminopropyl)-3-(1-piperidyl)propylamine (153): A Model Study

In order to test the proposed chain addition strategy a simple cyclic amine, piperidine, was chosen. Employing the method of Tomalia and co-workers,[78] piperidine (**154**) was added to methyl acrylate in a Michael fashion to afford, upon removal of excess reagents and solvent in vacuo, a β-amino ester (Scheme 22). Amidation of the β-amino ester with a ten-fold excess of 1,3-diaminopropane gave analytically pure amide **155** in a yield of 97% over two steps upon removal of excess reagent and solvent in vacuo. A ten-fold excess of 1,3-diaminopropane was required to suppress formation

of the diacylated product. None of the diacylated product was observed in the NMR spectra or the LRMS. Reduction of **155** with LAH revealed the spermidine-like unit to afford triamine **153** in 66% yield.

Scheme 22. Synthesis of *N*-(3-Aminopropyl)-3-(1-piperidyl)propylamine (**153**)[a]

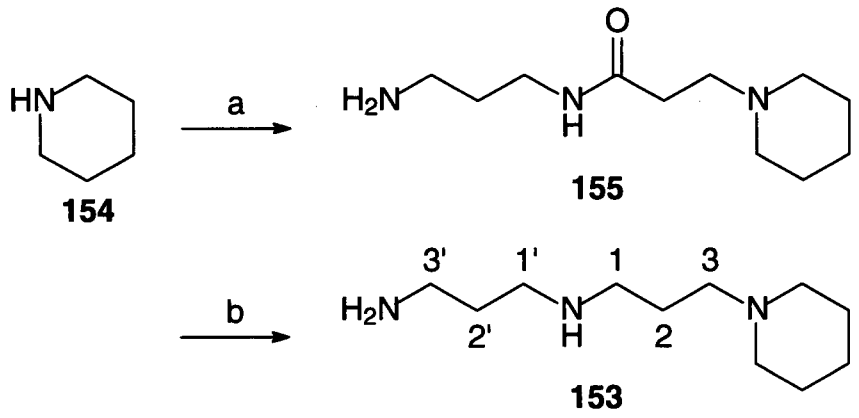

[a]Key: (a) $CH_3OCOCH{=}CH_2$, MeOH, rt; then $H_2N(CH_2)_3NH_2$, MeOH, rt, 97%; (b) LAH, THF, 70 °C, 66%.

The ^{1}H NMR spectrum of **153** contained three two-proton triplets at δ 2.67, 2.60 and 2.58 corresponding to the protons on the C-3', C-1', and C-1 methylene groups adjacent to the primary and secondary amine nitrogen atoms. The spectrum also contained resonances at δ 2.40-2.45 and 2.35 corresponding to the protons on the piperidine and C-3 methylene groups adjacent to the tertiary nitrogen atom. The ^{13}C NMR spectrum contained nine resonances consistent with the structure of **153**. In addition, the HRMS and chemical analysis results were consistent with the composition of triamine **153**. The synthesis of **153** established this chain addition strategy as a viable method for the assembly of a spermidine-like unit that could be applied in the synthesis of motuporamines A-C.

3.2 Synthesis of Diacetylmotuporamine A Trifluoroacetate (36·TFA)

The synthesis of diacetylmotuporamine A trifluoroacetate (**36**·TFA) began with the reduction of a simple lactam and subsequently employed conditions discussed in the previous section. Reduction of the commercially available 2-azacyclotridecanone (**65**) with LAH gave macrocyclic amine **66**[146] (Scheme 23). The spermidine-like unit was

assembled employing the method of Tomalia and co-workers.[78] In the initial step of a two-step one-pot process amine **66** was added in a Michael fashion to methyl acrylate. Upon removal of excess reagents and solvent in vacuo, amidation of the resulting β-amino ester with a ten-fold excess of 1,3-diaminopropane gave amide **156** in a yield of 99% over two steps. Removal of excess reagents and solvent in vacuo afforded analytically pure **156**. None of the diacylated product was observed. Reduction of amide **156** with LAH afforded motuporamine A (**33**) in 99% yield. The improved yield for the reduction of **156** over the analogous reduction of **155** was attributed to the increased reaction time from 6.5 to 19 hours. Acetylation of the natural product **33** followed by purification with reversed-phase chromatography, using 60% water and 1% trifluoroacetic acid in methanol as eluant, resulted in the formation of diacetylmotuporamine A trifluoroacetate (**36**·TFA) in 77% yield. This last step was conducted in the same manner as Andersen and co-workers.[58]

Scheme 23. Synthesis of Diacetylmotuporamine A Trifluoroacetate (**36**·TFA)[a]

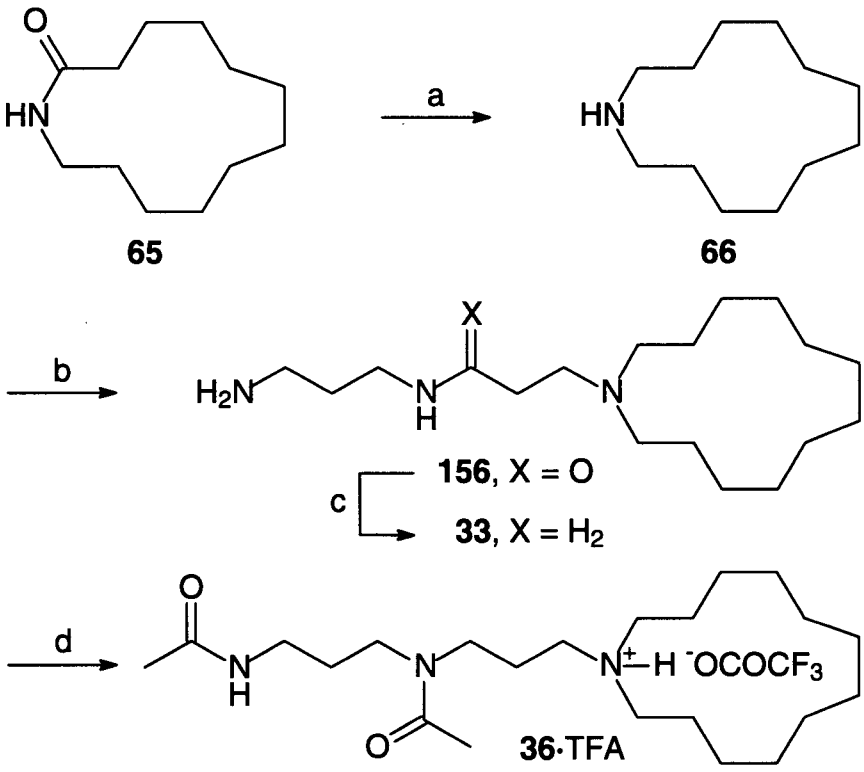

[a]Key: (a) LAH, THF, 70 °C, 87%; (b) $CH_3OCOCH{=}CH_2$, MeOH, rt; then $H_2N(CH_2)_3NH_2$, MeOH, rt, 99%; (c) LAH, THF, 70 °C, 99%; (d) Ac_2O, pyr, rt; then reversed-phase chromatography using H_2O, MeOH, and TFA (60:39:1), 77%.

Confirmation of the structure assigned to authentic diacetylmotuporamine A (**36**) was based on a comparison of the spectral data obtained for the natural and synthetic compounds. This comparison and analysis appears in the following section.

3.2.1 Structural Verification of Authentic Diacetylmotuporamine A (36)

In order to determine if the synthetically derived diacetylmotuporamine A trifluoroacetate (**36**·TFA) was identical to authentic compound **36**, it was necessary to make explicit comparisons between the two sets of spectral data. This was accomplished by collecting the data for the synthetic compound in the same manner and under the same conditions as that collected for the authentic material. Accordingly, all NMR spectra were recorded in methanol-d_4. 1D NMR spectra were recorded at 400 MHz and 500 MHz, and all 2D NMR spectra were recorded at 500 MHz. All low- and high-resolution mass spectra were recorded in positive-ion LSIMS mode. The comparison that follows predominantly focuses on the ^{1}H and ^{13}C NMR data from both compounds.

No distinct differences were observed between the ^{1}H NMR spectra of the authentic and synthetic compounds. The 400 MHz proton NMR spectra of authentic diacetylmotuporamine A (**36**) (Figure 40 a) and synthetic diacetylmotuporamine A trifluoroacetate (**36**·TFA) (Figure 40 b) were nearly identical. The only notable difference was a resonance at δ 3.30 due to the solvent CD_3OD, which was present in both spectra. In the spectrum of the authentic compound this resonance was more intense relative to the other signals present. This was simply due to different compound concentrations between the two samples. The similarity between these two spectra suggested authentic compound **36** was isolated as the ammonium salt and not the free base as reported.

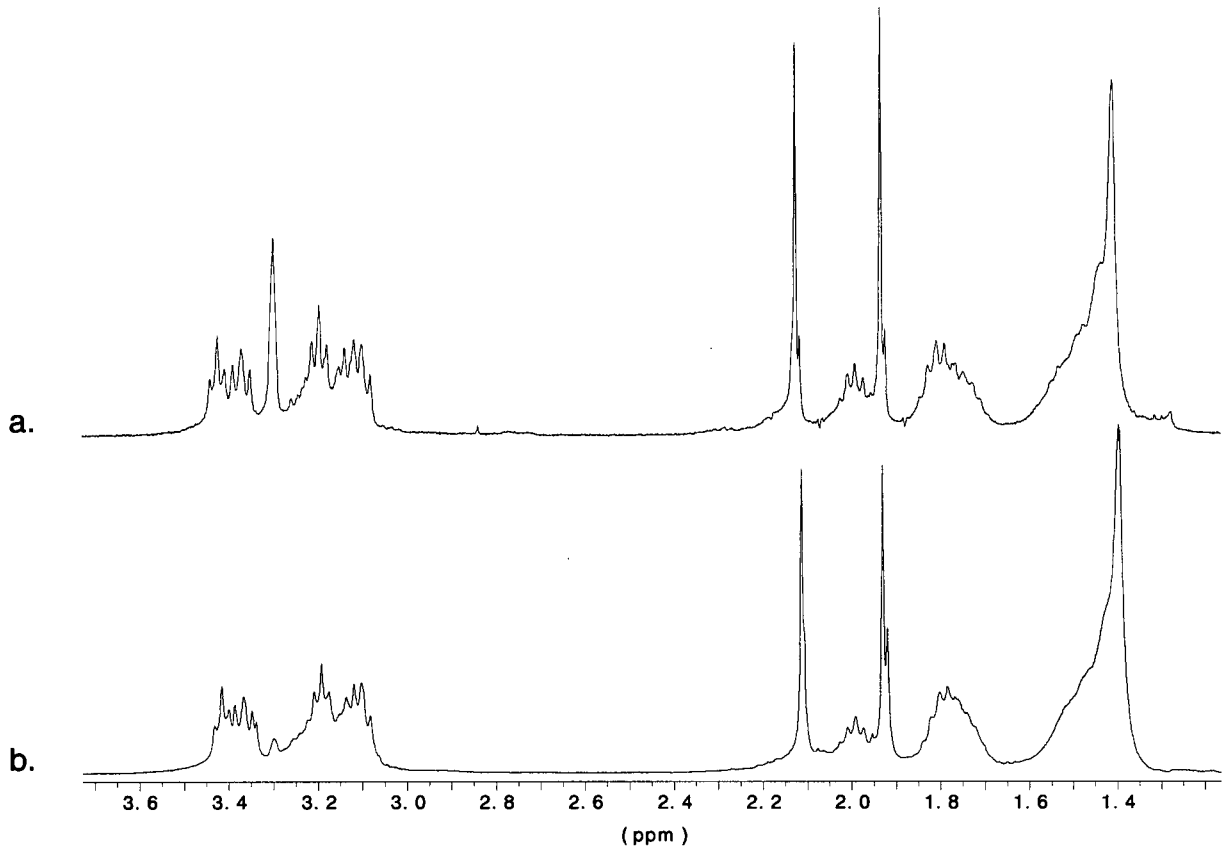

Figure 40. 400 MHz ^{1}H NMR spectra of (a) authentic diacetylmotuporamine A (**36**), and (b) synthetic diacetylmotuporamine A trifluoroacetate (**36**·TFA).

A detailed comparison of the 500 MHz ^{1}H and ^{13}C NMR spectral data for these compounds (Table 15) provided further evidence that these compounds were identical. The assignments provided in this table were based on those reported by Andersen and co-workers[58] and were confirmed by analysis of the 500 MHz COSY, HMQC, and HMBC data for **36**·TFA. Six methylene units (atoms 2, 4, 6, 8, 10 and 21) were identified as having an attached nitrogen atom based on the proton and carbon chemical shift data. Analysis of the 2D NMR data clearly identified the spermidine-like unit. Figure 41 illustrates some of the COSY and HMBC correlations, where bold red bonds represent COSY correlations and the blue arrows represent HMBC correlations. For example, analysis of the COSY data suggested correlations between H-2 (δ 3.20) and H-3 (δ 1.78), which in turn was correlated to H-4 (δ 3.37). Additional correlations between H-6 (δ 3.42) and H-7 (δ 1.99), which in turn was correlated to H-8 (δ 3.10) provided the second of two three-carbon units. These units were attached to the same

nitrogen atom (N-5) by an HMBC correlation between H-6 (δ 3.42) and C-4 (δ 47.9), which confirmed the presence of the spermidine-like unit.

Table 15. 500 MHz ^{1}H and ^{13}C NMR Assignments for Authentic **36** and Synthetic Diacetylmotuporamine A Trifluoroacetate (**36**·TFA)[a]

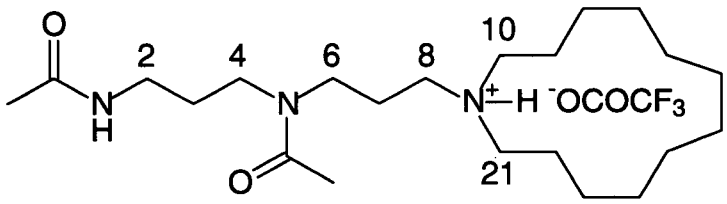

36·TFA

	Authentic Diacetylmotuporamine A (**36**)[58]		Synthetic Diacetylmotuporamine A Trifluoroacetate (**36**·TFA)	
Atom	δ ^{1}H[b]	δ ^{13}C[b]	δ ^{1}H[b]	δ ^{13}C[b]
2	3.20	37.8	3.20	37.8
3	1.80	29.6	1.78	29.4
4	3.37	47.7	3.37	47.9
6	3.43	43.7	3.42	43.6
7	1.99	24.2	1.99	24.1
8	3.10	53.6	3.10	53.6
10, 21	3.13, 3.21	53.2	3.14, 3.22	53.1
11, 20	1.72-1.78	22.5	1.71-1.84	22.4
12, 19	1.48, 1.53	25.3	1.35-1.57	25.2
13, 18	1.41-1.44[c]	26.8	1.35-1.57	26.7[c]
14, 17	1.41-1.44[c]	26.0	1.35-1.57	26.0[c]
15, 16	1.41-1.44[c]	25.8	1.35-1.57	25.7[c]
CO (N1)		171.2		173.5
CH_3 (N1)	1.93	22.6	1.94	22.4
CO (N5)		174.5		174.3
CH_3 (N5)	2.13	21.2	2.12	21.2

[a] Due to acetamide rotamers, the majority of carbons and some protons appeared as two resonances. Only the δ value for the more intense resonance is represented.
[b] The chemical shift values are referenced to CD_2HOD (^{1}H) and CD_3OD (^{13}C).
[c] Assignments within a column are interchangeable.

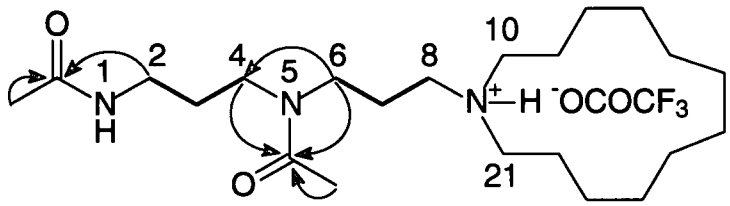

36·TFA

Figure 41. Partial 500 MHz COSY (bold red bonds) and HMBC (blue arrows) correlations for diacetylmotuporamine A trifluoroacetate (**36**·TFA).

Due to an overlap of the proton resonances at δ 1.35-1.57, assignment of the remaining methylene units within the macrocyclic amine could not be made.

The assignment of both acetamide groups was confirmed by an analysis of the HMBC data. HMBC correlations between the protons H-4 (δ 3.37), H-6 (δ 3.42), the methyl protons at δ 2.12 and the carbonyl at δ 174.3 identified the acetamide group attached to N-5 (Figure 41). Similarly, HMBC correlations between the protons H-2 (δ 3.20), the methyl protons at δ 1.94 and the carbonyl at δ 173.5 identified the second acetamide group attached to N-1.

In addition to the comparable NMR data discussed above, HRMS results obtained in positive-ion LSIMS mode were consistent with the composition of authentic diacetylmotuporamine A (**36**). However, combustion analysis results were not consistent with the composition of either **36**·TFA or **36**, and prompted further analysis of this compound. Recall that **36**·TFA was purified by reversed-phase chromatography using 60% water and 1% trifluoroacetic acid in methanol as eluant. The inconsistent combustion analysis results were not surprising when the method of purification for this compound was considered. The presence of a signal at δ 0.0 in the ^{19}F NMR spectrum, and LRMS results obtained in negative-ion LSIMS mode confirmed the presence of trifluoroacetate anion. This data suggested that **36**·TFA did indeed exist as the ammonium salt and might have contained a combination of water and trifluoroacetic acid as well, thus affecting the results from combustion analysis. Further evidence in support of this assignment was found in the ^{1}H NMR spectrum of **36**·TFA. Two resonances were observed for the protons attached to C-10 and C-21, thus indicating their diastereotopic relationship. Such a relationship is only possible for the ammonium salt. If the free base **36** was isolated, only one resonance would be observed for these

protons in the ^{1}H NMR spectrum due to rapid inversion about the nitrogen atom. Therefore, the diastereotopic nature of these protons, observed in the ^{1}H NMR spectrum of **36**·TFA, provided further evidence to support the assignment as the ammonium salt. Since the authentic and synthetic compounds were purified in the same manner it seems logical that they were both isolated as the ammonium salt. The consistency between the spectral data for these compounds suggested this to be true.

In conclusion, diacetylmotuporamine A trifluoroacetate (**36**·TFA) was synthesized from commercially available lactam **65** in excellent yield over four steps. The synthetic compound was identical to the authentic compound based on comparisons of the spectral data for both. This conclusion was primarily based upon comparable chemical shift assignments between the NMR spectra for both compounds. Further analysis of **36**·TFA confirmed this compound was isolated as the ammonium salt. Therefore, the authentic material **36** must have been isolated as the ammonium salt and not the free base as reported.

3.3 Synthesis of Diacetylmotuporamine B Trifluoroacetate (37·TFA)

The synthesis of diacetylmotuporamine B trifluoroacetate (**37**·TFA) followed a similar set of steps to those that were used in the synthesis of diacetylmotuporamine A trifluoroacetate (**36**·TFA). The macrocyclic amine portion of **37**·TFA was synthesized from the corresponding 14-membered lactam **62**. Although this lactam could have been formed via Beckmann rearrangement of the oxime derived from cyclotridecanone,[85] or by the methods employed by Baldwin and co-workers (see Section 1.5.5),[70] it seemed appropriate to utilize a number of the lactams synthesized as part of the RCM studies discussed in Chapter 2. Accordingly, the synthesis of **37**·TFA began with the hydrogenation of a mixture of 2-azacyclotetradecenones **83**, **85**, and **86** in a ratio of 41:28:31, respectively (Scheme 24). The resulting lactam **62**[147] was reduced with LAH to afford macrocyclic amine **63**[146] in 89% yield over two steps. The spermidine-like unit was assembled employing the method of Tomalia and co-workers.[78] Following the same two-step one-pot process used in the synthesis of diacetylmotuporamine A trifluoroacetate (**36**·TFA), macrocyclic amine **63** was converted into amide **157** via Michael addition with methyl acrylate followed by amidation with 1,3-diaminopropane in a yield of 96% over two steps. Reduction of amide **157** with LAH afforded

motuporamine B (**34**) in 87% yield. As discussed earlier, the improved yield for this reduction over that of the analogous reduction of **155** was attributed to an increase in reaction time (see Section 3.2). Acetylation of triamine **34** followed by purification with reversed-phase chromatography, using 60% water and 1% trifluoroacetic acid in methanol as eluant, resulted in the formation of diacetylmotuporamine B trifluoroacetate (**37**·TFA) in 77% yield. This last step was conducted in the same manner as Andersen and co-workers.[58]

Scheme 24. Synthesis of Diacetylmotuporamine B Trifluoroacetate (**37**·TFA)[a]

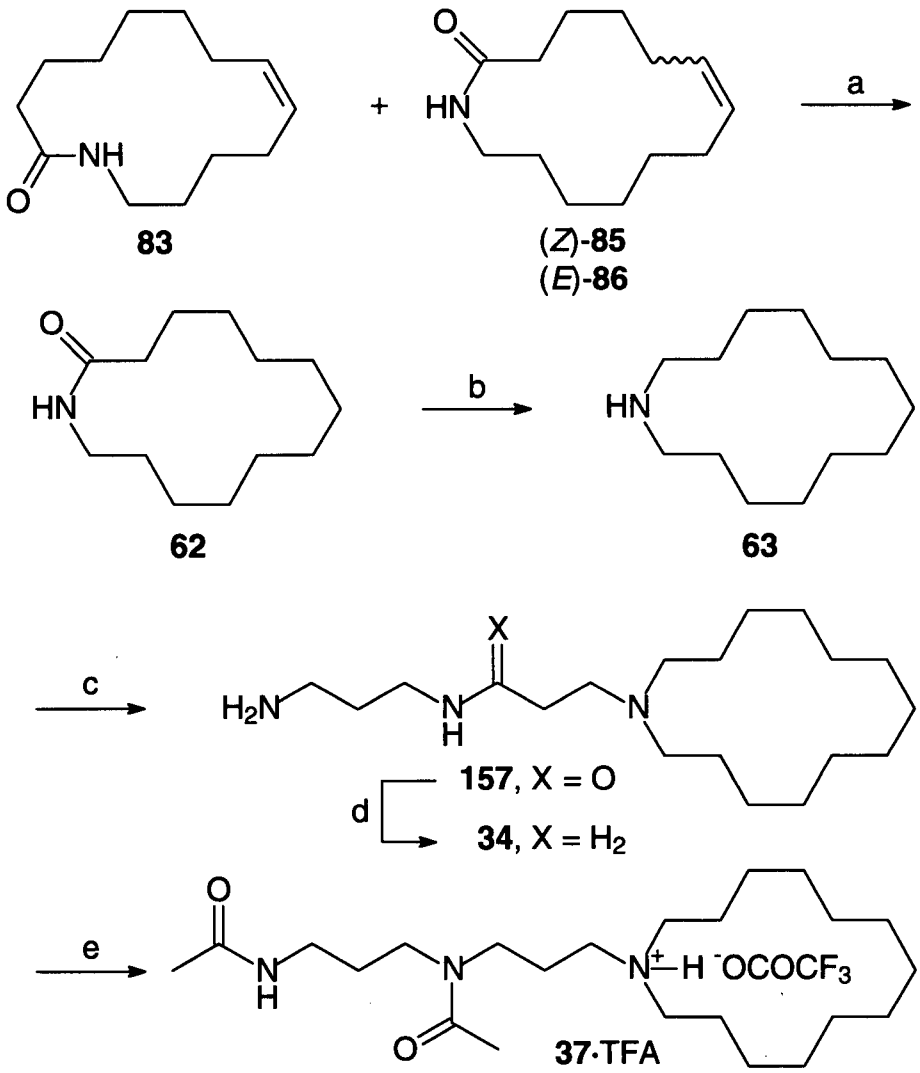

[a]Key: (a) H_2, 5% Pd/C, EtOH, rt, 97%; (b) LAH, THF, 70 °C, 92%; (c) $CH_3OCOCH{=}CH_2$, MeOH, rt; then $H_2N(CH_2)_3NH_2$, MeOH, rt, 96%; (d) LAH, THF, 70 °C, 87%; (e) Ac_2O, pyr, rt; then reversed-phase chromatography using H_2O, MeOH, and TFA (60:39:1), 77%.

Confirmation of the structure assigned to authentic diacetylmotuporamine B (**37**) was based on a comparison of the spectral data obtained for the authentic and synthetic compounds. This was conducted following the same analysis used for diacetylmotuporamine A (see Section 3.2.1).

3.3.1 Spectral Comparison Between Authentic Diacetylmotuporamine B (37) and Diacetylmotuporamine B Trifluoroacetate (37·TFA)

Confirmation of the structure assigned to authentic diacetylmotuporamine B (**37**) was complicated due to the lack of NMR data reported for this compound. Neither a ^{13}C NMR spectrum, nor any 2D NMR data were reported by Andersen and co-workers.[58] Although the HRMS results for both compounds were consistent with the composition of the assigned structure, obvious differences between the 400 MHz ^{1}H NMR spectra of authentic **37** (Figure 42 a) and synthetic **37**·TFA (Figure 42 b) were observed. For example, the resonances at δ 0.97 and δ 0.93 in the ^{1}H NMR spectrum of authentic **37** were absent in the spectrum of the synthetic compound. In addition, the pattern of resonances at δ 1.25-1.60 and δ 1.65-1.74 were distinctly different upon visual inspection. Minor differences throughout the remainder of these spectra were observed. The poor correlation between these spectra suggested these compounds were different.

Although similarities could be drawn between the ^{1}H NMR spectra of synthetic **37**·TFA and authentic **37**, the differences warranted a more detailed analysis of these spectra as well as the 125 MHz carbon NMR spectrum of synthetic compound **37**·TFA (Table 16). Assignments were based on those reported by Andersen and co-workers[58] and by analysis of the 500 MHz COSY, HMQC, and HMBC data for **37**·TFA. COSY correlations between H-2 (δ 3.20) and H-3 (δ 1.81), which in turn was correlated to H-4 (δ 3.37), and also between H-6 (δ 3.43) and H-7 (δ 1.99), which in turn was correlated to H-8 (δ 3.10) provided two three-carbon units. An HMBC correlation between H-6 (δ 3.43) and C-4 (δ 47.9) indicated that these units were attached to the same nitrogen atom (N-5), thus confirming the presence of the spermidine-like unit. Refer to Figure 41 for an illustration of some of these correlations. Both acetamide groups were assigned by HMBC correlations similar to those found for diacetylmotuporamine A trifluoroacetate (**36**·TFA) (see Section 3.2.1). Finally, overlap of the proton resonances at δ 1.29-1.55 prevented assignment of the remaining methylene units within the macrocyclic amine.

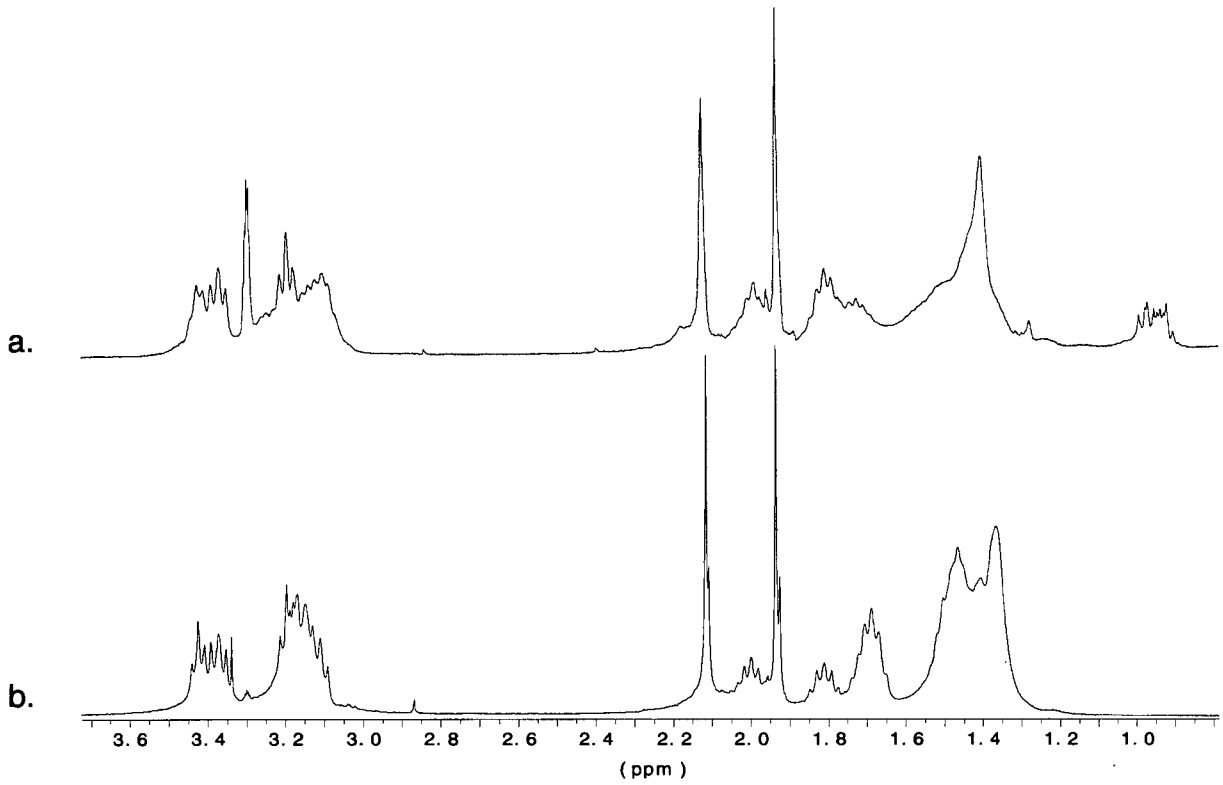

Figure 42. 400 MHz ^{1}H NMR spectra of (a) authentic diacetylmotuporamine B (**37**), and (b) synthetic diacetylmotuporamine B trifluoroacetate (**37**·TFA).

Although the HRMS results obtained in positive-ion LSIMS mode for **37**·TFA were consistent with the composition of the structure assigned to authentic **37**, combustion analysis was not. The inconsistent combustion analysis results were not surprising considering the method of purification for **37**·TFA, performed by reversed-phase chromatography using 60% water and 1% trifluoroacetic acid in methanol as eluant. The presence of a signal at δ 0.0 in the ^{19}F NMR spectrum, and LRMS results obtained in negative-ion LSIMS mode both confirmed the presence of trifluoroacetate anion. This data suggested that **37**·TFA did indeed exist as the ammonium salt and might have contained a combination of water and trifluoroacetic acid as well, thus affecting the combustion analysis results. In addition, an HMQC correlation between the chemically equivalent carbons C-10/C-22 (δ 51.3) and two separate signals within the multiplet at δ 3.13-3.18 indicated the diastereotopic relationship between the protons attached to these carbons. Therefore, this analysis provided further evidence to support the assignment of **37**·TFA as the ammonium salt.

Table 16. 400 MHz ^{1}H and 125 MHz ^{13}C NMR Assignments for Authentic **37** and Synthetic Diacetylmotuporamine B Trifluoroacetate (**37**·TFA)[a]

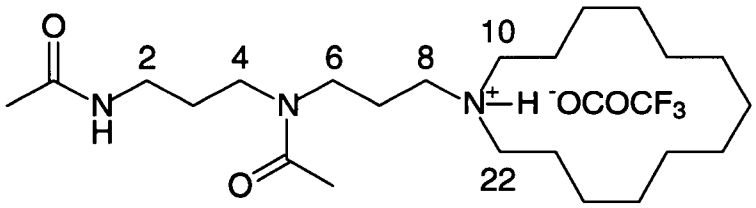

37·TFA

	Authentic Diacetylmotuporamine B (**37**)[58]		Synthetic Diacetylmotuporamine B Trifluoroacetate (**37**·TFA)	
Atom	δ ^{1}H[b]	δ ^{13}C[b]	δ ^{1}H[b]	δ ^{13}C[b]
2	3.20	NA	3.20	37.8
3	1.81	NA	1.81	29.5
4	3.37	NA	3.37	47.9
6	3.43	NA	3.43	43.5
7	2.00	NA	1.99	24.1
8	3.06-3.26	NA	3.10	52.9
10, 22	3.06-3.26	NA	3.13-3.18	51.3
11, 21	1.70-1.75, 0.97 (11), 0.93 (21)	NA	1.65-1.74	21.2
12, 20	1.25-1.60	NA	1.29-1.55	24.1
13, 19	1.25-1.60	NA	1.29-1.55	26.4[c]
14, 18	1.25-1.60	NA	1.29-1.55	24.8[c]
15, 17	1.25-1.60	NA	1.29-1.55	25.3[c]
16	1.25-1.60	NA	1.29-1.55	27.0
CO (N1)		NA		173.5
CH_3 (N1)	1.94	NA	1.94	22.5
CO (N5)		NA		174.5
CH_3 (N5)	2.13	NA	2.13	20.6

[a] Due to acetamide rotamers, the majority of carbons and some protons appeared as two resonances. Only the δ value for the more intense resonance is represented.
[b] The chemical shift values are referenced to CD_2HOD (^{1}H) and CD_3OD (^{13}C).
[c] Assignments within a column are interchangeable.

Since the authentic and synthetic compounds were purified in the same manner it seems logical that they were both isolated as the ammonium salt. However, this still did not account for the differences between the spectral data for these compounds. Previous studies in our laboratory of macrocyclic amines provided a necessary perspective on this problem.

A number of 13-, 14-, and 16-membered cyclic amines were previously synthesized in our laboratory[85] and the NMR studies of these compounds provided some insight regarding the structure of synthetic **37**·TFA and authentic **37**. Table 17 contains the proton and carbon NMR resonances due to the endocyclic methylenes adjacent to the nitrogen atom for a variety of these compounds, labelled as types **S-X**. The resonances for compounds of type **S-V** did not correlate with those for diacetylmotuporamine trifluoroacetate compounds of type **X**. The methylenes in type **X** compounds were in a different chemical environment than those in compounds of type **S-V**. The correlation of these resonances between compounds of type **W** and type **X** suggested that synthetic **37**·TFA and authentic **37** were obtained as the ammonium salt and not as the tertiary amine. This correlation also contributes to the evidence suggesting that authentic diacetylmotuporamine A (**36**) was obtained as the ammonium salt. The minor differences in the chemical shift values between these types of compounds could be attributed to the different anion (X^-), *N*-alkyl substituent, and NMR solvent. Although this information suggests authentic **37** was isolated as the ammonium salt, it does not provide any insight into the differences between it and synthetic compound **37**·TFA.

Regarding the proton resonances at δ 0.97 and δ 0.93 observed in the ^{1}H NMR spectrum of authentic **37**, such high field signals were absent in the corresponding spectra of compounds of type **S-W** (n = 1, 2, or 4) and synthetic **37**·TFA at room temperature. However, such high field signals were observed at low temperatures in the spectra of some of these compounds due to slower conformational processes. ^{1}H DNMR studies were conducted with compounds of type **S-U** (n = 2) as part of the aforementioned studies of macrocyclic amines.[85] High field signals similar to those found in the ^{1}H NMR spectrum of authentic **37** only appeared at temperatures lower than -70 °C for type **S** (n = 2), -95 °C for type **T** (n = 2), and -58 °C for type **U** (n = 2). These signals were assigned to protons that were shielded in specific ring conformations due to steric interactions and bond anisotropy.[148] The precedence set by

this research suggests that such high field signals should not have been observed in the ^{1}H NMR spectrum of authentic **37** at room temperature. Without additional data for the authentic compound, conclusions cannot be drawn as to whether these high field signals resulted from such shielding effects, the presence of impurities, or compounds isomeric to authentic **37**.

Table 17. 400 MHz ^{1}H and 100 MHz ^{13}C NMR Resonances due to the Endocyclic Methylenes Adjacent to Nitrogen in 13-, 14-, and 16-Membered Macrocyclic Amines and Ammonium Salts (from reference 85).

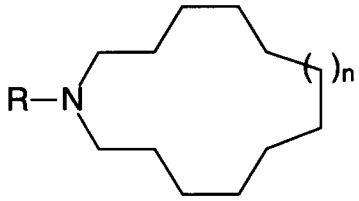

S: R = H
T: R = CH_3

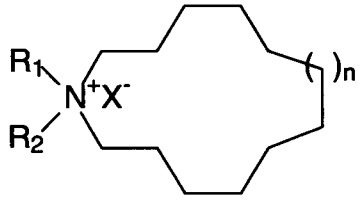

U: $R_1 = R_2 = CH_3$, X = I
V: $R_1 = R_2 = H$, X = Cl
W: $R_1 = CH_3$, $R_2 = H$, X = Cl

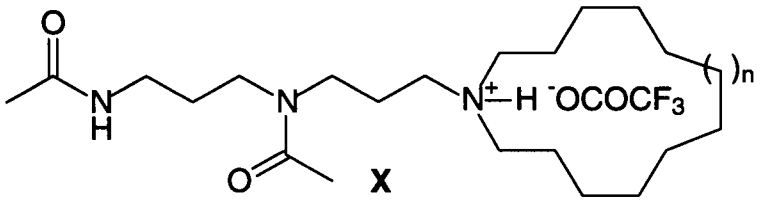

	n=1		n=2		n=4	
Type	δ ^{1}H[a]	δ ^{13}C[a]	δ ^{1}H[a]	δ ^{13}C[a]	δ ^{1}H[a]	δ ^{13}C[a]
S	2.61	47.9	2.61	46.1	2.61	47.6
T	2.27	56.8	2.28	55.1	2.27	56.2
U	3.4-3.5	62.0	3.4-3.5	61.7	3.35-3.55	62.3
V	3.02	42.2	2.97	42.9	2.95	44.2
W	2.84-3.00, 3.00-3.18	52.7	2.70-2.90, 3.00-3.20	54.5	2.89, 3.08	52.6
X[b]	3.14, 3.22	53.1	3.13-3.18	51.3	NA	NA

[a] The chemical shift values are referenced to $CHCl_3$ (^{1}H) and $CDCl_3$ (^{13}C), with the exception of type **X** compounds for which the chemical shift values are referenced to CD_2HOD (^{1}H) and CD_3OD (^{13}C).

[b] Data collected for synthetic compounds **36**·TFA and **37**·TFA.

The comparison of chemical shift data and DNMR studies discussed above provided some insight into the structures of and differences between synthetic **37**·TFA and authentic **37**. It appeared that the authentic compound was isolated as the ammonium salt and not the tertiary amine. The inconsistency between the spectral data and the precedence set by the ^{1}H DNMR studies of macrocyclic amines[85] suggested that the peaks at δ 0.97 and δ 0.93 in the ^{1}H NMR spectrum of the authentic compound should not be observed at room temperature for **37** or **37**·TFA. Furthermore, the minor differences between the ^{1}H NMR spectra might be explained by considering partially protonated forms of these compounds. For example, if the authentic sample was obtained in a partially protonated form the ^{1}H NMR spectrum would appear as an average of the protonated and non-protonated forms. This would result in a spectrum with a similar profile to that of **37**·TFA, but with minor differences in the arrangement of signals.

Trifluoroacetic acid and water were removed from **37**·TFA in order to obtain spectral data of the free base **37**. Compound **37**·TFA in diethyl ether was washed with saturated aqueous sodium carbonate followed by brine to give **37**, the free base of **37**·TFA. Analysis of the 500 MHz ^{1}H and ^{13}C NMR spectra as well as the 500 MHz COSY, HMQC, and HMBC data confirmed the structure of **37**. Some of the proton and most of the carbon resonances in the ^{1}H and ^{13}C NMR spectra of **37** were doubled. This was attributed to the slow conformational processes of acetamide rotamers. A detailed analysis of the 2D NMR data will not be discussed in the interest of brevity, however this data provided correlations similar to those found for **37**·TFA. The most striking difference between the ^{1}H NMR spectra of **37**·TFA and **37** was the high field shift of the signals assigned to the three methylenes attached to the tertiary nitrogen atom. For synthetic **37**, the chemical shift data for these signals (ca. δ 2.40) were more consistent with compounds of type **T**, the free base (see Table 17). In addition to the spectral data discussed above, the ^{19}F NMR spectrum did not contain any signals. The spectral data of synthetic **37** confirmed that trifluoroacetic acid was removed and the free base was formed. A comparison between the spectral data for authentic and synthetic **37** indicated that these compounds were different. It is interesting to note that ^{1}H NMR spectra obtained at various stages during the titration of synthetic **37** with trifluoroacetic acid did not correlate with the spectrum of the authentic compound.[149]

Furthermore, HPLC analysis of authentic and synthetic **37** by co-injection also indicated these compounds were different.

In conclusion, diacetylmotuporamine B trifluoroacetate (**37**·TFA) was synthesized from a mixture of 2-azacyclotetradecenones **83**, **85**, and **86** in excellent yield over five steps. Synthetic compound **37**·TFA was different than authentic diacetylmotuporamine B based on comparisons of the respective spectral data. Further analysis of **37**·TFA confirmed the presence of trifluoroacetate anion indicating this compound was isolated as the ammonium salt. Extraction of **37**·TFA in aqueous base provided the free base **37**, which was also different than the authentic material. The results discussed throughout this section indicated three possibilities that could account for the differences between the spectral data of synthetic **37**·TFA and authentic **37**:

(1) The structure assigned to the authentic compound was incorrect. The composition of the authentic compound from mass spectral data[58] was consistent with the structure of, but not limited to that of **37**. A number of constitutional isomers of **37** could be considered that possess different ring sizes and spermidine-like units of varying carbon chain length. Without further analysis of the authentic compound, especially using 2D NMR, these isomers cannot be identified or eliminated.

(2) The authentic compound contained impurities. The ^{1}H DNMR studies discussed earlier suggested that the high field signals present in the ^{1}H NMR spectrum of the authentic compound should not be present at room temperature and are possibly due to impurities. Although this accounts for the presence of these high field peaks, it does not account for the differences throughout the remainder of the spectra between the authentic and synthetic compounds.

(3) The authentic sample was partially protonated. This would result in an averaged ^{1}H NMR spectrum due to contributions from the protonated and non-protonated compounds. However, titration of synthetic **37** with trifluoroacetic acid did not support this conclusion based on differences between the spectral data of synthetic **37** at various stages of the titration, and that of the authentic compound.

Ongoing studies in the Andersen laboratory suggest that the authentic material might contain a mixture of two compounds, one of which possesses a cyclopropane group.[149] Further analysis of the authentic material will be required to provide a more conclusive assignment of its structure and/or composition.

3.4 Synthesis and Structural Verification of Authentic Diacetylmotuporamine C

The structure of naturally occurring motuporamine C (**35**) is somewhat similar to the structures assigned to motuporamines A (**33**) and B (**34**). Much like the smaller ring size members of this family it contains a spermidine-like unit, but has a 15-membered cyclic amine. It also contains an olefin within the macrocyclic amine, however the position of the olefin was not conclusively determined from the spectroscopic data as reported by Andersen and co-workers.[58] Proton homonuclear decoupling NMR experiments determined the olefin configuration to be of the *Z* geometry, with J = 10.9 Hz. Analysis of the 2D NMR data eliminated all but two of the possible ring positions for the olefin. These positions are represented by the dashed lines in the structure of the naturally occurring compound **35** and its diacetylated derivative **38**. The isomeric compounds **42**·TFA and **41**·TFA, containing an olefin in the C-15/C-16 and C-14/C-15 bond positions respectively, were synthesized in an attempt to unambiguously determine the position of the olefin in the natural product. The correct structural identity of naturally occurring motuporamine C (**35**) was determined by a comparison of the spectral data between both isomeric compounds and the authentic diacetylated derivative **38**.

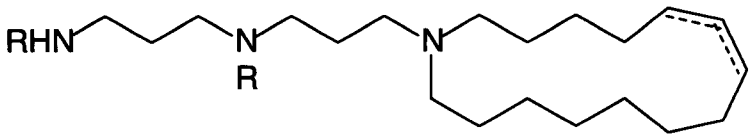

35 R = H (motuporamine C)
38 R = Ac

3.4.1 Syntheses of Diene-amides 159 and 161

Expanding on the RCM methodology discussed in Chapter 2, the 15-membered macrocyclic amine portions of isomers **42**·TFA and **41**·TFA were obtained from the corresponding lactams, which in turn were constructed from diene-amides **159** and **161** via RCM. In terms of the methods applicable for constructing the diene-amides, a few amide bond forming methods were employed in the syntheses of the nine diene-amides used in the RCM studies discussed in Chapter 2 (see Section 2.5). However, one of the more prevalent problems encountered during the synthesis of these compounds was the inconsistent and frequent low yields obtained from the amidation reactions. This

prompted a survey of methods available for amide bond formation via the coupling of an amine and a carboxylic acid. Through this survey a reliable and efficient method was chosen for the construction of **159** and **161**, the diene-amides required for the synthesis of isomers **42**·TFA and **41**·TFA.

The coupling of 4-pentenoic acid (**136**) with benzylamine was examined using five different coupling reagents. The combination of DCC and 1-hydroxybenzotriazole (HOBt) as coupling reagents provided the highest yield of amide **158** (Table 18, Entry 1). The least effective method involved the use of DCC alone (Entry 5), and intermediate yields were obtained using pyridinium reagents and amidation via reaction of the acid chloride (Entries 2-4). Although these results illustrate the relative efficiency of these methods, they do not explain the low and inconsistent yields observed when applied to the synthesis of the nine diene-amides described earlier (see Section 2.5). However, the exclusive use of DCC could only have had a negative impact on the yield observed from the amidation reactions to which it was applied. From this survey, coupling of the requisite carboxylic acid and amine with DCC and HOBt appeared to be the most efficient method. Accordingly, this method was applied in the syntheses of diene-amides **159** and **161**.

Table 18. Comparison of Reaction Conditions Applied in the Formation of Amide **158** from 4-Pentenoic acid (**136**) and Benzylamine

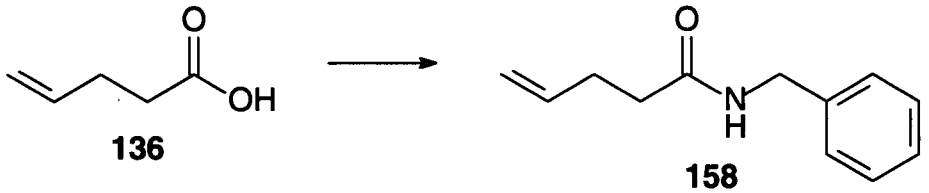

136 **158**

Entry	Reaction Conditions	Yield (%)[a]
1	DCC, HOBt, CH_2Cl_2, 0 °C to rt	94
2	TEA, 2-bromo-1-methylpyridinium fluorosulphonate, CH_2Cl_2, 40 °C	86
3	TEA, 2-chloro-1-methylpyridinium iodide, CH_2Cl_2, 40 °C	76
4	TEA, $(ClOC)_2$, CH_2Cl_2, 0 °C to rt; then amine	76
5	DCC, CH_2Cl_2, rt	53

[a] Refers to isolated yields after chromatography.

The synthetic approach to diene-amide **159** required the formation of amine **134**. This amine was obtained by LAH reduction of either nitrile **128** or amide **130**, both previously synthesized during the RCM studies (see Section 2.5.4). The first attempted synthesis of diene-amide **159** began with the LAH reduction of nitrile **128** to afford amine **134** (Scheme 25). It should be noted that amine **134** was not obtained analytically pure, even upon Kugelrohr distillation. The resulting amine was coupled with acid **131** using DCC and HOBt to afford diene-amide **159** in 43% yield.

Scheme 25. Synthesis of Diene-Amide **159**[a]

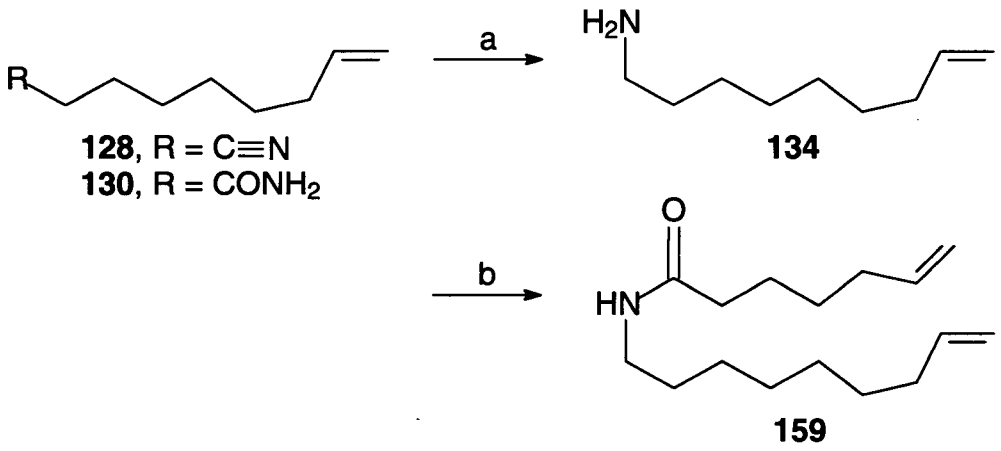

[a]Key: (a) LAH, THF, 70 °C; (b) acid **131**, DCC, HOBt, CH_2Cl_2, 0 °C to rt. See Table 19 for product yields.

In an attempt to improve the yield of the amide bond forming reaction the same series of steps were carried out starting with amide **130**. Reduction of **130** with LAH, followed by Kugelrohr distillation gave analytically pure amine **134** (Scheme 25). Coupling of amine **134** with acid **131** using DCC and HOBt gave diene-amide **159** in an improved yield of 83%. The results for the two separate syntheses of diene-amide **159** are summarized in Table 19.

Table 19. Comparison of Yield in the Formation of Diene-Amide **159** from Amine **134** Obtained from the Reduction of Nitrile **128** or Amide **130**

Entry	R	Yield **134** (%)[a]	Yield **159** (%)[b]
1	$CONH_2$	68	83
2	C≡N	84	43

[a] Refers to isolated yield after Kugelrohr distillation.
[b] Refers to isolated yield after chromatography.

Concurrent to the synthesis of diene-amide **159** from nitrile **128**, similar results were obtained for the analogous syntheses of diene-amide **161**. Nitrile **160** was prepared by the addition of lithioacetonitrile to 8-bromooctene (**127**) (Scheme 26). Lithioacetonitrile was generated by the addition of *n*-butyllithium to acetonitrile in THF. The resulting nitrile **160** was reduced with LAH to afford amine **138**. Much like the formation of amine **134** by reduction of the corresponding nitrile, **138** was not obtained analytically pure even upon Kugelrohr distillation. None of the desired diene-amide **161** was obtained after the coupling of amine **138** with acid **135**[100] using DCC and HOBt.

Scheme 26. Synthesis of Diene-Amide **161**[a]

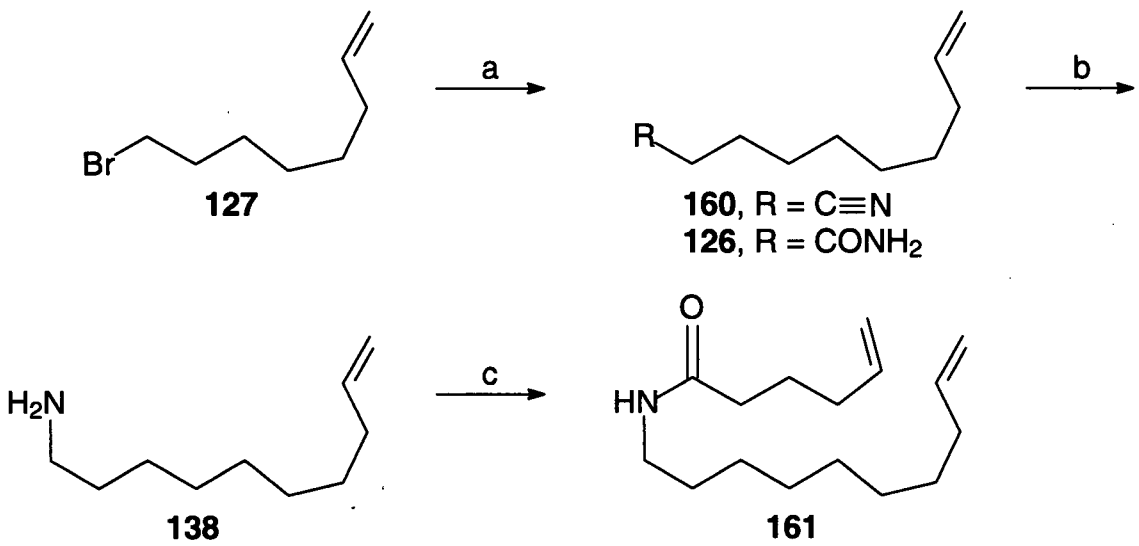

127 **160**, R = C≡N; **126**, R = $CONH_2$ **138** **161**

[a]Key: (a) $LiCH_2CN$, THF, -78 °C to rt, 57% (**160**); (b) LAH, THF, 70 °C; (c) acid **135**, DCC, HOBt, CH_2Cl_2, 0 °C to rt. See Table 20 for product yields.

The successful synthesis of diene-amide **159**, from amide **130**, suggested that amide **126** should be used as the starting material in an attempt to improve the yield of the amide bond forming reaction. Reduction of **126** with LAH, followed by Kugelrohr distillation, gave analytically pure amine **138** (Scheme 26). Coupling of **138** with acid **135**[100] using DCC and HOBt gave diene-amide **161** in an excellent yield of 90%. The results for the two separate syntheses of diene-amide **161** are summarized in Table 20.

Table 20. Comparison of Yield in the Formation of Diene-Amide **161** from Amine **138** Obtained by the Reduction of Nitrile **160** or Amide **126**

Entry	R	Yield **138** (%)[a]	Yield **161** (%)[b]
1	$CONH_2$	88	90
2	C≡N	82	0

[a] Refers to isolated yield after Kugelrohr distillation.
[b] Refers to isolated yield after chromatography.

The results from the syntheses of diene-amides **159** and **161** indicated that the amines formed by the reduction of the corresponding nitriles were the problematic component in the diene-amide synthetic strategy. The carboxylic acids and the coupling conditions and reagents (DCC and HOBt) were eliminated as the sources of impediment to the amide bond forming reactions. The reaction conditions remained constant and the carboxylic acids were used from the same batch of compound, as were the coupling reagents. Thus, if any impurity or problematic reactivity existed with any of these compounds or conditions the lower yields should have been more consistently observed regardless of the method of amine formation.

The reduction of a nitrile to a primary amine is often complicated by the formation of secondary and tertiary amines. By catalytic hydrogenation, the ratio of these products was often dependent on the metal catalyst, reaction conditions, and the structure of the nitrile.[150,151] In fact, in the absence of any catalyst or reducing agent an amidine, the intermediate in the reductions described above, can be formed upon reaction of an α-halogenated nitrile with an amine.[152] However, under these conditions non-halogenated nitriles, such as acetonitrile, were not reactive. An example more closely related to our work involved the reduction of a nitrile with sodium borohydride in

the presence of a primary or secondary amine to afford the corresponding secondary or tertiary amine.[153] For example, reaction of phenylacetonitrile with dimethylamine, followed by reduction of the resulting amidine intermediate, led to the formation of 2-phenyl-*N*,*N*-dimethylethylamine (Figure 43).

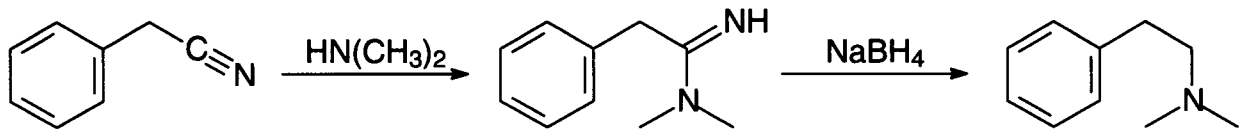

Figure 43. Reduction of phenylacetonitrile with $NaBH_4$ in the presence of dimethylamine (from reference 153).

This reactivity could conceivably be extended to the reduction of nitriles with LAH. A primary amine, formed by reduction of a nitrile with LAH, could react with a molecule of the initial nitrile to form an amidine (Figure 44). Reduction of the resulting amidine with LAH would afford a secondary amine. Addition of the newly formed secondary amine to another molecule of the initial nitrile, followed by reduction of the resulting amidine with LAH, would provide a tertiary amine. These series of steps would clearly lead to a complex mixture of primary, secondary, and tertiary amines.

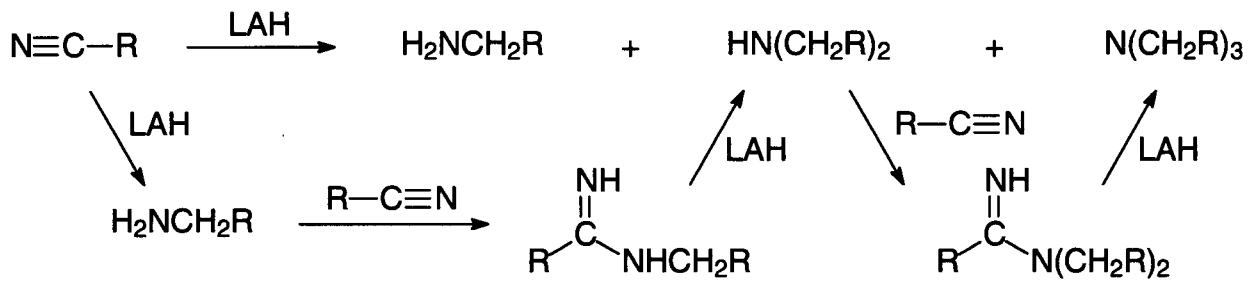

Figure 44. Proposed reduction of a nitrile with LAH in the presence of a primary amine.

When the reduction of nitriles **128** and **160** with LAH is considered in the context of these examples the conclusion could easily be drawn that the resulting product was a mixture of the primary, secondary, and tertiary amines. This would explain why the amide bond forming reactions proceeded in poor yield, and also why primary amines **134** and **138** could not be obtained analytically pure when formed by reduction of the

corresponding nitriles. However, signals indicative of the undesired secondary or tertiary amines were not observed in the NMR and mass spectral data obtained from either amine. At this point it remains unclear why the amide bond forming reactions using amines derived from nitriles did not proceed as well as those using amines derived from primary amides.

3.4.2 Synthesis of Diacetylisomotuporamine C Trifluoroacetate (42·TFA)

Diacetylisomotuporamine C trifluoroacetate (**42**·TFA) was prepared using similar strategies to those employed in the syntheses of diacetylmotuporamine trifluoroacetates A (**36**·TFA) and B (**37**·TFA). Beginning with diene-amide **159**, this compound was cyclized via RCM using ruthenium benzylidene **3** (Scheme 27). The same RCM conditions developed for the formation of 14-membered lactams in Chapter 2 were applied to this cyclization. Specifically, separate solutions of **159** and **3**, both in dichloromethane, were slowly combined over 3 hours under high dilution conditions using a syringe pump. Using these cyclization conditions the isomeric macrocyclic lactams **162** and **163** were obtained in an overall yield of 70% and in a ratio of 37:63 respectively. Column and radial chromatography were ineffective in completely separating these isomers. Silver nitrate impregnated silica gel has often been used to more effectively separate olefin isomers.[154] Chromatography conducted under these conditions normally causes the *Z* isomer to be more strongly retained to the stationary phase than the *E* isomer. This process is quite effective when the order of elution is first the *E* isomer and then the *Z* isomer. Unfortunately, in this instance (*Z*)-lactam **162** elutes first followed by (*E*)-lactam **163**. Consequently, purification of the mixture using silver nitrate impregnated silica gel resulted in the complete co-elution of these isomers. Approximately 40 mg, or 14% of the mixture, of the desired (*Z*)-lactam **162** was isolated by conventional chromatography and carried on to the next step in the synthesis of diacetylisomotuporamine C trifluoroacetate (**42**·TFA).

Reduction of lactam **162** with LAH followed by Michael addition of the resulting macrocyclic amine **167** to methyl acrylate gave β-amino ester **164** in a yield of 65% over two steps. Amidation of **164** with 1,3-diaminopropane followed by reduction of the resulting amide with LAH gave isomotuporamine C (**40**) in a yield of 99% over two steps. Acetylation of triamine **40** followed by purification with reversed-phase

chromatography, using 60% water and 1% trifluoroacetic acid in methanol as eluant, gave diacetylisomotuporamine C trifluoroacetate (**42**·TFA) in 73% yield. This last step was conducted in the same manner as Andersen and co-workers.[58]

Scheme 27. Synthesis of Diacetylisomotuporamine C Trifluoroacetate (**42**·TFA)[a]

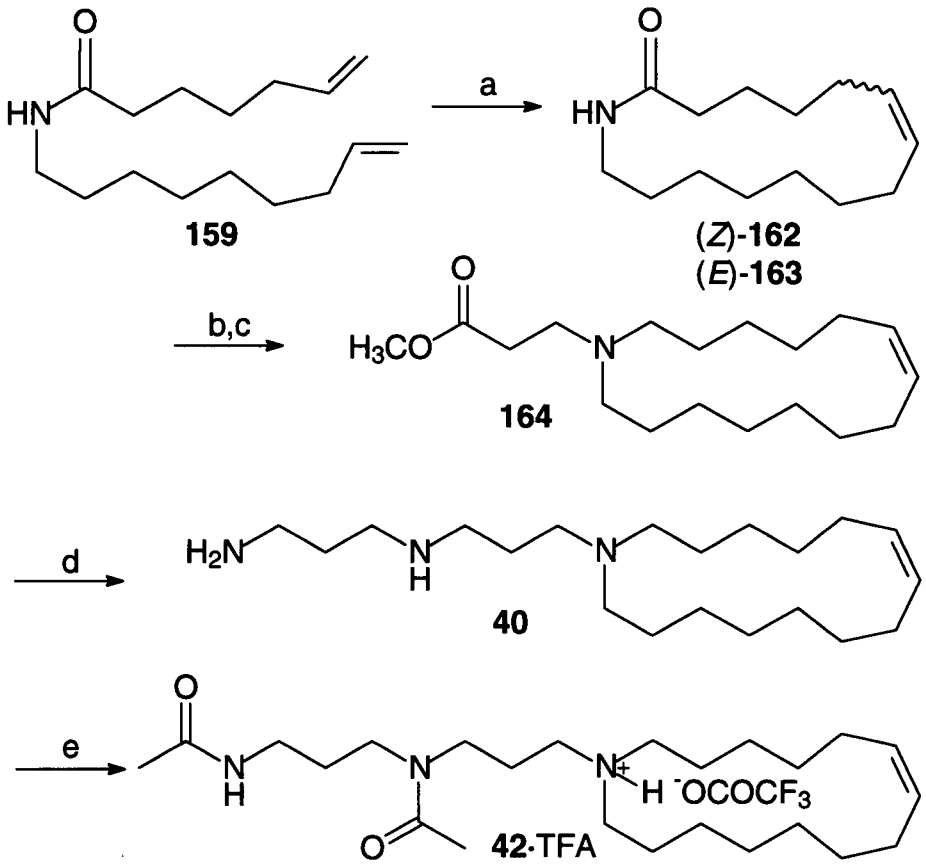

[a]Key: (a) 5 mol% **3**, CH_2Cl_2, 45 °C, 70% (**162** and **163**); (b) radial chromatography; (c) LAH, THF, 70 °C; then $CH_3OCOCH{=}CH_2$, MeOH, rt, (65% for two steps); (d) $H_2N(CH_2)_3NH_2$, MeOH, rt; LAH, THF, 70 °C, (99% for two steps); (e) Ac_2O, pyr, rt; then reversed-phase chromatography using H_2O, MeOH, and TFA (60:39:1), 73%.

Subsequent to our published results describing this work,[69] an alternate route to isomotuporamine C (**40**) appeared in the literature.[71] The key step of this route involved cyclization of diyne **165** via RCM followed by Lindlar-type reduction resulting in the stereoselective formation of macrocyclic amine **166** (Scheme 28). Following cleavage of the Fmoc group, the remainder of triamine **40** was assembled following the route established by Baldwin and co-workers.[70] This example illustrated an indirect solution

to the fundamental problem associated with alkene RCM; formation of the olefin without control of the resulting stereochemistry.

Scheme 28. Key Step in an Alternate Synthesis of Isomotuporamine C (**40**) (from reference 71)[a]

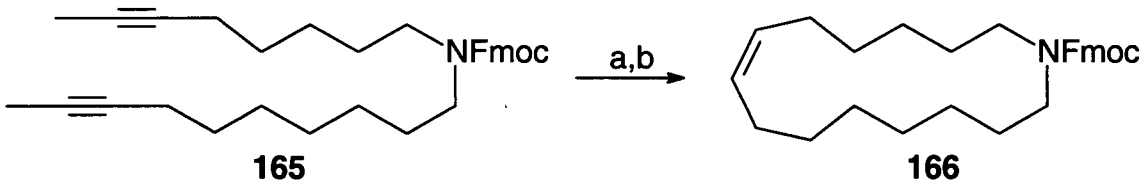

165 **166**

[a]Key: (a) 5 mol% $Mo(CO)_6$, *p*-chlorophenol, chlorobenzene, 140 °C, 67%;
(b) Lindlar catalyst, quinoline, H_2, MeOH, 98%.

Returning to the inseparable mixture of lactams **162** and **163**, the separation of these isomers at a later stage in the synthesis was considered. The mixture of lactams **162** and **163**, in a ratio of 44:56, were reduced with LAH to afford a mixture of macrocyclic amines **167** and **168** in an overall yield of 94% (Scheme 29). The mixture of **167** and **168** was added to methyl acrylate in a Michael fashion. Removal of the excess reagent and solvent in vacuo gave a mixture of isomeric β-amino esters **164** and **169** in an overall yield of 66% and in a ratio of 47:53 respectively. These isomers were more readily separated by conventional chromatography than the isomeric lactams, **162** and **163**, from which they were derived. The possibility of olefin isomerization, either in configuration or position, was considered when the synthetic strategy for these compounds was developed. A comparison between the isomeric ratios (*Z*:*E*) of the original mixture of lactams **162** and **163** and of the separable β-amino ester products **164** and **169** indicated that little or no isomerization of either olefin took place during the reduction or Michael addition. Therefore, this suggested that these reactions did not lead to olefin isomerization.

Scheme 29. Synthesis of Methyl 3-((*Z*/*E*)-1-azacyclopentadec-7-enyl)propionates (**164**) and (**169**)[a]

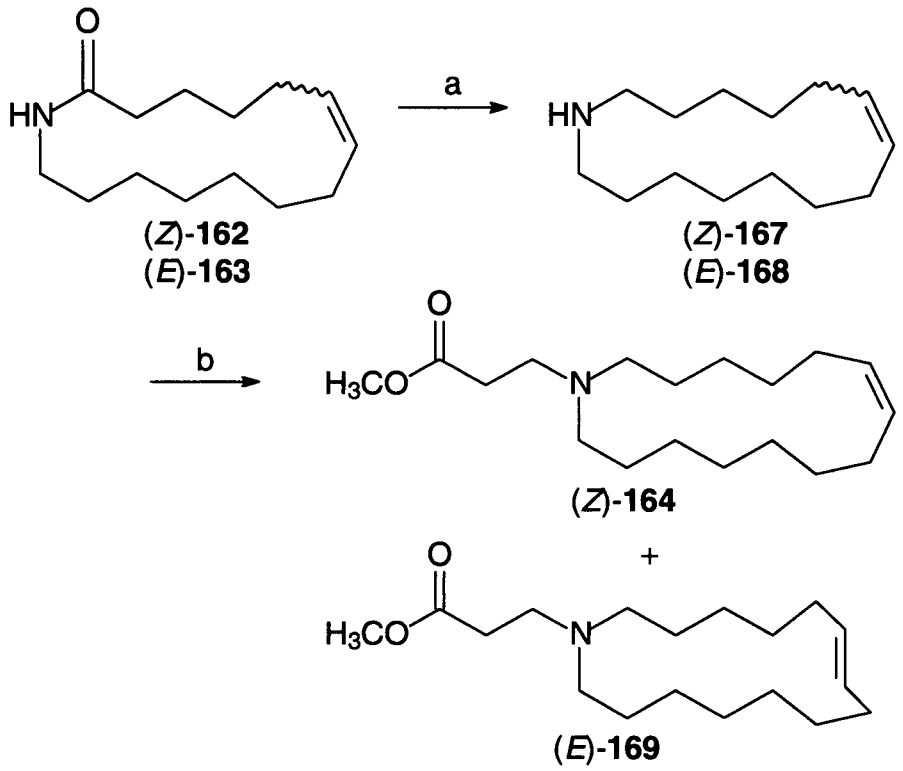

[a]Key: (a) LAH, THF, 70 °C, 94%; (b) $CH_3OCOCH{=}CH_2$, MeOH, rt, 31% (**164**) and 35% (**169**).

Having completed the synthesis of diacetylisomotuporamine C trifluoroacetate (**42**·TFA), what remained was a detailed analysis and comparison between the spectral data of **42**·TFA and the authentic compound **38**. Following the previous analyses performed for diacetylmotuporamine trifluoroacetates A (**36**·TFA) and B (**37**·TFA), this comparison focussed on the NMR data from both compounds. Regardless of the results from this analysis the comparison was not complete until the other positional isomer, compound **41**·TFA, was synthesized and subsequently compared to the authentic compound through their respective spectral data. The following analysis can only confirm or disprove the C-15/C-16 bond as a valid position for the olefin within the authentic compound.

3.4.2.1 Spectral Comparison Between Authentic Diacetylmotuporamine C (38) and Diacetylisomotuporamine C Trifluoroacetate (42·TFA)

Spectral data for synthetic compound **42**·TFA was obtained in a similar manner to the corresponding data from the authentic compound **38**. HRMS results for both the synthetic and authentic compounds were consistent with the composition of the assigned structure. Unfortunately this information did not lead to a better understanding of the location of the olefin within the macrocyclic amine. A more detailed analysis of the NMR spectral data was required.

Inspection of the 400 MHz ^{1}H NMR spectra for authentic diacetylmotuporamine C (**38**) (Figure 45 a) and synthetic diacetylisomotuporamine C trifluoroacetate (**42**·TFA) (Figure 45 b) illustrated numerous differences between these spectra. The most obvious differences were observed between the resonances in the olefinic region (ca. δ 5.20-5.50) and in the methylene envelope (ca. δ 1.20-1.60). Immediately, it appeared from the incomplete correlation between these spectra that the two compounds were different.

Proton homonuclear decoupling NMR experiments were conducted in order to determine the configuration of the olefin in synthetic compound **42**·TFA. The decoupling experiments were performed by irradiation of one of the two allylic proton resonances (ca. δ 2.0-2.3) resulting in simplification of the adjacent olefinic proton resonance to a doublet. These experiments indicated that the olefin had the *Z* configuration, with J = 11.1 Hz. This result, although not surprising considering this compound was derived from (*Z*)-lactam **162**, did indicate that the chemistry utilized to make **42**·TFA from **162** did not lead to isomerization of the olefin. The olefin in the authentic compound also had the *Z* configuration, with J = 10.9 Hz.[58] The differences between the coupling constants and the chemical shift data indicated that the pair of olefinic protons in authentic **38** were in a different chemical environment than the corresponding protons in **42**·TFA, and therefore must be in a different position within the macrocyclic amine.

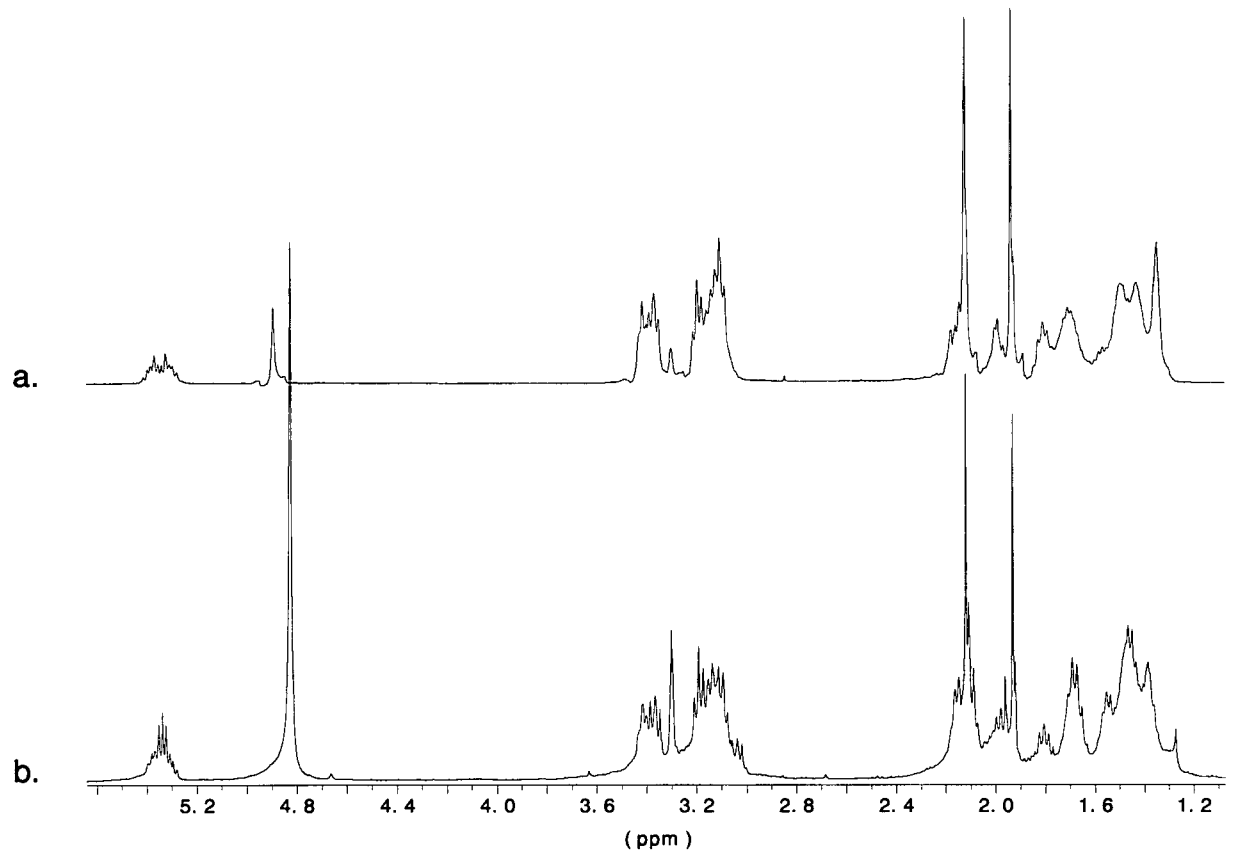

Figure 45. 400 MHz ^{1}H NMR spectra of (a) authentic diacetylmotuporamine C (**38**), and (b) synthetic diacetylisomotuporamine C trifluoroacetate (**42**·TFA).

Although the spectral data presented thus far suggested that these two compounds were different, a more concrete conclusion was based on a comparison between the ^{13}C and 2D NMR spectral data from **42**·TFA and **38**. Indeed, inspection of the 500 MHz ^{1}H and ^{13}C NMR spectral data for these compounds provided further evidence that they were different (Table 21). The assignments provided for compound **42**·TFA were based on analyses of the 500 MHz COSY, HMQC, and HMBC data. The proton and carbon resonances from the atoms within the spermidine-like unit of **42**·TFA were in agreement with the corresponding resonances from authentic **38**. Although this suggested the similarity of these compounds, it was not surprising considering how far removed these atoms were from the olefin and thus the effects of its chemical environment. Comparison between the ^{13}C NMR resonances from **38** and **42**·TFA, especially when viewed in numerical order, showed poor correlation between the resonances for the carbon atoms within the macrocyclic amine.

Table 21. 500 MHz ^{1}H and ^{13}C NMR Assignments for Authentic Diacetylmotuporamine C (**38**) and Synthetic Diacetylisomotuporamine C Trifluoroacetate (**42**·TFA)[a] (Part 1)

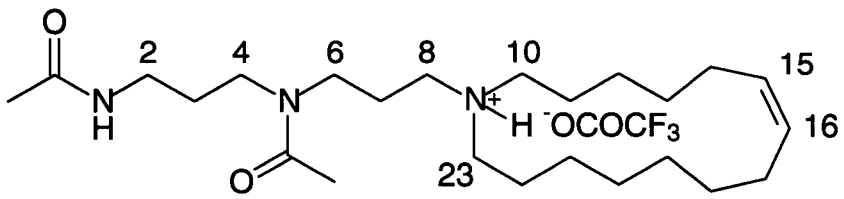

42·TFA

Atom	Authentic Diacetylmotuporamine C (**38**)[58]		Synthetic Diacetylisomotuporamine C Trifluoroacetate (**42**·TFA)	
	δ $^{1}H^{b}$	δ $^{13}C^{b}$	δ $^{1}H^{b}$	δ $^{13}C^{b}$
2	3.20	37.8	3.19	37.8
3	1.81	29.5	1.81	29.5
4	3.37	48.0	3.37	48.0
6	3.42	43.7	3.42	43.6
7	1.99	24.1	1.99	24.1
8	3.11	53.9	3.10	53.2
10	3.11	53.6	3.10	52.5
11	1.71	23.1[c]	1.67	23.0
12	1.49, 1.57	23.7[c]	1.43-1.51	25.5[c]
13	2.16	27.0	1.55	28.6
14	5.32	130.6	2.14	26.1
15	5.37	133.0	5.31	131.0
16	2.12	26.6	5.36	132.0
17	1.49	29.2	2.10	27.2
18	1.35	27.8	1.42	29.4
19	1.35-1.43	27.0[d]	1.32-1.41	27.8[d]
20	1.35-1.43	26.6[d]	1.32-1.41	27.5[d]

[a] Due to acetamide rotamers, the majority of carbons and some protons appeared as two resonances. Only the δ value for the more intense resonance is represented.
[b] The chemical shift values are referenced to CD_2HOD (^{1}H) and CD_3OD (^{13}C).
[c,d] Assignments within a column are interchangeable.

Table 21. 500 MHz ^{1}H and ^{13}C NMR Assignments for Authentic Diacetylmotuporamine C (**38**) and Synthetic Diacetylisomotuporamine C Trifluoroacetate (**42**·TFA)[a] (Part 2)

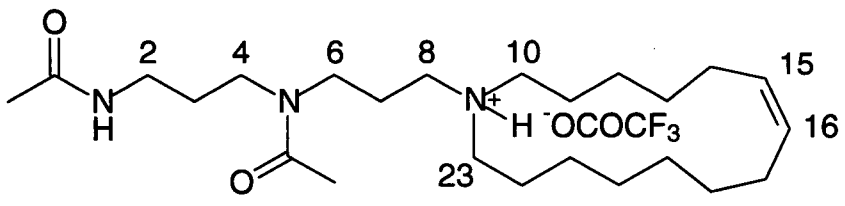

42·TFA

	Authentic Diacetylmotuporamine C (**38**)[58]		Synthetic Diacetylisomotuporamine C Trifluoroacetate (**42**·TFA)	
Atom	δ $^{1}H^{b}$	δ $^{13}C^{b}$	δ $^{1}H^{b}$	δ $^{13}C^{b}$
21	1.43	27.5[d]	1.43-1.51	25.9[c]
22	1.71	25.0[c]	1.70	22.2
23	3.15	52.9	3.14	53.0
CO (N1)		173.5		173.6
CH_3 (N1)	1.93	22.6	1.93	22.6
CO (N5)		174.4		174.6
CH_3 (N5)	2.12	21.2	2.12	21.2

[a] Due to acetamide rotamers, the majority of carbons and some protons appeared as two resonances. Only the δ value for the more intense resonance is represented.
[b] The chemical shift values are referenced to CD_2HOD (^{1}H) and CD_3OD (^{13}C).
[c,d] Assignments within a column are interchangeable.

The differences between the ^{13}C NMR spectra provided further evidence that the olefins in these compounds were situated in different positions within the ring, thus resulting in different chemical shift values due to the different chemical environments.

Recall that the ^{1}H and ^{13}C NMR assignments made for **42**·TFA were based on the analysis of COSY, HMQC, and HMBC data. The relationship and connectivity between the proton and carbon resonances corresponding to the atoms within the spermidine-like unit and the two acetamide groups were established and mapped out by a detailed analysis of this 2D NMR data (see Figure 41). The details and results from this analysis were similar to those established for diacetylmotuporamine trifluoroacetates A (**36**·TFA) and B (**37**·TFA) and do not require any further elaboration.

The position of the olefin within the macrocyclic amine was identified by a detailed analysis of the 2D NMR data. Figure 46 illustrates some of the COSY and HMBC correlations, where bold red bonds represent COSY correlations and the blue arrows represent HMBC correlations. For simplicity structure **42**, the free base of **42**·TFA, is shown in this figure. Subsequent to the identification of the spermidine-like unit, two low field proton resonances at δ 3.10 and δ 3.14 remained unassigned. HMBC correlations between both of these proton resonances and C-8 (δ 53.2) identified these as the methylene groups at C-10 and C-23 both attached to N-9. COSY correlations between H-10/H-10' (δ 3.10) and H-11/H-11' (δ 1.67), and also between H-22/H-22' (δ 1.70) and H-23/H-23' (δ 3.14) readily identified a portion of the macrocyclic amine extending from N-9. Additional COSY correlations between H-13/H-13' (δ 1.55) and H-14/H-14' (δ 2.14), which in turn was correlated to H-15/H-15' (δ 5.31), which was correlated to H-16/H-16' (δ 5.36) followed by H-17/H-17' (δ 2.10) and finally to H-18/H-18' (δ 1.42) identified a second linear substructure within this ring. HMBC correlations between H-13/H-13' (δ 1.55) and C-11 (δ 23.0), C-14 (δ 26.1), C-15 (δ 131.0), and a resonance at δ 25.5 suggested that carbons C-11 and C-13 were attached to a common methylene unit which must be C-12 (δ 25.5). The assignment of C-12 resolved ambiguous correlations observed in the COSY and HMQC spectra. It appeared that COSY correlations existed between the resonances from H-12/H-12' and H-21/H-21', both contained within the multiplet at δ 1.43-1.51, and the proton resonances H-11/H-11' (δ 1.67) and H-22/H-22' (δ 1.70). This problem was further complicated by unresolved HMQC correlations between both proton resonances at δ 1.43-1.51 and the carbon resonances δ 25.5 and δ 25.9. The assignment of the methylene unit C-12 (δ 25.5) allowed the assignment of the resonance at δ 25.9 to C-21, by a process of elimination. Finally, HMBC correlations were observed between H-17/H-17' (δ 2.10) and a carbon resonance at either δ 27.5 or δ 27.8, and also between one of these carbons and H-21/H-21' (δ 1.43-1.51) and H-22/H-22' (δ 1.70). This suggested that carbons C-18 and C-21 were attached through two carbons, C-19 and C-20. Due to the complexity of the spectral data the carbon resonances at δ 27.5 or δ 27.8 were arbitrarily assigned to C-20 and C-19 respectively.

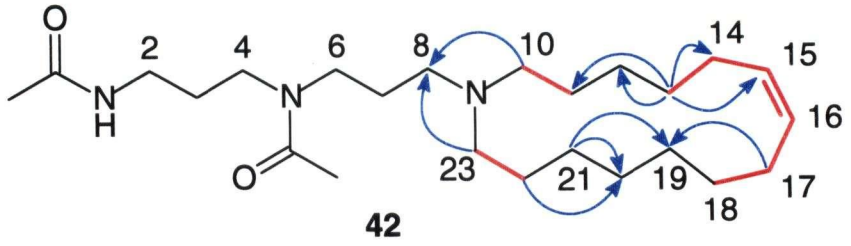

42

Figure 46. Partial 500 MHz COSY (bold red bonds) and HMBC (blue arrows) correlations for diacetylisomotuporamine C trifluoroacetate (**42**·TFA).

Combustion analysis results were not consistent with the composition of **42**·TFA. Much like diacetylmotuporamine trifluoroacetates A (**36**·TFA) and B (**37**·TFA) the presence of a signal at δ 0.0 in the ^{19}F NMR spectrum and LRMS results obtained in negative-ion LSIMS mode for **42**·TFA confirmed the presence of trifluoroacetate anion. This data suggested that **42**·TFA existed as the ammonium salt and might have contained a combination of water and trifluoroacetic acid as well, thus affecting the results from combustion analysis. The chemical shift values for protons H-10/H-10' (δ 3.10) and H-23/H-23' (δ 3.14) were consistent with the corresponding proton resonances from compounds of type **W** (see Table 17). This provided further evidence that **42**·TFA was obtained as the ammonium salt. Since **42**·TFA and the authentic material were purified in the same manner they both must have been isolated in this form and not as the free base. Therefore differences between these compounds were solely due to different olefin positions.

In conclusion, diacetylisomotuporamine C trifluoroacetate (**42**·TFA) was synthesized from diene-amide **159** in six steps in an overall yield of 12%. The spectral data presented in this section clearly illustrated the differences between **42**·TFA and the authentic compound **38**. Consequently, these results eliminated the C-15/C-16 bond position as one of the possibilities for the location of the olefin. Further analysis of **42**·TFA confirmed this compound was isolated as the ammonium salt. In order to conclusively determine the structure of the authentic material, the synthesis of the C-14/C-15 olefin isomer **41**·TFA and subsequent comparison of the spectral data for these compounds was required.

3.4.3 Synthesis of Diacetylmotuporamine C Trifluoroacetate (41·TFA)

The same set of steps were carried out in the synthesis of diacetylmotuporamine C trifluoroacetate (**41**·TFA) as those applied in the synthesis of diacetylisomotuporamine C trifluoroacetate (**42**·TFA). Lactams **170** and **171** were synthesized using the same reaction conditions that were applied in the formation of lactams **162** and **163** (Section 3.4.2). Accordingly, diene-amide **161** was cyclized via RCM with ruthenium benzylidene **3** (Scheme 30). Isomeric lactams **170** and **171** were formed in an overall yield of 76% and in a ratio of 53:47 respectively. Column and radial chromatography of the mixture of isomers was not effective and only a small amount of both were obtained. Unlike the order of elution of their positional neighbours, lactams **162** and **163**, (*E*)-lactam **170** would elute first followed by (*Z*)-lactam **171**. As discussed earlier, chromatography with silver nitrate impregnated silica gel should be effective with this order of elution. Accordingly, the separation of isomeric lactams **170** and **171** was achieved by application of this purification technique.

The desired isomer, lactam **171**, was carried on to the next step. Reduction of **171** with LAH gave macrocyclic amine **172** in a yield of 87%. An alternate route to **172**, via alkyne RCM, recently appeared in the literature (see Scheme 28).[71] β-Amino ester **173** was formed by Michael addition of **172** to methyl acrylate in a yield of 72%, after chromatography. Amidation of **173** with 1,3-diaminopropane followed by reduction of the resulting amide with LAH gave motuporamine C (**39**) in a yield of 95% over two steps. Acetylation of **39** followed by purification with reversed-phase chromatography, using 60% water and 1% trifluoroacetic acid in methanol as eluant, gave diacetylmotuporamine C trifluoroacetate (**41**·TFA) in 78% yield. This last step was conducted in the same manner as Andersen and co-workers.[58]

With the synthesis of compound **41**·TFA complete a detailed comparison of the spectral data from this compound to that of the authentic compound **38** was conducted. Since the spectral analysis of **38** only allowed for two possible positional isomers, and one isomer was eliminated based on an unfavourable comparison with isomeric compound **42**·TFA, it was expected that **41**·TFA would compare favourably to **38**.

Scheme 30. Synthesis of Diacetylmotuporamine C Trifluoroacetate (**41**·TFA)[a]

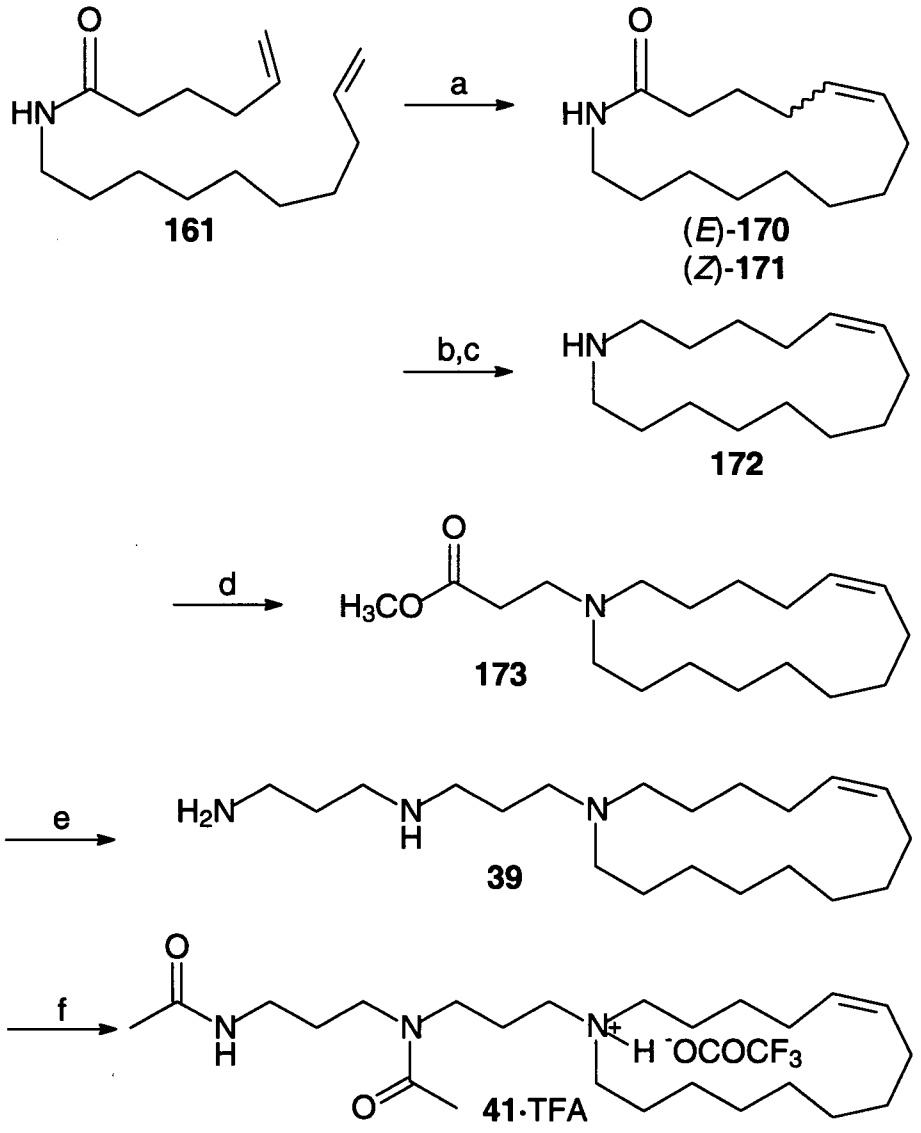

[a]Key: (a) 5 mol% **3**, CH_2Cl_2, 45 °C, 76% (**170** and **171**) ; (b) radial chromatography; (c) LAH, THF, 70 °C, 87%; (d) $CH_3OCOCH{=}CH_2$, MeOH, rt, 72%; (e) $H_2N(CH_2)_3NH_2$, MeOH, rt; LAH, THF, 70 °C, (95% for two steps); (f) Ac_2O, pyr, rt; then reversed-phase chromatography using H_2O, MeOH, and TFA (60:39:1), 78%.

3.4.4 Structural Determination of Authentic Diacetylmotuporamine C (38)

The spectral analysis of **41**·TFA followed a process similar to that used in the analysis of the olefin isomer **42**·TFA. The HRMS results for the synthetic and authentic compounds were consistent with the composition of the assigned structure. However, a more detailed analysis of the NMR spectral data was required to clearly compare the synthetic and authentic compounds.

Inspection of the 400 MHz ^{1}H NMR spectra for authentic diacetylmotuporamine C (**38**) (Figure 47 b) and synthetic diacetylmotuporamine C trifluoroacetate (**41**·TFA) (Figure 47 c) illustrated the similarity between these compounds. For comparison the 400 MHz ^{1}H NMR spectrum for diacetylisomotuporamine C trifluoroacetate (**42**·TFA) (Figure 47 a) is included. The spectrum of **41**·TFA resembled the spectrum of **38**, especially in the region containing the olefinic resonances (ca. δ 5.20-5.50) and the methylene envelope (ca. δ 1.20-1.60), which did not compare well in the spectrum of **42**·TFA. So far it appeared that **41**·TFA and authentic **38** were the identical based on the correlation between their respective proton NMR spectra.

Proton homonuclear decoupling NMR experiments were conducted in order to determine the configuration of the olefin in synthetic **41**·TFA. These experiments were performed in a manner similar to those used for the same determination of isomeric **42**·TFA. These experiments indicated that the olefin had the *Z* configuration, with $J = 10.9$ Hz. This result, although not surprising considering that this compound was derived from (*Z*)-lactam **171**, did indicate that the chemistry utilized to make **41**·TFA from **171** did not lead to any isomerization of the olefin. The olefin in the authentic compound also had the *Z* configuration with $J = 10.9$ Hz.[58] The similarity of the coupling constants and the chemical shift data indicated that the pair of olefinic protons in authentic **38** and the corresponding protons in **41**·TFA were in a similar chemical environment and thus must be in the same position within the macrocyclic amine.

The spectral data thus far suggested that these two compounds were identical. In order to provide a more solid basis for this conclusion the ^{13}C and 2D NMR spectral data from **41**·TFA were compared to the authentic compound **38**.

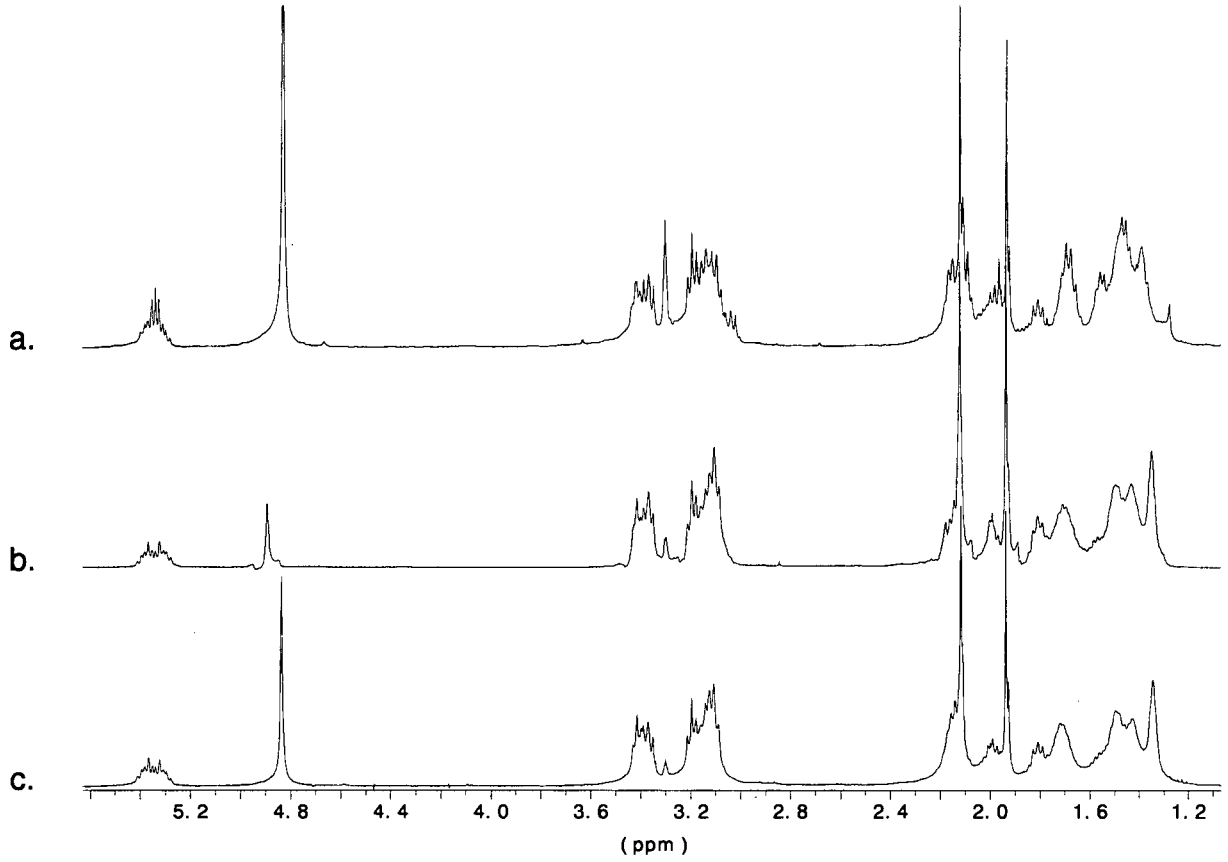

Figure 47. 400 MHz ^{1}H NMR spectra of (a) synthetic diacetylisomotuporamine C trifluoroacetate (**42**·TFA), (b) authentic diacetylmotuporamine C (**38**), and (c) synthetic diacetylmotuporamine C trifluoroacetate (**41**·TFA).

A detailed comparison of the 500 MHz NMR spectral data for **38** and **41**·TFA provided further evidence that these compounds were identical (Table 22). The assignments provided for compound **41**·TFA were based on those reported by Andersen and co-workers[58] and on the analysis of the 500 MHz COSY, HMQC, and HMBC data for the synthetic compound. The proton and carbon resonances for the atoms within the spermidine-like unit of **41**·TFA were in agreement with the corresponding resonances from **38**. The correlation between the two sets of spectra in this region did not necessarily indicate that these compounds were the same considering how far removed the olefin was from this unit. Recall that correlations in the same region were made between authentic **38** and the isomeric compound **42**·TFA despite the fact that these compounds were found to be different. A detailed comparison of the proton and carbon resonances as well as the 2D NMR data corresponding to the macrocyclic amine region provided more conclusive evidence.

Table 22. 500 MHz ^{1}H and ^{13}C NMR Assignments for Authentic Diacetylmotuporamine C (**38**) and Synthetic Diacetylmotuporamine C Trifluoroacetate (**41**·TFA)[a] (Part 1)

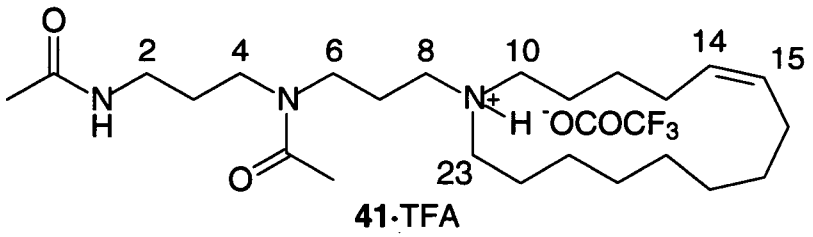

41·TFA

Atom	Authentic Diacetylmotuporamine C (**38**)[58]		Synthetic Diacetylmotuporamine C Trifluoroacetate (**41**·TFA)	
	δ ^{1}H[b]	δ ^{13}C[b]	δ ^{1}H[b]	δ ^{13}C[b]
2	3.20	37.8	3.19	37.8
3	1.81	29.5	1.80	29.4
4	3.37	48.0	3.37	47.9
6	3.42	43.7	3.41	43.7
7	1.99	24.1	1.98	24.0
8	3.11	53.9	3.11	53.9
10	3.11	53.6	3.15	52.8
11	1.71	23.1[c]	1.72	23.0
12	1.49, 1.57	23.7[c]	1.47, 1.57	26.5
13	2.16	27.0	2.16	27.0
14	5.32	130.6	5.31	130.6
15	5.37	133.0	5.38	133.0
16	2.12	26.6	2.12	26.5
17	1.49	29.2	1.49	29.2
18	1.35	27.8	1.31-1.38	27.5[c]
19	1.35-1.43	27.0[d]	1.39-1.48	24.9[d]
20	1.35-1.43	26.6[d]	1.31-1.38	26.9[c]

[a] Due to acetamide rotamers, the majority of carbons and some protons appeared as two resonances. Only the δ value for the more intense resonance is represented.
[b] The chemical shift values are referenced to CD_2HOD (^{1}H) and CD_3OD (^{13}C).
[c,d] Assignments within a column are interchangeable.

Table 22. 500 MHz ^{1}H and ^{13}C NMR Assignments for Authentic Diacetylmotuporamine C (**38**) and Synthetic Diacetylmotuporamine C Trifluoroacetate (**41**·TFA)[a] (Part 2)

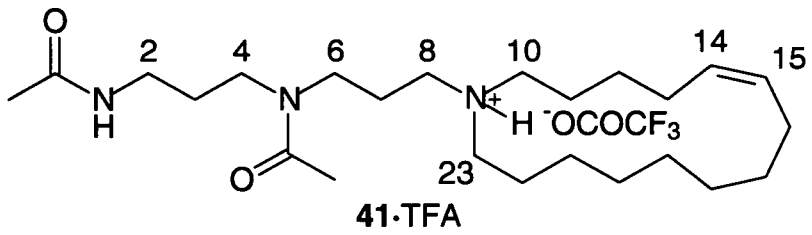

41·TFA

	Authentic Diacetylmotuporamine C (**38**)[58]		Synthetic Diacetylmotuporamine C Trifluoroacetate (**41**·TFA)	
Atom	δ $^{1}H^{b}$	δ $^{13}C^{b}$	δ $^{1}H^{b}$	δ $^{13}C^{b}$
21	1.43	27.5[d]	1.39-1.48	27.7[d]
22	1.71	25.0[c]	1.68	23.6
23	3.15	52.9	3.11	53.5
CO (N1)		173.5		173.6
CH_3 (N1)	1.93	22.6	1.94	22.5
CO (N5)		174.4		174.4
CH_3 (N5)	2.12	21.2	2.12	21.2

[a] Due to acetamide rotamers, the majority of carbons and some protons appeared as two resonances. Only the δ value for the more intense resonance is represented.
[b] The chemical shift values are referenced to CD_2HOD (^{1}H) and CD_3OD (^{13}C).
[c,d] Assignments within a column are interchangeable.

Nearly identical numerically ordered lists of proton and carbon data illustrated the similarity between the authentic and synthetic compounds. Changes to the assignments of some of the carbon resonances within the macrocyclic amine, from those of the authentic compound, were made based on analysis of the 500 MHz COSY, HMQC, and HMBC data from **41**·TFA. Assignments of the proton and carbon resonances corresponding to the atoms within the spermidine-like unit and the two acetamide groups were established and mapped out by a detailed analysis of the 2D NMR data (see Figure 41). The details and results from this analysis were similar to those discussed in previous sections and do not require any further elaboration. Verification of the position of the olefin within the macrocyclic amine unit of **41**·TFA, by

analysis of the 2D NMR data, led to a reassignment of certain carbon resonances in relation to those assignments provided for the authentic compound. Figure 48 illustrates some of the COSY and HMBC correlations that assisted in verifying the position of the olefin within the macrocyclic amine of **41**·TFA. For simplicity structure **41**, the free base of **41**·TFA, is shown in this figure. HMBC correlations between H-10/H-10' (δ 3.15) and C-8 (δ 53.9), between H-8/H-8' (δ 3.11) and C-10 (δ 52.8), and between H-23/H-23' (δ 3.11) and C-10 (δ 52.8) suggested the methylene carbons C-8, C-10, and C-23 were all attached to a common nitrogen atom (N-9). Two sets of COSY correlations between H-10/H-10' (δ 3.15) and H-11/H-11' (δ 1.72) and between H-21/H-21' (δ 1.39-1.48) and H-22/H-22' (δ 1.68), which in turn was correlated to H-23/H-23' (δ 3.11) readily identified a portion of the macrocyclic amine extending from N-9. Additional COSY correlations between H-12/H-12' (δ 1.47, 1.57) and H-13/H-13' (δ 2.16), which in turn was correlated to H-14/H-14' (δ 5.31) and then to H-15/H-15' (δ 5.38) identified a subunit that contained the olefin. Further COSY correlations between H-15/H-15' (δ 5.38) and H-16/H-16' (δ 2.12), which in turn was correlated to H-17/H-17' (δ 1.49) and finally to H-18/H-18' (δ 1.31-1.38) identified a linear substructure within the macrocyclic amine that included the olefin. HMBC correlations between H-13/H-13' (δ 2.16) and C-11 (δ 23.0) and C-12 (δ 26.5) and between H-12/H-12' (δ 1.47, 1.57) and C-10 (δ 52.8) and C-11 (δ 23.0) suggested a bond connection between carbons C-11 and C-12 despite the absence of COSY correlations between these methylene units. Thus far the 2D NMR data correlated a single chain of atoms connected by N-9 extending to C-18 in one direction and to C-21 in the other.

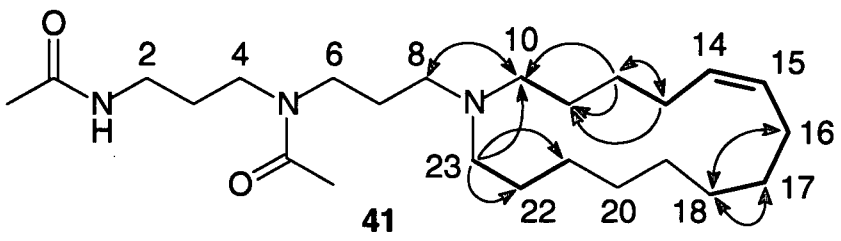

41

Figure 48. Partial 500 MHz COSY (bold red bonds) and HMBC (blue arrows) correlations for diacetylmotuporamine C trifluoroacetate (**41**·TFA).

The assignment of a particular carbon resonance to C-18 was complicated by an overlap of two proton resonances at δ 1.31-1.38. In this region HMQC correlations suggested the two carbon resonances at δ 26.9 and 27.5 for C-18. HMBC correlations were observed between H-16/H-16' (δ 2.12) and a carbon resonance at δ 27.5 and between H-17/H-17' (δ 1.49) and the same carbon resonance. These results suggested the assignment of the carbon resonance at δ 27.5 to C-18. Similar difficulties were encountered with the assignment of a carbon resonance to C-21. HMQC correlations suggested two possible carbon resonances at δ 24.9 or 27.7. HMBC correlations between H-23/H-23' (δ 3.10) and C-22 (δ 23.6) and a carbon resonance at δ 27.7 allowed the assignment of the latter resonance to C-21. The assignment of the remaining two carbon resonances, at δ 24.9 and 26.9, was not possible due to the complexity of the spectral data. Accordingly these resonances were arbitrarily assigned to C-19 and C-20 respectively.

The preceding discussion revealed two details concerning the macrocyclic amine unit of synthetic diacetylmotuporamine C (**41**·TFA). First, the analysis allowed the assignment of most of the proton and carbon resonances thus confirming the C-14/C-15 bond position of the olefin within the macrocyclic amine. Second, the analysis led to the reassignment of a number of carbon resonances from those provided for the authentic compound. Recall that the same carbon resonances appeared in the spectra of the authentic and synthetic compounds. Therefore, this did not lead to a different conclusion as to the olefin position within authentic diacetylmotuporamine C (**38**), but hopefully to a more accurate assignment of the carbon resonances.

As was discussed earlier, HRMS results obtained in positive-ion LSIMS mode were consistent with the composition of authentic diacetylmotuporamine C (**38**) and synthetic **41**·TFA. However, combustion analysis results were not consistent with the composition of either synthetic **41**·TFA or authentic **38**. Similar to the data obtained for ammonium trifluoroacetates **36**·TFA, **37**·TFA, and **42**·TFA the presence of a signal at δ 0.0 in the ^{19}F NMR spectrum and LRMS results obtained in negative-ion LSIMS mode for **41**·TFA confirmed the presence of trifluoroacetate anion. These results suggested that **41**·TFA existed as the ammonium salt and might have contained a combination of water and trifluoroacetic acid as well, thus affecting the results from combustion analysis. The chemical shift values for protons H-10/H-10' (δ 3.15) and H-23/H-23'

(δ 3.11) were consistent with the corresponding proton resonances from compounds of type **W** (see Table 17). This provided further evidence that **41**·TFA was obtained as the ammonium salt. Since the authentic and synthetic compounds were purified in the same manner it seems logical that they were both isolated as the ammonium salt and not the free base. The consistency between the spectral data for authentic **38** and synthetic **41**·TFA suggested this to be true.

In conclusion, diacetylmotuporamine C trifluoroacetate (**41**·TFA) was synthesized from diene-amide **161** in six steps in an overall yield of 17%. The data presented in this section clearly illustrated that synthetic compound **41**·TFA and authentic compound **38** were identical. Consequently, these results allowed the identification of the C-14/C-15 bond position as the location of the olefin within the macrocyclic amine unit of authentic motuporamine C (**35**). Subsequent to our published results,[69] a report of an alternate synthesis of isomeric triamines **39** and **40** fully confirmed our conclusions with regard to the position of the olefin in authentic motuporamine C (**35**).[71] Further analysis of **41**·TFA confirmed this compound was isolated as the ammonium salt. Therefore, the authentic compound **38** must have been isolated as the ammonium salt and not the free base as reported.

3.5 Conclusions

This chapter described the total syntheses of the marine alkaloids motuporamines A (**33**), B (**34**), and C (**35**), and their respective diacetylated derivatives **36**, **37**, and **38**. Furthermore, the structures assigned to the authentic compounds were verified by comparing the spectral data for the authentic and synthetic compounds. Recall that motuporamines A-C were isolated from *Xestospongia exigua* (Kirkpatrick) as an inseparable mixture that required the formation of the diacetylated derivatives to allow their separation.[58] Accordingly, the syntheses of the diacetylated derivatives was required to allow a comparison between the spectral data of the synthetic and authentic material. Also recall that the position of the olefin within the macrocyclic amine unit of authentic diacetylmotuporamine C (**38**) was not readily identified from the spectral data. However, the data did allow the investigators to narrow down the possibilities to the C-14/C-15 and the C-15/C-16 bond positions. Accordingly, the two isomeric compounds **41**·TFA and **42**·TFA were synthesized and compared to the authentic compound in an attempt to determine the position of the olefin within motuporamine C.

Two key strategies were employed in the syntheses of these compounds. The first utilized the RCM reaction to form the lactam precursors to the macrocyclic amine units. Studies of this reaction were presented in Chapter 2. The second strategy utilized Michael addition and amidation chemistry to form the spermidine-like unit from the nitrogen atom of the macrocyclic amine. The synthesis of the model compound **153** established this strategy as a simple and efficient method. Note that this strategy did not require the use of protective groups, and the purification simply involved evaporation of the solvent and excess reagents.

The synthesis of diacetylmotuporamine A trifluoroacetate (**36**·TFA) proceeded in excellent yield over four steps from lactam **65**. A comparison between the spectral data of the synthetic and authentic compounds indicated that they were identical. The synthesis of diacetylmotuporamine B trifluoroacetate (**37**·TFA) also proceeded in excellent yield over five steps from lactams **83**, **85**, and **86**, which in turn were synthesized as part of the studies presented in Chapter 2. A comparison between the spectral data of the synthetic and authentic compounds indicated they were different. Distinct differences between the spectral data of the free base **37** and the authentic compound indicated these compounds were also different. Ongoing studies in the Andersen laboratory confirmed that the structure assigned to the authentic material was

incorrect, however a related compound that possesses a cyclopropane ring was suggested.[149]

The syntheses of diacetylmotuporamine C trifluoroacetate (**41**·TFA) and the positional isomer diacetylisomotuporamine C trifluoroacetate (**42**·TFA) both proceeded in modest yield over six steps from diene-amides **161** and **159**, respectively. Comparisons between the spectral data from these compounds and authentic compound **38** indicated that **41**·TFA and the authentic compound were identical. Thus, the position of the olefin in diacetylmotuporamine C (**38**) was assigned to the C-14/C-15 bond position. This conclusion was later confirmed by an alternate synthesis of isomeric triamines **39** and **40**.[71]

Further analysis of **36**·TFA, **37**·TFA, **42**·TFA, and **41**·TFA, in addition to the formation of the free base **37**, suggested that the initial four compounds were isolated as the ammonium trifluoroacetates. Compounds **36**·TFA and **41**·TFA were found to be identical to authentic diacetylmotuporamines A (**36**) and C (**38**), respectively. This indicated that the authentic diacetylated compounds were in fact isolated as the ammonium salts and not as the free bases as they were originally reported.[58,69,70]

The productive application of the RCM reaction to the formation of a 15-membered lactam was illustrated in the syntheses of **41**·TFA and **42**·TFA. It should be noted that the diene-amide precursors used in these reactions possessed terminal double bonds that were sufficiently remote from the amide functionality. The good yield and low catalyst loading suggested that factors inhibiting the reaction, such as the conformational strain of a 15-membered ring, were not significant. The yields of 76% and 70% in the cyclization step for both compounds could be improved upon, however a greater problem was the lack of stereoisomeric control in these reactions. This led to a significant loss of product due to the formation of the undesired olefin isomer. An indirect solution to this fundamental problem of RCM was illustrated by an alternate synthesis of isomeric triamines **39** and **40** via diyne RCM.[71]

A lack of stereoisomeric control was also encountered in the studies of 14-membered lactam formation via RCM, which was presented in Chapter 2. In the last few years the RCM reaction has become a popular method for macrocyclization. Numerous application studies have appeared, but a surprising lack of attention has been paid to the issue of stereoisomeric control. More recently the Fürstner research

group developed a general alkyne ring-closing metathesis methodology allowing entry to macrocyclic alkynes containing a number of different functional groups.[155,156] Reduction of the alkyne allowed exclusive formation of the (*Z*)-alkene, however this constitutes an indirect solution to the fundamental problem in alkene RCM. Efforts towards elucidating the stereoselectivity of this reaction appear to be the next challenge the synthetic organic chemist faces in the development of RCM as a truly efficient and versatile macrocyclization method.

CHAPTER 4
EXPERIMENTAL

4.1 General

Unless stated otherwise, all reactions were performed under a nitrogen atmosphere in flame- or oven-dried glassware. Elevated temperature reactions were performed in a silicone oil bath heated to the desired temperature. Low temperature reactions were performed in a cold bath prepared as follows: -78 °C (dry ice, acetone), -42 °C (dry ice, acetonitrile), -15 °C (dry ice, ethylene glycol), 0 °C (ice, water).

Anhydrous solvents were obtained by distillation. Diethyl ether, tetrahydofuran (THF), benzene, and toluene were distilled from sodium. Methanol was distilled from magnesium. Dichloromethane, acetonitrile, and pyridine were distilled from calcium hydride. Triethylamine (TEA) was distilled at reduced pressure from calcium hydride. *N,N*-Dimethyl formamide (DMF) was distilled at reduced pressure from magnesium sulfate. The low boiling fraction of petroleum ether (bp 35-60 °C) was used. Dichloromethane and methanol were deoxygenated by sparging with nitrogen for 20 minutes. Otherwise the solvent was used as received from the supplier.

Unless noted otherwise, reagents were purchased from the Aldrich Chemical Co. Sodium hydride, in oil, was washed with pentane (3X) and dried under vacuum. *n*–Butyllithium was standardized by titration against diphenylacetic acid in THF at 0 °C to a faint yellow colour indicative of the endpoint.[157] Jones' reagent was prepared according to the method of Eisenbraun.[158] Dichlorotris(triphenylphosphine)ruthenium was prepared by Mr. André Hodder according to the method of Stephenson and Wilkinson.[159] Other reagents were purified according to the procedure given in the literature.[160]

A brine solution refers to a saturated NaCl solution. The concentration or evaporation of solvents under reduced pressure refers to the use of a Büchi rotary evaporator.

Thin layer chromatography (TLC) was performed on commercially available aluminum backed plates of silica gel 60 F_{254} (EM Science 5554, 0.25 mm thickness). TLC plates were visualized with ultraviolet light (254 nm) or 1% *p*-anisaldehyde spray. Flash chromatography[161] was performed using silica gel 60, 230-400 mesh, supplied by E. Merck Co. In most cases, a solvent system was chosen such that the desired product had an R_f of approximately 0.30-0.40 on TLC. Radial chromatography was performed using a Harrison Chromatotron™ model 8924. The adsorbent used was silica gel 60 PF_{254} with gypsum binder supplied by EM Science. Silver nitrate impregnated silica was prepared by the method of Morris.[154] In most cases, a solvent system was chosen such that the desired product had an R_f of approximately 0.10-0.20 on TLC. Reversed-phase chromatography was performed using a Sep-Pak® Vac 35cc (10 g) C_{18} cartridge supplied by Millipore Co.

Analytical gas-liquid chromatography (GC) was performed on a Hewlett-Packard model 5880A gas chromatograph, equipped with a split mode capillary injection system and a flame ionization detector. The stationary phase consisted of an OV-101 capillary column of dimensions 0.2 mm X 2 m. Helium was used as the carrier gas. GC analyses were performed isothermally.

Melting points were performed using a Mel-Temp II™ apparatus and are uncorrected. In the cases where Kugelrohr distillation was performed, boiling points are reported as the oven temperature and are uncorrected.

Infrared (IR) spectra were recorded on a Bomem Michelson 100 FT-IR spectrometer with internal calibration. IR spectra were taken of either a neat liquid or a carbontetrachloride solution of the analyte between two NaCl plates of 4 mm thickness with an internal well of 0.2 mm thickness. IR spectra of solids insoluble in carbontetrachloride were taken as KBr disks.

Proton nuclear magnetic resonance (^{1}H NMR) spectra were recorded in deuteriochlorofrom, benzene-d_6 or methanol-d_4 solutions using a Bruker AC-200 (200 MHz), a Bruker WH-400 (400 MHz) or a Bruker AMX-500 (500 MHz) spectrometer. Chemical shifts are given in parts per million (ppm) on the δ scale, referenced to

chloroform (δ 7.24), benzene (δ 7.15) or methanol (δ 3.30) as an internal standard. Signal multiplicity, coupling constants, and integration ratios are indicated in parentheses. The abbreviations used to denote NMR signal multiplicity appear as follows: bs (broad singlet), s (singlet), d (doublet), t (triplet), q (quartet), quint (quintet), m (multiplet), dd (doublet of doublets), dt (doublet of triplets), ddt (doublet of doublet of triplets), etc. Carbon nuclear magnetic resonance (^{13}C NMR) spectra were recorded in deuteriochlorofrom, benzene-d_6 or methanol-d_4 solutions using a Bruker AC-200 (50 MHz), a Bruker WH-400 (100 MHz) or a Bruker AMX-500 (125 MHz) spectrometer. Chemical shifts are given in parts per million (ppm) on the δ scale, referenced to chloroform (δ 77.0), benzene (δ 128.0) or methanol (δ 49.0) as an internal standard.

Low resolution mass spectra (LRMS) in electron ionization (EI) mode were recorded on a Kratos-AEI model MS 50 spectrometer. LRMS in desorption chemical ionization (DCI) mode were recorded on a Delsi Nermag R10-10 C spectrometer. LRMS in chemical ionization (CI) mode were recorded on either a Kratos MS 80 spectrometer or a Kratos Concept II HQ spectrometer. LRMS in liquid secondary ion mass spectrometry (LSIMS) mode were recorded on a Kratos Concept II HQ spectrometer. Only peaks with greater than 20% relative intensity or those that were analytically useful were reported.

High resolution mass spectra (HRMS) in EI mode were recorded on a Kratos-AEI model MS 50 spectrometer. HRMS in CI mode were recorded on either a Kratos MS 80 spectrometer or a Kratos Concept II HQ spectrometer. HRMS in LSIMS mode were recorded on a Kratos Concept II HQ spectrometer.

Microanalyses were performed by Mr. Peter Borda in the Microanalytical Laboratory at the University of British Columbia on a Fisons CHN-O Elemental Analyzer Model 1108.

4.2 Conformational Analysis Methods

Conformational searches and energy minimizations were performed using Macromodel version 4.5, a molecular modelling program developed by Still and co-workers.[107] The MM3* force field, without solvation, was implemented in Macromodel for all calculations. The MM3* force field was based on the MM3[162] parameter set developed by Allinger and co-workers. Energy minimizations were conducted using the Polak-Ribiere conjugate gradient (PRCG) first derivative method.[163] Minimum energy conformations were obtained by conformational searches using the Monte Carlo Multiple Minimum Search (MCMM) method of Goodman and Still.[164] Ring closure bonds were chosen at positions removed by at least one carbon atom from any functional groups. Those with bond closure distances outside 1-2 Å were considered energetically improbable and rejected. Amide bonds and olefins with the *E* configuration were required to be *trans*. Olefins with the *Z* configuration were required to be *cis*. For each of these cases those deviating by more than 90° were considered energetically improbable and rejected. This method began with the generation and minimization of 1,000 starting structures by application of random variations to the internal co-ordinates (torsional angles). Duplicate structures and those greater than 50 kJ/mol above the global minimum were discarded.

4.3 Chemical Methods

Dichlorobis(tricyclohexylphosphine)ruthenium benzylidene (Grubbs' benzylidene) (3)

$$Cl_2Ru(=CHPh)(P(C_6H_{11})_3)_2$$

An aqueous 3.8 M sodium hydroxide solution (66.0 mL, 251 mol) was added to a solution of benzaldehyde *p*-toluenesulfonylhydrazone (**107**) (2.16 g, 7.87 mmol) and benzyltriethylammonium chloride (0.32 g, 1.40 mmol) dissolved in hexane (16.0 mL) and toluene (3.2 mL) and the reaction was stirred, behind a protective shield, for two hours at 70 °C. After cooling to room temperature the reaction, containing a clear colourless aqueous layer and a clear red organic layer, was carefully poured into a 500 mL separatory funnel half filled with ice. The mixture was shaken gently until all of the ice melted and the aqueous layer was discarded and the organic layer was washed with water (2X) (70 mL each). Crude phenyldiazomethane, in hexane and toluene, was dried over Na_2SO_4, filtered, sparged with N_2 gas for 20 minutes, and stored at -42 °C. The crude phenyldiazomethane solution was added via cannula over 15 minutes to a sparged solution of $RuCl_2(PPh_3)_3$ (3.02 g, 3.14 mmol) in CH_2Cl_2 (95.0 mL) stirred at -42 °C. Tricyclohexylphosphine (1.94 g, 6.92 mmol) in sparged CH_2Cl_2 (10.0 mL) at 0 °C was added via cannula over 15 minutes to the reaction stirred at -42 °C. The purple reaction mixture was warmed to -15 °C and stirred for 20 minutes. The reaction was warmed to room temperature and diluted with sparged methanol (20 mL) and concentrated under vacuum. Sparged methanol (200 mL) was added to the residue and a purple solid precipitated. The solids were filtered, flushing with N_2 gas, and washed with sparged methanol (10X) (10 mL each) and dried under vacuum overnight to afford **3** (1.07g, 41%) a purple solid.

Analysis calculated for $C_{43}H_{72}RuP_2Cl_2$: C, 62.76; H, 8.82. Found: C, 62.80; H, 8.64.

5-Hexenyl 10-undecenoate (5)

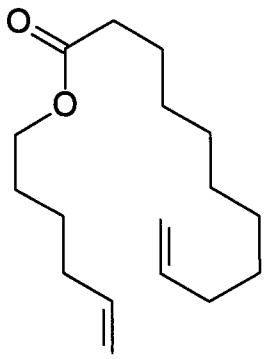

Triethylamine (1.13 mL, 8.14 mmol) and dicyclohexylcarbodiimide (1.23 g, 5.97 mmol) were sequentially added to a solution of ω-undecylenic acid (1.00 mL, 5.43 mmol) in CH_3CN (13.6 mL) and the solution was stirred for 30 minutes. 5-hexen-1-ol (0.65 mL, 5.43 mmol) was added and the reaction was stirred for 48 hours. The reaction was diluted with diethyl ether (100 mL) and sequentially washed with water, 1 M HCl, saturated $NaHCO_3$ solution, and brine (25 mL each). Each aqueous layer was washed with diethyl ether (100 mL). The combined organic layers were dried over $MgSO_4$, filtered, and concentrated. The residue was vacuum filtered through silica gel and washed with diethyl ether and concentrated. Purification of the residue by flash column chromatography with 10% ethyl acetate in petroleum ether as eluant afforded **5** (207.8 mg, 14%) as a yellow oil.

R_f = 1.0 (petroleum ether-ethyl acetate 4:1);

IR (neat): 3076, 2928, 2854, 1738, 1641, 1454, 1170, 987, 910 cm^{-1};

^1H NMR (200 MHz, $CDCl_3$) δ: 5.81 (ddt, J = 17.0, 10.2, 6.6 Hz, 1 H), 5.80 (ddt, J = 17.1, 10.2, 6.6 Hz, 1 H), 4.86-5.04 (m, 4 H), 4.04 (t, J = 6.6 Hz, 2 H), 2.26 (t, J = 7.4 Hz, 2 H), 1.95-2.11 (m, 4 H), 1.52-1.69 (m, 4 H), 1.20-1.50 (m, 12 H);

^{13}C NMR (50 MHz, $CDCl_3$) δ: 173.89, 139.11, 138.31, 114.76, 114.10, 64.09, 34.33, 33.75, 33.25, 29.25, 29.17, 29.09, 29.02, 28.86, 28.06, 25.18, 24.96;

LRMS (EI) *m/z* (relative intensity): 266 (M^+, 2), 225 (1), 124 (5), 114 (4), 100 (3), 97 (5), 96 (6), 83 (44), 82 (100), 69 (19), 67 (42), 55 (74), 54 (34);

HRMS (EI) *m/z* calculated for $C_{17}H_{30}O_2$: 266.2246, found: 266.2247;

Analysis calculated for $C_{17}H_{30}O_2$: C, 76.64; H, 11.35. Found: C, 76.63; H, 11.42.

N-(3-Aminopropyl)-3-(1-azacyclotridecyl)propylamine (motuporamine A) (33)

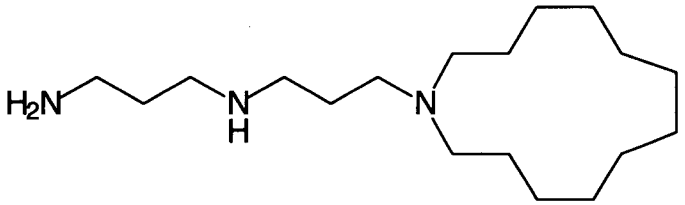

Lithium aluminum hydride (0.44 g, 11.6 mmol) was added to a solution of *N*-(3-aminopropyl)-3-(1-azacyclotridecyl)propanamide (**156**) (727.2 mg, 2.334 mmol) in THF (15.0 mL) and the reaction was stirred for 19 hours at 70 °C. The reaction was cooled to 0 °C and a solution of THF (2.5 mL) and water (0.5 mL) was added and stirred for 15 minutes. Aqueous 3 M NaOH solution was added dropwise until a white precipitate formed and the solution was stirred for 15 minutes. The slurry was vacuum filtered through celite and the filtrate was dried over $MgSO_4$, filtered, and concentrated to afford **33** (687.8 mg, 99%) as a colourless oil.

R_f = 0.0 (dichloromethane-methanol 1:1);

IR (neat): 3367, 3292, 2926, 2854, 2799, 1580, 1460, 1126, 1090, 1061, 814 cm^{-1};

^1H NMR (500 MHz, CD_3OD) δ: 2.66 (t, J = 7.2 Hz, 2 H), 2.64 (bs, 1 H), 2.61 (t, J = 7.3 Hz, 2 H), 2.60 (t, J = 7.4 Hz, 2 H), 2.39 (t, J = 6.9 Hz, 2 H), 2.38 (t, J = 6.0 Hz, 4 H), 1.63-1.69 (m, 4 H), 1.35-1.48 (m, 22 H);

^{13}C NMR (125 MHz, CD_3OD) δ: 54.97, 54.26, 49.49, 48.45, 40.72, 33.72, 28.04, 27.18, 27.00, 26.87, 26.57, 26.48;

LRMS (EI) *m/z* (relative intensity): 298 (M^++1, 21), 297 (M^+, 45), 196 (100), 194 (74), 184 (35), 182 (22), 84 (21);

HRMS (EI) *m/z* calculated for $C_{18}H_{39}N_3$: 297.3144, found: 297.3139;

Analysis calculated for $C_{18}H_{39}N_3$: C, 72.66; H, 13.21; N, 14.12. Found: C, 72.29; H, 12.95; N, 13.87.

N-(3-Aminopropyl)-3-(1-azacyclotetradecyl)propylamine (motuporamine B) (34)

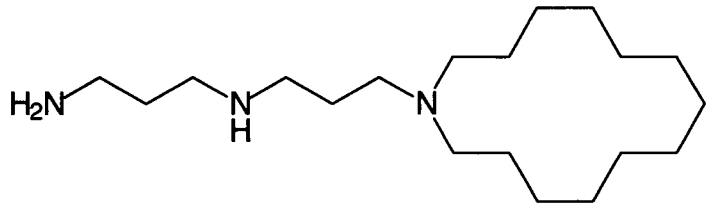

Lithium aluminum hydride (0.29 g, 7.6 mmol) was added to a solution of *N*-(3-aminopropyl)-3-(1-azacyclotetradecyl)propanamide (**157**) (503.7 mg, 1.547 mmol) in THF (10.0 mL) and the reaction was stirred for 24 hours at 70 °C. The reaction was cooled to 0 °C and a solution of THF (1.4 mL) and water (0.4 mL) was added and stirred for 15 minutes. Aqueous 3 M NaOH solution was added dropwise until a white precipitate formed and the solution was stirred for 15 minutes. The slurry was vacuum filtered through celite and the filtrate was dried over $MgSO_4$, filtered, and concentrated to afford **34** (419.0 mg, 87%) as a colourless oil.

R_f = 0.12 (dichloromethane-methanol 1:1);

IR (neat): 3362, 3288, 2926, 2858, 2797, 1639, 1591, 1462, 1128, 1095, 814, 714 cm^{-1};

^1H NMR (500 MHz, CD_3OD) δ: 2.66 (t, J = 7.2 Hz, 2 H), 2.62 (bs, 1 H), 2.60 (t, J = 7.4 Hz, 4 H), 2.43 (t, J = 7.0 Hz, 6 H), 1.63-1.70 (m, 4 H), 1.45-1.50 (m, 4 H), 1.32-1.41 (m, 20 H);

^{13}C NMR (125 MHz, CD_3OD) δ: 53.80, 52.67, 49.56, 48.45, 40.73, 33.75, 27.64, 26.81, 26.26, 26.13, 25.79, 25.50, 25.09;

LRMS (EI) *m/z* (relative intensity): 311 (M^+, 10), 210 (100), 208 (63), 198 (38), 196 (23);

HRMS (EI) *m/z* calculated for $C_{19}H_{41}N_3$: 311.3301, found: 311.3294;

Analysis calculated for $C_{19}H_{41}N_3$: C, 73.25; H, 13.26; N, 13.49. Found: C, 73.56; H, 12.96; N, 13.00.

_N_-((_N_-Acetyl)-3-aminopropyl)-_N_-acetyl-3-(1-azacyclotridecyl)propylammonium trifluoroacetate (diacetylmotuporamine A trifluoroacetate) (36·TFA)

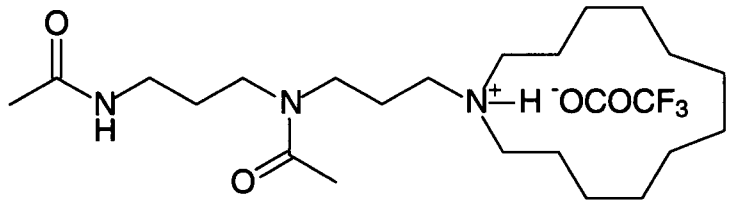

Acetic anhydride (0.59 mL, 6.2 mmol) was added to a solution of _N_-(3-aminopropyl)-3-(1-azacyclotridecyl)propylamine (**33**) (98.0 mg, 0.3293 mmol) in pyridine (1.70 mL) and stirred for 72 hours. The reaction was concentrated and the residue was purified by reverse phase chromatography with 60% water and 1% trifluoroacetic acid in methanol as eluant to afford **36**·TFA (125.5 mg, 77%) as a colourless oil.

R_f = 0.41 (dichloromethane-methanol 1:1);

IR (neat): 3458, 3315, 2935, 2864, 1682, 1651, 1634, 1556, 1464, 1427, 1383, 1202, 1138, 831, 798, 721 cm^{-1};

^1H NMR (500 MHz, CD_3OD) δ: 3.42 (t, J = 6.6 Hz, 2 H), 3.37 (t, J = 7.7 Hz, 2 H), 3.20-3.25 (m, 2 H), 3.20 (t, J = 6.7 Hz, 2 H), 3.13-3.16 (m, 2 H), 3.10 (t, J = 7.5 Hz, 2 H), 2.12 (s, 3 H), 1.96-2.02 (m, 2 H), 1.94 (s, 3 H), 1.71-1.84 (m, 6 H), 1.35-1.57 (m, 16 H);

^{13}C NMR (125 MHz, CD_3OD) δ: 174.34, 173.49, 53.62, 53.07, 47.89, 43.63, 37.79, 29.42, 26.73, 25.97, 25.69, 25.25, 24.07, 22.55, 22.39, 21.21;

^{19}F NMR (188 MHz, CD_3OD) δ: 0.0 (s);

LRMS (LSIMS(+), thioglycerol/methanol) *m/z* (relative intensity): 382 (M^++1, 100), 381 (M^+, 3), 196 (23), 100 (40);

LRMS (LSIMS(-), 3-nitrobenzyl alcohol) *m/z* (relative intensity): 494 (M+TFA^-, 7), 266 (23), 113 (100);

HRMS (LSIMS(+), thioglycerol/methanol) *m/z* calculated for $C_{22}H_{44}O_2N_3$ (M^++1): 382.3434, found: 382.3434.

_N_-((_N_-Acetyl)-3-aminopropyl)-_N_-acetyl-3-(1-azacyclotetradecyl)propylammonium trifluoroacetate (diacetylmotuporamine B trifluoroacetate) (37·TFA) and Diacetylmotuporamine B (37)

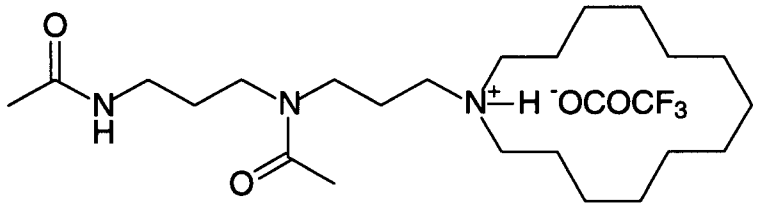

Acetic anhydride (0.61 mL, 6.5 mmol) was added to a solution of _N_-(3-aminopropyl)-3-(1-azacyclotetradecyl)propylamine (**34**) (105.6 mg, 0.3390 mmol) in pyridine (1.78 mL) and stirred for 72 hours. The reaction was concentrated and the residue was purified by reverse phase chromatography with 60% water and 1% trifluoroacetic acid in methanol as eluant to afford **37**·TFA (113.6 mg, 77%) as a colourless oil. A sample of **37**·TFA was diluted with diethyl ether and washed sequentially with saturated Na_2CO_3 solution (4X) and brine. The organic layer was dried over $MgSO_4$, filtered, and concentrated to afford the free base **37**.

37·TFA

R_f = 0.38 (dichloromethane-methanol 1:1);

IR (neat): 3312, 2935, 2864, 1668, 1636, 1464, 1446, 1381, 1200, 1178, 798 cm^{-1};

^1H NMR (500 MHz, CD_3OD) δ: 3.43 (t, J = 6.7 Hz, 2 H), 3.37 (t, J = 7.7 Hz, 2 H), 3.20 (t, J = 6.9 Hz, 2 H), 3.13-3.18 (m, 4 H), 3.10 (t, J = 7.4 Hz, 2 H), 2.13 (s, 3 H), 1.96-2.02 (m, 2 H), 1.94 (s, 3 H), 1.78-1.84 (m, 2 H), 1.65-1.74 (m, 4 H), 1.29-1.55 (m, 18 H);

^{13}C NMR (125 MHz, CD_3OD) δ: 174.46, 173.52, 52.90, 51.27, 47.92, 43.54, 37.81, 29.47, 26.97, 26.40, 25.26, 24.79, 24.14, 24.10, 22.54, 21.21, 20.61;

^{19}F NMR (188 MHz, CD_3OD) δ: 0.0 (s);

LRMS (LSIMS(+), thioglycerol/methanol) _m/z_ (relative intensity): 396 (M^++1, 100), 395 (M^+, 3), 210 (26), 100 (39);

LRMS (LSIMS(-), 3-nitrobenzyl alcohol) _m/z_ (relative intensity): 508 (M+TFA^-, 5), 266 (20), 113 (100);

HRMS (LSIMS(+), thioglycerol/methanol) _m/z_ calculated for $C_{23}H_{46}O_2N_3$ (M^++1): 396.3590, found: 396.3582.

37

IR (neat): 3299, 3081, 2932, 2859, 2795, 1635, 1462, 1370, 1095, 715 cm^{-1};

^1H NMR (500 MHz, CD_3OD) δ: 3.32-3.38 (m, 4 H), 3.19 (t, J = 7.0 Hz, 1 H), 3.14 (t, J = 7.0 Hz, 1 H), 2.39-2.49 (m, 6 H), 2.11 (s, 1.5 H), 2.08 (s, 1.5 H), 1.93 (s, 1.5 H), 1.92 (s, 1.5 H), 1.68-1.82 (m, 4 H), 1.44-1.52 (m, 4 H), 1.32-1.44 (m, 18 H);

^{13}C NMR (125 MHz, CD_3OD) δ: 173.19, 52.90 (52.80), 52.53 (52.45), 48.49 (47.85), 45.51 (44.47), 38.06 (37.92), 30.90, 29.69 (28.52), 27.30 (25.73), 26.76, 26.30 (26.13), 25.78 (25.57), 25.40 (25.38), 24.63, 22.60 (22.54), 21.46 (21.31);

LRMS (DCI(+), ammonia) *m/z* (relative intensity): 396 (M^++1, 100), 395 (M^+, 10), 225 (26), 210 (37), 198 (50);

HRMS (DCI(+), methane/ammonia) *m/z* calculated for $C_{23}H_{46}O_2N_3$ (M^++1): 396.3590, found: 396.3587;

Analysis calculated for $C_{23}H_{45}O_2N_3$: C, 69.83; H, 11.46; N, 10.62. Found: C, 69.91; H, 11.57; N, 9.78.

_N_-(3-Aminopropyl)-3-((_Z_)-1-azacyclopentadec-6-enyl)propylamine (motuporamine C) (39)

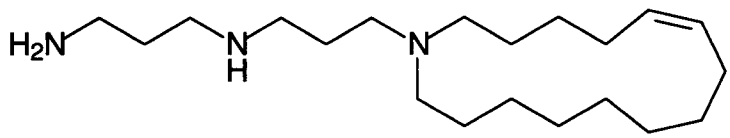

1,3-Diaminopropane (0.37 mL, 4.4 mmol) was added to a solution of methyl 3-((*Z*)-1-azacyclopentadec-6-enyl)propionate (**173**) (132.1 mg, 0.4471 mmol) in methanol (0.9 mL) and the reaction was stirred for 72 hours. The reaction was concentrated and excess reagents were removed under vacuum. Lithium aluminum hydride (85.0 mg, 2.24 mmol) was added to a solution of the residue (150.7 mg) in THF (2.8 mL) and the reaction was stirred for 19 hours at 70 °C. The reaction was cooled to 0 °C and a solution of THF (0.34 mL) and water (0.07 mL) was added and stirred for 15 minutes. Aqueous 3 M NaOH solution was added dropwise until a white precipitate formed and the solution was stirred for 15 minutes. The slurry was vacuum filtered through celite and the filtrate was dried over $MgSO_4$, filtered, and concentrated to afford **39** (137.9 mg, 95%) as a colourless oil.

R_f = 0.05 (dichloromethane-methanol 1:1);

IR (neat): 3367, 3296, 3001, 2928, 2854, 2800, 1651, 1582, 1462, 1126, 1076, 716 cm^{-1};

^1H NMR (500 MHz, CD_3OD) δ: 5.35 (dt, J = 10.9, 5.1 Hz, 1 H), 5.32 (dt, J = 10.9, 5.0 Hz, 1 H), 2.66 (t, J = 7.2 Hz, 2 H), 2.61 (bs, 1 H), 2.60 (t, J = 7.1 Hz, 2 H), 2.59 (t, J = 7.4 Hz, 2 H), 2.42 (t, J = 7.1 Hz, 2 H), 2.38 (t, J = 6.7 Hz, 2 H), 2.37 (t, J = 6.5 Hz, 2 H), 2.06-2.09 (m, 4 H), 1.62-1.68 (m, 4 H), 1.28-1.56 (m, 18 H);

^{13}C NMR (125 MHz, CD_3OD) δ: 131.54, 131.37, 55.12, 54.94, 54.01, 49.60, 48.44, 40.70, 33.68, 29.41, 28.62, 28.35, 28.18, 28.04, 28.02, 27.92, 27.05, 26.86, 26.71;

LRMS (EI) *m/z* (relative intensity): 323 (M^+, 26), 223 (23), 222 (100), 220 (58), 210 (40), 208 (29), 110 (22), 98 (24), 96 (22), 84 (53), 70 (38), 58 (23), 57 (28), 56 (30), 55 (29);

HRMS (EI) *m/z* calculated for $C_{20}H_{41}N_3$: 323.3301, found: 323.3303;

Analysis calculated for $C_{20}H_{41}N_3$: C, 74.24; H, 12.77; N, 12.99. Found: C, 74.55; H, 12.68; N, 12.23.

_N_-(3-Aminopropyl)-3-((_Z_)-1-azacyclopentadec-7-enyl)propylamine (40)

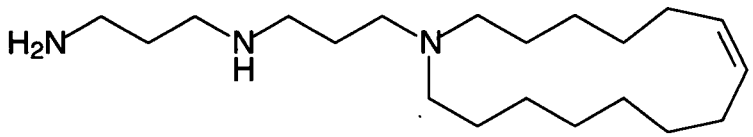

1,3-Diaminopropane (0.08 mL, 1.0 mmol) was added to a solution of methyl 3-((*Z*)-1-azacyclopentadec-7-enyl)propionate (**164**) (27.4 mg, 0.0937 mmol) in methanol (0.20 mL) and the reaction was stirred for 72 hours. The reaction was concentrated and excess reagents were removed under vacuum. Lithium aluminum hydride (17.6 mg, 0.464 mmol) was added to a solution of the residue (31.3 mg) in THF (0.60 mL) and the reaction was stirred for 19 hours at 70 °C. The reaction was cooled to 0 °C and a solution of THF (0.03 mL) and water (0.01 mL) was added and stirred for 15 minutes. Aqueous 3 M NaOH solution was added dropwise until a white precipitate formed and the solution was stirred for 15 minutes. The slurry was vacuum filtered through celite and the filtrate was dried over $MgSO_4$, filtered, and concentrated to afford **40** (29.8 mg, 99%) as a colourless oil.

R_f = 0.04 (dichloromethane-methanol-triethylamine 10:10:1);

IR (neat): 3294, 2999, 2926, 2853, 2800, 1651, 1634, 1460, 1126, 1078, 715 cm^{-1};

^1H NMR (500 MHz, CD_3OD) δ: 5.34 (dt, J = 11.0, 6.5 Hz, 1 H), 5.31 (dt, J = 11.1, 6.3 Hz, 1 H), 3.56 (bs, 1 H), 2.66 (t, J = 7.1 Hz, 2 H), 2.60 (t, J = 7.3 Hz, 2 H), 2.59 (t, J = 7.4 Hz, 2 H), 2.40 (t, J = 7.1 Hz, 2 H), 2.38 (t, J = 5.8 Hz, 4 H), 2.10 (dt, J = 6.3, 6.6 Hz, 2 H), 2.07 (q, J = 6.5 Hz, 2 H), 1.61-1.68 (m, 4 H), 1.28-1.55 (m, 18 H);

^{13}C NMR (125 MHz, CD_3OD) δ: 131.36, 131.28, 55.01, 54.62, 54.52, 49.50, 48.47, 40.70, 33.67, 29.90, 29.46, 28.49, 28.36, 28.11, 28.00, 27.55, 27.43, 27.36, 27.14, 26.66;

LRMS (EI) *m/z* (relative intensity): 323 (M^+, 23), 222 (100), 220 (35), 210 (32), 208 (21), 126 (22), 85 (30), 84 (45), 70 (31), 58 (43), 57 (21), 56 (21), 55 (26);

HRMS (EI) *m/z* calculated for $C_{20}H_{41}N_3$: 323.3301, found: 323.3296;

Analysis calculated for $C_{20}H_{41}N_3$: C, 74.24; H, 12.77; N, 12.99. Found: C, 74.59; H, 12.88; N, 11.36.

_N_-((_N_-Acetyl)-3-aminopropyl)-_N_-acetyl-3-((_Z_)-1-azacyclopentadec-6-enyl)propyl-ammonium trifluoroacetate (diacetylmotuporamine C trifluoroacetate) (41·TFA)

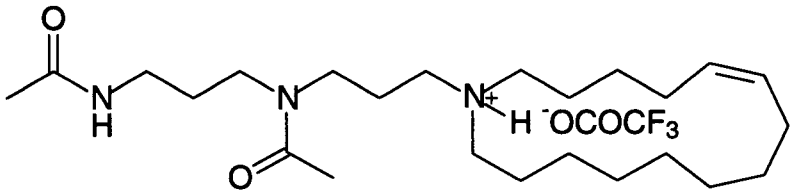

Acetic anhydride (0.39 mL, 4.1 mmol) was added to a solution of *N*-(3-aminopropyl)-3-((*Z*)-1-azacyclopentadec-6-enyl)propylamine (**39**) (70.0 mg, 0.2163 mmol) in pyridine (1.14 mL) and stirred for 68 hours. The reaction was concentrated and the residue was purified by reverse phase chromatography with 60% water and 1% trifluoroacetic acid in methanol as eluant to afford **41**·TFA (88.0 mg, 78%) as a colourless oil.

R_f = 0.72 (dichloromethane-methanol-triethylamine 50:50:1);

IR (neat): 3439, 3312, 2934, 2862, 1664, 1630, 1460, 1439, 1379, 1200, 1176, 1130, 839, 719 cm^{-1};

^1H NMR (500 MHz, CD_3OD) δ: 5.38 (dt, J = 10.9, 6.6 Hz, 1 H), 5.31 (dt, J = 10.9, 6.8 Hz, 1 H), 3.41 (t, J = 6.6 Hz, 2 H), 3.37 (t, J = 7.8 Hz, 2 H), 3.19 (t, J = 6.8 Hz,

2 H), 3.08-3.16 (m, 6 H), 2.10-2.19 (m, 4 H), 2.12 (s, 3 H), 1.96-2.01 (m, 2 H), 1.94 (s, 3 H), 1.78-1.83 (m, 2 H), 1.64-1.76 (m, 4 H), 1.55-1.60 (m, 2 H), 1.39-1.53 (m, 6 H), 1.31-1.37 (m, 4 H);

^{13}C NMR (125 MHz, CD_3OD) δ: 174.36, 173.59, 133.02, 130.55, 53.89, 53.50, 52.78, 47.90, 43.68, 37.81, 29.36, 29.18, 27.74, 27.46, 26.96, 26.93, 26.49, 26.47, 24.92, 24.02, 23.55, 23.03, 22.52, 21.19;

^{19}F NMR (188 MHz, CD_3OD) δ: 0.0 (s);

LRMS (LSIMS(+), thioglycerol) *m/z* (relative intensity): 408 (M^++1, 100), 407 (M^+, 5), 100 (26);

LRMS (LSIMS(-), glycerol/methanol) *m/z* (relative intensity): 113 (100);

HRMS (LSIMS(+), thioglycerol) *m/z* calculated for $C_{24}H_{46}O_2N_3$ (M^++1): 408.3590, found: 408.3585.

_N_-((_N_-Acetyl)-3-aminopropyl)-_N_-acetyl-3-((_Z_)-1-azacyclopentadec-7-enyl)propyl-ammonium trifluoroacetate (diacetylisomotuporamine C trifluoroacetate) (42·TFA)

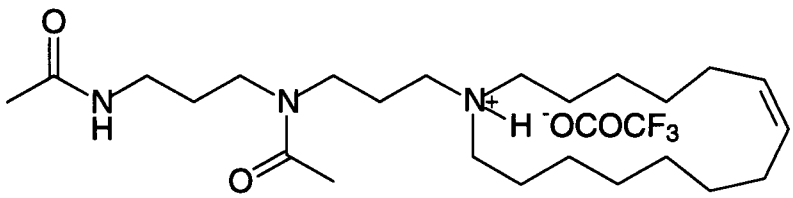

Acetic anhydride (0.09 mL, 1.0 mmol) was added to a solution of _N_-(3-aminopropyl)-3-((_Z_)-1-azacyclopentadec-7-enyl)propylamine (**40**) (16.4 mg, 0.0507 mmol) in pyridine (0.27 mL) and stirred for 71 hours. The reaction was concentrated and the residue was purified by reverse phase chromatography with 60% water and 1% trifluoroacetic acid in methanol as eluant to afford **42**·TFA (19.4 mg, 73%) as a colourless oil.

R_f = 0.54 (dichloromethane-methanol-triethylamine 50:50:1);

IR (CCl_4): 3335, 2930, 2858, 1668, 1460, 1425, 1379, 1186, 1140 cm^{-1};

^{1}H NMR (500 MHz, CD_3OD) δ: 5.36 (dt, J = 11.1, 7.0 Hz, 1 H), 5.31 (dt, J = 11.1, 6.5 Hz, 1 H), 3.42 (t, J = 6.8 Hz, 2 H), 3.37 (t, J = 7.8 Hz, 2 H), 3.19 (t, J = 6.9 Hz, 2 H), 3.14 (t, J = 7.6 Hz, 2 H), 3.10 (t, J = 7.4 Hz, 2 H), 3.10 (t, J = 7.8 Hz, 2 H), 2.12 (s, 3 H), 2.08-2.16 (m, 4 H), 1.96-2.01 (m, 2 H), 1.93 (s, 3 H), 1.78-1.84 (m, 2 H), 1.64-1.74 (m, 4 H), 1.53-1.58 (m, 2 H), 1.32-1.51 (m, 10 H);

^{13}C NMR (125 MHz, CD_3OD) δ: 174.57, 173.64, 131.96, 131.01, 53.25, 53.00, 52.52, 47.97, 43.62, 37.82, 29.52, 29.44, 28.57, 27.81, 27.49, 27.22, 26.06, 25.95, 25.50, 24.09, 23.04, 22.57, 22.17, 21.21;

^{19}F NMR (188 MHz, CD_3OD) δ: 0.0 (s);

LRMS (LSIMS(+), thioglycerol) *m/z* (relative intensity): 408 (M^++1, 97), 407 (M^+, 4), 186 (52), 100 (100), 84 (23), 72 (29), 70 (39);

LRMS (LSIMS(-), glycerol/methanol) *m/z* (relative intensity): 113 (100);

HRMS (LSIMS(+), thioglycerol) *m/z* calculated for $C_{24}H_{46}O_2N_3$ (M^++1): 408.3590, found: 408.3593.

2-Azacyclotetradecanone (62)[147]

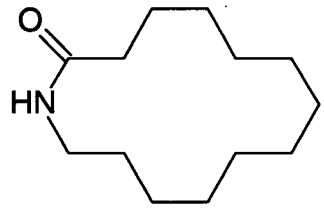

Palladium, 5% on carbon, (0.18 g) was added to a solution of (*Z*)-2-azacyclotetradec-7-enone (**83**) (0.20 g, 0.96 mmol) and a mixture of (*Z*/*E*)-2-azacyclotetradec-9-enone (**85**) and (**86**) (^{1}H NMR ratio **85**:**86**, 48:52) (0.29 g, 1.39 mmol) in ethanol (23.0 mL) and the flask was flushed with H_2 gas (4X). The reaction was stirred under a hydrogen atmosphere for 21 hours. The reaction was filtered through celite and concentrated to afford **62** (478.7 mg, 97%) as a white solid. Spectral data for **62** are identical to those reported.[147]

R_f = 0.58 (petroleum ether-ethyl acetate 3:1);

Melting point: 154.5-155.0 °C (ethanol);

IR (CCl_4): 3454, 3304, 3082, 2932, 2860, 1680, 1643, 1504, 1460, 1443, 908 cm^{-1};

^{1}H NMR (200 MHz, $CDCl_3$) δ: 5.63 (bs, 1 H), 3.29 (dt, J = 4.9, 5.9 Hz, 2 H), 2.16-2.22 (m, 2 H), 1.57-1.70 (m, 2 H), 1.22-1.52 (m, 18 H);

^{13}C NMR (50 MHz, $CDCl_3$) δ: 173.11, 38.45, 36.21, 28.30, 26.49, 25.79, 25.73, 25.65, 25.38, 25.29, 24.01, 23.75, 23.15;

LRMS (EI) *m/z* (relative intensity): 211 (M^+, 100), 170 (26), 168 (23), 128 (21), 114 (31), 112 (39), 100 (32), 98 (30), 87 (22), 86 (30), 73 (33), 72 (24), 55 (49);

HRMS (EI) *m/z* calculated for $C_{13}H_{25}ON$: 211.1936, found: 211.1939;

Analysis calculated for $C_{13}H_{25}ON$: C, 73.88; H, 11.92; N, 6.63. Found: C, 73.82; H, 11.86; N, 6.76.

Azacyclotetradecane (63)[146]

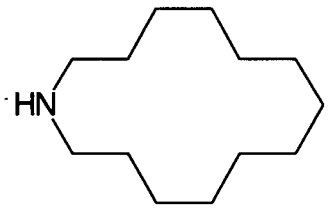

Lithium aluminum hydride (0.17 g, 4.4 mmol) was added to a solution of 2-azacyclotetradecanone (**62**) (461.4 mg, 2.183 mmol) in THF (9.0 mL) and the reaction was stirred for 19 hours at 70 °C. The reaction was cooled to 0 °C and a solution of THF (0.8 mL) and water (0.2 mL) was added and stirred for 15 minutes. Aqueous 3 M NaOH solution was added dropwise until a white precipitate formed and the solution was stirred for 15 minutes. The slurry was vacuum filtered through celite and concentrated. Kugelrohr distillation of the residue at 110 °C at 0.2 mm Hg afforded **63** (395.4 mg, 92%) as a white solid. Spectral data for **63** are identical to those reported.[146]

R_f = 0.08 (petroleum ether-ethyl acetate 1:1);

Boiling point: 110 °C at 0.2 mm Hg;

Melting point: 38.0-39.5 °C (tetrahydrofuran);

IR (CCl_4): 3404, 2928, 2860, 2810, 1462, 1443, 1134, 908 cm^{-1};

^1H NMR (200 MHz, $CDCl_3$) δ: 2.56 (t, J = 5.8 Hz, 4 H), 1.39-1.50 (m, 4 H), 1.14-1.34 (m, 18 H), 1.02 (bs, 1 H);

^{13}C NMR (50 MHz, $CDCl_3$) δ: 45.97, 27.13, 25.90, 25.03, 24.15, 23.65, 23.14;

LRMS (EI) *m/z* (relative intensity): 197 (M^+, 100), 168 (25), 154 (55), 140 (37), 126 (36), 112 (65), 98 (57), 84 (49), 70 (85), 56 (97);

HRMS (EI) *m/z* calculated for $C_{13}H_{27}N$: 197.2144, found: 197.2138;

Analysis calculated for $C_{13}H_{27}N$: C, 79.11; H, 13.79; N, 7.10. Found: C, 78.99; H, 13.75; N, 7.24.

Azacyclotridecane (66)[146]

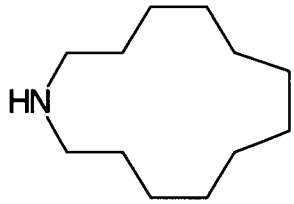

Lithium aluminum hydride (0.77 g, 20.3 mmol) was added to a solution of 2-azacyclotridecanone (2.00 g, 10.14 mmol) in THF (41.0 mL) and the reaction was stirred for 8 hours at 70 °C. The reaction was cooled to 0 °C and a solution of THF (3.8 mL) and water (0.8 mL) was added and stirred for 15 minutes. Aqueous 3 M NaOH solution was added dropwise until a white precipitate formed and the solution was stirred for 15 minutes. The slurry was vacuum filtered through celite and concentrated. Kugelrohr distillation of the residue at 95 °C at 0.2 mm Hg afforded **66** (1.61 g, 87%) as a colourless oil. Spectral data for **66** are identical to those reported.[146]

R_f = 0.12 (petroleum ether-ethyl acetate 1:1);

Boiling point: 95.0 °C at 0.2 mm Hg;

IR (neat): 3310, 2926, 2856, 2808, 1460, 1447, 1132 cm^{-1};

^1H NMR (200 MHz, $CDCl_3$) δ: 2.59 (t, J = 5.2 Hz, 4 H), 1.27-1.47 (m, 20 H), 1.06 (bs, 1 H);

^{13}C NMR (50 MHz, $CDCl_3$) δ: 47.85, 27.83, 26.49, 25.93, 25.36, 24.53;

LRMS (EI) *m/z* (relative intensity): 183 (M^+, 100), 154 (26), 142 (41), 140 (41), 126 (31), 112 (32), 100 (25), 98 (29), 86 (25), 84 (22) 72 (20), 70 (42), 56 (52), 55 (28);

HRMS (EI) *m/z* calculated for $C_{12}H_{25}N$: 183.1987, found: 183.1985;

Analysis calculated for $C_{12}H_{25}N$: C, 78.62; H, 13.74; N, 7.64. Found: C, 79.03; H, 13.82; N, 7.33.

N-(2-Propenyl)-11-dodecenamide (68)

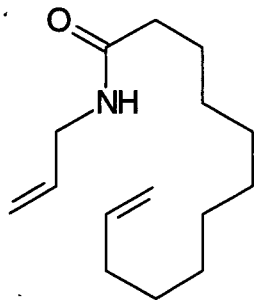

11-Dodecenoic acid (**124**) (1.95 g, 9.83 mmol) and 1,3-dicyclohexylcarbodiimide (2.03 g, 9.84 mmol) were sequentially added to a solution of allylamine (0.74 mL, 9.8 mmol) in CH_2Cl_2 (12.3 mL) at 0 °C and the reaction was stirred for 3 hours with warming to room temperature. The reaction was filtered and washed with ethyl acetate (40 mL). The filtrate was washed sequentially with saturated $NaHCO_3$ solution and brine (50 mL each). The combined aqueous layers were successively washed with ethyl acetate (2X) (50 mL each). The combined organic extracts were dried over $MgSO_4$, filtered, and concentrated. Purification of the residue by flash column chromatography with 30% ethyl acetate in petroleum ether as eluant afforded **68** (792.6 mg, 34%) as a white solid.

R_f = 0.25 (petroleum ether-ethyl acetate 4:1);

Melting point: 44.0-45.0 °C (ethyl acetate);

IR (CCl_4): 3456, 3300, 3078, 2932, 2856, 1641, 1464, 1418, 1269, 991, 912 cm^{-1};

^1H NMR (200 MHz, $CDCl_3$) δ: 5.82 (ddt, J = 17.1, 10.2, 5.6 Hz, 1 H), 5.79 (ddt, J = 16.9, 10.3, 6.7 Hz, 1 H), 5.46 (bs, 1 H), 5.07-5.21 (m, 2 H), 4.86-5.02 (m, 2 H), 3.86 (tt, J = 5.7, 1.5 Hz, 2 H), 2.17 (t, J = 7.5 Hz, 2 H), 2.01 (q, J = 7.1 Hz, 2 H), 1.54-1.69 (m, 2 H), 1.20-1.38 (m, 12 H);

^{13}C NMR (50 MHz, C_6D_6) δ: 172.00, 139.21, 135.49, 115.35, 114.48, 41.88, 36.53, 34.18, 29.88, 29.85, 29.81, 29.72, 29.48, 29.31, 26.06;

LRMS (EI) *m/z* (relative intensity): 237 (M^+, 1), 112 (27), 99 (100), 98 (29), 84 (20), 58 (32), 57 (85), 55 (32), 41 (62);

HRMS (EI) *m/z* calculated for $C_{15}H_{27}ON$: 237.2093, found: 237.2088;

Analysis calculated for $C_{15}H_{27}ON$: C, 75.88; H, 11.47; N, 5.90. Found: C, 75.83; H, 11.51; N, 5.85.

_N_-(3-Butenyl)-10-undecenamide (69)

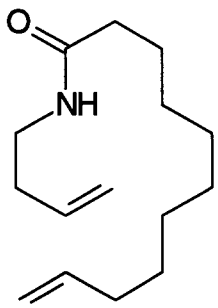

Potassium phthalimide (2.27 g, 12.3 mmol) was added to a solution of 4-bromo-1-butene (2.0 mL, 11.1 mmol) in DMF (12.0 mL) and the reaction was stirred for 3 hours at 90 °C. The reaction was cooled to room temperature and filtered. The filtrate was diluted with water and brine (1:1) and successively extracted with portions of diethyl ether (3X) (15 mL each). The combined organic extracts were washed with brine (2X), dried over $MgSO_4$, filtered, and concentrated. Hydrazine monohydrate (0.54 mL, 11.1 mmol) was added to a solution of crude *N*-phthaloyl-4-aminobut-1-ene in ethanol (13.5 mL) and the reaction was stirred for 16 hours at 60 °C. The reaction was cooled to room temperature, conc. HCl (4 mL) was added and the reaction was stirred for 2 hours at 60 °C. The reaction was cooled to room temperature, then filtered and concentrated. The residue was diluted with water, made alkaline with KOH, and extracted with diethyl ether (4X) (20 mL each). The combined organic extracts were washed with brine (2X), dried over $MgSO_4$ and filtered. The filtrated was treated with HCl gas and concentrated. Crude 3-butenylammonium chloride (454.5 mg, 4.227 mmol), undecylenic acid (0.885 mL, 4.802 mmol), and triethylamine (1.42 mL, 10.23 mmol) were sequentially added to a solution of 2-bromo-1-methylpyridinium fluorosulphonate (1.38 g, 5.07 mmol) in CH_2Cl_2 (42.0 mL) and the reaction was stirred for three hours at 40 °C. The reaction was cooled to room temperature and diluted with diethyl ether (80 mL) and sequentially washed with 1 M HCl (3X), saturated $NaHCO_3$ solution (2X), and water (200 mL each). The organic layer was dried over $MgSO_4$, filtered, and concentrated. Purification of the residue by flash column chromatography with 25% ethyl acetate in petroleum ether as eluant afforded **69** (362.1 mg, 36%) as a white solid.

R_f = 0.17 (petroleum ether-ethyl acetate 4:1);

Melting point: 31.5-32.5 °C (ethyl acetate);

IR (CCl_4): 3456, 3344, 3080, 2928, 2856, 1682, 1504, 1464, 993, 910 cm^{-1};

^1H NMR (200 MHz, $CDCl_3$) δ: 5.60-5.84 (m, 3 H), 4.84-5.07 (m, 4 H), 3.26 (q, J = 6.4 Hz, 2 H), 2.20 (q, J = 6.6 Hz, 2 H), 2.10 (t, J = 7.5 Hz, 2 H), 1.97 (q, J = 6.5 Hz, 2 H), 1.46-1.62 (m, 2 H), 1.15-1.38 (m, 10 H);

^{13}C NMR (50 MHz, $CDCl_3$) δ: 173.07, 139.02, 135.26, 116.93, 114.03, 38.24, 36.69, 33.72, 33.66, 29.20, 29.17, 28.95, 28.77, 25.70;

LRMS (EI) *m/z* (relative intensity): 237 (M^+, 22), 196 (100), 126 (34), 113 (79), 98 (23), 83 (23), 81 (20), 72 (22), 55 (41), 41 (27), 30 (33);

HRMS (EI) *m/z* calculated for $C_{15}H_{27}ON$: 237.2093, found: 237.2089;

Analysis calculated for $C_{15}H_{27}ON$: C, 75.90; H, 11.46; N, 5.90. Found: C, 75.77; H, 11.49; N, 5.82.

_N_-(4-Pentenyl)-9-decenamide (70)

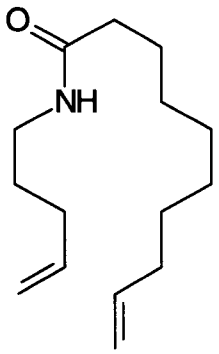

5-Bromopentene (5.4 mL, 45.6 mmol) was added to a solution of 9-decenamide (**126**) (5.19 g, 30.66 mmol), sodium hydroxide (4.29 g, 107.2 mmol), potassium carbonate (8.48 g, 61.36 mmol), and tetrabutylammonium hydrogen sulfate (1.04 g, 3.06 mmol) in toluene (38.0 mL) and the reaction was stirred for 30 minutes at 120 °C. The reaction was cooled to room temperature and diluted with ethyl acetate (100 mL) and washed with water (3X) (40 mL each). The organic layer was dried over $MgSO_4$, filtered, and concentrated. Purification of the residue by flash column chromatography with 20% ethyl acetate in petroleum ether as eluant afforded **70** (5.16 g, 71%) as a colourless oil.

R_f = 0.46 (petroleum ether-ethyl acetate 1:1);

IR (neat): 3296, 3078, 2928, 2856, 1643, 1556, 1441, 993, 910 cm^{-1};

^{1}H NMR (200 MHz, $CDCl_3$) δ: 5.84 (bs, 1 H), 5.74 (ddt, J = 17.1, 10.2, 6.8 Hz, 2 H), 4.84-5.02 (m, 4 H), 3.19 (q, J = 7.1 Hz, 2 H), 2.10 (t, J = 7.5 Hz, 2 H), 1.92-2.08 (m, 4 H), 1.47-1.62 (m, 2 H), 1.20-1.31 (m, 10 H);

^{13}C NMR (50 MHz, $CDCl_3$) δ: 173.06, 138.96, 137.70, 115.02, 114.08, 38.88, 36.71, 33.63, 31.03, 29.16, 29.10, 28.84, 28.73, 28.71, 25.72;

LRMS (EI) *m/z* (relative intensity): 237 (M^+, 8), 182 (21), 140 (45), 127 (26), 99 (50), 98 (23), 86 (29), 85 (56), 84 (25), 73 (48), 69 (64), 68 (20), 67 (29), 55 (57), 44 (38), 41 (100);

HRMS (EI) *m/z* calculated for $C_{15}H_{27}ON$: 237.2093, found: 237.2087;

Analysis calculated for $C_{15}H_{27}ON$: C, 75.90; H, 11.46; N, 5.90. Found: C, 76.19; H, 11.55; N, 6.04.

_N_-(5-Hexenyl)-8-nonenamide (71)

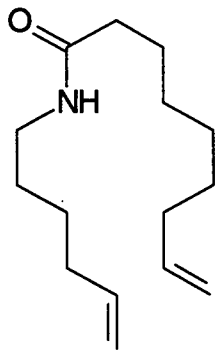

6-Bromohexene (1.82 g, 11.16 mmol) was added to a solution of 8-nonenamide (**130**) (1.65 g, 10.63 mmol), sodium hydroxide (1.28 g, 32.0 mmol), potassium carbonate (2.94 g, 21.27 mmol), and tetrabutylammonium hydrogen sulfate (0.36 g, 1.06 mmol) in toluene (13.0 mL) and the reaction was stirred for 30 minutes at 120 °C. The reaction was cooled to room temperature and diluted with ethyl acetate (30 mL) and washed with water (3X) (15 mL each). The organic layer was dried over $MgSO_4$, filtered, and concentrated. Purification of the residue by flash column chromatography with 30% ethyl acetate in petroleum ether as eluant afforded **71** (0.69 g, 27%) as a colourless oil.

R_f = 0.55 (petroleum ether-ethyl acetate 1:1);

IR (neat): 3292, 3078, 2928, 2856, 1643, 1556, 1456, 1371, 993, 910 cm^{-1};

^{1}H NMR (200 MHz, $CDCl_3$) δ: 5.99 (bs, 1 H), 5.72 (ddt, J = 17.0, 10.4, 6.6 Hz, 1 H), 5.71 (ddt, J = 17.0, 10.1, 6.7 Hz, 1 H), 4.81-4.98 (m, 4 H), 3.16 (q, J = 6.8 Hz, 2 H), 2.09 (t, J = 7.5 Hz, 2 H), 1.90-2.04 (m, 4 H), 1.18-1.62 (m, 12 H);

^{13}C NMR (50 MHz, $CDCl_3$) δ: 173.11, 138.78, 138.22, 114.56, 114.09, 39.15, 36.59, 33.53, 33.18, 28.99, 28.93, 28.67, 28.57, 26.02, 25.65;

LRMS (EI) *m/z* (relative intensity): 237 (M^+, 9), 196 (50), 154 (60), 126 (29), 100 (31), 99 (37), 98 (38), 84 (32), 82 (24), 73 (33), 72 (25), 70 (20), 69 (57), 67 (24), 60 (22), 58 (31), 56 (45), 55 (95), 44 (21), 44 (100);

HRMS (EI) *m/z* calculated for $C_{15}H_{27}ON$: 237.2093, found: 237.2095;

Analysis calculated for $C_{15}H_{27}ON$: C, 75.90; H, 11.46; N, 5.90. Found: C, 75.72; H, 11.51; N, 6.10.

_N_-(6-Heptenyl)-7-octenamide (72)

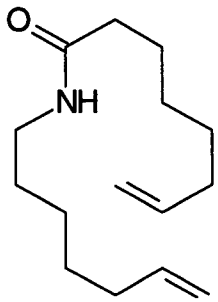

(a) <u>2-Bromo-1-methylpyridinium Fluorosulphonate Coupling of 6-Heptenylamine (**94**) and 7-Octenoic acid (**93**)</u>

6-Heptenylamine (**94**) (1.41 g, 12.46 mmol), 7-octenoic acid (**93**) (1.77 g, 12.45 mmol), and triethylamine (4.15 mL, 29.77 mmol) were sequentially added to a solution of 2-bromo-1-methylpyridinium fluorosulphonate (4.07 g, 14.96 mmol) in CH_2Cl_2 (125.0 mL) and the reaction was stirred for three hours at 40 °C. The reaction was cooled to room temperature and diluted with diethyl ether (250 mL) and sequentially washed with 1 M HCl (3X), saturated $NaHCO_3$ solution (2X), and water (500 mL each). The organic layer was dried over $MgSO_4$, filtered, and concentrated. Purification of the residue by flash column chromatography with 25% ethyl acetate in petroleum ether as eluant afforded **72** (2.3475 g, 79%) as a colourless oil.

R_f = 0.16 (petroleum ether-ethyl acetate 4:1);

IR (neat): 3294, 3078, 2930, 2856, 1643, 1555, 1462, 1439, 993, 910, 729 cm^{-1};

^{1}H NMR (200 MHz, $CDCl_3$) δ: 5.74 (ddt, J = 17.1, 10.2, 6.6 Hz, 2 H), 5.69 (bs, 1 H), 4.84-4.99 (m, 4 H), 3.18 (q, J = 6.8 Hz, 2 H), 2.11 (t, J = 7.5 Hz, 2 H), 1.94-2.05 (m, 4 H), 1.17-1.66 (m, 12 H);

^{13}C NMR (50 MHz, $CDCl_3$) δ: 172.95, 138.73, 138.63, 114.38, 114.30, 39.33, 36.68, 33.51, 33.49, 29.43, 28.67, 28.52, 28.42, 26.26, 25.58;

LRMS (EI) *m/z* (relative intensity): 237 (M^+, 14), 196 (63), 168 (29), 155 (47), 154 (26), 142 (24), 140 (100), 114 (53), 113 (33), 112 (59), 100 (31), 98 (36), 97 (27), 55 (68), 41 (35), 30 (23);

HRMS (EI) *m/z* calculated for $C_{15}H_{27}ON$: 237.2093, found: 237.2094;

Analysis calculated for $C_{15}H_{27}ON$: C, 75.88; H, 11.47; N, 5.90. Found: C, 75.91; H, 11.51; N, 5.90.

(b) 2-Chloro-1-methylpyridinium Iodide Coupling of 6-Heptenylamine (**94**) and 7-Octenoic acid (**93**)

6-Heptenylamine (**94**) (0.55 g, 4.86 mmol), 7-octenoic acid (**93**) (0.69 g, 4.85 mmol), and triethylamine (1.65 mL, 11.84 mmol) were sequentially added to a solution of 2-chloro-1-methylpyridinium iodide (1.49 g, 5.83 mmol) in CH_2Cl_2 (49.0 mL) and the reaction was stirred for three hours at 40 °C. The reaction was cooled to room temperature and diluted with diethyl ether (80 mL) and sequentially washed with 1 M HCl (3X), saturated $NaHCO_3$ solution (2X), and water (150 mL each). The organic layer was dried over $MgSO_4$, filtered, and concentrated. Purification of the residue by flash column chromatography with 25% ethyl acetate in petroleum ether as eluant afforded **72** (0.51 g, 44%) with spectral data in agreement with that reported above.

N-(7-Octenyl)-6-heptenamide (73)

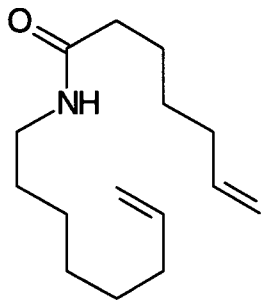

(a) Alkylation of 6-Heptenamide (**132**) with 8-Bromooctene

8-Bromooctene (1.88 mL, 11.20 mmol) was added to a solution of 6-heptenamide (**132**) (0.95 g, 7.47 mmol), crushed sodium hydroxide (1.05 g, 26.2 mmol), potassium carbonate (2.06 g, 14.90 mmol), and tetrabutylammonium hydrogen sulfate (0.25 g, 0.74 mmol) in toluene (9.5 mL) and the reaction was stirred for 30 minutes at 120 °C. The reaction was cooled to room temperature and diluted with ethyl acetate (25 mL) and washed with water (3X) (10 mL each). The organic layer was dried over $MgSO_4$, filtered, and concentrated. Purification of the residue by flash column chromatography with 15% ethyl acetate in petroleum ether as eluant afforded **73** (0.80 g, 45%) as a colourless oil.

R_f = 0.14 (petroleum ether-ethyl acetate 4:1);

IR (neat): 3290, 3076, 2928, 2856, 1641, 1553, 1437, 1373, 991, 908 cm^{-1};

^1H NMR (200 MHz, $CDCl_3$) δ: 5.77 (bs, 1 H), 5.74 (ddt, J = 17.1, 10.3, 6.6 Hz, 1 H), 5.74 (ddt, J = 17.0, 10.1, 6.7 Hz, 1 H), 4.84-5.00 (m, 4 H), 3.17 (q, J = 6.8 Hz, 2 H), 2.12 (t, J = 7.5 Hz, 2 H), 1.93-2.06 (m, 4 H), 1.52-1.67 (m, 2 H), 1.19-1.47 (m, 10 H);

^{13}C NMR (50 MHz, $CDCl_3$) δ: 172.90, 138.82, 138.36, 114.54, 114.20, 39.36, 36.53, 33.56, 33.36, 29.51, 28.66, 28.64, 28.42, 26.67, 25.20;

LRMS (EI) *m/z* (relative intensity): 237 (M^+, 13), 182 (24), 169 (24), 154 (39), 140 (29), 128 (28), 126 (28), 112 (30), 111 (26), 110 (20), 98 (30), 87 (23), 86 (23), 84 (21), 83 (35), 73 (36), 72 (29), 69 (50), 67 (26), 60 (36), 56 (23), 55 (100), 44 (54), 43 (20), 41 (89);

HRMS (EI) *m/z* calculated for $C_{15}H_{27}ON$: 237.2093, found: 237.2098;

Analysis calculated for $C_{15}H_{27}ON$: C, 75.90; H, 11.46; N, 5.90. Found: C, 75.62; H, 11.35; N, 6.02.

(b) 2-Chloro-1-methylpyridinium Iodide Coupling of 7-Octenylamine (**133**) and 6-Heptenoic acid (**131**)

7-Octenylamine (**133**) (1.70 g, 13.36 mmol), 6-heptenoic acid (**131**) (1.71 g, 13.34 mmol), and triethylamine (4.50 mL, 32.29 mmol) were sequentially added to a solution of 2-chloro-1-methylpyridinium iodide (4.10 g, 16.05 mmol) in CH_2Cl_2 (135.0 mL) and the reaction was stirred for one hour at 40 °C. The reaction was cooled to room temperature and diluted with diethyl ether (150 mL) and sequentially washed with 1 M HCl (3X), saturated $NaHCO_3$ solution (2X), and water (300 mL each). The organic layer was dried over $MgSO_4$, filtered, and concentrated. Purification of the residue by flash column chromatography with 30% ethyl acetate in petroleum ether as eluant afforded **73** (960.4 mg, 30%) with spectral data in agreement with that reported above.

***N*-(8-Nonenyl)-5-hexenamide (74)**

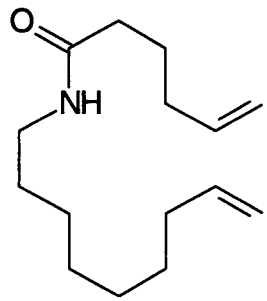

8-Nonenylamine (**134**) (123.8 mg, 0.8765 mmol), 5-hexenoic acid (**135**) (0.10 g, 0.88 mmol), and triethylamine (0.30 mL, 2.15 mmol) were sequentially added to a solution of 2-chloro-1-methylpyridinium iodide (0.27 g, 1.06 mmol) in CH_2Cl_2 (9.0 mL) and the reaction was stirred for two hours at 40 °C and for 15 hours at room temperature. The reaction was cooled to room temperature and diluted with ethyl acetate (20 mL) and sequentially washed with 1 M HCl (3X), saturated $NaHCO_3$ solution (2X), and water (50 mL each). The organic layer was dried over $MgSO_4$, filtered, and concentrated. Purification of the residue by flash column chromatography with 25% ethyl acetate in petroleum ether as eluant afforded **74** (155.6 mg, 75%) as a colourless oil.

R_f = 0.11 (petroleum ether-ethyl acetate 4:1);

IR (neat): 3294, 3078, 2928, 2856, 1643, 1555, 1439, 1371, 991, 910, 723 cm^{-1};

^1H NMR (200 MHz, $CDCl_3$) δ: 5.76 (ddt, J = 17.1, 10.3, 6.7 Hz, 1 H), 5.74 (ddt, J = 17.1, 10.3, 6.6 Hz, 1 H), 5.58 (bs, 1 H), 4.85-5.03 (m, 4 H), 3.18 (q, J = 7.1 Hz, 2 H),

2.12 (t, J = 7.5 Hz, 2 H), 1.94-2.10 (m, 4 H), 1.62-1.77 (m, 2 H), 1.20-1.52 (m, 10 H);

^{13}C NMR (50 MHz, $CDCl_3$) δ: 172.69, 139.00, 137.90, 115.17, 114.15, 39.42, 35.93, 33.67, 33.10, 29.60, 29.06, 28.93, 28.75, 26.81, 24.76;

LRMS (EI) *m/z* (relative intensity): 237 (M^+, 43), 196 (30), 168 (20), 154 (28), 140 (33), 127 (30), 126 (42), 114 (32), 100 (27), 98 (32), 97 (41), 87 (25), 86 (24), 73 (37), 72 (32), 69 (73), 55 (59), 44 (41), 41 (100);

HRMS (EI) *m/z* calculated for $C_{15}H_{27}ON$: 237.2093, found: 237.2091;

Analysis calculated for $C_{15}H_{27}ON$: C, 75.90; H, 11.46; N, 5.90. Found: C, 76.12; H, 11.61; N, 6.04.

_N_-(9-Decenyl)-4-pentenamide (75)

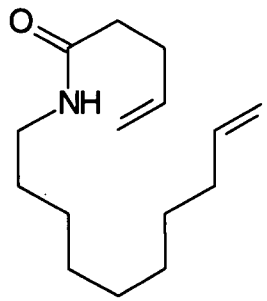

(a) DCC Coupling of 4-Pentenoic Acid and 9-Decenylamine (**138**)

4-Pentenoic acid (0.125 mL, 1.225 mmol) and 1,3-dicyclohexylcarbodiimide (0.26 g, 1.26 mmol) were sequentially added to a solution of 9-decenylamine (**138**) (191.8 mg, 1.24 mmol) in CH_2Cl_2 (2.5 mL) at 0 °C and the reaction was stirred for 30 minutes at 0 °C and stirred for 16 hours with warming to room temperature. The reaction was filtered and washed with ethyl acetate (10 mL). The filtrate was washed sequentially with saturated $NaHCO_3$ solution and brine (12 mL each). The combined aqueous layers were successively washed with ethyl acetate (2X) (12 mL each). The combined organic extracts were dried over $MgSO_4$, filtered, and concentrated. Purification of the residue by flash column chromatography with 20% ethyl acetate in petroleum ether as eluant afforded **75** (215.2 mg, 74%) as a colourless oil.

R_f = 0.35 (petroleum ether-ethyl acetate 4:1);

IR (CCl_4): 3454, 3317, 3080, 2930, 2856, 1643, 1439, 1270, 993, 912 cm^{-1};

^{1}H NMR (200 MHz, C_6D_6) δ: 5.80 (ddt, J = 16.8, 10.3, 6.6 Hz, 2 H), 5.43 (bs, 1 H), 4.92-5.10 (m, 4 H), 3.15 (q, J = 6.6 Hz, 2 H), 2.39 (q, J = 7.1 Hz, 2 H), 1.94-2.04 (m, 4 H), 1.14-1.40 (m, 12 H);

^{13}C NMR (50 MHz, C_6D_6) δ: 171.40, 139.17, 137.89, 115.13, 114.52, 39.59, 35.81, 34.16, 30.18, 30.08, 29.79, 29.65, 29.41, 29.28, 27.24;

LRMS (EI) *m/z* (relative intensity): 237 (M^+, 40), 196 (26), 140 (23), 113 (28), 100 (22), 83 (28), 56 (24), 55 (100), 44 (22), 41 (47);

HRMS (EI) *m/z* calculated for $C_{15}H_{27}ON$: 237.2093, found: 237.2088;

Analysis calculated for $C_{15}H_{27}ON$: C, 75.88; H, 11.47; N, 5.90. Found: C, 75.98; H, 11.59; N, 6.09.

(b) Alkylation of 4-Pentenamide (**137**) with 10-Iododecene (**116**)

10-iododecene (**116**) (3.22 g, 12.10 mmol) was added to a solution of 4-pentenamide (**137**) (0.80 g, 8.1 mmol), crushed sodium hydroxide (1.13 g, 28.2 mmol), potassium carbonate (2.23 g, 16.13 mmol), and tetrabutylammonium hydrogen sulfate (0.27 g, 0.80 mmol) in toluene (10.0 mL) and the reaction was stirred for 1.5 hours at 120 °C. The reaction was cooled to room temperature and diluted with ethyl acetate (10 mL) and washed with water (3X) (10 mL each). The organic layer was dried over $MgSO_4$, filtered, and concentrated. Purification of the residue by flash column chromatography with 15% ethyl acetate in petroleum ether as eluant afforded **75** (0.53 g, 28%) with spectral data in agreement with that reported above.

***N*-(10-Undecenyl)-3-butenamide (76)**

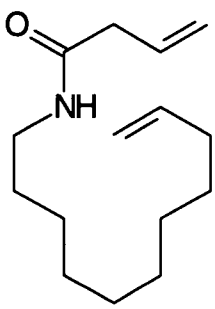

(a) DCC Coupling of Vinylacetic Acid and 10-Undecenylamine (**118**)

Vinylacetic acid (0.46 mL, 5.4 mmol) and 1,3-dicyclohexylcarbodiimide (1.10 g, 5.33 mmol) were sequentially added to a solution of 10-undecenylamine (**118**) (905.5 mg, 5.349 mmol) in CH_2Cl_2 (11.0 mL) at 0 °C and the reaction was stirred for 30 minutes at

0 °C and stirred for 23 hours with warming to room temperature. The reaction was filtered and washed with ethyl acetate (40 mL). The filtrate was washed sequentially with saturated $NaHCO_3$ solution and brine (50 mL each). The combined aqueous layers were successively washed with ethyl acetate (2X) (50 mL each). The combined organic extracts were dried over $MgSO_4$, filtered, and concentrated. Purification of the residue by flash column chromatography with 20% ethyl acetate in petroleum ether as eluant afforded **76** (419.4 mg, 33%) as a white solid.

R_f = 0.16 (petroleum ether-ethyl acetate 4:1);

Melting point: 31.0-32.0 °C (ethyl acetate);

IR (CCl_4): 3448, 3308, 3080, 2930, 2856, 1681, 1650, 1464, 1439, 993, 912 cm^{-1};

^1H NMR (200 MHz, C_6D_6) δ: 5.90 (ddt, J = 17.8, 9.5, 7.1 Hz, 1 H), 5.80 (ddt, J = 17.1, 10.3, 6.6 Hz, 1 H), 5.18 (bs, 1 H), 4.91-5.10 (m, 4 H), 3.11 (q, J = 6.6 Hz, 2 H), 2.73 (dt, J = 7.1, 1.3 Hz, 2 H), 2.00 (dt, J = 7.3, 6.8 Hz, 2 H), 1.17-1.39 (m, 14 H);

^{13}C NMR (50 MHz, C_6D_6) δ: 169.79, 139.19, 132.77, 116.07, 114.48, 41.78, 39.71, 34.17, 30.09, 29.89, 29.80, 29.68, 29.46, 29.30, 27.23;

LRMS (EI) *m/z* (relative intensity): 237 (M^+, 6), 196 (46), 140 (18), 126 (20), 99 (26), 98 (31), 97 (21), 86 (18), 83 (34), 69 (56), 55 (100), 43 (39), 41 (76);

HRMS (EI) *m/z* calculated for $C_{15}H_{27}ON$: 237.2093, found: 237.2086;

Analysis calculated for $C_{15}H_{27}ON$: C, 75.88; H, 11.47; N, 5.90. Found: C, 75.55; H, 11.61; N, 5.72.

(b) Alkylation of 3-Butenamide (**115**) with 11-Iodoundecene (**113**)

11-iodoundecene (**113**) (1.48 g, 5.28 mmol) was added to a solution of 3-butenamide (**115**) (0.30 g, 3.5 mmol), crushed sodium hydroxide (0.49 g, 12.2 mmol), potassium carbonate (0.97 g, 7.02 mmol), and tetrabutylammonium hydrogen sulfate (0.12 g, 0.35 mmol) in toluene (4.5 mL) and the reaction was stirred for 4 hours at 120 °C. The reaction was cooled to room temperature and diluted with ethyl acetate (5 mL) and washed with water (3X) (5 mL each). The organic layer was dried over $MgSO_4$, filtered, and concentrated. Purification of the residue by flash column chromatography with 20% ethyl acetate in petroleum ether as eluant afforded **76** (0.21 g, 25%) with spectral data in agreement with that reported above.

(*E*)-2-Azacyclotetradec-4-enone (77)

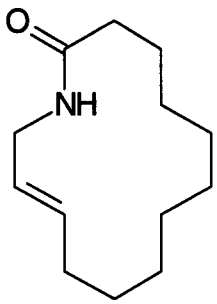

(a) Ring-Closing Metathesis of *N*-(2-Propenyl)-11-dodecenamide (**68**)

A solution of *N*-(2-propenyl)-11-dodecenamide (**68**) (49.6 mg, 0.2090 mmol) in sparged CH_2Cl_2 (12.5 mL) and a solution of Grubbs' benzylidene (**3**) (9.0 mg, 0.0109 mmol) in sparged CH_2Cl_2 (12.5 mL) were added simultaneously using a syringe pump to sparged CH_2Cl_2 (80.0 mL) stirred over 3 hours. After the addition, the reaction was stirred for an additional 23.5 hours. The solution in the receiver flask was gently sparged with N_2 gas during the addition and reaction. Triethylamine (1 mL) was added to the reaction and stirred for 15 minutes and a spatula of silica was added. The solution was concentrated and purification of the silica absorbed residue by flash column chromatography with 50% ethyl acetate in petroleum ether as eluant afforded **77** (2.9 mg, 7%) as a white solid.

R_f = 0.36 (petroleum ether-ethyl acetate 1:1);

Melting point: 125.0-125.5 °C (ethyl acetate);

IR (CCl_4): 3454, 3319, 2930, 2856, 1682, 1499, 1456, 1441, 970, 891 cm^{-1};

^1H NMR (500 MHz, $CDCl_3$) δ: 5.68 (bs, 1 H), 5.54 (dt, J = 15.4, 6.4 Hz, 1 H), 5.48 (dt, J = 15.4, 6.7 Hz, 1 H), 3.73 (t, J = 6.4 Hz, 2 H), 2.16-2.18 (m, 2 H), 2.03 (dt, J = 5.9, 6.4 Hz, 2 H), 1.59-1.64 (m, 2 H), 1.38-1.43 (m, 2 H), 1.30-1.34 (m, 2 H), 1.17-1.27 (m, 8 H);

^{13}C NMR (125 MHz, $CDCl_3$) δ: 173.03, 133.36, 127.49, 41.11, 36.18, 30.08, 27.47, 26.65, 26.59, 26.11, 25.99, 24.97, 24.89;

LRMS (CI(+), ammonia) *m/z* (relative intensity): 210 (M^++1, 100), 209 (M^+, 99), 180 (22), 166 (34);

HRMS (CI(+), isobutane) *m/z* calculated for $C_{13}H_{24}ON$ (M^++1): 210.1858, found: 210.1858;

Analysis calculated for $C_{13}H_{23}ON$: C, 74.59; H, 11.07; N, 6.69. Found: C, 74.32; H, 10.98; N, 6.48.

(b) Ring-Closing Metathesis of *N*-*tert*-Butoxycarbonyl-*N*-(2-propenyl)-11-dodecenamide (**139**)

A solution of *N*-*tert*-butoxycarbonyl-*N*-(2-propenyl)-11-dodecenamide (**139**) (153.9 mg, 0.4560 mmol) in sparged CH_2Cl_2 (25.0 mL) and a solution of Grubbs' benzylidene (**3**) (18.8 mg, 0.0228 mmol) in sparged CH_2Cl_2 (25.0 mL) were added simultaneously using a syringe pump to sparged CH_2Cl_2 (178.0 mL) stirred over 3 hours. After the addition, the reaction was stirred for an additional 21 hours. The solution in the receiver flask was gently sparged with N_2 gas during the addition and reaction. Triethylamine (1 mL) was added to the reaction and stirred overnight. The solution was concentrated and the residue was dissolved in trifluoroacetic acid (1.15 mL) and CH_2Cl_2 (1.15 mL) and stirred for 30 minutes. The reaction was diluted with methanol (2 mL) and concentrated. This dilution and concentration was repeated twice more and a spatula of silica was added before the final concentration. Purification of the silica absorbed residue by flash column chromatography with 45% ethyl acetate in petroleum ether as eluant afforded **77** (19.0 mg, 20%) with spectral data in agreement with that reported above.

(*Z*/*E*)-2-Azacyclotetradec-5-enone (78) and (79)

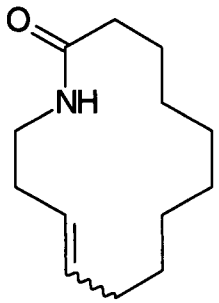

(a) Ring-Closing Metathesis of *N*-(3-Butenyl)-10-undecenamide (**69**)

A solution of *N*-(3-butenyl)-10-undecenamide (**69**) (51.0 mg, 0.2148 mmol) in sparged CH_2Cl_2 (12.5 mL) and a solution of Grubbs' benzylidene (**3**) (9.4 mg, 0.0114 mmol) in sparged CH_2Cl_2 (12.5 mL) were added simultaneously using a syringe pump to sparged CH_2Cl_2 (82.0 mL) stirred over 3 hours. After the addition, the reaction was stirred for an additional 17 hours. The solution in the receiver flask was gently sparged with N_2 gas during the addition and reaction. Triethylamine (1 mL) was added to the reaction and

stirred for 15 minutes and a spatula of silica was added. The solution was concentrated and purification of the silica absorbed residue (^{1}H NMR ratio **78**:**79**, 28:72) by flash column chromatography with 50% ethyl acetate in petroleum ether as eluant afforded **78** (4.0 mg, 9%) and **79** (10.4 mg, 23%) both as white solids.

78 (*Z*)

R_f = 0.25 (petroleum ether-ethyl acetate 1:1);

Melting point: 149.5-150.0 °C (ethyl acetate);

IR (CCl_4): 3456, 3358, 3003, 2932, 2860, 1682, 1504, 1460, 1443, 910 cm^{-1};

^{1}H NMR (500 MHz, $CDCl_3$) δ: 5.61 (bs, 1 H), 5.58 (dt, J = 11.0, 7.8 Hz, 1 H), 5.26 (dt, J = 11.0, 7.6 Hz, 1 H), 3.37 (dt, J = 4.3, 5.7 Hz, 2 H), 2.22-2.25 (m, 2 H), 2.15 (t, J = 5.2 Hz, 2 H), 1.95-1.99 (m, 2 H), 1.62-1.69 (m, 2 H), 1.20-1.37 (m, 10 H);

^{13}C NMR (125 MHz, $CDCl_3$) δ: 172.71, 133.42, 127.05, 38.22, 35.01, 28.05, 27.87, 26.18, 25.93, 25.82, 25.18, 24.68, 24.16;

LRMS (DCI(+), ammonia) *m/z* (relative intensity): 210 (M^++1, 100), 209 (M^+, 83), 112 (33), 98 (62), 81 (62), 67 (89), 55 (67);

HRMS (DCI(+), methane) *m/z* calculated for $C_{13}H_{24}ON$ (M^++1): 210.1858, found: 210.1859;

Analysis calculated for $C_{13}H_{23}ON$: C, 74.59; H, 11.07; N, 6.69. Found: C, 74.80; H, 11.05; N, 6.54.

79 (*E*)

R_f = 0.18 (petroleum ether-ethyl acetate 1:1);

Melting point: 112.5-114.0 °C (ethyl acetate);

IR (CCl_4): 3450, 3337, 2932, 2860, 1678, 1504, 1439, 970 cm^{-1};

^{1}H NMR (500 MHz, $CDCl_3$) δ: 5.52 (bs, 1 H), 5.43 (dt, J = 15.4, 7.2 Hz, 1 H), 5.27 (dt, J = 15.4, 7.0 Hz, 1 H), 3.30 (dt, J = 5.9, 5.4 Hz, 2 H), 2.20 (t, J = 6.1 Hz, 2 H), 2.19-2.23 (m, 2 H), 1.95-2.01 (m, 2 H), 1.48-1.54 (m, 2 H), 1.21-1.35 (m, 10 H);

^{13}C NMR (125 MHz, $CDCl_3$) δ: 172.96, 133.69, 128.46, 38.39, 36.44, 32.13, 31.54, 26.79, 25.70, 25.59, 25.54, 24.27, 24.07;

LRMS (DCI(+), ammonia) *m/z* (relative intensity): 210 (M^++1, 100), 209 (M^+, 71), 98 (41), 81 (40), 67 (48), 57 (37);

HRMS (DCI(+), methane) *m/z* calculated for $C_{13}H_{24}ON$ (M^++1): 210.1858, found: 210.1859;

Analysis calculated for $C_{13}H_{23}ON$: C, 74.59; H, 11.07; N, 6.69. Found: C, 74.42; H, 11.16; N, 6.52.

(b) Ring-Closing Metathesis of *N-tert*-Butoxycarbonyl-*N*-(3-butenyl)-10-undecenamide (**140**)

A solution of *N-tert*-butoxycarbonyl-*N*-(3-butenyl)-10-undecenamide (**140**) (152.4 mg, 0.4516 mmol) in sparged CH_2Cl_2 (25.0 mL) and a solution of Grubbs' benzylidene (**3**) (18.6 mg, 0.0226 mmol) in sparged CH_2Cl_2 (25.0 mL) were added simultaneously using a syringe pump to sparged CH_2Cl_2 (176.0 mL) stirred over 3 hours. After the addition, the reaction was stirred for an additional 14 hours. The solution in the receiver flask was gently sparged with N_2 gas during the addition and reaction. Triethylamine (2 mL) was added to the reaction and stirred for one hour. The solution was concentrated and the residue was dissolved in trifluoroacetic acid (1.1 mL) and CH_2Cl_2 (1.1 mL) and stirred for 30 minutes. The reaction was diluted with methanol (2 mL) and concentrated. This dilution and concentration was repeated twice more and a spatula of silica was added before the final concentration. Purification of the silica absorbed residue (^{1}H NMR ratio **78**:**79**, 36:64) by flash column chromatography with 45% ethyl acetate in petroleum ether as eluant afforded **78** (19.1 mg, 20%) and **79** (34.4 mg, 36%) with spectral data in agreement with that reported above.

(*Z*/*E*)-2-Azacyclotetradec-6-enone (80) and (81)

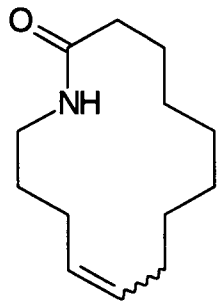

(a) Ring-Closing Metathesis of *N*-(4-Pentenyl)-9-decenamide (**70**)

A solution of *N*-(4-pentenyl)-9-decenamide (**70**) (100.1 mg, 0.4217 mmol) in sparged CH_2Cl_2 (25.0 mL) and a solution of Grubbs' benzylidene (**3**) (17.4 mg, 0.0211 mmol) in sparged CH_2Cl_2 (25.0 mL) were added simultaneously using a syringe pump to sparged

CH_2Cl_2 (161.0 mL) stirred over 3 hours. After the addition, the reaction was stirred for an additional 19 hours. The solution in the receiver flask was gently sparged with N_2 gas during the addition and reaction. Triethylamine (2 mL) was added to the reaction and stirred for 15 minutes and a spatula of silica was added. The solution was concentrated and purification of the silica absorbed residue (GC ratio **80**:**81**, 84:16) by flash column chromatography with 50% ethyl acetate in petroleum ether as eluant afforded **80** (36.5 mg, 41%) and a mixture of **80** and **81** (4.9 mg, 6%) both as white solids.

80 (*Z*)

R_f = 0.22 (petroleum ether-ethyl acetate 1:1);

Melting point: 153.5-154.5 °C (ethyl acetate);

IR (CCl_4): 3464, 3358, 3009, 2932, 2856, 1682, 1504, 1443, 1360, 912 cm^{-1};

^1H NMR (500 MHz, $CDCl_3$) δ: 6.12 (bs, 1 H), 5.39 (dt, J = 11.0, 7.6 Hz, 1 H), 5.34 (dt, J = 11.0, 7.5 Hz, 1 H), 3.25 (dt, J = 4.8, 5.9 Hz, 2 H), 2.19-2.22 (m, 2 H), 2.03-2.08 (m, 2 H), 1.91-1.96 (m, 2 H), 1.62-1.67 (m, 2 H), 1.45-1.50 (m, 2 H), 1.24-1.36 (m, 8 H);

^{13}C NMR (125 MHz, $CDCl_3$) δ: 172.97, 130.17, 128.75, 38.52, 35.56, 30.27, 26.98, 26.73, 25.92, 25.63, 25.17, 25.07, 24.52;

LRMS (DCI(+), ammonia) *m/z* (relative intensity): 210 (M^++1, 100), 209 (M^+, 51);

HRMS (DCI(+), methane/ammonia) *m/z* calculated for $C_{13}H_{24}ON$ (M^++1): 210.1858, found: 210.1854; calculated for $C_{13}H_{23}ON$: 209.1780, found: 209.1787;

Analysis calculated for $C_{13}H_{23}ON$: C, 74.59; H, 11.07; N, 6.69. Found: C, 74.39; H, 11.15; N, 6.63.

The following data was obtained from a mixture of **80 (*Z*)** and **81 (*E*)**, the latter of which was the major component. Only those peaks in the NMR spectra corresponding to **81 (*E*)** are reported.

R_f = 0.22 (petroleum ether-ethyl acetate 1:1);

Melting point: 112.5-118.0 °C (ethyl acetate);

IR (KBr): 3295, 3079, 2932, 2850, 1638, 1552, 1459, 1431, 981, 717 cm^{-1};

^{1}H NMR (500 MHz, $CDCl_3$) δ: 5.67 (bs, 1 H), 5.48 (dt, J = 15.4, 6.1 Hz, 1 H), 5.45 (dt, J = 15.4, 5.9 Hz, 1 H), 3.34 (q, J = 5.2 Hz, 2 H), 2.14-2.22 (m, 4 H), 2.06-2.12 (m, 2 H), 1.86 (bs, 2 H), 1.63-1.68 (m, 4 H), 1.43-1.50 (m, 2 H), 1.21-1.36 (m, 4 H);

^{13}C NMR (125 MHz, $CDCl_3$) δ: 172.98, 132.05, 130.88, 40.37, 35.06, 32.49, 30.52, 28.20, 26.79, 26.48, 26.39, 24.78, 24.22;

LRMS (DCI(+), isobutane) *m/z* (relative intensity): 210 (M^++1, 100), 209 (M^+, 62);

HRMS (DCI(+), isobutane) *m/z* calculated for $C_{13}H_{24}ON$ (M^++1): 210.1858, found: 210.1855;

Analysis calculated for $C_{13}H_{23}ON$: C, 74.59; H, 11.07; N, 6.69. Found: C, 74.89; H, 11.00; N, 6.74.

(b) Ring-Closing Metathesis of *N-tert*-Butoxycarbonyl-*N*-(4-pentenyl)-9-decenamide (**141**)

A solution of *N-tert*-butoxycarbonyl-*N*-(4-pentenyl)-9-decenamide (**141**) (149.0 mg, 0.4415 mmol) in sparged CH_2Cl_2 (25.0 mL) and a solution of Grubbs' benzylidene (**3**) (18.2 mg, 0.0221 mmol) in sparged CH_2Cl_2 (25.0 mL) were added simultaneously using a syringe pump to sparged CH_2Cl_2 (171.0 mL) stirred over 3 hours. After the addition, the reaction was stirred for an additional 5 hours. The solution in the receiver flask was gently sparged with N_2 gas during the addition and reaction. Air was bubbled into the reaction and stirred for 45 minutes. The solution was concentrated and the residue was dissolved in trifluoroacetic acid (1.1 mL) and CH_2Cl_2 (1.1 mL) and stirred for 30 minutes. The reaction was diluted with methanol (2 mL) and concentrated. This dilution and concentration was repeated twice more and a spatula of silica was added before the final concentration. Purification of the silica absorbed residue (GC ratio **80**:**81**, 87:13) by flash column chromatography with 45% ethyl acetate in petroleum ether as eluant afforded **80** (50.9 mg, 55%), a mixture of **80** and **81** (5.0 mg, 5%), and **81** (1.8 mg, 2%) with spectral data in agreement with that reported above.

(c) Isomerization of (*Z*)-2-Azacyclotetradec-6-enone (**80**) with Ruthenium Methylidene **4**

Ethylene gas was bubbled into a solution of Grubbs' benzylidene (**3**) (1.0 mg, 1.2 μmol) in sparged CH_2Cl_2 (6.0 mL) and stirred for 5 minutes. The resulting black solution of ruthenium methylidene **4** was transferred via cannula to a solution of (*Z*)-2-azacyclotetradec-6-enone (**80**) (5.0 mg, 0.024 mmol) in sparged CH_2Cl_2 (6.0 mL)

and stirred for 20 hours. The reaction mixture was gently sparged with N_2 gas during the reaction. The reaction mixture was concentrated and the residue was purified by flash column chromatography with 50% ethyl acetate in petroleum ether as eluant to afford a mixture of **80** and **81** (4.4 mg, 88%; GC ratio **80**:**81**, 83:17).

(*E*/*Z*)-2-Azacyclotetradec-7-enone (82) and (83)

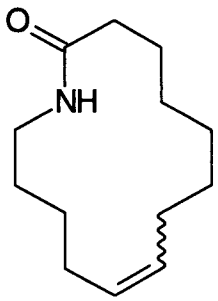

A solution of *N*-(5-hexenyl)-8-nonenamide (**71**) (52.5 mg, 0.2212 mmol) in sparged CH_2Cl_2 (12.5 mL) and a solution of Grubbs' benzylidene (**3**) (9.1 mg, 0.0110 mmol) in sparged CH_2Cl_2 (12.5 mL) were added simultaneously using a syringe pump to sparged CH_2Cl_2 (86.0 mL) stirred over 3 hours. After the addition, the reaction was stirred for an additional 4 hours. The solution in the receiver flask was gently sparged with N_2 gas during the addition and reaction. Triethylamine (1 mL) was added to the reaction and stirred for 15 minutes and a spatula of silica was added. The solution was concentrated and purification of the silica absorbed residue (GC ratio **82**:**83**, 54:46) by flash column chromatography with 40% ethyl acetate in petroleum ether as eluant afforded **82** (21.5 mg, 46%) and **83** (18.4 mg, 40%) both as white solids.

82 (*E*)

R_f = 0.21 (petroleum ether-ethyl acetate 1:1);

Melting point: 143.0-144.5 °C (ethyl acetate);

IR (CCl_4): 3468, 3321, 2926, 2854, 1680, 1504, 1454, 1439, 972, 908 cm^{-1};

^1H NMR (500 MHz, $CDCl_3$) δ: 5.95 (bs, 1 H), 5.48 (dt, J = 15.1, 7.3 Hz, 1 H), 5.26 (dt, J = 15.1, 6.9 Hz, 1 H), 3.16 (dt, J = 5.1, 6.0 Hz, 2 H), 2.09-2.12 (m, 2 H), 1.99 (dt, J = 5.5, 6.4 Hz, 2 H), 1.92 (dt, J = 5.0, 6.9 Hz, 2 H), 1.62-1.67 (m, 2 H), 1.48-1.53 (m, 2 H), 1.33-1.41 (m, 4 H), 1.16-1.30 (m, 4 H);

^{13}C NMR (125 MHz, $CDCl_3$) δ: 173.07, 131.81, 130.56, 39.02, 36.02, 31.51, 30.51, 28.28, 28.25, 27.97, 27.41, 27.03, 25.26;

LRMS (DCI(+), ammonia) *m/z* (relative intensity): 210 (M^++1, 100), 209 (M^+, 97), 166 (25);

HRMS (DCI(+), methane/ammonia) *m/z* calculated for $C_{13}H_{24}ON$ (M^++1): 210.1858, found: 210.1854; calculated for $C_{13}H_{23}ON$: 209.1780, found: 209.1779;

Analysis calculated for $C_{13}H_{23}ON$: C, 74.59; H, 11.07; N, 6.69. Found: C, 74.62; H, 10.98; N, 6.53.

83 (*Z*)

R_f = 0.17 (petroleum ether-ethyl acetate 1:1);

Melting point: 141.0-143.5 °C (ethyl acetate);

IR (CCl_4): 3454, 3339, 3005, 2930, 2858, 1680, 1506, 1462, 1441, 908 cm^{-1};

^1H NMR (500 MHz, $CDCl_3$) δ: 5.47 (bs, 1 H), 5.45 (dt, J = 10.7, 8.0 Hz, 1 H), 5.22 (dt, J = 10.7, 7.8 Hz, 1 H), 3.30 (q, J = 5.6 Hz, 2 H), 2.17 (t, J = 5.9 Hz, 2 H), 2.04 (q, J = 6.6 Hz, 2 H), 1.96 (dt, J = 8.0, 7.8 Hz, 2 H), 1.53-1.63 (m, 4 H), 1.21-1.44 (m, 8 H);

^{13}C NMR (125 MHz, $CDCl_3$) δ: 173.51, 130.36, 129.52, 37.95, 36.95, 27.94, 27.34, 26.85, 26.64, 26.50, 26.04, 26.01, 24.66;

LRMS (DCI(+), ammonia) *m/z* (relative intensity): 210 (M^++1, 100), 209 (M^+, 76), 166 (23);

HRMS (DCI(+), methane/ammonia) *m/z* calculated for $C_{13}H_{24}ON$ (M^++1): 210.1858, found: 210.1856; calculated for $C_{13}H_{23}ON$: 209.1780, found: 209.1779;

Analysis calculated for $C_{13}H_{23}ON$: C, 74.59; H, 11.07; N, 6.69. Found: C, 74.50; H, 11.13; N, 6.59.

(a) Isomerization of (*E*)-2-Azacyclotetradec-7-enone (**82**) with Ruthenium Methylidene **4**

Ethylene gas was bubbled into a solution of Grubbs' benzylidene (**3**) (0.8 mg, 1.06 μmol) in sparged CH_2Cl_2 (5.1 mL) and stirred for 5 minutes. The resulting black solution of ruthenium methylidene **4** was transferred via cannula to a solution of (*E*)-2-azacyclotetradec-7-enone (**82**) (4.3 mg, 0.021 mmol) in sparged CH_2Cl_2 (5.1 mL) and stirred for 20 hours. The reaction mixture was gently sparged with N_2 gas during the reaction. The reaction mixture was concentrated and the residue was purified by

flash column chromatography with 50% ethyl acetate in petroleum ether as eluant to afford a mixture of **82** and **83** (3.7 mg, 86%; GC ratio **82**:**83**, 82:18).

(*E*)-2-Azacyclotetradec-8-enone (84)

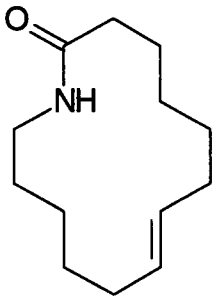

A solution of *N*-(6-heptenyl)-7-octenamide (**72**) (26.4 mg, 0.1112 mmol) in sparged CH_2Cl_2 (10.0 mL) and a solution of Grubbs' benzylidene (**3**) (4.6 mg, 0.0056 mmol) in sparged CH_2Cl_2 (10.0 mL) were added simultaneously via cannula to sparged CH_2Cl_2 (36.0 mL) and the reaction was stirred for one hour. The solution in the receiver flask was gently sparged with N_2 gas during the reaction. Triethylamine (1 mL) was added to the reaction and stirred for 15 minutes and a spatula of silica was added. The solution was concentrated and purification of the silica absorbed residue by flash column chromatography with 40% ethyl acetate in petroleum ether as eluant afforded **84** (20.3 mg, 87%) as a white solid.

R_f = 0.19 (petroleum ether-ethyl acetate 1:1);

Melting point: 152.0-153.0 °C (ethyl acetate);

IR (CCl_4): 3454, 3346, 2928, 2856, 1680, 1508, 1460, 1441, 974, 914, 777 cm^{-1};

^1H NMR (500 MHz, $CDCl_3$) δ: 5.53 (bs, 1 H), 5.20 (dt, J = 14.2, 6.2 Hz, 1 H), 5.16 (dt, J = 14.2, 6.2 Hz, 1 H), 3.30 (dt, J = 5.2, 5.8 Hz, 2 H), 2.12 (t, J = 6.0 Hz, 2 H), 1.94-2.01 (m, 4 H), 1.56-1.62 (m, 2 H), 1.21-1.42 (m, 10 H);

^{13}C NMR (125 MHz, $CDCl_3$) δ: 173.13, 131.67, 131.43, 38.42, 37.00, 32.00, 31.24, 29.00, 28.03, 27.60, 26.97, 25.54, 24.13;

LRMS (DCI(+), ammonia) *m/z* (relative intensity): 210 (M^++1, 100), 209 (M^+, 46), 112 (33), 81 (23), 67 (34), 56 (46);

HRMS (DCI(+), methane) *m/z* calculated for $C_{13}H_{24}ON$ (M^++1): 210.1858, found: 210.1860;

Analysis calculated for $C_{13}H_{23}ON$: C, 74.59; H, 11.07; N, 6.69. Found: C, 74.81; H, 11.15; N, 6.68.

(*Z*/*E*)-2-Azacyclotetradec-9-enone (85) and (86)

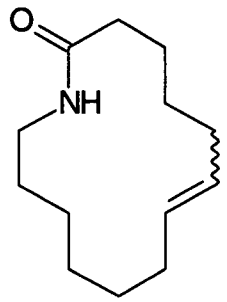

A solution of *N*-(7-octenyl)-6-heptenamide (**73**) (51.7 mg, 0.2178 mmol) in sparged CH_2Cl_2 (12.5 mL) and a solution of Grubbs' benzylidene (**3**) (9.9 mg, 0.0120 mmol) in sparged CH_2Cl_2 (12.5 mL) were added simultaneously using a syringe pump to sparged CH_2Cl_2 (84.0 mL) stirred over 3 hours. After the addition, the reaction was stirred for an additional hour. The solution in the receiver flask was gently sparged with N_2 gas during the addition and reaction. Triethylamine (1 mL) was added to the reaction and stirred for 15 minutes and a spatula of silica was added. The solution was concentrated and purification of the silica absorbed residue (^{1}H NMR ratio **85**:**86**, 42:58) by flash column chromatography with 50% ethyl acetate in petroleum ether as eluant afforded **85** (14.0 mg, 31%) and **86** (19.6 mg, 43%) both as white solids.

85 (*Z*)

R_f = 0.18 (petroleum ether-ethyl acetate 1:1);

Melting point: 120.0-122.0 °C (ethyl acetate);

IR (CCl_4): 3466, 3346, 3007, 2928, 2856, 1682, 1504, 1460, 1439, 912 cm^{-1};

^{1}H NMR (500 MHz, $CDCl_3$) δ: 5.65 (bs, 1 H), 5.44 (dt, J = 10.7, 7.8 Hz, 1 H), 5.25 (dt, J = 10.7, 7.7 Hz, 1 H), 3.27 (dt, J = 4.8, 6.7 Hz, 2 H), 2.21-2.23 (m, 2 H), 2.05 (dt, J = 6.6, 7.0 Hz, 2 H), 1.99 (dt, J = 8.4, 8.0 Hz, 2 H), 1.65-1.72 (m, 2 H), 1.24-1.48 (m, 10 H);

^{13}C NMR (125 MHz, $CDCl_3$) δ: 172.74, 129.89, 129.56, 39.00, 35.90, 28.97, 28.80, 27.14, 26.81, 26.57, 25.56, 24.71, 24.46;

LRMS (DCI(+), ammonia) *m/z* (relative intensity): 210 (M^++1, 100), 209 (M^+, 58), 126 (22), 112 (42), 98 (58), 86 (81), 67 (36), 56 (64);

HRMS (DCI(+), methane) *m/z* calculated for $C_{13}H_{24}ON$ (M^++1): 210.1858, found: 210.1856;

Analysis calculated for $C_{13}H_{23}ON$: C, 74.59; H, 11.07; N, 6.69. Found: C, 74.58; H, 10.99; N, 6.54.

86 (*E*)

R_f = 0.16 (petroleum ether-ethyl acetate 1:1);

Melting point: 123.5-126.0 °C (ethyl acetate);

IR (CCl_4): 3454, 3325, 2930, 2854, 1678, 1504, 1458, 1441, 974, 908 cm^{-1};

^1H NMR (500 MHz, $CDCl_3$) δ: 5.47 (dt, J = 15.4, 7.2 Hz, 1 H), 5.43 (bs, 1 H), 5.31 (dt, J = 15.4, 7.0 Hz, 1 H), 3.26 (dt, J = 5.8, 5.4 Hz, 2 H), 2.19 (t, J = 6.7 Hz, 2 H), 2.05 (dt, J = 5.5, 6.6 Hz, 2 H), 1.98 (dt, J = 5.4, 6.8 Hz, 2 H), 1.58-1.64 (m, 2 H), 1.49-1.53 (m, 2 H), 1.26-1.47 (m, 8 H);

^{13}C NMR (125 MHz, $CDCl_3$) δ: 173.05, 131.90, 130.51, 38.94, 36.29, 31.55, 30.68, 28.74, 27.76, 27.34, 25.98, 24.33;

LRMS (DCI(+), ammonia) *m/z* (relative intensity): 210 (M^++1, 100), 209 (M^+, 41), 112 (34), 98 (62), 86 (74), 67 (78), 56 (34);

HRMS (DCI(+), methane) *m/z* calculated for $C_{13}H_{24}ON$ (M^++1): 210.1858, found: 210.1857;

Analysis calculated for $C_{13}H_{23}ON$: C, 74.59; H, 11.07; N, 6.69. Found: C, 74.54; H, 10.96; N, 6.54.

(*Z*/*E*)-2-Azacyclotetradec-10-enone (87) and (88)

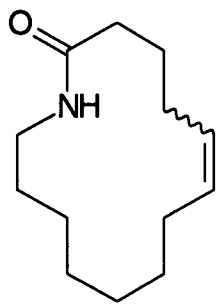

(a) Ring-Closing Metathesis of *N*-(8-Nonenyl)-5-hexenamide (**74**)

A solution of *N*-(8-nonenyl)-5-hexenamide (**74**) (53.6 mg, 0.2258 mmol) in sparged CH_2Cl_2 (12.5 mL) and a solution of Grubbs' benzylidene (**3**) (9.0 mg, 0.0109 mmol) in sparged CH_2Cl_2 (12.5 mL) were added simultaneously using a syringe pump to sparged

CH_2Cl_2 (85.0 mL) stirred over 3 hours. After the addition, the reaction was stirred for an additional 22 hours. The solution in the receiver flask was gently sparged with N_2 gas during the addition and reaction. Triethylamine (1 mL) was added to the reaction and stirred for 15 minutes and a spatula of silica was added. The solution was concentrated and purification of the silica absorbed residue (^{1}H NMR ratio **87**:**88**, 89:11) by flash column chromatography with 50% ethyl acetate in petroleum ether as eluant removed ruthenium compounds. Purification of the residue by radial chromatography with 45% ethyl acetate in petroleum ether as eluant afforded **87** (3.6 mg, 8%) and a mixture of **87** and **88** (14.8 mg, 31%) both as white solids.

87 (*Z*)

R_f = 0.18 (petroleum ether-ethyl acetate 1:1);

Melting point: 141.0-143.0 °C (ethyl acetate);

IR (CCl_4): 3452, 3350, 3003, 2930, 2860, 1682, 1506, 1460, 1443, 775 cm^{-1};

^{1}H NMR (500 MHz, $CDCl_3$) δ: 5.44 (bs, 1 H), 5.42 (dt, J = 10.7, 7.6 Hz, 1 H), 5.29 (dt, J = 10.7, 7.4 Hz, 1 H), 3.31 (dt, J = 5.8, 5.7 Hz, 2 H), 2.18-2.20 (m, 2 H), 2.10 (dt, J = 7.9, 7.5 Hz, 2 H), 1.93 (dt, J = 6.9, 7.6 Hz, 2 H), 1.64-1.69 (m, 2 H), 1.51-1.56 (m, 2 H), 1.27-1.36 (m, 8 H);

^{13}C NMR (125 MHz, $CDCl_3$) δ: 172.93, 130.81, 129.03, 37.91, 35.77, 27.25, 27.09, 26.27, 26.22, 26.05, 25.20, 24.83, 23.61;

LRMS (DCI(+), ammonia) *m/z* (relative intensity): 210 (M^++1, 100), 209 (M^+, 32);

HRMS (DCI(+), methane) *m/z* calculated for $C_{13}H_{24}ON$ (M^++1): 210.1858, found: 210.1856;

Analysis calculated for $C_{13}H_{23}ON$: C, 74.59; H, 11.07; N, 6.69. Found: C, 74.77; H, 11.13; N, 6.52.

The following data was obtained from a mixture of **87 (*Z*)** and **88 (*E*)**, the latter of which was the minor component. Only those peaks in the NMR spectra corresponding to **88 (*E*)** are reported, and the remainder of the data was a mixture of **87 (*Z*)** and **88 (*E*)**.

R_f = 0.18 (petroleum ether-ethyl acetate 1:1);

Melting point: 108.0-118.0 °C (ethyl acetate);

IR (KBr): 3294, 3088, 2927, 2855, 1646, 1558, 1461, 1435, 973, 714 cm^{-1};

^{1}H NMR (500 MHz, $CDCl_3$) δ: 3.26 (q, J = 5.6 Hz, 0.5 H), 2.00 (q, J = 6.0 Hz, 0.5 H), 1.76-1.81 (m, 0.5 H);

^{13}C NMR (125 MHz, $CDCl_3$) δ: 172.92, 132.13, 129.60, 38.43, 32.16, 31.05, 27.27, 26.91, 25.93, 25.15, 25.04, 24.88, 23.00;

LRMS (DCI(+), isobutane) *m/z* (relative intensity): 210 (M^++1, 100), 209 (M^+, 47);

HRMS (DCI(+), isobutane) *m/z* calculated for $C_{13}H_{24}ON$ (M^++1): 210.1858, found: 210.1858;

Analysis calculated for $C_{13}H_{23}ON$: C, 74.59; H, 11.07; N, 6.69. Found: C, 74.77; H, 10.99; N, 6.56.

(b) Ring-Closing Metathesis of *N-tert*-Butoxycarbonyl-*N*-(8-nonenyl)-5-hexenamide (**142**)

A solution of *N-tert*-butoxycarbonyl-*N*-(8-nonenyl)-5-hexenamide (**142**) (49.1 mg, 0.1455 mmol) in sparged CH_2Cl_2 (12.5 mL) and a solution of Grubbs' benzylidene (**3**) (6.0 mg, 0.0073 mmol) in sparged CH_2Cl_2 (12.5 mL) were added simultaneously using a syringe pump to sparged CH_2Cl_2 (48.0 mL) stirred over 3 hours. After the addition, the reaction was stirred for an additional 7 hours. The solution in the receiver flask was gently sparged with N_2 gas during the addition and reaction. Triethylamine (1 mL) was added to the reaction and stirred for one hour. The solution was concentrated and the residue was dissolved in trifluoroacetic acid (0.75 mL) and CH_2Cl_2 (0.75 mL) and stirred for 30 minutes. The reaction was diluted with methanol (2 mL) and concentrated. This dilution and concentration was repeated twice more and a spatula of silica was added before the final concentration. Purification of the silica absorbed residue (^{1}H NMR ratio **87**:**88**, 20:80) by flash column chromatography with 45% ethyl acetate in petroleum ether as eluant afforded a mixture of **87** and **88** (21.4 mg, 70%) with spectral data in agreement with that reported above.

(*E*/*Z*)-2-Azacyclotetradec-11-enone (89) and (90)

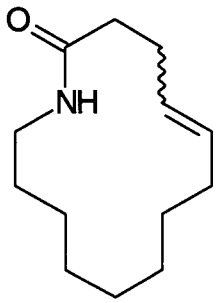

(a) Ring-Closing Metathesis of *N*-(9-Decenyl)-4-pentenamide (**75**)

A solution of *N*-(9-decenyl)-4-pentenamide (**75**) (49.7 mg, 0.2094 mmol) in sparged CH_2Cl_2 (12.5 mL) and a solution of Grubbs' benzylidene (**3**) (8.6 mg, 0.0104 mmol) in sparged CH_2Cl_2 (12.5 mL) were added simultaneously using a syringe pump to sparged CH_2Cl_2 (80.0 mL) stirred over 3 hours. After the addition, the reaction was stirred for an additional 21 hours. The solution in the receiver flask was gently sparged with N_2 gas during the addition and reaction. Triethylamine (1 mL) was added to the reaction and stirred for 15 minutes and a spatula of silica was added. The solution was concentrated and purification of the silica absorbed residue (GC ratio **89**:**90**, 80:20) by flash column chromatography with 40% ethyl acetate in petroleum ether as eluant afforded **89** (0.9 mg, 2%) and a mixture of **89** and **90** (3.8 mg, 9%) both as white solids.

89 (*E*)

R_f = 0.18 (petroleum ether-ethyl acetate 1:1);

Melting point: 135.0-136.0 °C (ethyl acetate);

IR (CCl_4): 3468, 3346, 2930, 2860, 1682, 1506, 1456, 1441, 972, 908 cm^{-1};

^1H NMR (500 MHz, $CDCl_3$) δ: 5.71 (bs, 1 H), 5.43 (dt, J = 15.4, 6.9 Hz, 1 H), 5.30 (dt, J = 15.4, 6.7 Hz, 1 H), 3.23 (dt, J = 4.8, 5.9 Hz, 2 H), 2.34 (dt, J = 5.5, 6.3 Hz, 2 H), 2.20-2.23 (m, 2 H), 1.95 (dt, J = 4.5, 6.5 Hz, 2 H), 1.14-1.40 (m, 12 H);

^{13}C NMR (125 MHz, $CDCl_3$) δ: 172.23, 132.17, 129.23, 39.06, 36.63, 31.48, 28.36, 27.39, 26.46, 25.25, 24.96, 23.74, 22.98;

LRMS (DCI(+), ammonia) *m/z* (relative intensity): 210 (M^++1, 100), 209 (M^+, 3);

HRMS (CI(+), isobutane) *m/z* calculated for $C_{13}H_{24}ON$ (M^++1): 210.1858, found: 210.1859;

Analysis calculated for $C_{13}H_{23}ON$: C, 74.59; H, 11.07; N, 6.69. Found: C, 74.51; H, 11.13; N, 6.74.

The following data was obtained from a mixture of **89 (*E*)** and **90 (*Z*)**, the latter of which was the minor component.

R_f = 0.18 (petroleum ether-ethyl acetate 1:1);

Melting point: 114.0-118.0 °C (ethyl acetate);

IR (KBr): 3305, 3078, 2921, 2858, 1646, 1548, 1456, 1437, 966, 711 cm^{-1};

LRMS (DCI(+), isobutane) *m/z* (relative intensity): 210 (M^++1, 100) , 209 (M^+, 46);

HRMS (DCI(+), isobutane) *m/z* calculated for $C_{13}H_{24}ON$ (M^++1): 210.1858, found: 210.1860;

Analysis calculated for $C_{13}H_{23}ON$: C, 74.59; H, 11.07; N, 6.69. Found: C, 74.75; H, 11.12; N, 6.60.

An impure sample of **90 (*Z*)** was obtained from the mixture reported above, and only those peaks in the NMR spectrum corresponding to **90 (*Z*)** are reported. The remainder of the data was a mixture of **90 (*Z*)** and other unidentified compounds.

^{1}H NMR (500 MHz, $CDCl_3$) δ: 5.54 (dt, J = 11.2, 7.5 Hz, 1 H), 5.34 (dt, J = 11.2, 7.2 Hz, 1 H), 5.34 (bs, 1 H), 3.29-3.32 (m, 2 H), 2.40 (dt, J = 5.0, 6.1 Hz, 2 H), 2.26-2.28 (m, 2 H), 2.00-2.04 (m, 2 H).

(b) Ring-Closing Metathesis of *N-tert*-Butoxycarbonyl-*N*-(9-decenyl)-4-pentenamide (**143**)

A solution of *N-tert*-butoxycarbonyl-*N*-(9-decenyl)-4-pentenamide (**143**) (146.6 mg, 0.4344 mmol) in sparged CH_2Cl_2 (25.0 mL) and a solution of Grubbs' benzylidene (**3**) (17.9 mg, 0.0218 mmol) in sparged CH_2Cl_2 (25.0 mL) were added simultaneously using a syringe pump to sparged CH_2Cl_2 (167.0 mL) stirred over 3 hours. After the addition, the reaction was stirred for an additional 21 hours. The solution in the receiver flask was gently sparged with N_2 gas during the addition and reaction. Air was bubbled into the reaction and stirred for 45 minutes. The solution was concentrated and the residue was dissolved in trifluoroacetic acid (1.1 mL) and CH_2Cl_2 (1.1 mL) and stirred for 30 minutes. The reaction was diluted with methanol (2 mL) and concentrated. This dilution and concentration was repeated twice more and a spatula of silica was added before the final concentration. Purification of the silica absorbed residue (GC ratio **89**:**90**, 82:18) by flash column chromatography with 45% ethyl acetate in petroleum ether as

eluant afforded **89** (5.2 mg, 6%) and a mixture of **89** and **90** (22.4 mg, 25%) with spectral data in agreement with that reported above.

(*E*/*Z*)-2-Azacyclotetradec-12-enone (91) and (92)

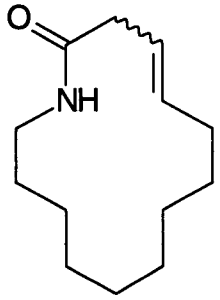

(a) Ring-Closing Metathesis of (*Z*)-*N*-(10-Undecenyl)-3-hexenamide (**148**)

A solution of (*Z*)-*N*-(10-undecenyl)-3-hexenamide (**148**) (51.2 mg, 0.193 mmol) in sparged CH_2Cl_2 (12.5 mL) and a solution of Grubbs' benzylidene (**3**) (31.7 mg, 0.0386 mmol) in sparged CH_2Cl_2 (12.5 mL) were added simultaneously using a syringe pump to sparged CH_2Cl_2 (71.0 mL) stirred over 3 hours. After the addition, the reaction was stirred for an additional 21 hours. The solution in the receiver flask was gently sparged with N_2 gas during the addition and reaction. Triethylamine (1 mL) was added to the reaction and stirred for 15 minutes and a spatula of silica was added. The solution was concentrated and purification of the silica absorbed residue (^{1}H NMR ratio **91**:**92**, 80:20) by flash column chromatography with 50% ethyl acetate in petroleum ether as eluant afforded a mixture of **91** and **92** (14.9 mg, 37%) as a white solid.

91 (*E*) in a mixture containing minor isomer **92 (*Z*)**

R_f = 0.24 (petroleum ether-ethyl acetate 1:1);

Melting point: 111.5-114.5 °C (ethyl acetate);

IR (KBr): 3309, 3081, 2927, 2855, 1645, 1551, 1462, 1439, 977, 739, 709 cm^{-1};

^{1}H NMR (500 MHz, $CDCl_3$) δ: 5.74 (bs, 1 H), 5.47-5.64 (m, 2 H), 3.25-3.29 (m, 2 H), 3.01 (d, J = 7.7 Hz, 0.4 H), 2.89 (d, J = 6.2 Hz, 1.6 H), 2.07-2.13 (m, 2 H), 1.42-1.51 (m, 4 H), 1.35-1.39 (m, 2 H), 1.18-1.30 (m, 8 H);

^{13}C NMR (125 MHz, $CDCl_3$) δ: 171.25, 136.38, 124.82, 41.25, 37.43, 30.93, 27.25, 27.14, 26.53, 25.55, 25.26, 24.82, 22.77;

LRMS (DCI(+), isobutane) *m/z* (relative intensity): 210 (M^++1, 100), 209 (M^+, 28);

HRMS (DCI(+), isobutane) *m/z* calculated for $C_{13}H_{24}ON$ (M^++1): 210.1858, found: 210.1859;

Analysis calculated for $C_{13}H_{23}ON$: C, 74.59; H, 11.07; N, 6.69. Found: C, 74.40; H, 11.13; N, 6.49.

Minor isomer **92 (*Z*)** in a mixture with major isomer **91 (*E*)**

^{13}C NMR (125 MHz, $CDCl_3$) δ: 170.82, 136.52, 121.79, 38.51, 35.17, 27.58, 26.86, 26.64, 25.76, 25.62, 25.60, 25.44, 23.10.

(b) Ring-Closing Metathesis of (*E*)-*N*-(10-Undecenyl)-3-hexenamide (**145**)

A solution of (*E*)-*N*-(10-undecenyl)-3-hexenamide (**145**) (53.2 mg, 0.2004 mmol) in sparged CH_2Cl_2 (12.5 mL) and a solution of Grubbs' benzylidene (**3**) (36.9 mg, 0.0448 mmol) in sparged CH_2Cl_2 (12.5 mL) were added simultaneously using a syringe pump to sparged CH_2Cl_2 (87.0 mL) stirred over 3 hours. After the addition, the reaction was stirred for an additional 21 hours. The solution in the receiver flask was gently sparged with N_2 gas during the addition and reaction. Triethylamine (1 mL) was added to the reaction and stirred for 15 minutes and a spatula of silica was added. The solution was concentrated and purification of the silica absorbed residue (^1H NMR ratio **91**:**92**, 77:23) by flash column chromatography with 50% ethyl acetate in petroleum ether as eluant afforded a mixture of **91** and **92** (4.7 mg, 11%) with spectral data in agreement with that reported above.

7-Octenoic acid (93)

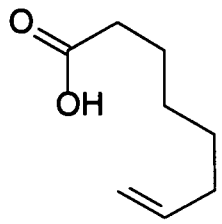

(a) Hydrolysis and Decarboxylation of Dimethyl (5-Hexenyl)malonate (**119**)

Potassium hydroxide (161.5 mg, 2.88 mmol) was added to a solution of dimethyl (5-hexenyl)malonate (**119**) (154.2 mg, 0.720 mmol) in water (0.5 mL) and the reaction was stirred for 4.5 hours at 90 °C. The reaction was cooled to room temperature and concentrated HCl (0.15 mL) was added in parts. The mixture was washed with diethyl

ether (3X) (10 mL each). The combined organic layers were dried over $MgSO_4$, filtered, and concentrated. The crude product was stirred for 10 hours at 100 °C. The crude product was cooled to room temperature and diluted with water (5 mL) and successively extracted with portions of diethyl ether (3X) (10 mL each). The combined organic layers were dried over $MgSO_4$, filtered, and concentrated. Purification of the residue by flash column chromatography with 50% diethyl ether in petroleum ether as eluant afforded **93** (97.4 mg, 95%) as a pale yellow oil.

R_f = 0.31 (petroleum ether-ethyl acetate 9:1);

IR (neat): 3078, 2932, 2858, 1712, 1641, 1414, 1279, 993, 910, 731 cm^{-1};

^1H NMR (200 MHz, $CDCl_3$) δ: 11.33 (bs, 1 H), 5.77 (ddt, J = 17.0, 10.1, 6.6 Hz, 1 H), 4.88-5.02 (m, 2 H), 2.33 (t, J = 7.4 Hz, 2 H), 2.03 (q, J = 6.8 Hz, 2 H), 1.62 (quint, J = 7.3 Hz, 2 H), 1.23-1.47 (m, 4 H);

^{13}C NMR (50 MHz, $CDCl_3$) δ: 175.27, 133.46, 109.21, 28.81, 28.26, 23.23, 19.24;

LRMS (EI) *m/z* (relative intensity): 142 (M^+, 4), 125 (15), 124 (100), 101 (10), 100 (27), 96 (47), 87 (7), 83 (23), 82 (39), 73 (8), 69 (4), 68 (7), 67 (9), 60 (8), 55 (19), 41 (6);

HRMS (EI) *m/z* calculated for $C_8H_{14}O_2$: 142.0994, found: 142.0996;

Analysis calculated for $C_8H_{14}O_2$: C, 67.56; H, 9.93. Found: C, 67.75; H, 9.87.

(b) Hydrolysis of 7-Octenenitrile (**95**)

Ground KOH (1.84 g, 32.8 mmol) was added to a solution of 7-octenenitrile (**95**) (1.01 g, 8.21 mmol) in ethylene glycol (11.0 mL) and the reaction was stirred for 3 hours at 120 °C, then for 17 hours at 45 °C and then for 6 hours at 150 °C. The reaction was cooled to room temperature and diluted with water (20 mL) and washed with diethyl ether (3X) (20 mL each). The aqueous solution was acidified with concentrated HCl and the crude product was successively extracted with portions of diethyl ether (4X) (50 mL each). The combined organic layers were dried over $MgSO_4$, filtered, and concentrated. Purification of the residue by flash column chromatography with 30% diethyl ether in petroleum ether as eluant afforded **93** (1.03 g, 88%) with spectral data in agreement with that reported above.

6-Heptenylamine (94)

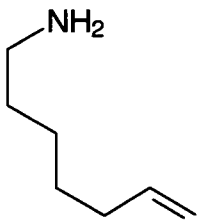

Lithium aluminum hydride (1.75 g, 46.1 mmol) was added to a solution of 6-heptenenitrile (**96**) (2.51 g, 23.0 mmol) in THF (92 mL) at 0 °C and the reaction was stirred for 3.5 hours at 70 °C. The reaction was cooled to 0 °C and a solution of THF (8.8 mL) and water (1.8 mL) was added and stirred for 15 minutes. Aqueous 3 M NaOH solution was added dropwise until a white precipitate formed and the solution was stirred for 15 minutes. The slurry was vacuum filtered and concentrated. Kugelrohr distillation of the residue at 80 °C at 10 mm Hg afforded **94** (2.28 g, 88%) as a colourless oil.

R_f = 0.0 (petroleum ether-ethyl acetate 4:1);

Boiling point: 80 °C at 10 mm Hg;

IR (neat): 3369, 3290, 3076, 2928, 2854, 1641, 1462, 1072, 993, 910, 816, 733 cm^{-1};

^1H NMR (200 MHz, $CDCl_3$) δ: 5.74 (ddt, J = 17.1, 10.2, 6.6 Hz, 1 H), 4.83-4.98 (m, 2 H), 2.61 (t, J = 6.8 Hz, 2 H), 1.98 (q, J = 6.8 Hz, 2 H), 1.23-1.44 (m, 8 H);

^{13}C NMR (50 MHz, $CDCl_3$) δ: 138.83, 114.19, 42.07, 33.62, 33.57, 28.64, 26.25;

LRMS (EI) *m/z* (relative intensity): 114 (M^++1, 93), 113 (M^+, 3), 98 (22), 70 (29), 56 (33), 30 (100);

HRMS (EI) *m/z* calculated for $C_7H_{15}N$: 113.1205, found: 113.1202.

7-Octenenitrile (95)

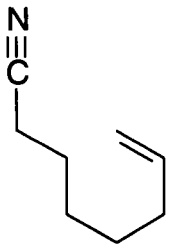

A solution of *n*-butyllithium in hexanes (13.6 mL, 21.8 mmol) was added dropwise to a solution of CH_3CN (1.10 mL, 21.1 mmol) in THF (31.5 mL) at -78 °C and the reaction

was stirred for two hours. 6-Iodohexene (**97**) (4.58 g, 21.80 mmol) was added and the reaction was stirred for two hours at -78 °C and stirred for 16 hours warming to room temperature. The reaction was concentrated and the residue was purified by flash column chromatography with 10% diethyl ether in petroleum ether as eluant to afford **95** (2.35 g, 90%) as a colourless oil.

R_f = 0.78 (petroleum ether-ethyl acetate 4:1);

Boiling point: 130 °C at 15 mm Hg;

IR (neat): 3078, 2934, 2860, 2245, 1641, 1462, 995, 912, 729 cm^{-1};

^1H NMR (200 MHz, $CDCl_3$) δ: 5.74 (ddt, J = 17.0, 10.2, 6.8 Hz, 1 H), 4.88-5.02 (m, 2 H), 2.30 (t, J = 6.9 Hz, 2 H), 2.02 (q, J = 6.8 Hz, 2 H), 1.55-1.69 (m, 2 H), 1.31-1.50 (m, 4 H);

^{13}C NMR (50 MHz, $CDCl_3$) δ: 138.15, 119.63, 114.67, 33.21, 27.93, 27.85, 25.10, 16.95;

LRMS (DCI(+), ammonia) *m/z* (relative intensity): 141 (M^++NH_4, 18), 124 (M^++1, 64), 95 (37), 94 (100), 80 (27), 58 (21), 55 (40);

HRMS (CI(+), isobutane) *m/z* calculated for $C_8H_{14}N$ (M^++1): 124.1126, found: 124.1127;

Analysis calculated for $C_8H_{13}N$: C, 77.99; H, 10.64; N, 11.37. Found: C, 77.76; H, 10.66; N, 11.31.

6-Heptenenitrile (96)

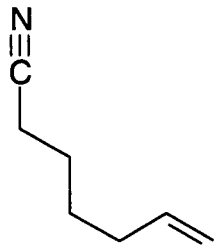

Recrystallized potassium cyanide (4.65 g, 71.4 mmol) was added to a solution of 6-iodo-1-hexene (**97**) (10.0 g, 47.6 mmol) in CH_3CN (26.0 mL) and the reaction was stirred for 33 hours at 90 °C. The reaction was cooled to room temperature and diluted with CH_2Cl_2 (30 mL) and vacuum filtered through celite and concentrated. Purification of the residue by flash column chromatography with 5% diethyl ether in petroleum ether as eluant afforded **96** (4.88 g, 94%) as a colourless oil.

R_f = 0.77 (petroleum ether-ethyl acetate 4:1);

IR (neat): 3078, 2935, 2864, 2247, 1641, 1427, 995, 916, 735 cm^{-1};

^1H NMR (200 MHz, $CDCl_3$) δ: 5.72 (ddt, J = 17.1, 10.2, 6.6 Hz, 1 H), 4.90-5.03 (m, 2 H), 2.30 (t, J = 6.9 Hz, 2 H), 2.05 (dt, J = 7.1, 6.6 Hz, 2 H), 1.41-1.70 (m, 4 H);

^{13}C NMR (50 MHz, $CDCl_3$) δ: 137.41, 119.52, 115.14, 32.57, 27.53, 24.54, 16.79;

LRMS (DCI(+), ammonia) *m/z* (relative intensity): 110 (M^++1, 100), 109 (8), 108 (12), 82 (7), 81 (17);

HRMS (CI(+), isobutane) *m/z* calculated for $C_7H_{12}N$ (M^++1): 110.0970, found: 110.0969;

Analysis calculated for $C_7H_{11}N$: C, 77.01; H, 10.16; N, 12.83. Found: C, 76.94; H, 10.35; N, 13.00.

6-Iodo-1-hexene (97)

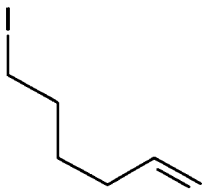

Crushed iodine (41.21 g, 162.36 mmol) was added in parts to a solution of 5-hexen-1-ol (15.0 mL, 124.9 mmol), triphenylphosphine (42.59 g, 162.38 mmol), and imidazole (11.17 g, 162.2 mmol) in CH_2Cl_2 (500.0 mL) stirred at 0 °C and the reaction was stirred for 22 hours with warming to room temperature. The reaction mixture was vacuum filtered through silica gel and washed with CH_2Cl_2 (600 mL). The filtrate was sequentially washed with saturated $Na_2S_2O_3$ solution and saturated $CuSO_4$ solution (600 mL each). The aqueous layers were separately washed with CH_2Cl_2 (600 mL each). The combined organic layers were dried over $MgSO_4$, filtered, and concentrated. Purification of the residue by vacuum liquid chromatography with petroleum ether as eluant afforded **97** (25.21 g, 96%) as a yellow oil.

R_f = 0.78 (petroleum ether-ethyl acetate 4:1);

IR (neat): 3076, 2932, 2854, 1641, 1427, 1215, 991, 912, 723 cm^{-1};

^1H NMR (200 MHz, $CDCl_3$) δ: 5.76 (ddt, J = 17.0, 10.2, 6.8 Hz, 1 H), 4.90-5.04 (m, 2 H), 3.16 (t, J = 6.9 Hz, 2 H), 2.05 (q, J = 7.1 Hz, 2 H), 1.81 (dt, J = 15.1, 6.8 Hz, 2 H), 1.47 (dt, J = 14.4, 7.1 Hz, 2 H);

^{13}C NMR (50 MHz, $CDCl_3$) δ: 138.00, 114.93, 32.83, 32.54, 29.62, 6.74;

LRMS (EI) *m/z* (relative intensity): 210 (M^+, 4), 83 (75), 55 (100), 41 (68);

HRMS (EI) *m/z* calculated for $C_6H_{11}I$: 209.9906, found: 209.9902.

9-Decenyl acetate (104)

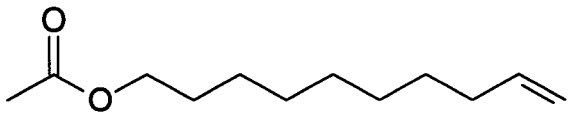

Acetyl chloride (0.52 mL, 7.3 mmol) was added dropwise to a solution of 9-decen-1-ol (1.00 mL, 5.61 mmol), *N,N*-dimethylaminopyridine (342.0 mg, 2.799 mmol), and triethylamine (2.34 mL) in CH_2Cl_2 (28 mL) at 0 °C and the reaction was stirred for two hours at room temperature. The reaction was diluted with CH_2Cl_2 (75 mL) and washed with water (50 mL). The aqueous layer was washed with CH_2Cl_2 (2X) (100 mL each). The combined organic layers were dried over $MgSO_4$, filtered, and concentrated. Purification of the residue by flash column chromatography with petroleum ether as eluant afforded **104** (1.0033 g, 90%) as a colourless oil.

R_f = 0.90 (petroleum ether-ethyl acetate 9:1);

IR (neat): 3076, 2928, 2856, 1744, 1641, 1465, 1366, 1240, 1040, 993, 910, 723 cm^{-1};

^{1}H NMR (200 MHz, $CDCl_3$) δ: 5.77 (ddt, J = 17.0, 10.1, 6.6 Hz, 1 H), 4.85-5.00 (m, 2 H), 4.01 (t, J = 6.7 Hz, 2 H), 2.00 (s, 3 H), 2.00 (q, J = 6.8 Hz, 2 H), 1.51-1.64 (m, 2 H), 1.20-1.37 (m, 10 H);

^{13}C NMR (50 MHz, $CDCl_3$) δ: 171.10, 139.04, 114.10, 64.55, 33.71, 29.28, 29.13, 28.96, 28.82, 28.54, 25.83, 20.92;

LRMS (DCI(+), ammonia) *m/z* (relative intensity): 199 (M^++1, 17), 139 (18), 138 (100), 110 (48), 109 (57), 97 (27), 96 (74), 95 (82), 83 (33), 82 (60), 81 (76), 69 (25), 68 (47), 67 (66), 61 (10), 55 (46), 54 (21);

HRMS (DCI(+), methane/ammonia) *m/z* calculated for $C_{12}H_{23}O_2$ (M^++1): 199.1698, found: 199.1696;

Analysis calculated for $C_{12}H_{22}O_2$: C, 72.68; H, 11.18. Found: C, 72.43; H, 11.10.

Benzaldehyde *p*-toluenesulfonylhydrazone (107)

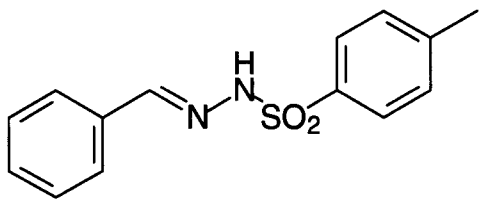

Benzaldehyde (1.8 mL, 17.7 mmol) was added to a solution of *p*-toluenesulfonylhydrazide (3.33 g, 17.88 mmol) in methanol (6.0 mL) and stirred for 30 minutes at 50 °C. The reaction was cooled to 0 °C for 20 minutes, filtered, and washed with ice-cold methanol to afford **107** (2.19 g, 45%) as a white solid.

R_f = 0.10 (petroleum ether-ethyl acetate 4:1);

Melting point: 126.0-127.0 °C (methanol);

IR (KBr): 3227, 3084, 3067, 3032, 2989, 2864, 1664, 1597, 1438, 1367, 1325, 1167, 1094, 959, 816, 750 cm^{-1};

^1H NMR (200 MHz, $CDCl_3$) δ: 8.40 (bs, 1 H), 7.87 (d, J = 8.3 Hz, 2 H), 7.77 (s, 1 H), 7.51-7.57 (m, 2 H), 7.26-7.37 (m, 5 H), 2.37 (s, 3 H);

^{13}C NMR (50 MHz, $CDCl_3$) δ: 147.93, 144.22, 135.21, 133.16, 130.34, 129.33, 128.56, 127.89, 127.32, 21.52;

LRMS (DCI(+), ammonia) *m/z* (relative intensity): 275 (M^++1, 100), 274 (M^+, 49), 119 (38), 118 (67), 92 (21), 90 (40);

HRMS (DCI(+), methane/ammonia) *m/z* calculated for $C_{14}H_{14}O_2N_2S$: 274.0776, found: 274.0776;

Analysis calculated for $C_{14}H_{14}O_2N_2S$: C, 61.29; H, 5.14; N, 10.21. Found: C, 60.97; H, 5.09; N, 10.23.

N-Benzyl-10-undecenamide (109)

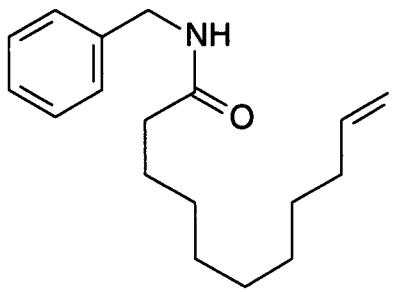

Undecylenic acid (7.36 mL, 36.42 mmol) and 1,3-dicyclohexylcarbodiimide (7.52 g, 36.45 mmol) were sequentially added to a solution of benzylamine (4.0 mL, 36.6 mmol) in CH_2Cl_2 (73 mL) and the reaction was stirred for 43 hours. The reaction was filtered and washed with ethyl acetate (250 mL). The filtrate was washed sequentially with saturated $NaHCO_3$ solution and brine (250 mL each). The combined aqueous layers were successively washed with ethyl acetate (2X) (300 mL each). The combined organic extracts were dried over $MgSO_4$, filtered, and concentrated. Purification of the residue by flash column chromatography with 35% ethyl acetate in petroleum ether as eluant afforded **109** (6.51 g, 65%) as a white solid.

R_f = 0.26 (petroleum ether-ethyl acetate 4:1);

Melting point: 62.5-63.0 °C (ethyl acetate);

IR (CCl_4): 3452, 3342, 3067, 3032, 2928, 2856, 1682, 1454, 912 cm^{-1};

^1H NMR (200 MHz, $CDCl_3$) δ: 7.21-7.36 (m, 5 H), 5.79 (ddt, J = 17.1, 10.2, 6.7 Hz, 1 H), 5.75 (bs, 1 H), 4.87-5.02 (m, 2 H), 4.41 (d, J = 5.6 Hz, 2 H), 2.19 (t, J = 7.6 Hz, 2 H), 2.01 (q, J = 6.9 Hz, 2 H), 1.63 (quint, J = 7.3 Hz, 2 H), 1.23-1.37 (m, 10 H);

^{13}C NMR (50 MHz, $CDCl_3$) δ: 172.98, 139.15, 138.38, 128.68, 127.80, 127.48, 114.12, 43.58, 36.77, 33.75, 29.26, 29.02, 28.86, 25.72;

LRMS (EI) *m/z* (relative intensity): 273 (M^+, 19), 162 (22), 149 (81), 107 (21), 106 (61), 91 (100), 55 (22), 41 (30);

HRMS (EI) *m/z* calculated for $C_{18}H_{27}ON$: 273.2093, found: 273.2091;

Analysis calculated for $C_{18}H_{27}ON$: C, 79.06; H, 9.96; N, 5.13. Found: C, 79.18; H, 10.13; N, 5.15.

N-Benzyl-10-undecenylamine (110)

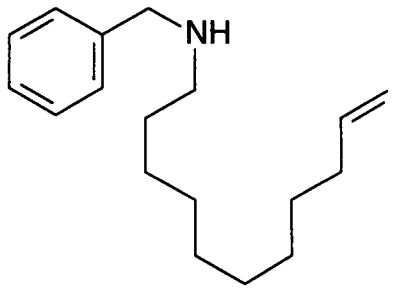

Lithium aluminum hydride (0.14 g, 3.7 mmol) was added to a solution of *N*-benzyl-10-undecenamide (**109**) (0.50 g, 1.83 mmol) in THF (7.3 mL) and the reaction was stirred for 3 hours at 70 °C. The reaction was cooled to 0 °C and a solution of THF (0.7 mL) and water (0.1 mL) was added and stirred for 15 minutes. Aqueous 3 M NaOH solution was added dropwise until a white precipitate formed and the solution was stirred for 15 minutes. The slurry was vacuum filtered and concentrated to afford **110** (486.9 mg, 90%) as a colourless oil. This material was used in subsequent reactions without further purification. Precipitation of the hydrochloride salt in CH_2Cl_2 gave pure **110**·HCl for analysis.

R_f = 0.0 (petroleum ether-ethyl acetate 4:1);

Melting point ($C_{18}H_{30}NCl$): 182.0-183.5 °C (dichloromethane);

IR (neat): 3323, 3063, 3028, 2926, 2853, 1641, 1497, 1454, 1121, 993, 908, 733 cm^{-1};

^1H NMR (200 MHz, $CDCl_3$) δ: 7.31 (s, 5 H), 5.82 (ddt, J = 17.0, 10.1, 6.6 Hz, 1 H), 4.89-5.05 (m, 2 H), 3.78 (s, 2 H), 2.62 (t, J = 7.0 Hz, 2 H), 2.04 (q, J = 6.8 Hz, 2 H), 1.23-1.58 (m, 15 H);

^{13}C NMR (50 MHz, $CDCl_3$) δ: 140.54, 139.12, 128.28, 128.02, 126.76, 114.06, 54.05, 49.47, 33.74, 30.26, 30.06, 29.48, 29.37, 29.06, 28.87, 27.29;

LRMS (EI) *m/z* (relative intensity): 259 (M^+, 4), 120 (100), 91 (100);

HRMS (EI) *m/z* calculated for $C_{18}H_{29}N$: 259.2300, found: 259.2298;

Analysis calculated for $C_{18}H_{30}NCl$: C, 73.17; H, 10.24; N, 4.74. Found: C, 72.98; H, 9.99; N, 4.78.

_N_-Benzyl-_N_-(3-butenyl)-10-undecenylamine (111)

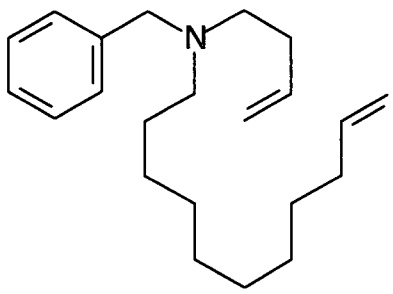

4-Bromo-1-butene (0.37 mL, 3.64 mmol) was added to a solution of _N_-benzyl-10-undecenylamine (**110**) (475.0 mg, 1.612 mmol) and potassium carbonate (0.51 g, 3.69 mmol) in CH_3CN (5.6 mL) and the reaction was stirred for 23 hours. Another portion of potassium carbonate (0.25 g, 1.81 mmol) was added to the reaction and stirred for an additional 17 hours. The reaction mixture was concentrated and diluted with diethyl ether (10 mL) and sequentially washed with water (7 mL) and brine (7 mL). The organic layer was dried over $MgSO_4$, filtered, and concentrated. Purification of the residue by flash column chromatography with 5% ethyl acetate in petroleum ether as eluant afforded **111** (246.7 mg, 49%) as a colourless oil.

R_f = 0.93 (petroleum ether-ethyl acetate 4:1);

IR (neat): 3076, 3026, 2926, 2854, 2799, 1641, 1454, 1070, 993, 910, 735 cm^{-1};

^1H NMR (200 MHz, $CDCl_3$) δ: 7.19-7.38 (m, 5 H), 5.83 (ddt, J = 17.1, 10.2, 6.6 Hz, 1 H), 5.81 (ddt, J = 17.1, 10.2, 6.6 Hz, 1 H), 4.91-5.09 (m, 4 H), 3.59 (s, 2 H), 2.53 (t, J = 7.5 Hz, 2 H), 2.44 (t, J = 7.1 Hz, 2 H), 2.25 (dt, J = 6.3, 7.6 Hz, 2 H), 2.06 (dt, J = 6.8, 7.3 Hz, 2 H), 1.22-1.55 (m, 14 H);

^{13}C NMR (50 MHz, $CDCl_3$) δ: 140.05, 139.15, 137.11, 128.74, 128.03, 126.61, 115.19, 114.08, 58.50, 53.69, 53.26, 33.79, 31.52, 29.55, 29.51, 29.43, 29.11, 28.92, 27.36, 26.98;

LRMS (EI) _m/z_ (relative intensity): 313 (M^+, 1), 272 (75), 91 (100);

HRMS (EI) _m/z_ calculated for $C_{22}H_{35}N$: 313.2770, found: 313.2766;

Analysis calculated for $C_{22}H_{35}N$: C, 84.27; H, 11.26; N, 4.47. Found: C, 84.04; H, 11.20; N, 4.68.

10-Undecen-1-ol (112)[97]

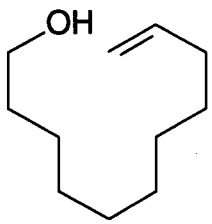

A solution of undecylenic acid (10.0 mL, 49.5 mmol) in THF (30 mL) was added dropwise to a solution of lithium aluminum hydride (2.82 g, 74.2 mmol) in THF (170 mL) at -78 °C and the reaction was stirred overnight with slow warming to room temperature. The reaction was cooled to 0 °C and water (100 mL) and 1 M HCl (50 mL) were sequentially added dropwise and the mixture was stirred for 1 hour. The organic layer was removed, and the aqueous layer was washed with diethyl ether (200 mL). The combined organic layers were dried over $MgSO_4$, filtered, and concentrated to afford **112** (8.38 g, 99%) as a pale yellow oil. This material was used in subsequent reactions without further purification. Column chromatography of a sample of **112** with 20% ethyl acetate in petroleum ether as eluant gave pure **112** for analysis.

R_f = 0.60 (petroleum ether-ethyl acetate 4:1);

IR (neat): 3334, 3076, 2928, 2854, 1641, 1464, 1057, 993, 908, 721 cm^{-1};

^1H NMR (200 MHz, $CDCl_3$) δ: 5.77 (ddt, J = 17.1, 10.2, 6.6 Hz, 1 H), 4.85-5.00 (m, 2 H), 3.85 (t, J = 6.6 Hz, 2 H), 1.98 (m, 3 H), 1.45-1.59 (m, 2 H), 1.20-1.40 (m, 12 H);

^{13}C NMR (50 MHz, $CDCl_3$) δ: 139.12, 114.04, 62.86, 33.73, 32.69, 29.49, 29.36, 29.05, 28.86, 25.68;

LRMS (EI) *m/z* (relative intensity): 170 (M^+, 1), 152 (18), 124 (60), 110 (64), 96 (87), 82 (85), 69 (34), 55 (39), 41 (16);

HRMS (EI) *m/z* calculated for $C_{11}H_{22}O$: 170.1671, found: 170.1672;

Analysis calculated for $C_{11}H_{22}O$: C, 77.58; H, 13.02. Found: C, 77.42; H, 12.99.

11-Iodo-1-undecene (113)

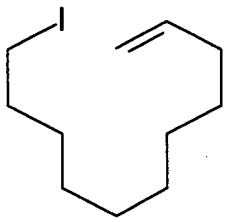

Crushed iodine (6.59 g, 25.96 mmol) was added in parts to a solution of 10-undecen-1-ol (**112**) (4.0 mL, 20.0 mmol), triphenylphosphine (6.81 g, 25.96 mmol), and imidazole (1.79 g, 26.0 mmol) in CH_2Cl_2 (80.0 mL) stirred at 0 °C and the reaction was stirred overnight with warming to room temperature. The reaction mixture was vacuum filtered through silica gel and washed with CH_2Cl_2 (100 mL). The filtrate was sequentially washed with saturated $Na_2S_2O_3$ solution and saturated $CuSO_4$ solution (100 mL each). The aqueous layers were separately washed with CH_2Cl_2 (200 mL each). The combined organic layers were dried over $MgSO_4$, filtered, and concentrated. Purification of the residue by vacuum liquid chromatography with petroleum ether as eluant afforded **113** (5.54 g, 99%) as a yellow oil.

R_f = 0.83 (petroleum ether-ethyl acetate 4:1);

IR (neat): 3076, 2925, 2853, 1639, 1462, 993, 908, 719 cm^{-1};

^1H NMR (200 MHz, $CDCl_3$) δ: 5.79 (ddt, J = 17.1, 10.3, 6.6 Hz, 1 H), 4.87-5.02 (m, 2 H), 3.16 (t, J = 7.1 Hz, 2 H), 2.02 (dt, J = 7.1, 6.8 Hz, 2 H), 1.72-1.87 (m, 2 H), 1.20-1.45 (m, 12 H);

^{13}C NMR (50 MHz, $CDCl_3$) δ: 139.14, 114.15, 33.79, 33.57, 30.50, 29.37, 29.07, 28.91, 28.53, 7.23;

LRMS (EI) *m/z* (relative intensity): 280 (M^+, 9), 238 (7), 155 (5), 127 (3), 111 (14), 97 (55), 83 (59), 69 (74), 55 (100), 41 (52);

HRMS (EI) *m/z* calculated for $C_{11}H_{21}I$: 280.0688, found: 280.0681;

Analysis calculated for $C_{11}H_{21}I$: C, 47.15; H, 7.55. Found: C, 47.22; H, 7.66.

3-Butenamide (115)

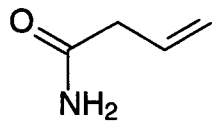

DMF (0.18 mL, 2.3 mmol) and a 2.0 M solution of oxalyl chloride in CH_2Cl_2 (12.9 mL, 26 mmol) were sequentially added to a solution of vinylacetic acid (2.0 mL, 24.0 mmol) in CH_2Cl_2 (118.0 mL) at 0 °C and the reaction was stirred for one hour with slow warming to room temperature. The reaction was cooled to 0 °C and NH_3 gas was bubbled into the solution with stirring for 20 minutes. The reaction was warmed to room temperature and diluted with ethyl acetate (75 mL) and sequentially washed with saturated $NaHCO_3$ solution, water, and brine (75 mL each). The combined aqueous layers were successively washed with ethyl acetate (3X) (120 mL each). The combined organic layers were dried over $MgSO_4$, filtered, and concentrated to afford **115** (0.93 g, 47%) as a white solid.

R_f = 0.06 (petroleum ether-ethyl acetate 4:1);

Melting point: 69.0-70.0 °C (diethyl ether/petroleum ether);

IR (CCl_4): 3358, 3192, 3082, 1693, 1641, 1406, 995, 914, 879 cm^{-1};

^1H NMR (200 MHz, $CDCl_3$) δ: 6.08 (bs, 1 H), 5.91 (ddt, J = 17.8, 9.3, 7.1 Hz, 1 H), 5.70 (bs, 1 H), 5.14-5.25 (m, 2 H), 2.99 (dt, J = 7.1, 1.2 Hz, 2 H);

^{13}C NMR (50 MHz, $CDCl_3$) δ: 173.66, 131.11, 119.61, 40.90;

LRMS (EI) *m/z* (relative intensity): 85 (M^+, 25), 84 (21), 44 (100), 42 (95), 41 (36), 39 (27);

HRMS (EI) *m/z* calculated for C_4H_7ON: 85.0528, found: 85.0524;

Analysis calculated for C_4H_7ON: C, 56.45; H, 8.29; N, 16.46. Found: C, 56.53; H, 8.21; N, 16.54.

10-Iodo-1-decene (116)

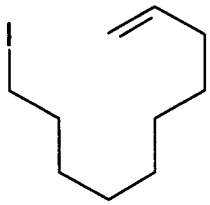

Crushed iodine (18.50 g, 72.89 mmol) was added in parts to a solution of 9-decen-1-ol (10.0 mL, 56.06 mmol), triphenylphosphine (19.11 g, 72.86 mmol), and imidazole (5.01 g, 72.8 mmol) in CH_2Cl_2 (224.0 mL) stirred at 0 °C and the reaction was stirred for 22 hours with warming to room temperature. The reaction mixture was vacuum filtered through silica gel and washed with CH_2Cl_2 (250 mL). The filtrate was sequentially washed with saturated $Na_2S_2O_3$ solution and saturated $CuSO_4$ solution (250 mL each). The aqueous layers were separately washed with CH_2Cl_2 (250 mL each). The combined organic layers were dried over $MgSO_4$, filtered, and concentrated. Purification of the residue by vacuum liquid chromatography with petroleum ether as eluant afforded **116** (14.90 g, quantitative) as a yellow oil.

R_f = 0.92 (petroleum ether-ethyl acetate 9:1);

IR (neat): 3076, 2926, 2854, 1639, 1462, 1194, 993, 910, 721 cm^{-1};

^1H NMR (200 MHz, $CDCl_3$) δ: 5.78 (ddt, J = 17.0, 10.2, 6.6 Hz, 1 H), 4.86-5.02 (m, 2 H), 3.15 (t, J = 7.1 Hz, 2 H), 2.01 (dt, J = 6.8, 7.1 Hz, 2 H), 1.72-1.86 (m, 2 H), 1.21-1.45 (m, 10 H);

^{13}C NMR (50 MHz, $CDCl_3$) δ: 139.00, 114.14, 33.71, 33.50, 30.44, 29.20, 28.95, 28.81, 28.43, 7.13;

LRMS (EI) *m/z* (relative intensity): 266 (M^+, 3), 224 (4), 155 (5), 127 (4), 97 (21), 83 (50), 69 (38), 55 (100), 41 (58);

HRMS (EI) *m/z* calculated for $C_{10}H_{19}I$: 266.0532, found: 266.0527;

Analysis calculated for $C_{10}H_{19}I$: C, 45.10; H, 7.20. Found: C, 44.98; H, 7.27.

10-Undecenenitrile (117)

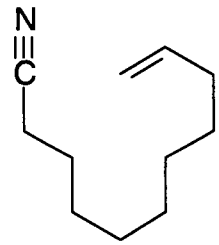

Recrystallized potassium cyanide (2.44 g, 37.5 mmol) was added to a solution of 10-iodo-1-decene (**116**) (6.66 g, 25.02 mmol) in CH_3CN (14.0 mL) and the reaction was stirred for 50 hours at 90 °C. The reaction was cooled to room temperature, diluted with CH_2Cl_2 (20 mL) and vacuum filtered through celite and concentrated. Purification of the residue by flash column chromatography with 5% diethyl ether in petroleum ether as eluant afforded **117** (3.87 g, 93%) as a colourless oil.

R_f = 0.89 (petroleum ether-ethyl acetate 4:1);

IR (neat): 3076, 2928, 2856, 2247, 1641, 1464, 1427, 995, 910, 723 cm^{-1};

^1H NMR (200 MHz, $CDCl_3$) δ: 5.78 (ddt, J = 17.1, 10.2, 6.6 Hz, 1 H), 4.87-5.01 (m, 2 H), 2.31 (t, J = 7.1 Hz, 2 H), 2.01 (q, J = 6.8 Hz, 2 H), 1.56-1.70 (m, 2 H), 1.20-1.50 (m, 10 H);

^{13}C NMR (50 MHz, $CDCl_3$) δ: 138.95, 119.75, 114.15, 33.65, 29.05, 28.85, 28.74, 28.62, 28.55, 25.28, 17.03;

LRMS (DCI(+), ammonia) *m/z* (relative intensity): 184 (M^++NH_4, 32), 183 (M^++NH_3, 100), 166 (M^++1, 20);

HRMS (CI(+), isobutane) *m/z* calculated for $C_{11}H_{20}N$ (M^++1): 166.1596, found: 166.1596;

Analysis calculated for $C_{11}H_{19}N$: C, 79.93; H, 11.59; N, 8.48. Found: C, 80.13; H, 11.68; N, 8.50.

10-Undecenylamine (118)

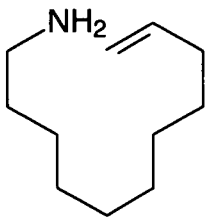

Lithium aluminum hydride (1.00 g, 26.4 mmol) was added to a solution of 10-undecenenitrile (**117**) (869.8 mg, 5.263 mmol) in THF (26 mL) at -78 °C and stirred for 6.5 hours at room temperature. The reaction was cooled to 0 °C and aqueous 1 M NaOH solution (3.7 mL) was added dropwise and stirred for 30 minutes. The slurry was vacuum filtered and sequentially washed with THF (3X), petroleum ether, and ethyl acetate (50 mL each). The solution was dried over $MgSO_4$, filtered, and concentrated to afford **118** (905.5 mg, 100% crude) as a colourless oil. This material was used in subsequent reactions without further purification.

R_f = 0.0 (petroleum ether-ethyl acetate 4:1);

IR (neat): 3346, 3300, 3076, 2926, 2854, 1641, 1464, 993, 908, 721 cm^{-1};

^1H NMR (200 MHz, $CDCl_3$) δ: 5.78 (ddt, J = 17.1, 10.2, 6.6 Hz, 1 H), 4.86-5.01 (m, 2 H), 2.64 (t, J = 6.7 Hz, 2 H), 2.01 (q, J = 6.9 Hz, 2 H), 1.15-1.46 (m, 16 H);

^{13}C NMR (50 MHz, C_6D_6) δ: 139.21, 114.48, 42.53, 34.19, 30.54, 30.02, 29.93, 29.87, 29.51, 29.33, 27.25;

LRMS (EI) *m/z* (relative intensity): 169 (M^+, 15), 168 (M^++1, 100), 95 (21), 71 (58), 70 (51), 69 (29), 67 (28), 58 (30), 56 (44), 55 (58), 44 (21), 41 (41);

HRMS (EI) *m/z* calculated for $C_{11}H_{23}N$: 169.1830, found: 169.1792.

Dimethyl (5-hexenyl)malonate or **7,7-dimethoxycarbonylhept-1-ene (119)**

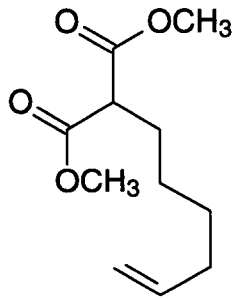

Sodium hydride (0.13 g, 5.4 mmol) was added in parts to a solution of 6-iodo-1-hexene (**97**) (1.00 g, 4.76 mmol) and dimethyl malonate (0.60 mL, 5.25 mmol) in THF (4.0 mL) and DMF (4.0 mL) stirred at 0 °C and the reaction was stirred for 20 hours at 60 °C. The reaction was cooled to room temperature and diluted with ethyl acetate (50 mL) and was sequentially washed with water, 1 M HCl, saturated $NaHCO_3$ solution, and brine (25 mL each). The aqueous layers were washed separately with ethyl acetate (50 mL each). The combined organic layers were dried over $MgSO_4$, filtered, and concentrated. Purification of the residue by flash column chromatography with 10% ethyl acetate in petroleum ether as eluant afforded **119** (866.8 mg, 85%) as a colourless oil.

R_f = 0.77 (petroleum ether-ethyl acetate 4:1);

IR (neat): 3078, 2955, 2930, 2860, 1738, 1641, 1435, 1344, 1153, 1063, 997, 912 cm^{-1};

^1H NMR (200 MHz, $CDCl_3$) δ: 5.74 (ddt, J = 16.8, 10.3, 6.7 Hz, 1 H), 4.86-5.00 (m, 2 H), 3.69 (s, 6 H), 3.32 (t, J = 7.6 Hz, 1 H), 2.01 (q, J = 6.8 Hz, 2 H), 1.87 (q, J = 7.6 Hz, 2 H), 1.19-1.46 (m, 4 H);

^{13}C NMR (50 MHz, $CDCl_3$) δ: 169.83, 138.43, 114.54, 52.36, 51.59, 33.30, 28.62, 28.35, 26.69;

LRMS (DCI(+), ammonia) *m/z* (relative intensity): 215 (M^++1, 100), 122 (10);

HRMS (CI(+), isobutane) *m/z* calculated for $C_{11}H_{19}O_4$ (M^++1): 215.1283, found: 215.1283;

Analysis calculated for $C_{11}H_{18}O_4$: C, 61.65; H, 8.47. Found: C, 61.60; H, 8.58.

Dimethyl (9-decenyl)malonate (123)

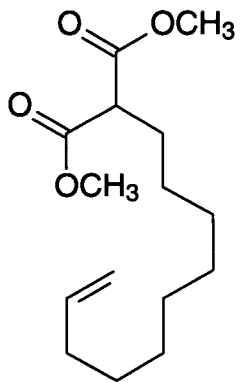

Washed and dried sodium hydride (0.51 g, 21.1 mmol) was added in parts to a solution of 10-iodo-1-decene (**116**) (5.10 g, 19.16 mmol) and dimethyl malonate (2.4 mL, 20.9 mmol) in THF (16.0 mL) and DMF (16.0 mL) stirred at 0 °C and the reaction was stirred for 22 hours at 60 °C. The reaction was cooled to room temperature and diluted with ethyl acetate (200 mL) and was sequentially washed with water, 1 M HCl, saturated $NaHCO_3$ solution, and brine (100 mL each). The aqueous layers were washed separately with ethyl acetate (200 mL). The combined organic layers were dried over $MgSO_4$, filtered, and concentrated. Purification of the residue by flash column chromatography with 5% ethyl acetate in petroleum ether as eluant afforded **123** (4.80 g, 93%) as a colourless oil.

R_f = 0.81 (petroleum ether-ethyl acetate 4:1);

IR (neat): 3076, 2930, 2854, 1738, 1641, 1435, 1153, 997, 910, 723 cm^{-1};

^1H NMR (200 MHz, $CDCl_3$) δ: 5.77 (ddt, J = 17.0, 10.3, 6.6 Hz, 1 H), 4.85-4.99 (m, 2 H), 3.69 (s, 6 H), 3.31 (t, J = 7.6 Hz, 1 H), 1.98 (q, J = 6.8 Hz, 2 H), 1.84 (q, J = 7.3 Hz, 2 H), 1.15-1.35 (m, 12 H);

^{13}C NMR (50 MHz, $CDCl_3$) δ: 169.88, 139.07, 114.06, 52.33, 51.64, 33.70, 29.25, 29.15, 29.08, 28.97, 28.81, 28.77, 27.25;

LRMS (EI) *m/z* (relative intensity): 270 (M^+, 2), 238 (18), 206 (17), 161 (22), 145 (83), 133 (20), 132 (100), 100 (28), 95 (25), 81 (28), 68 (20), 67 (30), 55 (49), 41 (48);

HRMS (EI) *m/z* calculated for $C_{15}H_{26}O_4$: 270.1831, found: 270.1829;

Analysis calculated for $C_{15}H_{26}O_4$: C, 66.62; H, 9.70. Found: C, 66.75; H, 9.85.

11-Dodecenoic acid (124)[100]

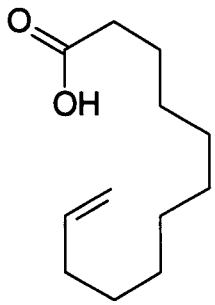

Potassium hydroxide (0.90 g, 16.0 mmol) was added to a solution of dimethyl (10-decenyl)malonate (**123**) (1.5550 g, 5.752 mmol) in water (1.3 mL) and the reaction was stirred for two hours at 90 °C. The reaction was cooled to room temperature and concentrated HCl (1.3 mL) was added in parts. The mixture was washed with diethyl ether (3X) (100 mL each). The combined organic layers were dried over $MgSO_4$, filtered, and concentrated. The crude product was stirred for 18 hours at 140 °C. The crude product was cooled to room temperature and diluted with water (50 mL) and successively extracted with portions of diethyl ether (3X) (100 mL each). The combined organic layers were dried over $MgSO_4$, filtered, and concentrated. Purification of the residue by flash column chromatography with 50% ethyl acetate in petroleum ether as eluant afforded **124** (1.0586 g, 93%) as a pale yellow oil.

R_f = 0.74 (petroleum ether-ethyl acetate 4:1);

IR (neat): 3076, 2928, 2854, 2679, 1711, 1641, 1464, 1414, 1286, 993, 910, 723 cm^{-1};

^1H NMR (200 MHz, $CDCl_3$) δ: 10.71 (bs, 1 H), 5.79 (ddt, J = 17.1, 10.3, 6.6 Hz, 1 H), 4.86-5.02 (m, 2 H), 2.32 (t, J = 7.4 Hz, 2 H), 2.01 (q, J = 6.8 Hz, 2 H), 1.61 (quint, J = 7.3 Hz, 2 H), 1.19-1.42 (m, 12 H);

^{13}C NMR (50 MHz, $CDCl_3$) δ: 175.22, 133.93, 108.87, 28.86, 28.54, 24.15, 24.11, 23.96, 23.84, 23.96, 23.84, 23.79, 23.66, 19.41;

LRMS (EI) *m/z* (relative intensity): 198 (M^+, 4), 180 (53), 151 (21), 139 (23), 138 (100), 137 (35), 136 (36), 124 (26), 123 (33), 114 (44), 111 (25), 110 (46), 101 (20), 98 (36), 97 (58), 96 (65), 95 (21), 84 (28), 83 (35), 69 (28), 55 (28);

HRMS (EI) *m/z* calculated for $C_{12}H_{22}O_2$: 198.1620, found: 198.1624;

Analysis calculated for $C_{12}H_{22}O_2$: C, 72.67; H, 11.19. Found: C, 72.93; H, 11.31.

9-Decenoic acid (125)[102]

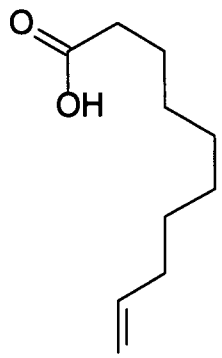

A solution of Jones' reagent (ca. 32.0 mL) was added to a solution of 9-decen-1-ol (6.0 mL, 33.6 mmol) in acetone (336 mL) and stirred at room temperature until an orange colour persisted. The reaction was filtered through celite and back titrated with 2-propanol (ca. 6.0 mL) until a blue colour persisted. This mixture was filtered through celite and concentrated. Purification of the residue by flash column chromatography with 20% diethyl ether in petroleum ether as eluant afforded **125** (5.58 g, 97%) as a pale yellow oil. Spectral data for **125** are identical to those reported.[102]

R_f = 0.52 (petroleum ether-ethyl acetate 4:1);

IR (neat): 3078, 2928, 2856, 2671, 1711, 1641, 1464, 1414, 1284, 993, 910, 725 cm^{-1};

^1H NMR (200 MHz, $CDCl_3$) δ: 11.60 (bs, 1 H), 5.78 (ddt, J = 17.0, 10.1, 6.6 Hz, 1 H), 4.86-5.02 (m, 2 H), 2.32 (t, J = 7.4 Hz, 2 H), 2.01 (q, J = 6.8 Hz, 2 H), 1.61 (quint, J = 7.3 Hz, 2 H), 1.21-1.42 (m, 8 H);

^{13}C NMR (50 MHz, $CDCl_3$) δ: 180.59, 139.01, 114.18, 34.10, 33.71, 29.03, 28.95, 28.85, 28.80, 24.60;

LRMS (EI) *m/z* (relative intensity): 170 (M^+, 1), 110 (21), 84 (34), 83 (22), 82 (28), 73 (28), 69 (89), 68 (57), 67 (22), 60 (33), 56 (22), 55 (100), 41 (79), 39 (26);

HRMS (EI) *m/z* calculated for $C_{10}H_{18}O_2$: 170.1307, found: 170.1303;

Analysis calculated for $C_{10}H_{18}O_2$: C, 70.55; H, 10.66. Found: C, 70.72; H, 10.81.

9-Decenamide (126)

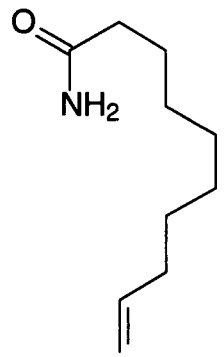

DMF (60 μL, 0.77 mmol) and a 2.0 M solution of oxalyl chloride in CH_2Cl_2 (4.3 mL, 8.6 mmol) were sequentially added to a solution of 9-decenoic acid (**125**) (1.32 g, 7.75 mmol) in CH_2Cl_2 (39.0 mL) at 0 °C and the reaction was stirred for 1.5 hours with slow warming to room temperature. The reaction was cooled to 0 °C and NH_3 gas was bubbled into the solution with stirring for 20 minutes. The reaction was warmed to room temperature and diluted with ethyl acetate (20 mL) and sequentially washed with saturated $NaHCO_3$ solution, water, and brine (20 mL each). The combined aqueous layers were successively washed with ethyl acetate (3X) (30 mL each). The combined organic layers were dried over $MgSO_4$, filtered, and concentrated to afford **126** (1.25 g, 95%) as a white solid.

R_f = 0.17 (petroleum ether-ethyl acetate 4:1);

Melting point: 79.0-80.0 °C (diethyl ether/petroleum ether);

IR (CCl_4): 3358, 3186, 3076, 2928, 2854, 1690, 1468, 1410, 912 cm^{-1};

^1H NMR (200 MHz, $CDCl_3$) δ: 5.77 (ddt, J = 17.0, 10.1, 6.6 Hz, 1 H), 5.71 (bs, 1 H), 5.46 (bs, 1 H), 4.86-5.01 (m, 2 H), 2.19 (t, J = 7.5 Hz, 2 H), 2.01 (q, J = 6.9 Hz, 2 H), 1.53-1.67 (m, 2 H), 1.22-1.38 (m, 8 H);

^{13}C NMR (50 MHz, $CDCl_3$) δ: 175.70, 139.06, 114.17, 35.90, 33.70, 29.12, 28.88, 28.80, 25.46;

LRMS (EI) *m/z* (relative intensity): 169 (M^+, 1), 72 (43), 59 (100);

HRMS (EI) *m/z* calculated for $C_{10}H_{19}ON$: 169.1467, found: 169.1465;

Analysis calculated for $C_{10}H_{19}ON$: C, 70.96; H, 11.31; N, 8.27. Found: C, 70.95; H, 11.38; N, 8.19.

8-Nonenenitrile (128)

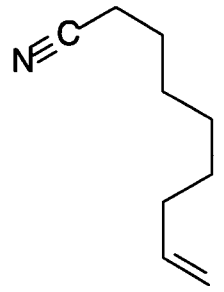

Recrystallized potassium cyanide (1.48 g, 22.7 mmol) and recrystallized 18-crown-6 (0.24 g, 0.91 mmol) were sequentially added to a solution of 8-bromo-1-octene (1.9 mL, 11.3 mmol) in CH_3CN (6.3 mL) and the reaction was stirred for 22 hours at 90 °C. The reaction was cooled to room temperature, diluted with CH_2Cl_2 (10 mL) and vacuum filtered through celite and concentrated. Purification of the residue by flash column chromatography with 7% diethyl ether in petroleum ether as eluant afforded **128** (1.55 g, quantitative) as a colourless oil.

R_f = 0.61 (petroleum ether-ethyl acetate 4:1);

IR (neat): 3078, 2932, 2858, 2245, 1641, 1464, 995, 912, 727 cm^{-1};

^1H NMR (200 MHz, $CDCl_3$) δ: 5.76 (ddt, J = 17.1, 10.2, 6.6 Hz, 1 H), 4.87-5.02 (m, 2 H), 2.30 (t, J = 7.1 Hz, 2 H), 2.02 (q, J = 6.8 Hz, 2 H), 1.55-1.69 (m, 2 H), 1.24-1.49 (m, 6 H);

^{13}C NMR (50 MHz, $CDCl_3$) δ: 138.59, 119.71, 114.43, 33.46, 28.41, 28.39, 28.08, 25.22, 17.01;

LRMS (DCI(+), ammonia) *m/z* (relative intensity): 138 (M^++1, 40), 122 (100), 109 (30), 108 (84), 96 (28), 94 (39);

HRMS (DCI(+), methane) *m/z* calculated for $C_9H_{16}N$ (M^++1): 138.1283, found: 138.1282;

Analysis calculated for $C_9H_{15}N$: C, 78.78; H, 11.02; N, 10.21. Found: C, 78.73; H, 10.97; N, 10.36.

8-Nonenoic acid (129)

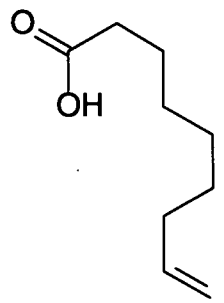

Ground KOH (4.62 g, 82.3 mmol) was added to a solution of 8-nonenenitrile (**128**) (2.82 g, 20.55 mmol) in ethylene glycol (28.0 mL) and the reaction was stirred for 3 hours at 170 °C and for 15 hours at 65 °C. The reaction was cooled to room temperature and diluted with water (60 mL) and washed with diethyl ether (3X) (60 mL each). The aqueous solution was acidified with concentrated HCl and the crude product was successively extracted with portions of diethyl ether (4X) (100 mL each). The combined organic layers were dried over $MgSO_4$, filtered, and concentrated. Purification of the residue by flash column chromatography with 30% diethyl ether in petroleum ether as eluant afforded **129** (3.08 g, 96%) as a pale yellow oil.

R_f = 0.31 (petroleum ether-ethyl acetate 4:1);

IR (neat): 3076, 2928, 2856, 2671, 1709, 1641, 1458, 1414, 1288, 995, 910, 727 cm^{-1};

^1H NMR (200 MHz, $CDCl_3$) δ: 11.78 (bs, 1 H), 5.77 (ddt, J = 16.8, 10.3, 6.6 Hz, 1 H), 4.88-5.01 (m, 2 H), 2.32 (t, J = 7.3 Hz, 2 H), 2.02 (q, J = 6.7 Hz, 2 H), 1.61 (quint, J = 7.1 Hz, 2 H), 1.26-1.44 (m, 6 H);

^{13}C NMR (50 MHz, $CDCl_3$) δ: 180.59, 138.83, 114.24, 34.05, 33.62, 28.81, 28.62, 28.61, 24.54;

LRMS (EI) *m/z* (relative intensity): 156 (M^+, 1), 138 (33), 96 (37), 81 (20), 73 (28), 69 (60), 68 (45), 60 (41), 55 (100), 41 (63), 39 (23);

HRMS (EI) *m/z* calculated for $C_9H_{16}O_2$: 156.1150, found: 156.1147;

Analysis calculated for $C_9H_{16}O_2$: C, 69.19; H, 10.32. Found: C, 69.38; H, 10.43.

8-Nonenamide (130)

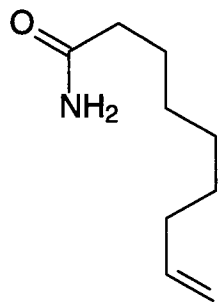

DMF (0.10 mL, 1.3 mmol) and a 2.0 M solution of oxalyl chloride in CH_2Cl_2 (7.4 mL, 14.8 mmol) were sequentially added to a solution of 8-nonenoic acid (**129**) (2.10 g, 13.44 mmol) in CH_2Cl_2 (67.0 mL) at 0 °C and the reaction was stirred for one hour with slow warming to room temperature. The reaction was cooled to 0 °C and NH_3 gas was bubbled into the solution with stirring for 20 minutes. The reaction was warmed to room temperature and diluted with ethyl acetate (40 mL) and sequentially washed with saturated $NaHCO_3$ solution, water, and brine (40 mL each). The combined aqueous layers were successively washed with ethyl acetate (3X) (50 mL each). The combined organic layers were dried over $MgSO_4$, filtered, and concentrated to afford **130** (2.08 g, quantitative) as a white solid.

R_f = 0.16 (petroleum ether-ethyl acetate 4:1);

Melting point: 88.0-88.5 °C (diethyl ether/petroleum ether);

IR (CCl_4): 3358, 3178, 3080, 2927, 2856, 1688, 1466, 1412, 993, 912 cm^{-1};

^1H NMR (200 MHz, $CDCl_3$) δ: 5.86 (bs, 1 H), 5.76 (ddt, J = 17.0, 10.1, 6.6 Hz, 1 H), 5.52 (bs, 1 H), 4.86-5.01 (m, 2 H), 2.18 (t, J = 7.5 Hz, 2 H), 2.00 (q, J = 6.8 Hz, 2 H), 1.52-1.67 (m, 2 H), 1.23-1.42 (m, 6 H);

^{13}C NMR (50 MHz, $CDCl_3$) δ: 175.80, 138.93, 114.24, 35.88, 33.63, 29.00, 28.72, 28.65, 25.42;

LRMS (EI) *m/z* (relative intensity): 155 (M^+, 1), 72 (46), 59 (100), 44 (23), 41 (25);

HRMS (EI) *m/z* calculated for $C_9H_{17}ON$: 155.1310, found: 155.1309;

Analysis calculated for $C_9H_{17}ON$: C, 69.63; H, 11.04; N, 9.02. Found: C, 69.66; H, 10.98; N, 9.12.

6-Heptenoic acid (131)

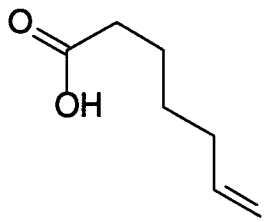

Ground KOH (2.41 g, 43.0 mmol) was added to a solution of 6-heptenenitrile (**96**) (1.17 g, 10.72 mmol) in ethylene glycol (15.0 mL) and the reaction was stirred for 5 hours at 150 °C and for 20 hours at 45 °C. The reaction was cooled to room temperature and diluted with water (30 mL) and washed with diethyl ether (3X) (30 mL each). The aqueous solution was acidified with concentrated HCl and the crude product was successively extracted with portions of diethyl ether (4X) (50 mL each). The combined organic layers were dried over $MgSO_4$, filtered, and concentrated. Purification of the residue by flash column chromatography with 30% diethyl ether in petroleum ether as eluant afforded **131** (1.28 g, 93%) as a pale yellow oil.

R_f = 0.36 (petroleum ether-ethyl acetate 4:1);

IR (neat): 3078, 2934, 2862, 2677, 1711, 1641, 1414, 1288, 993, 912 cm^{-1};

^1H NMR (200 MHz, $CDCl_3$) δ: 11.22 (bs, 1 H), 5.77 (ddt, J = 17.1, 10.3, 6.6 Hz, 1 H), 4.90-5.05 (m, 2 H), 2.34 (t, J = 7.3 Hz, 2 H), 2.05 (q, J = 7.1 Hz, 2 H), 1.56-1.71 (m, 2 H), 1.34-1.49 (m, 2 H);

^{13}C NMR (50 MHz, $CDCl_3$) δ: 180.34, 138.26, 114.76, 33.90, 33.29, 28.19, 24.06;

LRMS (EI) *m/z* (relative intensity): 128 (M^+, 34), 111 (21), 110 (100), 82 (25), 69 (23), 68 (30);

HRMS (EI) *m/z* calculated for $C_7H_{12}O_2$: 128.0837, found: 128.0839;

Analysis calculated for $C_7H_{12}O_2$: C, 65.60; H, 9.44. Found: C, 65.52; H, 9.53.

6-Heptenamide (132)

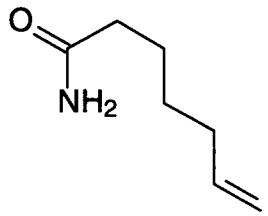

DMF (80 μL, 1.03 mmol) and oxalyl chloride (0.94 mL, 10.8 mmol) were sequentially added to a solution of 6-heptenoic acid (**131**) (1.26 g, 9.83 mmol) in CH_2Cl_2 (49.0 mL) at 0 °C and the reaction was stirred for one hour with slow warming to room temperature. The reaction was cooled to 0 °C and NH_3 gas was bubbled into the solution with stirring for 20 minutes. The reaction was warmed to room temperature and diluted with ethyl acetate (35 mL) and sequentially washed with saturated $NaHCO_3$ solution, water, and brine (35 mL each). The combined aqueous layers were successively washed with ethyl acetate (3X) (50 mL each). The combined organic layers were dried over $MgSO_4$, filtered, and concentrated to afford **132** (1.08 g, 86%) as a white solid.

R_f = 0.15 (petroleum ether-ethyl acetate 4:1);

Melting point: 84.0-85.0 °C (ethyl acetate);

IR (CCl_4): 3362, 3186, 3080, 2937, 2862, 1688, 1639, 1460, 1412, 914 cm^{-1};

^1H NMR (200 MHz, $CDCl_3$) δ: 6.14 (bs, 1 H), 5.75 (ddt, J = 17.0, 10.2, 6.6 Hz, 1 H), 5.69 (bs, 1 H), 4.88-5.00 (m, 2 H), 2.18 (t, J = 7.4 Hz, 2 H), 2.02 (q, J = 7.1 Hz, 2 H), 1.53-1.67 (m, 2 H), 1.32-1.46 (m, 2 H);

^{13}C NMR (50 MHz, $CDCl_3$) δ: 175.88, 138.32, 114.64, 35.69, 33.33, 28.33, 24.88;

LRMS (EI) *m/z* (relative intensity): 127 (M^+, 5), 72 (24), 59 (100), 44 (32), 41 (24);

HRMS (EI) *m/z* calculated for $C_7H_{13}ON$: 127.0997, found: 127.0995;

Analysis calculated for $C_7H_{13}ON$: C, 66.11; H, 10.30; N, 11.01. Found: C, 65.95; H, 10.41; N, 11.05.

7-Octenylamine (133)

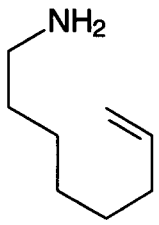

Lithium aluminum hydride (1.21 g, 31.9 mmol) was added to a solution of 7-octenenitrile (**95**) (1.96 g, 15.91 mmol) in THF (64 mL) at 0 °C and the reaction was stirred for 3.5 hours at room temperature. The reaction was cooled to 0 °C and a solution of THF (6.1 mL) and water (1.2 mL) was added and stirred for 15 minutes. Aqueous 3 M NaOH solution was added dropwise until a white precipitate formed and the solution was stirred for 15 minutes. The slurry was vacuum filtered and concentrated. Kugelrohr distillation of the residue at 60 °C at 8 mm Hg afforded **133** (1.72 g, 85%) as a colourless oil.

R_f = 0.0 (petroleum ether-ethyl acetate 4:1);
Boiling point: 60 °C at 8 mm Hg;
IR (neat): 3364, 3076, 2928, 2854, 1641, 1574, 1466, 993, 908, 820, 725 cm^{-1};
^1H NMR (200 MHz, $CDCl_3$) δ: 5.71 (ddt, J = 17.1, 10.0, 6.8 Hz, 1 H), 4.79-4.95 (m, 2 H), 2.58 (t, J = 6.8 Hz, 2 H), 1.95 (q, J = 6.8 Hz, 2 H), 1.16-1.41 (m, 10 H);
^{13}C NMR (50 MHz, $CDCl_3$) δ: 138.86, 114.02, 42.03, 33.59, 33.55, 28.78, 28.70, 26.55;
LRMS (DCI(+), ammonia) *m/z* (relative intensity): 128 (M^++1, 100), 127 (M^+, 5);
HRMS (CI(+), isobutane) *m/z* calculated for $C_8H_{18}N$ (M^++1): 128.1439, found: 128.1440.

8-Nonenylamine (134)

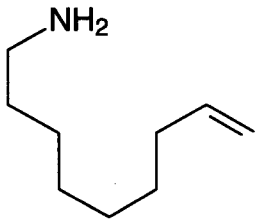

(a) Reduction of 8-Nonenenitrile (**128**)

Lithium aluminum hydride (1.73 g, 45.6 mmol) was added to a solution of 8-nonenenitrile (**128**) (2.99 g, 21.79 mmol) in THF (91 mL) at 0 °C and the reaction was

stirred for 4 hours at 70 °C. The reaction was cooled to 0 °C and a solution of THF (8.6 mL) and water (1.8 mL) was added and stirred for 15 minutes. Aqueous 3 M NaOH solution was added dropwise until a white precipitate formed and the solution was stirred for 15 minutes. The slurry was vacuum filtered and concentrated. Kugelrohr distillation of the residue at 100 °C at 10 mm Hg afforded **134** (2.70 g, 84%) as a colourless oil.

R_f = 0.0 (petroleum ether-ethyl acetate 4:1);

Boiling point: 100 °C at 10 mm Hg;

IR (neat): 3369, 3296, 3076, 2926, 2854, 1639, 1591, 1464, 1070, 993, 910, 815, 723 cm^{-1};

^1H NMR (200 MHz, $CDCl_3$) δ: 5.75 (ddt, J = 17.0, 10.1, 6.6 Hz, 1 H), 4.83-4.99 (m, 2 H), 2.62 (t, J = 6.7 Hz, 2 H), 1.98 (q, J = 6.9 Hz, 2 H), 1.17-1.44 (m, 12 H);

^{13}C NMR (50 MHz, $CDCl_3$) δ: 139.05, 114.06, 42.19, 33.79, 33.69, 29.25, 29.01, 28.79, 26.76;

LRMS (EI) *m/z* (relative intensity): 141 (M^+, 4), 100 (100), 96 (29), 95 (21), 86 (34), 83 (59), 82 (51), 81 (32), 67 (22), 56 (27), 55 (25), 45 (23), 44 (24), 41 (23), 30 (96);

HRMS (EI) *m/z* calculated for $C_9H_{19}N$: 114.1518, found: 114.1513;

Analysis calculated for $C_9H_{19}N$: C, 76.53; H, 13.56; N, 9.92. Found: C, 76.59; H, 13.51; N, 9.71.

(b) Reduction of 8-Nonenamide (**130**)

Lithium aluminum hydride (0.74 g, 19.5 mmol) was added to a solution of 8-nonenamide (**130**) (1.52 g, 9.79 mmol) in THF (39.0 mL) at 0 °C and the reaction was stirred for 4 hours at 70 °C. The reaction was cooled to 0 °C and a solution of THF (3.8 mL) and water (0.8 mL) was added and stirred for 15 minutes. Aqueous 3 M NaOH solution was added dropwise until a white precipitate formed and the solution was stirred for 15 minutes. The slurry was vacuum filtered and concentrated. Kugelrohr distillation of the residue at 110 °C at 10 mm Hg afforded **134** (0.94 g, 68%) with spectral data in agreement with that reported above.

5-Hexenoic acid (135)[100]

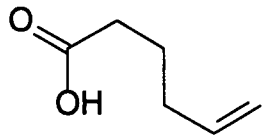

A solution of Jones' reagent (ca. 24.0 mL) was added to a solution of 5-hexen-1-ol (3.0 mL, 25.0 mmol) in acetone (250 mL) and stirred at room temperature until an orange colour persisted. The reaction was filtered through celite and back titrated with 2-propanol (ca. 4.0 mL) until a blue colour persisted. This mixture was filtered through celite and concentrated. Purification of the residue by flash column chromatography with 20% diethyl ether in petroleum ether as eluant afforded **135** (2.80 g, 98%) as a pale yellow oil.

R_f = 0.29 (petroleum ether-ethyl acetate 4:1);

IR (neat): 3078, 2935, 2669, 1709, 1641, 1414, 1244, 993, 914 cm^{-1};

^1H NMR (200 MHz, $CDCl_3$) δ: 10.94 (bs, 1 H), 5.76 (ddt, J = 17.1, 10.2, 6.6 Hz, 1 H), 4.94-5.07 (m, 2 H), 2.35 (t, J = 7.4 Hz, 2 H), 2.10 (q, J = 6.6 Hz, 2 H), 1.72 (quint, J = 7.1 Hz, 2 H);

^{13}C NMR (50 MHz, $CDCl_3$) δ: 180.17, 137.44, 115.52, 33.26, 32.88, 23.69;

LRMS (EI) *m/z* (relative intensity): 114 (M^+, 8), 73 (22), 68 (41), 60 (100), 55 (82), 54 (21), 41 (53), 39 (38);

HRMS (EI) *m/z* calculated for $C_6H_{10}O_2$: 114.0681, found: 114.0683.

4-Pentenamide (137)

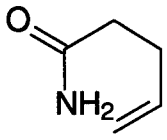

DMF (0.15 mL, 1.9 mmol) and a 2.0 M solution of oxalyl chloride in CH_2Cl_2 (10.8 mL, 22 mmol) were sequentially added to a solution of 4-pentenoic acid (2.0 mL, 19.6 mmol) in CH_2Cl_2 (98.0 mL) at 0 °C and the reaction was stirred for one hour with slow warming to room temperature. The reaction was cooled to 0 °C and NH_3 gas was bubbled into the solution with stirring for 20 minutes. The reaction was warmed to room temperature and diluted with ethyl acetate (70 mL) and sequentially washed with saturated $NaHCO_3$ solution, water, and brine (70 mL each). The combined aqueous layers were

successively washed with ethyl acetate (2X) (100 mL each). The combined organic layers were dried over $MgSO_4$, filtered, and concentrated to afford **137** (1.56 g, 80%) as a white solid.

R_f = 0.14 (petroleum ether-ethyl acetate 4:1);

Melting point: 102.0-102.5 °C (diethyl ether/petroleum ether);

IR (CCl_4): 3358, 3186, 3082, 1690, 1634, 1418, 997, 910 cm^{-1};

^1H NMR (200 MHz, $CDCl_3$) δ: 5.83 (bs, 1 H), 5.81 (ddt, J = 17.1, 10.3, 6.2 Hz, 1 H), 5.57 (bs, 1 H), 4.96-5.11 (m, 2 H), 2.24-2.43 (m, 4 H);

^{13}C NMR (50 MHz, $CDCl_3$) δ: 175.16, 136.82, 115.57, 34.97, 29.25;

LRMS (EI) *m/z* (relative intensity): 99 (M^+, 3), 56 (100), 55 (29), 44 (45), 41 (29);

HRMS (EI) *m/z* calculated for C_5H_9ON: 99.0684, found: 99.0684;

Analysis calculated for C_5H_9ON: C, 60.58; H, 9.15; N, 14.13. Found: C, 60.67; H, 9.20; N, 13.98.

9-Decenylamine (138)

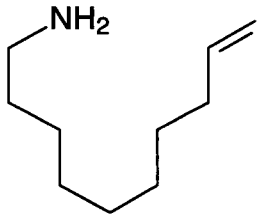

(a) Reduction of 9-Decenamide (**126**)

Lithium aluminum hydride (0.56 g, 14.8 mmol) was added to a solution of 9-decenamide (**126**) (1.24 g, 7.33 mmol) in THF (29 mL) at 0 °C and the reaction was stirred for 4 hours at 70 °C. The reaction was cooled to 0 °C and a solution of THF (2.8 mL) and water (0.6 mL) was added and stirred for 15 minutes. Aqueous 3 M NaOH solution was added dropwise until a white precipitate formed and the solution was stirred for 15 minutes. The slurry was vacuum filtered and concentrated. Kugelrohr distillation of the residue at 130 °C at 10 mm Hg afforded **138** (1.00 g, 88%) as a colourless oil.

R_f = 0.0 (petroleum ether-ethyl acetate 4:1);

Boiling point: 130 °C at 10 mm Hg;

IR (neat): 3373, 3294, 3076, 2926, 2854, 1641, 1464, 993, 908, 723 cm^{-1};

^{1}H NMR (200 MHz, $CDCl_3$) δ: 5.76 (ddt, J = 17.0, 10.3, 6.6 Hz, 1 H), 4.84-5.00 (m, 2 H), 2.63 (t, J = 6.5 Hz, 2 H), 1.99 (q, J = 6.8 Hz, 2 H), 1.19-1.42 (m, 14 H);

^{13}C NMR (50 MHz, $CDCl_3$) δ: 139.11, 114.05, 42.19, 33.72, 29.39, 29.01, 28.85, 26.81;

LRMS (EI) *m/z* (relative intensity): 155 (M^+, 29), 114 (44), 100 (27), 97 (32), 96 (31), 95 (22), 86 (39), 82 (28), 81 (30), 72 (28), 69 (23), 67 (39), 56 (72), 55 (85), 54 (23), 45 (50), 44 (40), 43 (25), 42 (20), 41 (100);

HRMS (EI) *m/z* calculated for $C_{10}H_{21}N$: 155.1674, found: 155.1679;

Analysis calculated for $C_{10}H_{21}N$: C, 77.35; H, 13.63; N, 9.02. Found: C, 76.96; H, 13.79; N, 9.01.

(b) Reduction of 9-Decenenitrile (**160**)

Lithium aluminum hydride (0.89 g, 23.4 mmol) was added to a solution of 9-decenenitrile (**160**) (1.77 g, 11.70 mmol) in THF (47.0 mL) at 0 °C and the reaction was stirred for 5 hours at 70 °C. The reaction was cooled to 0 °C and a solution of THF (4.4 mL) and water (0.9 mL) was added and stirred for 15 minutes. Aqueous 3 M NaOH solution was added dropwise until a white precipitate formed and the solution was stirred for 15 minutes. The slurry was vacuum filtered and concentrated. Kugelrohr distillation of the residue at 150 °C at 10 mm Hg afforded **138** (1.50 g, 82%) with spectral data in agreement with that reported above.

***N*-*tert*-Butoxycarbonyl-*N*-(2-propenyl)-11-dodecenamide (139)**

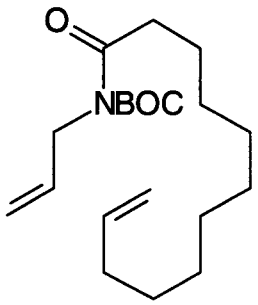

4-Dimethylaminopyridine (0.69 g, 5.65 mmol) and di-*tert*-butyl dicarbonate (0.92 g, 4.22 mmol) were sequentially added to a solution of *N*-(2-propenyl)-11-dodecenamide (**68**) (0.67 g, 2.82 mmol) in THF (17.6 mL) and the reaction was stirred for 21 hours. The reaction was diluted with diethyl ether (50 mL) and sequentially washed with saturated $NaHCO_3$ solution and brine (50 mL each). The aqueous layers were separately washed with diethyl ether (120 mL). The combined organic extracts were dried over $MgSO_4$,

filtered, and concentrated. Purification of the residue by flash column chromatography with 3% diethyl ether in petroleum ether as eluant afforded **139** (0.87 g, 92%) as a colourless oil.

R_f = 0.72 (petroleum ether-ethyl acetate 4:1);

IR (neat): 3074, 2978, 2928, 2854, 1734, 1699, 1641, 1456, 1435, 1369, 1146, 991, 910 cm^{-1};

^1H NMR (200 MHz, $CDCl_3$) δ: 5.77 (ddt, J = 17.1, 10.2, 6.6 Hz, 1 H), 5.76 (ddt, J = 17.1, 10.2, 5.4 Hz, 1 H), 5.03-5.14 (m, 2 H), 4.85-5.00 (m, 2 H), 4.24 (dt, J = 5.6, 1.5 Hz, 2 H), 2.82 (t, J = 7.5 Hz, 2 H), 2.00 (dt, J = 7.1, 5.6 Hz, 2 H), 1.52-1.69 (m, 2 H), 1.47 (s, 9 H), 1.20-1.37 (m, 12 H);

^{13}C NMR (50 MHz, $CDCl_3$) δ: 175.78, 152.99, 139.16, 133.56, 116.25, 114.04, 82.74, 46.37, 38.23, 33.75, 29.37, 29.19, 29.07, 28.88, 27.94, 25.10;

LRMS (DCI(+), ammonia) *m/z* (relative intensity): 338 (M^++1, 26), 282 (100), 238 (100), 237 (20), 99 (21), 57 (22);

HRMS (DCI(+), methane/ammonia) *m/z* calculated for $C_{20}H_{36}O_3N$ (M^++1): 338.2695, found: 338.2696;

Analysis calculated for $C_{20}H_{35}O_3N$: C, 71.18; H, 10.45; N, 4.15. Found: C, 71.47; H, 10.25; N, 4.04.

_N_-(3-Butenyl)-_N_-*tert*-butoxycarbonyl-10-undecenamide (140)

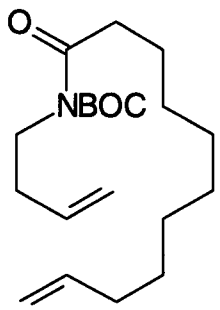

4-Dimethylaminopyridine (0.32 g, 2.62 mmol) and di-*tert*-butyl dicarbonate (0.43 g, 1.97 mmol) were sequentially added to a solution of *N*-(3-butenyl)-10-undecenamide (**69**) (0.31 g, 1.31 mmol) in THF (8.2 mL) and the reaction was stirred for 27 hours. The reaction was diluted with diethyl ether (20 mL) and sequentially washed with saturated $NaHCO_3$ solution and brine (20 mL each). The aqueous layers were separately washed with diethyl ether (50 mL). The combined organic extracts were dried over $MgSO_4$,

filtered, and concentrated. Purification of the residue by flash column chromatography with 3% diethyl ether in petroleum ether as eluant afforded **140** (0.26 g, 59%) as a colourless oil.

R_f = 0.75 (petroleum ether-ethyl acetate 4:1);

IR (neat): 3078, 2978, 2928, 2854, 1734, 1697, 1641, 1450, 1369, 1146, 993, 910 cm^{-1};

^1H NMR (200 MHz, $CDCl_3$) δ: 5.75 (ddt, J = 17.1, 10.0, 6.6 Hz, 1 H), 5.70 (ddt, J = 17.1, 10.0, 7.1 Hz, 1 H), 4.83-5.03 (m, 4 H), 3.68 (t, J = 7.2 Hz, 2 H), 2.76 (t, J = 7.5 Hz, 2 H), 2.22 (dt, J = 7.1, 7.3 Hz, 2 H), 1.92-2.02 (m, 2 H), 1.50-1.63 (m, 2 H), 1.47 (s, 9 H), 1.20-1.37 (m, 10 H);

^{13}C NMR (50 MHz, $CDCl_3$) δ: 175.94, 153.10, 139.07, 135.15, 116.55, 114.02, 82.55, 43.53, 38.32, 33.71, 33.21, 29.32, 29.25, 29.14, 28.99, 28.82, 27.94, 25.11;

LRMS (DCI(+), ammonia) *m/z* (relative intensity): 338 (M^++1, 24), 282 (100), 238 (78), 196 (80), 149 (25), 57 (25);

HRMS (DCI(+), methane/ammonia) *m/z* calculated for $C_{20}H_{36}O_3N$ (M^++1): 338.2695, found: 338.2695;

Analysis calculated for $C_{20}H_{35}O_3N$: C, 71.18; H, 10.45; N, 4.15. Found: C, 70.87; H, 10.49; N, 4.27.

_N_-*tert*-Butoxycarbonyl-_N_-(4-pentenyl)-9-decenamide (141)

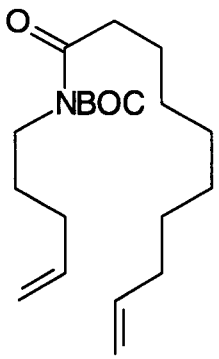

4-Dimethylaminopyridine (0.55 g, 4.50 mmol) and di-*tert*-butyl dicarbonate (0.73 g, 3.34 mmol) were sequentially added to a solution of *N*-(4-pentenyl)-9-decenamide (**70**) (0.53 g, 2.23 mmol) in THF (14.0 mL) and the reaction was stirred for 30 hours. The reaction was diluted with diethyl ether (35 mL) and sequentially washed with saturated $NaHCO_3$ solution and brine (35 mL each). The aqueous layers were separately washed with diethyl ether (80 mL). The combined organic extracts were dried over $MgSO_4$, filtered,

and concentrated. Purification of the residue by flash column chromatography with 5% diethyl ether in petroleum ether as eluant afforded **141** (0.45 g, 60%) as a colourless oil.

R_f = 0.86 (petroleum ether-ethyl acetate 4:1);

IR (neat): 3078, 2978, 2930, 2856, 1736, 1697, 1641, 1458, 1369, 1146, 993, 910, 721 cm^{-1};

^1H NMR (200 MHz, $CDCl_3$) δ: 5.76 (ddt, J = 17.1, 10.2, 6.6 Hz, 2 H), 4.84-5.03 (m, 4 H), 3.62 (t, J = 7.6 Hz, 2 H), 2.77 (t, J = 7.5 Hz, 2 H), 1.94-2.06 (m, 4 H), 1.50-1.64 (m, 2 H), 1.48 (s, 9 H), 1.21-1.38 (m, 10 H);

^{13}C NMR (50 MHz, $CDCl_3$) δ: 175.96, 153.22, 139.07, 137.80, 114.80, 114.06, 82.54, 44.00, 38.34, 33.71, 31.06, 29.24, 29.13, 28.91, 28.81, 27.98, 27.74, 25.11;

LRMS (DCI(+), ammonia) *m/z* (relative intensity): 338 (M^++1, 29), 337 (M^+, 2), 282 (95), 281 (33), 238 (100), 237 (54), 236 (37), 182 (23), 171 (25), 153 (25), 143 (55), 140 (47), 127 (46), 126 (40), 112 (28), 114 (49), 99 (28), 57 (31);

HRMS (DCI(+), methane/ammonia) *m/z* calculated for $C_{20}H_{36}O_3N$ (M^++1): 338.2695, found: 338.2696;

Analysis calculated for $C_{20}H_{35}O_3N$: C, 71.18; H, 10.45; N, 4.15. Found: C, 71.36; H, 10.32; N, 4.33.

_N_-*tert*-Butoxycarbonyl-_N_-(8-nonenyl)-5-hexenamide (142)

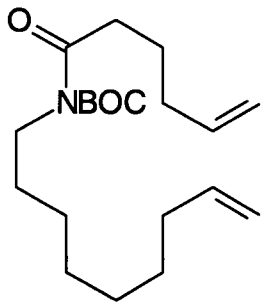

4-Dimethylaminopyridine (0.48 g, 3.93 mmol) and di-*tert*-butyl dicarbonate (0.65 g, 2.98 mmol) were sequentially added to a solution of *N*-(8-nonenyl)-5-hexenamide (**74**) (0.47 g, 1.98 mmol) in THF (10.0 mL) and the reaction was stirred for 65 hours. The reaction was diluted with diethyl ether (25 mL) and sequentially washed with saturated $NaHCO_3$ solution and brine (25 mL each). The aqueous layers were separately washed with diethyl ether (60 mL). The combined organic extracts were dried over $MgSO_4$, filtered,

and concentrated. Purification of the residue by flash column chromatography with 3% diethyl ether in petroleum ether as eluant afforded **142** (0.38 g, 57%) as a colourless oil.

R_f = 0.76 (petroleum ether-ethyl acetate 4:1);

IR (neat): 3076, 2978, 2930, 2856, 1732, 1697, 1641, 1456, 1369, 1148, 993, 910 cm^{-1};

^1H NMR (500 MHz, $CDCl_3$) δ: 5.77 (ddt, J = 16.9, 10.4, 6.6 Hz, 1 H), 5.76 (ddt, J = 17.0, 10.6, 6.6 Hz, 1 H), 4.87-5.00 (m, 4 H), 3.61 (t, J = 7.5 Hz, 2 H), 2.79 (t, J = 7.5 Hz, 2 H), 2.06 (dt, J = 7.2, 6.9 Hz, 2 H), 1.99 (q, J = 6.9 Hz, 2 H), 1.70 (quint, J= 7.4 Hz, 2 H), 1.49 (s, 9 H), 1.20-1.47 (m, 10 H);

^{13}C NMR (125 MHz, $CDCl_3$) δ: 175.76, 153.40, 139.12, 138.31, 114.94, 114.21, 82.60, 44.55, 37.75, 33.78, 33.24, 29.18, 29.05, 28.86, 28.74, 28.09, 26.91, 24.44;

LRMS (DCI(+), ammonia) *m/z* (relative intensity): 338 (M^++1, 88), 337 (M^+, 9), 282 (100), 281 (61), 238 (22), 237 (35);

HRMS (DCI(+), methane/ammonia) *m/z* calculated for $C_{20}H_{36}O_3N$ (M^++1): 338.2695, found: 338.2695; calculated for $C_{20}H_{35}O_3N$: 337.2617, found: 337.2609;

Analysis calculated for $C_{20}H_{35}O_3N$: C, 71.18; H, 10.45; N, 4.15. Found: C, 71.39; H, 10.60; N, 4.23.

***N*-*tert*-Butoxycarbonyl-*N*-(9-decenyl)-4-pentenamide (143)**

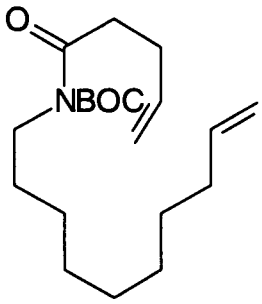

4-Dimethylaminopyridine (0.49 g, 4.01 mmol) and di-*tert*-butyl dicarbonate (0.66 g, 3.02 mmol) were sequentially added to a solution of *N*-(9-decenyl)-4-pentenamide (**75**) (0.48 g, 2.02 mmol) in THF (12.5 mL) and the reaction was stirred for 54 hours. The reaction was diluted with diethyl ether (30 mL) and sequentially washed with saturated $NaHCO_3$ solution and brine (30 mL each). The aqueous layers were separately washed with diethyl ether (75 mL). The combined organic extracts were dried over $MgSO_4$, filtered, and concentrated. Purification of the residue by flash column chromatography with 3% diethyl ether in petroleum ether as eluant afforded **143** (0.48 g, 72%) as a colourless oil.

R_f = 0.80 (petroleum ether-ethyl acetate 4:1);

IR (neat): 3078, 2976, 2928, 2854, 1734, 1697, 1641, 1456, 1443, 1369, 1148, 993, 910 cm^{-1};

^1H NMR (200 MHz, $CDCl_3$) δ: 5.79 (ddt, J = 17.0, 10.4, 6.6 Hz, 1 H), 5.74 (ddt, J = 17.1, 10.3, 6.6 Hz, 1 H), 4.82-5.04 (m, 4 H), 3.59 (t, J = 7.4 Hz, 2 H), 2.87 (t, J = 7.5 Hz, 2 H), 2.32 (q, J = 7.2 Hz, 2 H), 1.97 (q, J = 6.8 Hz, 2 H), 1.46 (s, 9 H), 1.15-1.41 (m, 12 H);

^{13}C NMR (50 MHz, $CDCl_3$) δ: 174.99, 153.20, 138.97, 137.40, 114.93, 114.04, 82.48, 44.41, 37.58, 33.67, 29.27, 29.13, 28.91, 28.78, 28.60, 27.92, 26.80;

LRMS (DCI(+), ammonia) *m/z* (relative intensity): 338 (M^++1, 21), 337 (M^+, 3), 282 (68), 281 (100), 238 (52), 237 (65), 196 (21), 182 (24), 113 (23), 57 (35);

HRMS (DCI(+), methane/ammonia) *m/z* calculated for $C_{20}H_{36}O_3N$ (M^++1): 338.2695, found: 338.2691;

Analysis calculated for $C_{20}H_{35}O_3N$: C, 71.18; H, 10.45; N, 4.15. Found: C, 71.43; H, 10.35; N, 4.00.

_N_-*tert*-Butoxycarbonyl-_N_-(10-undecenyl)-3-butenamide (144)

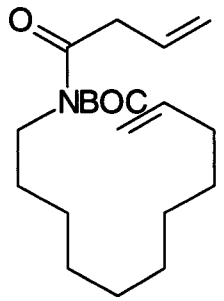

4-Dimethylaminopyridine (0.24 g, 1.96 mmol) and di-*tert*-butyl dicarbonate (0.32 g, 1.47 mmol) were sequentially added to a solution of *N*-(10-undecenyl)-3-butenamide (**76**) (234.5 mg, 0.9879 mmol) in THF (6.2 mL) and the reaction was stirred for 72 hours. The reaction was diluted with diethyl ether (15 mL) and sequentially washed with saturated $NaHCO_3$ solution and brine (15 mL each). The aqueous layers were separately washed with diethyl ether (35 mL). The combined organic extracts were dried over $MgSO_4$, filtered, and concentrated. Purification of the residue by flash column chromatography with 5% ethyl acetate in petroleum ether as eluant afforded **144** (217.9 mg, 65%) as a colourless oil.

R_f = 0.90 (petroleum ether-ethyl acetate 1:1);

IR (neat): 3078, 2978, 2928, 2854, 1732, 1697, 1641, 1456, 1369, 1148, 1089, 993, 910 cm^{-1};

^1H NMR (200 MHz, C_6D_6) δ: 6.20 (ddt, J = 17.1, 10.4, 6.7 Hz, 1 H), 5.78 (ddt, J = 17.0, 10.1, 6.6 Hz, 1 H), 4.94-5.12 (m, 4 H), 3.70 (t, J = 7.6 Hz, 2 H), 3.69 (d, J = 6.8 Hz, 2 H), 1.98 (q, J = 7.1 Hz, 2 H), 1.49-1.64 (m, 2 H), 1.30 (s, 9 H), 1.14-1.27 (m, 12 H);

^{13}C NMR (50 MHz, C_6D_6) δ: 173.10, 153.35, 139.20, 132.65, 117.33, 114.47, 82.02, 44.55, 43.47, 34.16, 29.85, 29.76, 29.64, 29.44, 29.28, 29.12, 27.83, 27.25;

LRMS (DCI(+), ammonia) *m/z* (relative intensity): 338 (M^++1, 40), 300 (44), 299 (100), 282 (28), 239 (27), 238 (69);

HRMS (CI(+), isobutane) *m/z* calculated for $C_{20}H_{36}O_3N$ (M^++1): 338.2695, found: 338.2696;

Analysis calculated for $C_{20}H_{35}O_3N$: C, 71.16; H, 10.46; N, 4.15. Found: C, 71.43; H, 10.60; N, 4.25.

(*E*)-*N*-(10-Undecenyl)-3-hexenamide (145)

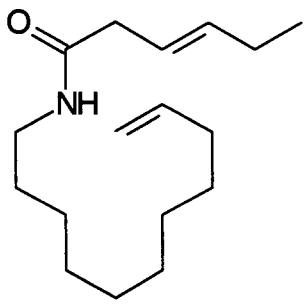

10-Undecenylamine (**118**) (0.86 g, 5.08 mmol), (*E*)-3-hexenoic acid (0.60 mL, 5.06 mmol), and triethylamine (1.70 mL, 12.20 mmol) were sequentially added to a solution of 2-chloro-1-methylpyridinium iodide (1.56 g, 6.11 mmol) in CH_2Cl_2 (51.0 mL) and the reaction was stirred for two hours at 40 °C and for 6 hours at room temperature. The reaction was cooled to room temperature and diluted with ethyl acetate (100 mL) and sequentially washed with 1 M HCl (3X), saturated $NaHCO_3$ solution (2X), and water (250 mL each). The organic layer was dried over $MgSO_4$, filtered, and concentrated. Purification of the residue by flash column chromatography with 20% ethyl acetate in petroleum ether as eluant afforded **145** (0.92 g, 69%) as a white solid.

R_f = 0.20 (petroleum ether-ethyl acetate 4:1);

Melting point: 35.5-36.5 °C (ethyl acetate);

IR (CCl_4): 3448, 3337, 3078, 2966, 2930, 2856, 1682, 1510, 1462, 1415, 972, 908 cm^{-1};

^1H NMR (200 MHz, $CDCl_3$) δ: 5.77 (ddt, J = 17.0, 10.1, 6.7 Hz, 1 H), 5.63 (bs, 1 H), 5.63 (dt, J = 15.4, 5.8 Hz, 1 H), 5.46 (dt, J = 15.4, 6.8 Hz, 1 H), 4.97 (ddt, J = 15.9, 2.2, 1.6 Hz, 1 H), 4.88 (ddt, J = 8.8, 2.2, 1.2 Hz, 1 H), 3.19 (q, J = 6.6 Hz, 2 H), 2.89 (d, J = 6.8 Hz, 2 H), 1.94-2.11 (m, 4 H), 1.17-1.51 (m, 14 H), 0.97 (t, J = 7.4 Hz, 3 H);

^{13}C NMR (50 MHz, $CDCl_3$) δ: 171.18, 139.13, 137.85, 121.77, 114.08, 40.51, 39.53, 33.74, 29.52, 29.42, 29.34, 29.21, 29.04, 28.86, 26.82, 25.54, 13.50;

LRMS (EI) *m/z* (relative intensity): 266 (M^++1, 26), 265 (M^+, 100), 196 (53), 70 (38), 69 (32), 55 (30);

HRMS (EI) *m/z* calculated for $C_{17}H_{31}ON$: 265.2406, found: 265.2405;

Analysis calculated for $C_{17}H_{31}ON$: C, 76.92; H, 11.77; N, 5.28. Found: C, 76.95; H, 11.78; N, 5.18.

(*Z*)-3-Hexenoic acid (147)

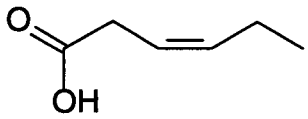

A solution of Jones' reagent (ca. 24.0 mL) was added to a solution of (*Z*)-3-hexen-1-ol (3.0 mL, 25.3 mmol) in acetone (253 mL) and stirred at room temperature until an orange colour persisted. The reaction was filtered through celite and back titrated with 2-propanol (ca. 4.0 mL) until a blue colour persisted. This mixture was filtered through celite and concentrated. Purification of the residue by flash column chromatography with 20% diethyl ether in petroleum ether as eluant afforded **147** (2.61 g, 90%) as a pale yellow oil.

R_f = 0.41 (petroleum ether-ethyl acetate 4:1);

IR (neat): 3028, 2966, 2935, 2878, 2719, 1713, 1456, 1418, 1296, 935 cm^{-1};

^1H NMR (200 MHz, $CDCl_3$) δ: 11.82 (bs, 1 H), 5.59 (dt, J = 10.7, 6.8 Hz, 1 H), 5.47 (dt, J = 10.8, 7.1 Hz, 1 H), 3.11 (d, J = 7.1 Hz, 2 H), 2.03 (quint, J = 7.3 Hz, 2 H), 0.95 (t, J = 7.4 Hz, 3 H);

^{13}C NMR (50 MHz, $CDCl_3$) δ: 178.78, 135.61, 119.32, 32.55, 20.66, 13.77;

LRMS (EI) *m/z* (relative intensity): 114 (M^+, 49), 73 (29), 69 (40), 68 (57), 67 (21), 60 (57), 57 (23), 55 (100), 41 (98), 39 (40);

HRMS (EI) *m/z* calculated for $C_6H_{10}O_2$: 114.0681, found: 114.0680;

Analysis calculated for $C_6H_{10}O_2$: C, 63.14; H, 8.83. Found: C, 63.35; H, 8.87.

(*Z*)-*N*-(10-Undecenyl)-3-hexenamide (148)

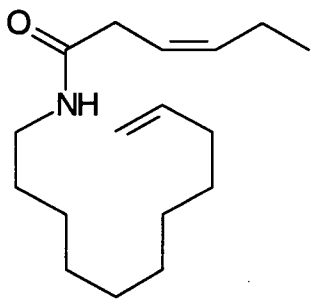

10-Undecenylamine (**118**) (0.83 g, 4.90 mmol), (*Z*)-3-hexenoic acid (**147**) (0.56 g, 4.91 mmol), and triethylamine (1.64 mL, 11.77 mmol) were sequentially added to a solution of 2-chloro-1-methylpyridinium iodide (1.50 g, 5.87 mmol) in CH_2Cl_2 (49.0 mL) and the reaction was stirred for two hours at 40 °C and for 6 hours at room temperature. The reaction was cooled to room temperature and diluted with ethyl acetate (100 mL) and sequentially washed with 1 M HCl (3X), saturated $NaHCO_3$ solution (2X), and water (250 mL each). The organic layer was dried over $MgSO_4$, filtered, and concentrated. Purification of the residue by flash column chromatography with 15% ethyl acetate in petroleum ether as eluant afforded **148** (0.76 g, 58%) as a colourless oil.

R_f = 0.63 (petroleum ether-ethyl acetate 1:1);

IR (neat): 3292, 3078, 2962, 2930, 2854, 1645, 1553, 1460, 1439, 1373, 993, 968, 908, 732 cm^{-1};

^{1}H NMR (500 MHz, $CDCl_3$) δ: 5.77 (ddt, J = 17.1, 10.3, 6.7 Hz, 1 H), 5.65 (bs, 1 H), 5.62 (dt, J = 15.2, 6.3 Hz, 1 H), 5.47 (dt, J = 15.3, 7.1 Hz, 1 H), 4.95 (ddt, J = 17.1, 2.1, 1.6 Hz, 1 H), 4.89 (ddt, J = 10.2, 2.1, 1.2 Hz, 1 H), 3.19 (q, J = 7.0 Hz, 2 H), 2.89 (d, J = 7.0 Hz, 2 H), 2.05 (dt, J = 7.6, 6.3 Hz, 2 H), 1.99 (dt, J = 7.6, 6.8 Hz, 2 H), 1.39-1.49 (m, 2 H), 1.16-1.34 (m, 12 H), 0.97 (t, J = 7.5 Hz, 3 H);

^{13}C NMR (125 MHz, $CDCl_3$) δ: 171.22, 139.13, 137.87, 121.73, 114.07, 40.48, 39.53, 33.73, 29.50, 29.41, 29.33, 29.19, 29.02, 28.85, 26.81, 15.53, 13.49;

LRMS (EI) *m/z* (relative intensity): 265 (M^+, 18), 83 (25), 70 (52), 69 (66), 67 (27), 57 (20), 56 (27), 55 (100), 43 (32), 41 (91), 39 (37);

HRMS (EI) *m/z* calculated for $C_{17}H_{31}ON$: 265.2406, found: 265.2407;

Analysis calculated for $C_{17}H_{31}ON$: C, 76.92; H, 11.77; N, 5.28. Found: C, 77.10; H, 11.67; N, 5.11.

N-(3-Aminopropyl)-3-(1-piperidyl)propylamine (153)

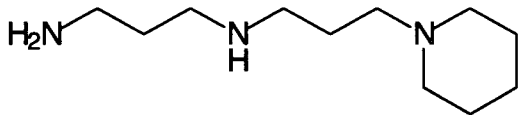

Lithium aluminum hydride (0.38 g, 10.0 mmol) was added to a solution of *N*-(3-aminopropyl)-3-(1-piperidyl)propanamide (**155**) (0.54 g, 2.53 mmol) in THF (10.0 mL) and the reaction was stirred for 6.5 hours at 70 °C. The reaction was cooled to 0 °C and a solution of THF (1.8 mL) and water (0.3 mL) was added and stirred for 15 minutes. Aqueous 3 M NaOH solution was added dropwise until a white precipitate formed and the solution was stirred for 15 minutes. The slurry was vacuum filtered through celite and the filtrate was dried over $MgSO_4$, filtered, and concentrated. Kugelrohr distillation of the residue at 110 °C at 0.2 mm Hg afforded **153** (0.33 g, 66%) as a colourless oil.

R_f = 0.16 (dichloromethane-methanol 1:1);

IR (neat): 3358, 3285, 2932, 2853, 2802, 1663, 1595, 1470, 1443, 1155, 1126, 858 cm^{-1};

^1H NMR (200 MHz, CD_3OD) δ: 2.67 (t, J = 7.0 Hz, 2 H), 2.60 (t, J = 7.4 Hz, 2 H), 2.59 (bs, 1 H), 2.58 (t, J = 7.3 Hz, 2 H), 2.40-2.45 (m, 4 H), 2.35 (t, J = 7.8 Hz, 2 H), 1.40-1.78 (m, 12 H);

^{13}C NMR (50 MHz, CD_3OD) δ: 58.58, 55.57, 49.36, 48.36, 40.72, 33.66, 27.42, 26.64, 25.32;

LRMS (EI) *m/z* (relative intensity): 199 (M^+, 12), 125 (32), 110 (37), 98 (100), 84 (29);

HRMS (EI) *m/z* calculated for $C_{11}H_{25}N_3$: 199.2049, found: 199.2046;

Analysis calculated for $C_{11}H_{25}N_3$: C, 66.28; H, 12.64; N, 21.08. Found: C, 66.36; H, 12.49; N, 20.87.

N-(3-Aminopropyl)-3-(1-piperidyl)propanamide (155)

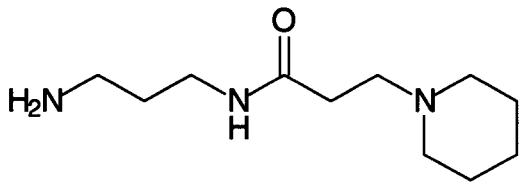

Methyl acrylate (0.96 mL, 10.7 mmol) was added to a solution of piperidine (1.10 mL, 11.1 mmol) in methanol (20 mL) and the reaction was stirred for 3 hours. Another portion of methyl acrylate (0.96 mL, 10.7 mmol) was added to the reaction and stirred for 26 hours. The reaction was concentrated and excess reagents were removed under vacuum. 1,3-Diaminopropane (8.4 mL, 100 mmol) was added to a solution of the residue (1.91 g) in methanol (20 mL) and the reaction was stirred for 67 hours. The reaction was concentrated and excess reagents were removed under vacuum to afford **155** (2.29 g, 97%) as a colourless oil.

R_f = 0.21 (dichloromethane-methanol 9:1);

IR (neat): 3285, 3072, 2934, 2853, 2804, 1647, 1560, 1470, 1443, 1377, 1117, 862, 760 cm^{-1};

^1H NMR (200 MHz, $CDCl_3$) δ: 8.56 (bs, 1 H), 3.16 (dt, J = 5.9, 6.7 Hz, 2 H), 2.61 (t, J = 6.7 Hz, 2 H), 2.41 (t, J = 6.0 Hz, 2 H), 2.24-2.32 (m, 4 H), 2.21 (t, J = 6.1 Hz, 2 H), 1.32-1.56 (m, 10 H);

^{13}C NMR (50 MHz, $CDCl_3$) δ: 172.49, 54.37, 53.51, 39.38, 36.09, 33.08, 31.87, 25.87, 23.98;

LRMS (EI) *m/z* (relative intensity): 213 (M^+, 9), 98 (100), 84 (35);

HRMS (EI) *m/z* calculated for $C_{11}H_{23}ON_3$: 213.1841, found: 213.1838;

Analysis calculated for $C_{11}H_{23}ON_3$: C, 61.93; H, 10.87; N, 19.70. Found: C, 61.71; H, 10.76; N, 20.00.

N-(3-Aminopropyl)-3-(1-azacyclotridecyl)propanamide (156)

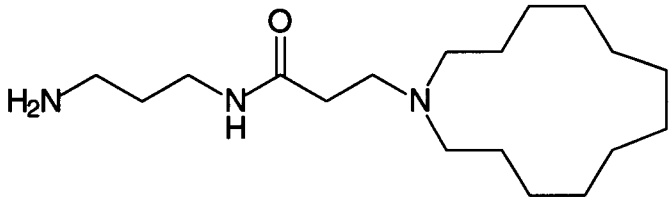

Methyl acrylate (0.51 mL, 5.7 mmol) was added to a solution of azacyclotridecane (**66**) (497.7 mg, 2.715 mmol) in methanol (5.4 mL) and the reaction was stirred for 24 hours. The reaction was concentrated and excess reagents were removed under vacuum. 1,3-Diaminopropane (2.25 mL, 27.0 mmol) was added to a solution of the residue (721.1 mg) in methanol (5.4 mL) and the reaction was stirred for 70 hours. Another portion of 1,3-diaminopropane (1.15 mL, 13.8 mmol) was added to the reaction and stirred for 52 hours. The reaction was concentrated and excess reagents were removed under vacuum to afford **156** (834.3 mg, 99%) as a colourless oil.

R_f = 0.04 (petroleum ether-ethyl acetate 1:1);

IR (neat): 3292, 3074, 2928, 2856, 2802, 1643, 1553, 1460, 1348, 1089 cm^{-1};

^1H NMR (200 MHz, $CDCl_3$) δ: 8.21 (bs, 1 H), 3.24 (dt, J = 6.1, 6.8 Hz, 2 H), 2.66 (t, J = 6.7 Hz, 2 H), 2.54 (t, J = 6.1 Hz, 2 H), 2.32 (t, J = 6.0 Hz, 4 H), 2.26 (t, J = 6.2 Hz, 2 H), 1.56 (quint, J = 6.8 Hz, 2 H), 1.18-1.44 (m, 22 H);

^{13}C NMR (50 MHz, $CDCl_3$) δ: 172.87, 53.21, 51.45, 39.46, 36.36, 33.44, 32.91, 25.84, 25.77, 25.41, 25.31, 25.23;

LRMS (EI) *m/z* (relative intensity): 311 (M^+, 33), 197 (20), 196 (86), 182 (100), 170 (41), 158 (41), 141 (41), 130 (23), 112 (21), 98 (27), 85 (20), 86 (20);

HRMS (EI) *m/z* calculated for $C_{18}H_{37}ON_3$: 311.2937, found: 311.2928;

Analysis calculated for $C_{18}H_{37}ON_3$: C, 69.40; H, 11.97; N, 13.49. Found: C, 69.58; H, 12.00; N, 13.21.

N-(3-Aminopropyl)-3-(1-azacyclotetradecyl)propanamide (157)

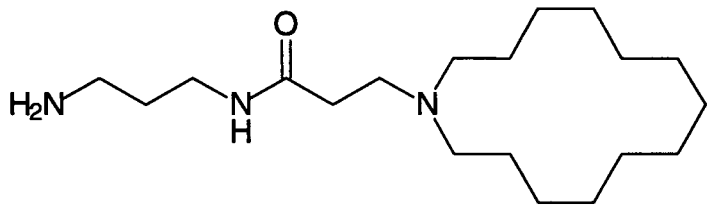

Methyl acrylate (0.33 mL, 3.7 mmol) was added to a solution of azacyclotetradecane (**63**) (348.3 mg, 1.765 mmol) in methanol (3.5 mL) and the reaction was stirred for 26 hours. The reaction was concentrated and excess reagents were removed under vacuum. 1,3-Diaminopropane (1.47 mL, 17.6 mmol) was added to a solution of the residue (485.9 mg) in methanol (3.5 mL) and the reaction was stirred for 64 hours. Another portion of 1,3-diaminopropane (0.74 mL, 8.9 mmol) was added to the reaction and stirred for 23 hours. The reaction was concentrated and excess reagents were removed under vacuum to afford **157** (553.5 mg, 96%) as a colourless oil.

R_f = 0.10 (petroleum ether-ethyl acetate 1:1);

IR (CCl_4): 3294, 3059, 2934, 2860, 2812, 1666, 1462, 1371, 1040, 891 cm^{-1};

^1H NMR (500 MHz, CD_3OD) δ: 3.34 (bs, 1 H), 3.23 (t, J = 6.8 Hz, 2 H), 2.71 (t, J = 7.1 Hz, 2 H), 2.66 (t, J = 6.9 Hz, 2 H), 2.44 (t, J = 6.8 Hz, 4 H), 2.32 (t, J = 7.2 Hz, 2 H), 1.65 (quint, J = 6.9 Hz, 2 H), 1.49 (quint, J = 6.7 Hz, 4 H), 1.34-1.42 (m, 20 H);

^{13}C NMR (125 MHz, CD_3OD) δ: 175.36, 52.39, 51.39, 39.65, 37.53, 34.01, 33.22, 26.67, 26.39, 25.95, 25.81, 25.52, 25.43;

LRMS (EI) *m/z* (relative intensity): 325 (M^+, 9), 210 (70), 197 (22), 196 (100), 158 (21), 112 (22), 70 (20), 58 (28), 56 (33), 55 (32), 44 (73), 42 (25);

HRMS (EI) *m/z* calculated for $C_{19}H_{39}ON_3$: 325.3093, found: 325.3089.

N-Benzyl-4-pentenamide (158)

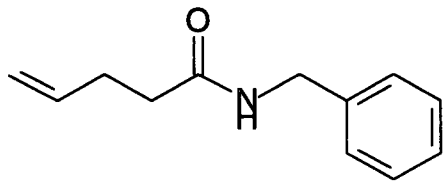

(a) DCC/HOBt Coupling of 4-Pentenoic Acid and Benzylamine

1,3-Dicyclohexylcarbodiimide (16.38 g, 79.39 mmol) was added to a solution of 4-pentenoic acid (5.4 mL, 52.9 mmol), benzylamine (5.8 mL, 53.1 mmol) and 1-hydroxybenzotriazole hydrate (8.10 g, 52.90 mmol) in CH_2Cl_2 (410 mL) stirred at 0 °C and the reaction was stirred for two hours with warming to room temperature. The reaction was diluted with CH_2Cl_2 (400 mL) and washed sequentially with 1 M HCl (2X), saturated $NaHCO_3$ solution (2X) and brine (400 mL each). The organic layer was dried over $MgSO_4$, filtered, and concentrated. Purification of the residue by vacuum liquid chromatography with 20% ethyl acetate in petroleum ether as eluant afforded **158** (9.42 g, 94%) as a white solid.

R_f = 0.23 (petroleum ether-ethyl acetate 4:1);

Melting point: 38.0-39.0 °C (ethyl acetate);

IR (CCl_4): 3452, 3344, 3067, 3032, 2928, 1682, 1504, 1454, 916 cm^{-1};

^1H NMR (200 MHz, $CDCl_3$) δ: 7.20-7.36 (m, 5 H), 5.83 (bs, 1 H), 5.81 (ddt, J = 17.1, 10.2, 6.4 Hz, 1 H), 4.95-5.10 (m, 2 H), 4.41 (d, J = 5.6 Hz, 2 H), 2.24-2.47 (m, 4 H);

^{13}C NMR (50 MHz, $CDCl_3$) δ: 172.08, 138.26, 136.97, 128.66, 127.79, 127.48, 115.63, 43.57, 35.82, 29.57;

LRMS (EI) *m/z* (relative intensity): 189 (M^+, 11), 107 (27), 106 (31), 91 (100), 55 (20);

HRMS (EI) *m/z* calculated for $C_{12}H_{15}ON$: 189.1154, found: 189.1146;

Analysis calculated for $C_{12}H_{15}ON$: C, 76.14; H, 7.99; N, 7.40. Found: C, 75.98; H, 8.00; N, 7.38.

(b) 2-Bromo-1-methylpyridinium Fluorosulphonate Coupling of 4-Pentenoic Acid and Benzylamine

Benzylamine (0.215 mL, 1.968 mmol), 4-pentenoic acid (0.20 mL, 1.96 mmol), and triethylamine (0.66 mL, 4.74 mmol) were sequentially added to a solution of 2-bromo-1-methylpyridinium fluorosulphonate (0.64 g, 2.35 mmol) in CH_2Cl_2 (20.0 mL) and the reaction was stirred for four hours at 40 °C. The reaction was cooled to room temperature and diluted with diethyl ether (50 mL) and sequentially washed with 1 M HCl (3X), saturated $NaHCO_3$ solution (2X), and water (100 mL each). The organic layer was dried over $MgSO_4$, filtered, and concentrated. Purification of the residue by flash column chromatography with 30% ethyl acetate in petroleum ether as eluant afforded **158** (317.5 mg, 86%) with spectral data in agreement with that reported above.

(c) 2-Chloro-1-methylpyridinium Iodide Coupling of 4-Pentenoic Acid and Benzylamine

Benzylamine (0.215 mL, 1.968 mmol), 4-pentenoic acid (0.20 mL, 1.96 mmol), and triethylamine (0.66 mL, 4.74 mmol) were sequentially added to a solution of 2-chloro-1-methylpyridinium iodide (0.60 g, 2.35 mmol) in CH_2Cl_2 (20.0 mL) and the reaction was stirred for four hours at 40 °C. The reaction was cooled to room temperature and diluted with diethyl ether (50 mL) and sequentially washed with 1 M HCl (3X), saturated $NaHCO_3$ solution (2X), and water (100 mL each). The organic layer was dried over $MgSO_4$, filtered, and concentrated. Purification of the residue by flash column chromatography with 40% ethyl acetate in petroleum ether as eluant afforded **158** (282.8 mg, 76%) with spectral data in agreement with that reported above.

(d) Acid Chloride Formation of 4-Pentenoic Acid and Coupling with Benzylamine

Triethylamine (1.34 mL, 9.61 mmol) and oxalyl chloride (0.16 mL, 1.8 mmol) were sequentially added to a solution of 4-pentenoic acid (0.20 mL, 1.96 mmol) in CH_2Cl_2 (10.3 mL) at 0 °C and the reaction was stirred for 30 minutes with slow warming to room temperature. Benzylamine (0.215 mL, 1.968 mmol) in CH_2Cl_2 (5.0 mL) was added to the reaction mixture and stirred for 3.5 hours. The reaction was diluted with methanol (12.5 mL) and pyridine (2.0 mL) and concentrated. The residue was diluted in ethyl acetate (40 mL) and sequentially washed with 1 M HCl (2X), water, saturated $NaHCO_3$ solution, and brine (20 mL each). The organic layer was dried over $MgSO_4$, filtered, and concentrated. Purification of the residue by flash column chromatography with 30%

ethyl acetate in petroleum ether as eluant afforded **158** (282.5 mg, 76%) with spectral data in agreement with that reported above.

(e) DCC Coupling of 4-Pentenoic Acid and Benzylamine

1,3-Dicyclohexylcarbodiimide (10.90 g, 52.83 mmol) was added to a solution of 4-pentenoic acid (5.4 mL, 52.9 mmol) and benzylamine (5.8 mL, 53.1 mmol) in CH_2Cl_2 (107.0 mL) and the reaction was stirred for 43 hours. The reaction was filtered and washed with ethyl acetate (300 mL). The filtrate was washed sequentially with saturated $NaHCO_3$ solution and brine (300 mL each). The combined aqueous layers were successively washed with ethyl acetate (2X) (350 mL each). The combined organic extracts were dried over $MgSO_4$, filtered, and concentrated. Purification of the residue by flash column chromatography with 30% ethyl acetate in petroleum ether as eluant afforded **158** (5.27 g, 53%) with spectral data in agreement with that reported above.

***N*-(8-Nonenyl)-6-heptenamide (159)**

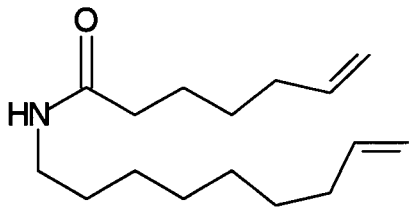

1,3-Dicyclohexylcarbodiimide (1.88 g, 9.11 mmol) was added to a solution of 6-heptenoic acid (**131**) (0.78 g, 6.09 mmol), 8-nonenylamine (**134**) (0.86 g, 6.09 mmol) and 1-hydroxybenzotriazole hydrate (0.82 g, 6.07 mmol) in CH_2Cl_2 (47.0 mL) stirred at 0 °C and the reaction was stirred for two hours with warming to room temperature. The reaction was diluted with CH_2Cl_2 (50 mL) and washed sequentially with 1 M HCl (2X), saturated $NaHCO_3$ solution (2X) and brine (50 mL each). The organic layer was dried over $MgSO_4$, filtered, and concentrated. Purification of the residue by flash column chromatography with 25% ethyl acetate in petroleum ether as eluant afforded **159** (1.27 g, 83%) as a colourless oil.

R_f = 0.50 (petroleum ether-ethyl acetate 1:1);

IR (neat): 3292, 3078, 2928, 2856, 1643, 1556, 1462, 1439, 991, 910 cm^{-1};

^{1}H NMR (200 MHz, $CDCl_3$) δ: 5.77 (ddt, J = 16.9, 10.4, 6.6 Hz, 1 H), 5.76 (ddt, J = 17.1, 10.2, 6.6 Hz, 1 H), 5.53 (bs, 1 H), 4.86-5.02 (m, 4 H), 3.19 (q, J = 6.6 Hz, 2 H), 2.13 (t, J = 7.5 Hz, 2 H), 1.95-2.08 (m, 4 H), 1.54-1.69 (m, 2 H), 1.20-1.48 (m, 12 H);

^{13}C NMR (50 MHz, $CDCl_3$) δ: 172.88, 139.01, 138.43, 114.60, 114.17, 39.46, 36.64, 33.68, 33.40, 29.61, 29.08, 28.94, 28.76, 28.47, 26.81, 25.23;

LRMS (EI) *m/z* (relative intensity): 251 (M^+, 22), 168 (21), 142 (20), 140 (32), 111 (20), 98 (27), 83 (38), 73 (24), 72 (20), 69 (33), 67 (21), 56 (20), 55 (97), 44 (44), 43 (28), 41 (100);

HRMS (EI) *m/z* calculated for $C_{16}H_{29}ON$: 251.2249, found: 251.2246;

Analysis calculated for $C_{16}H_{29}ON$: C, 76.44; H, 11.63; N, 5.57. Found: C, 76.40; H, 11.63; N, 5.60.

9-Decenenitrile (160)

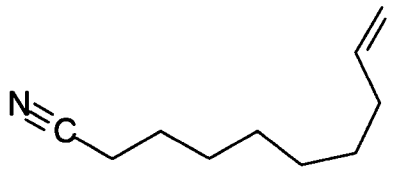

A solution of *n*-butyllithium in hexanes (11.6 mL, 23.8 mmol) was added dropwise to a solution of CH_3CN (1.19 mL, 22.8 mmol) in THF (36.0 mL) at -78 °C and the reaction was stirred for two hours. 8-bromooctene (4.0 mL, 23.8 mmol) was added to the solution and the reaction was stirred for two hours at -78 °C and stirred for three hours warming to room temperature. The reaction was concentrated and the residue was purified by flash column chromatography with 10% diethyl ether in petroleum ether as eluant to afford **160** (1.95 g, 57%) as a colourless oil.

R_f = 0.58 (petroleum ether-ethyl acetate 4:1);

IR (neat): 3076, 2930, 2856, 2247, 1639, 1464, 1427, 997, 910, 725 cm^{-1};

^{1}H NMR (200 MHz, $CDCl_3$) δ: 5.76 (ddt, J = 16.9, 10.1, 6.6 Hz, 1 H), 4.86-5.01 (m, 2 H), 2.30 (t, J = 7.0 Hz, 2 H), 2.01 (q, J = 6.6 Hz, 2 H), 1.55-1.69 (m, 2 H), 1.21-1.48 (m, 8 H);

^{13}C NMR (50 MHz, $CDCl_3$) δ: 138.80, 119.72, 114.24, 33.57, 28.62, 28.49, 25.24, 17.00;

LRMS (DCI(+), ammonia) *m/z* (relative intensity): 170 (M^++18, 26), 169 (M^++17, 100), 152 (M^+, 69), 122 (100), 110 (35), 108 (52), 95 (28), 94 (40), 80 (23), 58 (29);

HRMS (CI(+), methane/ammonia) *m/z* calculated for $C_{10}H_{18}N$ (M^++1): 152.1439, found: 152.1439;

Analysis calculated for $C_{10}H_{17}N$: C, 79.41; H, 11.33; N, 9.26. Found: C, 79.32; H, 11.37; N, 9.27.

N-(9-Decenyl)-5-hexenamide (161)

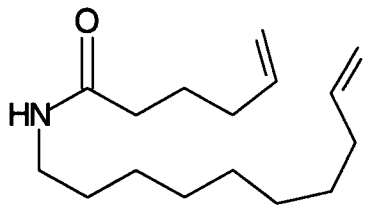

1,3-Dicyclohexylcarbodiimide (1.06 g, 5.14 mmol) was added to a solution of 5-hexenoic acid (**135**) (0.39 g, 3.42 mmol), 9-decenylamine (**138**) (0.53 g, 3.41 mmol) and 1-hydroxybenzotriazole hydrate (0.46 g, 3.40 mmol) in CH_2Cl_2 (26.0 mL) stirred at 0 °C and the reaction was stirred for 2.5 hours with warming to room temperature. The reaction was diluted with CH_2Cl_2 (30 mL) and washed sequentially with 1 M HCl (2X), saturated $NaHCO_3$ solution (2X) and brine (30 mL each). The organic layer was dried over $MgSO_4$, filtered, and concentrated. Purification of the residue by flash column chromatography with 25% ethyl acetate in petroleum ether as eluant afforded **161** (767.3 mg, 90%) as a colourless oil.

R_f = 0.39 (petroleum ether-ethyl acetate 1:1);

IR (neat): 3298, 3078, 2928, 2854, 1643, 1556, 1462, 1441, 991, 910 cm^{-1};

^1H NMR (200 MHz, $CDCl_3$) δ: 5.76 (ddt, J = 17.1, 10.2, 6.6 Hz, 1 H), 5.74 (ddt, J = 17.1, 10.3, 6.6 Hz, 1 H), 5.60 (bs, 1 H), 4.85-5.03 (m, 4 H), 3.18 (q, J = 6.6 Hz, 2 H), 2.12 (t, J = 7.5 Hz, 2 H), 1.94-2.06 (m, 4 H), 1.61-1.77 (m, 2 H), 1.18-1.51 (m, 12 H);

^{13}C NMR (50 MHz, $CDCl_3$) δ: 172.69, 139.06, 137.89, 115.16, 114.09, 39.44, 35.92, 33.70, 33.10, 29.61, 29.30, 29.17, 28.96, 28.81, 26.84, 24.77;

LRMS (EI) *m/z* (relative intensity): 251 (M^+, 100), 210 (64), 168 (24), 156 (22), 154 (43), 127 (20), 126 (23), 114 (22), 97 (20), 86 (22), 84 (34), 69 (23), 55 (26);

HRMS (EI) *m/z* calculated for $C_{16}H_{29}ON$: 251.2249, found: 251.2251;

Analysis calculated for $C_{16}H_{29}ON$: C, 76.44; H, 11.63; N, 5.57. Found: C, 76.32; H, 11.73; N, 5.68.

(*Z*/*E*)-2-Azacyclopentadec-10-enone (162) and (163)

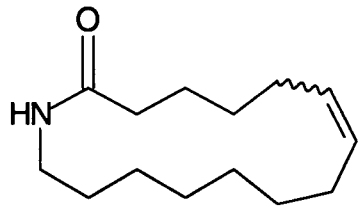

A solution of *N*-(8-nonenyl)-6-heptenamide (**159**) (103.0 mg, 0.4097 mmol) in sparged CH_2Cl_2 (25.0 mL) and a solution of Grubbs' benzylidene (**3**) (16.9 mg, 0.0205 mmol) in sparged CH_2Cl_2 (25.0 mL) were added simultaneously using a syringe pump to sparged CH_2Cl_2 (155.0 mL) stirred at 45 °C over 3 hours. After the addition, the reaction was stirred for an additional one hour at 45 °C. The solution in the receiver flask was gently sparged with N_2 gas during the addition and reaction. The reaction was cooled to room temperature and triethylamine (2 mL) was added and stirred for 15 minutes. The solution was concentrated. Purification of the residue (^{1}H NMR ratio **162:163**, 37:63) by radial chromatography, using silver nitrate impregnated silica, with 40% ethyl acetate in petroleum ether as eluant afforded **162** (8.9 mg, 10%), a mixture of **162** and **163** (45.9 mg, 50%) and **163** (8.9 mg, 10%) all as white solids.

162 (*Z*)

R_f = 0.23 (petroleum ether-ethyl acetate 1:1);

Melting point: 147.0-149.0 °C (ethyl acetate);

IR (CCl_4): 3452, 3321, 2930, 2856, 1682, 1651, 1504, 1460, 1441, 968 cm^{-1};

^{1}H NMR (500 MHz, $CDCl_3$) δ: 5.61 (bs, 1 H), 5.40 (dt, J = 10.8, 7.7 Hz, 1 H), 5.32 (dt, J = 10.8, 7.6 Hz, 1 H), 3.26 (dt, J = 5.5, 5.8 Hz, 2 H), 2.17 (t, J = 6.4 Hz, 2 H), 1.93-2.16 (m, 4 H), 1.63-1.69 (m, 2 H), 1.46-1.51 (m, 2 H), 1.26-1.37 (m, 10 H);

^{13}C NMR (125 MHz, $CDCl_3$) δ: 173.21, 130.83, 129.05, 38.90, 36.55, 29.36, 28.76, 27.95, 27.23, 27.20, 27.09, 26.16, 25.80, 25.09;

LRMS (DCI(+), ammonia) *m/z* (relative intensity): 224 (M^++1, 100), 223 (M^+, 100);

HRMS (DCI(+), methane/ammonia) *m/z* calculated for $C_{14}H_{26}ON$ (M^++1): 224.2015, found: 224.2014;

Analysis calculated for $C_{14}H_{25}ON$: C, 75.28; H, 11.28; N, 6.27. Found: C, 75.15; H, 11.21; N, 6.13.

163 (*E*)

R_f = 0.23 (petroleum ether-ethyl acetate 1:1);

Melting point: 140.0-141.0 °C (ethyl acetate);

IR (CCl_4): 3460, 3304, 3080, 2934, 2856, 1645, 1504, 1460, 1441, 1364, 968, 912 cm^{-1};

^1H NMR (500 MHz, $CDCl_3$) δ: 5.56 (bs, 1 H), 5.35 (dt, J = 15.5, 3.3 Hz, 1 H), 5.32 (dt, J = 15.8, 3.3 Hz, 1 H), 3.22 (dt, J = 5.1, 5.8 Hz, 2 H), 2.14 (t, J = 7.3 Hz, 2 H), 1.98-2.02 (m, 4 H), 1.56-1.63 (m, 2 H), 1.39-1.48 (m, 4 H), 1.33-1.38 (m, 2 H), 1.20-1.31 (m, 6 H);

^{13}C NMR (125 MHz, $CDCl_3$) δ: 173.57, 131.82, 130.55, 39.04, 37.05, 31.89, 31.58, 28.72, 28.55, 28.39, 28.18, 27.73, 26.54, 25.90;

LRMS (DCI(+), ammonia) *m/z* (relative intensity): 224 (M^++1, 100), 223 (M^+, 22);

HRMS (DCI(+), methane/ammonia) *m/z* calculated for $C_{14}H_{26}ON$ (M^++1): 224.2015, found: 224.2012;

Analysis calculated for $C_{14}H_{25}ON$: C, 75.28; H, 11.28; N, 6.27. Found: C, 75.25; H, 11.21; N, 6.32.

Methyl 3-((*Z*)-1-azacyclopentadec-7-enyl)propionate (164)

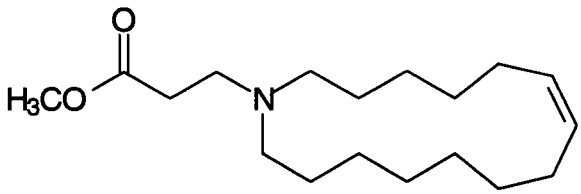

(a) Reduction/Michael Addition of (*Z*)-2-Azacyclopentadec-10-enone (**162**)

Lithium aluminum hydride (11.1 mg, 0.292 mmol) was added to a solution of (*Z*)-2-azacyclopentadec-10-enone (**162**) (32.8 mg, 0.1468 mmol) in THF (0.6 mL) and the reaction was stirred for 18 hours at 70 °C. The reaction was cooled to 0 °C and a solution of THF (0.06 mL) and water (0.01 mL) was added and stirred for 15 minutes. Aqueous 3 M NaOH solution was added dropwise until a white precipitate formed and the solution was stirred for 15 minutes. The slurry was vacuum filtered through celite

and concentrated. Methyl acrylate (0.02 mL, 0.2 mmol) was added to a solution of the residue (25.3 mg) in methanol (0.24 mL) and the reaction was stirred for 29 hours. The reaction was concentrated and excess reagents were removed under vacuum. Purification of the residue by flash column chromatography with 20% ethyl acetate and 0.2% triethylamine in petroleum ether as eluant afforded **164** (28.0 mg, 65%) as a colourless oil.

R_f = 0.69 (petroleum ether-ethyl acetate 1:1);

IR (neat): 2999, 2924, 2853, 2803, 1744, 1462, 1435, 1196, 1171, 841 cm^{-1};

^1H NMR (500 MHz, $CDCl_3$) δ: 5.32 (dt, J = 10.8, 6.1 Hz, 1 H), 5.29 (dt, J = 10.8, 6.2 Hz, 1 H), 3.64 (s, 3 H), 2.66 (t, J = 7.0 Hz, 2 H), 2.39 (t, J = 7.1 Hz, 2 H), 2.31 (t, J = 5.5 Hz, 2 H), 2.27 (t, J = 5.5 Hz, 2 H), 1.99-2.06 (m, 4 H), 1.23-1.40 (m, 16 H);

^{13}C NMR (125 MHz, $CDCl_3$) δ: 173.43, 130.24, 53.98, 53.80, 51.46, 50.36, 32.74, 29.01,28.17, 27.50, 27.37, 27.23, 26.90, 26.59, 26.10, 26.07;

LRMS (EI) *m/z* (relative intensity): 295 (M^+, 37), 222 (100), 130 (37), 116 (44), 55 (26);

HRMS (EI) *m/z* calculated for $C_{18}H_{33}O_2N$: 295.2511, found: 295.2519;

Analysis calculated for $C_{18}H_{33}O_2N$: C, 73.17; H, 11.26; N, 4.74. Found: C, 73.57; H, 11.32; N, 4.95.

(b) Michael Addition of (*Z*/*E*)-Azacyclopentadec-7-ene (**167**) and (**168**)

Methyl acrylate (0.16 mL, 1.8 mmol) was added to a solution of (*Z*/*E*)-azacyclopentadec-7-ene (**167**) and (**168**) (177.0 mg, 0.8454 mmol) in methanol (1.7 mL) and the reaction was stirred for 29 hours. The reaction was concentrated and excess reagents were removed under vacuum. Purification of the residue (^1H NMR ratio **164**:**169**, 47:53) by flash column chromatography with 20% ethyl acetate and 1% triethylamine in petroleum ether as eluant afforded **164** (56.4 mg, 23%) with spectral data in agreement with that reported above, a mixture of **164** and **169** (77.5 mg, 31%) and **169** (30.9 mg, 12%) all as colourless oils.

169 (*E*)

R_f = 0.60 (petroleum ether-ethyl acetate 1:1);

IR (neat): 2926, 2853, 2804, 1742, 1462, 1435, 1198, 1173, 968, 839 cm^{-1};

^{1}H NMR (500 MHz, $CDCl_3$) δ: 5.30 (dt, J = 14.9, 2.7 Hz, 1 H), 5.27 (dt, J = 14.9, 2.5 Hz, 1 H), 3.63 (s, 3 H), 2.68 (t, J = 7.2 Hz, 2 H), 2.39 (t, J = 7.2 Hz, 2 H), 2.33 (t, J = 5.7 Hz, 2 H), 2.25 (t, J = 6.2 Hz, 2 H), 1.97-2.03 (m, 4 H), 1.20-1.39 (m, 16 H);

^{13}C NMR (125 MHz, $CDCl_3$) δ: 173.39, 131.13, 131.08, 54.02, 52.92, 51.40, 50.57, 32.61, 32.18, 31.83, 28.64, 28.11, 27.70, 27.67, 26.82, 26.56, 26.29, 26.19;

LRMS (EI) *m/z* (relative intensity): 295 (M^+, 38), 222 (100), 130 (28), 116 (34);

HRMS (EI) *m/z* calculated for $C_{18}H_{33}O_2N$: 295.2511, found: 295.2512;

Analysis calculated for $C_{18}H_{33}O_2N$: C, 73.17; H, 11.26; N, 4.74. Found: C, 73.46; H, 11.33; N, 5.00.

(*Z*/*E*)-Azacyclopentadec-7-ene (167) and (168)

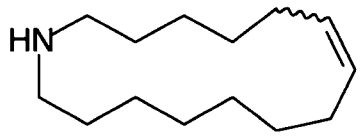

Lithium aluminum hydride (68.0 mg, 1.792 mmol) was added to a solution of a mixture of (*Z*/*E*)-2-azacyclopentadec-10-enone (**162**) and (**163**) (^{1}H NMR ratio **162**:**163**, 44:56) (200.0 mg, 0.8954 mmol) in THF (3.6 mL) and the reaction was stirred for 19 hours at 70 °C. The reaction was cooled to 0 °C and a solution of THF (0.34 mL) and water (0.07 mL) was added and stirred for 15 minutes. Aqueous 3 M NaOH solution was added dropwise until a white precipitate formed and the solution was stirred for 15 minutes. The slurry was vacuum filtered through celite and concentrated to afford a mixture of **167** and **168** (177.0 mg, 94%) as a pale yellow oil. This material was used in subsequent reactions without further purification.

R_f = 0.17 (petroleum ether-ethyl acetate-triethylamine 10:10:1);

IR (neat): 3317, 3001, 2926, 2853, 1666, 1652, 1460, 1130, 966 cm^{-1};

^{1}H NMR (200 MHz, $CDCl_3$) δ: 5.25-5.38 (m, 2 H), 2.49-2.67 (m, 4 H), 1.98-2.08 (m, 4 H), 1.22-1.80 (m, 17 H);

^{13}C NMR (50 MHz, $CDCl_3$) δ: 131.28, 131.12, 130.54, 130.06, 47.90, 47.41, 46.53, 31.69, 28.62, 28.34, 28.24, 27.73, 27.34, 26.83, 26.17, 25.93, 25.47, 24.75;

LRMS (EI) *m/z* (relative intensity): 209 (M^+, 96), 180 (23), 166 (44), 152 (26), 138 (24), 124 (24), 112 (46), 110 (40), 98 (54), 96 (52), 84 (59), 82 (35), 70 (80), 68 (21), 56 (100), 55 (71);

HRMS (EI) *m/z* calculated for $C_{14}H_{27}N$: 209.2144, found: 209.2142.

(*E/Z*)-2-Azacyclopentadec-11-enone (170) and (171)

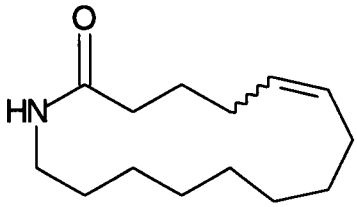

A solution of *N*-(9-decenyl)-5-hexenamide (**161**) (102.0 mg, 0.4057 mmol) in sparged CH_2Cl_2 (25.0 mL) and a solution of Grubbs' benzylidene (**3**) (16.7 mg, 0.0202 mmol) in sparged CH_2Cl_2 (25.0 mL) were added simultaneously using a syringe pump to sparged CH_2Cl_2 (153.0 mL) stirred at 45 °C over 3 hours. After the addition, the reaction was stirred for an additional 3 hours at 45 °C. The CH_2Cl_2 in the receiver flask was gently sparged with N_2 gas during the addition and reaction. The reaction was cooled to room temperature and triethylamine (2 mL) was added and stirred for 15 minutes. The solution was concentrated. Purification of the residue (GC ratio **170**:**171**, 53:47) by radial chromatography, using silver nitrate impregnated silica, with 40% ethyl acetate in petroleum ether as eluant afforded **170** (33.3 mg, 37%), a mixture of **170** and **171** (4.1 mg, 5%) and **171** (30.9 mg, 34%) all as white solids.

170 (*E*)

R_f = 0.23 (petroleum ether-ethyl acetate 1:1);

Melting point: 110.5-113.0 °C (ethyl acetate);

IR (CCl_4): 3448, 3350, 2930, 2856, 1682, 1504, 1456, 1441, 970 cm^{-1};

^1H NMR (500 MHz, $CDCl_3$) δ: 5.45 (bs, 1 H), 5.33 (dt, J = 15.4, 2.7 Hz, 1 H), 5.30 (dt, J = 15.1, 2.7 Hz, 1 H), 3.22 (dt, J = 5.4, 5.7 Hz, 2 H), 2.18 (t, J = 6.3 Hz, 2 H), 2.10 (dt, J = 6.2, 5.9 Hz, 2 H), 1.97 (q, J = 5.4 Hz, 2 H), 1.70-1.76 (m, 2 H), 1.38-1.43 (m, 2 H), 1.19-1.33 (m, 10 H);

^{13}C NMR (125 MHz, $CDCl_3$) δ: 172.94, 132.26, 130.00, 38.79, 34.48, 31.43, 31.42, 27.79, 27.53, 26.33, 26.13, 25.09, 23.69, 23.35;

LRMS (DCI(+), ammonia) *m/z* (relative intensity): 224 (M^++1, 100), 223 (M^+, 45);

HRMS (DCI(+), methane/ammonia) *m/z* calculated for $C_{14}H_{26}ON$ (M^++1): 224.2015, found: 224.2011;

Analysis calculated for $C_{14}H_{25}ON$: C, 75.28; H, 11.28; N, 6.27. Found: C, 75.48; H, 11.35; N, 6.22.

171 (*Z*)

R_f = 0.18 (petroleum ether-ethyl acetate 1:1);

Melting point: dec. 129.0 °C (ethyl acetate);

IR (CCl_4): 3452, 3350, 2930, 2858, 1682, 1504, 1456, 1441 cm^{-1};

^1H NMR (500 MHz, $CDCl_3$) δ: 5.59 (bs, 1 H), 5.38 (dt, J = 10.8, 7.7 Hz, 1 H), 5.25 (dt, J = 10.8, 6.5 Hz, 1 H), 3.28 (dt, J = 5.4, 5.8 Hz, 2 H), 2.17-2.19 (m, 2 H), 2.09 (dt, J = 7.6, 5.6 Hz, 2 H), 1.97 (q, J = 7.0 Hz, 2 H), 1.68-1.73 (m, 2 H), 1.46-1.51 (m, 2 H), 1.21-1.35 (m, 10 H);

^{13}C NMR (125 MHz, $CDCl_3$) δ: 172.89, 131.21, 129.51, 38.95, 35.37, 28.48, 27.94, 27.32, 26.97, 26.72, 26.69, 25.91, 25.42, 25.37;

LRMS (DCI(+), ammonia) *m/z* (relative intensity): 224 (M^++1, 100), 223 (M^+, 45);

HRMS (DCI(+), methane/ammonia) *m/z* calculated for $C_{14}H_{26}ON$ (M^++1): 224.2015, found: 224.2016;

Analysis calculated for $C_{14}H_{25}ON$: C, 75.28; H, 11.28; N, 6.27. Found: C, 75.59; H, 11.34; N, 6.21.

(*Z*)-Azacyclopentadec-6-ene (172)

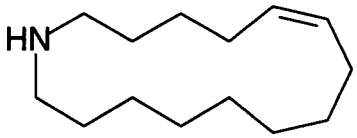

Lithium aluminum hydride (57.2 mg, 1.507 mmol) was added to a solution of (*Z*)-2-azacyclopentadec-11-enone (**171**) (168.4 mg, 0.7539 mmol) in THF (3.0 mL) and the reaction was stirred for 19 hours at 70 °C. The reaction was cooled to 0 °C and a solution of THF (0.28 mL) and water (0.06 mL) was added and stirred for 15 minutes. Aqueous 3 M NaOH solution was added dropwise until a white precipitate formed and the solution was stirred for 15 minutes. The slurry was vacuum filtered through celite and concentrated to afford **172** (137.6 mg, 87%) as a pale yellow oil. This material was used in subsequent reactions without further purification.

R_f = 0.0 (petroleum ether-ethyl acetate 1:1);

IR (neat): 3310, 3003, 2926, 2854, 1670, 1653, 1458, 1130, 717 cm^{-1};

^1H NMR (200 MHz, $CDCl_3$) δ: 5.36 (dt, J = 9.5, 4.6 Hz, 1 H), 5.32 (dt, J = 9.5, 4.9 Hz, 1 H), 2.61 (t, J = 5.8 Hz, 2 H), 2.60 (t, J = 6.5 Hz, 2 H), 1.92-2.08 (m, 4 H), 1.20-1.53 (m, 17 H);

^{13}C NMR (50 MHz, $CDCl_3$) δ: 125.13, 124.74, 42.23, 41.98, 23.08, 21.96, 21.85, 21.61, 21.49, 21.18, 21.09, 19.80;

LRMS (EI) *m/z* (relative intensity): 209 (M^+, 100), 208 (M^+-1, 41), 180 (28), 166 (51), 152 (23), 126 (20), 124 (23), 110 (30), 96 (32), 84 (32), 70 (23), 56 (22);

HRMS (EI) *m/z* calculated for $C_{14}H_{27}N$: 209.2144, found: 209.2143.

Methyl 3-((*Z*)-1-azacyclopentadec-6-enyl)propionate (173)

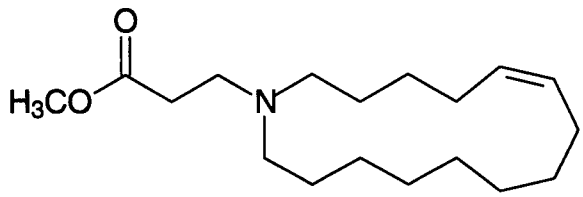

Methyl acrylate (0.12 mL, 1.3 mmol) was added to a solution of (*Z*)-azacyclopentadec-6-ene (**172**) (135.2 mg, 0.6457 mmol) in methanol (1.3 mL) and the reaction was stirred for 26 hours. The reaction was concentrated and excess reagents were removed under vacuum. Purification of the residue by flash column chromatography with 30% ethyl acetate and 0.2% triethylamine in petroleum ether as eluant afforded **173** (137.8 mg, 72%) as a colourless oil.

R_f = 0.64 (petroleum ether-ethyl acetate 1:1);

IR (neat): 3001, 2928, 2854, 2804, 1742, 1462, 1435, 1198, 1173, 841, 716 cm^{-1};

^1H NMR (200 MHz, $CDCl_3$) δ: 5.35 (dt, J = 9.0, 4.4 Hz, 1 H), 5.28 (dt, J = 9.0, 4.4 Hz, 1 H), 3.62 (s, 3 H), 2.68 (t, J = 7.1 Hz, 2 H), 2.38 (t, J = 7.3 Hz, 2 H), 2.30 (t, J = 6.0 Hz, 4 H), 1.96-2.05 (m, 4 H), 1.22-1.45 (m, 16 H);

^{13}C NMR (50 MHz, $CDCl_3$) δ: 173.35, 130.24, 53.94, 52.80, 51.39, 50.53, 32.54, 28.19, 27.73, 27.61, 27.29, 27.20, 27.17, 26.95, 26.72, 25.90, 25.66;

LRMS (EI) *m/z* (relative intensity): 295 (M^+, 37), 222 (100), 194 (20), 182 (29), 130 (22), 116 (28);

HRMS (EI) *m/z* calculated for $C_{18}H_{33}O_2N$: 295.2511, found: 295.2510;

Analysis calculated for $C_{18}H_{33}O_2N$: C, 73.17; H, 11.26; N, 4.74. Found: C, 73.23; H, 11.20; N, 4.90.

REFERENCES

1 Borman, S. *Chem. Eng. News* **2000**, *78* (5), 7.

2 For selected reviews on RCM see: (a) Grubbs, R. H.; Miller, S. J.; Fu, G. C. *Acc. Chem. Res.* **1995**, *28*, 446. (b) Schmalz, H.-G. *Angew. Chem. Int. Ed. Engl.* **1995**, *34*, 1833. (c) Fürstner, A. *Top. Catal.* **1997**, *4*, 285. (d) Schuster, M.; Blechert, S. *Angew. Chem. Int. Ed. Engl.* **1997**, *36*, 2036. (e) Fürstner, A. *Top. Organomet. Chem.* **1998**, *1*, 37. (f) Grubbs, R. H.; Chang, S. *Tetrahedron* **1998**, *54*, 4413.

3 Avis, W. S.; Drysdale, P. D.; Gregg, R. J.; Neufeldt, V. E.; Scargill, M. H. *Gage Canadian Dictionary*; Gage Educational Publishing Company: Toronto, 1983, p 720.

4 Villemin, D. *Tetrahedron Lett.* **1980**, *21*, 1715.

5 Tsuji, J.; Hashiguchi, S. *Tetrahedron Lett.* **1980**, *21*, 2955.

6 Tsuji, J.; Hashiguchi, S. *J. Organometal. Chem.* **1981**, *218*, 69.

7 Levisalles, J.; Rudler, H.; Cuzin, D.; Rull, T. *J. Mol. Catal.* **1984**, *26*, 231.

8 Schrock, R. R.; Murdzek, J. S.; Bazan, G. C.; Robbins, J.; DiMare, M.; O'Regan, M. *J. Am. Chem. Soc.* **1990**, *112*, 3875.

9 Nguyen, S. T.; Grubbs, R. H.; Ziller, J. W. *J. Am. Chem. Soc.* **1993**, *115*, 9858.

10 Schwab, P.; France, M. B.; Ziller, J. W.; Grubbs, R. H. *Angew. Chem. Int. Ed. Engl.* **1995**, *34*, 2039.

11 Schwab, P.; Grubbs, R. H.; Ziller, J. W. *J. Am. Chem. Soc.* **1996**, *118*, 100.

12 Kirkland, T. A.; Lynn, D. M.; Grubbs, R. H. *J. Org. Chem.* **1998**, *63*, 9904.

13 Kingsbury, J. S.; Harrity, J. P. A.; Bonitatebus, Jr., P. J.; Hoveyda, A. H. *J. Am. Chem. Soc.* **1999**, *121*, 791.

14 Fürstner, A.; Picquet, M.; Bruneau, C.; Dixneuf, P. H. *J. Chem. Soc., Chem. Commun.* **1998**, 1315.

15 For examples and applications of chiral molybdenum alkylidene complexes see: (a) Fujimura, O.; Grubbs, R. H. *J. Org. Chem.* **1998**, *63*, 824. (b) Alexander, J. B.; La, D. S.; Cefalo, D. R.; Hoveyda, A. H.; Schrock, R. R. *J. Am. Chem. Soc.* **1998**, *120*, 4041. (c) La, D. S.; Alexander, J. B.; Cefalo, D. R.; Graf, D. D.; Hoveyda, A. H.; Schrock, R. R. *J. Am. Chem. Soc.* **1998**, *120*, 9720.

16 Hérisson, J.-L.; Chauvin, Y. *Makromol. Chem.* **1970**, *141*, 161.

17 Crowe, W. E.; Zhang, Z. J. *J. Am. Chem. Soc.* **1993**, *115*, 10998.

18 Kirkland, T. A.; Grubbs, R. H. *J. Org. Chem.* **1997**, *62*, 7310.

19 Junga, H.; Blechert, S. *Tetrahedron Lett.* **1993**, *34*, 3731.

20 Fu, G. C.; Grubbs, R. H. *J. Am. Chem. Soc.* **1992**, *114*, 5426.

21 Fu, G. C.; Grubbs, R. H. *J. Am. Chem. Soc.* **1992**, *114*, 7324.

22 Fu, G. C.; Grubbs, R. H. *J. Am. Chem. Soc.* **1993**, *115*, 3800.

23 For recent reviews of the RCM reaction applied to the synthesis of macrocyclic compounds see: (a) Nicolaou, K. C.; King, N. P.; He, Y. *Top. Organomet. Chem.* **1998**, *1*, 73. (b) Hoveyda, A. H. *Top. Organomet. Chem.* **1999**, *1*, 105.

24 For examples of studies and applications of RCM in the total synthesis of Sch 38516 (Fluvirucin B_1) see: (a) Houri, A. F.; Xu, Z.; Cogan, D. A.; Hoveyda, A. H. *J. Am. Chem. Soc.* **1995**, *117*, 2943. (b) Xu, Z.; Johannes, C. W.; Salman, S. S.; Hoveyda, A. H. *J. Am. Chem. Soc.* **1996**, *118*, 10926. (c) Xu, Z.; Johannes, C. W.; Houri, A. F.; La, D. S.; Cogan, D. A.; Hofilena, G. E.; Hoveyda, A. H. *J. Am. Chem. Soc.* **1997**, *119*, 10302.

25 For examples of studies and applications of RCM towards the total synthesis of manzamine A see: (a) Martin, S. F.; Liao, Y.; Wong, Y.; Rein, T. *Tetrahedron Lett.* **1994**, *35*, 691. (b) Borer, B. C.; Deerenberg, S.; Bieräugel, H.; Pandit, U. K. *Tetrahedron Lett.* **1994**, *35*, 3191. (c) Pandit, U. K.; Borer, B. C.; Bieräugel, H. *Pure Appl. Chem.* **1996**, *68*, 659. (d) Martin, S. F.; Chen, H.-J.; Courtney, A. K.; Liao, Y.; Pätzel, M.; Ramser, M. N.; Wagman, A. S. *Tetrahedron* **1996**, *52*, 7251. (e) Martin, S. F.; Humphrey, J. M.; Ali, A.; Hillier, M. C. *J. Am. Chem. Soc.* **1999**, *121*, 866.

26 Miller, S. J.; Grubbs, R. H. *J. Am. Chem. Soc.* **1995**, *117*, 5855.

27 Miller, S. J.; Blackwell, H. E.; Grubbs, R. H. *J. Am. Chem. Soc.* **1996**, *118*, 9606.

28 Ravi, A.; Balaram, P. *Tetrahedron* **1984**, *40*, 2577.

29 Pernerstorfer, J.; Schuster, M.; Blechert, S. *J. Chem. Soc., Chem. Commun.* **1997**, 1949.

30 For applications of solid phase cyclization/cleavage RCM strategies in the construction of seven-membered lactams see: (a) van Maarseveen, J. H.; den Hartog, J. A. J.; Engelen, V.; Finner, E.; Visser, G.; Kruse, C. G. *Tetrahedron Lett.* **1996**, *37*, 8249. (b) Piscopio, A. D.; Miller, J. F.; Koch, K. *Tetrahedron Lett.* **1997**, *38*, 7143. (c) Piscopio, A. D.; Miller, J. F.; Koch, K. *Tetrahedron Lett.* **1998**, *39*, 2667.

31 Miller, S. J.; Kim, S.-H.; Chen, Z.-R.; Grubbs, R. H. *J. Am. Chem. Soc.* **1995**, *117*, 2108.

32 Zuercher, W. J.; Hashimoto, M.; Grubbs, R. H. *J. Am. Chem. Soc.* **1996**, *118*, 6634.

33 Clark, T. D.; Ghadiri, M. R. *J. Am. Chem. Soc.* **1995**, *117*, 12364.

34 Edwige, C.; Lattes, A.; Laval, J. P.; Mutin, R.; Basset, J. M.; Nouguier, R. *J. Mol. Catal.* **1980**, *8*, 297.

35 Shon, Y.-S.; Lee, T. R. *Tetrahedron Lett.* **1997**, *38*, 1283.

36 Chang, S.; Grubbs, R. H. *Tetrahedron Lett.* **1997**, *38*, 4757.

37 Meyer, C.; Cossy, J. *Tetrahedron Lett.* **1997**, *38*, 7861.

38 Evans, P. A.; Murthy, V. S. *J. Org. Chem.* **1998**, *63*, 6768.

39 Hoye, T. R.; Promo, M. A. *Tetrahedron Lett.* **1999**, *40*, 1429.

40 Hanson, P. R.; Stoianova, D. S. *Tetrahedron Lett.* **1998**, *39*, 3939.

41 Renaud, J.; Ouellet, S. G. *J. Am. Chem. Soc.* **1998**, *120*, 7995.

42 Linderman, R. J.; Siedlecki, J.; O'Neill, S. A.; Sun, H. *J. Am. Chem. Soc.* **1997**, *119*, 6919.

43 Fürstner, A.; Langemann, K. *J. Org. Chem.* **1996**, *61*, 3942.

44 Litinas, K. E.; Salteris, B. E. *J. Chem. Soc., Perkin Trans. 1* **1997**, 2869.

45 Fürstner, A.; Langemann, K. *Synthesis* **1997**, 792.

46 Arakawa, K.; Eguchi, T.; Kakinuma, K. *J. Org. Chem.* **1998**, *63*, 4741.

47 König, B.; Horn, C. *Synlett* **1996**, 1013.

48 Delgado, M.; Martín, J. D. *Tetrahedron Lett.* **1997**, *38*, 8387.

49 Descotes, G.; Ramza, J.; Basset, J.-M.; Pagano, S.; Gentil, E.; Banoub, J. *Tetrahedron* **1996**, *52*, 10903.

50 Huber-Buser, E.; Dunitz, J. D.; Venkatesan, K. *Proc. Chem. Soc.* **1961**, 463.

51 Dale, J. *J. Chem. Soc.* **1963**, 93.

52 Dale, J. *Acta Chem. Scand.* **1973**, *27*, 1115.

53 Groth, P. *Acta Chem. Scand. A* **1976**, *30*, 155.

54 (a) Borgen, G.; Dale, J. *J. Chem. Soc., Chem. Commun.* **1970**, 1340. (b) Anet, F. A. L.; Cheng, A. K.; Wagner, J. J. *J. Am. Chem. Soc.* **1972**, *94*, 9250.

55 Dale, J. *Acta Chem. Scand.* **1973**, *27*, 1149.

56 Dale, J. *Angew. Chem. Int. Ed. Engl.* **1966**, *5*, 1000.

57 For examples of studies and applications of RCM in the total synthesis of epothilone A see: (a) Nicolaou, K. C.; He, Y.; Vourloumis, D; Vallberg, H.; Yang, Z. *Angew. Chem. Int. Ed. Engl.* **1996**, *35*, 2399. (b) Bertinato, P.; Sorensen, E. J.; Meng, D.; Danishefsky, S. J. *J. Org. Chem.* **1996**, *61*, 8000. (c) Yang, Z.; He, Y.; Vourloumis, D.; Vallberg, H.; Nicolaou, K. C. *Angew. Chem. Int. Ed. Engl.* **1997**, *36*, 166. (d) Meng, D.; Su, D.-S.; Balog, A.; Bertinato, P.; Sorensen, E. J.; Danishefsky, S. J.; Zheng, Y.-H.; Chou, T.-C.; He, L.; Horwitz, S. B. *J. Am. Chem. Soc.* **1997**, *119*, 2733. (e) Schinzer, D.; Limberg, A.; Bauer, A.; Böhm, O. M.; Cordes, M. *Angew. Chem. Int. Ed. Engl.* **1997**, *36*, 523. (f) Nicolaou, K. C.; Winssinger, N.; Pastor, J.; Ninkovic, S.; Sarabia, F.; He, Y.; Vourloumis, D.; Yang, Z.; Li, T.; Giannakakou, P.; Hamel, E. *Nature* **1997**, *387*, 268. (g) Nicolaou, K. C.; He, Y.; Vourloumis, D.; Vallberg, H.; Roschangar, F.; Sarabia, F.; Ninkovic, S.; Yang, Z.; Trujillo, J. I. *J. Am. Chem. Soc.* **1997**, *119*, 7960. (h) Meng, D.; Bertinato, P.; Balog, A.; Su, D.-S.; Kamenecka, T.; Sorensen, E. J.; Danishefsky, S. J. *J. Am. Chem. Soc.* **1997**, *119*, 10073. (i) Schinzer, D.; Bauer, A.; Böhm, O. M.; Limberg, A.; Cordes, M. *Chemistry-A European Journal* **1999**, *5*, 2483.

58 Williams, D. E.; Lassota, P.; Andersen, R. J. *J. Org. Chem.* **1998**, *63*, 4838.

59 De Silva, E. D.; Williams, D. E.; Andersen, R. J.; Klix, H.; Holmes, C. F. B.; Allen, T. M. *Tetrahedron Lett.* **1992**, *33*, 1561.

60 Kong, F.; Andersen, R. J.; Allen, T. M. *Tetrahedron Lett.* **1994**, *35*, 1643.

61 Kong, F.; Andersen, R. J.; Allen, T. M. *J. Am. Chem. Soc.* **1994**, *116*, 6007.

62 Baldwin, J. E.; Whitehead, R. C. *Tetrahedron Lett.* **1992**, *33*, 2059.

63 Baldwin, J. E.; Claridge, T. D. W.; Culshaw, A. J.; Heupel, F. A.; Lee, V.; Spring, D. R.; Whitehead, R. C.; Boughtflower, R. J.; Mutton, I. M.; Upton, R. J. *Angew. Chem. Int. Ed. Engl.* **1998**, *37*, 2661.

64 Sakai, R.; Kohmoto, S.; Higa, T.; Jefford, C. W.; Bernardinelli, G. *Tetrahedron Lett.* **1987**, *28*, 5493.

65 Tsuda, M.; Kawasaki, N.; Kobayashi, J. *Tetrahedron Lett.* **1994**, *35*, 4387.

66 Koren-Goldshlager, G.; Kashman, Y.; Schleyer, M. *J. Nat. Prod.* **1998**, *61*, 282.

67 Kashman, Y.; Koren-Goldshlager, G.; Gravalos, M. D. G.; Schleyer, M. *Tetrahedron Lett.* **1999**, *40*, 997.

68 Silverstein, R. M.; Bassler, G. C.; Morrill, T. C. *Spectrometric Identification of Organic Compounds*; 5th ed.; John Wiley & Sons, Inc.: New York, 1991, p 208.

69 Goldring, W. P. D.; Weiler, L. *Org. Lett.* **1999**, *1*, 1471.

70 Baldwin, J. E.; Vollmer, H. R.; Lee, V. *Tetrahedron Lett.* **1999**, *40*, 5401.

71 Fürstner, A.; Rumbo, A. *J. Org. Chem.* **2000**, *65*, 2608.

72 Goldring, W. P. D.; Hodder, A. S.; Weiler, L. *Tetrahedron Lett.* **1998**, *39*, 4955.

73 Rukunga, G. M.; Waterman, P. G. *Phytochemistry* **1996**, *42*, 1211.

74 Kuroki, Y.; Ishihara, K.; Hanaki, N.; Ohara, S.; Yamamoto, H. *Bull. Chem. Soc. Jpn.* **1998**, *71*, 1221.

75 Horni, A.; Linden, A.; Hesse, M. *Helv. Chim. Acta* **1998**, *81*, 1303.

76 Pak, J. K.; Hesse, M. *J. Org. Chem.* **1998**, *63*, 8200.

77 For two examples see: Miyashita, M; Sato, H.; Matsushita, M; Kusumegi, Y.; Toki, T.; Yoshikoshi, A.; Yanami, T.; Kikuchi, Y.; Takasaki, C.; Nakajima, T.; Irie, H. *Tetrahedron Lett.* **1992**, *33*, 2837.

78 Tomalia, D. A.; Baker, H.; Dewald, J.; Hall, M.; Kallos, G.; Martin, S., Roeck, J.; Ryder, J.; Smith, P. *Macromolecules* **1986**, *19*, 2466.

79 El Sukkari, H.; Gesson, J.-P.; Renoux, B. *Tetrahedron Lett.* **1998**, *39*, 4043.

80 Ghosh, A. K.; Hussain, K. A. *Tetrahedron Lett.* **1998**, *39*, 1881.

81 Williams, R. M.; Liu, J. *J. Org. Chem.* **1998**, *63*, 2130.

82 For a similar synthesis of the symmetrical isomer (2S,7S)-2,7-diaminosuberic acid see: O'Leary, D. J.; Miller, S. J.; Grubbs, R. H. *Tetrahedron Lett.* **1998**, *39*, 1689.

83 Fürstner, A.; Koch, D.; Langemann, K.; Leitner, W.; Six, C. *Angew. Chem. Int. Ed. Engl.* **1997**, *36*, 2466.

84 For studies of the synthesis and conformational analysis of 14-membered cyclic ethers see: (a) Clyne, D. S. Ph. D. Thesis, University of British Columbia, January, 1998. (b) Clyne, D. S.; Weiler, L. *Tetrahedron* **1999**, *55*, 13659. (c) Clyne, D. S.; Weiler, L. *Tetrahedron* **2000**, *56*, 1281.

85 Lermer, L. Ph. D. Thesis, University of British Columbia, April, 1999.

86 Still, W. C.; Galynker, I. *Tetrahedron* **1981**, *37*, 3981.

87 Levisalles, J.; Villemin, D. *Tetrahedron* **1980**, *36*, 3181.

88 Grubbs, R. H., California Institute of Technology, personal communication, 1996.

89 Feldman, J.; Murdzek, J. S.; Davis, W. M.; Schrock, R. R. *Organometallics* **1989**, *8*, 2260.

90 Rutjes, F. P. J. T.; Schoemaker, H. E. *Tetrahedron Lett.* **1997**, *38*, 677.

91 For other examples of RCM using substrates containing an ammonium salt see: (a) Birman, V. B.; Rawal, V. H. *J. Org. Chem.* **1998**, *63*, 9146. (b) Fürstner, A.; Grabowski, J.; Lehmann, C. W. *J. Org. Chem.* **1999**, *64*, 8275.

92 Pierce, M. E.; Harris, G. D.; Islam, Q.; Radesca, L. A.; Storace, L.; Waltermire, R. E.; Wat, E.; Jadhav, P. K.; Emmett, G. C. *J. Org. Chem.* **1996**, *61*, 444.

93 Lampe, J. W.; Hughes, P. F.; Biggers, C. K.; Smith, S. H.; Hu, H. *J. Org. Chem.* **1996**, *61*, 4572.

94 Johnstone, R. A. W.; Rose, M. E. *Tetrahedron* **1979**, *35*, 2169.

95 Koziara, A.; Zawadzki, S.; Zwierzak, A. *Synthesis* **1979**, 527.

96 Pietzonka, T.; Seebach, D. *Angew. Chem. Int. Ed. Engl.* **1992**, *31*, 1481.

97 This compound was first prepared in our laboratory by Spracklin, D. K. Ph. D. Thesis, University of British Columbia, November, 1994.

98 Bald, E.; Saigo, K.; Mukaiyama, T. *Chem. Lett.* **1975**, 1163.

99 (a) Harrity, J. P. A.; Visser, M. S.; Gleason, J. D.; Hoveyda, A. H. *J. Am. Chem. Soc.* **1997**, *119*, 1488. (b) Harrity, J. P. A.; La, D. S.; Cefalo, D. R.; Visser, M. S.; Hoveyda, A. H. *J. Am. Chem. Soc.* **1998**, *120*, 2343.

100 This compound was first prepared in our laboratory using an alternate route by Spracklin, D. K. Ph. D. Thesis, University of British Columbia, November, 1994.

101 Gagné, M. R.; Stern, C. L.; Marks, T. J. *J. Am. Chem. Soc.* **1992**, *114*, 275.

102 This compound was first prepared in our laboratory by Clyne, D. S. Ph. D. Thesis, University of British Columbia, January, 1998.

103 Crowe, W. E.; Goldberg, D. R. *J. Am. Chem. Soc.* **1995**, *117*, 5162.

104 Visser, M. S.; Heron, N. M.; Didiuk, M. T.; Sagal, J. F., Hoveyda, A. H. *J. Am. Chem. Soc.* **1996**, *118*, 4291.

105 Oishi, T.; Nagumo, Y.; Hirama, M. *J. Chem. Soc., Chem. Commun.* **1998**, 1041.

106 Gibson, S. E.; Gibson, V. C.; Keen, S. P. *J. Chem. Soc., Chem. Commun.* **1997**, 1107.

107 Mohamadi, F.; Richards, N. G. J.; Guida, W. C.; Liskamp, R.; Lipton, M.; Caufield, C.; Chang, G.; Hendrickson, T.; Still, W. C. *J. Comput. Chem.* **1990**, *11*, 440.

108 See reference 68, p 221.

109 It is interesting to note that the opposite order, represented by the relationship $\delta_{\alpha(Z)} > \delta_{\alpha(E)}$, was provided in reference 68, p 238. However, the relationship $\delta_{\alpha(E)} > \delta_{\alpha(Z)}$ was proven to be correct after inspection of the data presented in this and other texts (see reference 110).

110 Breitmaier, E.; Voelter, W. *Carbon-13 NMR Spectroscopy*; 3rd ed.; VCH Publishers: New York, 1987, p 116 and 193.

111 Grant, D. M.; Cheney, B. V. *J. Am. Chem. Soc.* **1967**, *89*, 5315.

112 Clark, J. S.; Kettle, J. G. *Tetrahedron Lett.* **1997**, *38*, 123.

113 Joe, D.; Overman, L. E. *Tetrahedron Lett.* **1997**, *38*, 8635.

114 For a discussion of the use of polar maps in conformational analysis see: Ounsworth, J. P.; Weiler, L. *J. Chem. Ed.* **1987**, *64*, 568.

115 Dias, E. L.; Nguyen, S. T.; Grubbs, R. H. *J. Am. Chem. Soc.* **1997**, *119*, 3887.

116 Dias, E. L.; Grubbs, R. H. *Organometallics* **1998**, *17*, 2758.

117 Fürstner, A.; Langemann, K. *J. Am. Chem. Soc.* **1997**, *119*, 9130.

118 Ghosh, A. K.; Cappiello, J.; Shin, D. *Tetrahedron Lett.* **1998**, *39*, 4651.

119 Schuster, M.; Pernerstorfer, J.; Blechert, S. *Angew. Chem. Int. Ed. Engl.* **1996**, *35*, 1979.

120 Barrett, A. G. M.; Baugh, S. P. D.; Gibson, V. C.; Giles, M. R.; Marshall, E. L.; Procopiou, P. A. *J. Chem. Soc., Chem. Commun.* **1996**, 2231.

121 Sauriat-Dorizon, H.; Guibé, F. *Tetrahedron Lett.* **1998**, *39*, 6711.

122 Barrett, A. G. M.; Baugh, S. P. D.; Braddock, D. C.; Flack, K.; Gibson, V. C.; Giles, M. R.; Marshall, E. L.; Procopiou, P. A.; White, A. J. P.; Williams, D. J. *J. Org. Chem.* **1998**, *63*, 7893.

123 Kim, S.-H.; Zuercher, W. J.; Bowden, N. B.; Grubbs, R. H. *J. Org. Chem.* **1996**, *61*, 1073.

124 Huwe, C. M.; Velder, J.; Blechert, S. *Angew. Chem. Int. Ed. Engl.* **1996**, *35*, 2376.

125 Wilkinson, G., Ed. *Comprehensive Coordination Chemistry*; Vol. 5; Pergamon Press: New York, 1987.

126 Fujimura, O.; Fu, G. C.; Rothemund, P. W. K.; Grubbs, R. H. *J. Am. Chem. Soc.* **1995**, *117*, 2355.

127 Martin, S. F.; Liao, Y.; Chen, H.-J.; Pätzel, M.; Ramser, M. N. *Tetrahedron Lett.* **1994**, *35*, 6005.

128 Zuercher, W. J.; Scholl, M.; Grubbs, R. H. *J. Org. Chem.* **1998**, *63*, 4291.

129 HyperChem™; Version 3; Hypercube, Inc. and Autodesk, Inc., Waterloo, Ontario, Canada, 1993.

130 Pauling, L. *The Nature of the Chemical Bond*; Cornell University Press, 1960.

131 Fersht, A. R. *J. Am. Chem. Soc.* **1971**, *93*, 3504.

132 Huwe, C. M.; Kiehl, O. C.; Blechert, S. *Synlett* **1996**, 65.

133 Wiberg, K. B.; Bader, R. F. W.; Lau, C. D. H. *J. Am. Chem. Soc.* **1987**, *109*, 1001.

134 Zhang, L.; Jung, D.-Y.; Bittner, E. R.; Sommer, M. S.; Dias, E. L.; Lee, T. R. *J. Org. Chem.* **1998**, *63*, 8624.

135 For examples of chelation effects used in the RCM of macrocyclic compounds see: (a) Marsella, M. J.; Maynard, H. D.; Grubbs, R. H. *Angew. Chem. Int. Ed. Engl.* **1997**, *36*, 1101. (b) Mohr, B.; Weck, M.; Sauvage, J.-P.; Grubbs, R. H. *Angew. Chem. Int. Ed. Engl.* **1997**, *36*, 1308. (c) Dietrich-Buchecker, C.; Rapenne, G.; Sauvage, J.-P. *J. Chem. Soc., Chem. Commun.* **1997**, 2053. (d) Ng, P. L.; Lambert, J. N. *Synlett* **1999**, 1749.

136 Morehead, Jr., A.; Grubbs, R. *J. Chem. Soc., Chem. Commun.* **1998**, 275.

137 Crimmins, M. T.; Choy, A. L. *J. Org. Chem.* **1997**, *62*, 7548.

138 Illuminati, G.; Mandolini, L.; *Acc. Chem. Res.* **1981**, *14*, 95.

139 Irie, O.; Samizu, K.; Henry, J. R.; Weinreb, S. M. *J. Org. Chem.* **1999**, *64*, 587.

140 Curtin, D. Y. *Rec. Chem. Prog.* **1954**, *15*, 111.

141 Levine, I. N. *Physical Chemistry*; 3rd ed.; McGraw-Hill, Inc.: New York, 1988, p 779.

142 Fürstner, A., Müller, T. *J. Org. Chem.* **1998**, *63*, 424.

143 Fürstner, A. *Top. Organomet. Chem.* **1998**, *1*,37.

144 For examples of the serendipitous and exclusive formation of an (*E*)-alkene in the formation of a macrocyclic compound via RCM see: (a) References 26, 27, and 47. (b) Kim, S. H.; Figueroa, I.; Fuchs, P. L. *Tetrahedron Lett.* **1997**, *38*, 2601.

145 For other examples of the serendipitous and exclusive formation of a (*Z*)-alkene in the formation of a macrocyclic compound via RCM see: (a) References 25b, 25c, 25e, 80, and 135d. (b) Nishioka, T.; Iwabuchi, Y.; Irie, H.; Hatakeyama, S. *Tetrahedron Lett.* **1998**, *39*, 5597.

146 This compound was first prepared in our laboratory using an alternate method by Lermer, L. Ph. D. Thesis, University of British Columbia, April, 1999.

147 This compound was first prepared in our laboratory using an alternate route by Lermer, L. Ph. D. Thesis, University of British Columbia, April, 1999.

148 For a more thorough explanation of these two shielding effects see reference 85, p 122-128.

149 Williams, D. E., University of British Columbia, personal communication, 2000.

150 Galán, A.; De Mendoza, J.; Prados, P.; Rojo, J.; Echavarren, A. M. *J. Org. Chem.* **1991**, *56*, 452.

151 Freifelder, M. *J. Am. Chem. Soc.* **1960**, *82*, 2386.

152 Grivas, J. C.; Taurins, A. *Can. J. Chem.* **1961**, *39*, 761.

153 Rousselet, G.; Capdevielle, P.; Maumy, M. *Org. Synth.* **1998**, *76*, 133.

154 Morris, L. J. *Chem. Ind.* **1962**, 1238.

155 Fürstner, A.; Seidel, G. *Angew. Chem. Int. Ed. Engl.* **1998**, *37*,1734.

156 Fürstner, A.; Guth, O.; Rumbo, A.; Seidel, G. *J. Am. Chem. Soc.* **1999**, *121*, 11108.

157 Kofron, W. G.; Baclawski, L. M. J. *J. Org. Chem.* **1976**, *41*, 1879.

158 Eisenbraun, E. J. *Org. Synth.* **1965**, *45*, 28.

159 Stephenson, T. A.; Wilkinson, G. *J. Inorg. Nucl. Chem.* **1966**, *28*, 945.

160 Perrin, D. D.; Armarego, W. L. F. *Purification of Laboratory Chemicals*; 3rd ed.; Pergamon Press: New York, 1988.

161 Still, W. C.; Kahn, M.; Mitra, A. *J. Org. Chem.* **1978**, *43*, 2923.

162 Allinger, N. L.; Yuh, Y. H.; Lii, J.-H. *J. Am. Chem. Soc.* **1989**, *111*, 8551.

163 Polak, E.; Ribiere, G. *Revue Francaise Informat. Recherche Operationelle* **1969**, *16*, 35.

164 Goodman, J. M.; Still, W. C. *J. Comput. Chem.* **1991**, *12*, 1110.

SPECTRAL APPENDIX

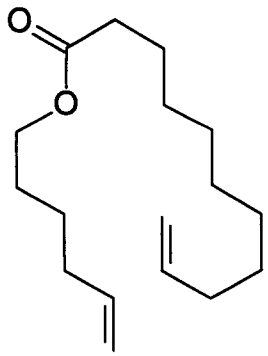

5

Integral
2.0003
3.9998
2.0010
5.9980
16.001
7.5 7.0 6.5 6.0 5.5 5.0 4.5 4.0 3.5 3.0 2.5 2.0 1.5 1.0 0.5
(ppm)

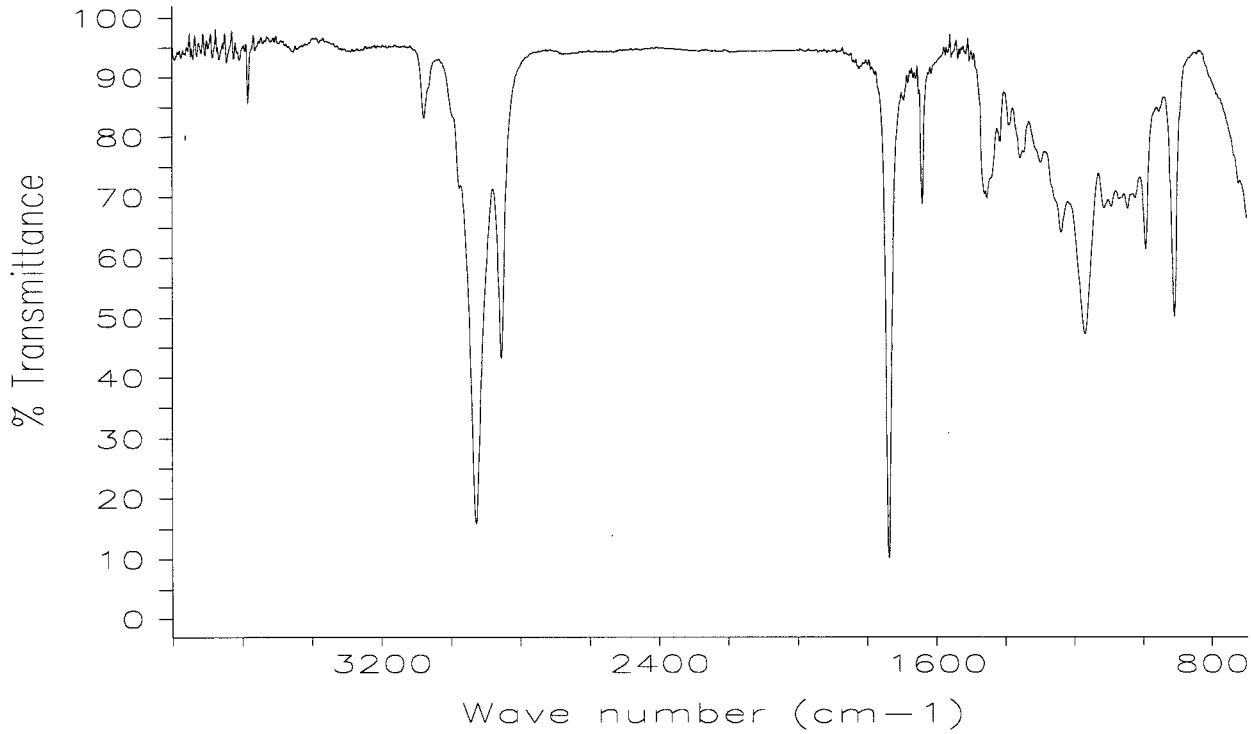
% Transmittance
100
90
80
70
60
50
40
30
20
10
0
3200
2400
1600
800
Wave number (cm−1)

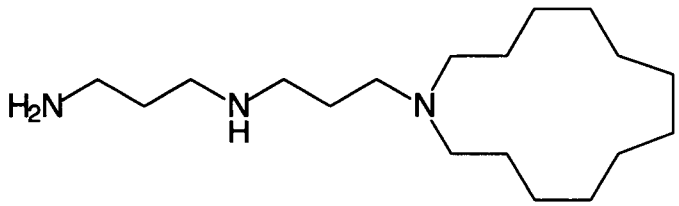
H2N
N
H
N

33

Int egral
7. 0000
6. 0007
26. 001
5.6
5.2
4.8
4.4
4.0
3.6
3.2
2.8
2.4
2.0
1.6
1.2
0.8
0.4
(ppm)

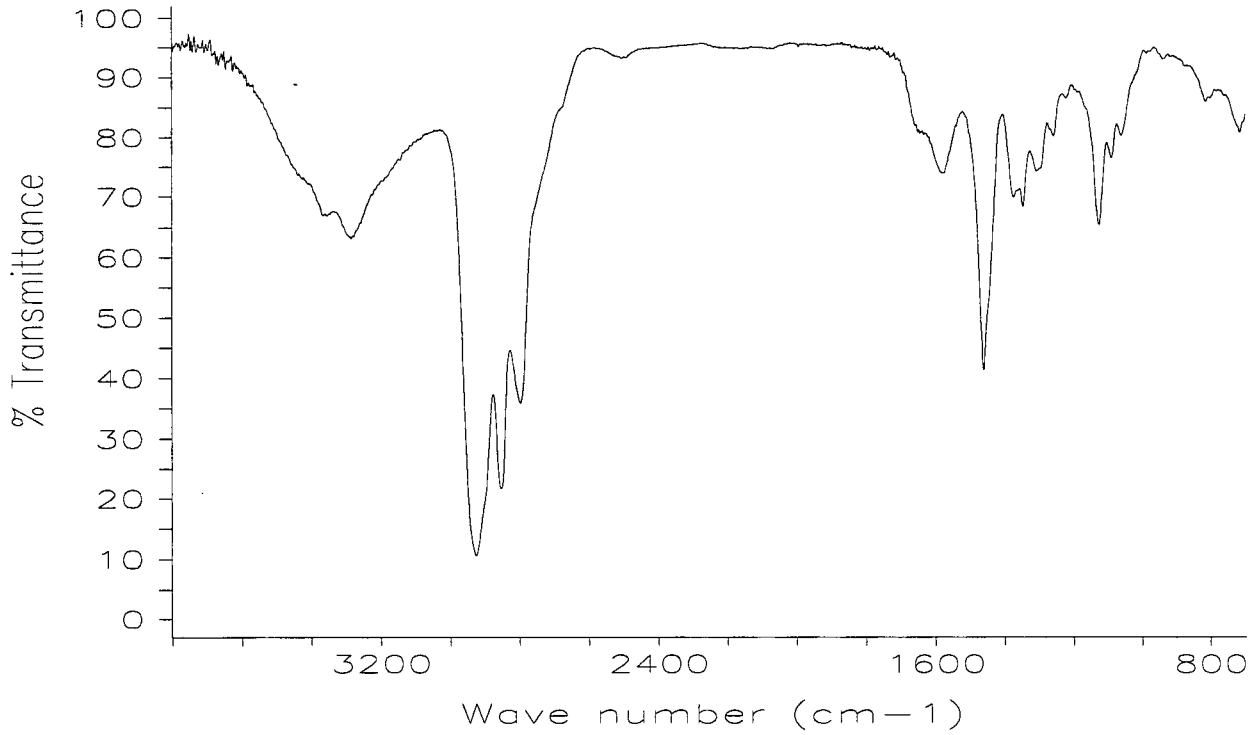
% Transmittance
100
90
80
70
60
50
40
30
20
10
0
3200
2400
1600
800
Wave number (cm−1)

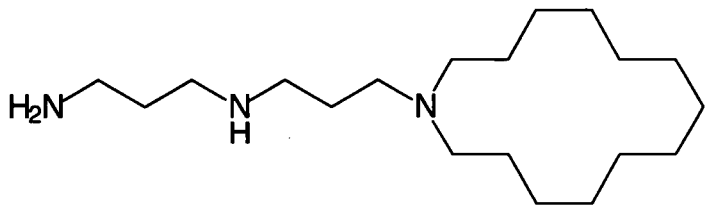
H2N
N
H
N

34

Integrial
6.9999
6.0003
28.000
5.6
5.2
4.8
4.4
4.0
3.6
3.2
2.8
2.4
2.0
1.6
1.2
0.8
0.4
(ppm)

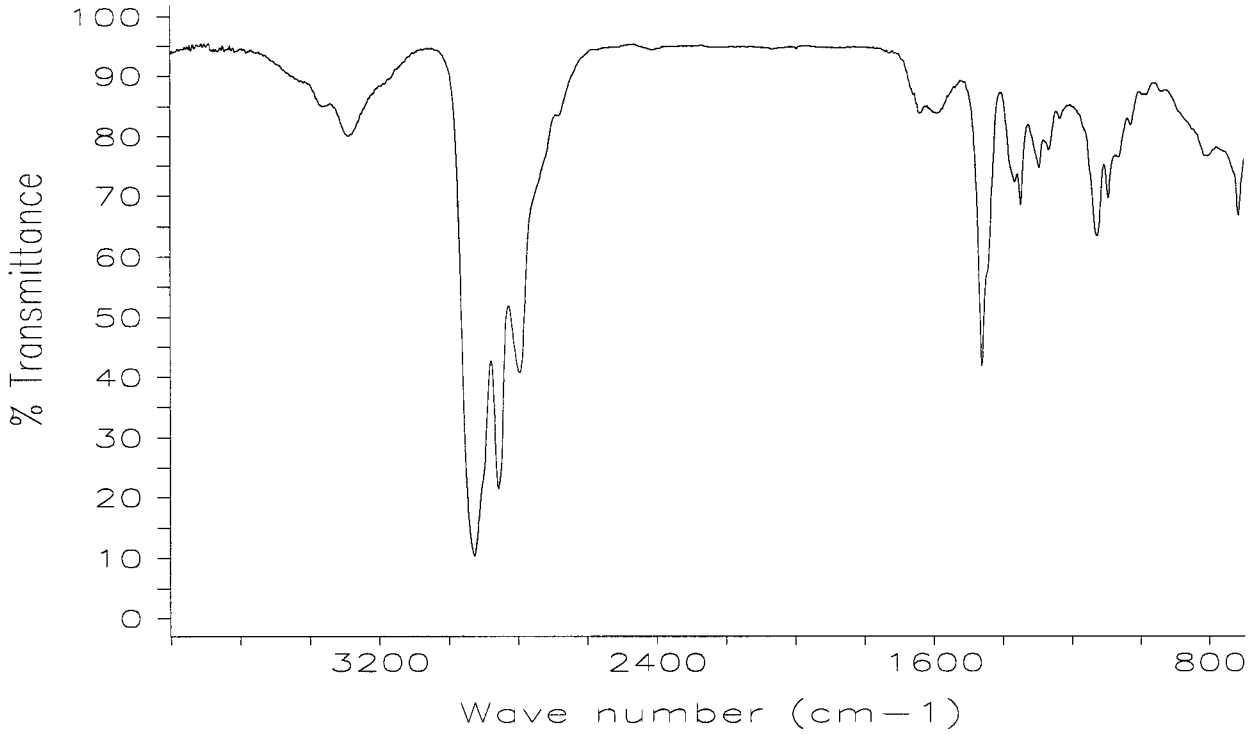
% Transmittance
100
90
80
70
60
50
40
30
20
10
0
3200
2400
1600
800
Wave number (cm−1)

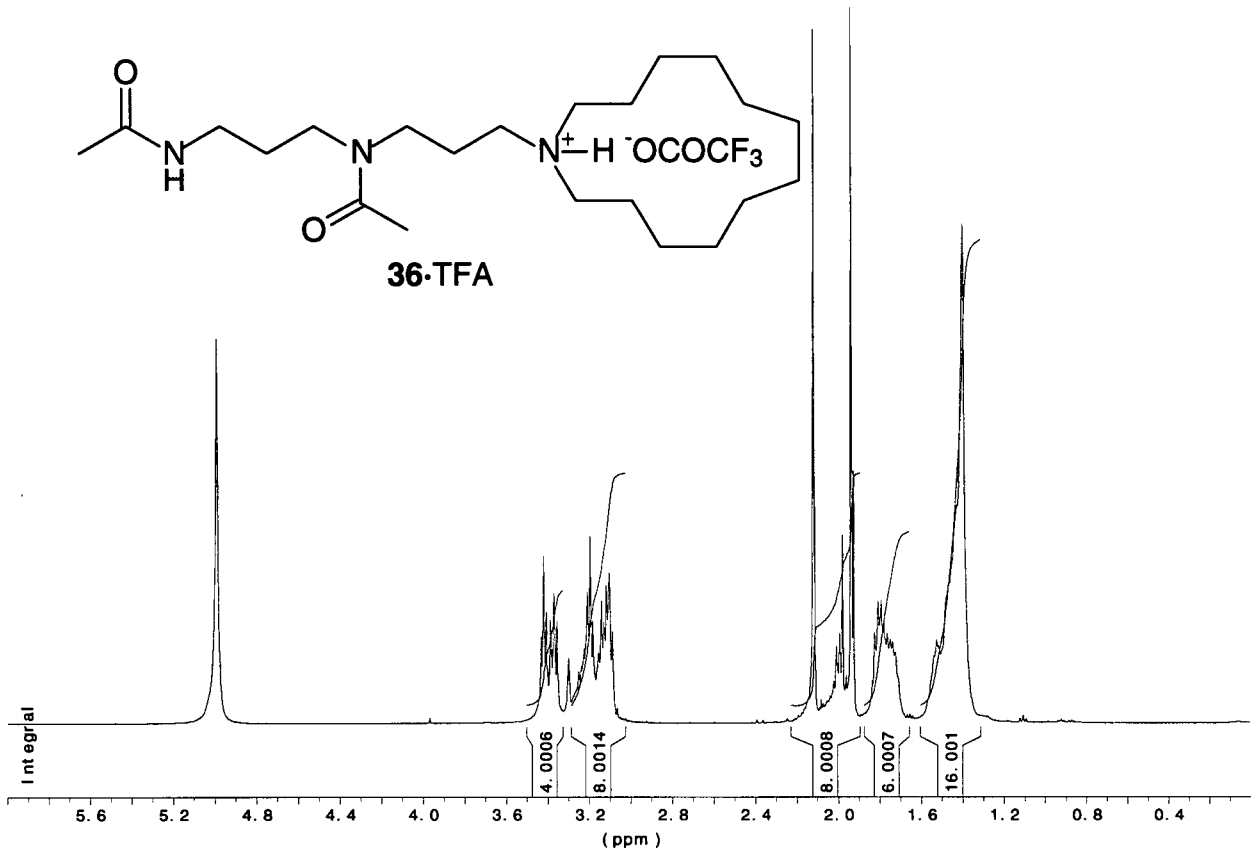
O
N
H
N
N
+
H
-OCOCF3
O
Int egral
4. 0006
8. 0014
8. 0008
6. 0007
16. 001
5.6
5.2
4.8
4.4
4.0
3.6
3.2
2.8
2.4
2.0
1.6
1.2
0.8
0.4
(ppm)

36·TFA

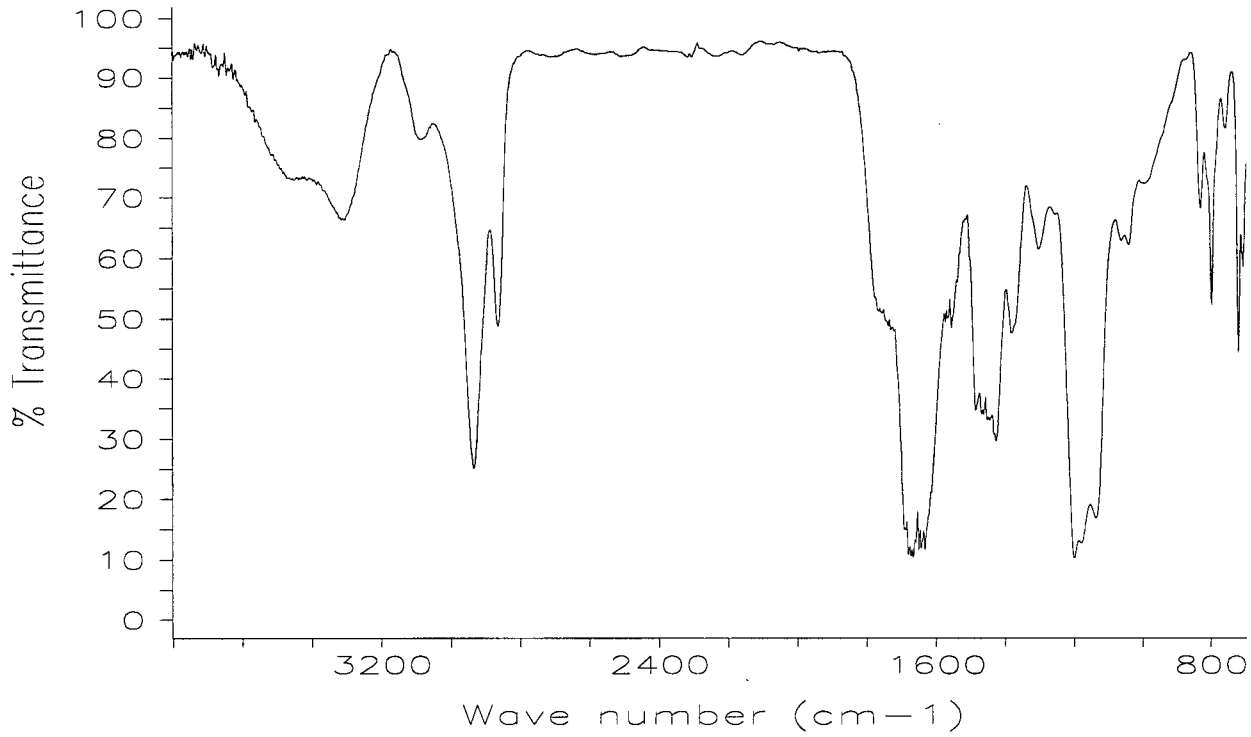
% Transmittance
100
90
80
70
60
50
40
30
20
10
0
3200
2400
1600
800
Wave number (cm−1)

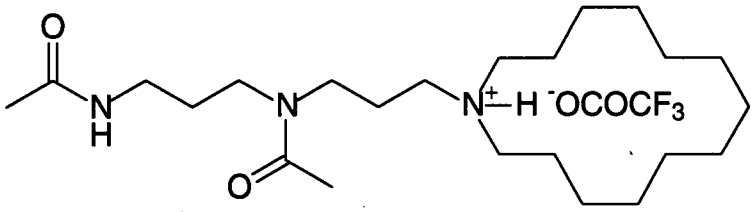
O
N
H
N
O
N+
H
-OCOCF3

37·TFA

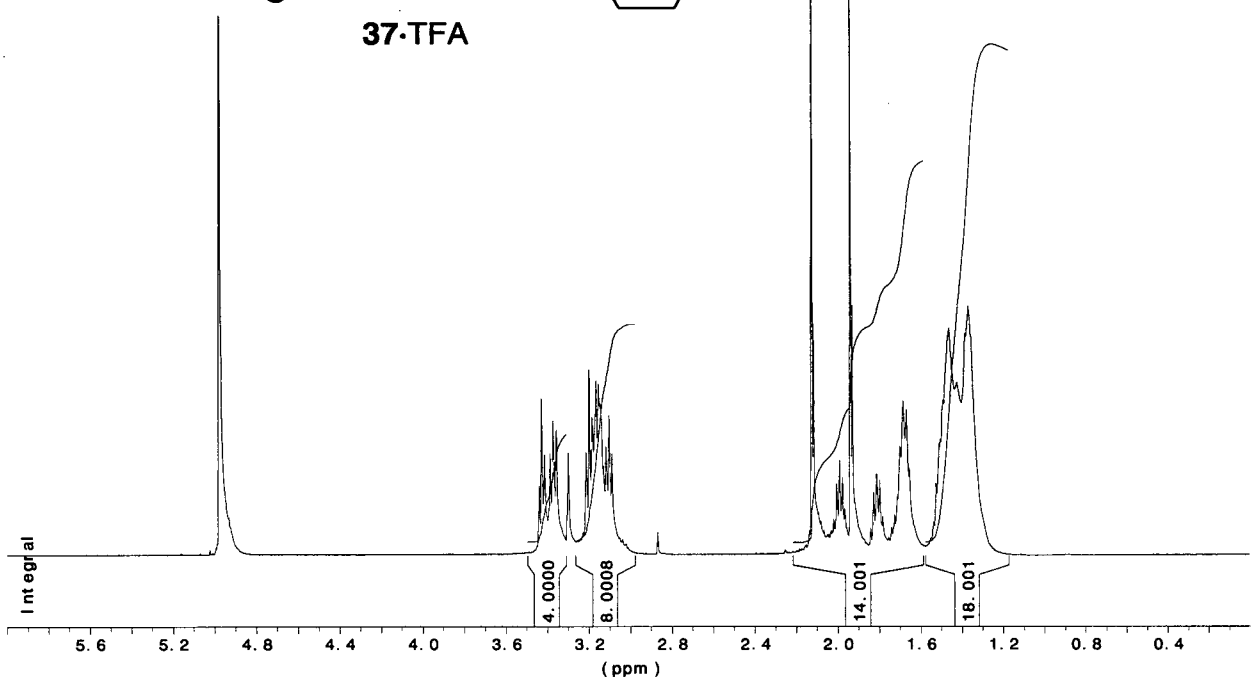
Integral
4.0000
8.0008
14.001
18.001
5.6
5.2
4.8
4.4
4.0
3.6
3.2
2.8
2.4
2.0
1.6
1.2
0.8
0.4
(ppm)

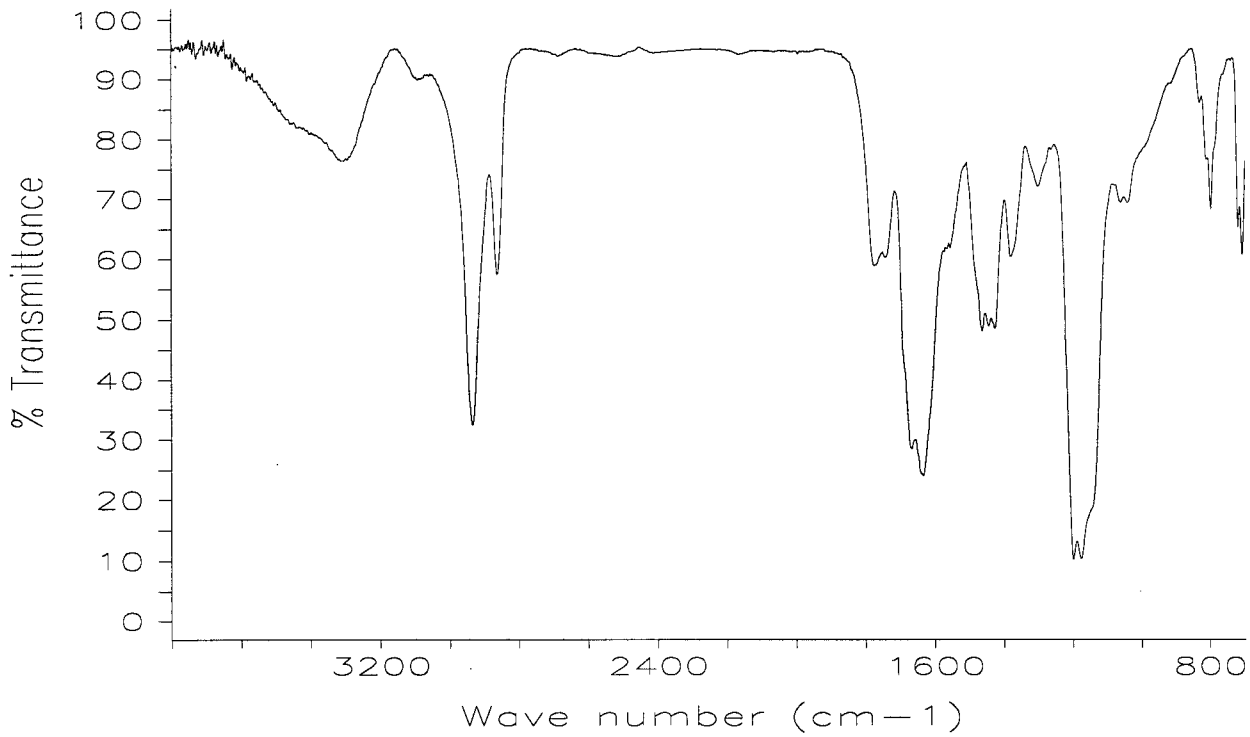
% Transmittance
100
90
80
70
60
50
40
30
20
10
0
3200
2400
1600
800
Wave number (cm−1)

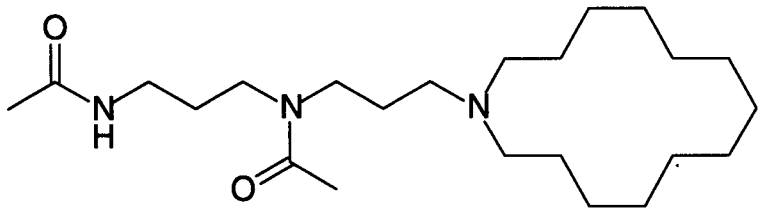

37

hegal
40022
20009
59999
30000
29999
40006
24495
56
52
48
44
40
36
32
28
24
20
16
12
08
04
ppm)

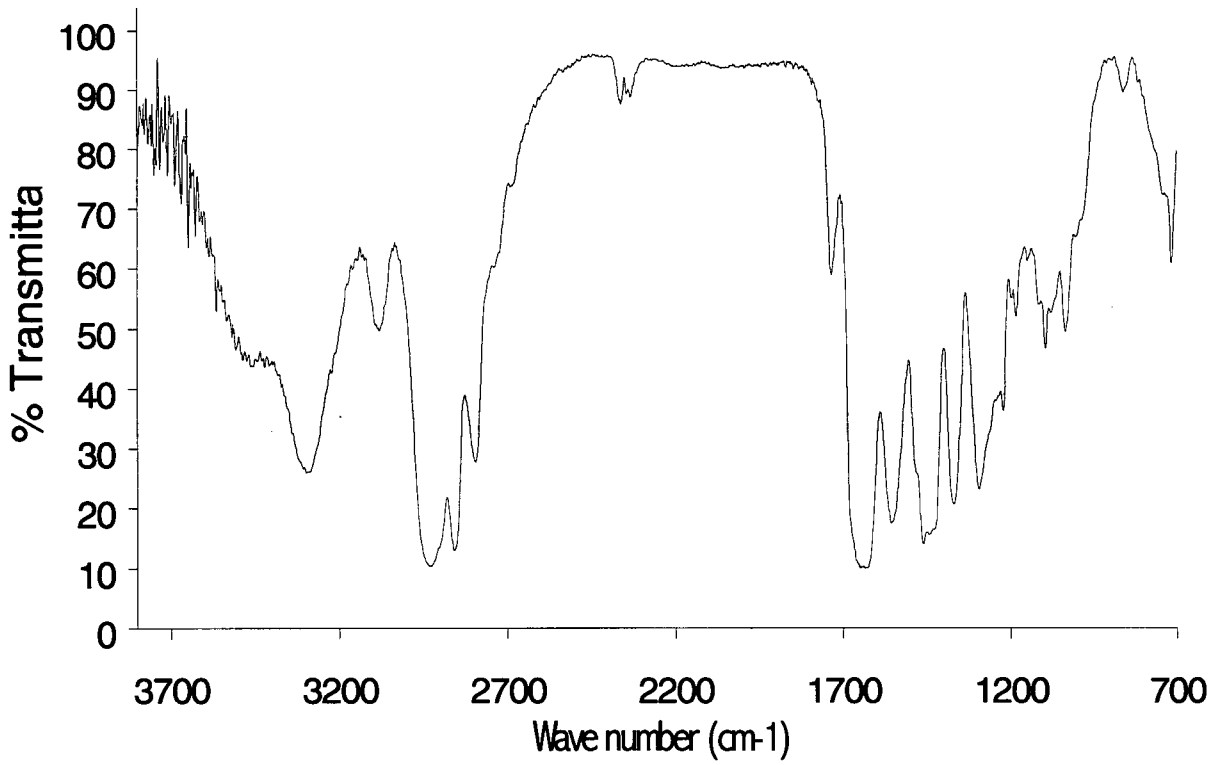
% Transmitta
100
90
80
70
60
50
40
30
20
10
0
3700
3200
2700
2200
1700
1200
700
Wave number (cm-1)

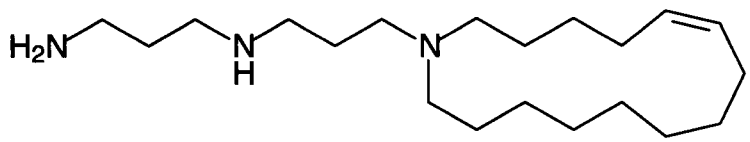
H2N
N
H
N

39

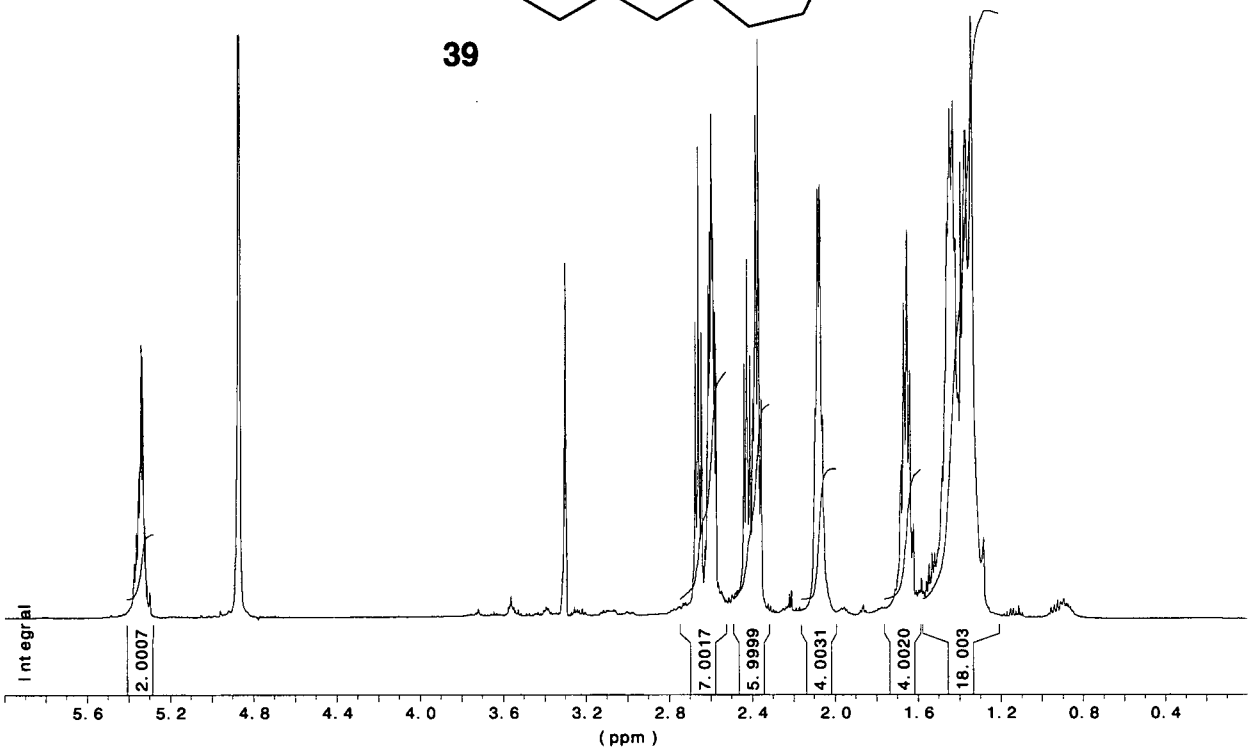
Integral
2.0007
7.0017
5.9999
4.0031
4.0020
18.003
5.6
5.2
4.8
4.4
4.0
3.6
3.2
2.8
2.4
2.0
1.6
1.2
0.8
0.4
(ppm)

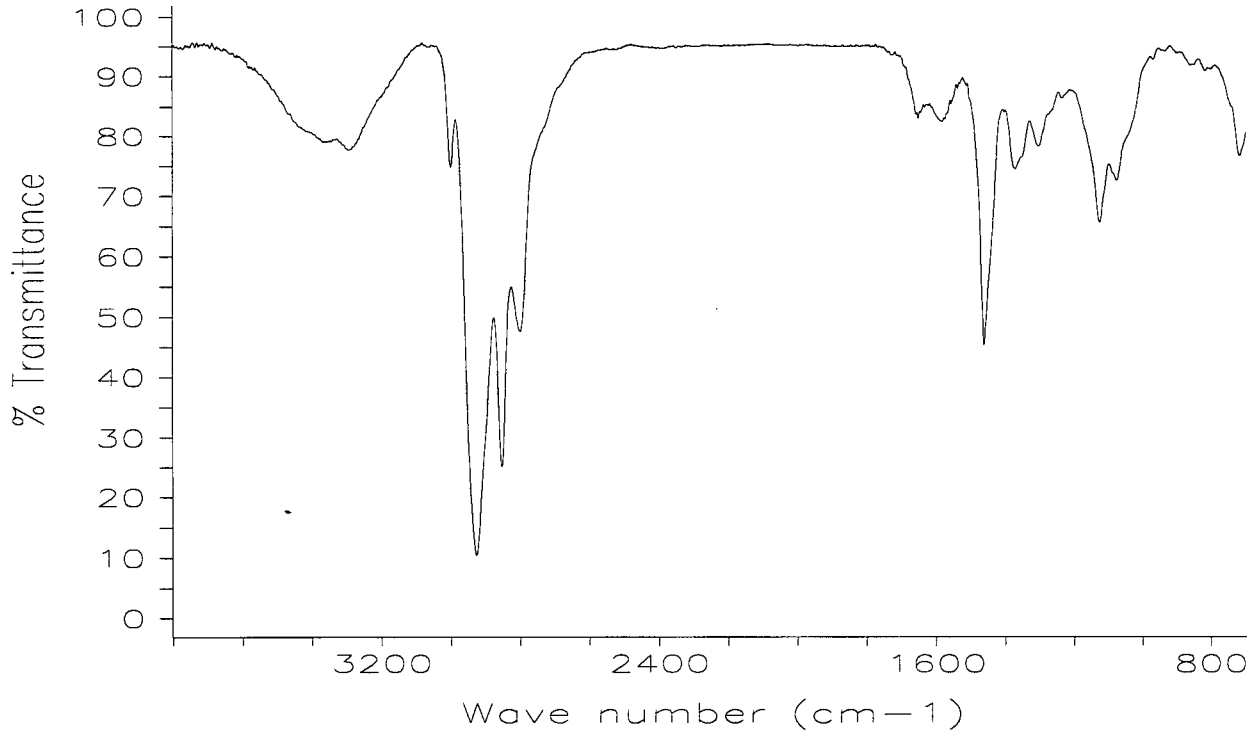
% Transmittance
100
90
80
70
60
50
40
30
20
10
0
3200
2400
1600
800
Wave number (cm−1)

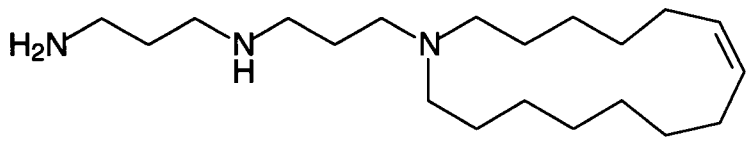
H2N
N
H
N

40

Int egral
2. 0012
1. 0007
6. 0016
5. 9999
4. 0011
4. 0012
18. 003
5.6
5.2
4.8
4.4
4.0
3.6
3.2
2.8
2.4
2.0
1.6
1.2
0.8
0.4
(ppm)

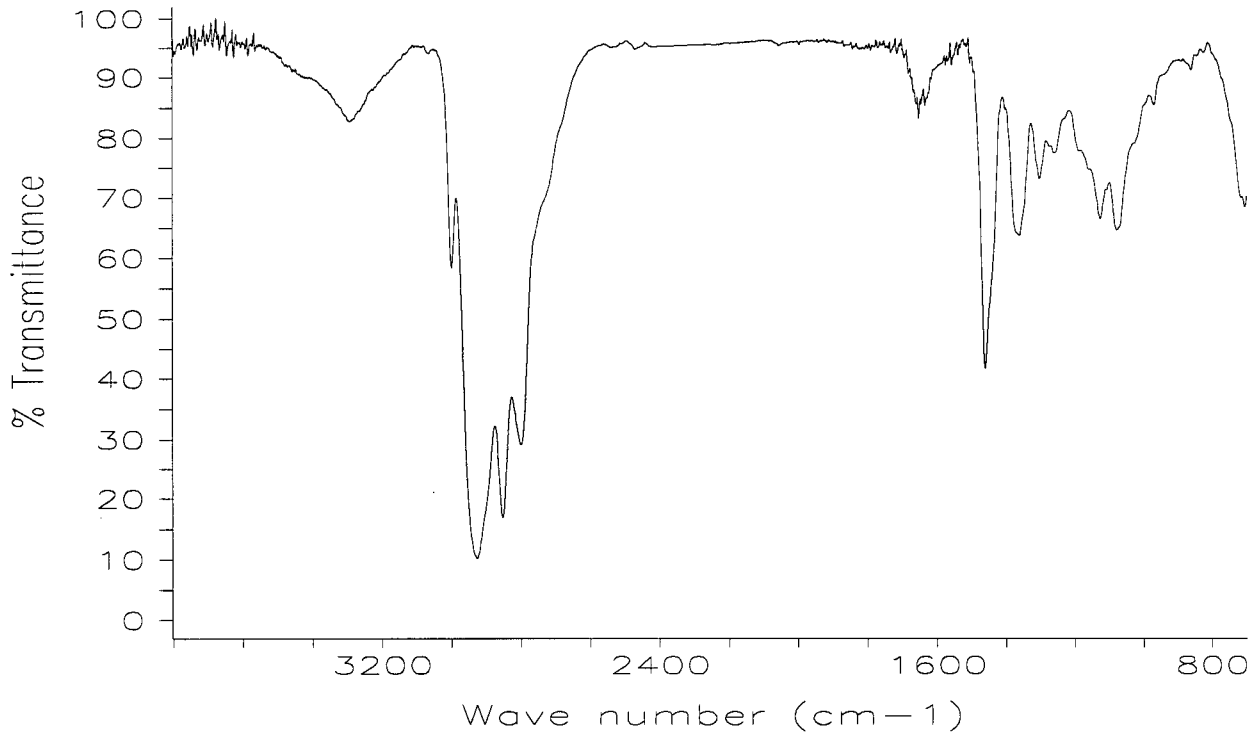
% Transmittance
100
90
80
70
60
50
40
30
20
10
0
3200
2400
1600
800
Wave number (cm−1)

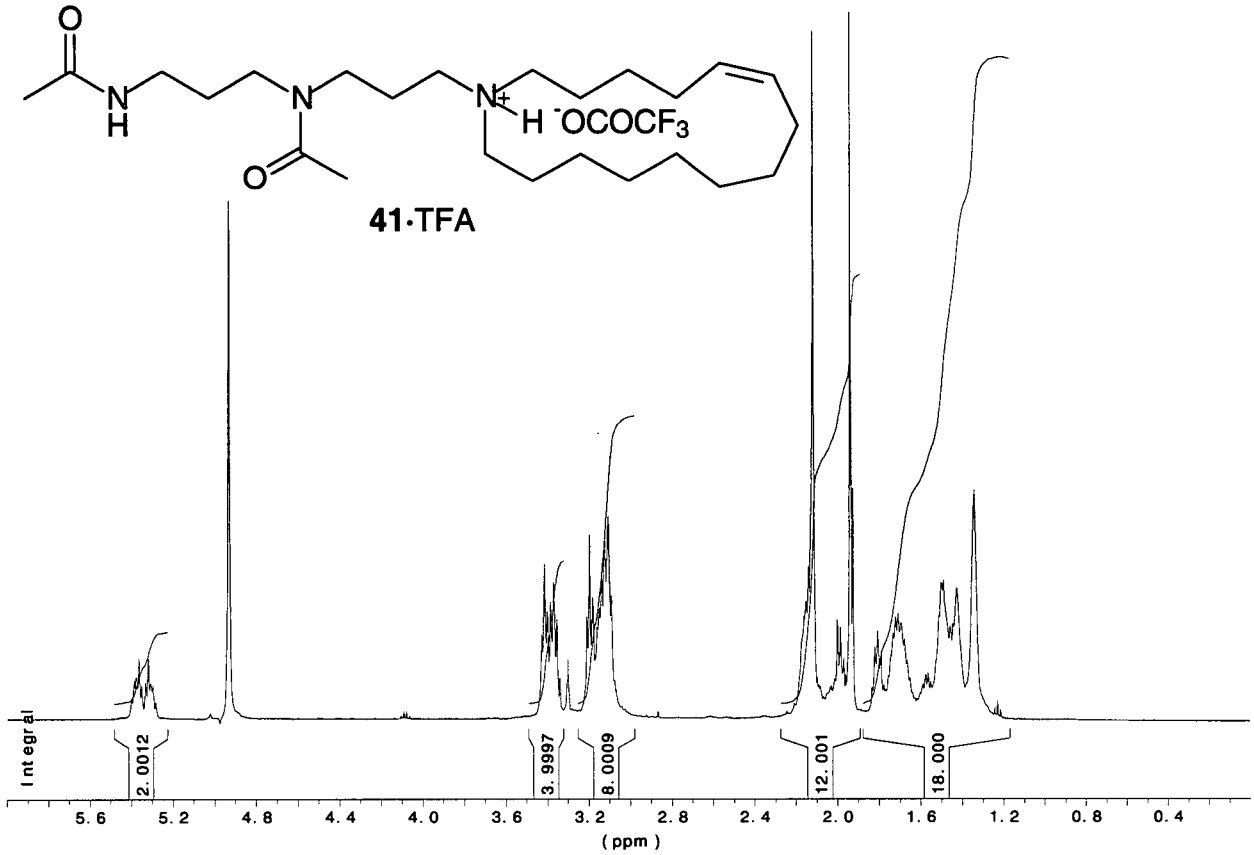
O
N
H
N
O
N+
H ⁻OCOCF3
Integral
2.0012
3.9997
8.0009
12.001
18.000
5.6
5.2
4.8
4.4
4.0
3.6
3.2
2.8
2.4
2.0
1.6
1.2
0.8
0.4
(ppm)

41·TFA

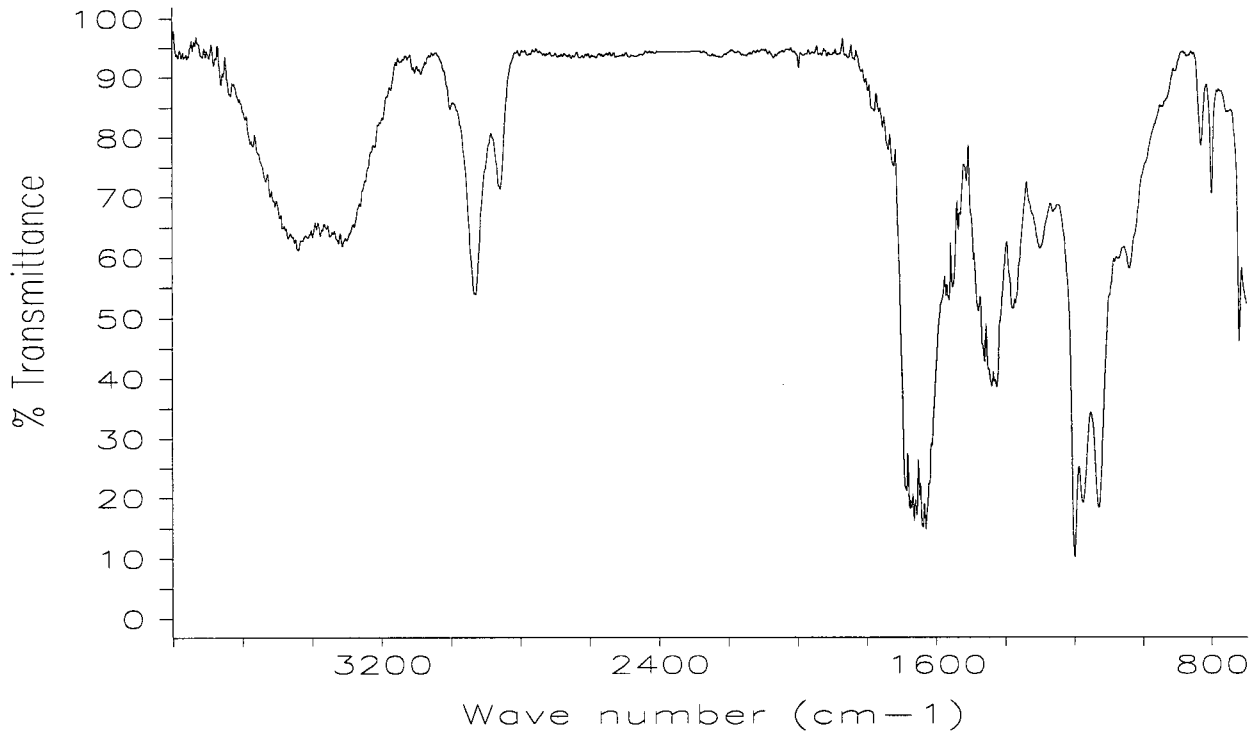
% Transmittance
100
90
80
70
60
50
40
30
20
10
0
3200
2400
1600
800
Wave number (cm−1)

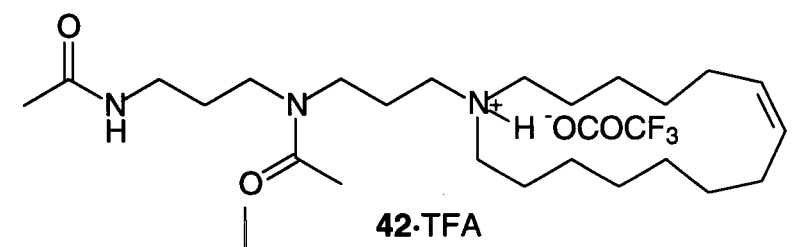
O
N
H
N
O
N+
H ⁻OCOCF3

42·TFA

Integral
1.9999
4.0012
8.0020
12.002
18.001
5.6
5.2
4.8
4.4
4.0
3.6
3.2
2.8
2.4
2.0
1.6
1.2
0.8
0.4
(ppm)

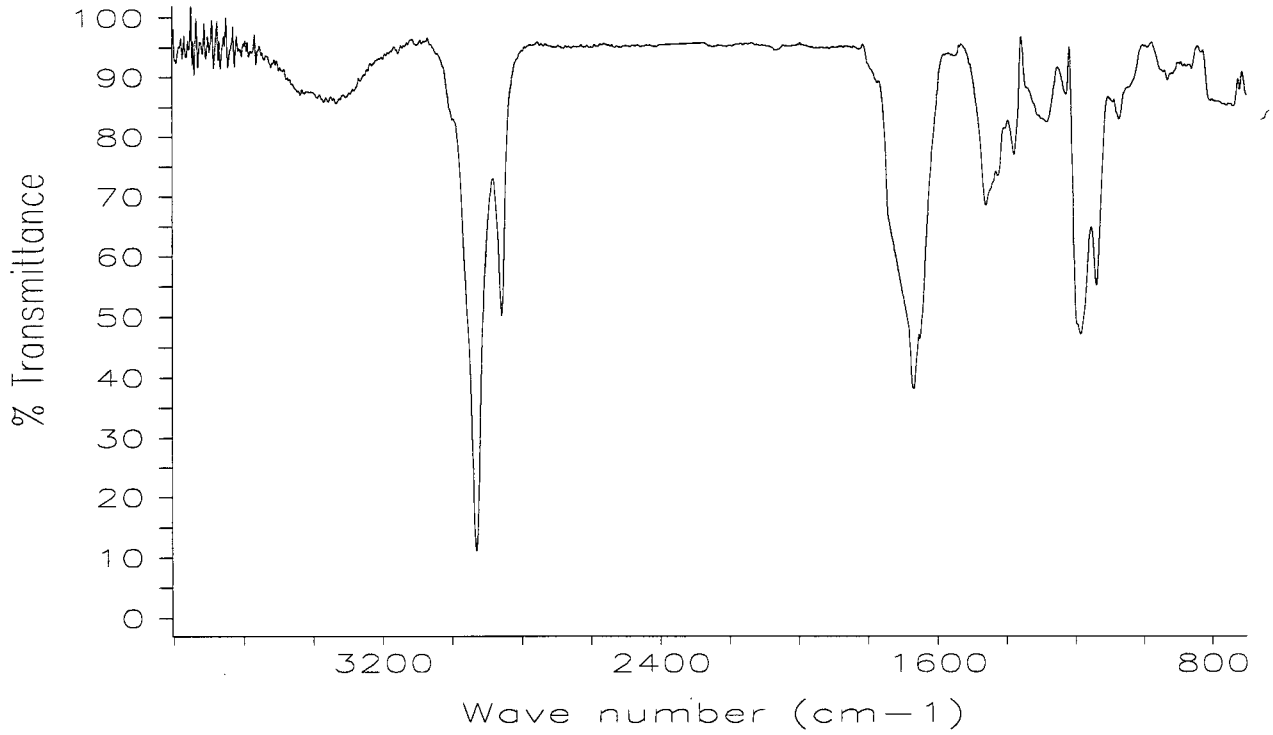
% Transmittance
100
90
80
70
60
50
40
30
20
10
0
3200
2400
1600
800
Wave number (cm−1)

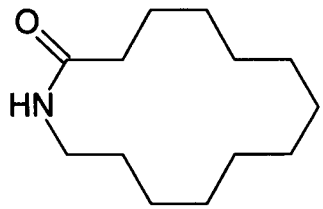
O
HN

62

Integral
1.0003
2.0011
2.0000
20.001
7.5 7.0 6.5 6.0 5.5 5.0 4.5 4.0 3.5 3.0 2.5 2.0 1.5 1.0 0.5
(ppm)

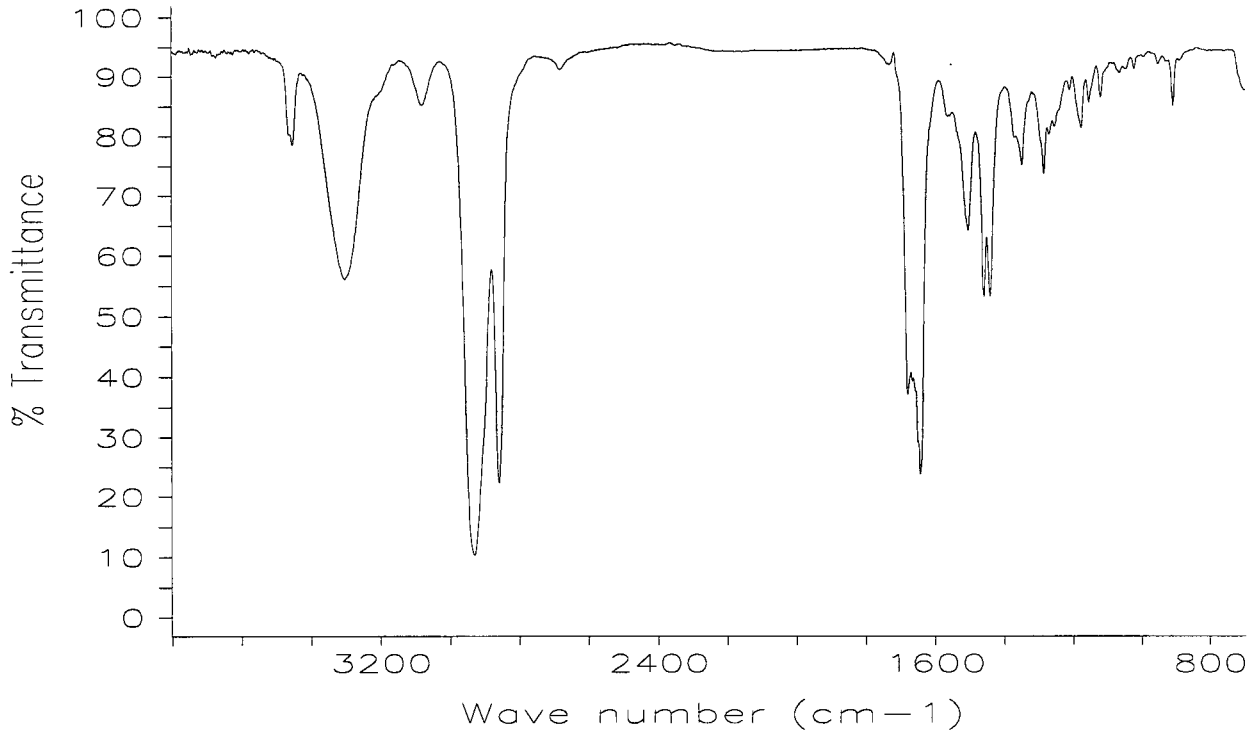
% Transmittance
100
90
80
70
60
50
40
30
20
10
0
3200
2400
1600
800
Wave number (cm−1)

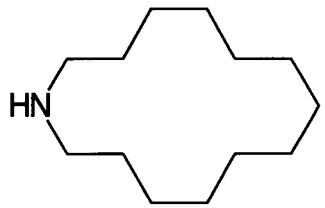
HN

63

Integral
4.0000
23.002
7.5
7.0
6.5
6.0
5.5
5.0
4.5
4.0
3.5
3.0
2.5
2.0
1.5
1.0
0.5
(ppm)

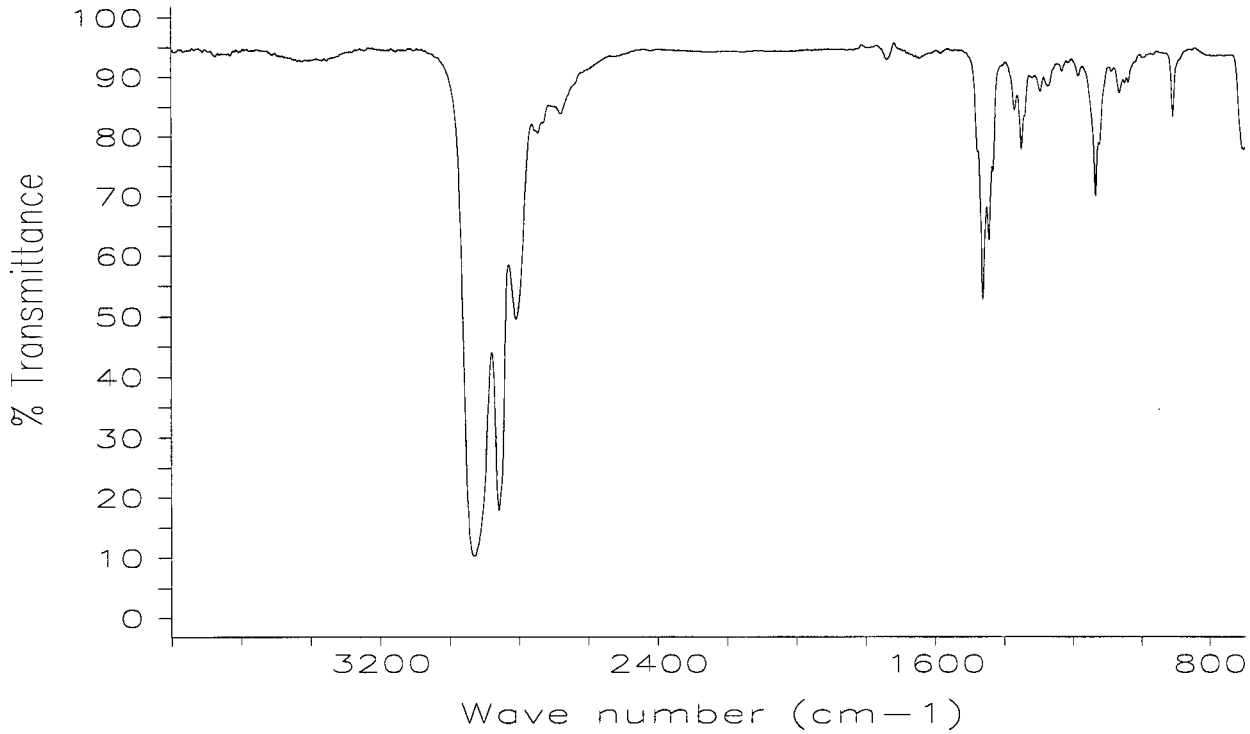
% Transmittance
100
90
80
70
60
50
40
30
20
10
0
3200
2400
1600
800
Wave number (cm−1)

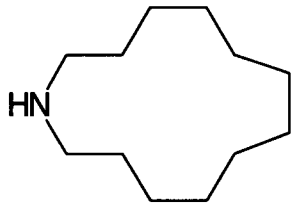
HN

66

Integrial
4.0000
21.001
7.5
7.0
6.5
6.0
5.5
5.0
4.5
4.0
3.5
3.0
2.5
2.0
1.5
1.0
0.5
(ppm)

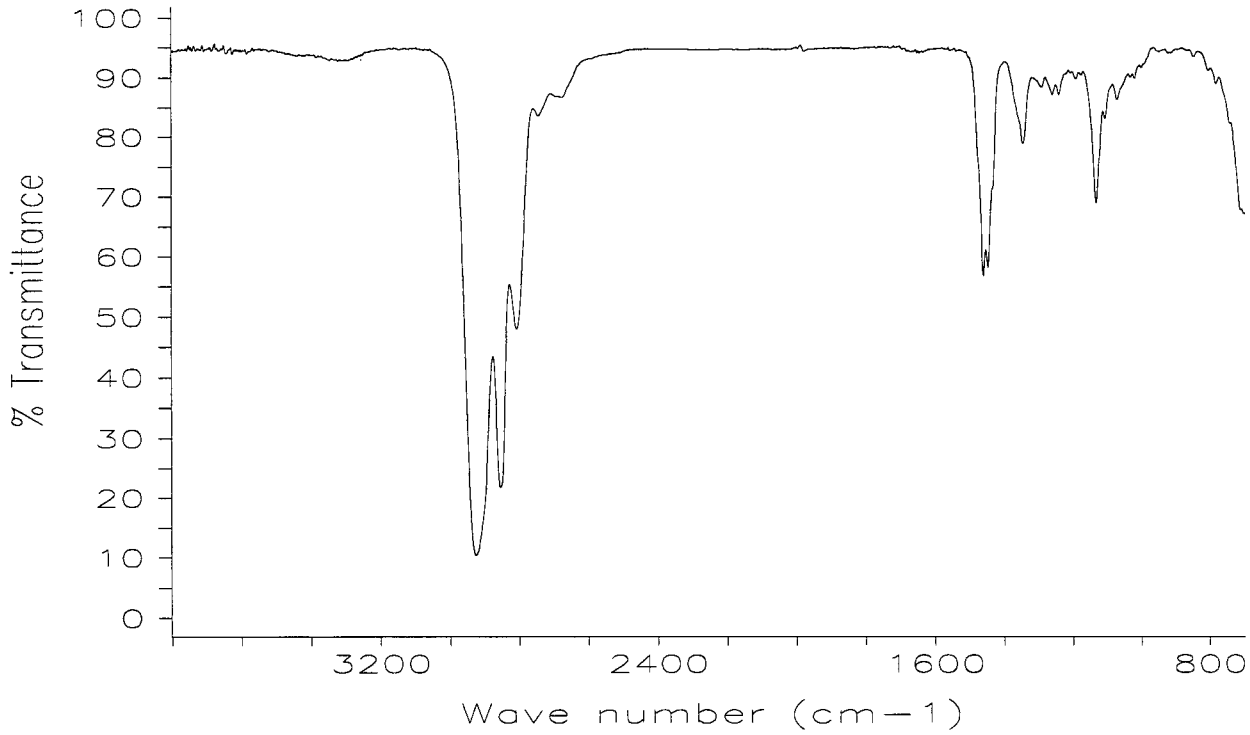
% Transmittance
100
90
80
70
60
50
40
30
20
10
0
3200
2400
1600
800
Wave number (cm−1)

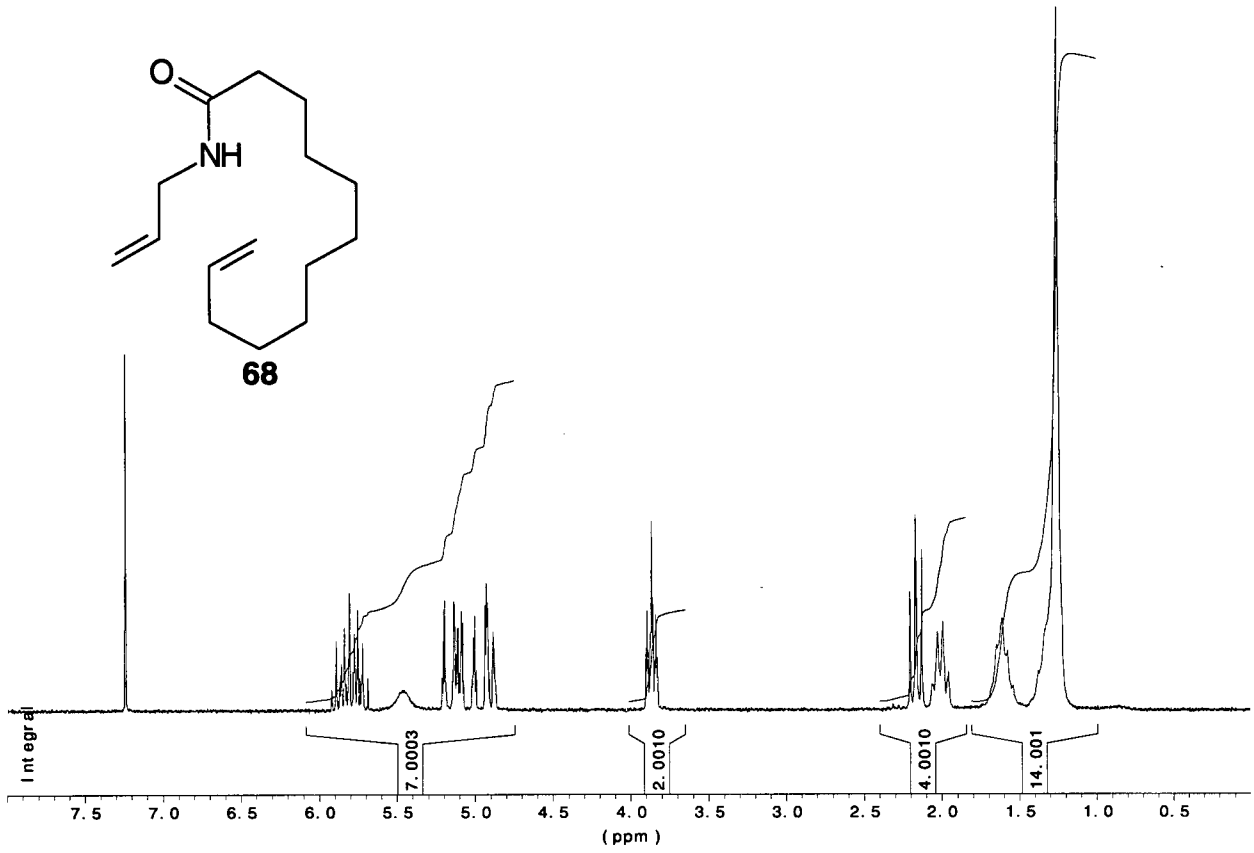
O
NH
68
Integral
7.0003
2.0010
4.0010
14.001
7.5 7.0 6.5 6.0 5.5 5.0 4.5 4.0 3.5 3.0 2.5 2.0 1.5 1.0 0.5
(ppm)

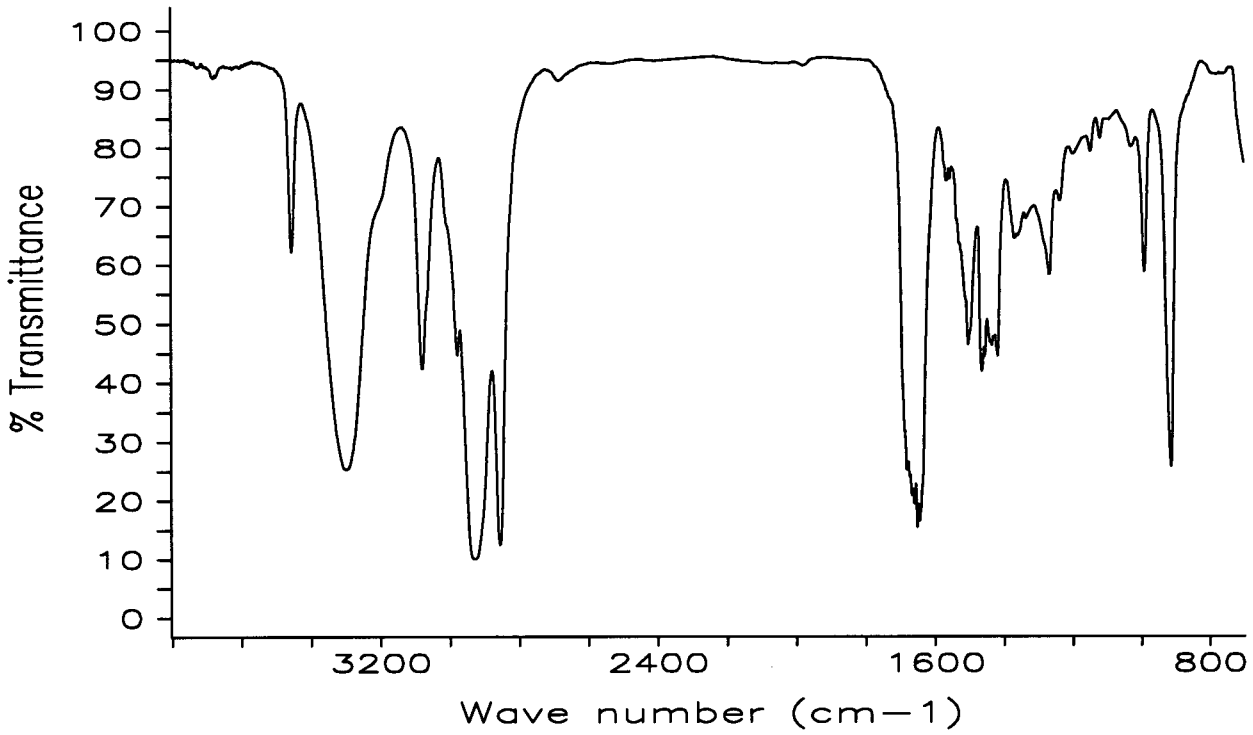
% Transmittance
100
90
80
70
60
50
40
30
20
10
0
3200
2400
1600
800
Wave number (cm−1)

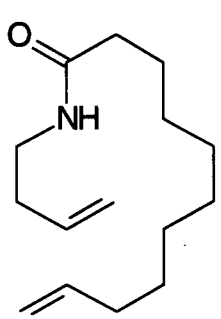
O
NH

69

Integral
3.0000
3.9995
2.0011
18.000
7.5 7.0 6.5 6.0 5.5 5.0 4.5 4.0 3.5 3.0 2.5 2.0 1.5 1.0 0.5
(ppm)

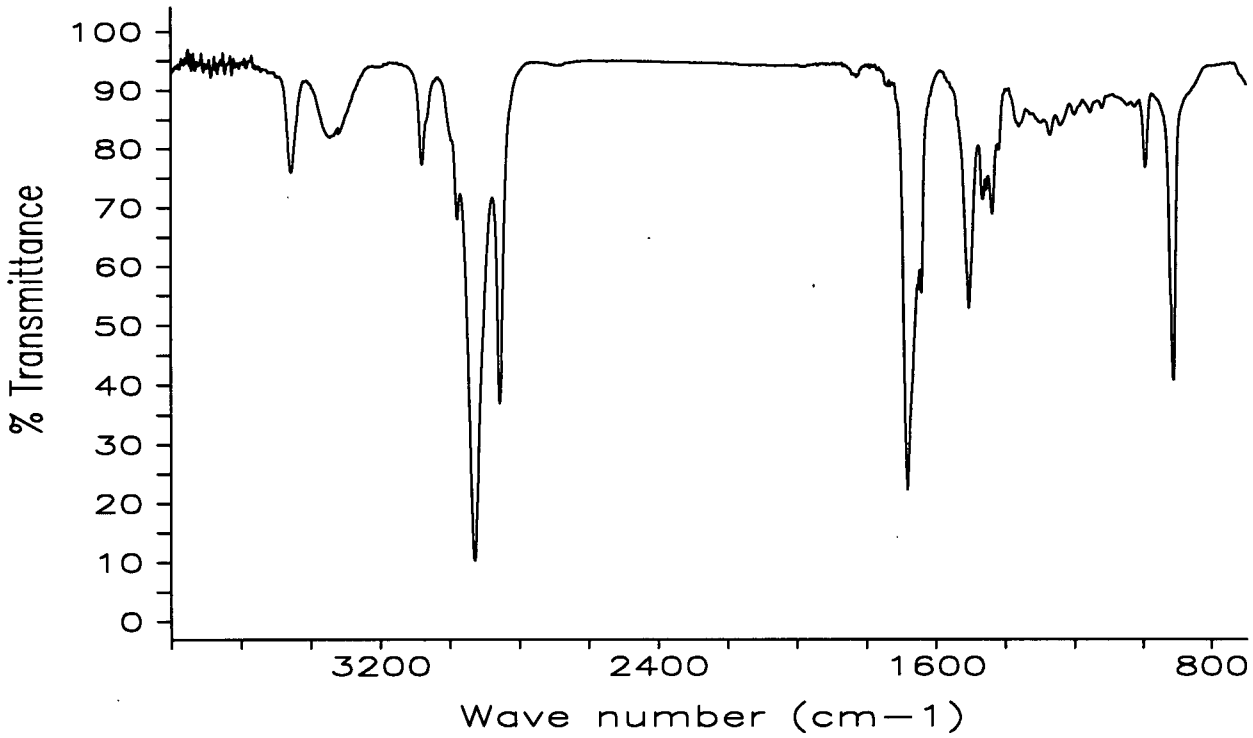
% Transmittance
100
90
80
70
60
50
40
30
20
10
0
3200
2400
1600
800
Wave number (cm−1)

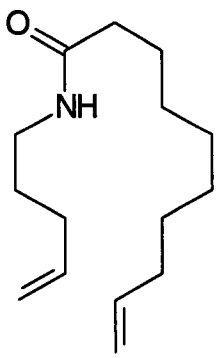
O
NH

70

Integral
3.0012
3.9999
2.0000
6.0010
12.002
7.5 7.0 6.5 6.0 5.5 5.0 4.5 4.0 3.5 3.0 2.5 2.0 1.5 1.0 0.5
(ppm)

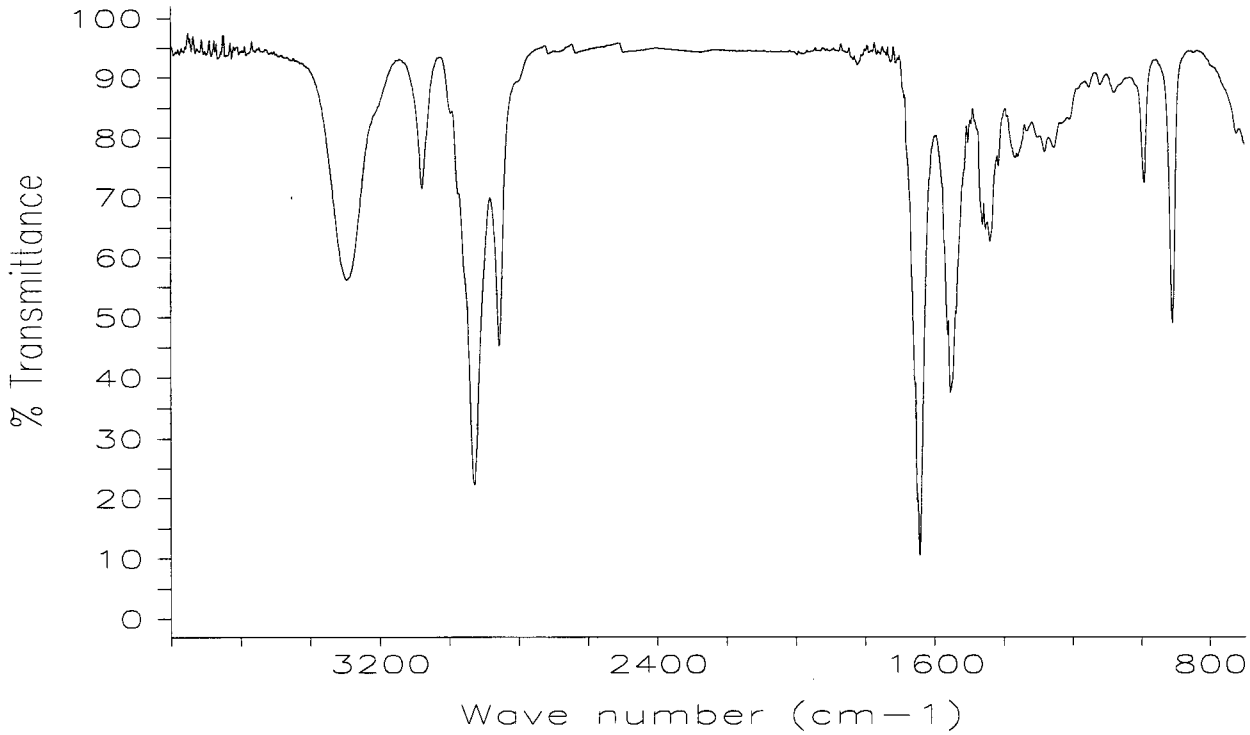
% Transmittance
100
90
80
70
60
50
40
30
20
10
0
3200
2400
1600
800
Wave number (cm−1)

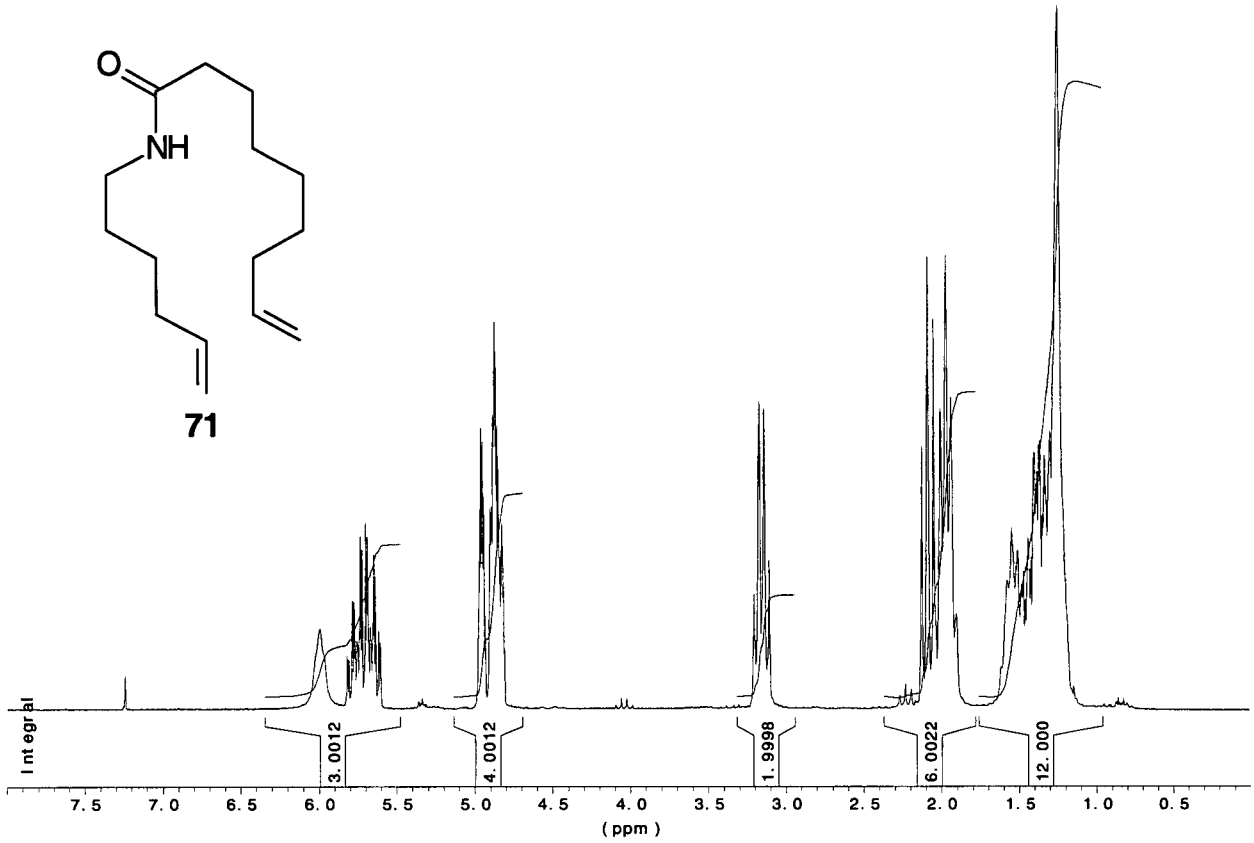
O
NH
71
Integral
3.0012
4.0012
1.9998
6.0022
12.000
7.5 7.0 6.5 6.0 5.5 5.0 4.5 4.0 3.5 3.0 2.5 2.0 1.5 1.0 0.5
(ppm)

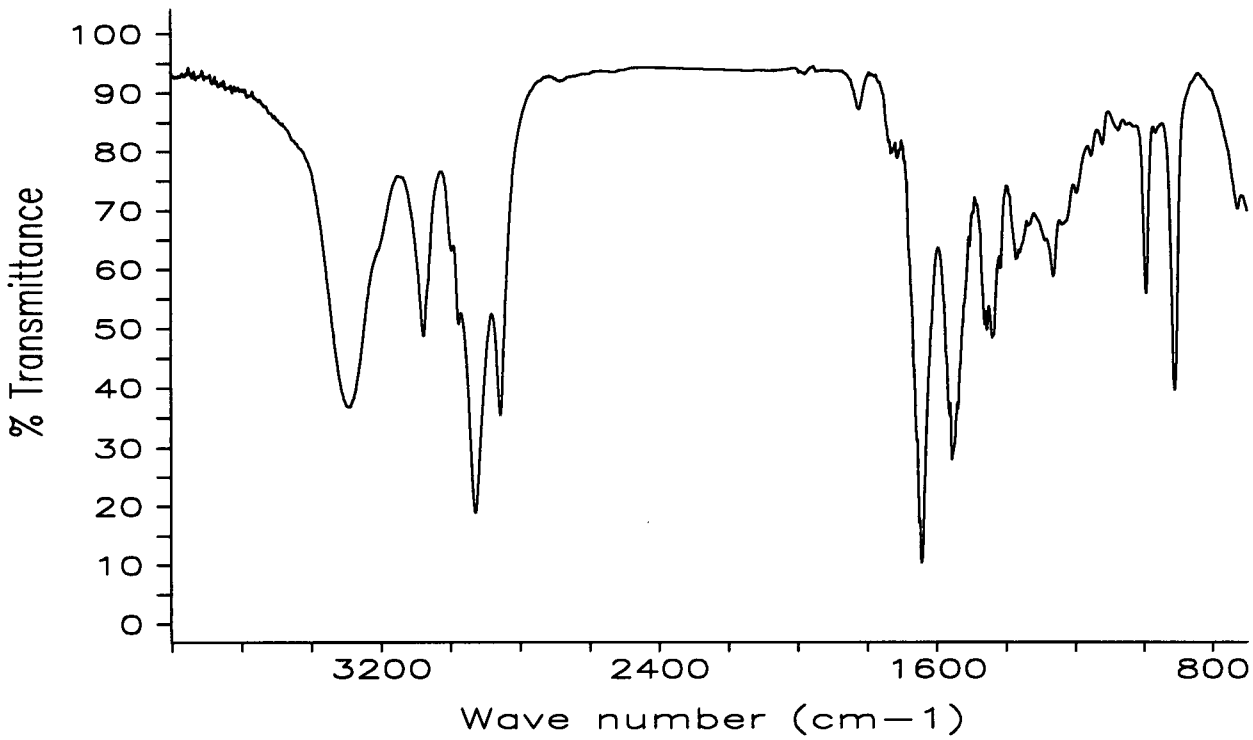
% Transmittance
100
90
80
70
60
50
40
30
20
10
0
3200
2400
1600
800
Wave number (cm−1)

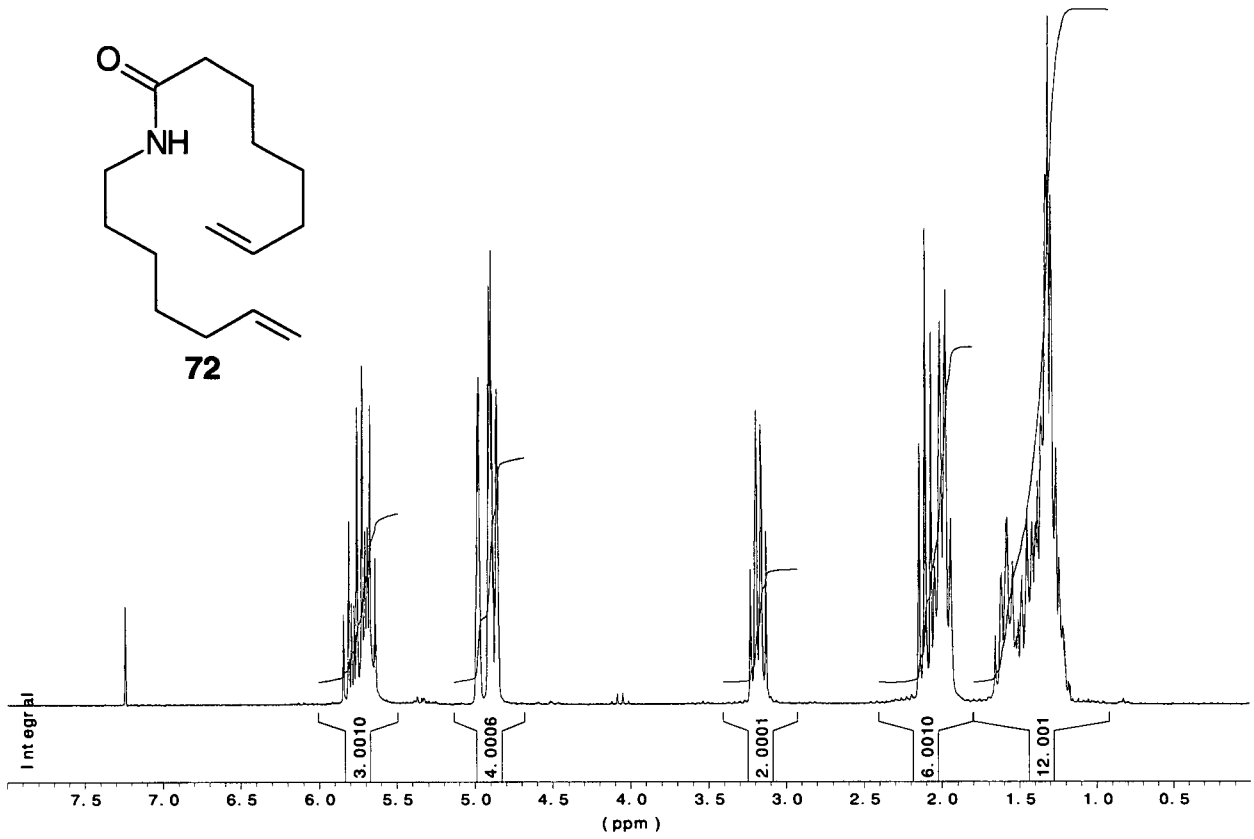
O
NH
72
Integral
3.0010
4.0006
2.0001
6.0010
12.001
7.5 7.0 6.5 6.0 5.5 5.0 4.5 4.0 3.5 3.0 2.5 2.0 1.5 1.0 0.5
(ppm)

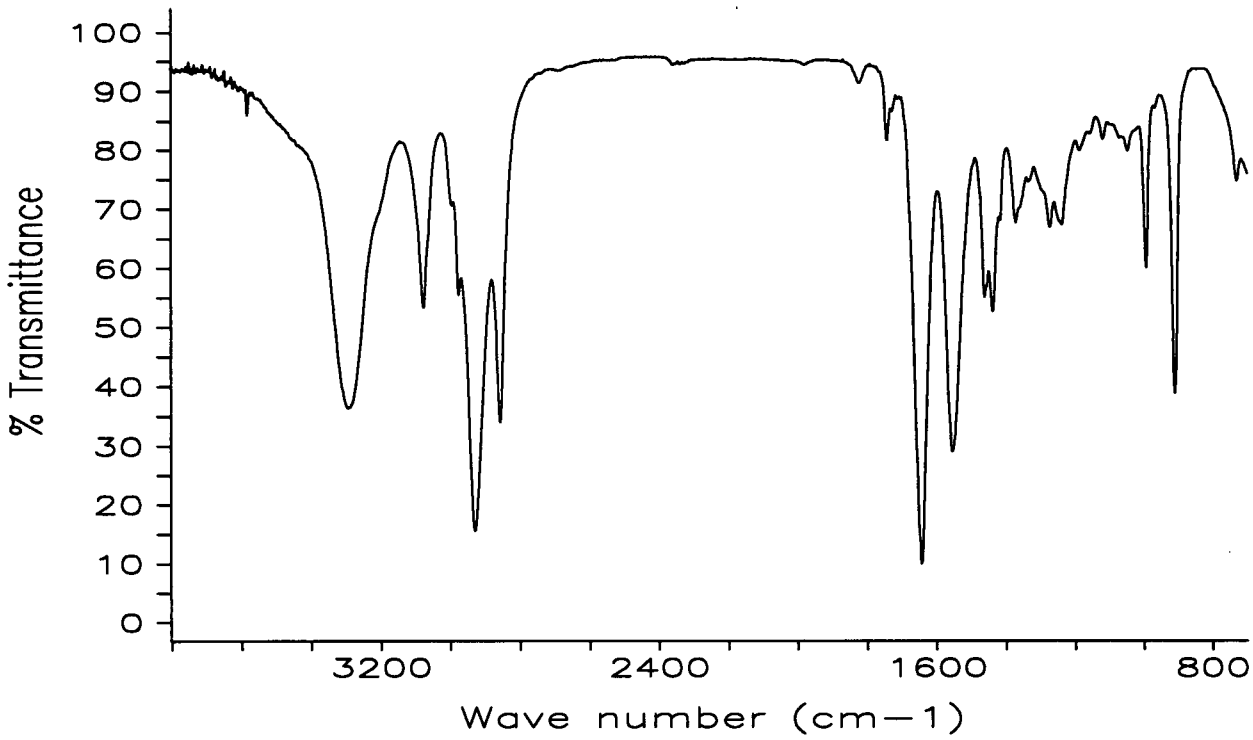
% Transmittance
100
90
80
70
60
50
40
30
20
10
0
3200
2400
1600
800
Wave number (cm−1)

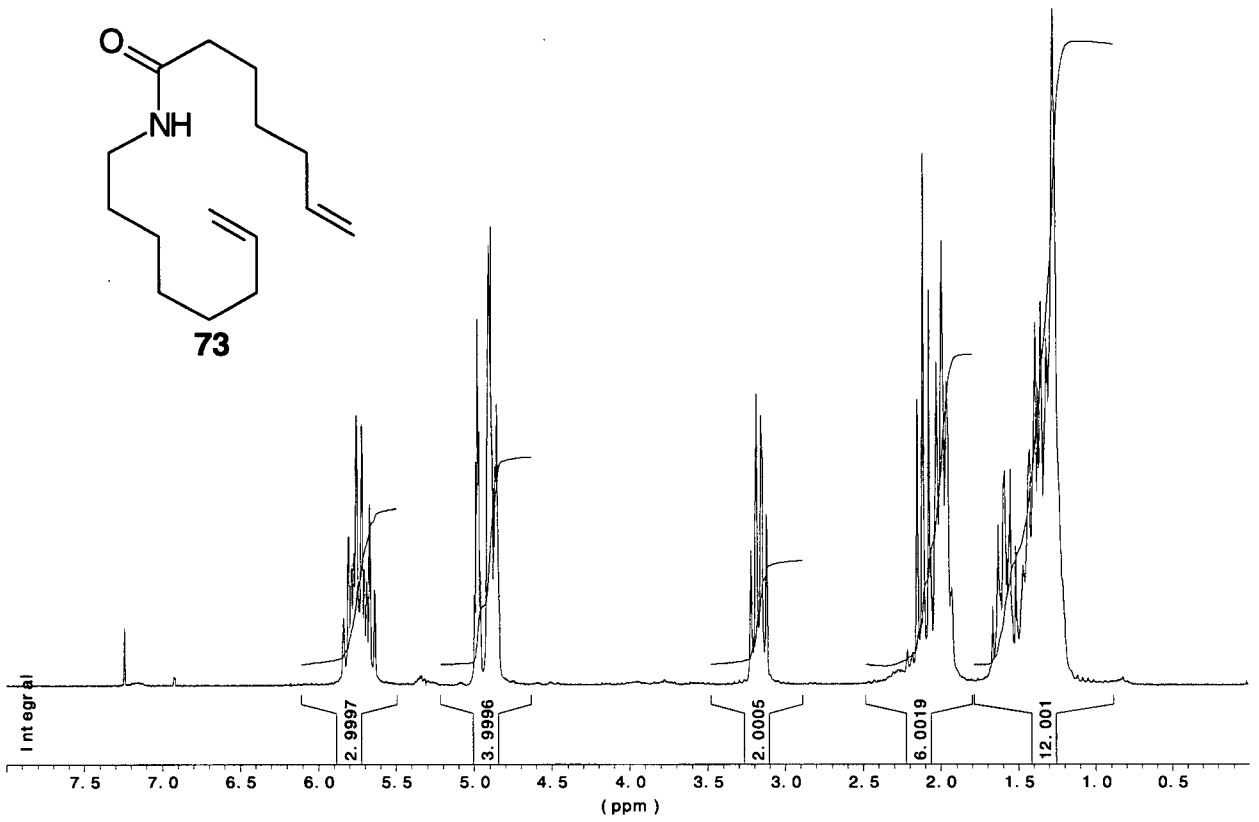
O
NH
73
Integral
2.9997
3.9996
2.0005
6.0019
12.001
7.5 7.0 6.5 6.0 5.5 5.0 4.5 4.0 3.5 3.0 2.5 2.0 1.5 1.0 0.5
(ppm)

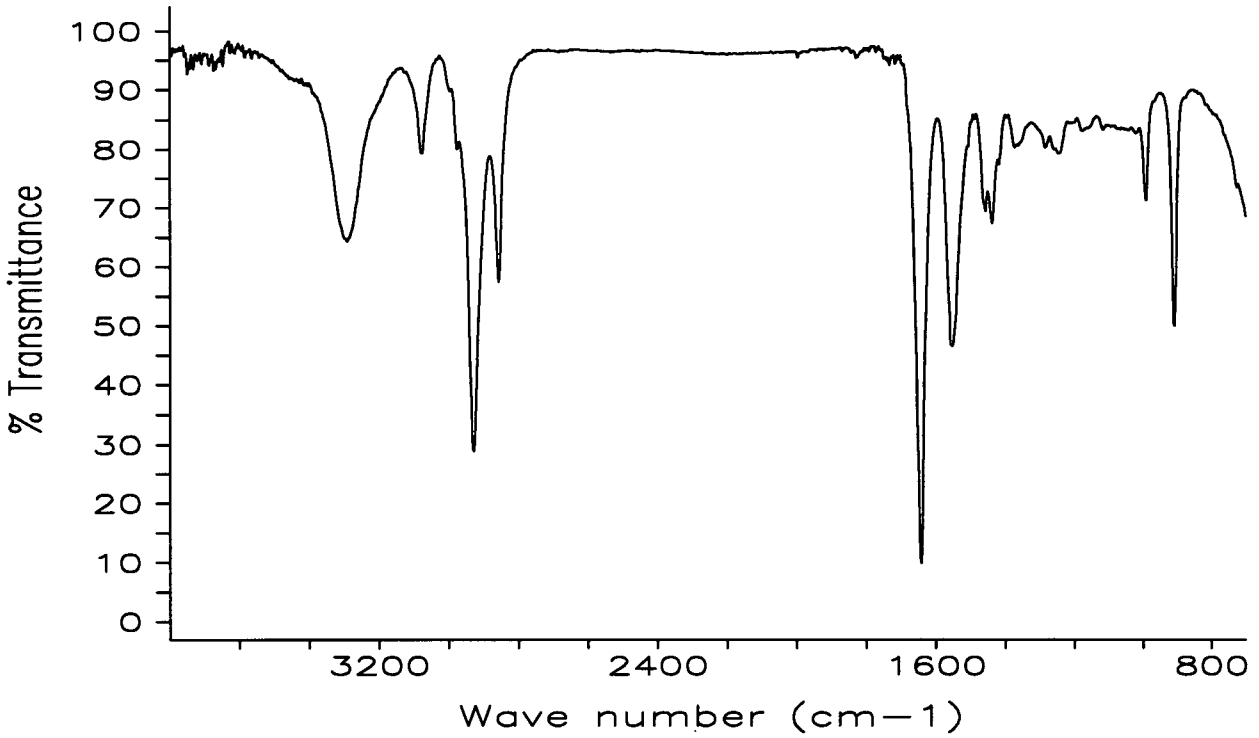
% Transmittance
100
90
80
70
60
50
40
30
20
10
0
3200
2400
1600
800
Wave number (cm−1)

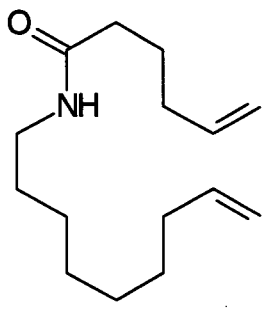
O
NH

74

Int egral
3. 0006
4. 0022
2. 0000
6. 0006
12. 001
7.5 7.0 6.5 6.0 5.5 5.0 4.5 4.0 3.5 3.0 2.5 2.0 1.5 1.0 0.5
(ppm)

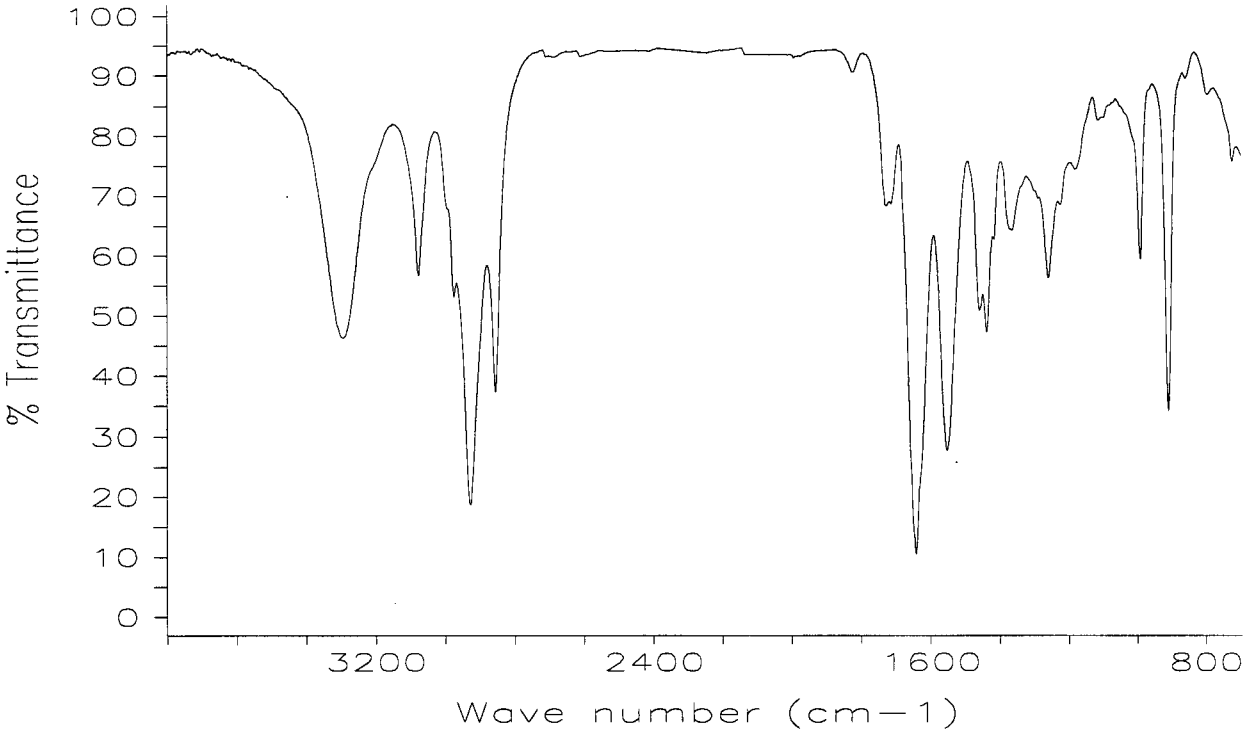
% Transmittance
100
90
80
70
60
50
40
30
20
10
0
3200
2400
1600
800
Wave number (cm−1)

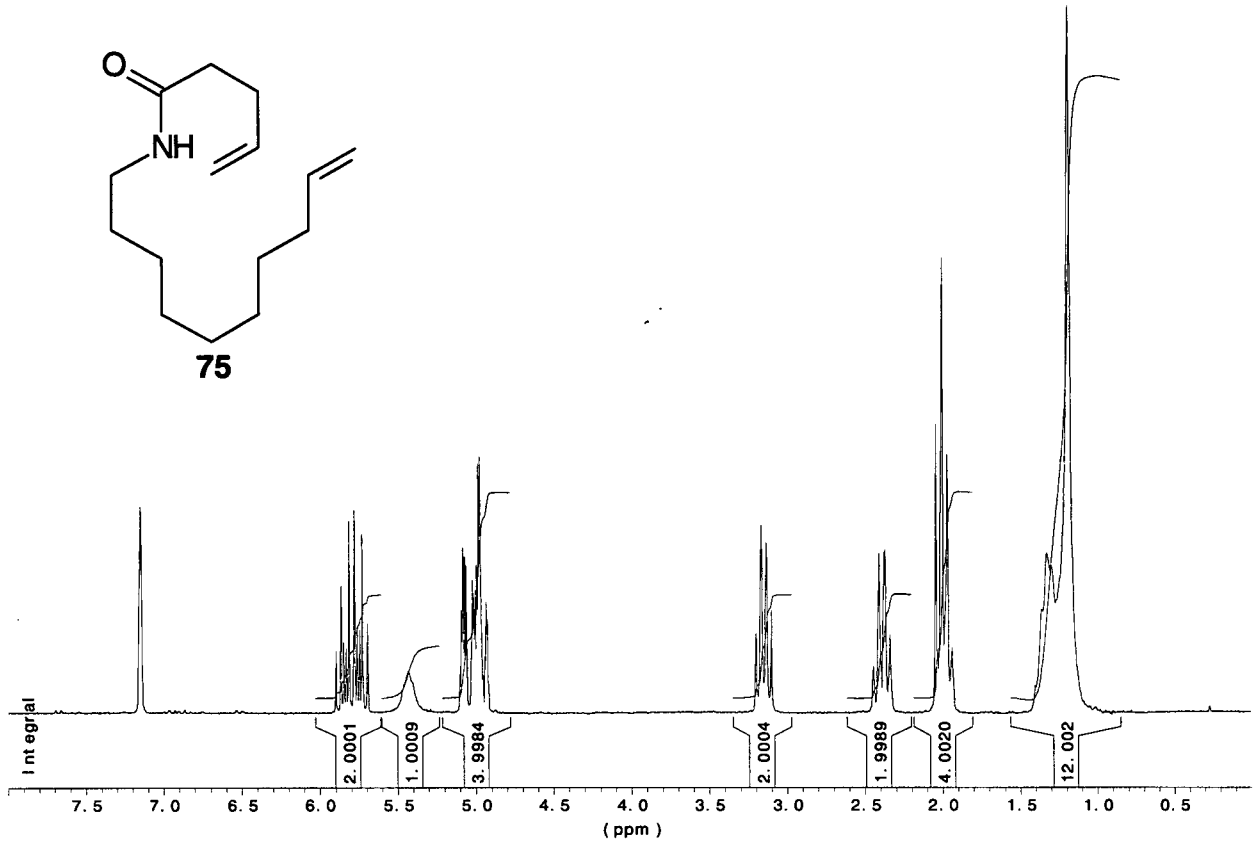
O
NH
75
Int egral
2.0001
1.0009
3.9984
2.0004
1.9989
4.0020
12.002
7.5 7.0 6.5 6.0 5.5 5.0 4.5 4.0 3.5 3.0 2.5 2.0 1.5 1.0 0.5
(ppm)

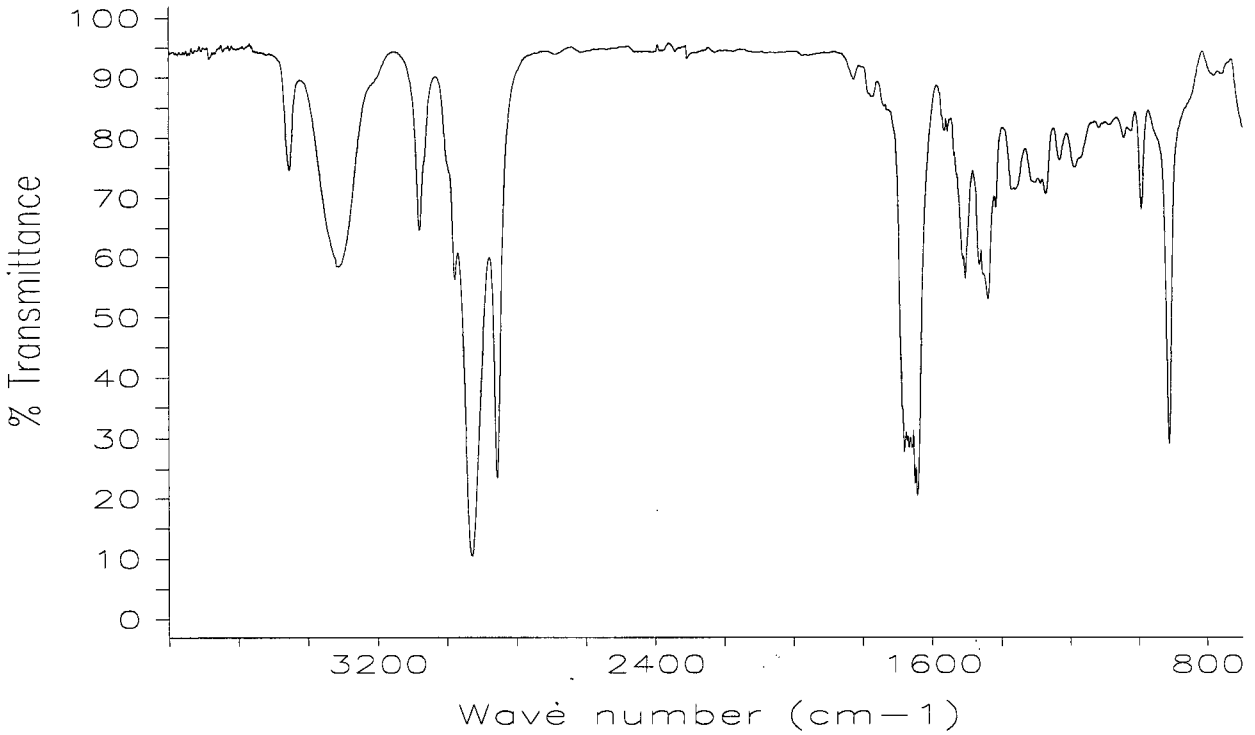
% Transmittance
100
90
80
70
60
50
40
30
20
10
0
3200
2400
1600
800
Wavė number (cm−1)

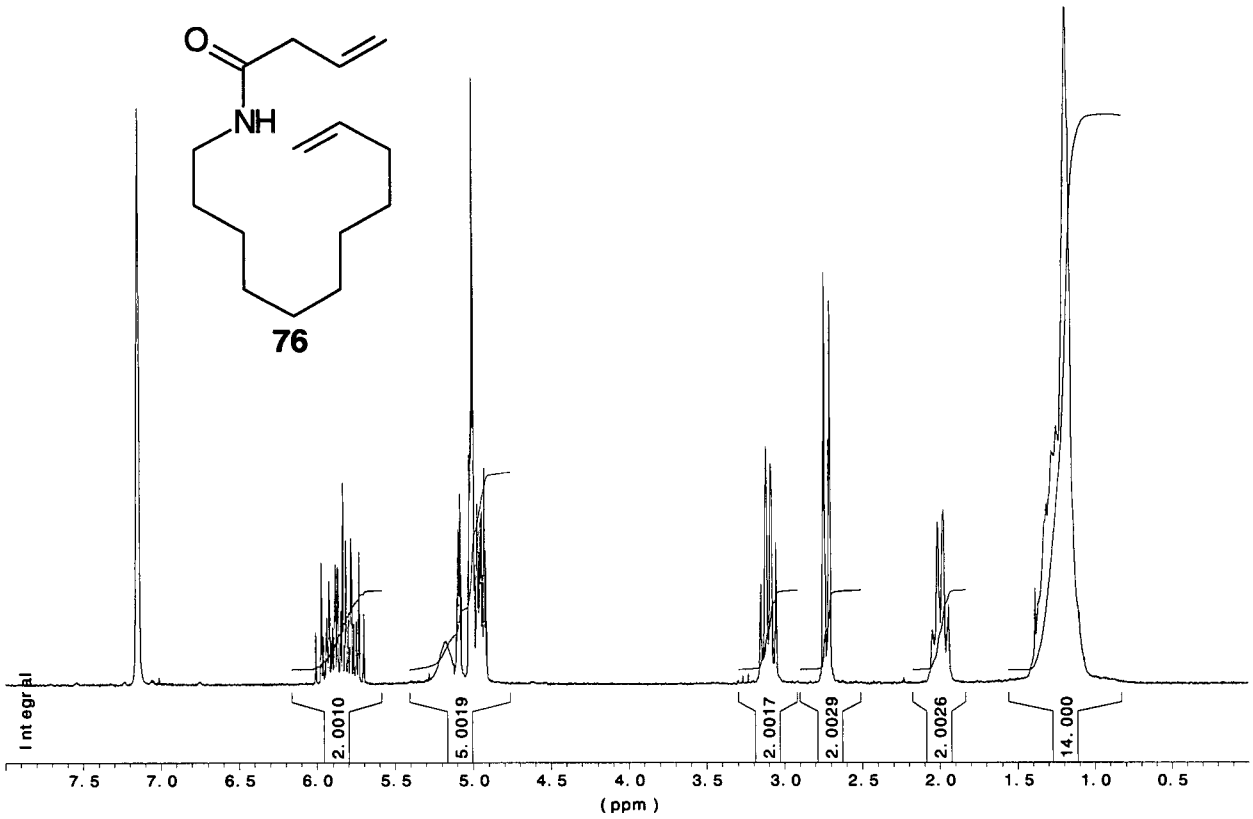
O
NH
76
Integral
2.0010
5.0019
2.0017
2.0029
2.0026
14.000
7.5 7.0 6.5 6.0 5.5 5.0 4.5 4.0 3.5 3.0 2.5 2.0 1.5 1.0 0.5
(ppm)

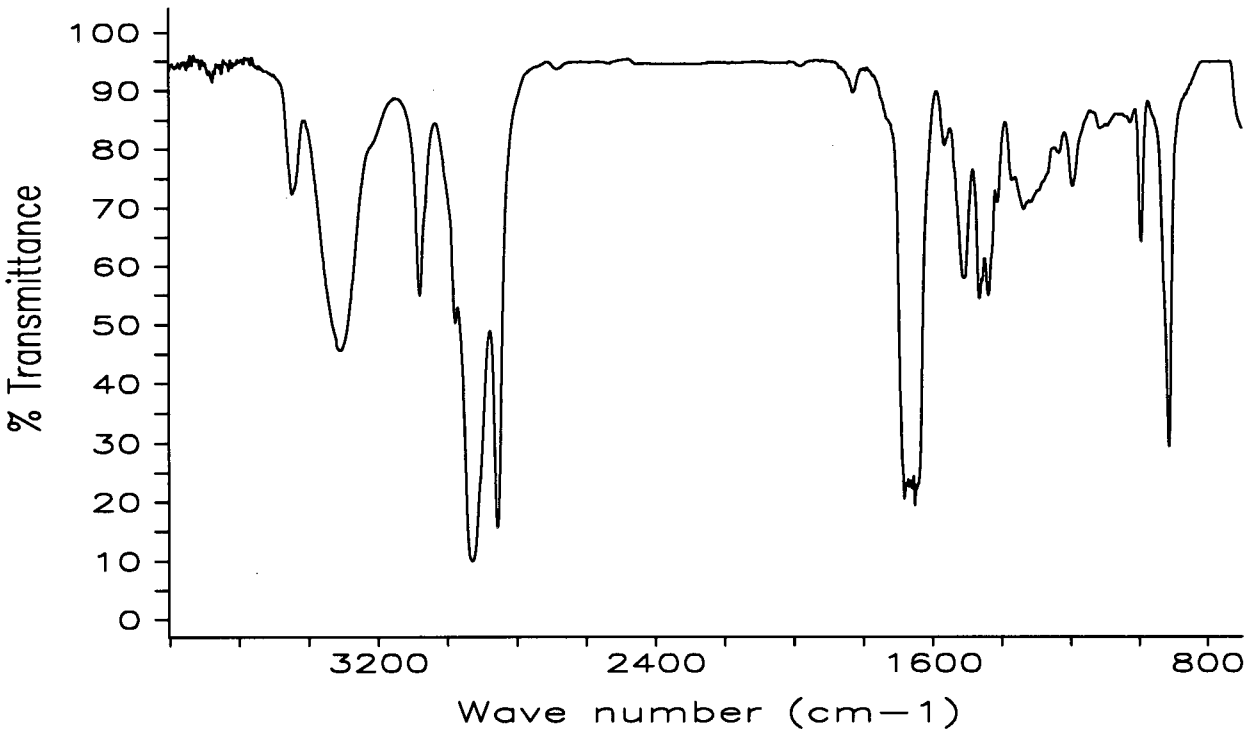
% Transmittance
100
90
80
70
60
50
40
30
20
10
0
3200
2400
1600
800
Wave number (cm−1)

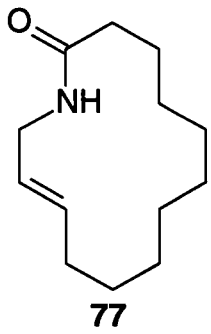
O
NH

77

Integral
3.0010
2.0005
4.0008
14.001
7.5
7.0
6.5
6.0
5.5
5.0
4.5
4.0
3.5
3.0
2.5
2.0
1.5
1.0
0.5
(ppm)

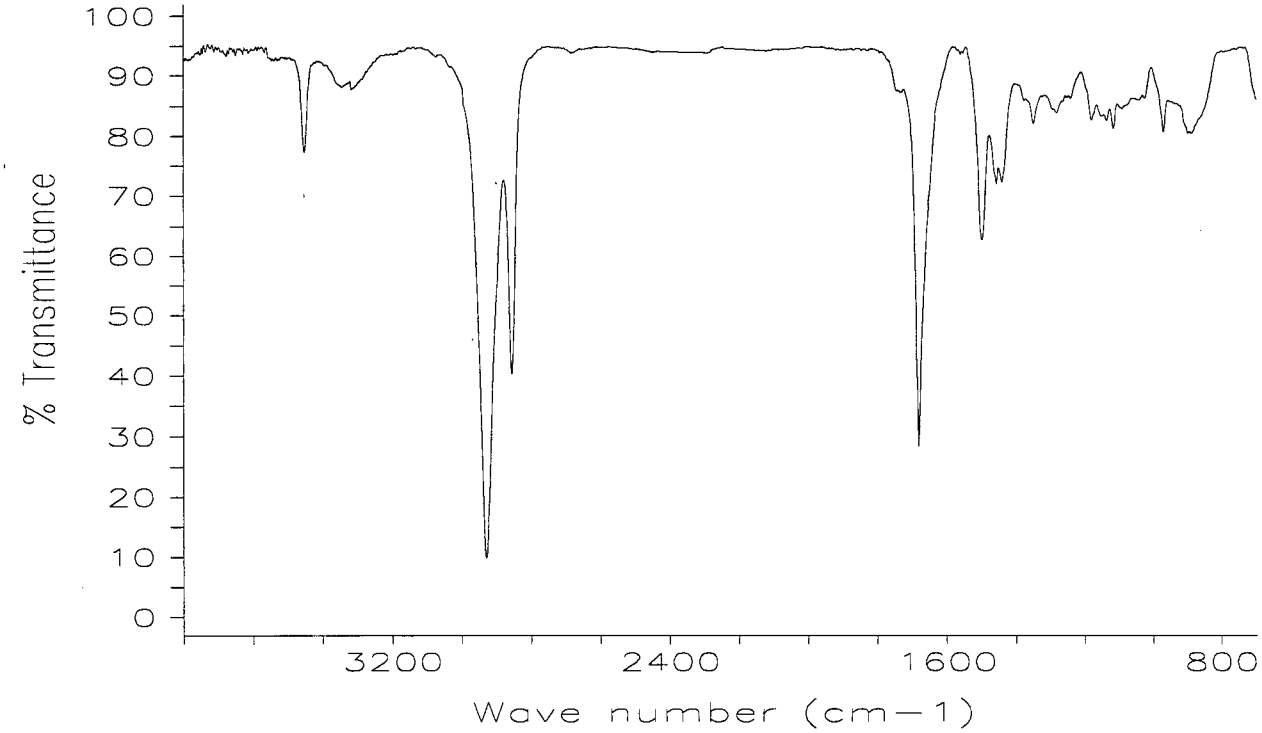
% Transmittance
100
90
80
70
60
50
40
30
20
10
0
3200
2400
1600
800
Wave number (cm−1)

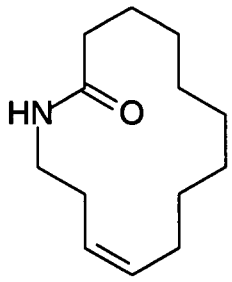
HN
O

78

Integral
3.0001
2.0000
6.0013
12.000
7.5 7.0 6.5 6.0 5.5 5.0 4.5 4.0 3.5 3.0 2.5 2.0 1.5 1.0 0.5
(ppm)

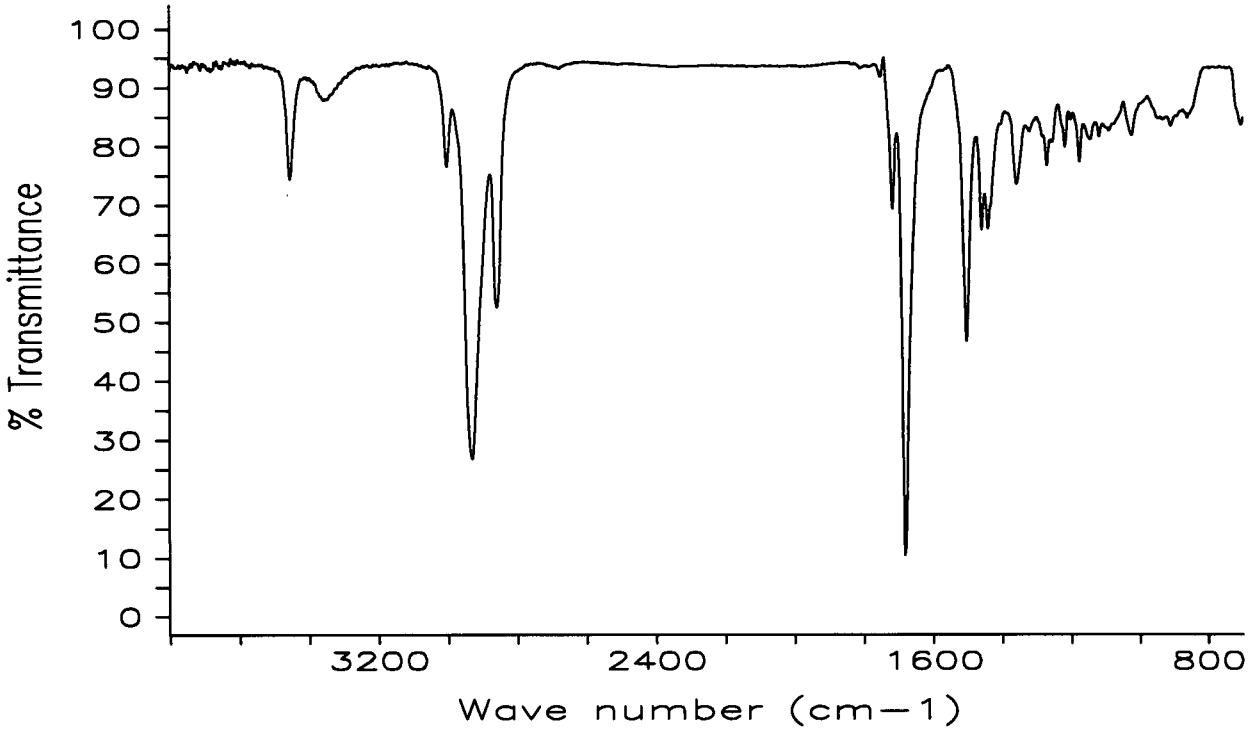
% Transmittance
100
90
80
70
60
50
40
30
20
10
0
3200
2400
1600
800
Wave number (cm−1)

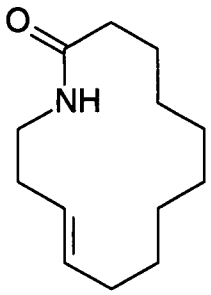
O
NH

79

Integral
3.0011
2.0014
6.0027
12.001
7.5 7.0 6.5 6.0 5.5 5.0 4.5 4.0 3.5 3.0 2.5 2.0 1.5 1.0 0.5
(ppm)

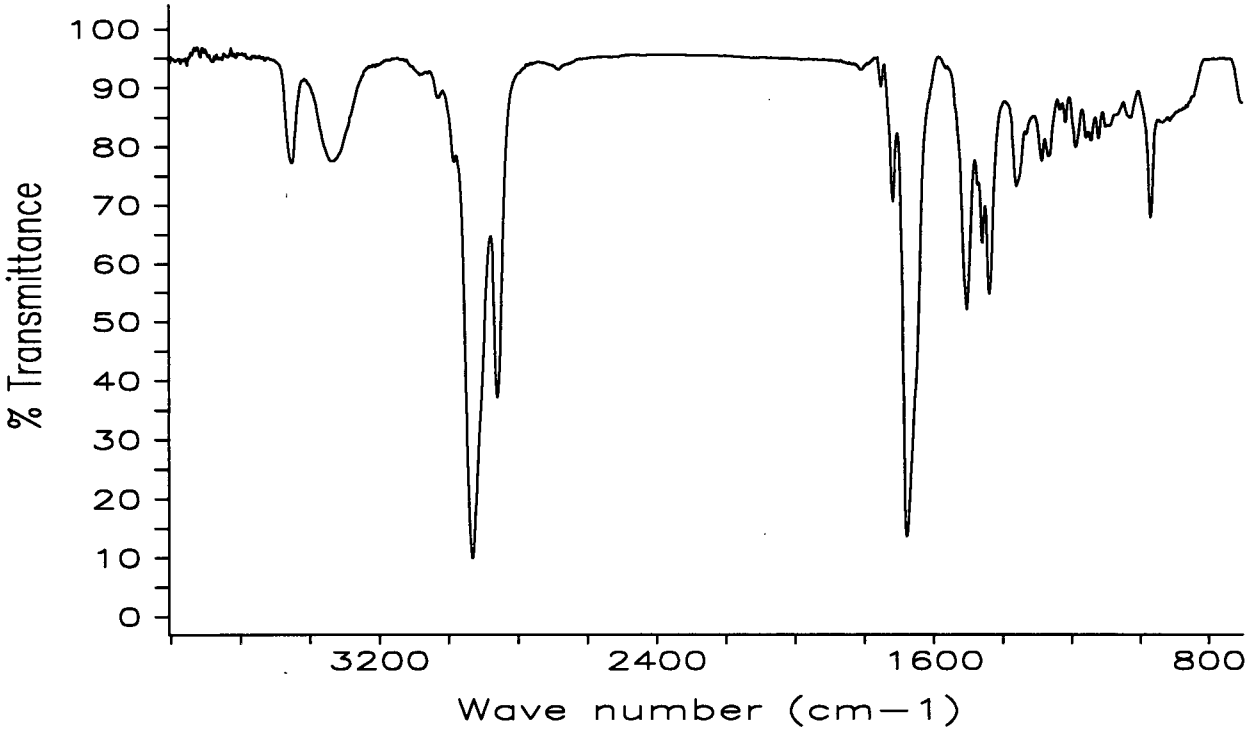
% Transmittance
100
90
80
70
60
50
40
30
20
10
0
3200
2400
1600
800
Wave number (cm−1)

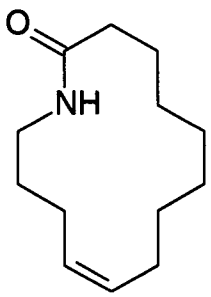
O
NH

80

Integral
1.0000
2.0016
2.0015
6.0033
12.001
7.5
7.0
6.5
6.0
5.5
5.0
4.5
4.0
3.5
3.0
2.5
2.0
1.5
1.0
0.5
(ppm)

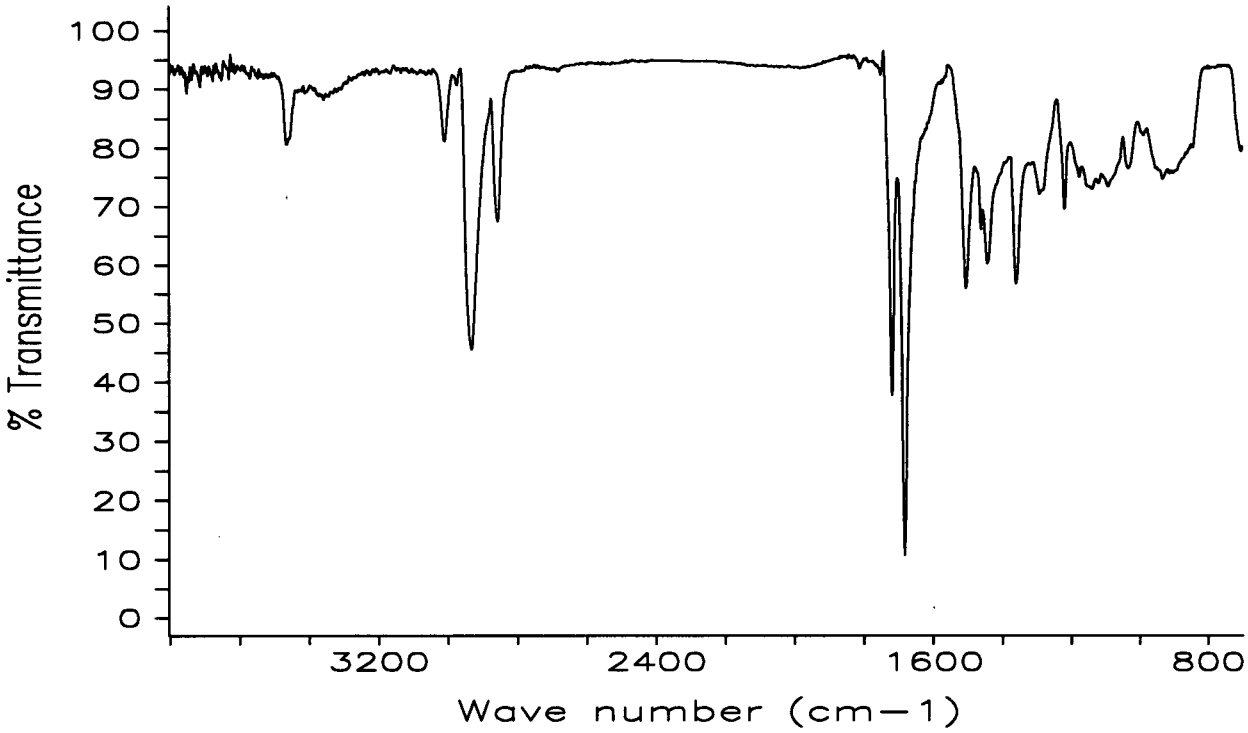
% Transmittance
100
90
80
70
60
50
40
30
20
10
0
3200
2400
1600
800
Wave number (cm−1)

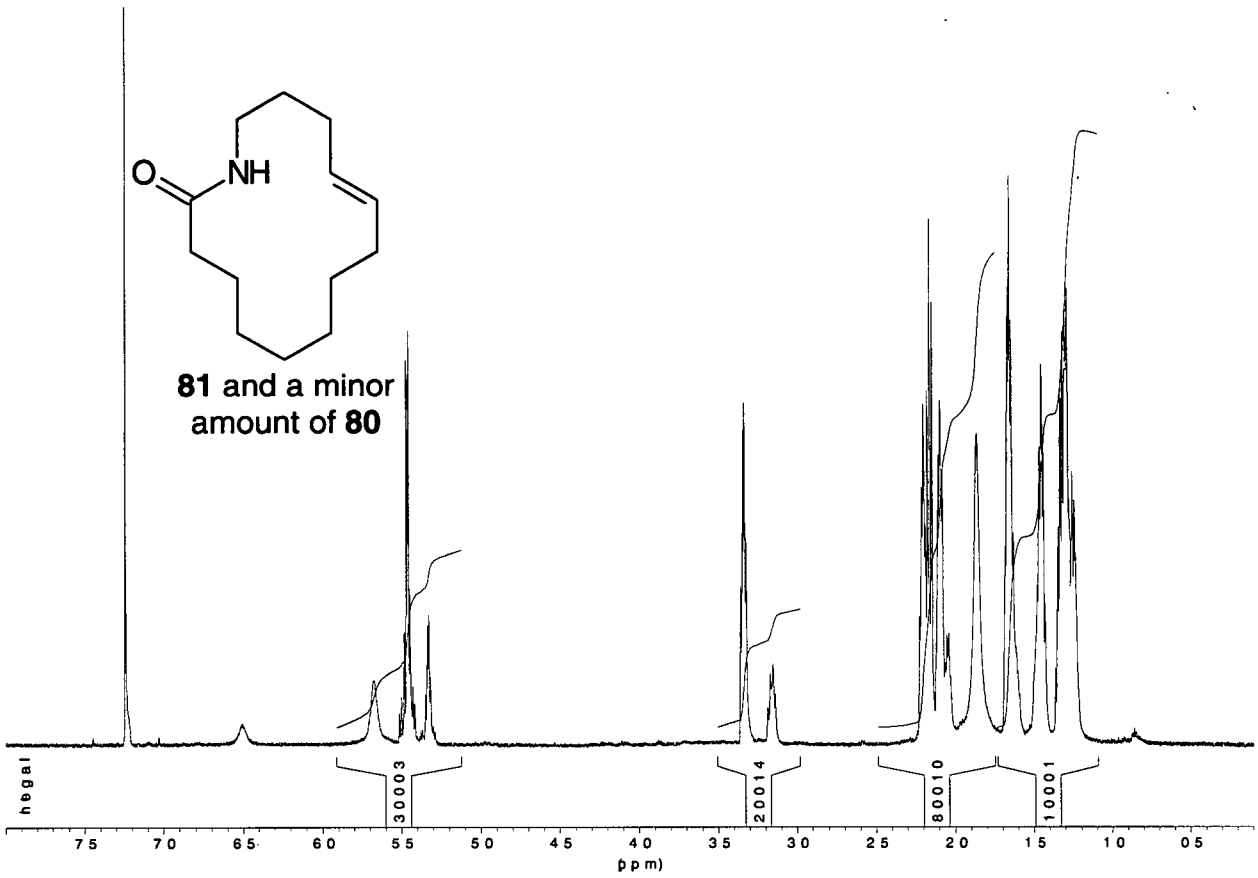
O
NH
81 and a minor amount of 80
hbgal
30003
20014
80010
10001
75 70 65 60 55 50 45 40 35 30 25 20 15 10 05
ppm)

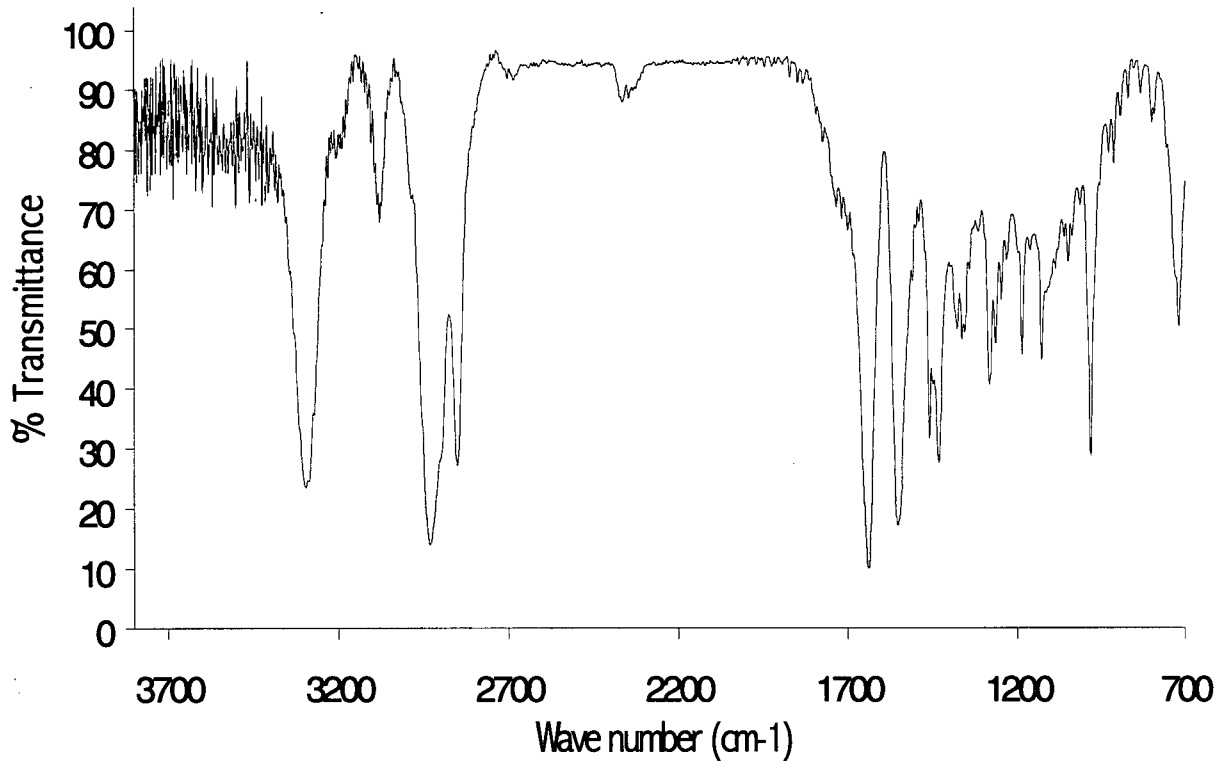
% Transmittance
100
90
80
70
60
50
40
30
20
10
0
3700
3200
2700
2200
1700
1200
700
Wave number (cm-1)

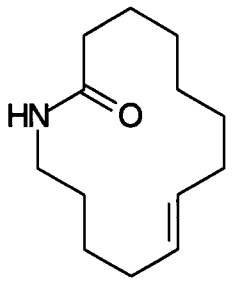
HN
O

82

Integral
1.0010
2.0015
2.0011
6.0019
12.004
7.5
7.0
6.5
6.0
5.5
5.0
4.5
4.0
3.5
3.0
2.5
2.0
1.5
1.0
0.5
(ppm)

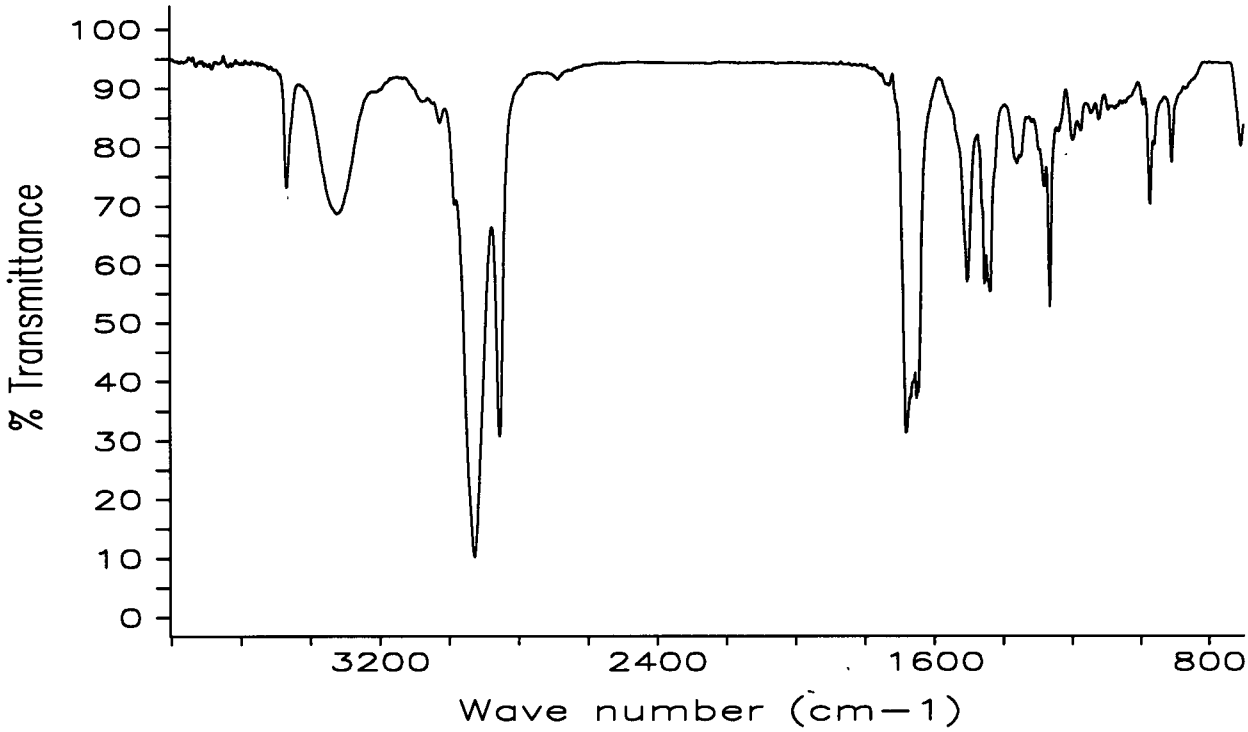
% Transmittance
100
90
80
70
60
50
40
30
20
10
0
3200
2400
1600
800
Wave number (cm−1)

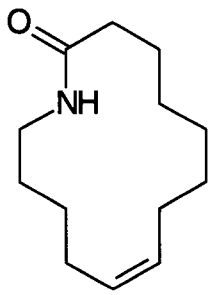
O
NH

83

Integral
3.0010
1.9999
6.0009
12.001
7.5
7.0
6.5
6.0
5.5
5.0
4.5
4.0
3.5
3.0
2.5
2.0
1.5
1.0
0.5
(ppm)

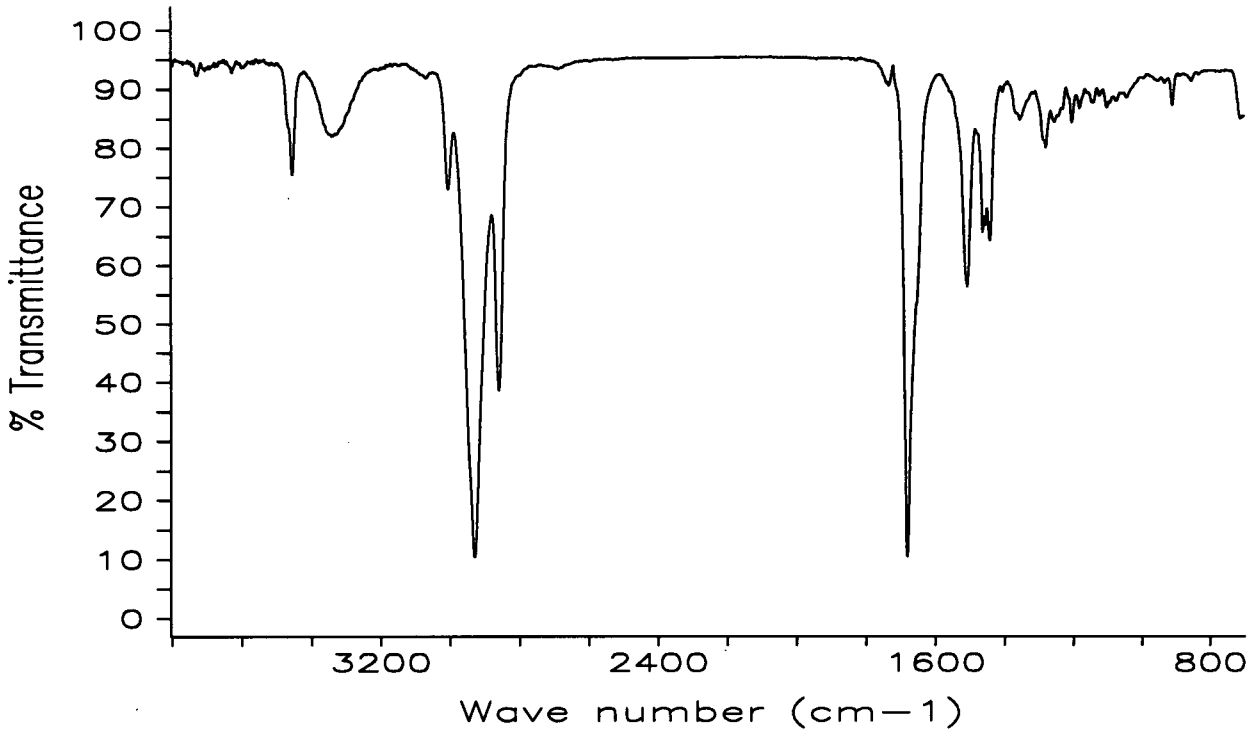
% Transmittance
100
90
80
70
60
50
40
30
20
10
0
3200
2400
1600
800
Wave number (cm−1)

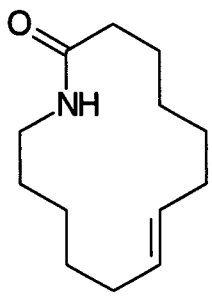
O
NH

84

Integral
3.0010
1.9995
6.0003
12.001
7.5 7.0 6.5 6.0 5.5 5.0 4.5 4.0 3.5 3.0 2.5 2.0 1.5 1.0 0.5
(ppm)

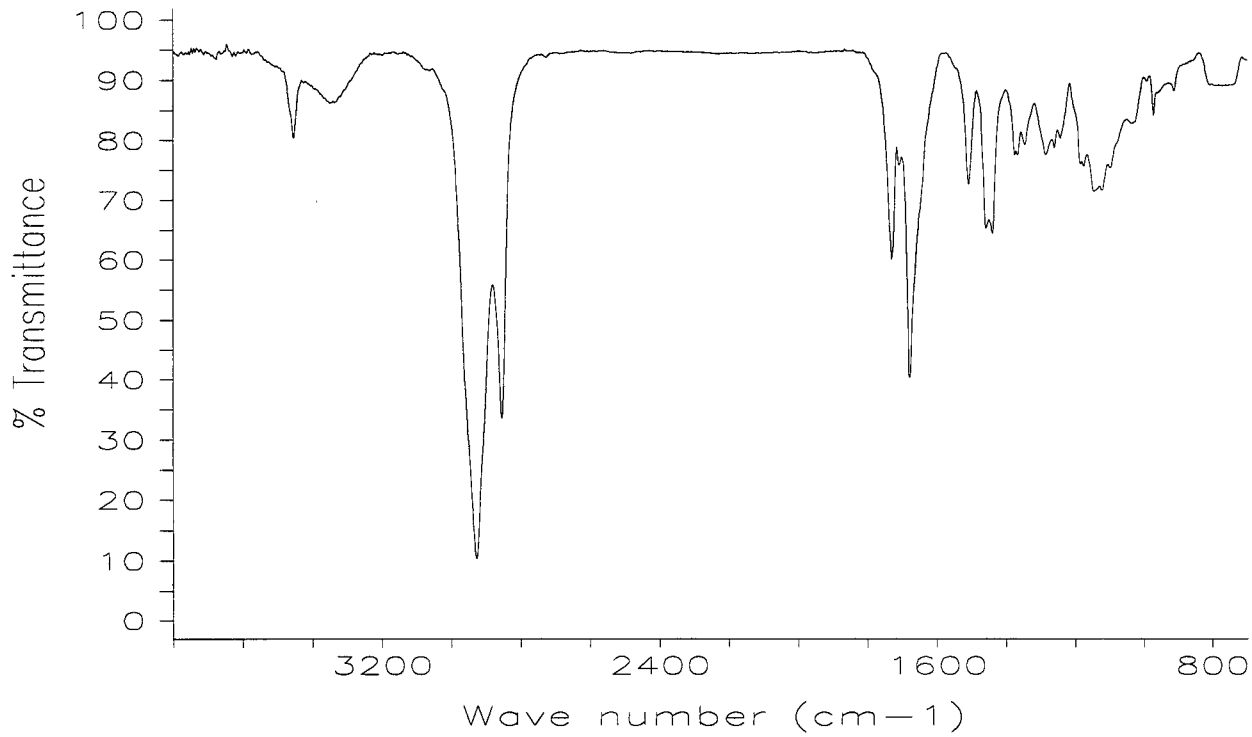
% Transmittance
100
90
80
70
60
50
40
30
20
10
0
3200
2400
1600
800
Wave number (cm−1)

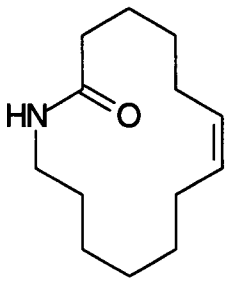
HN
O

85

Integral
3.0008
1.9996
6.0009
12.001
7.5
7.0
6.5
6.0
5.5
5.0
4.5
4.0
3.5
3.0
2.5
2.0
1.5
1.0
0.5
(ppm)

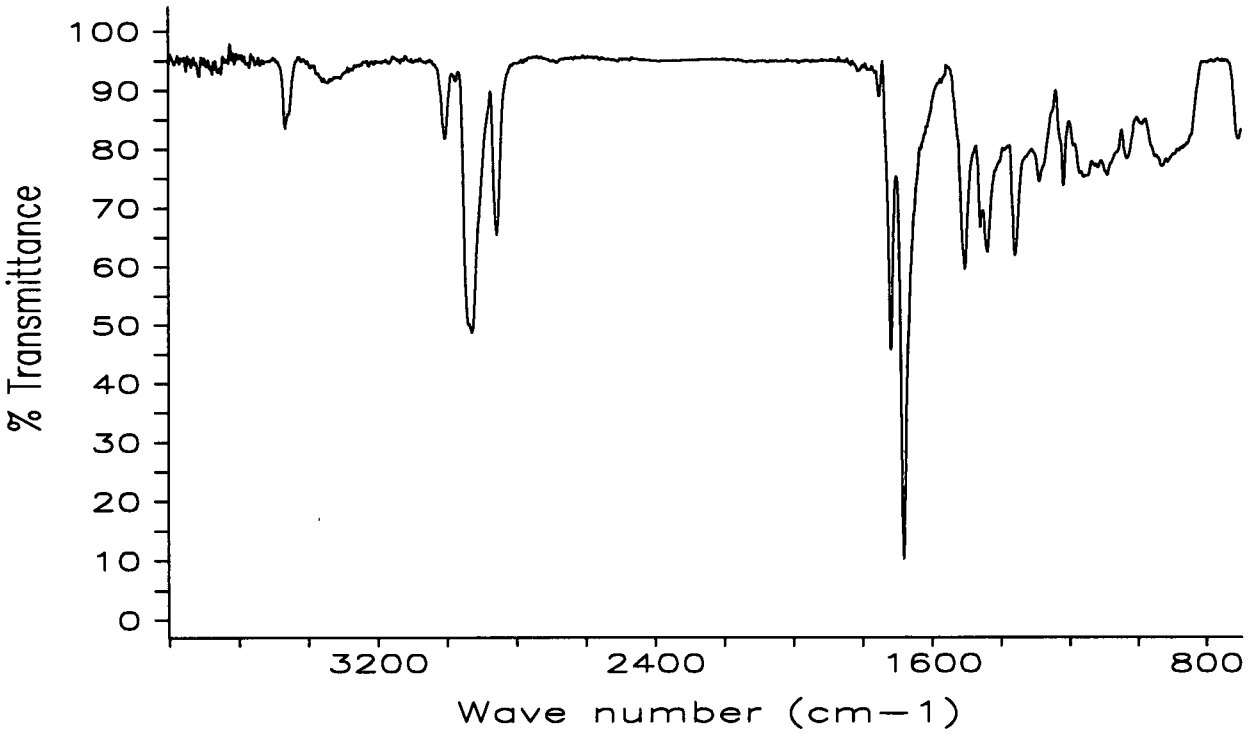
% Transmittance
100
90
80
70
60
50
40
30
20
10
0
3200
2400
1600
800
Wave number (cm−1)

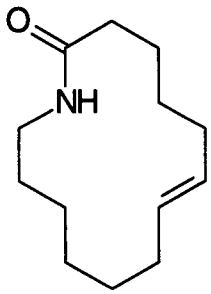
O
NH

86

Integral
3.0010
1.9997
6.0001
12.000
7.5
7.0
6.5
6.0
5.5
5.0
4.5
4.0
3.5
3.0
2.5
2.0
1.5
1.0
0.5
(ppm)

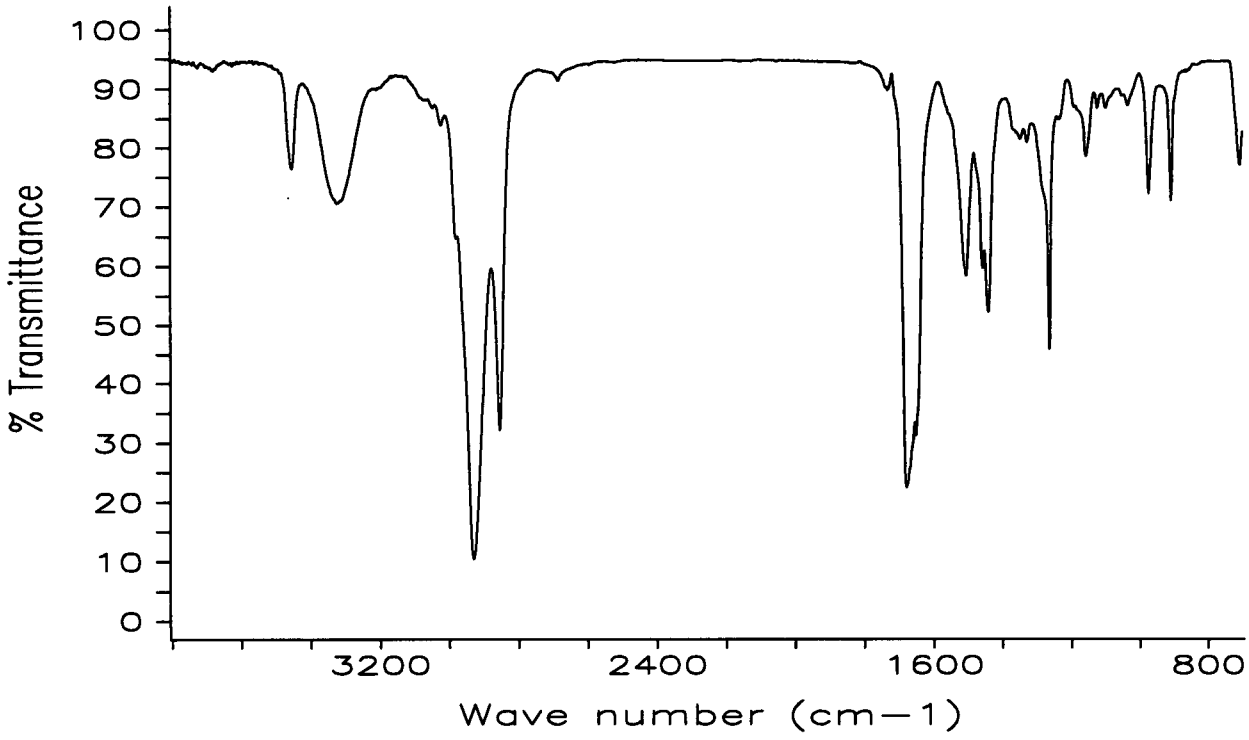
% Transmittance
100
90
80
70
60
50
40
30
20
10
0
3200
2400
1600
800
Wave number (cm−1)

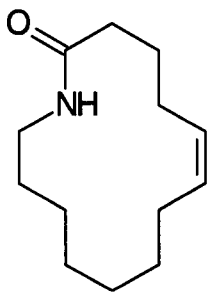
O
NH

87

Integral
3.0009
2.0008
6.0008
12.000
7.5 7.0 6.5 6.0 5.5 5.0 4.5 4.0 3.5 3.0 2.5 2.0 1.5 1.0 0.5
(ppm)

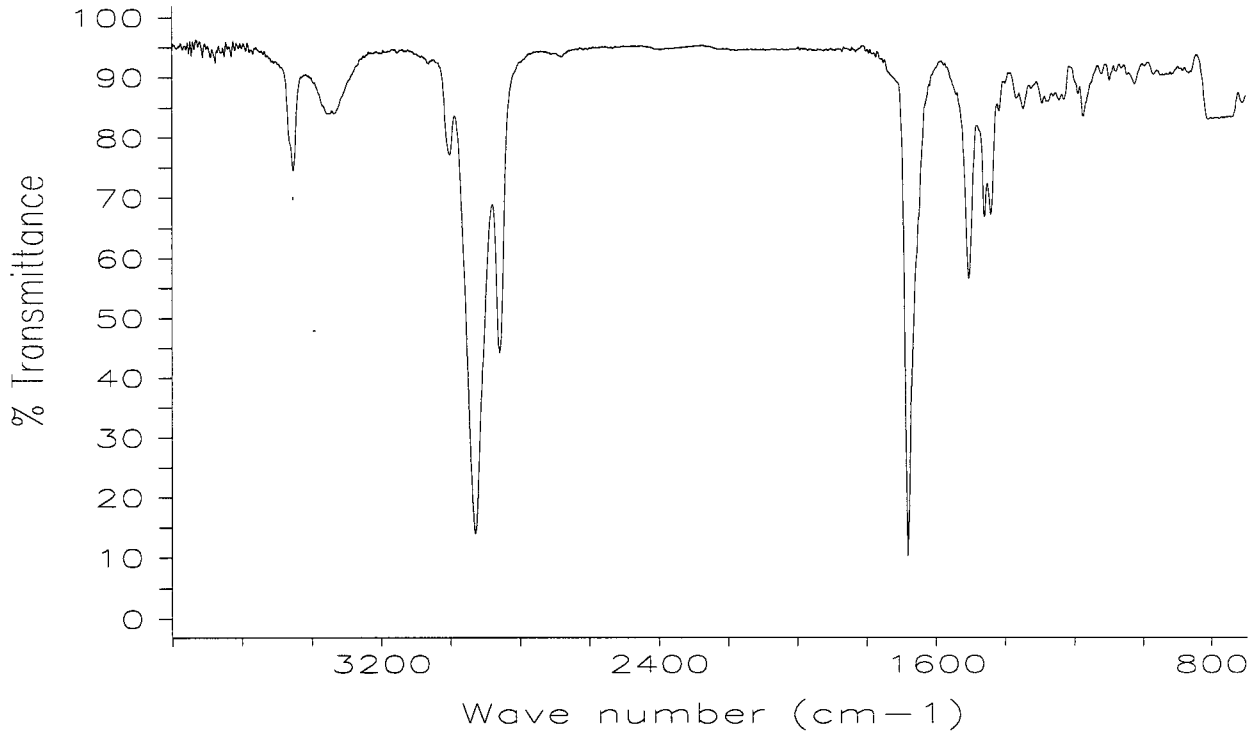
% Transmittance
100
90
80
70
60
50
40
30
20
10
0
3200
2400
1600
800
Wave number (cm−1)

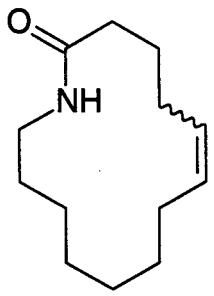

87 and a minor amount of **88**

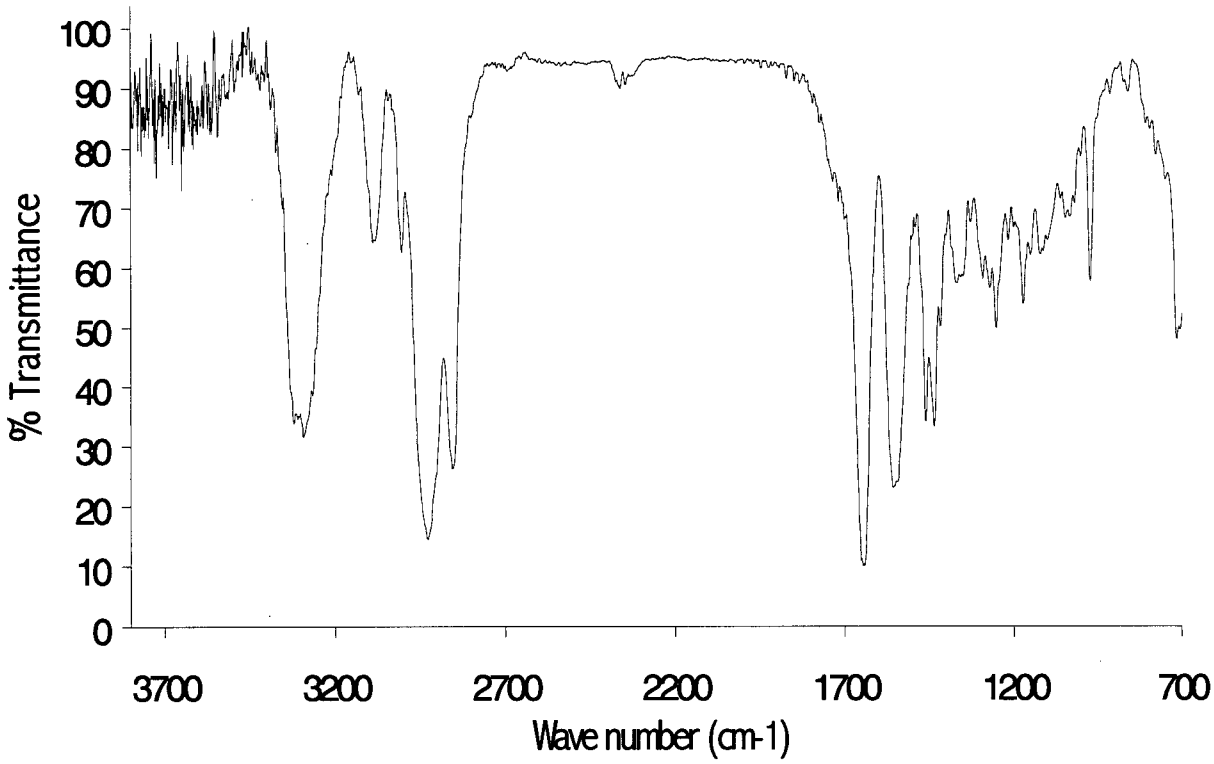

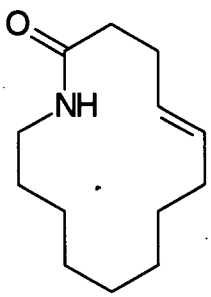
O
NH

89

Integral
3.0009
2.0004
6.0009
12.001
7.5 7.0 6.5 6.0 5.5 5.0 4.5 4.0 3.5 3.0 2.5 2.0 1.5 1.0 0.5
(ppm)

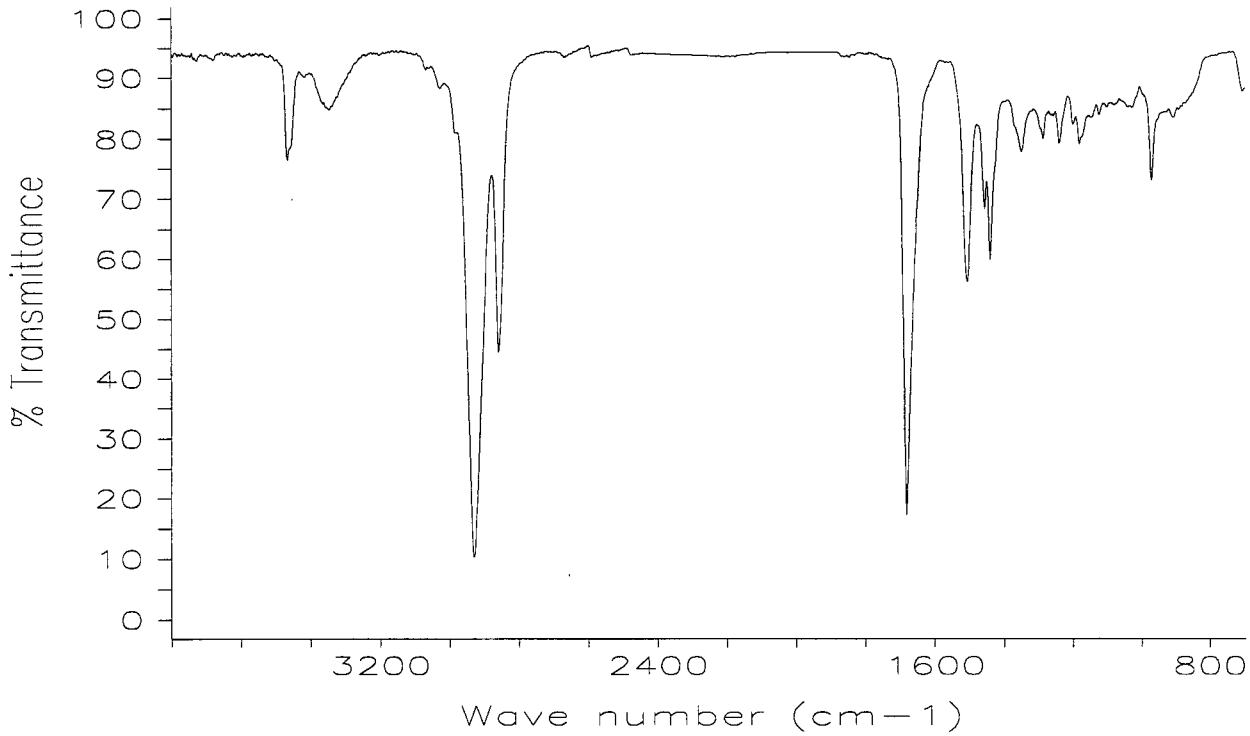
% Transmittance
100
90
80
70
60
50
40
30
20
10
0
3200
2400
1600
800
Wave number (cm−1)

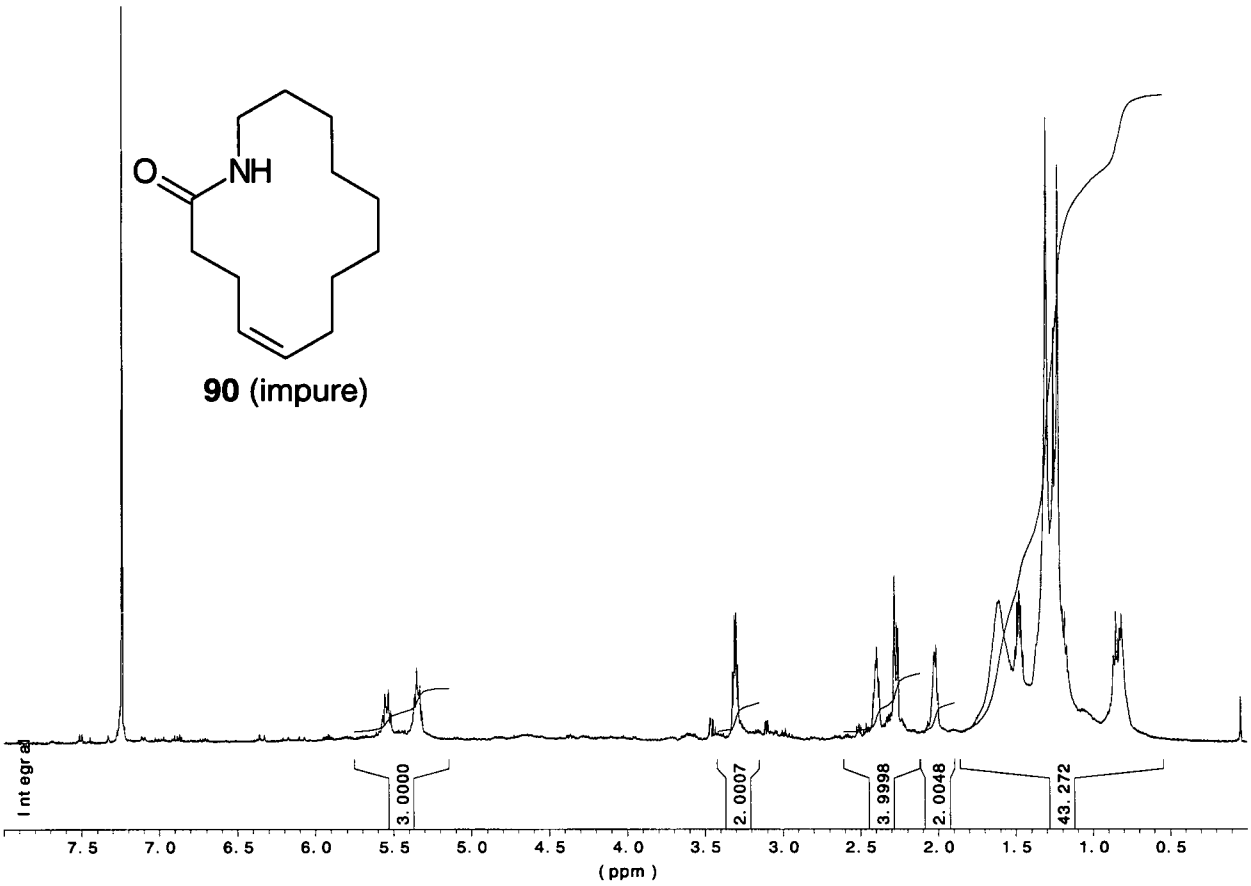
O
NH
Int egral
3.0000
2.0007
3.9998
2.0048
43.272
7.5 7.0 6.5 6.0 5.5 5.0 4.5 4.0 3.5 3.0 2.5 2.0 1.5 1.0 0.5
(ppm)

90 (impure)

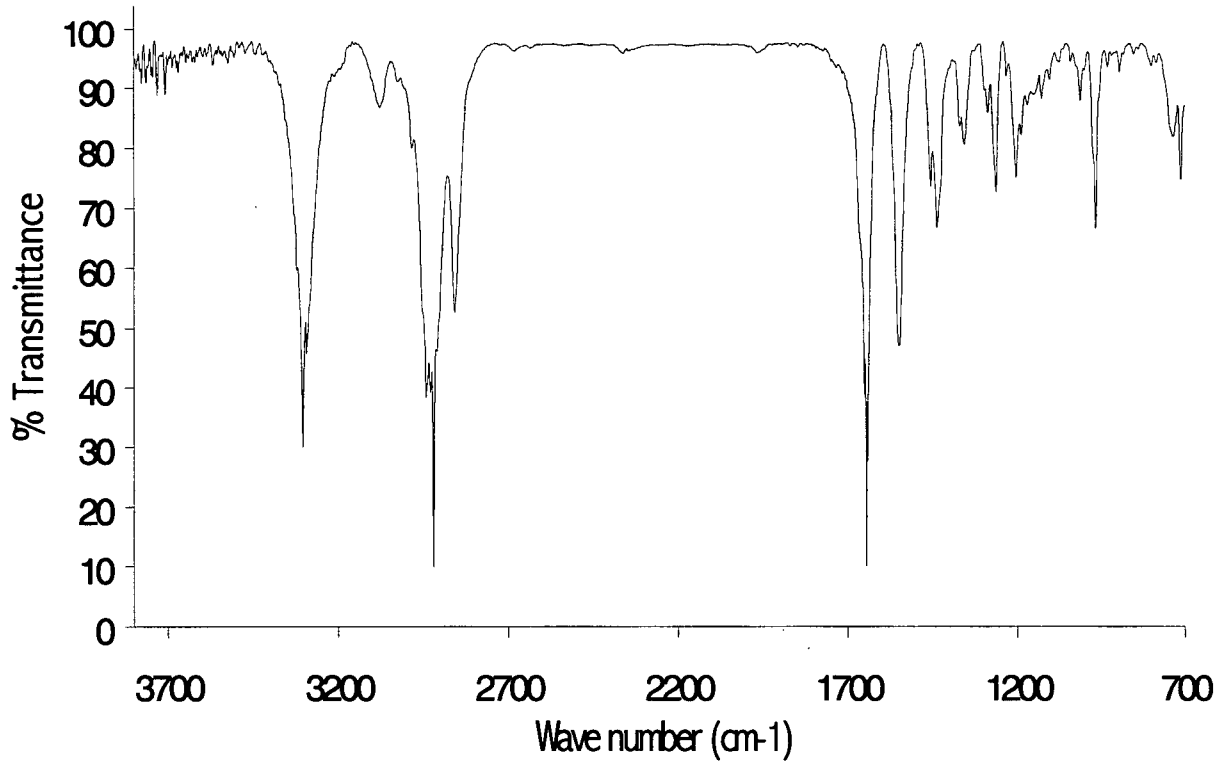
% Transmittance
100
90
80
70
60
50
40
30
20
10
0
3700
3200
2700
2200
1700
1200
700
Wave number (cm-1)

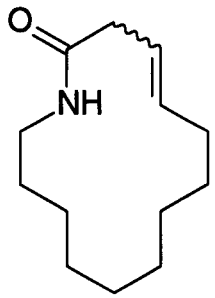

(*E*)-**91** (major)
and
(*Z*)-**92** (minor)

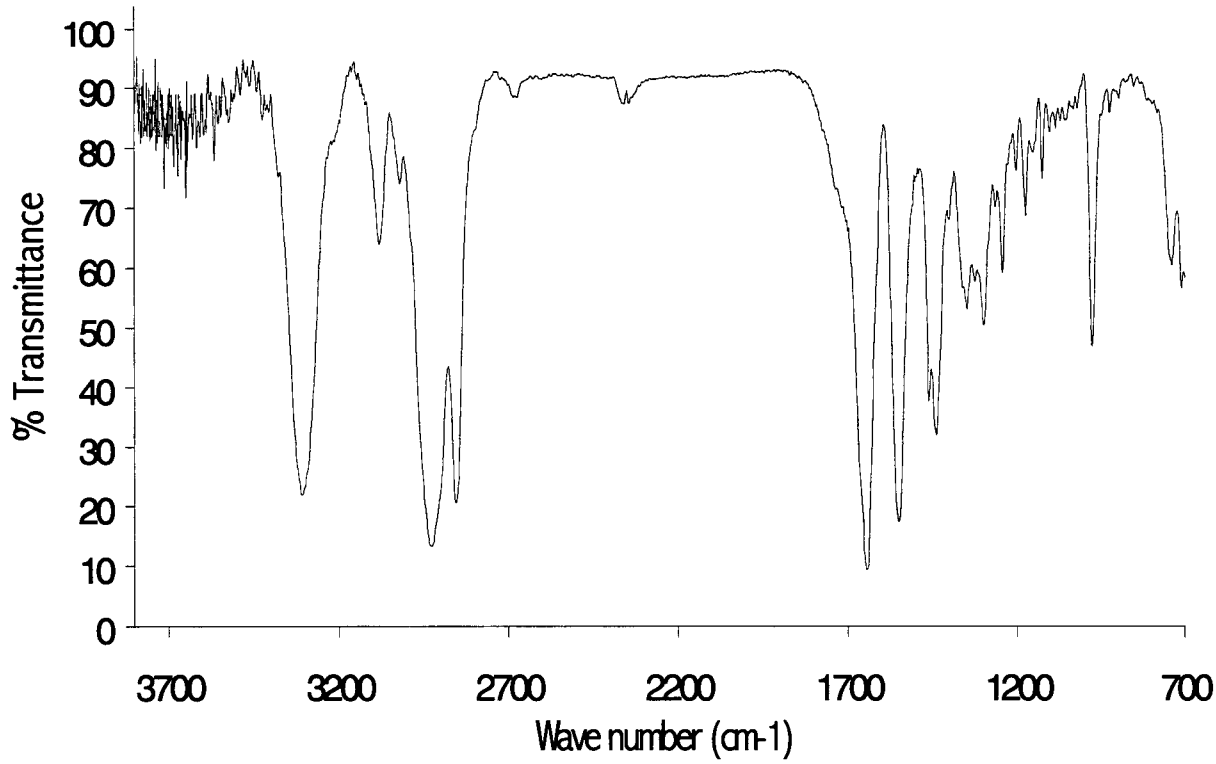

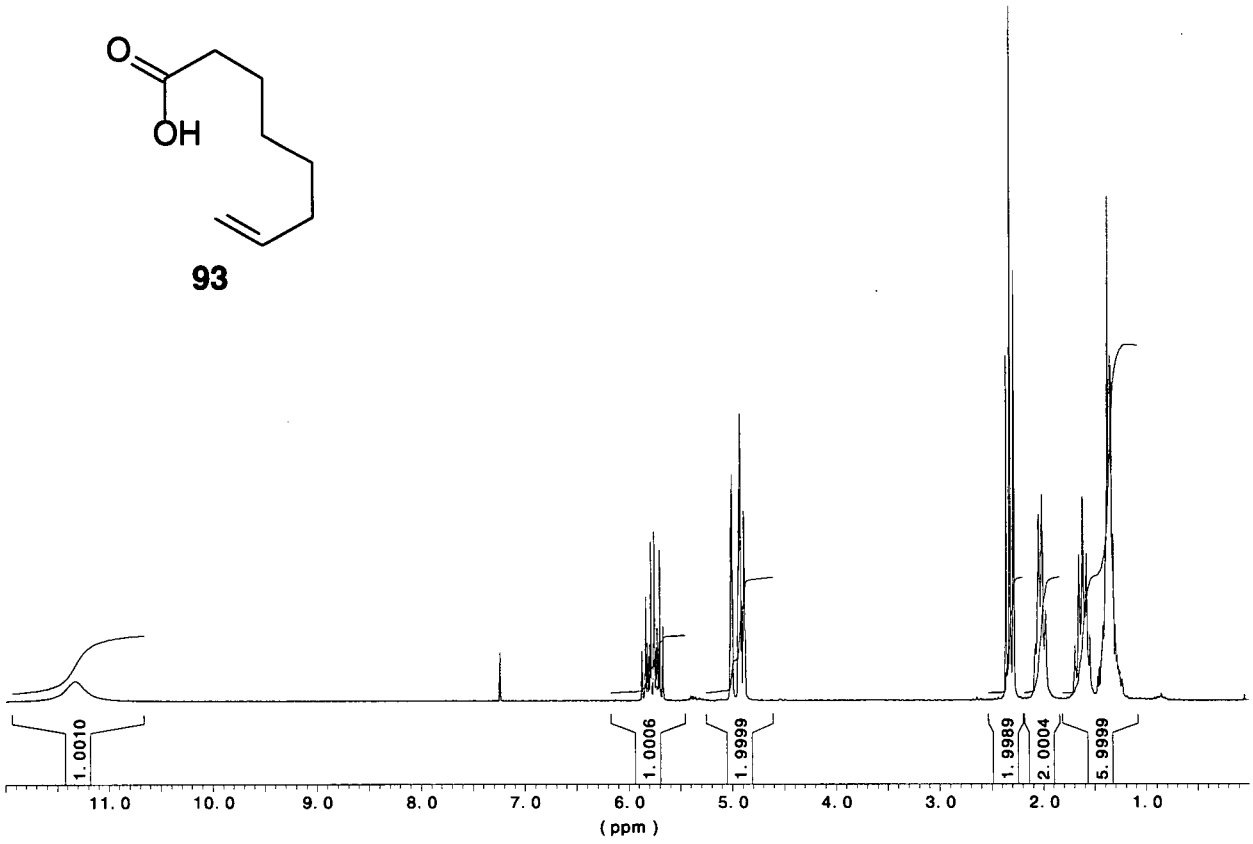
O
OH
93
1.0010
1.0006
1.9999
1.9989
2.0004
5.9999
11.0
10.0
9.0
8.0
7.0
6.0
5.0
4.0
3.0
2.0
1.0
(ppm)

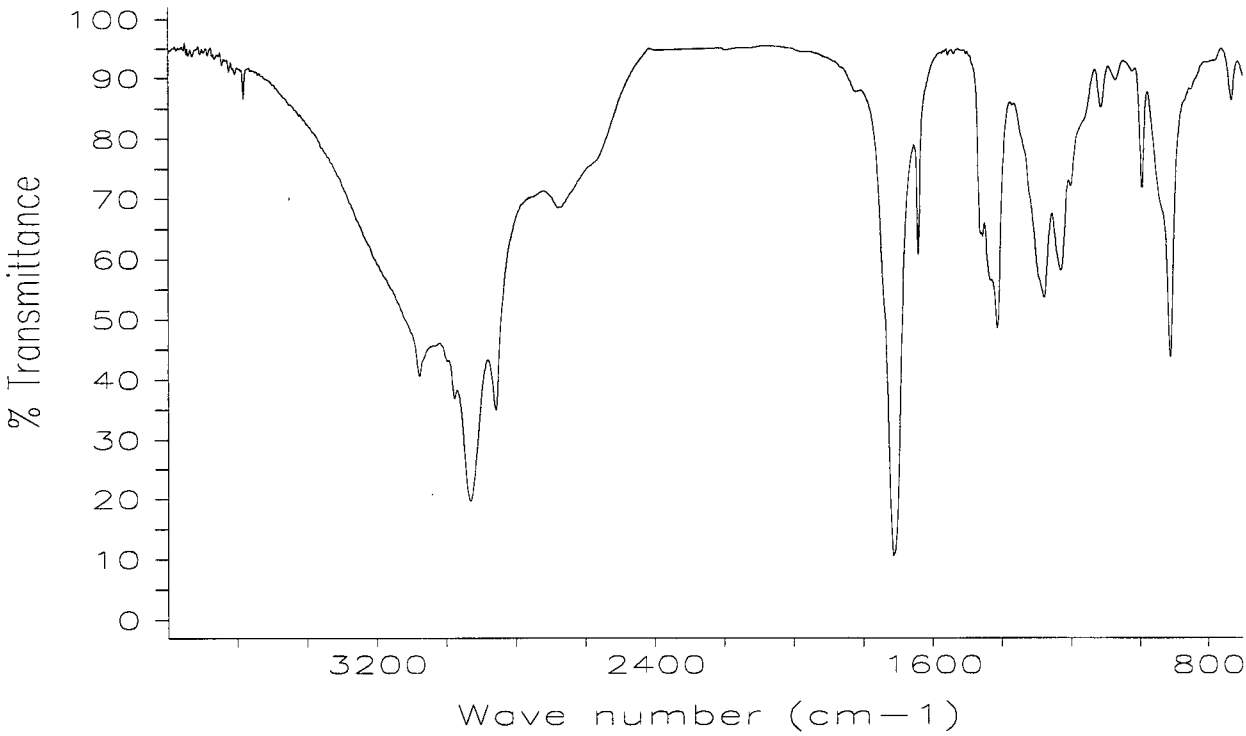
% Transmittance
100
90
80
70
60
50
40
30
20
10
0
3200
2400
1600
800
Wave number (cm−1)

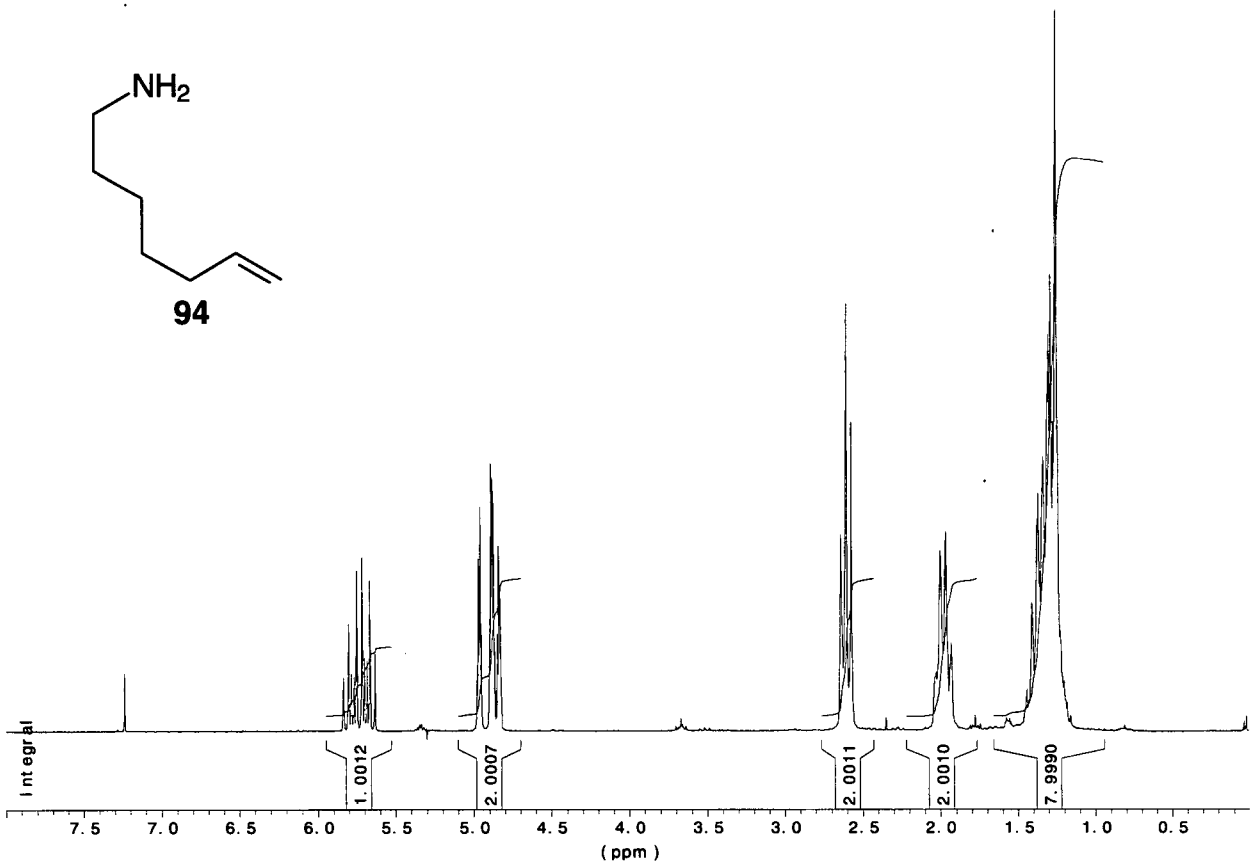
NH2
94
Integral
1.0012
2.0007
2.0011
2.0010
7.9990
7.5 7.0 6.5 6.0 5.5 5.0 4.5 4.0 3.5 3.0 2.5 2.0 1.5 1.0 0.5
(ppm)

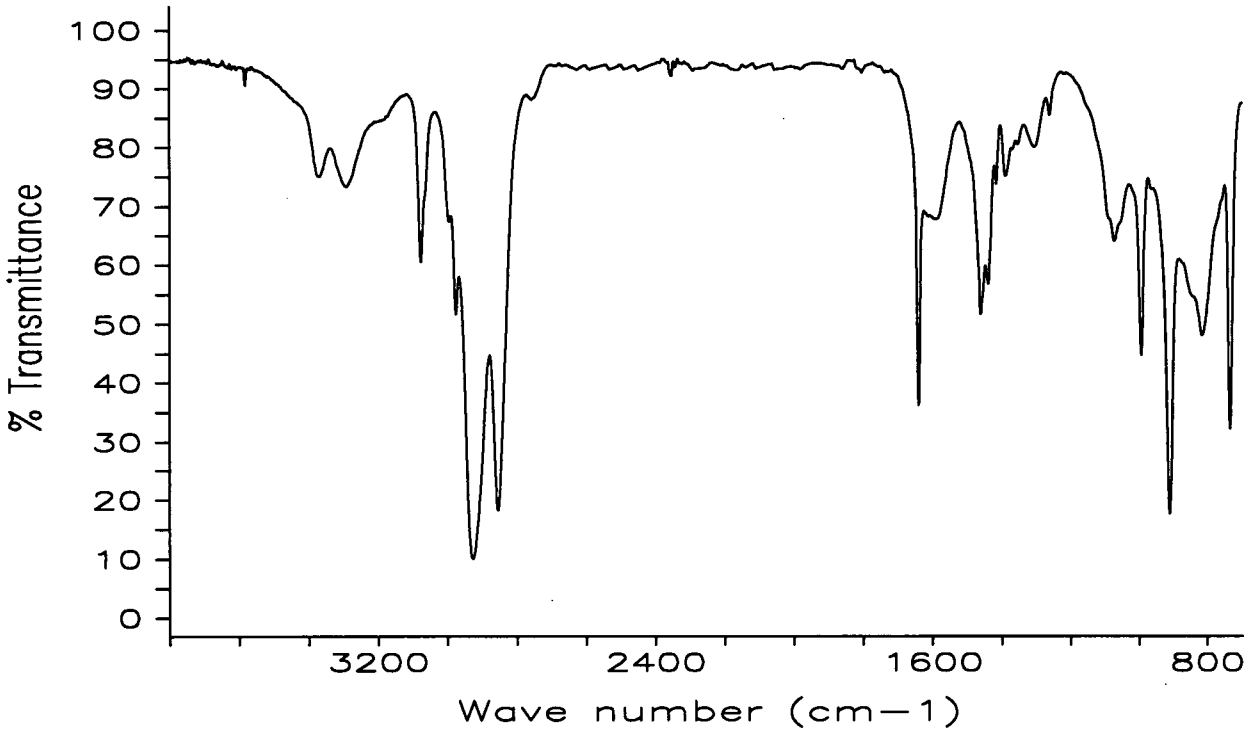
% Transmittance
100
90
80
70
60
50
40
30
20
10
0
3200
2400
1600
800
Wave number (cm−1)

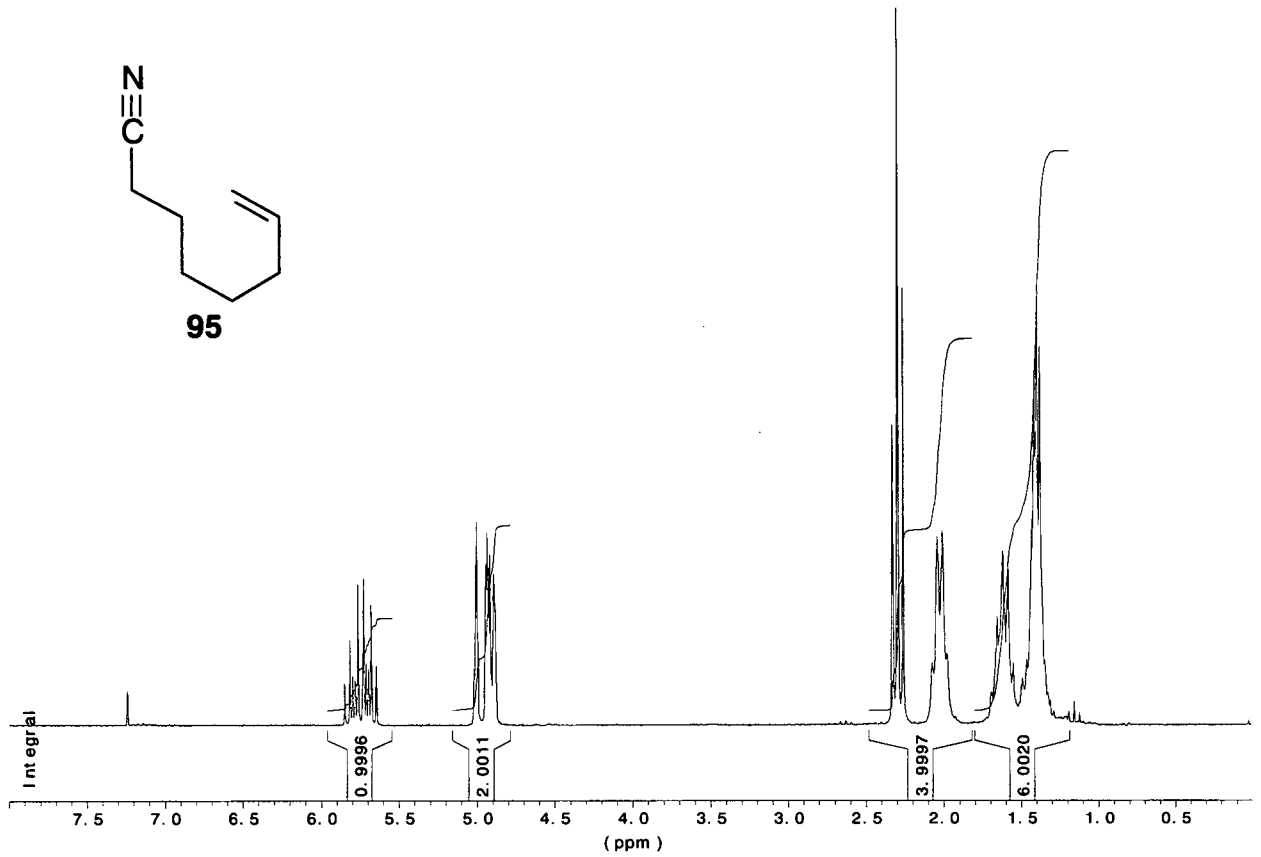
N
C
95
Integral
0.9996
2.0011
3.9997
6.0020
7.5 7.0 6.5 6.0 5.5 5.0 4.5 4.0 3.5 3.0 2.5 2.0 1.5 1.0 0.5
(ppm)

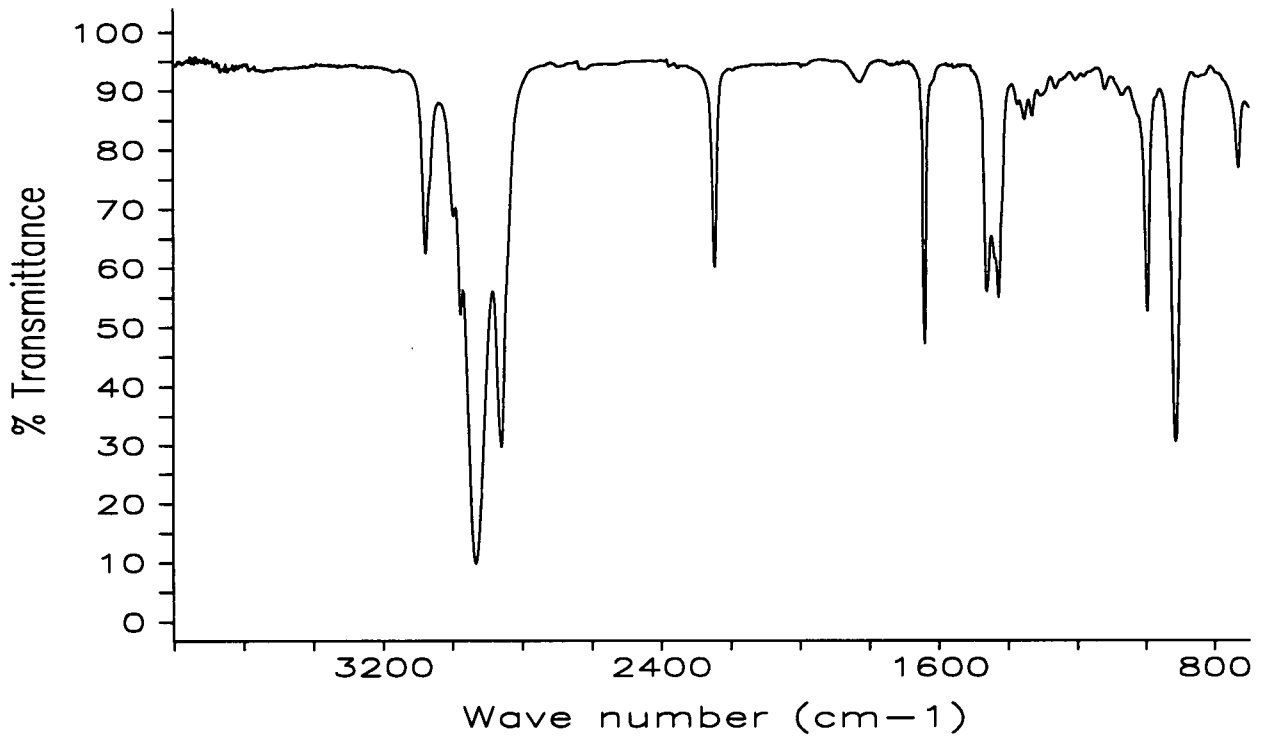
% Transmittance
100
90
80
70
60
50
40
30
20
10
0
3200
2400
1600
800
Wave number (cm−1)

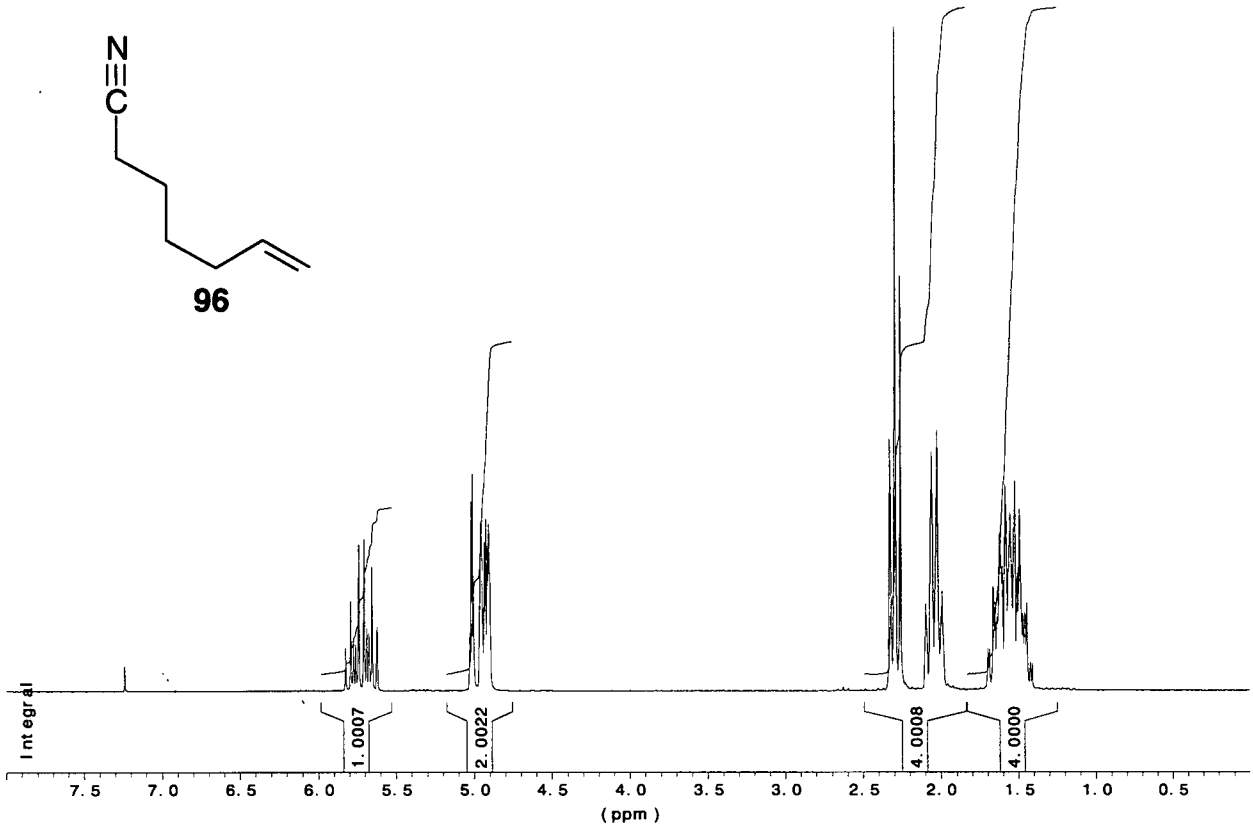
N
C
96
Integral
1.0007
2.0022
4.0008
4.0000
7.5 7.0 6.5 6.0 5.5 5.0 4.5 4.0 3.5 3.0 2.5 2.0 1.5 1.0 0.5
(ppm)

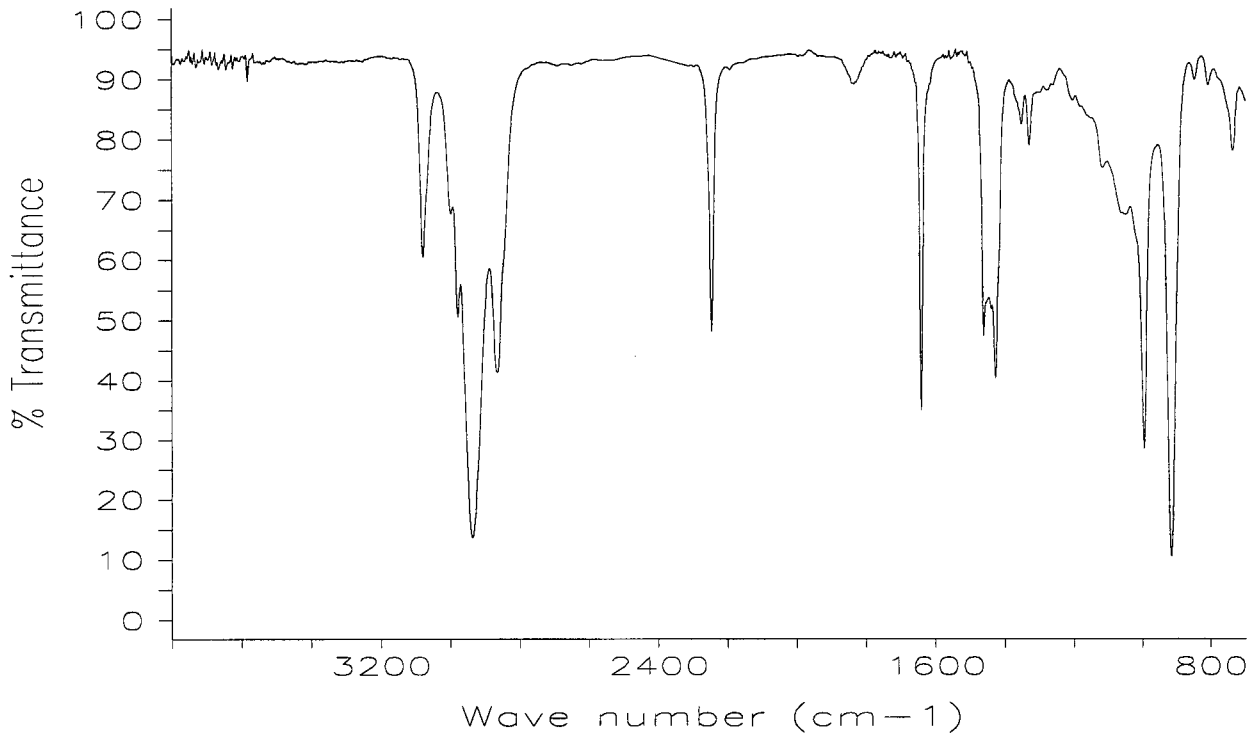
% Transmittance
100
90
80
70
60
50
40
30
20
10
0
3200
2400
1600
800
Wave number (cm−1)

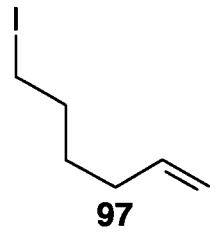

97

Integral
1.0013
2.0012
2.0007
4.0020
2.0010
7.5 7.0 6.5 6.0 5.5 5.0 4.5 4.0 3.5 3.0 2.5 2.0 1.5 1.0 0.5
(ppm)

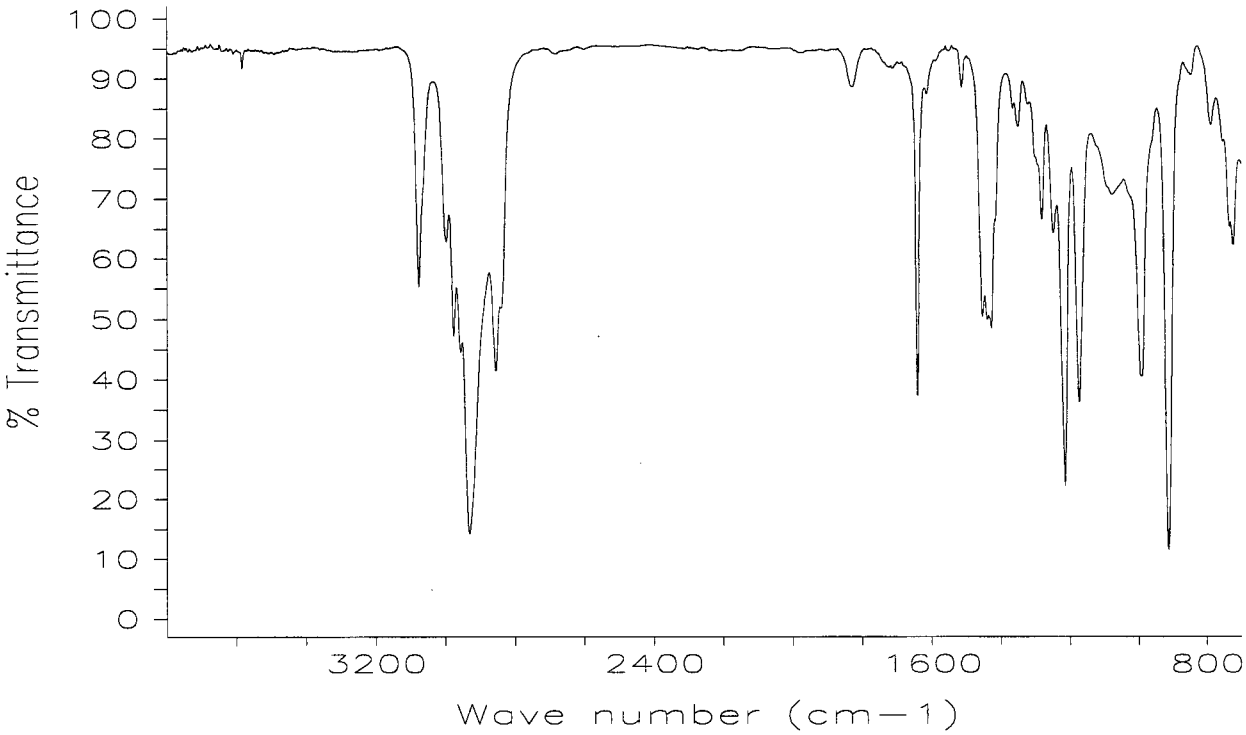
% Transmittance
100
90
80
70
60
50
40
30
20
10
0
3200
2400
1600
800
Wave number (cm−1)

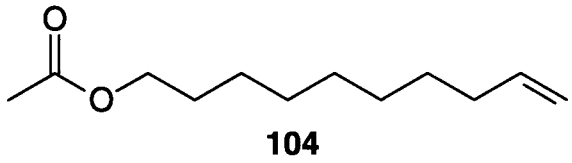

104

Integral
1.0009
2.0024
2.0006
5.0023
12.002
7.5 7.0 6.5 6.0 5.5 5.0 4.5 4.0 3.5 3.0 2.5 2.0 1.5 1.0 0.5
(ppm)

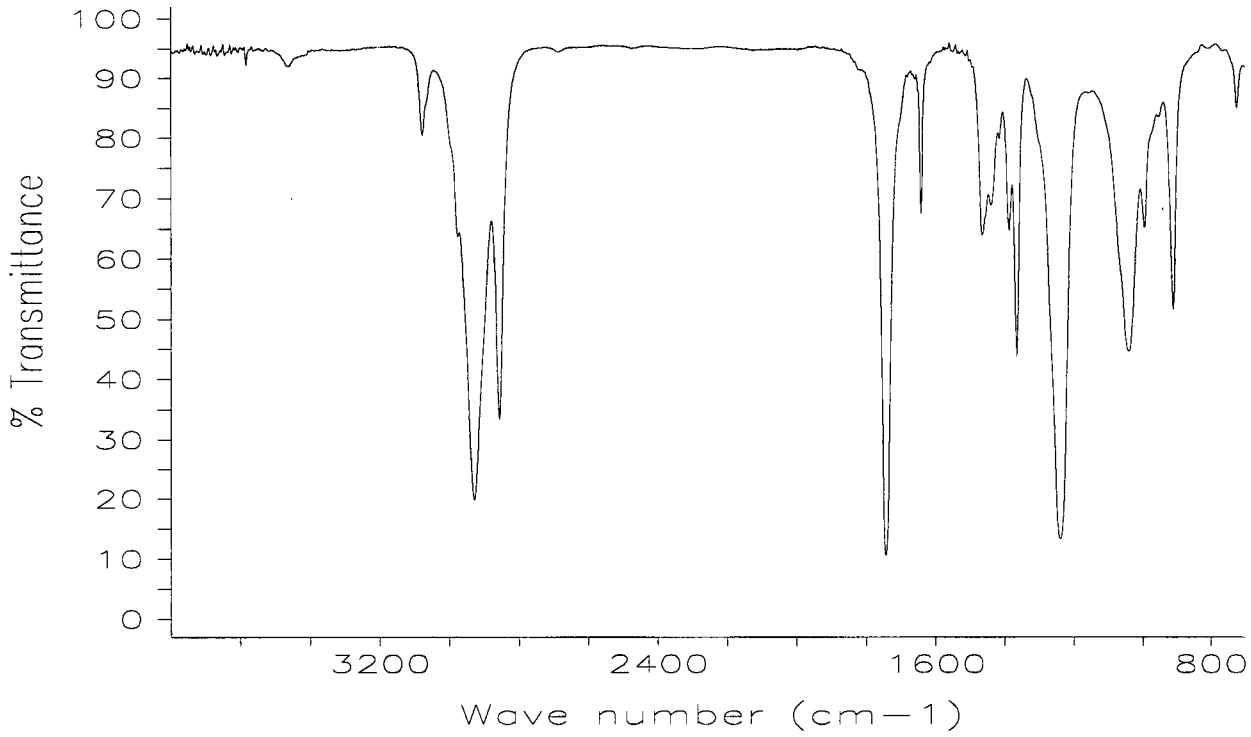
% Transmittance
100
90
80
70
60
50
40
30
20
10
0
3200
2400
1600
800
Wave number (cm−1)

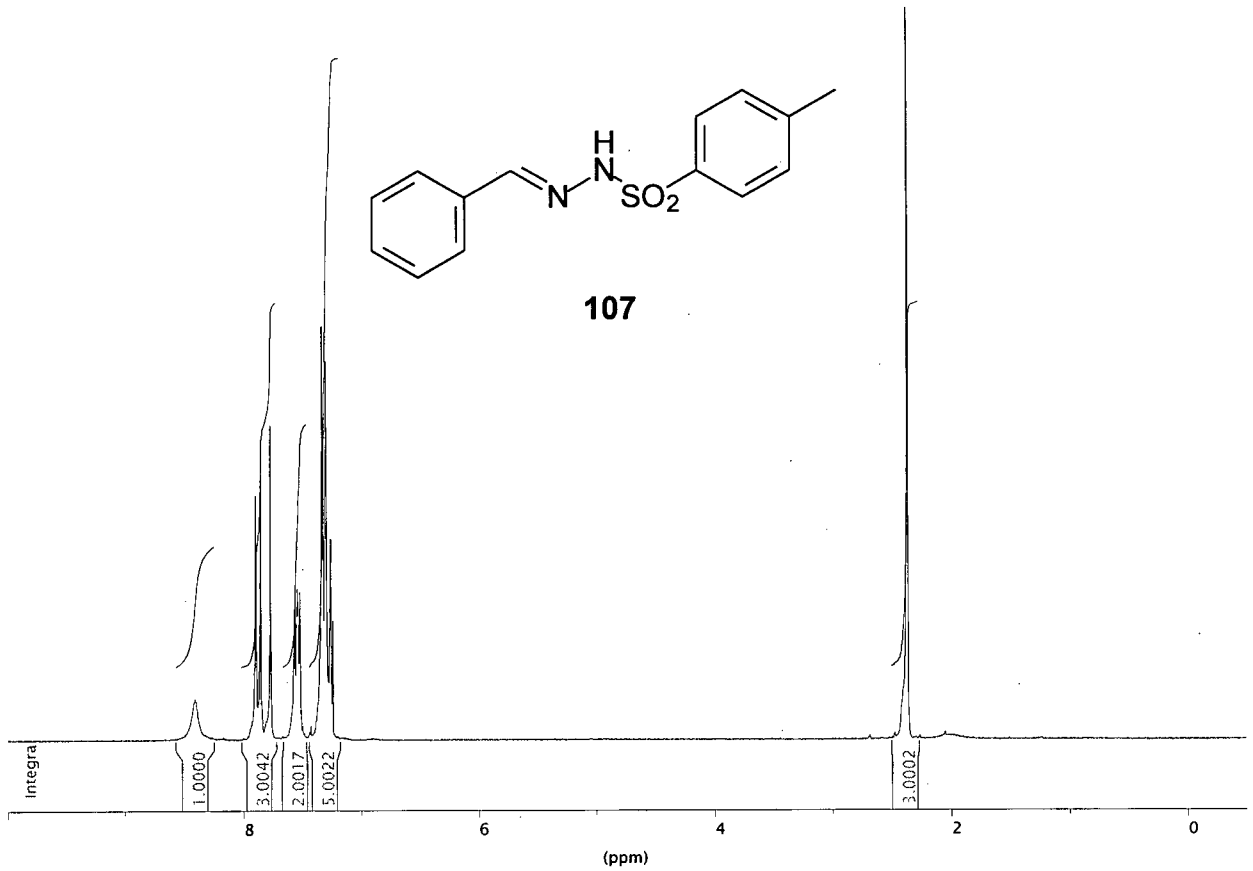
H
N
N
SO2
Integra
1.0000
3.0042
2.0017
5.0022
3.0002
8
6
4
2
0
(ppm)

107

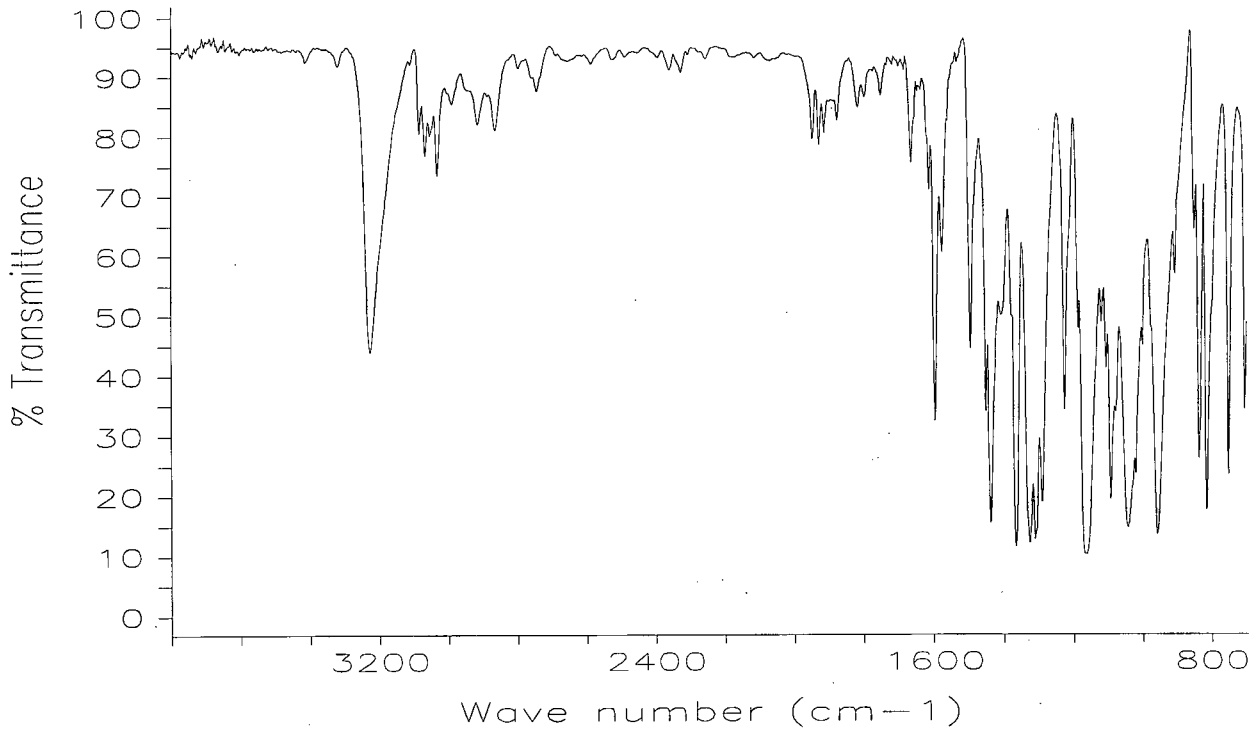
% Transmittance
100
90
80
70
60
50
40
30
20
10
0
3200
2400
1600
800
Wave number (cm−1)

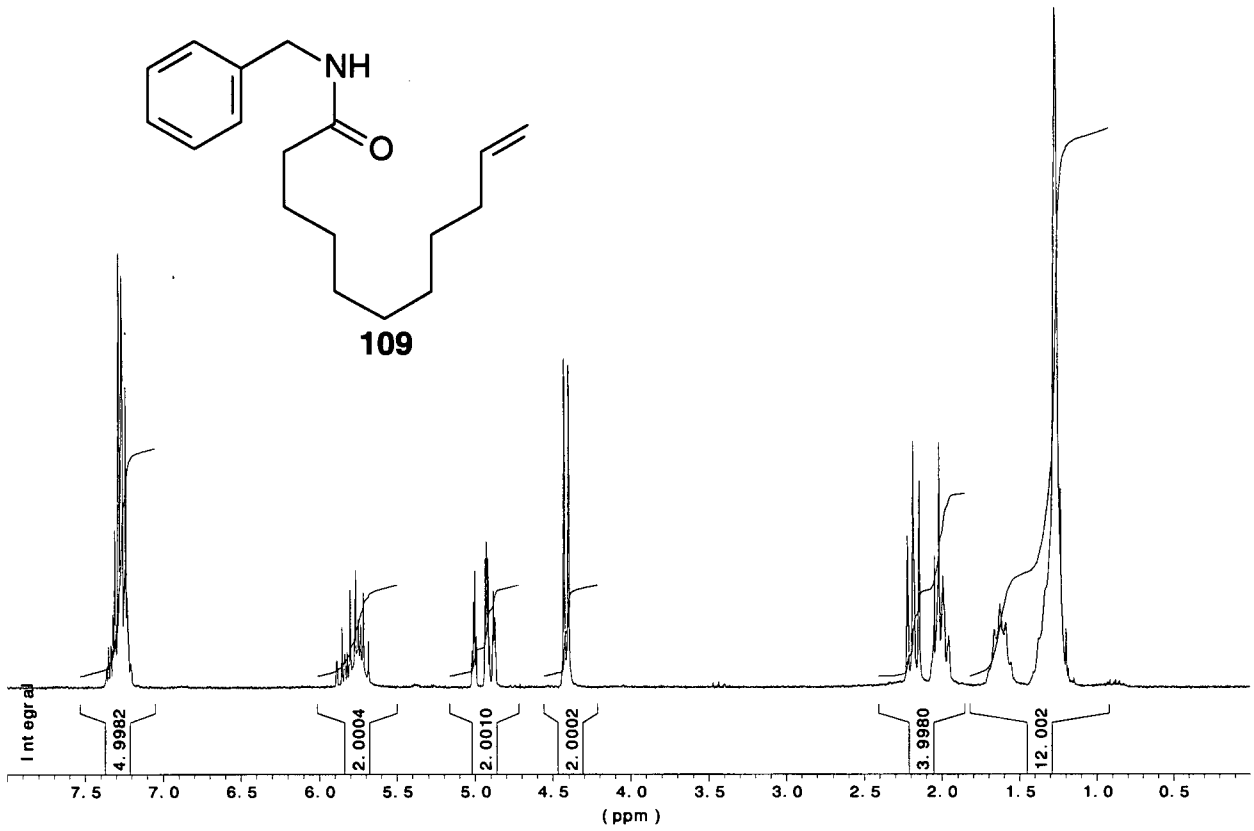
NH
O
109
Integral
4.9982
2.0004
2.0010
2.0002
3.9980
12.002
7.5
7.0
6.5
6.0
5.5
5.0
4.5
4.0
3.5
3.0
2.5
2.0
1.5
1.0
0.5
(ppm)

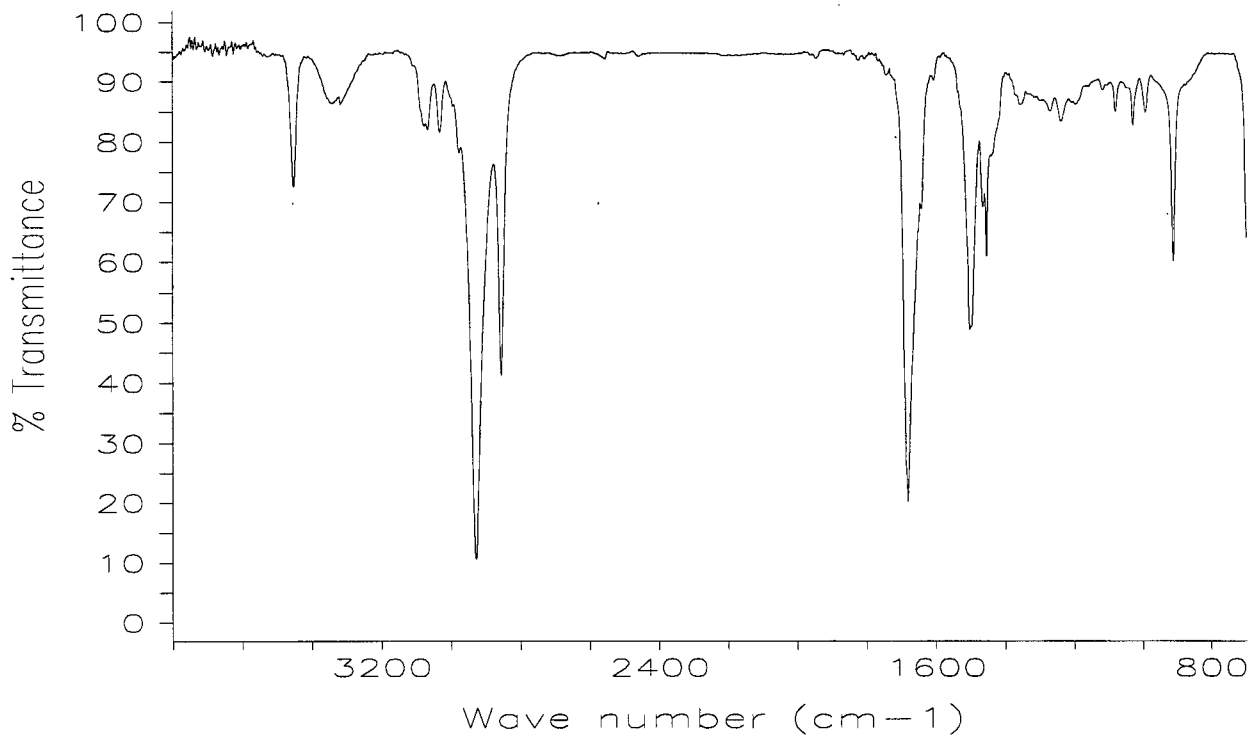
% Transmittance
100
90
80
70
60
50
40
30
20
10
0
3200
2400
1600
800
Wave number (cm−1)

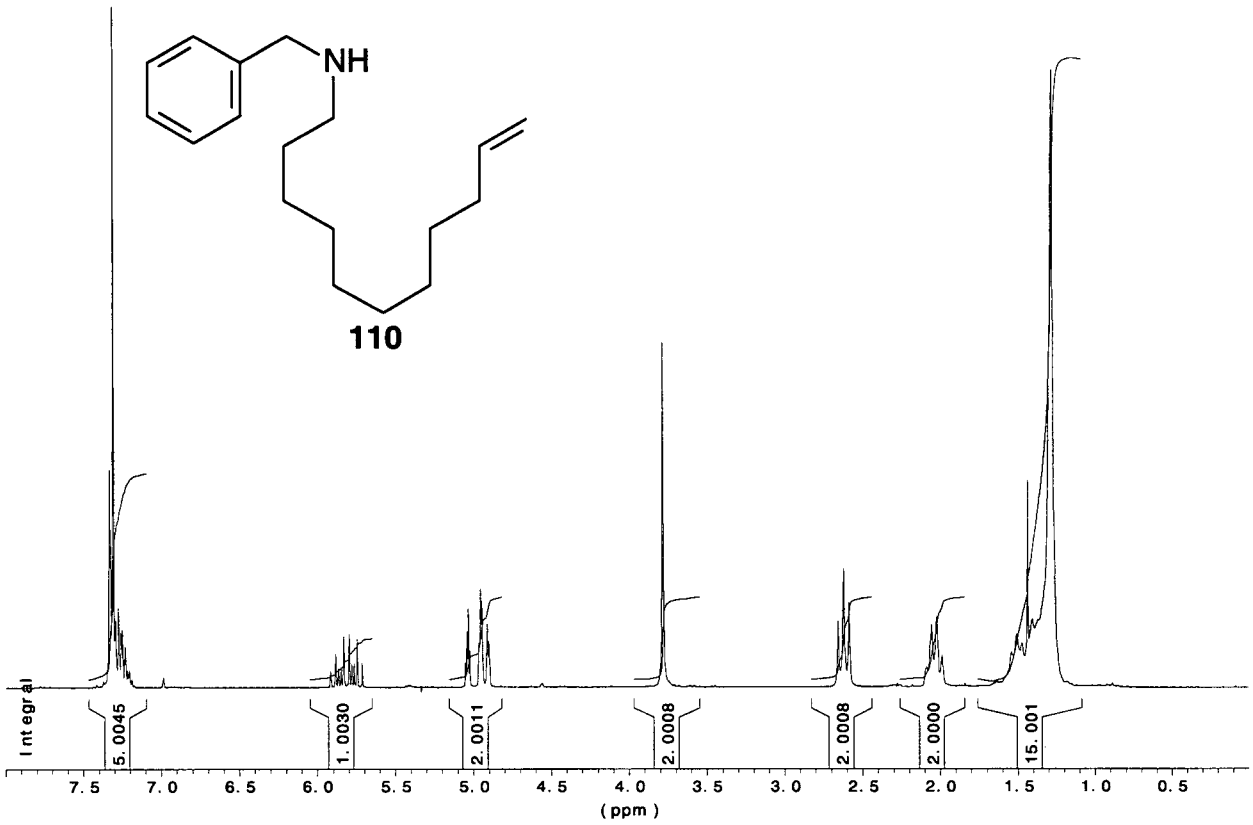
NH
110
Integral
5.0045
1.0030
2.0011
2.0008
2.0008
2.0000
15.001
7.5 7.0 6.5 6.0 5.5 5.0 4.5 4.0 3.5 3.0 2.5 2.0 1.5 1.0 0.5
(ppm)

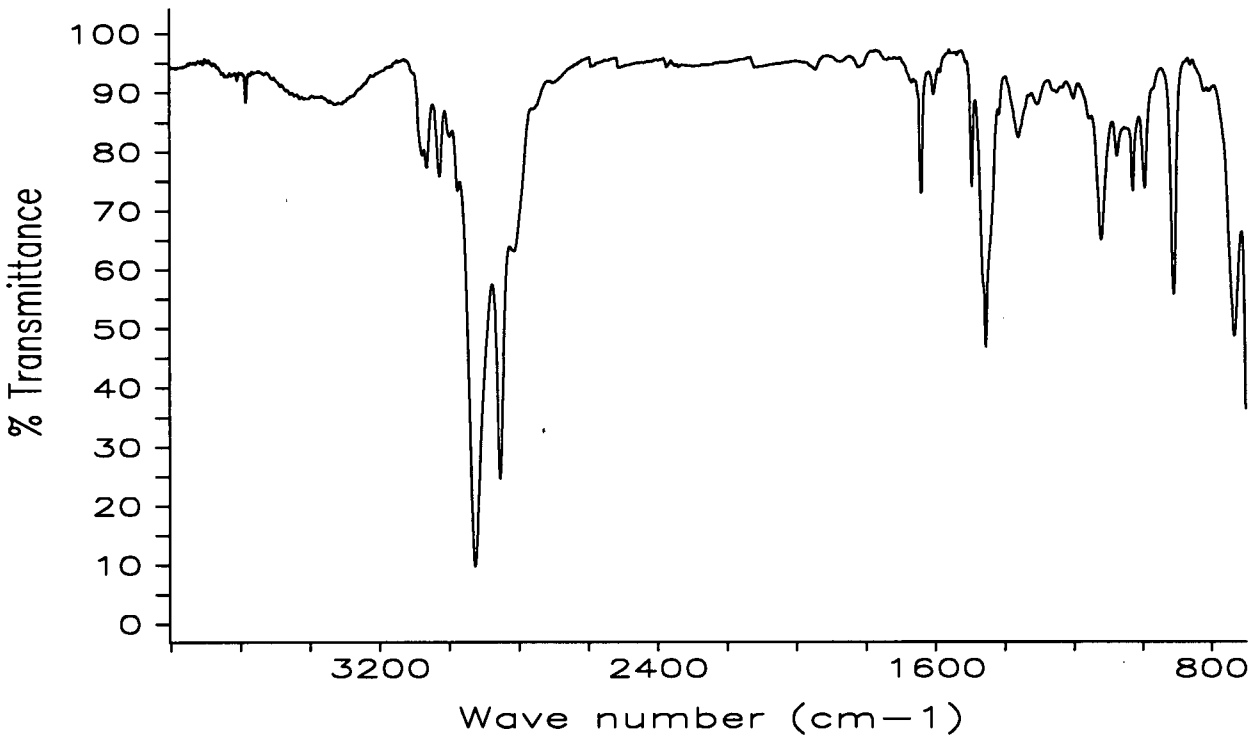
% Transmittance
100
90
80
70
60
50
40
30
20
10
0
3200
2400
1600
800
Wave number (cm−1)

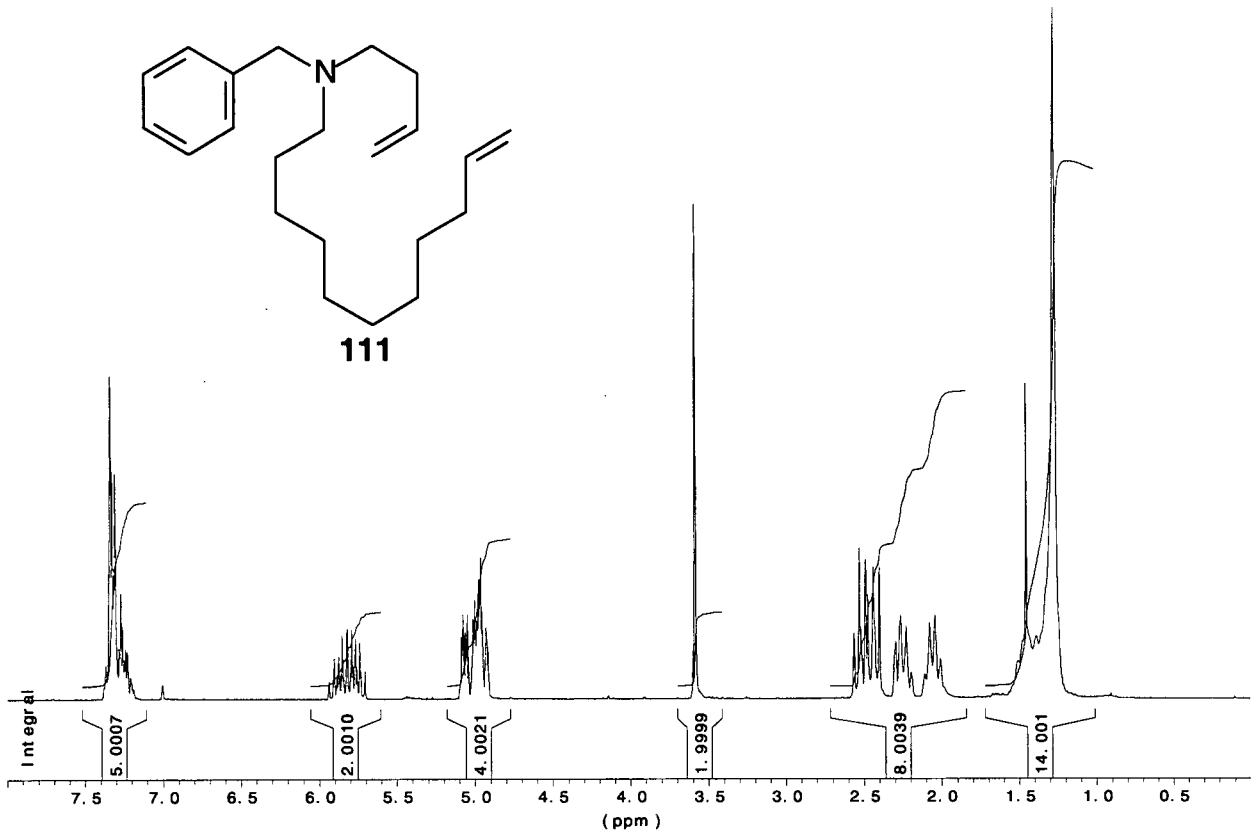
N
111
Integral
5.0007
2.0010
4.0021
1.9999
8.0039
14.001
7.5 7.0 6.5 6.0 5.5 5.0 4.5 4.0 3.5 3.0 2.5 2.0 1.5 1.0 0.5
(ppm)

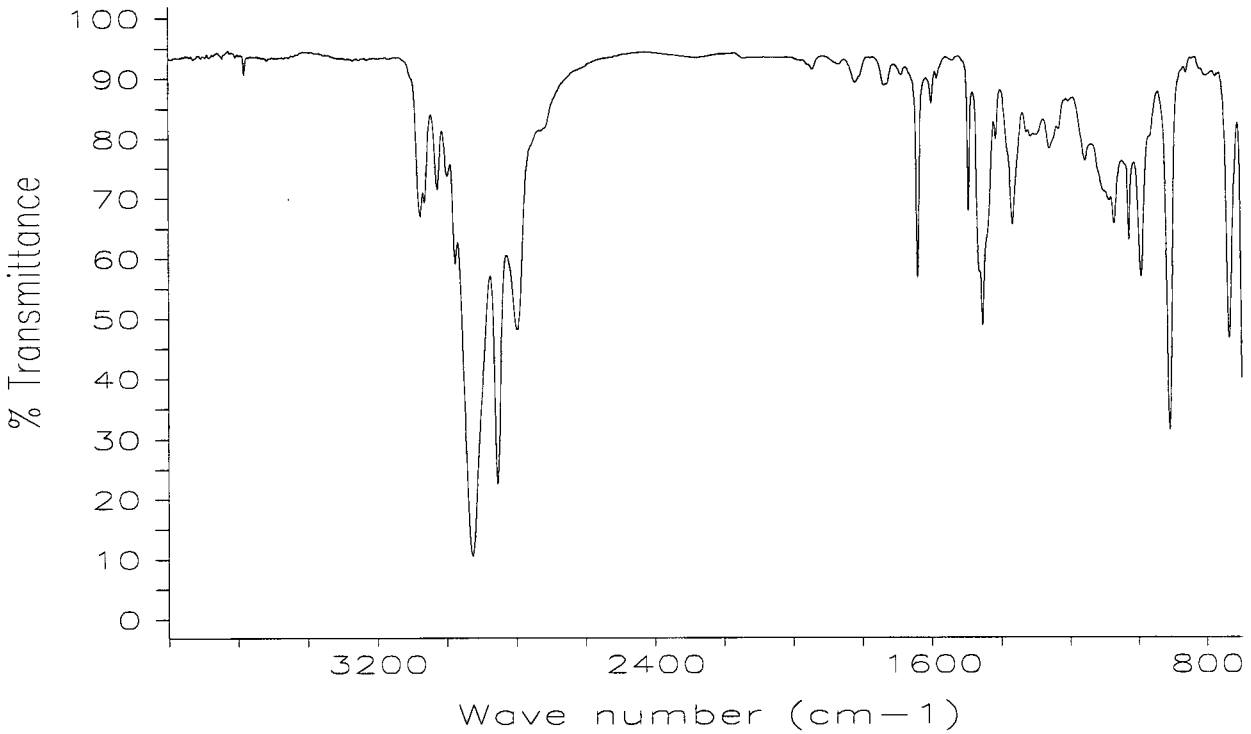
% Transmittance
100
90
80
70
60
50
40
30
20
10
0
3200
2400
1600
800
Wave number (cm−1)

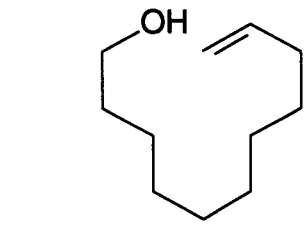
OH

112

Integral
0.9996
2.0008
1.9986
2.9999
14.001
7.5 7.0 6.5 6.0 5.5 5.0 4.5 4.0 3.5 3.0 2.5 2.0 1.5 1.0 0.5
(ppm)

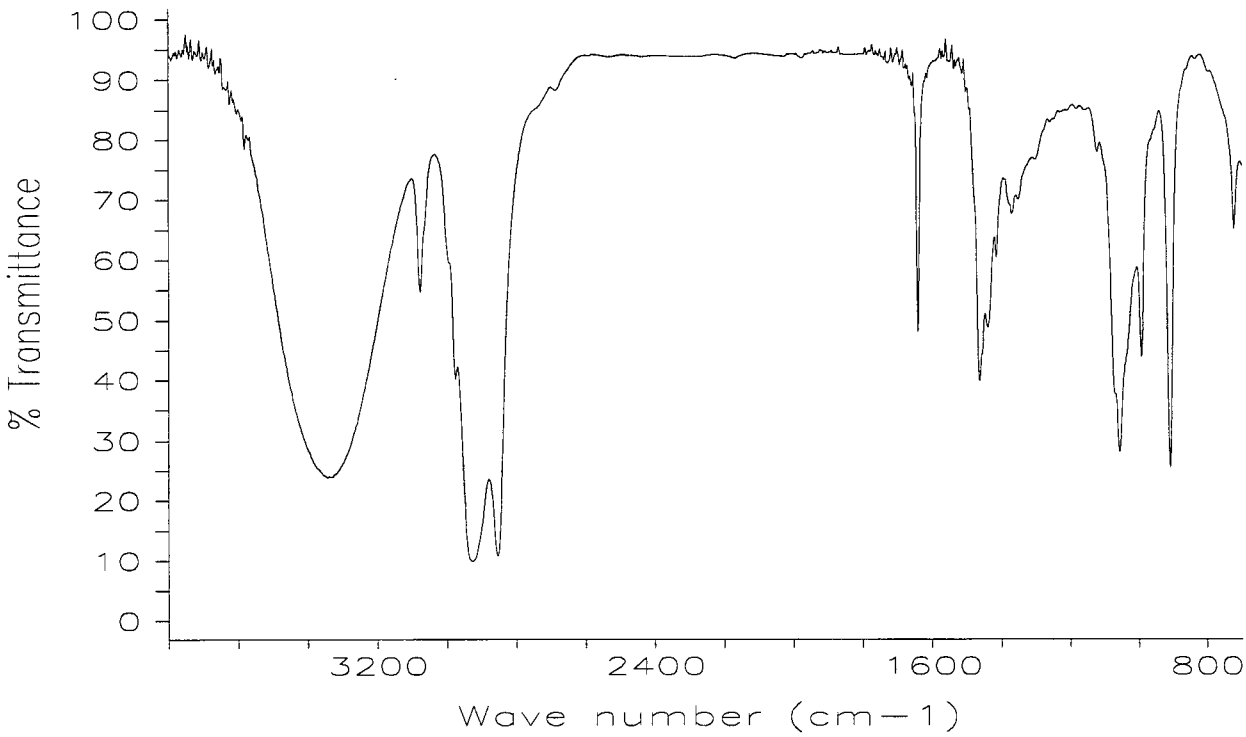
% Transmittance
100
90
80
70
60
50
40
30
20
10
0
3200
2400
1600
800
Wave number (cm−1)

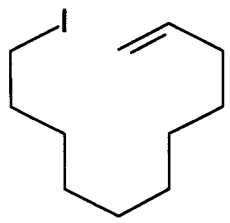

113

I nt egral
1.0011
2.0012
2.0000
4.0003
12.001
7.5 7.0 6.5 6.0 5.5 5.0 4.5 4.0 3.5 3.0 2.5 2.0 1.5 1.0 0.5
(ppm)

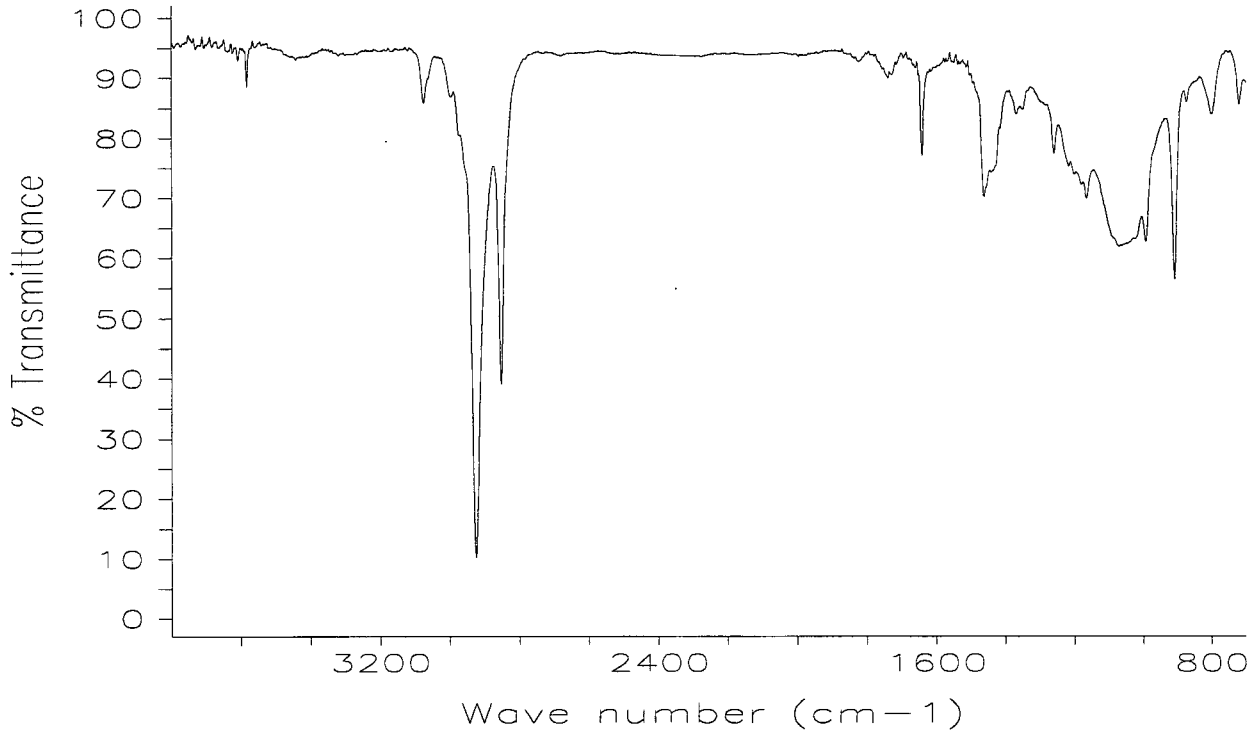
% Transmittance
100
90
80
70
60
50
40
30
20
10
0
3200
2400
1600
800
Wave number (cm−1)

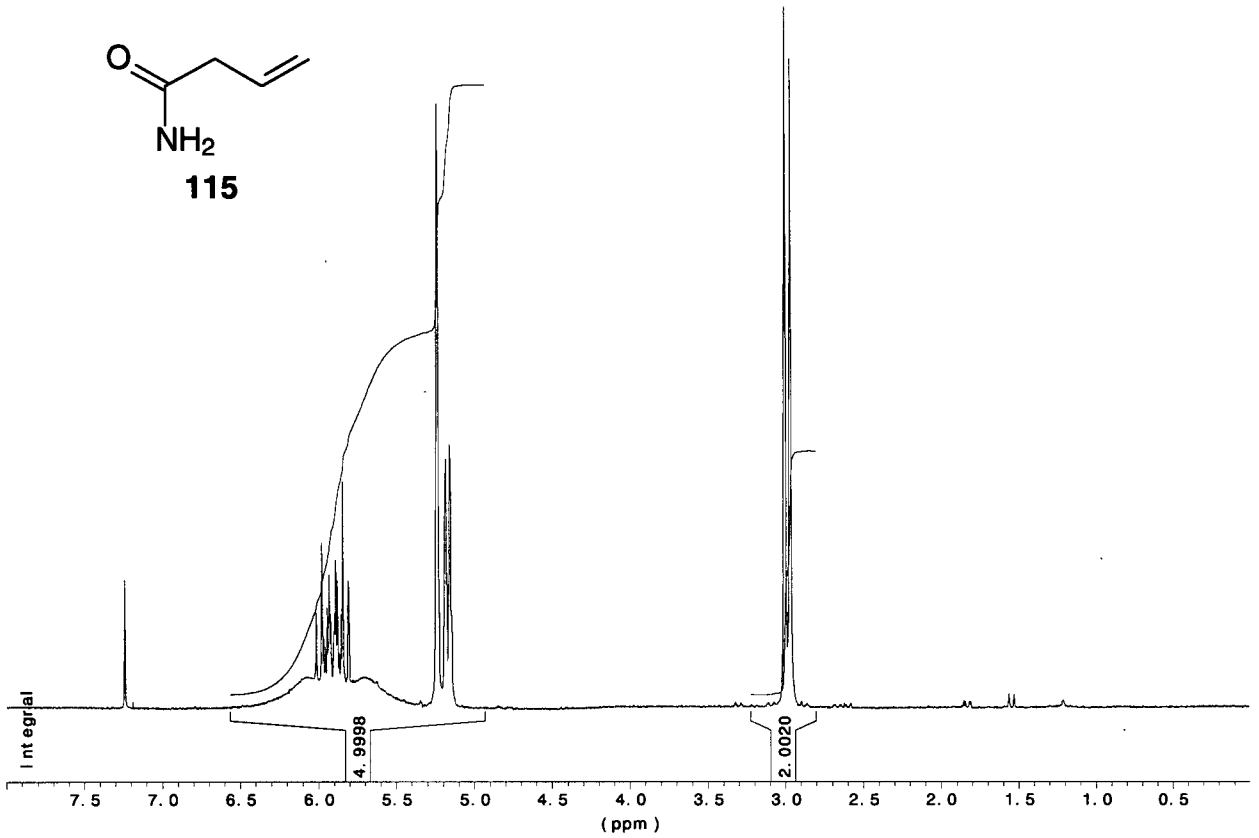
O
NH2
115
Integral
4.9998
2.0020
7.5
7.0
6.5
6.0
5.5
5.0
4.5
4.0
3.5
3.0
2.5
2.0
1.5
1.0
0.5
(ppm)

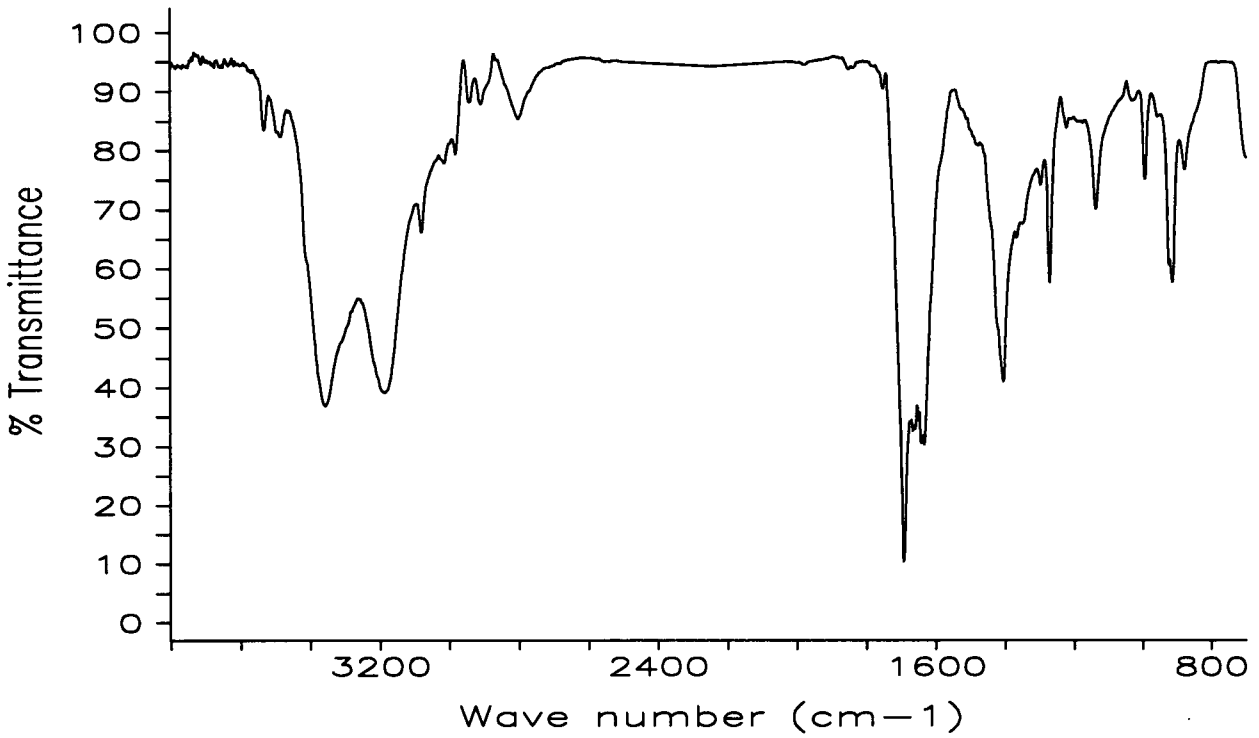
% Transmittance
100
90
80
70
60
50
40
30
20
10
0
3200
2400
1600
800
Wave number (cm—1)

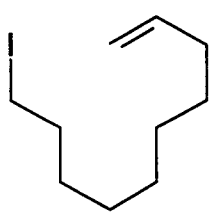

116

Integral
1.0009
2.0023
2.0007
3.9999
10.000
7.5 7.0 6.5 6.0 5.5 5.0 4.5 4.0 3.5 3.0 2.5 2.0 1.5 1.0 0.5
(ppm)

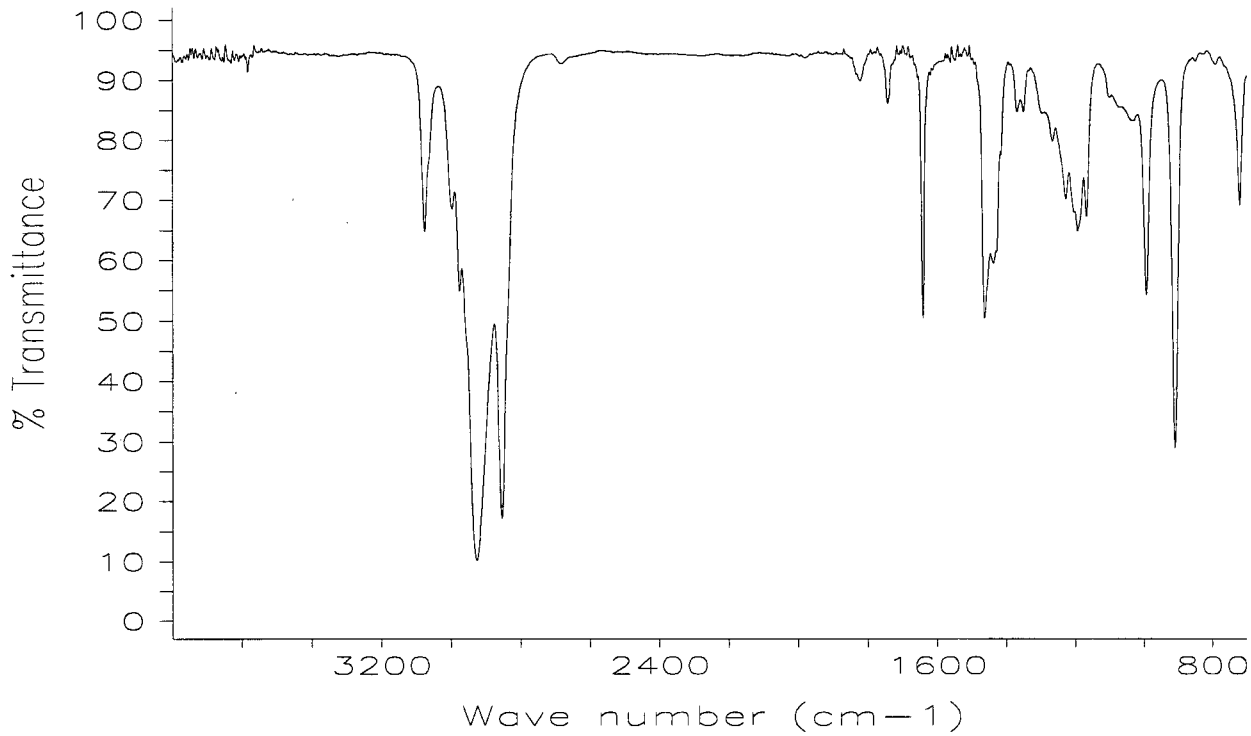
% Transmittance
100
90
80
70
60
50
40
30
20
10
0
3200
2400
1600
800
Wave number (cm−1)

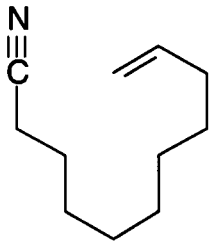
N
C

117

Int egral
1.0008
2.0009
4.0000
12.001
7.5 7.0 6.5 6.0 5.5 5.0 4.5 4.0 3.5 3.0 2.5 2.0 1.5 1.0 0.5
(ppm)

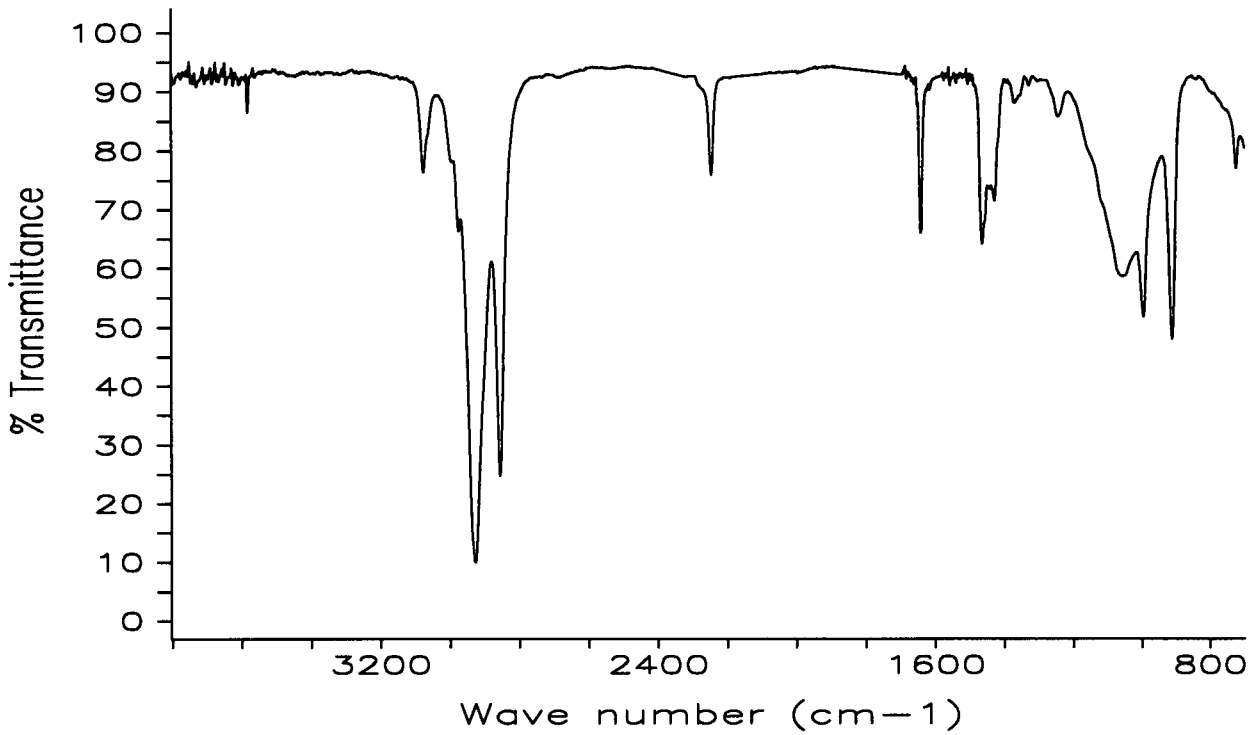
% Transmittance
100
90
80
70
60
50
40
30
20
10
0
3200
2400
1600
800
Wave number (cm−1)

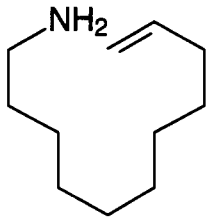
NH2

118

Integral
1.0000
2.0004
1.9973
1.9976
16.000
7.5 7.0 6.5 6.0 5.5 5.0 4.5 4.0 3.5 3.0 2.5 2.0 1.5 1.0 0.5
(ppm)

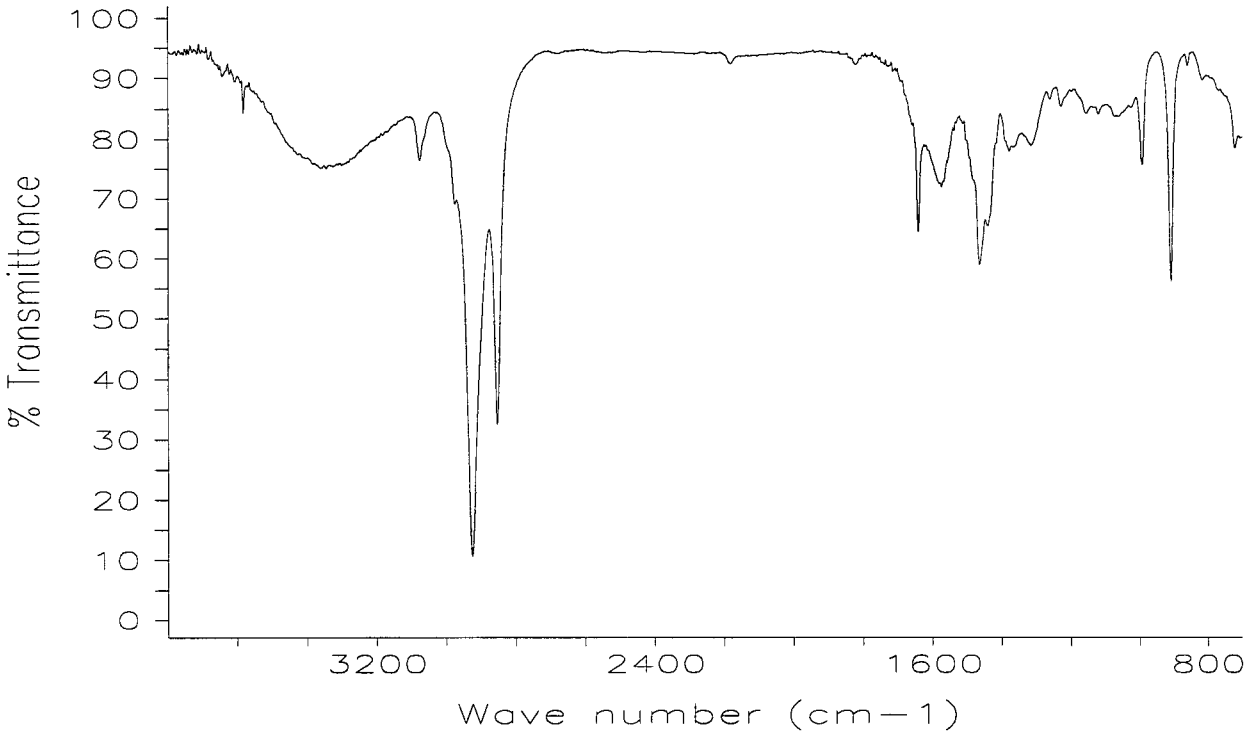
% Transmittance
100
90
80
70
60
50
40
30
20
10
0
3200
2400
1600
800
Wave number (cm−1)

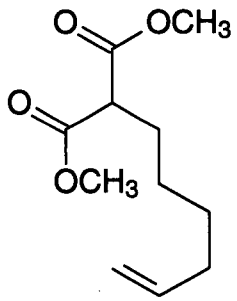
O
OCH3
O
OCH3

119

Integral
1.0011
2.0013
6.0030
1.0012
3.9980
3.9984
7.5 7.0 6.5 6.0 5.5 5.0 4.5 4.0 3.5 3.0 2.5 2.0 1.5 1.0 0.5
(ppm)

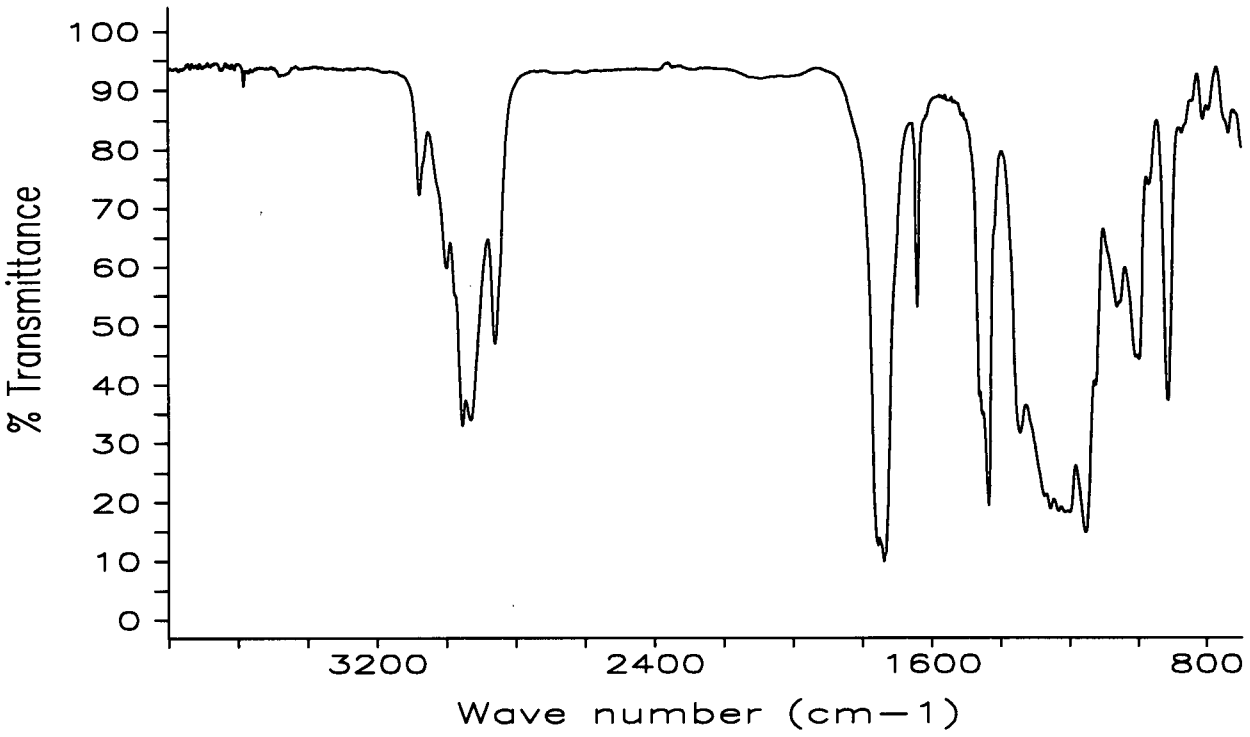
% Transmittance
100
90
80
70
60
50
40
30
20
10
0
3200
2400
1600
800
Wave number (cm−1)

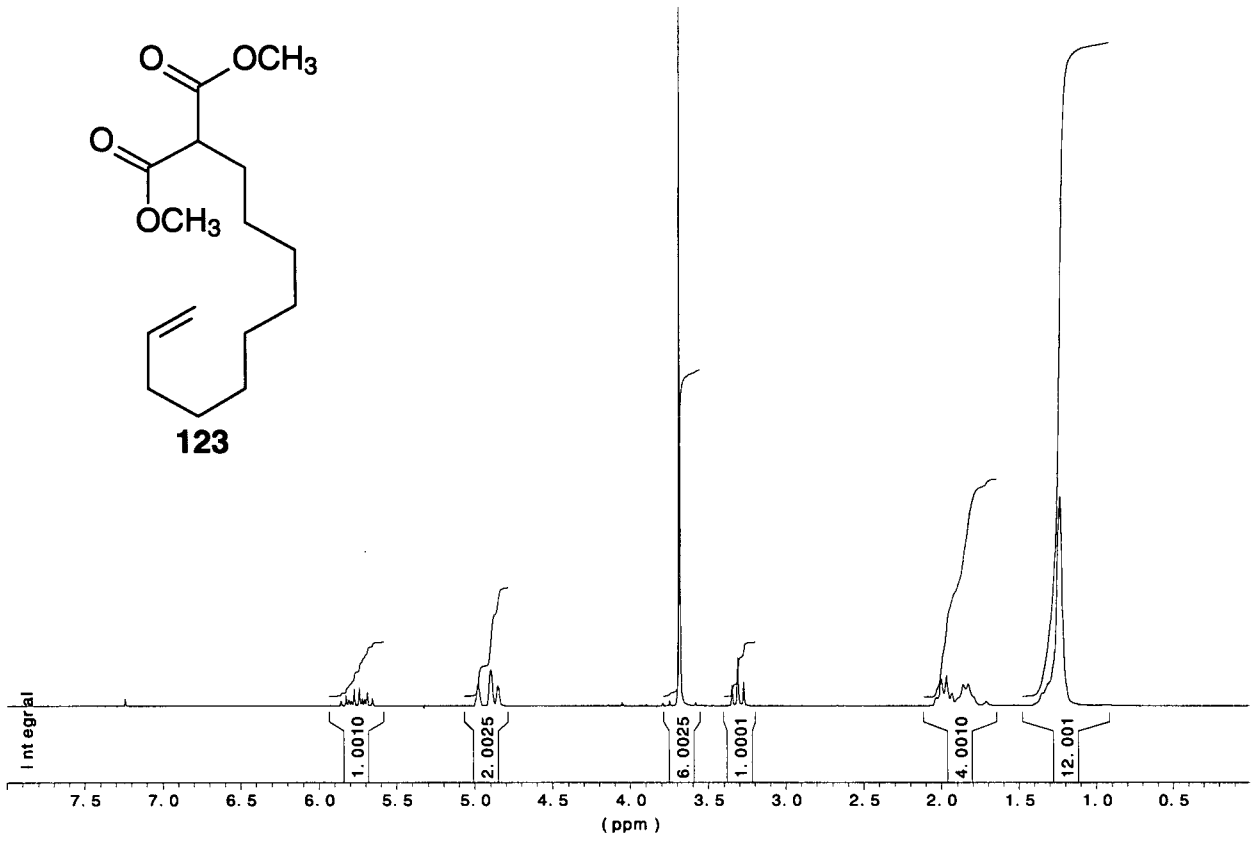
O
OCH3
O
OCH3
Integral
1.0010
2.0025
6.0025
1.0001
4.0010
12.001
7.5 7.0 6.5 6.0 5.5 5.0 4.5 4.0 3.5 3.0 2.5 2.0 1.5 1.0 0.5
(ppm)

123

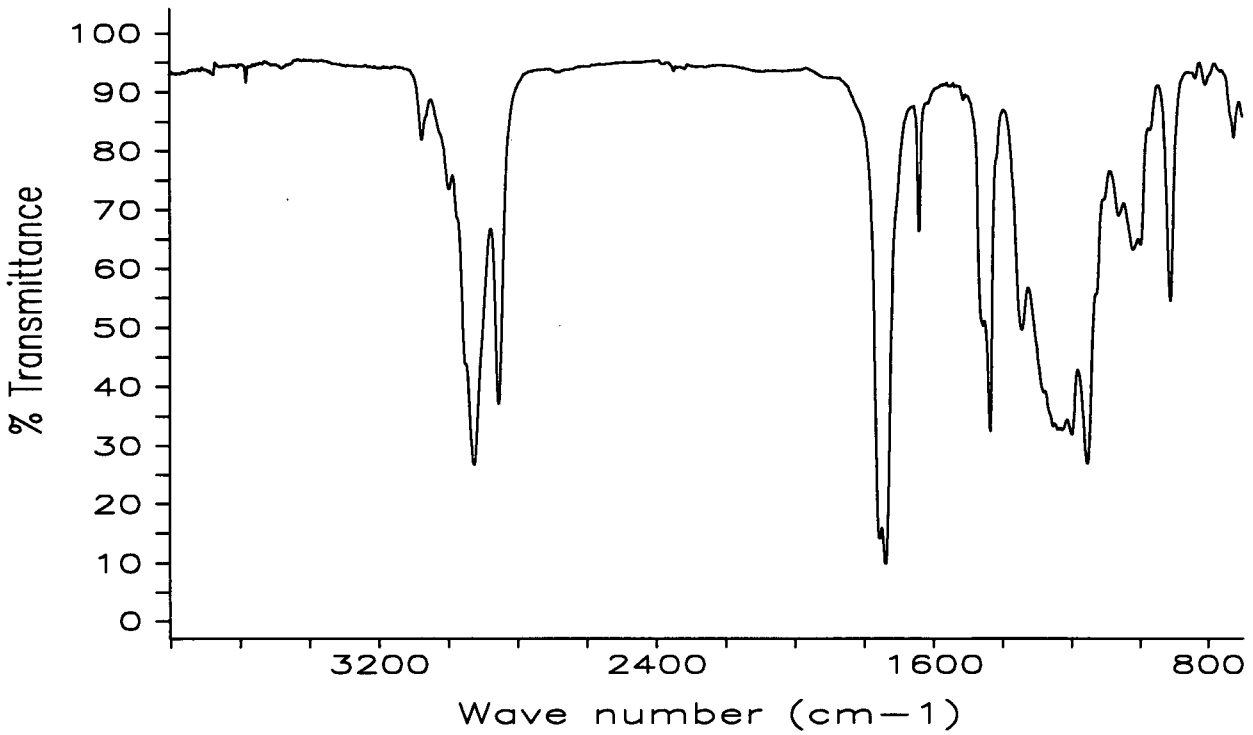
% Transmittance
100
90
80
70
60
50
40
30
20
10
0
3200
2400
1600
800
Wave number (cm−1)

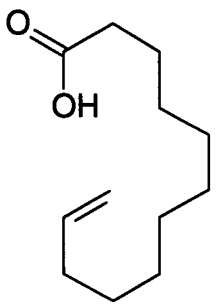
O
OH

124

Integral
1.0014
1.0010
2.0014
2.0005
2.0005
14.006
11.0
10.0
9.0
8.0
7.0
6.0
5.0
4.0
3.0
2.0
1.0
(ppm)

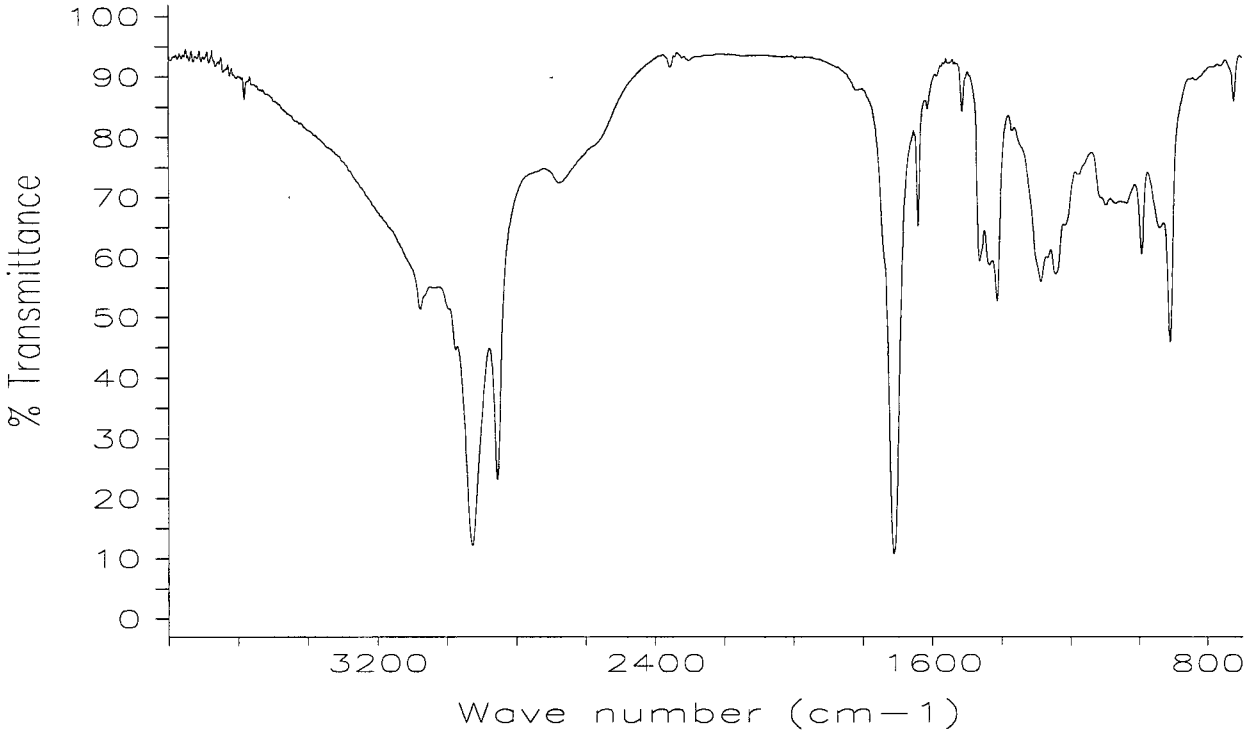
% Transmittance
100
90
80
70
60
50
40
30
20
10
0
3200
2400
1600
800
Wave number (cm−1)

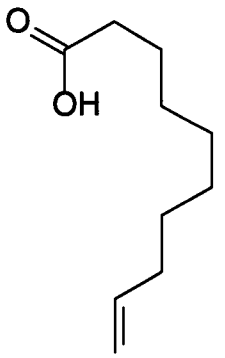
O
OH

125

1.0010
1.0022
2.0009
4.0001
10.000
11.0
10.0
9.0
8.0
7.0
6.0
5.0
4.0
3.0
2.0
1.0
(ppm)

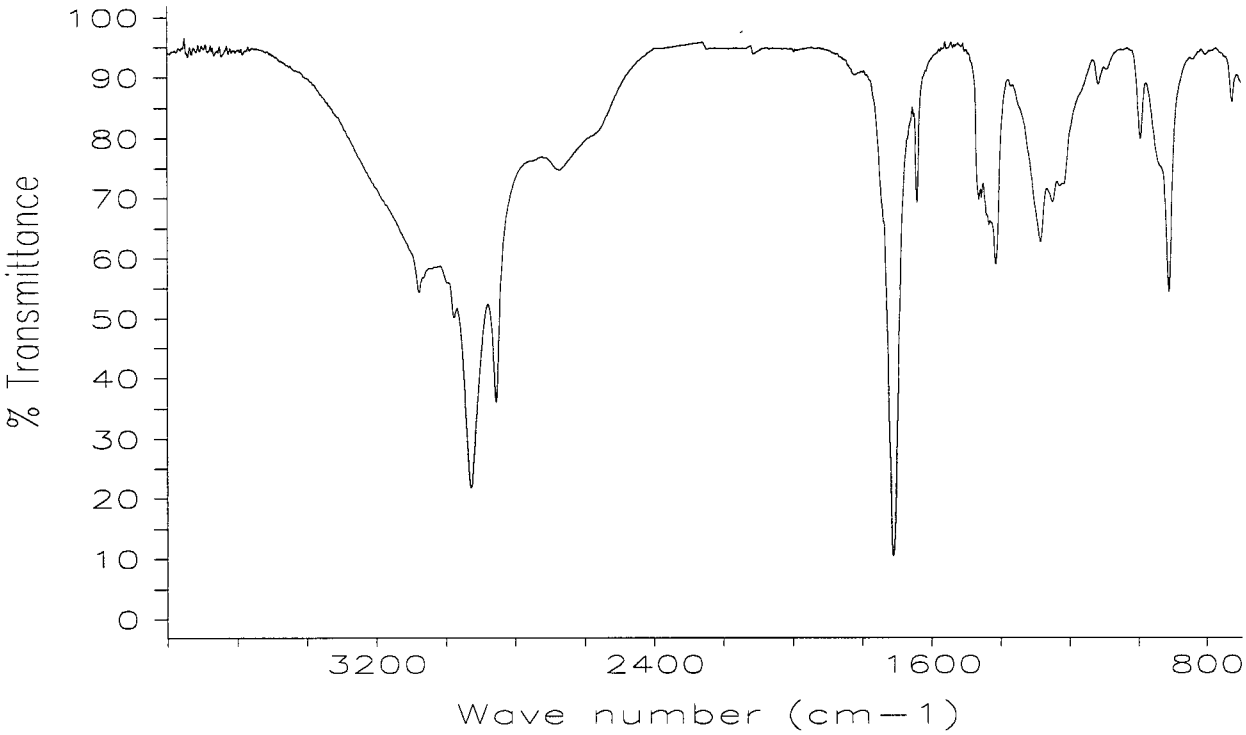
% Transmittance
100
90
80
70
60
50
40
30
20
10
0
3200
2400
1600
800
Wave number (cm−1)

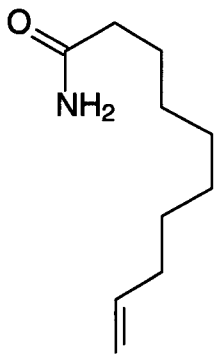
O
NH2

126

Integral
3.0010
2.0026
4.0027
10.004
7.5 7.0 6.5 6.0 5.5 5.0 4.5 4.0 3.5 3.0 2.5 2.0 1.5 1.0 0.5
(ppm)

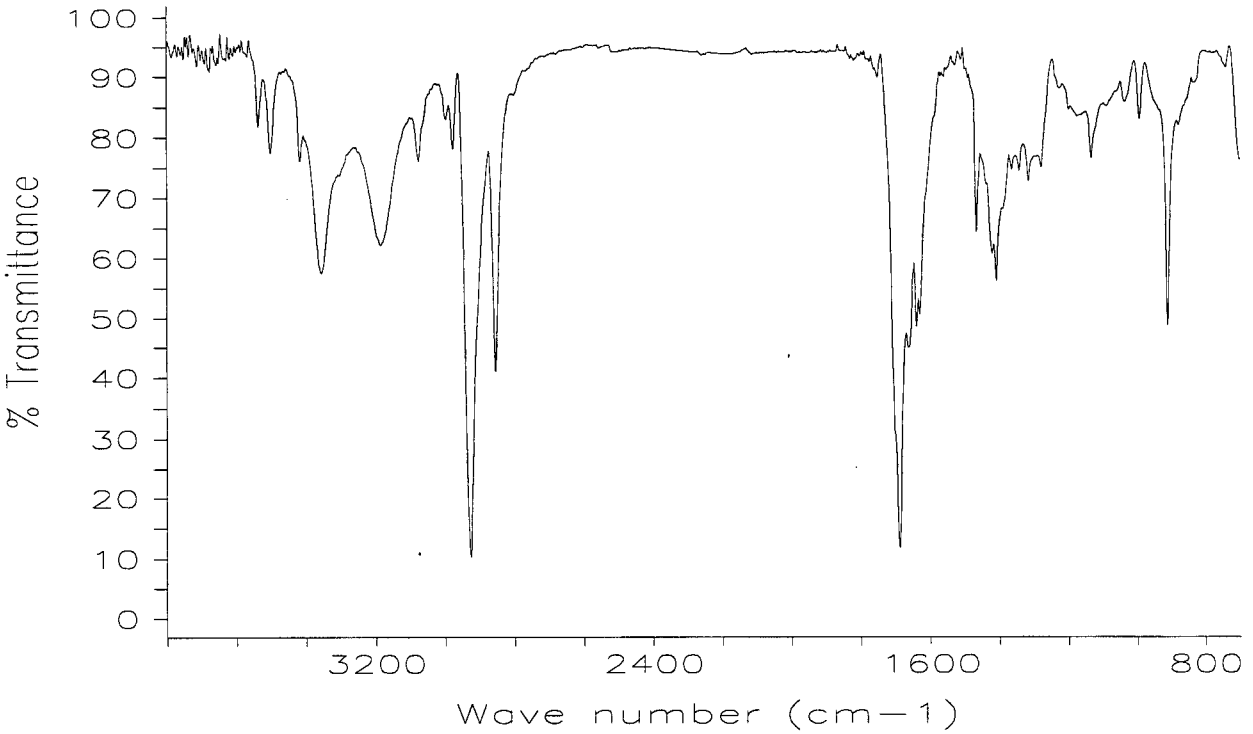
% Transmittance
100
90
80
70
60
50
40
30
20
10
0
3200
2400
1600
800
Wave number (cm−1)

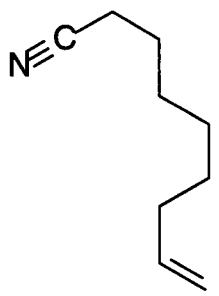

128

Integral
1.0010
2.0010
4.0012
8.0031
7.5 7.0 6.5 6.0 5.5 5.0 4.5 4.0 3.5 3.0 2.5 2.0 1.5 1.0 0.5
(ppm)

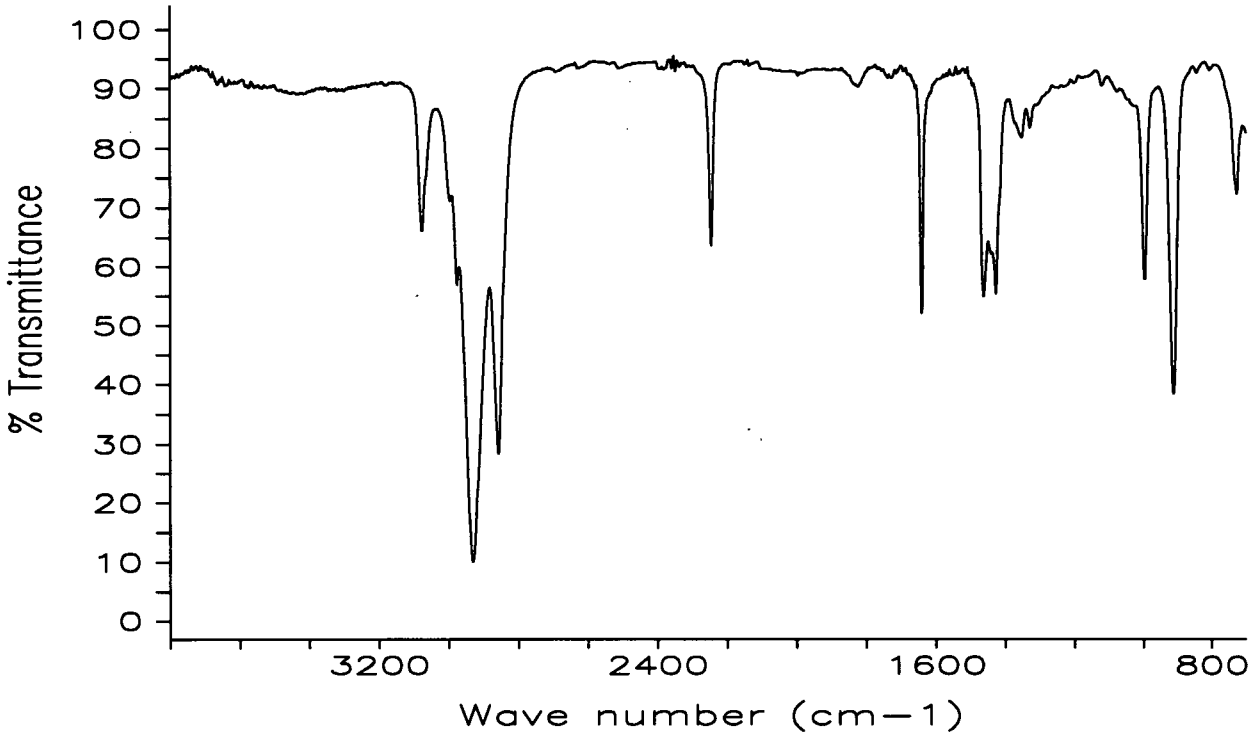
% Transmittance
100
90
80
70
60
50
40
30
20
10
0
3200
2400
1600
800
Wave number (cm−1)

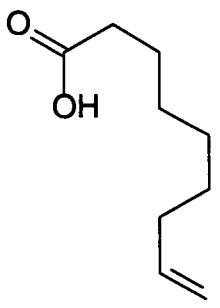
O
OH

129

Integral
1.0010
1.0007
2.0009
3.9980
7.9969
12.0
11.0
10.0
9.0
8.0
7.0
6.0
5.0
4.0
3.0
2.0
1.0
(ppm)

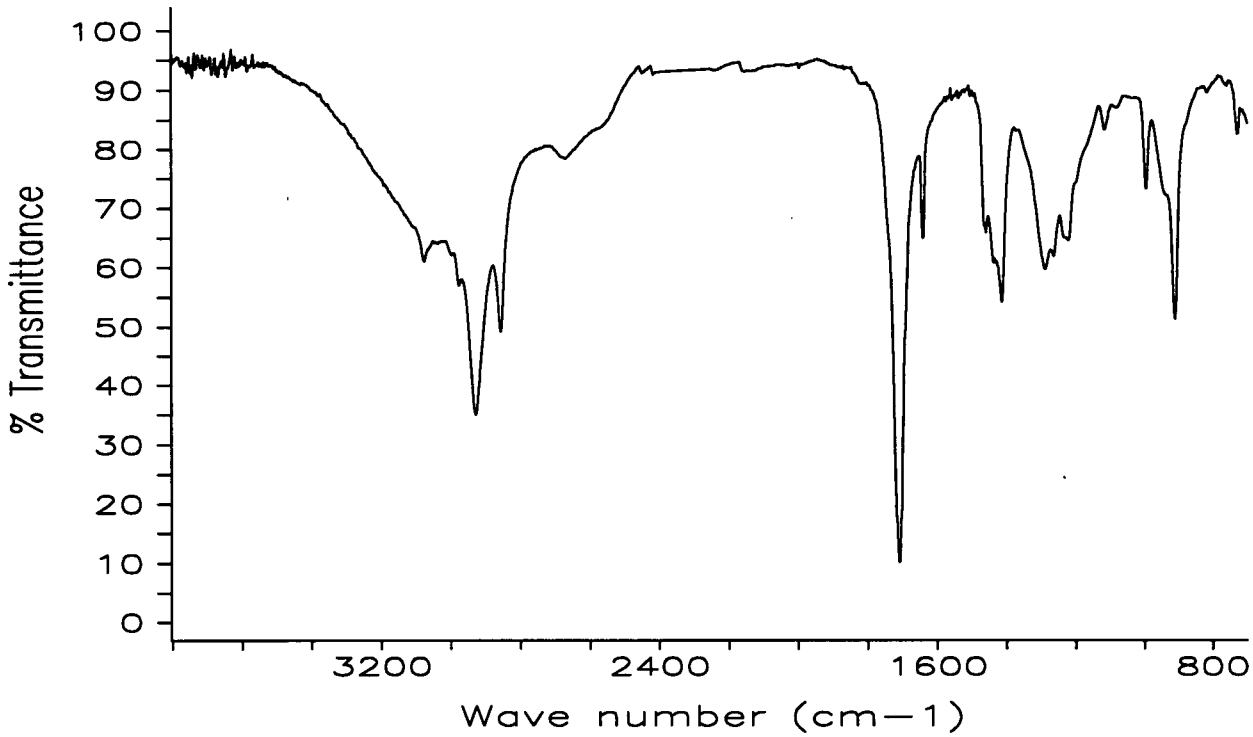
% Transmittance
100
90
80
70
60
50
40
30
20
10
0
3200
2400
1600
800
Wave number (cm−1)

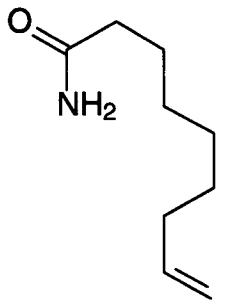
O
NH2

130

Integral
3.0000
2.0015
4.0012
8.0024
7.5
7.0
6.5
6.0
5.5
5.0
4.5
4.0
3.5
3.0
2.5
2.0
1.5
1.0
0.5
(ppm)

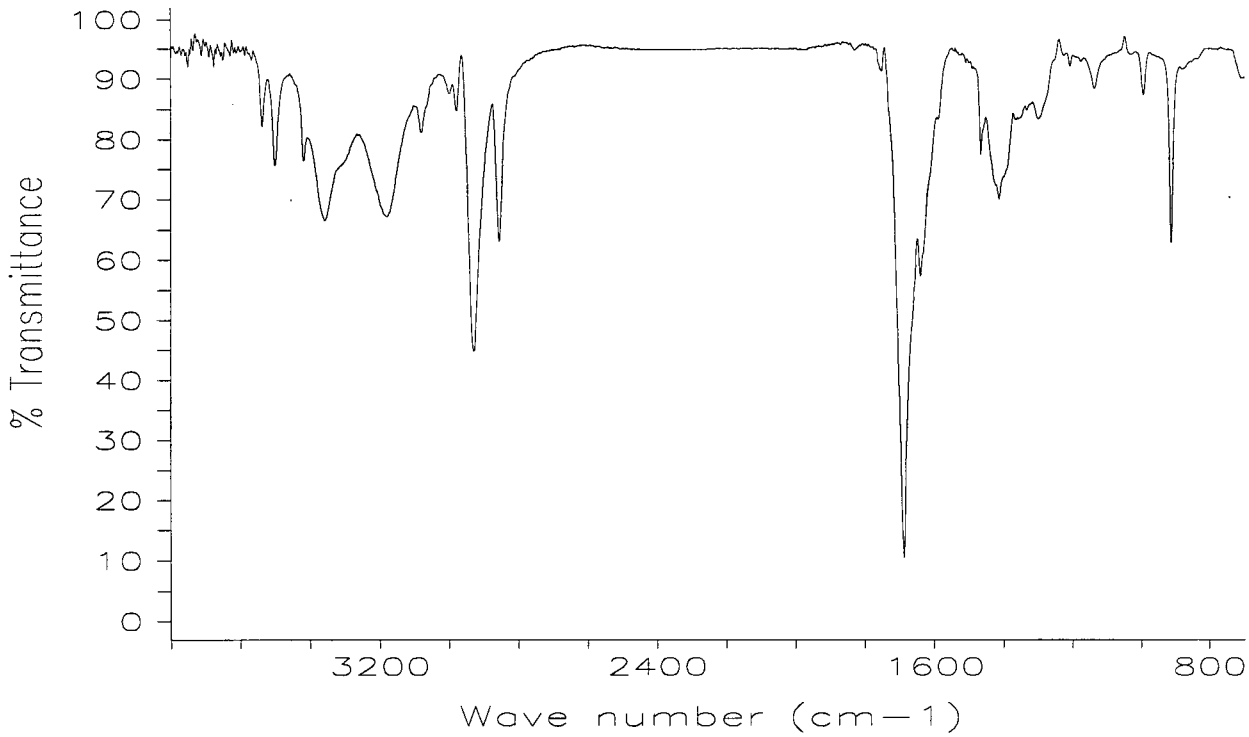
% Transmittance
100
90
80
70
60
50
40
30
20
10
0
3200
2400
1600
800
Wave number (cm−1)

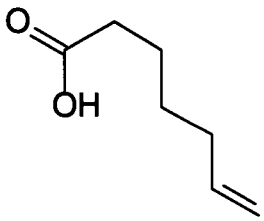
O
OH

131

1.0010
1.0005
2.0006
3.9986
3.9988
11.0
10.0
9.0
8.0
7.0
6.0
5.0
4.0
3.0
2.0
1.0
(ppm)

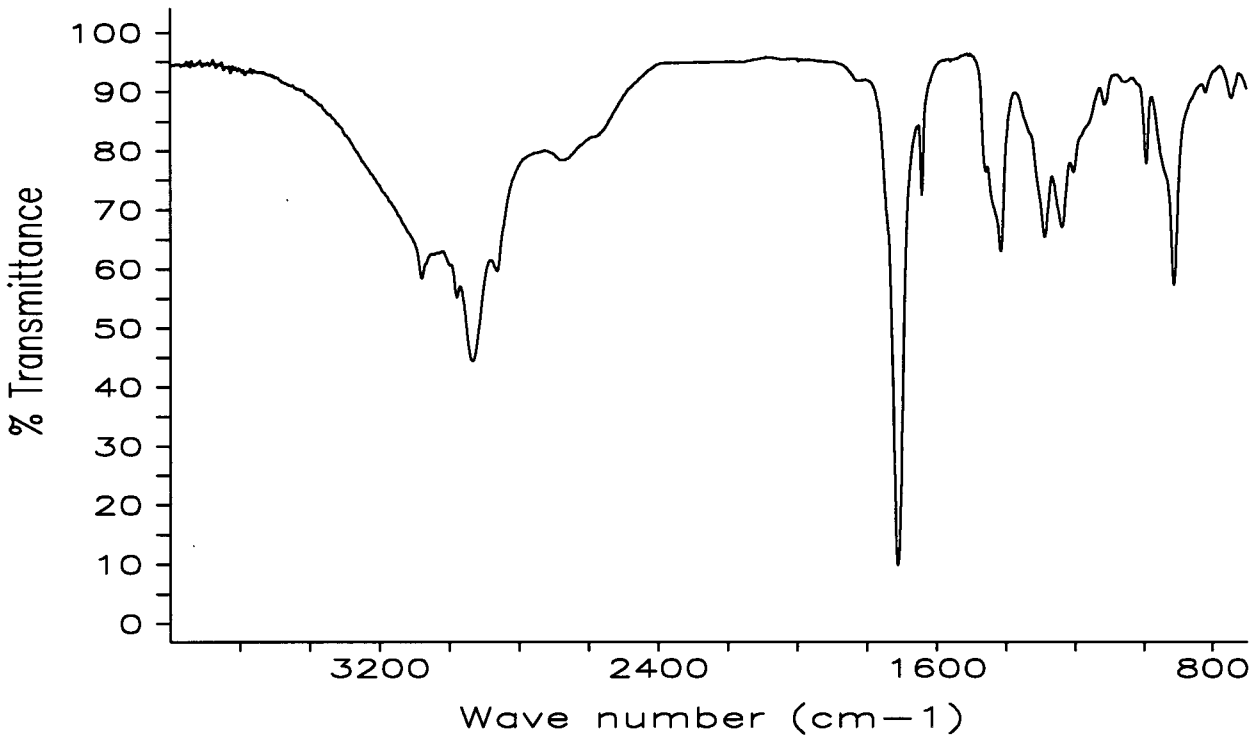
% Transmittance
100
90
80
70
60
50
40
30
20
10
0
3200
2400
1600
800
Wave number (cm−1)

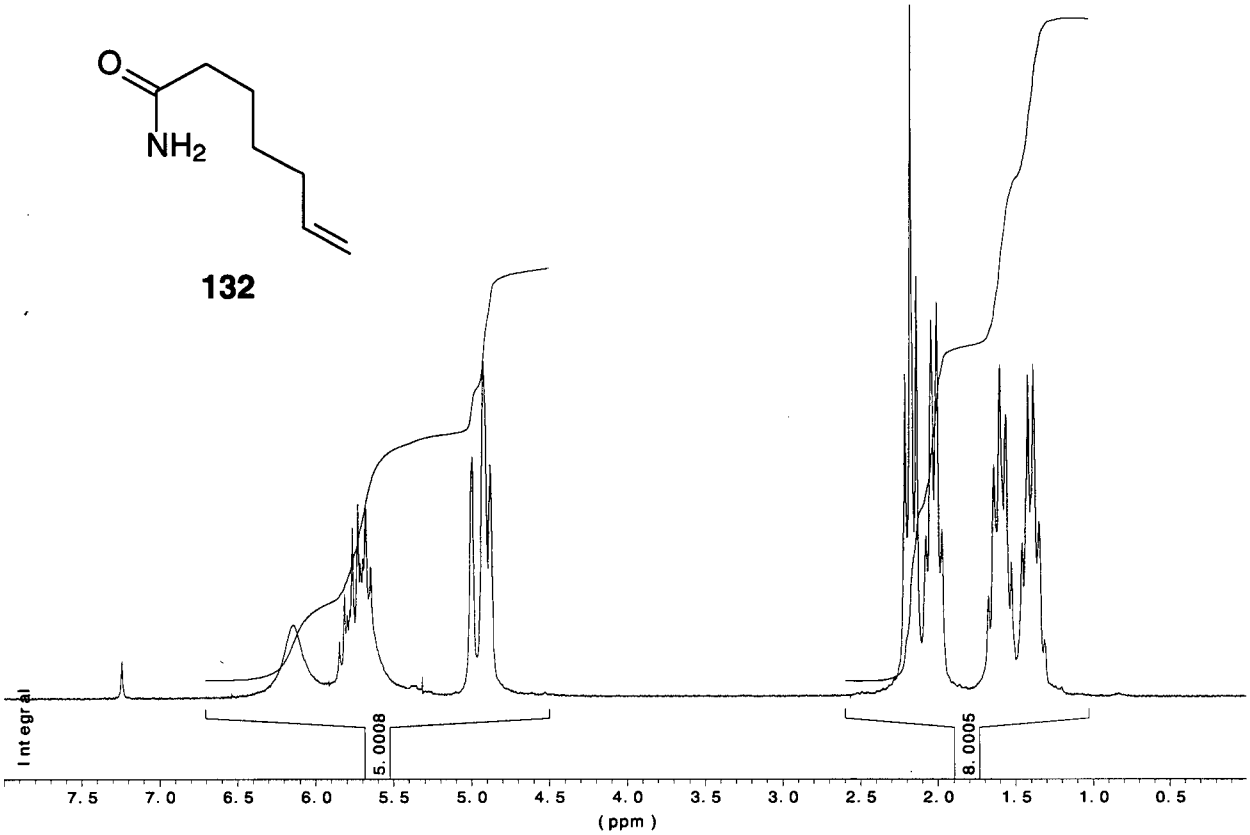
O
NH2
Integral
5.0008
8.0005
7.5 7.0 6.5 6.0 5.5 5.0 4.5 4.0 3.5 3.0 2.5 2.0 1.5 1.0 0.5
(ppm)

132

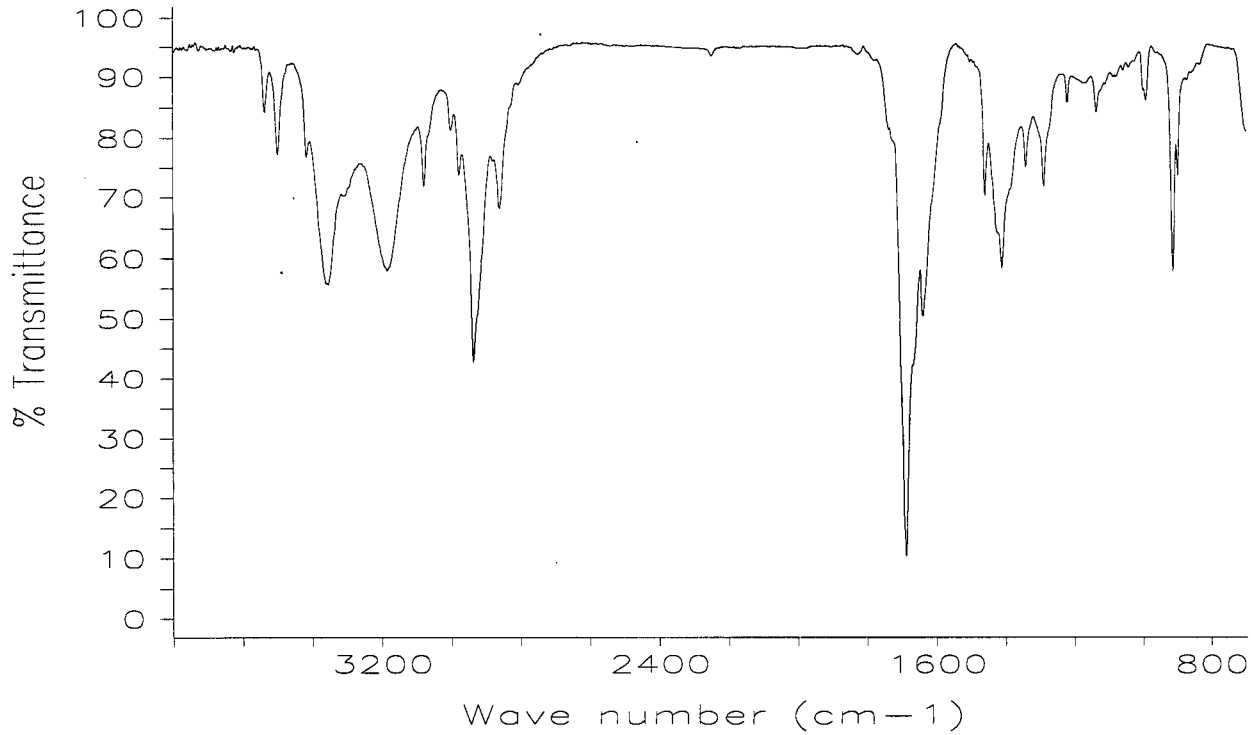
% Transmittance
100
90
80
70
60
50
40
30
20
10
0
3200
2400
1600
800
Wave number (cm−1)

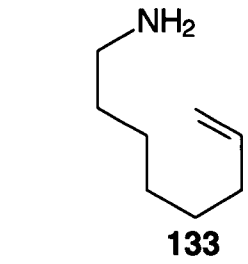
NH2

133

Integrial
1.0018
2.0021
2.0002
2.0016
10.002
7.5 7.0 6.5 6.0 5.5 5.0 4.5 4.0 3.5 3.0 2.5 2.0 1.5 1.0 0.5
(ppm)

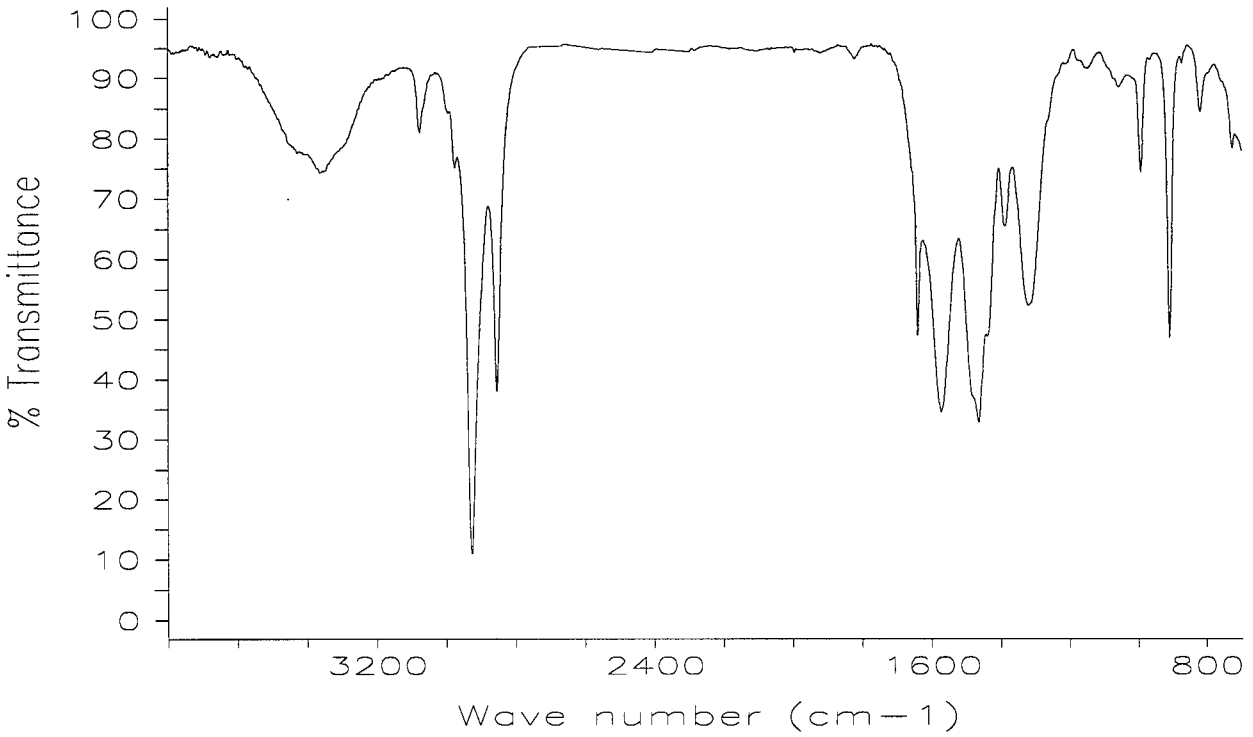
% Transmittance
100
90
80
70
60
50
40
30
20
10
0
3200
2400
1600
800
Wave number (cm−1)

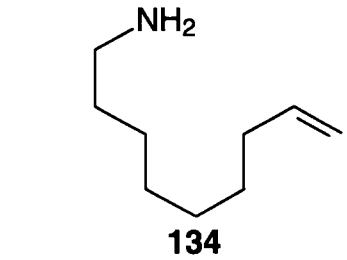
NH2

134

Integral
1.0007
2.0038
2.0000
2.0010
12.001
7.5 7.0 6.5 6.0 5.5 5.0 4.5 4.0 3.5 3.0 2.5 2.0 1.5 1.0 0.5
(ppm)

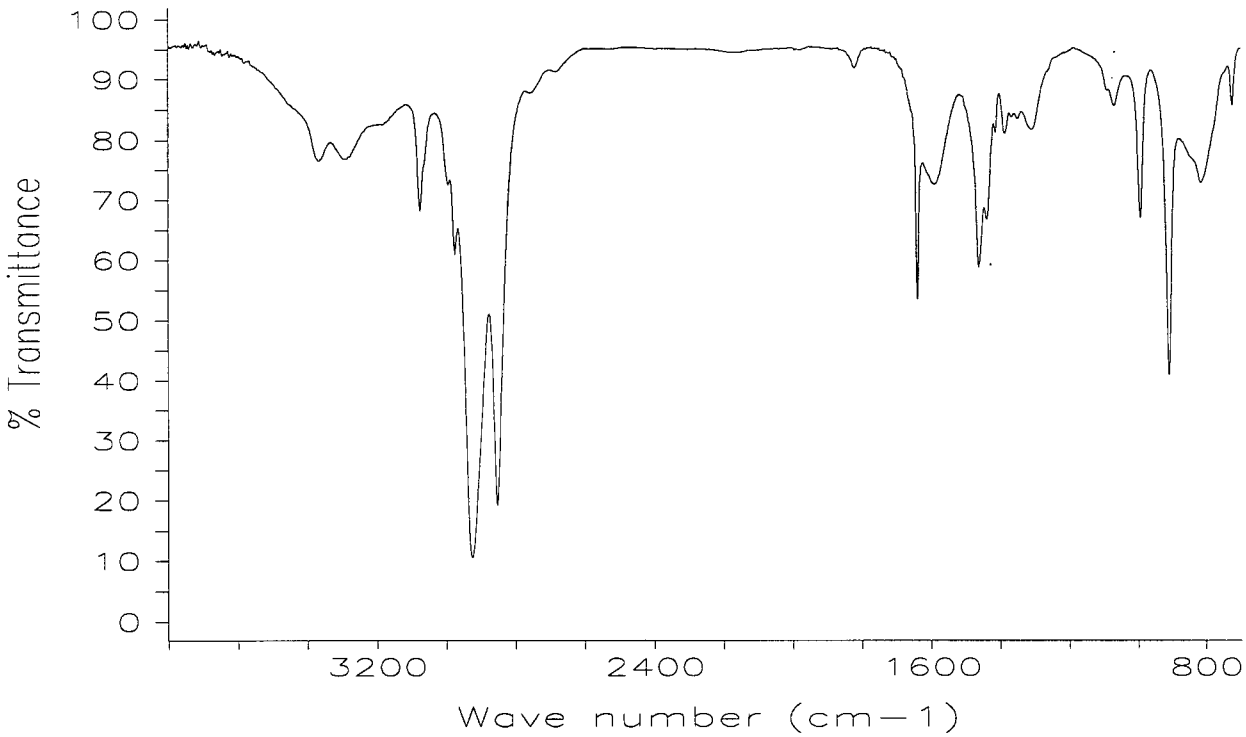
% Transmittance
100
90
80
70
60
50
40
30
20
10
0
3200
2400
1600
800
Wave number (cm−1)

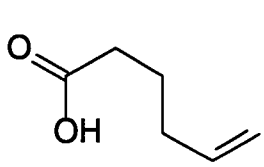
O
OH

135

1.0000
1.0013
2.0029
4.0017
2.0043
11.0
10.0
9.0
8.0
7.0
6.0
5.0
4.0
3.0
2.0
1.0
(ppm)

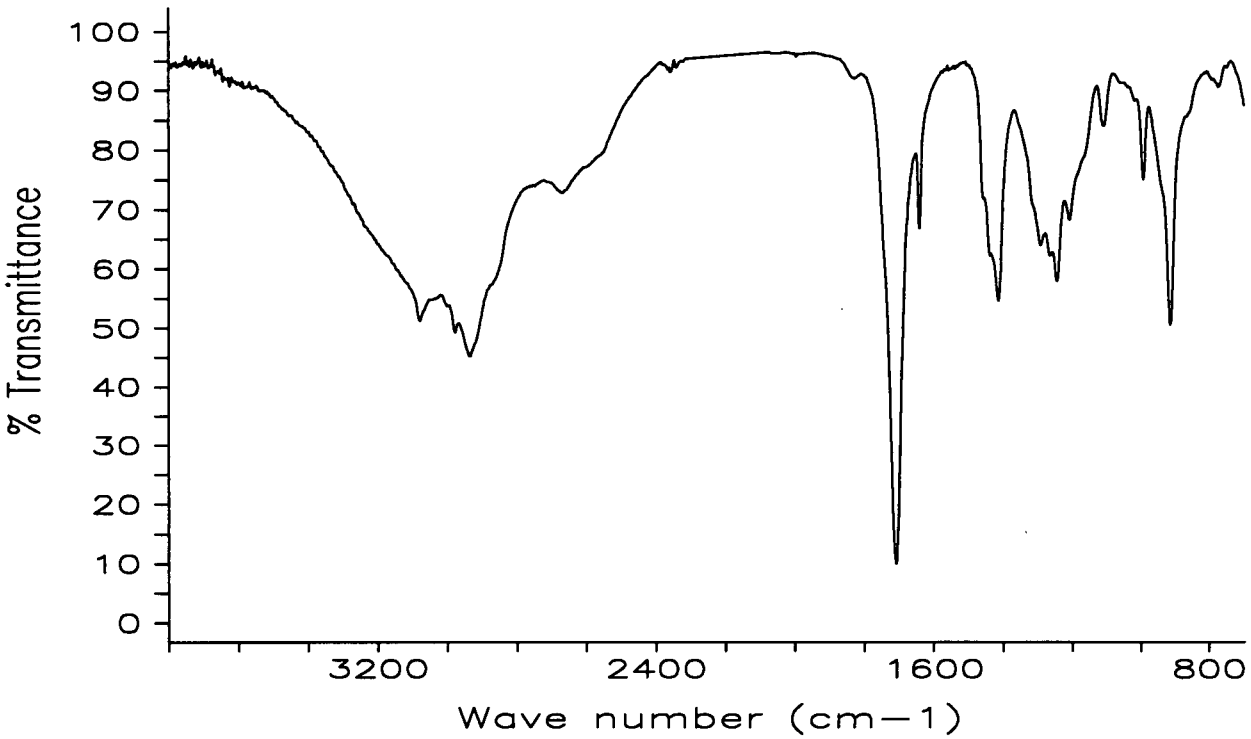
% Transmittance
100
90
80
70
60
50
40
30
20
10
0
3200
2400
1600
800
Wave number (cm−1)

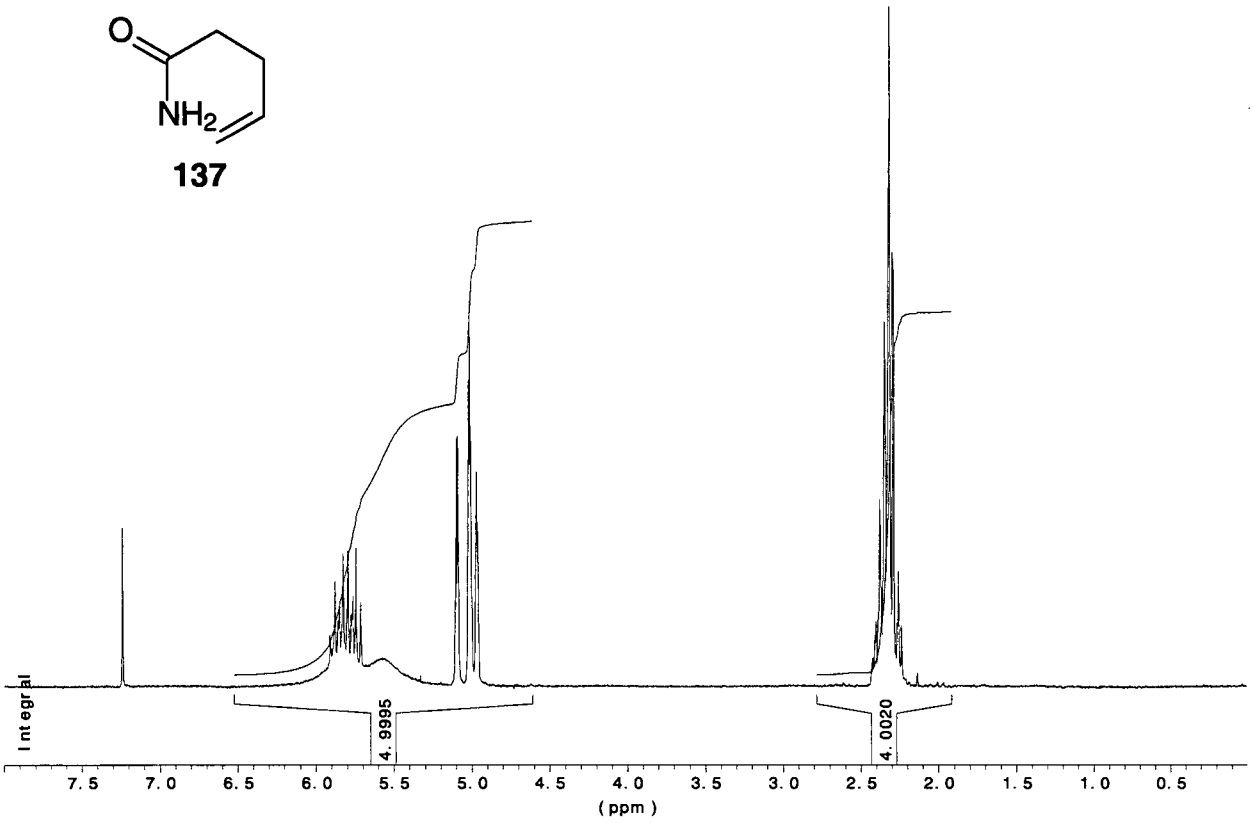
O
NH2
Integral
4.9995
4.0020
7.5 7.0 6.5 6.0 5.5 5.0 4.5 4.0 3.5 3.0 2.5 2.0 1.5 1.0 0.5
(ppm)

137

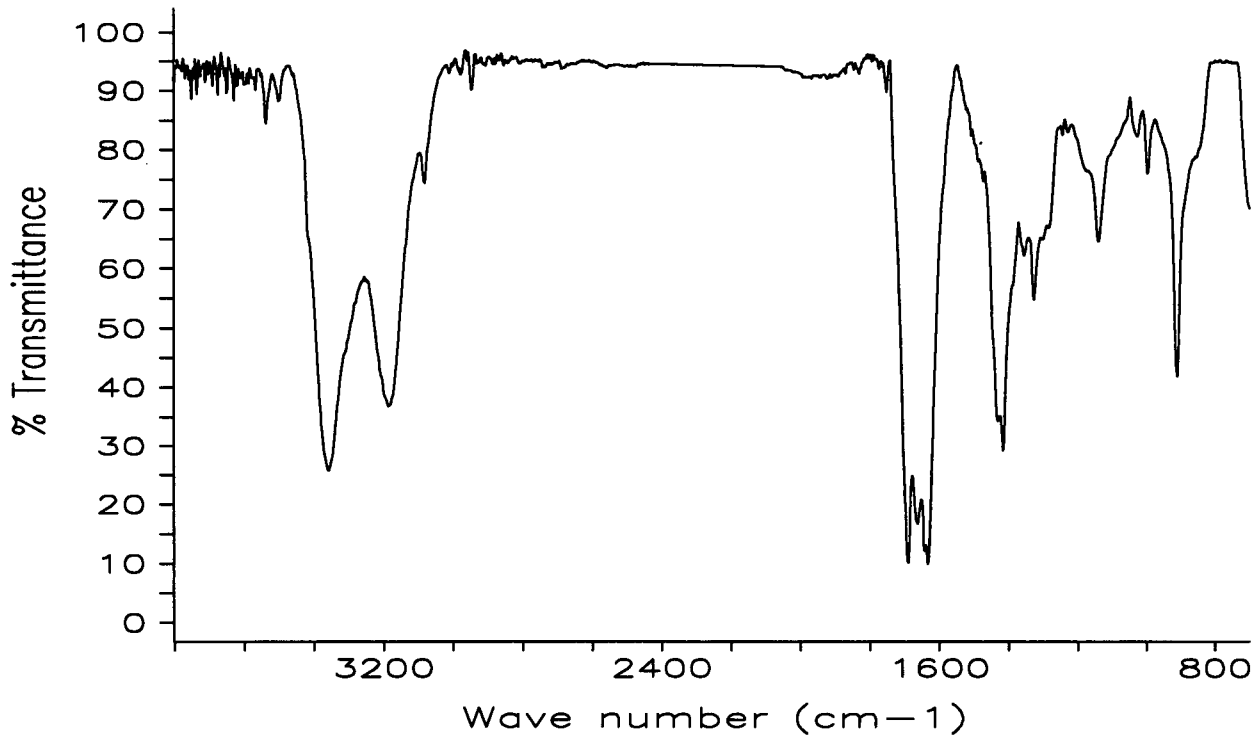
% Transmittance
100
90
80
70
60
50
40
30
20
10
0
3200
2400
1600
800
Wave number (cm−1)

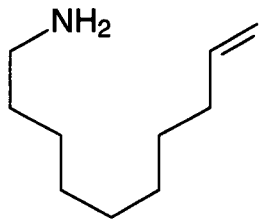
NH2

138

Integral
1.0012
2.0007
2.0011
2.0010
7.9990
7.5 7.0 6.5 6.0 5.5 5.0 4.5 4.0 3.5 3.0 2.5 2.0 1.5 1.0 0.5
(ppm)

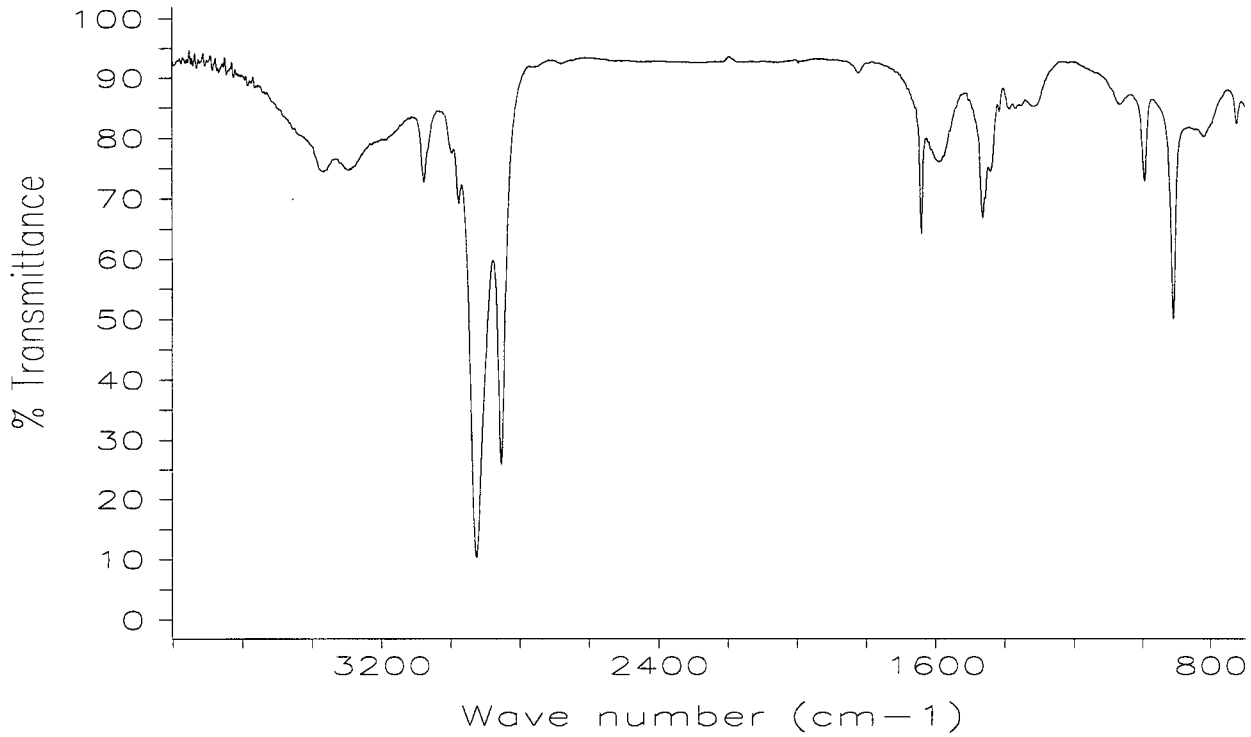
% Transmittance
100
90
80
70
60
50
40
30
20
10
0
3200
2400
1600
800
Wave number (cm−1)

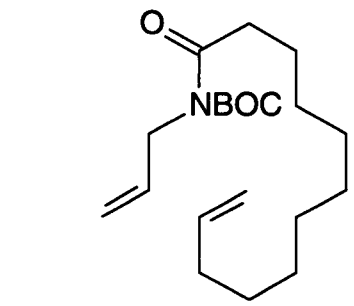
O
NBOC

139

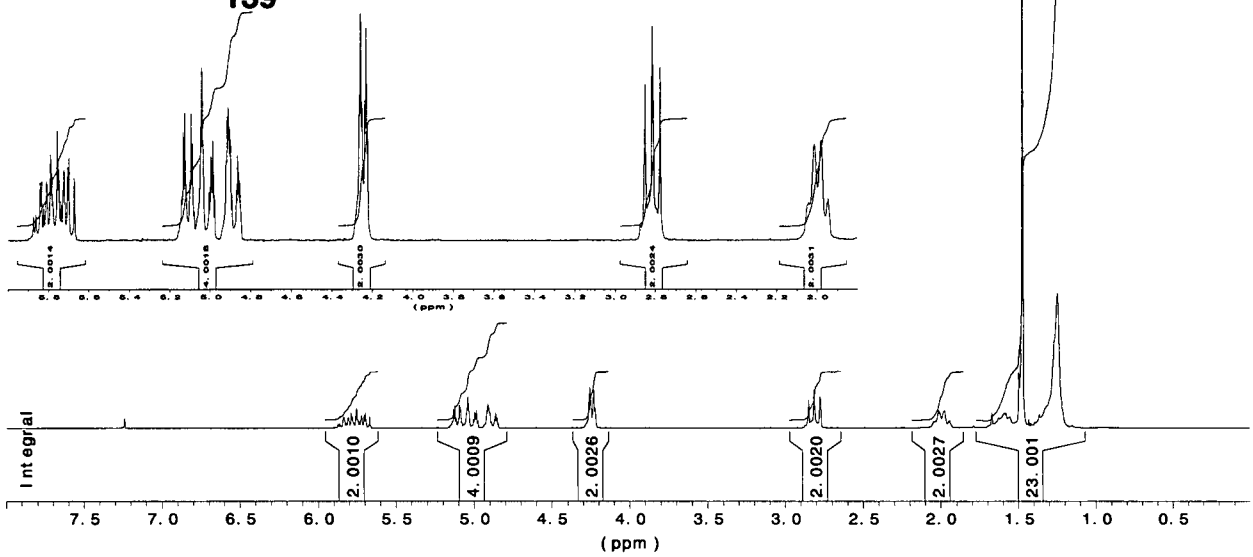
Integral
2.0010
4.0009
2.0026
2.0020
2.0027
23.001
7.5 7.0 6.5 6.0 5.5 5.0 4.5 4.0 3.5 3.0 2.5 2.0 1.5 1.0 0.5
(ppm)

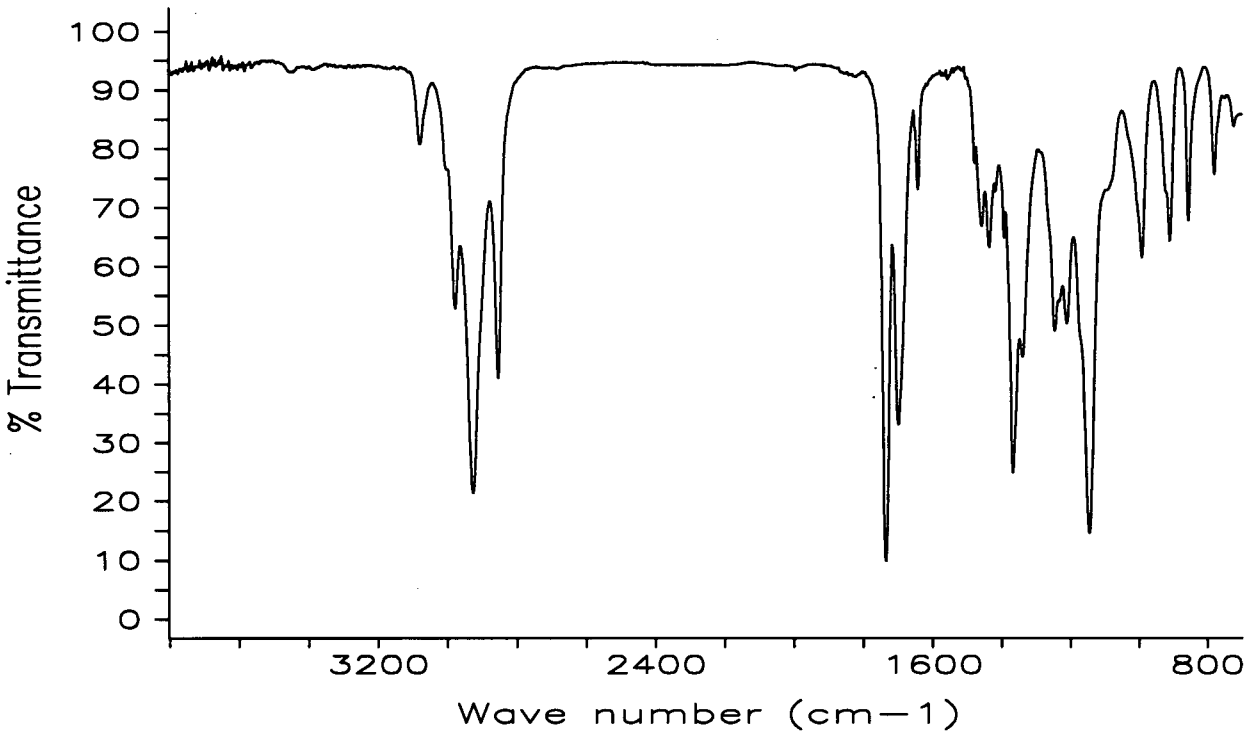
% Transmittance
100
90
80
70
60
50
40
30
20
10
0
3200
2400
1600
800
Wave number (cm−1)

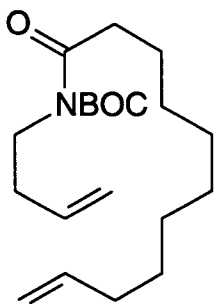
O
NBOC

140

Integral
1.9994
3.9997
2.0008
2.0013
1.9992
2.0010
21.002
7.5 7.0 6.5 6.0 5.5 5.0 4.5 4.0 3.5 3.0 2.5 2.0 1.5 1.0 0.5
(ppm)

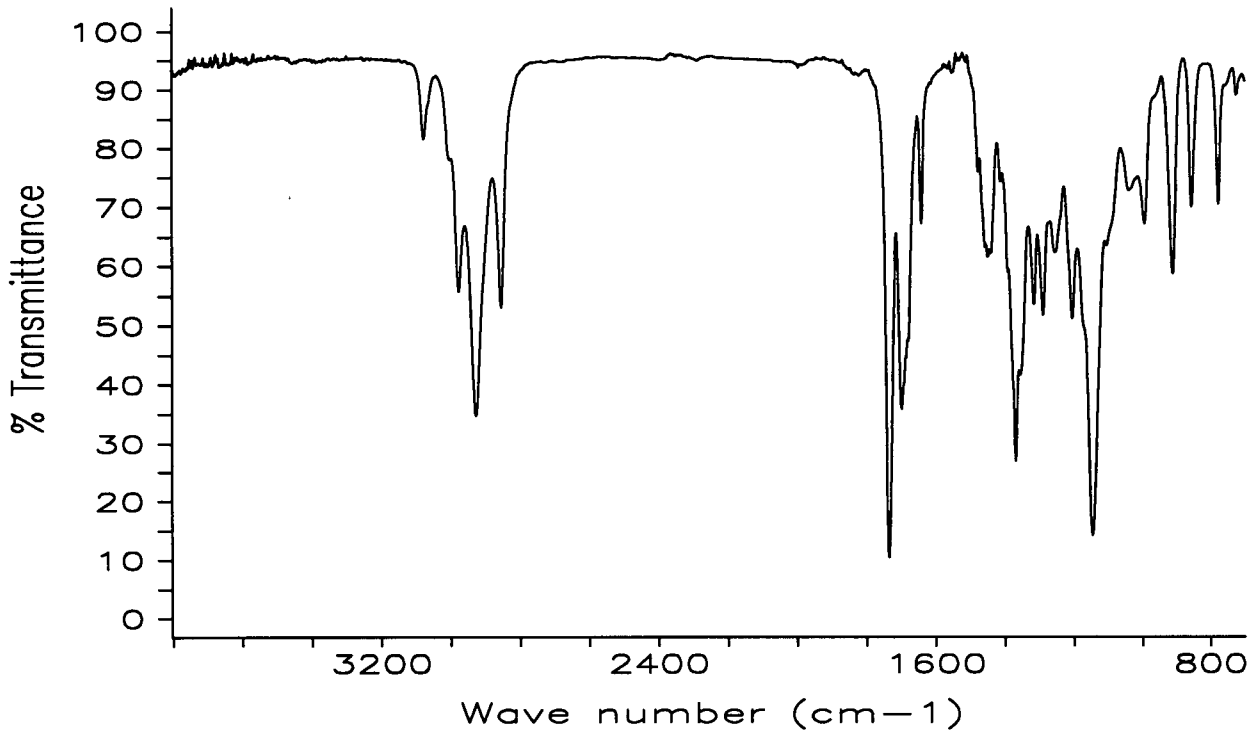
% Transmittance
100
90
80
70
60
50
40
30
20
10
0
3200
2400
1600
800
Wave number (cm−1)

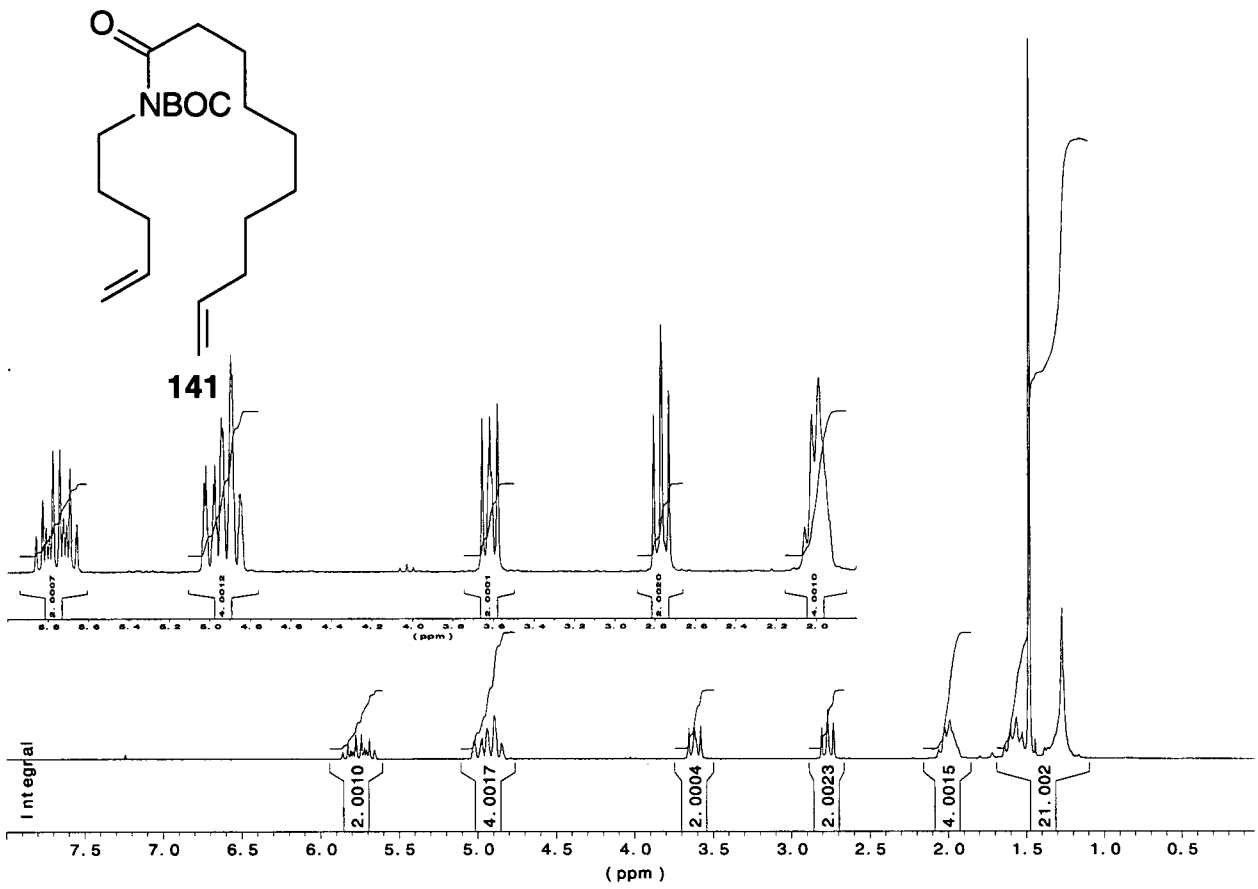
O
NBOC
141
Integral
2.0010
4.0017
2.0004
2.0023
4.0015
21.002
7.5 7.0 6.5 6.0 5.5 5.0 4.5 4.0 3.5 3.0 2.5 2.0 1.5 1.0 0.5
(ppm)

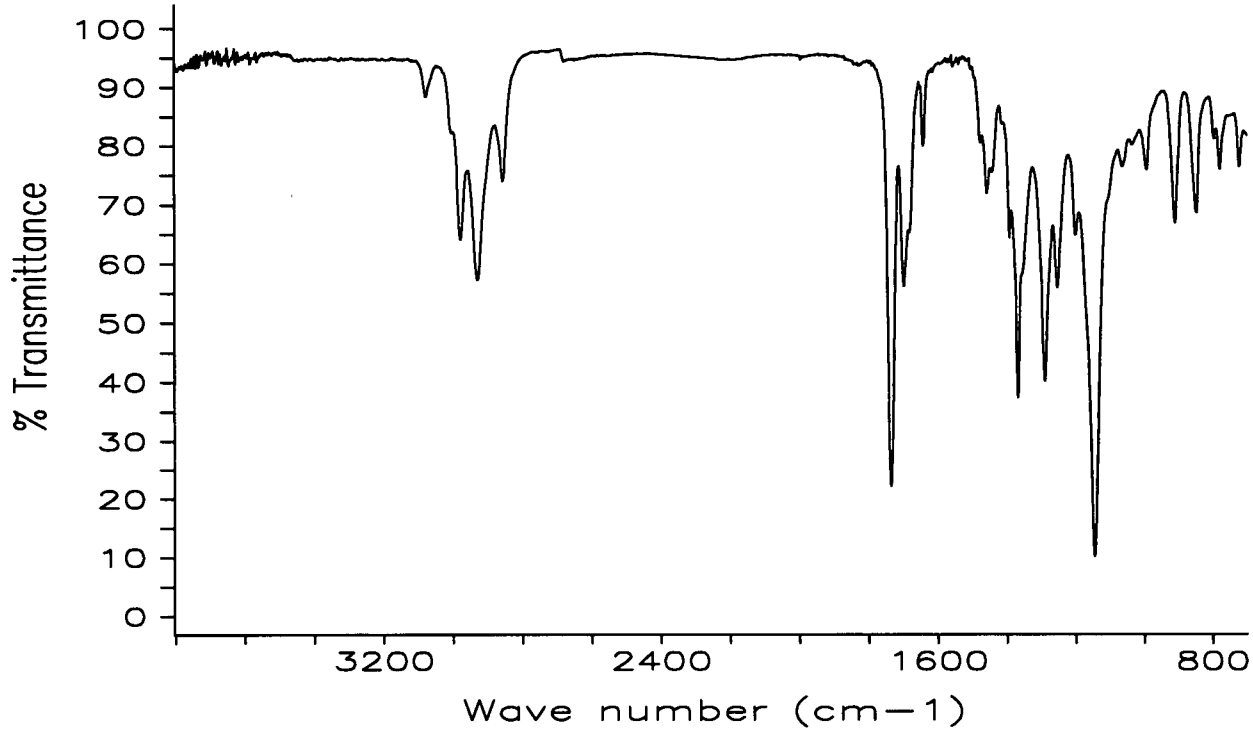
% Transmittance
100
90
80
70
60
50
40
30
20
10
0
3200
2400
1600
800
Wave number (cm−1)

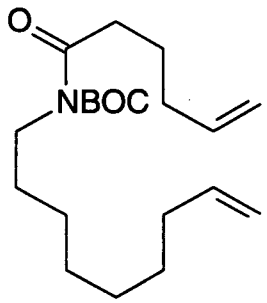
O
NBOC

142

Integral
2.0020
4.0021
2.0007
2.0009
4.0017
21.001
7.5 7.0 6.5 6.0 5.5 5.0 4.5 4.0 3.5 3.0 2.5 2.0 1.5 1.0 0.5
(ppm)

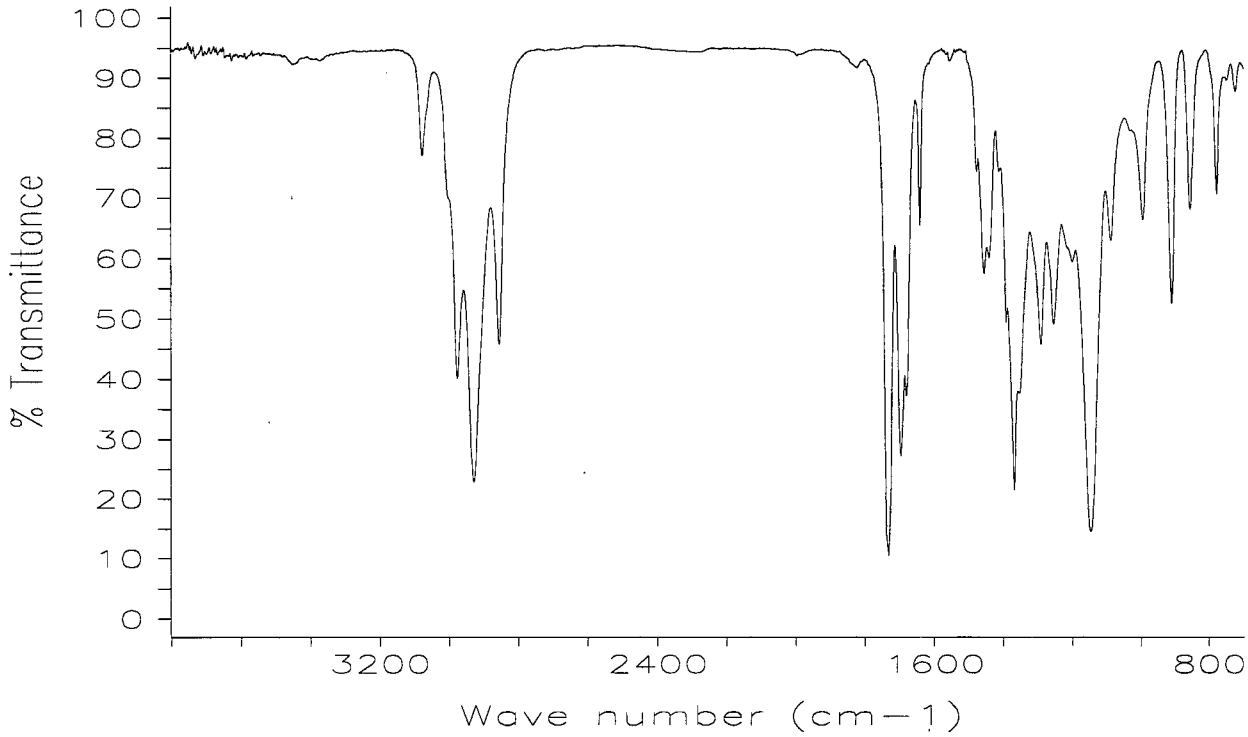
% Transmittance
100
90
80
70
60
50
40
30
20
10
0
3200
2400
1600
800
Wave number (cm−1)

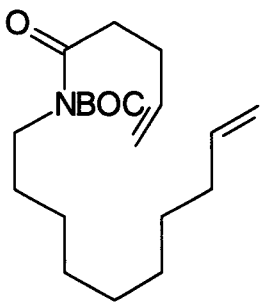
O
NBOC

143

Int egral
2.0020
4.0039
2.0022
2.0017
2.0025
2.0010
21.004
7.5 7.0 6.5 6.0 5.5 5.0 4.5 4.0 3.5 3.0 2.5 2.0 1.5 1.0 0.5
(ppm)

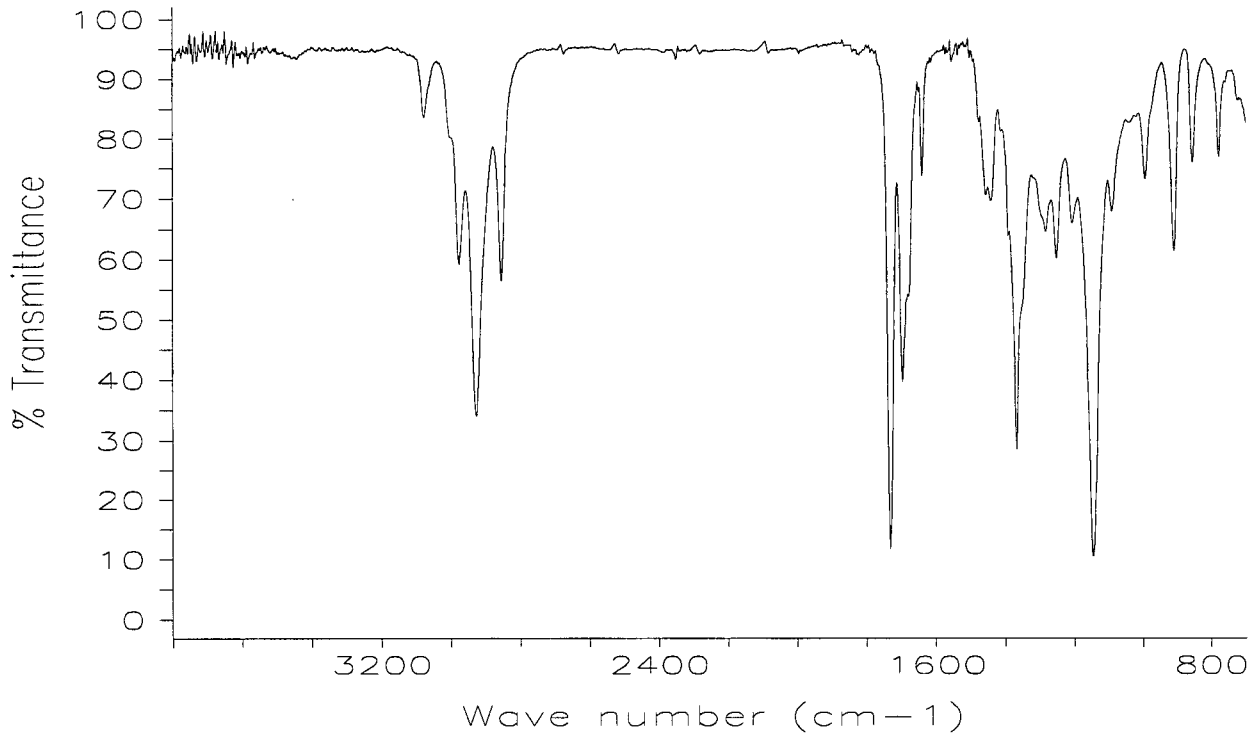
% Transmittance
100
90
80
70
60
50
40
30
20
10
0
3200
2400
1600
800
Wave number (cm−1)

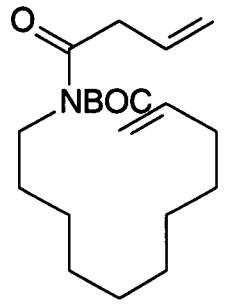
O
NBOC

144

Integral
1.0011
1.0013
4.0011
4.0016
2.0000
23.001
7.5 7.0 6.5 6.0 5.5 5.0 4.5 4.0 3.5 3.0 2.5 2.0 1.5 1.0 0.5
(ppm)

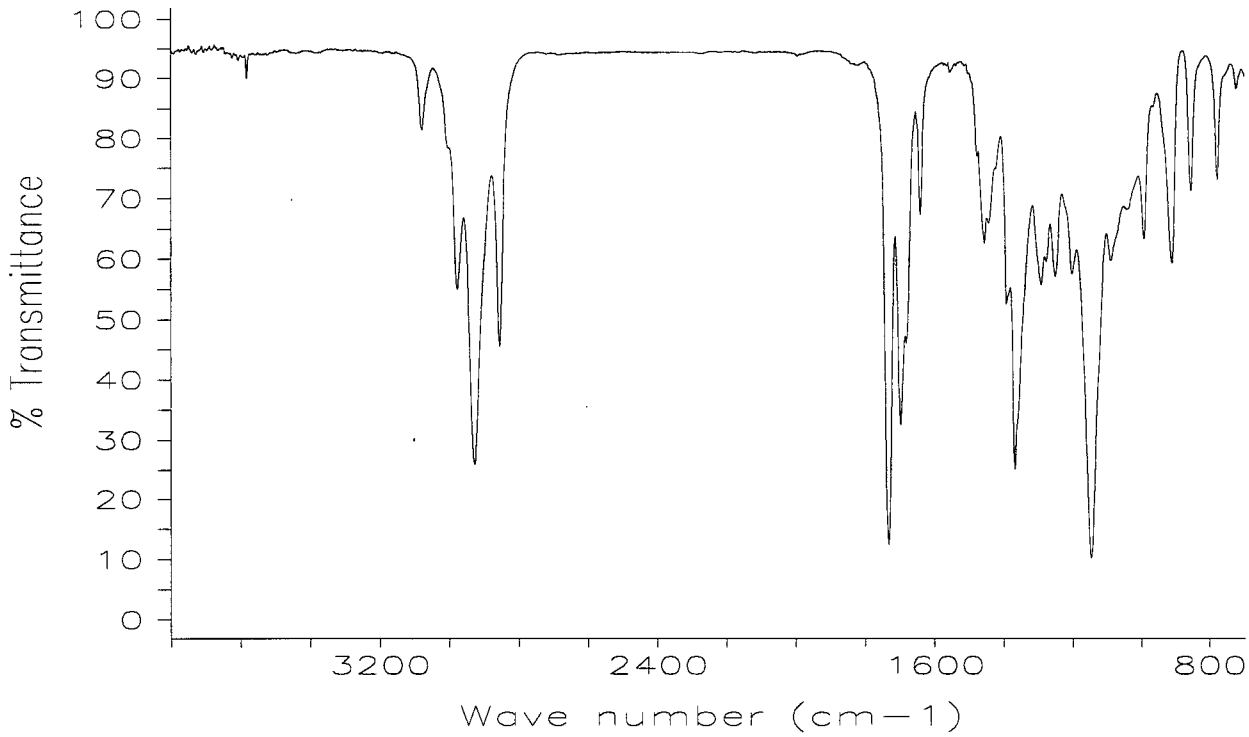
% Transmittance
100
90
80
70
60
50
40
30
20
10
0
3200
2400
1600
800
Wave number (cm−1)

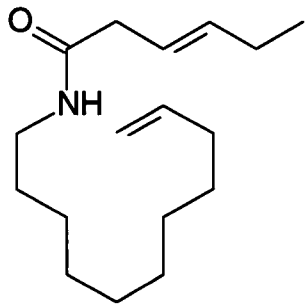
O
NH

145

Integral
4.0006
2.0023
2.0006
2.0009
4.0011
17.000
7.5 7.0 6.5 6.0 5.5 5.0 4.5 4.0 3.5 3.0 2.5 2.0 1.5 1.0 0.5
(ppm)

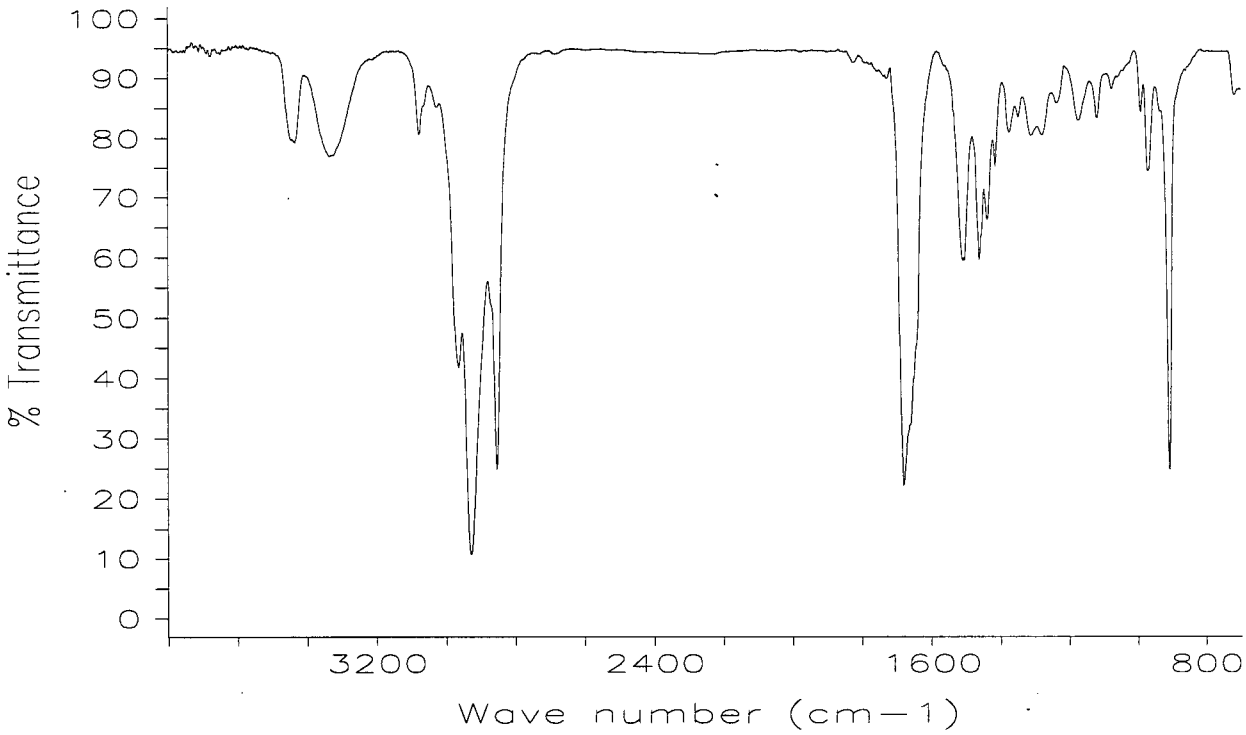
% Transmittance
100
90
80
70
60
50
40
30
20
10
0
3200
2400
1600
800
Wave number (cm−1)

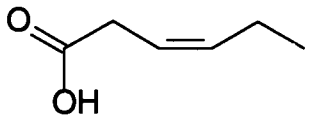
O
OH

147

1.0020
1.9998
2.0001
2.0005
2.9998
12.0
11.0
10.0
9.0
8.0
7.0
6.0
5.0
4.0
3.0
2.0
1.0
(ppm)

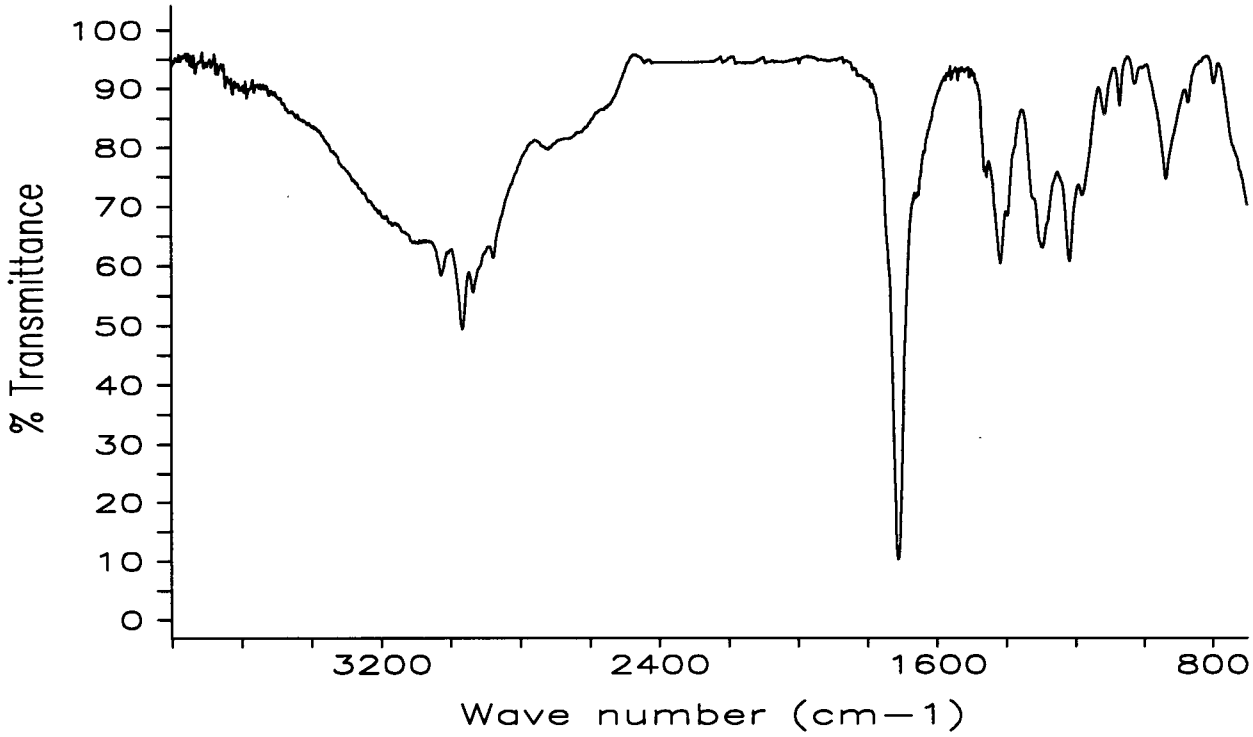
% Transmittance
100
90
80
70
60
50
40
30
20
10
0
3200
2400
1600
800
Wave number (cm−1)

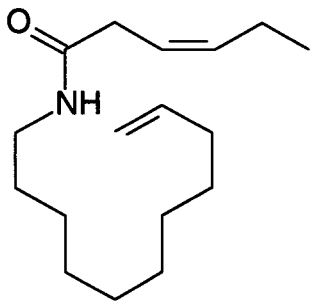
O
NH

148

Integral
4.0011
2.0010
2.0019
2.0014
4.0020
17.001
7.5 7.0 6.5 6.0 5.5 5.0 4.5 4.0 3.5 3.0 2.5 2.0 1.5 1.0 0.5
(ppm)

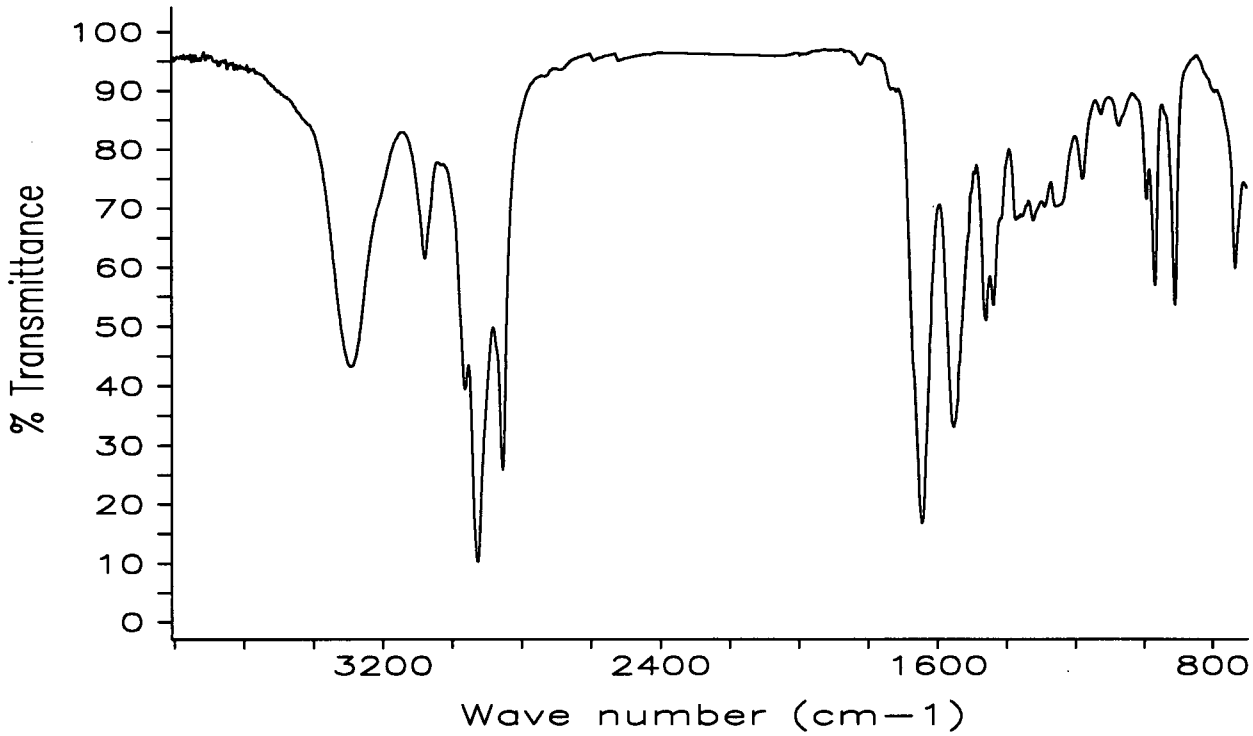
% Transmittance
100
90
80
70
60
50
40
30
20
10
0
3200
2400
1600
800
Wave number (cm−1)

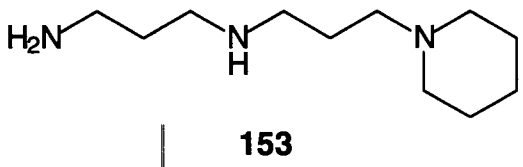

153

Integral
13.000
12.001
5.6
5.2
4.8
4.4
4.0
3.6
3.2
2.8
2.4
2.0
1.6
1.2
0.8
0.4
(ppm)

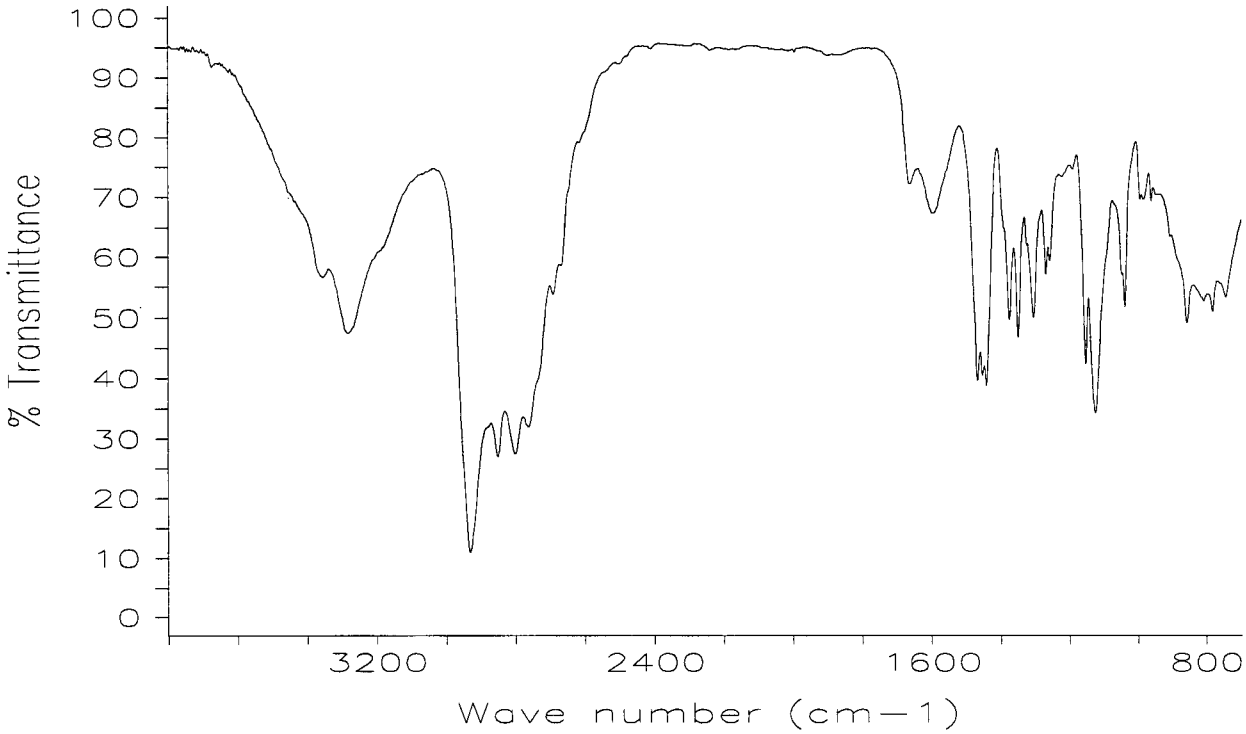
% Transmittance
100
90
80
70
60
50
40
30
20
10
0
3200
2400
1600
800
Wave number (cm−1)

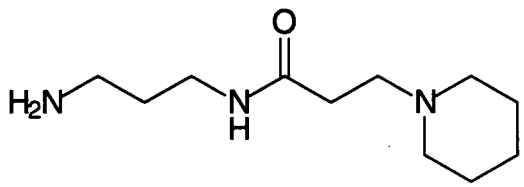
O
H2N
N
H
N

155

Integral
1.0005
2.0014
10.000
10.001
9.5 9.0 8.5 8.0 7.5 7.0 6.5 6.0 5.5 5.0 4.5 4.0 3.5 3.0 2.5 2.0 1.5 1.0 0.5
(ppm)

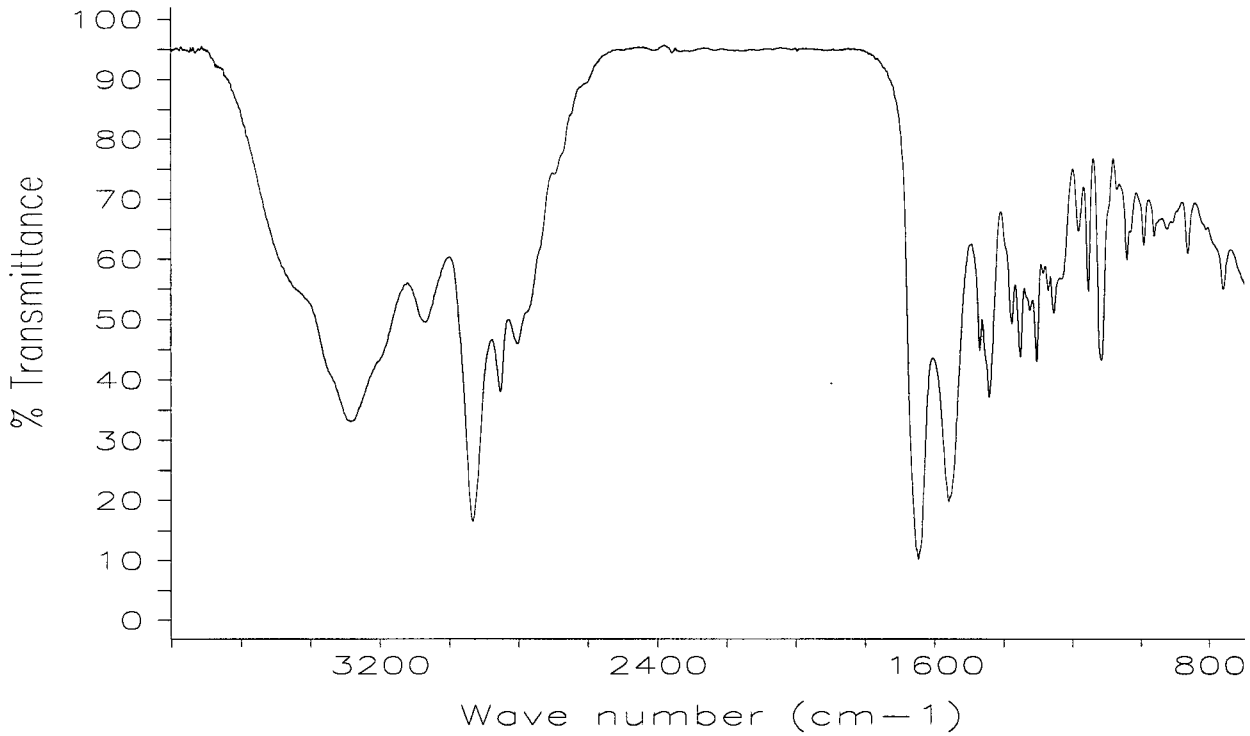
% Transmittance
100
90
80
70
60
50
40
30
20
10
0
3200
2400
1600
800
Wave number (cm−1)

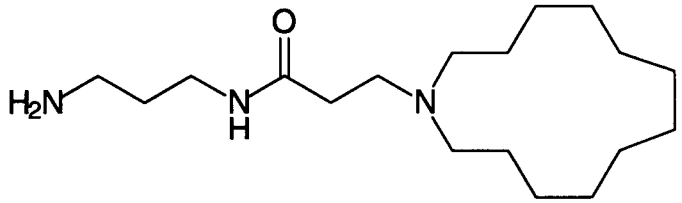
O
H2N
N
H
N

156

Int egral
1.0000
2.0008
10.000
24.002
9.5 9.0 8.5 8.0 7.5 7.0 6.5 6.0 5.5 5.0 4.5 4.0 3.5 3.0 2.5 2.0 1.5 1.0 0.5
(ppm)

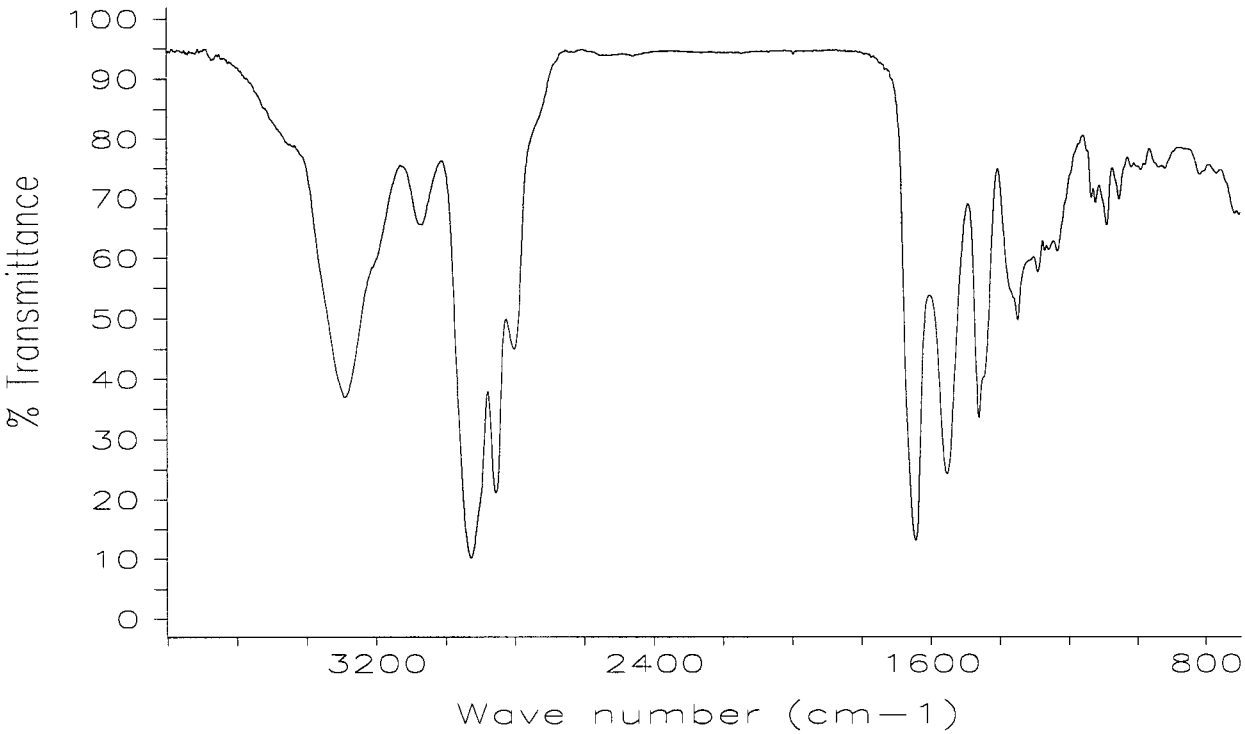
% Transmittance
100
90
80
70
60
50
40
30
20
10
0
3200
2400
1600
800
Wave number (cm−1)

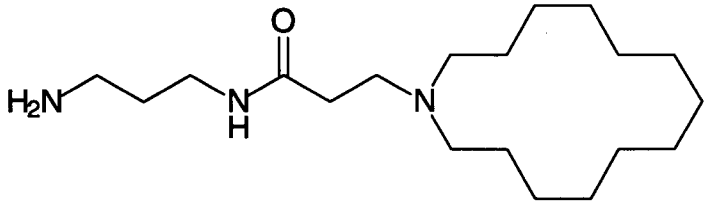
O
H2N
N
H
N

157

Integral
0.9998
2.0009
4.0000
4.0013
2.0017
26.001
5.6
5.2
4.8
4.4
4.0
3.6
3.2
2.8
2.4
2.0
1.6
1.2
0.8
0.4
(ppm)

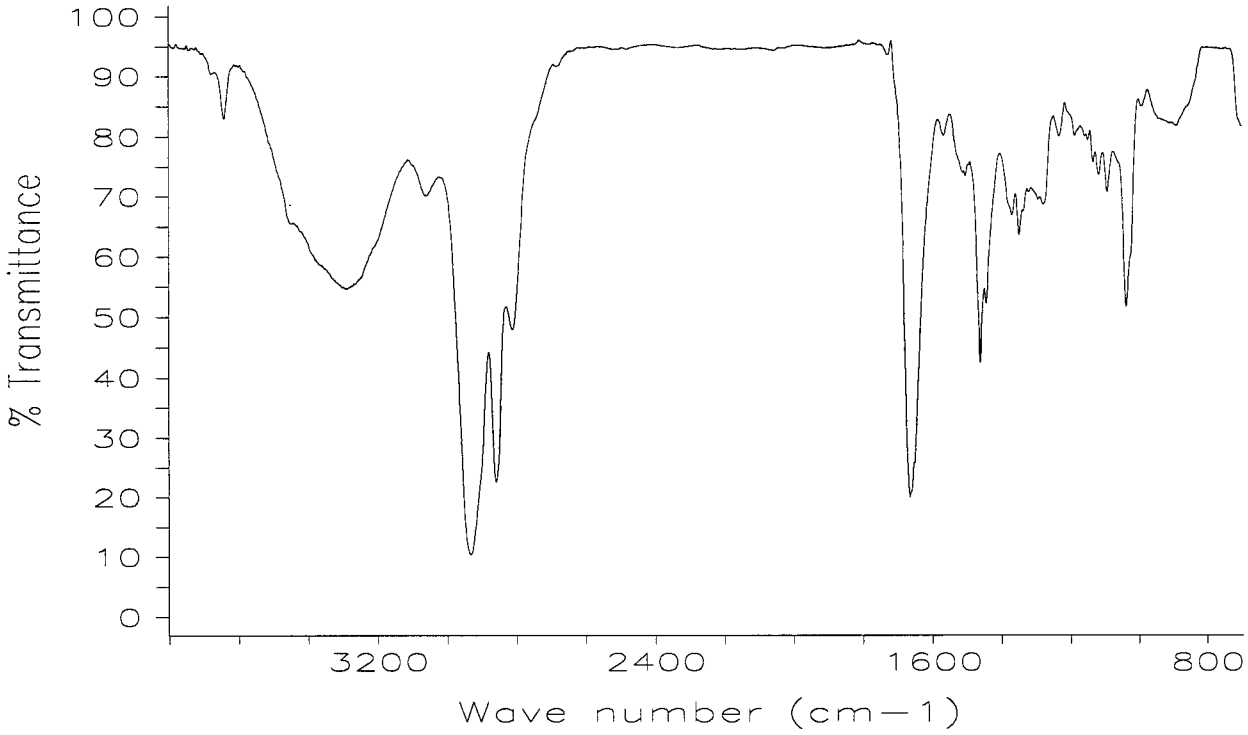
% Transmittance
100
90
80
70
60
50
40
30
20
10
0
3200
2400
1600
800
Wave number (cm−1)

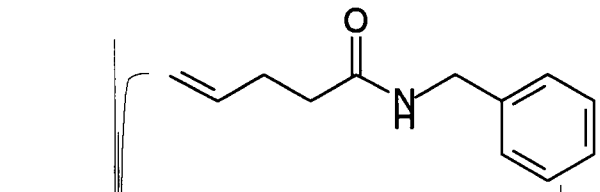

158

Integral
5.0950
2.0009
2.0009
2.0005
4.0013
7.5
7.0
6.5
6.0
5.5
5.0
4.5
4.0
3.5
3.0
2.5
2.0
1.5
1.0
0.5
(ppm)

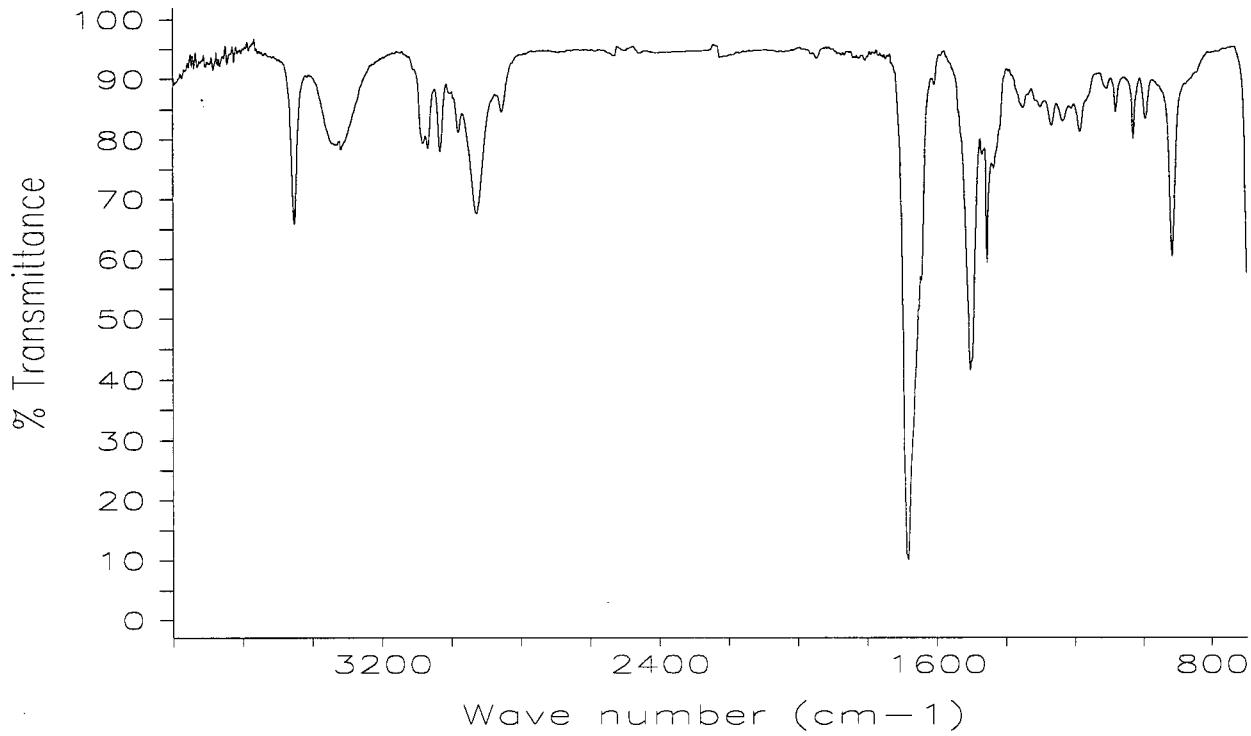
% Transmittance
100
90
80
70
60
50
40
30
20
10
0
3200
2400
1600
800
Wave number (cm−1)

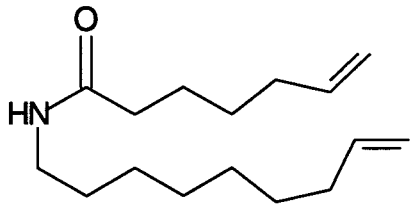
O
HN

159

Integral
3.0008
4.0007
2.0004
6.0000
14.001
7.5 7.0 6.5 6.0 5.5 5.0 4.5 4.0 3.5 3.0 2.5 2.0 1.5 1.0 0.5
(ppm)

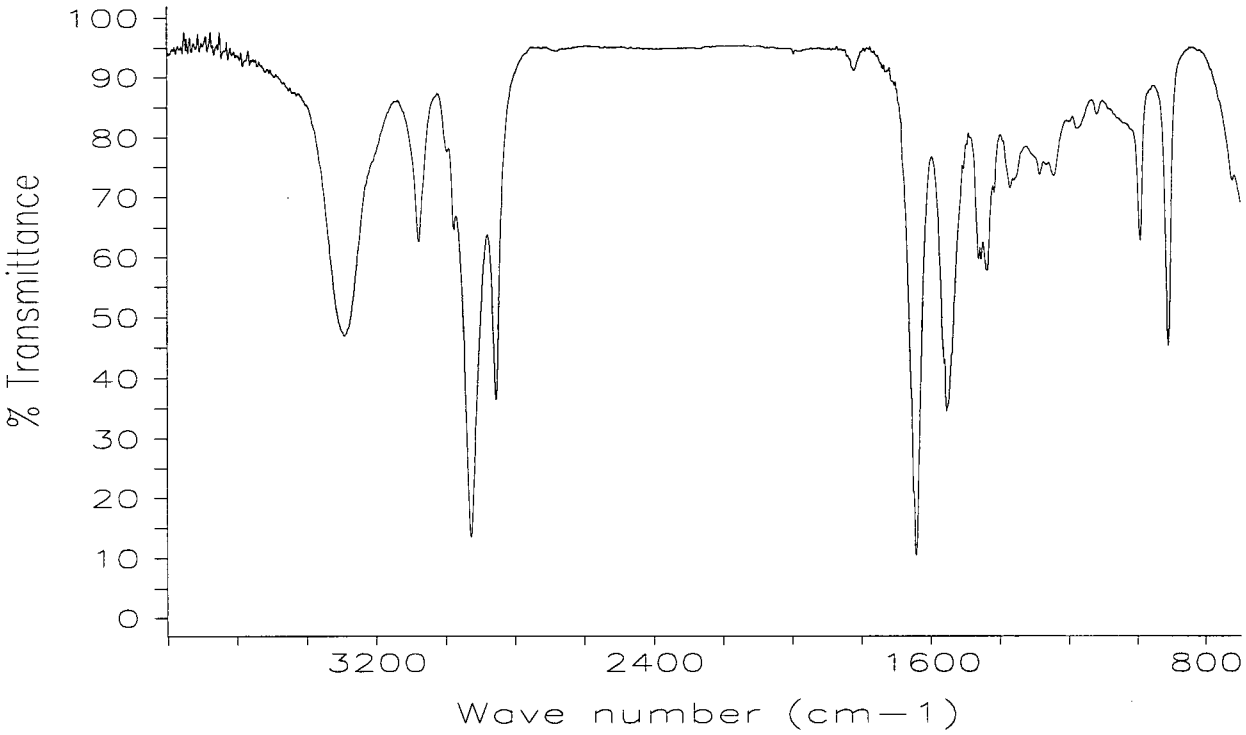
% Transmittance
100
90
80
70
60
50
40
30
20
10
0
3200
2400
1600
800
Wave number (cm−1)

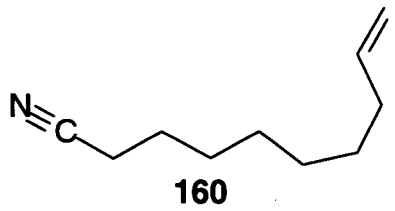
N≡C

160

Integral
1.0010
2.0015
4.0000
10.003
7.5 7.0 6.5 6.0 5.5 5.0 4.5 4.0 3.5 3.0 2.5 2.0 1.5 1.0 0.5
(ppm)

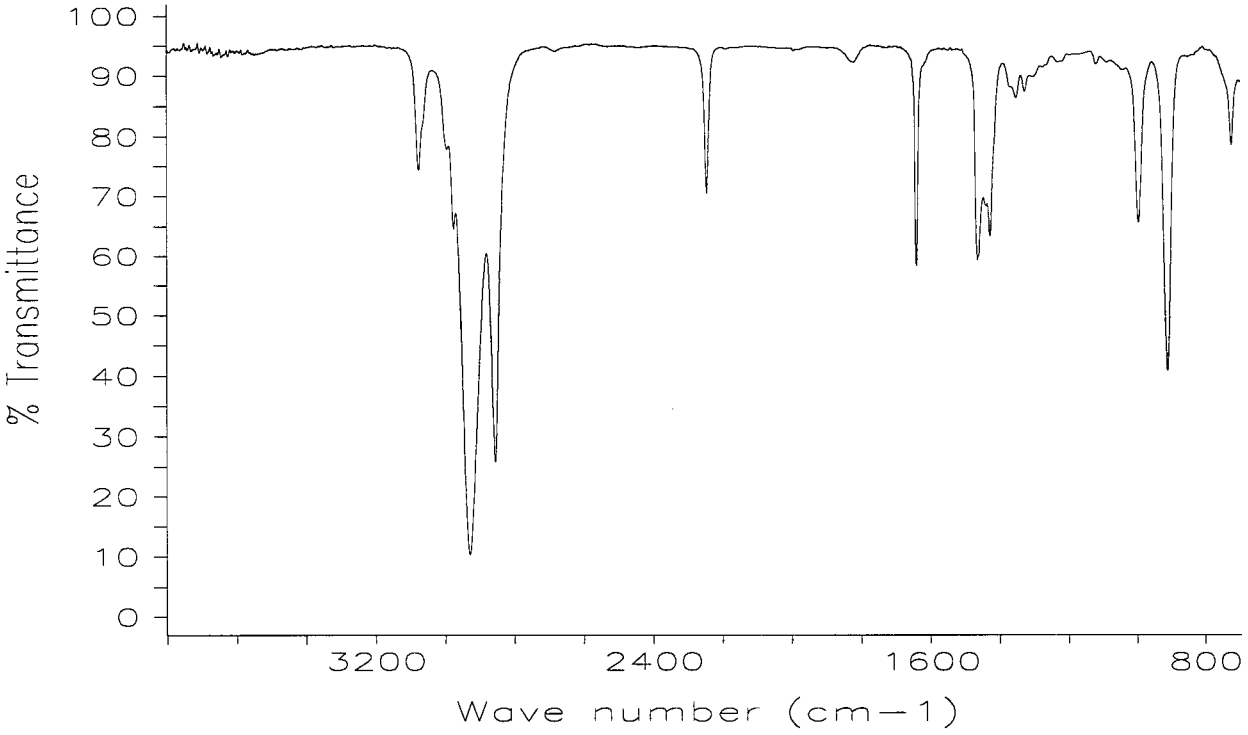
% Transmittance
100
90
80
70
60
50
40
30
20
10
0
3200
2400
1600
800
Wave number (cm−1)

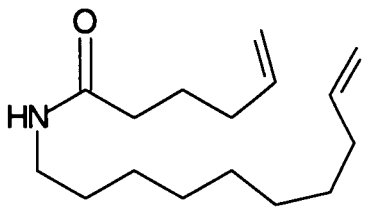
O
HN

161

Integral
3.0011
4.0023
2.0000
20.002
7.5 7.0 6.5 6.0 5.5 5.0 4.5 4.0 3.5 3.0 2.5 2.0 1.5 1.0 0.5
(ppm)

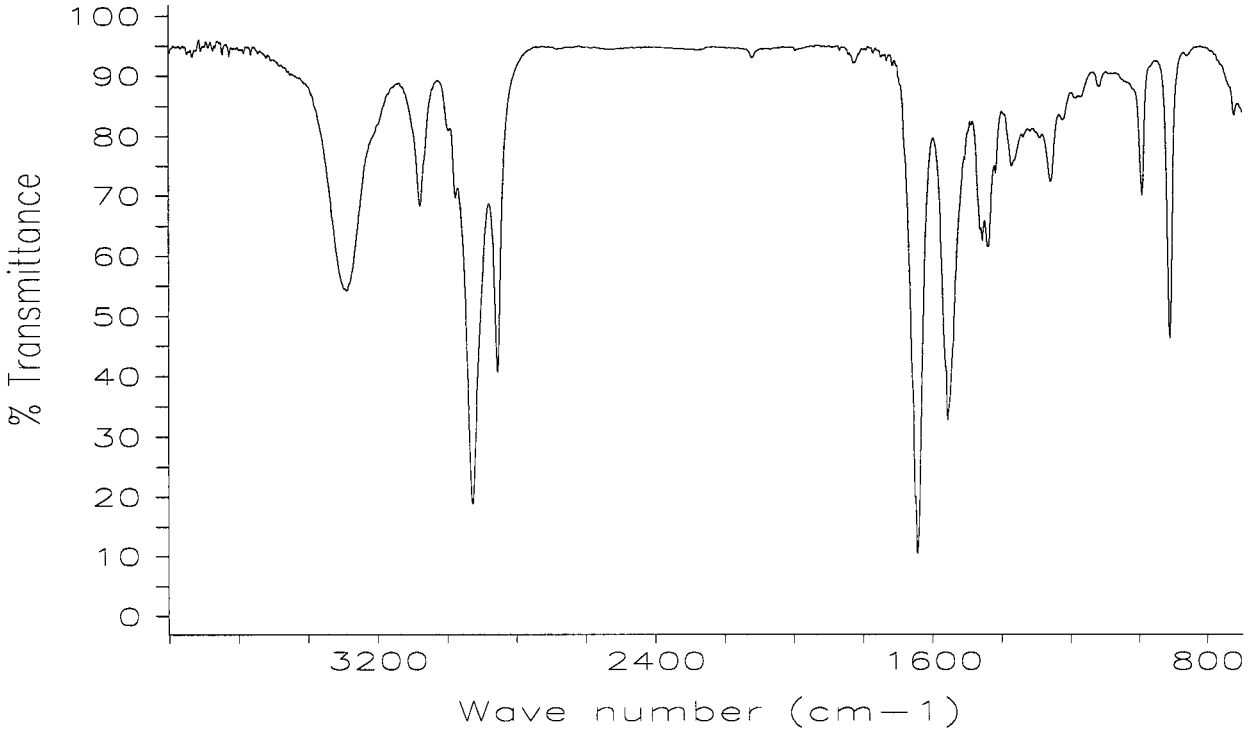
% Transmittance
100
90
80
70
60
50
40
30
20
10
0
3200
2400
1600
800
Wave number (cm−1)

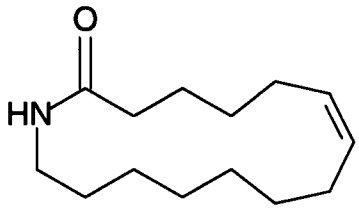
O
HN

162

Integral
3.0000
2.0009
6.0001
14.002
7.5
7.0
6.5
6.0
5.5
5.0
4.5
4.0
3.5
3.0
2.5
2.0
1.5
1.0
0.5
(ppm)

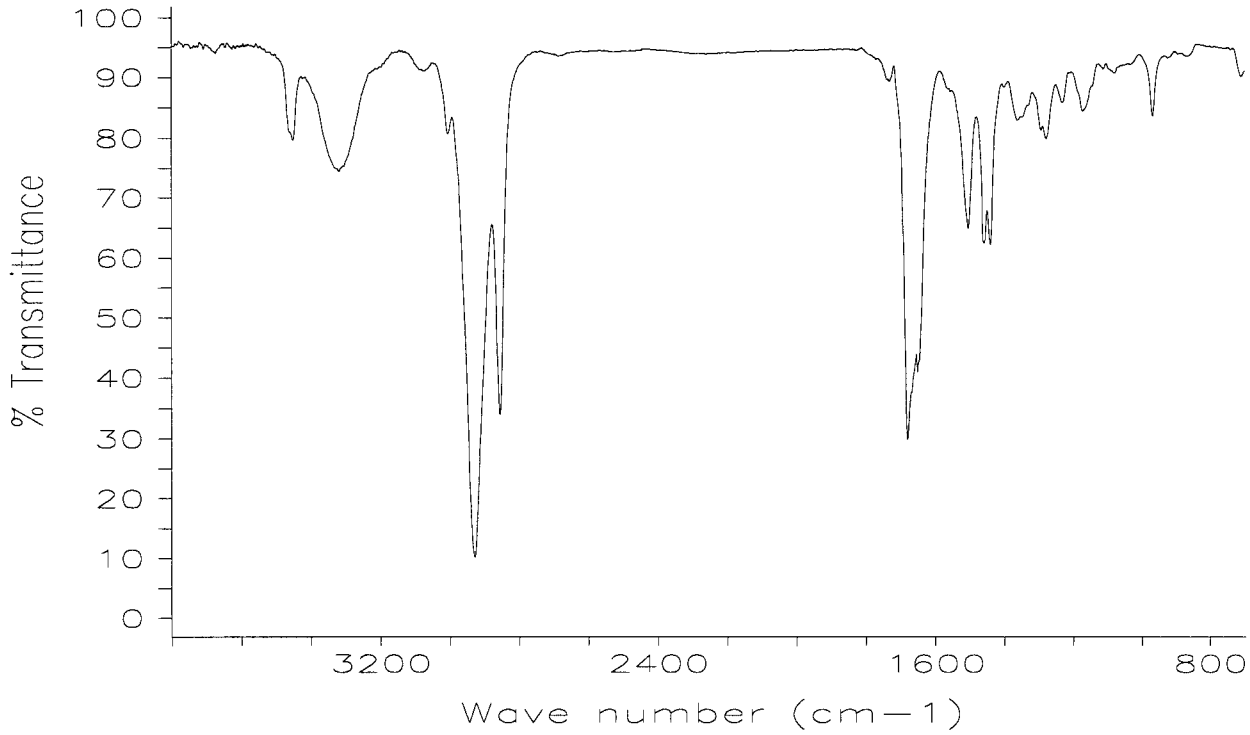
% Transmittance
100
90
80
70
60
50
40
30
20
10
0
3200
2400
1600
800
Wave number (cm−1)

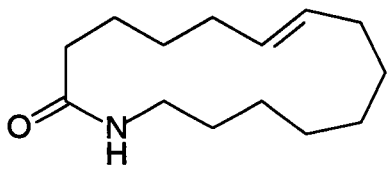
O
N
H

163

Integral
3.0008
2.0009
6.0000
14.001
7.5 7.0 6.5 6.0 5.5 5.0 4.5 4.0 3.5 3.0 2.5 2.0 1.5 1.0 0.5
(ppm)

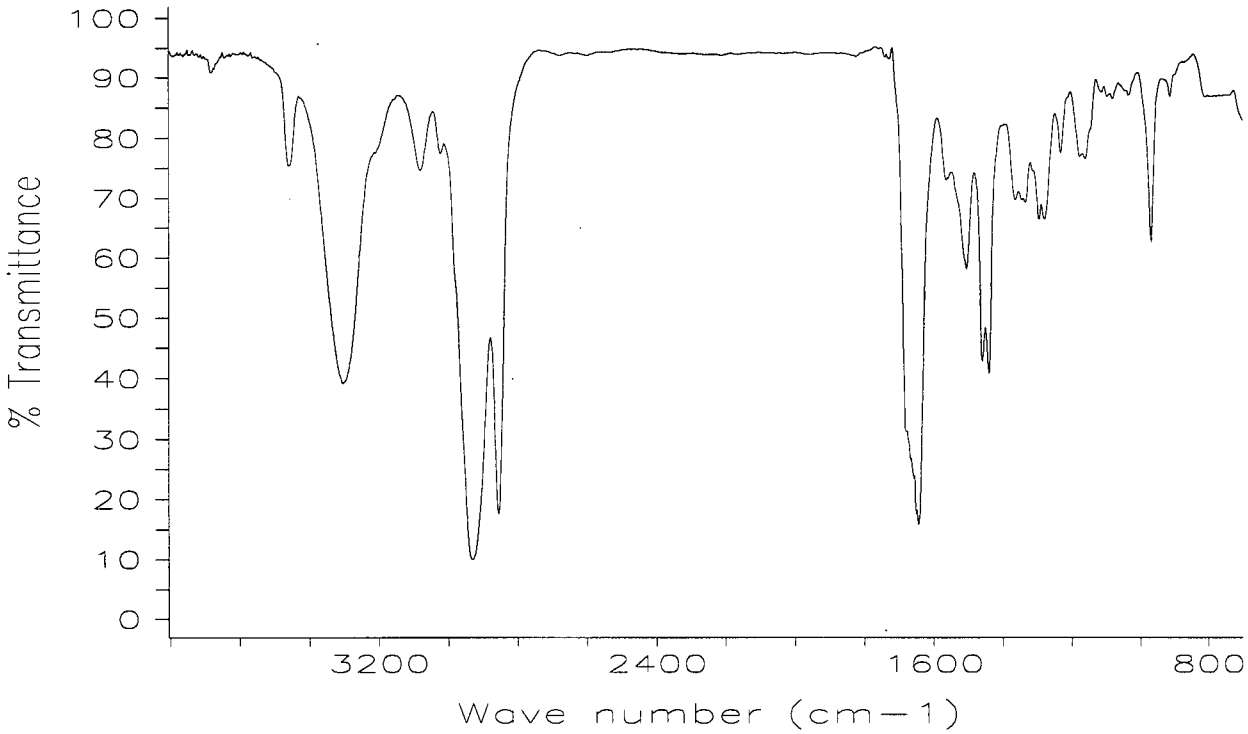
% Transmittance
100
90
80
70
60
50
40
30
20
10
0
3200
2400
1600
800
Wave number (cm−1)

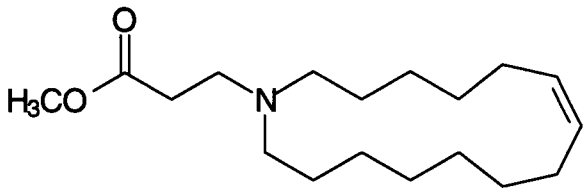
O
H3CO
N

164

Integral
2.0010
3.0008
2.0009
5.9987
3.9996
16.001
7.5 7.0 6.5 6.0 5.5 5.0 4.5 4.0 3.5 3.0 2.5 2.0 1.5 1.0 0.5
(ppm)

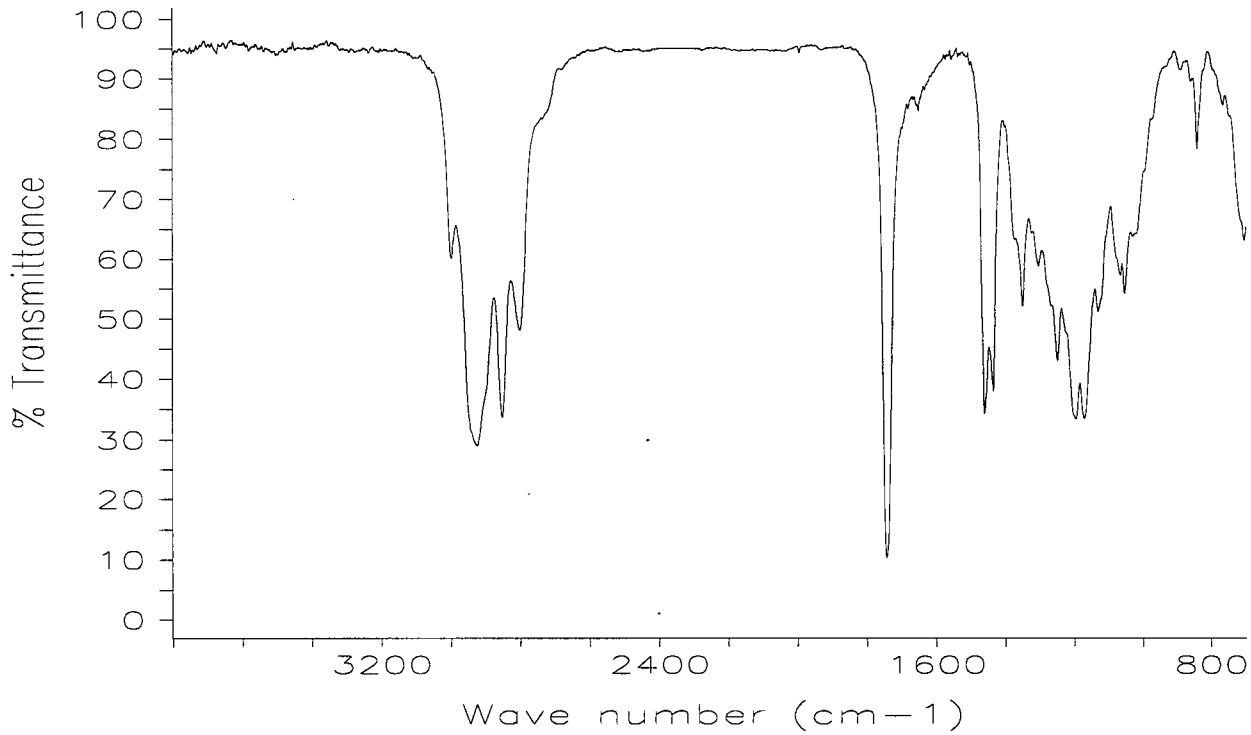
% Transmittance
100
90
80
70
60
50
40
30
20
10
0
3200
2400
1600
800
Wave number (cm−1)

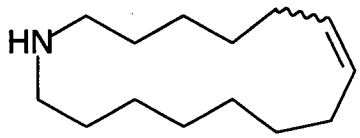
HN

167 and **168**

Integral
2.0007
4.0000
21.001
7.5
7.0
6.5
6.0
5.5
5.0
4.5
4.0
3.5
3.0
2.5
2.0
1.5
1.0
0.5
(ppm)

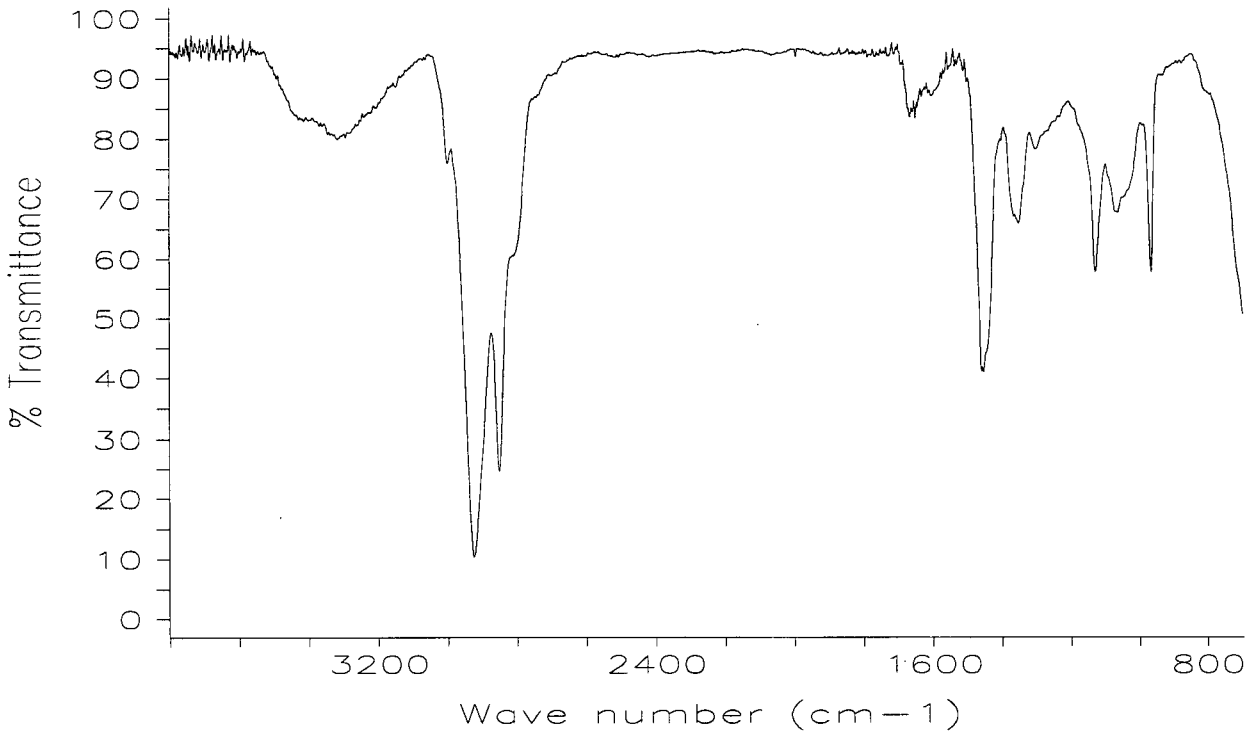
% Transmittance
100
90
80
70
60
50
40
30
20
10
0
3200
2400
1600
800
Wave number (cm−1)

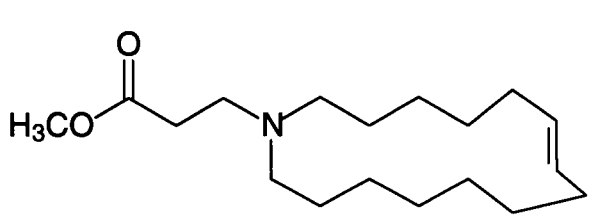
O
H3CO
N

169

Integral
1.9998
2.9993
1.9996
6.0003
4.0010
16.001
7.5 7.0 6.5 6.0 5.5 5.0 4.5 4.0 3.5 3.0 2.5 2.0 1.5 1.0 0.5
(ppm)

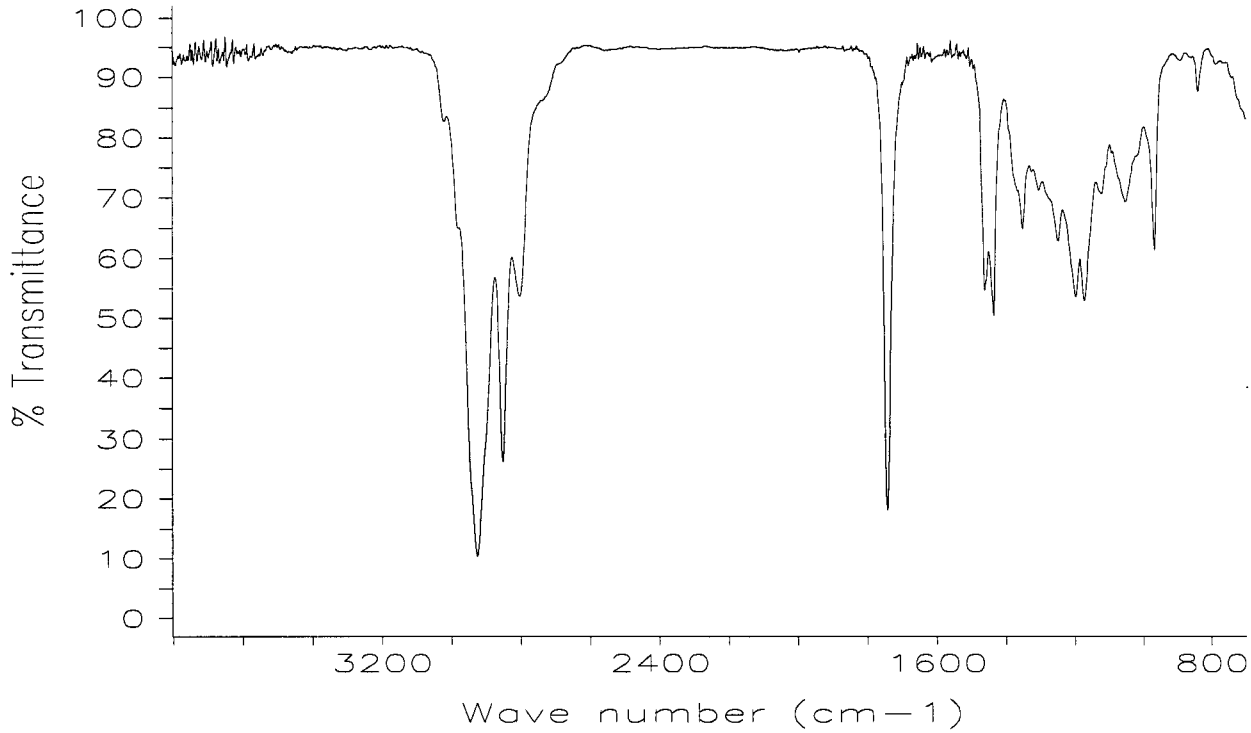
% Transmittance
100
90
80
70
60
50
40
30
20
10
0
3200
2400
1600
800
Wave number (cm−1)

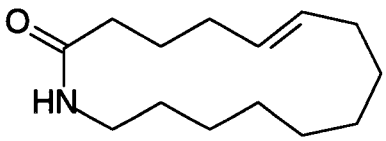
O
HN

170

Integral
3.0011
2.0009
6.0006
2.0011
12.002
7.5 7.0 6.5 6.0 5.5 5.0 4.5 4.0 3.5 3.0 2.5 2.0 1.5 1.0 0.5
(ppm)

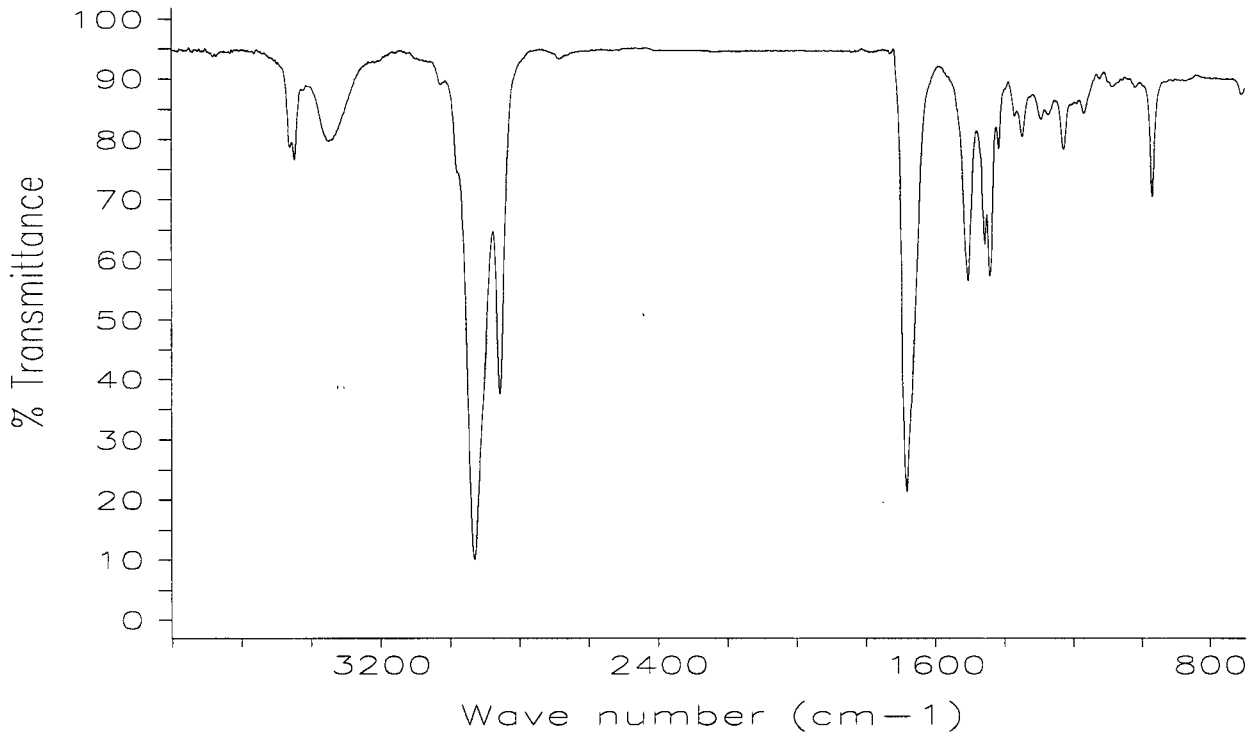
% Transmittance
100
90
80
70
60
50
40
30
20
10
0
3200
2400
1600
800
Wave number (cm−1)

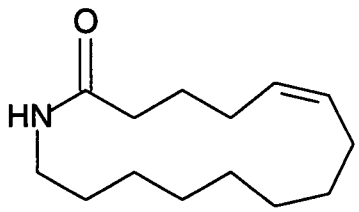
O
HN

171

Integral
3.0010
2.0012
6.0000
2.0011
12.001
7.5 7.0 6.5 6.0 5.5 5.0 4.5 4.0 3.5 3.0 2.5 2.0 1.5 1.0 0.5
(ppm)

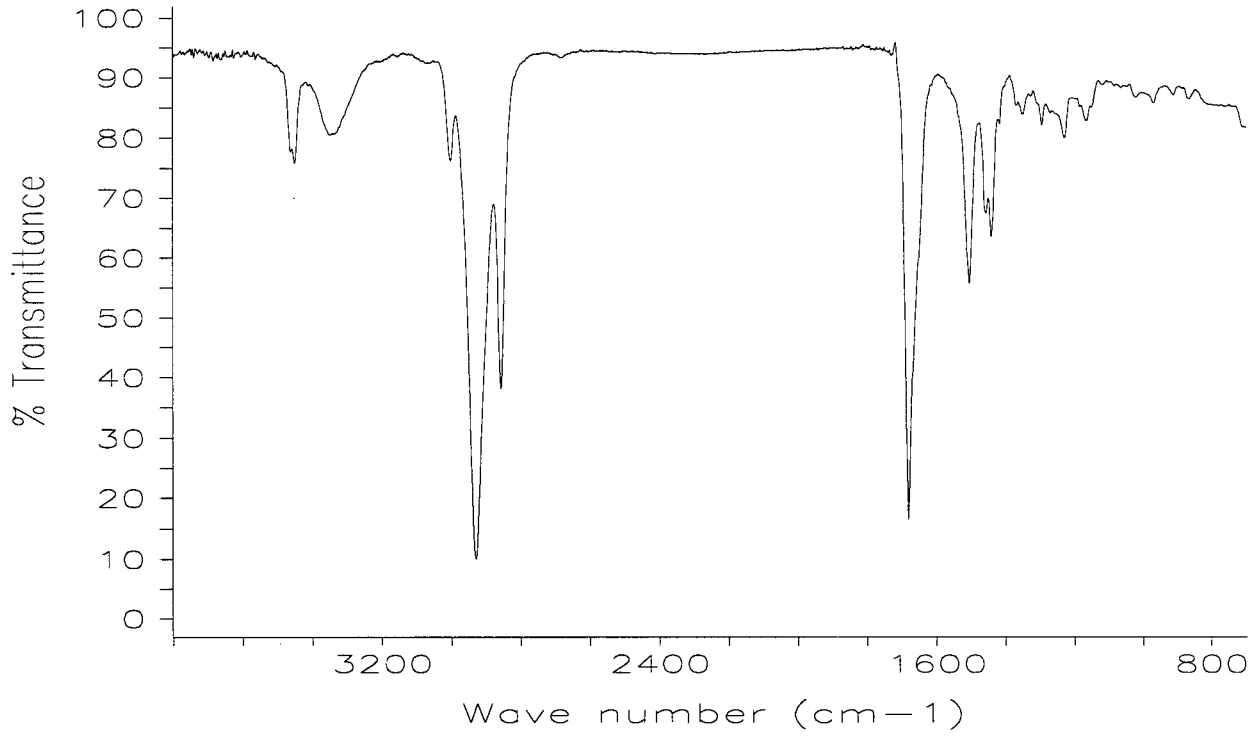
% Transmittance
100
90
80
70
60
50
40
30
20
10
0
3200
2400
1600
800
Wave number (cm−1)

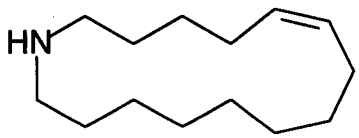
HN

172

Integral
2.0007
4.0000
4.0007
17.001
7.5
7.0
6.5
6.0
5.5
5.0
4.5
4.0
3.5
3.0
2.5
2.0
1.5
1.0
0.5
(ppm)

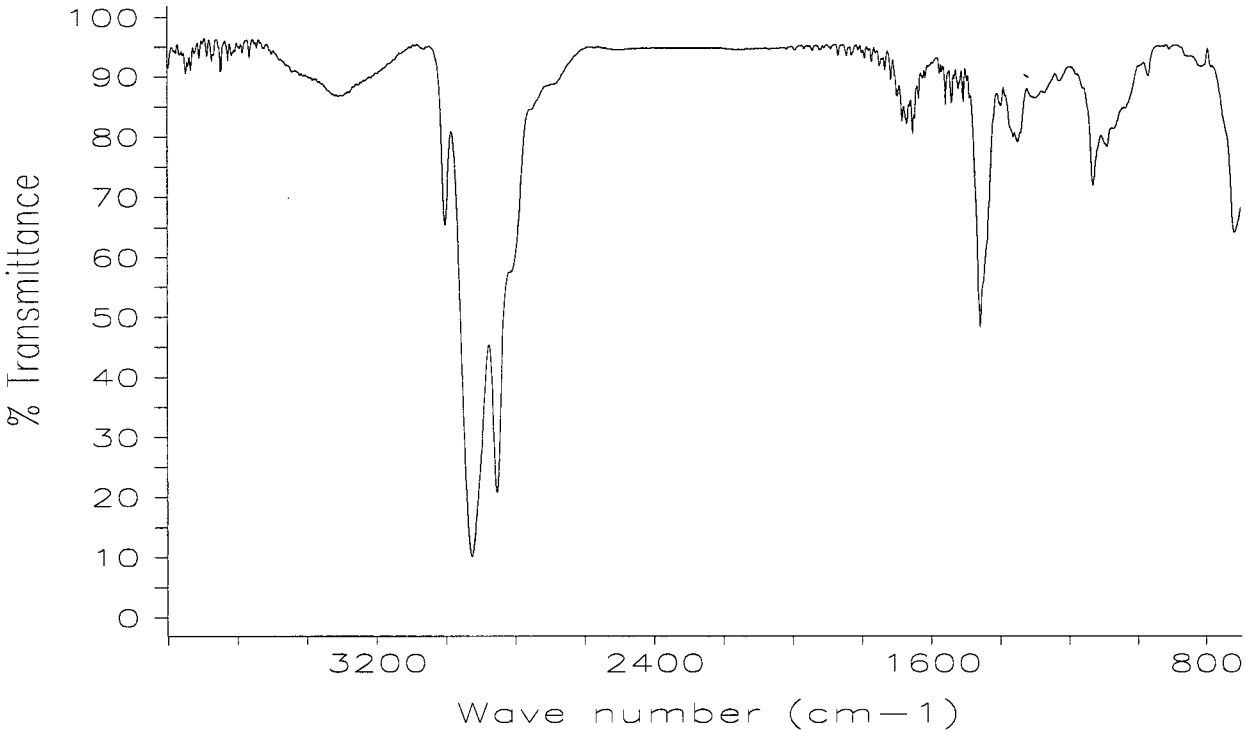
% Transmittance
100
90
80
70
60
50
40
30
20
10
0
3200
2400
1600
800
Wave number (cm−1)

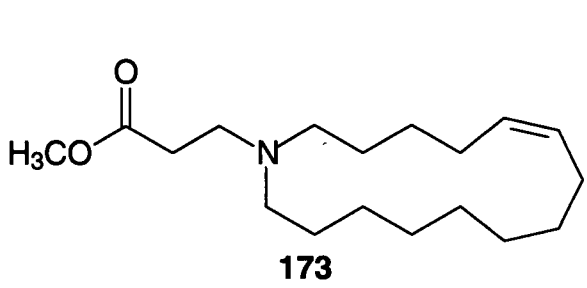
O
H3CO
N

173

Integral
2.0010
3.0013
2.0000
6.0009
4.0010
16.001
7.5 7.0 6.5 6.0 5.5 5.0 4.5 4.0 3.5 3.0 2.5 2.0 1.5 1.0 0.5
(ppm)

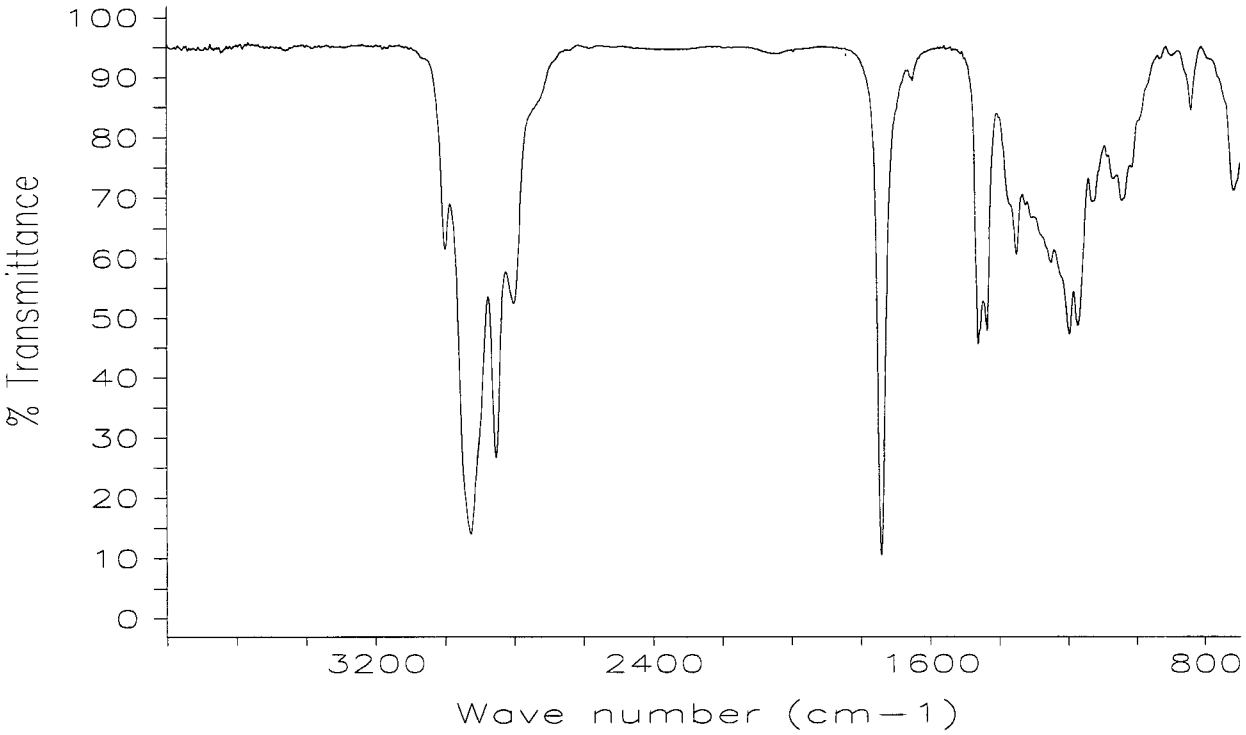
% Transmittance
100
90
80
70
60
50
40
30
20
10
0
3200
2400
1600
800
Wave number (cm−1)